RECEIVED
LAWRENCE
BERKELEY LABORATORY

NOV 1 8 1988

LIBRARY AND
DOCUMENTS SECTION

LBL-24242 c.1
UC-400

MATERIALS AND CHEMICAL SCIENCES DIVISION

Annual Report 1987

July 1988

Lawrence Berkeley Laboratory
University of California
Berkeley, California 94720

Prepared for the
U.S. Department of Energy under Contract DE-AC03-76SF00098

LBL-24242 c.1

DISCLAIMER

This document was prepared as an account of work sponsored by the United States Government. While this document is believed to contain correct information, neither the United States Government nor any agency thereof, nor the Regents of the University of California, nor any of their employees, makes any warranty, express or implied, or assumes any legal responsibility for the accuracy, completeness, or usefulness of any information, apparatus, product, or process disclosed, or represents that its use would not infringe privately owned rights. Reference herein to any specific commercial product, process, or service by its trade name, trademark, manufacturer, or otherwise, does not necessarily constitute or imply its endorsement, recommendation, or favoring by the United States Government or any agency thereof, or the Regents of the University of California. The views and opinions of authors expressed herein do not necessarily state or reflect those of the United States Government or any agency thereof or the Regents of the University of California.

LBL-24242

MATERIALS AND CHEMICAL SCIENCES DIVISION

Annual Report 1987
July 1988

Norman E. Phillips, Division Head
Mark Alper, Associate Division Head
Rolf H. Muller, Associate Division Head
Conway V. Peterson, Associate Division Head

Lawrence Berkeley Laboratory
University of California
Berkeley, California 94720

Materials Sciences

Chemical Sciences

Nuclear Sciences

Fossil Energy

Energy Storage Systems

Health and Environmental Sciences

Program Development Funds

Work for Others

Appendices

Contents

REMARKS BY THE DIVISION HEAD

Norman E. Phillips xi

MATERIALS SCIENCES

Metallurgy and Ceramics

Structure of Materials

Structure and Properties of Transformation Interfaces
Ronald Gronsky, Investigator 1

Microstructure, Properties, and Alloy Design: Inorganic Materials
Gareth Thomas, Investigator 5

Solid-State Phase Transformation Mechanisms
Kenneth H. Westmacott, Investigator 16

National Center for Electron Microscopy
Gareth Thomas, Ronald Gronsky, and Kenneth H. Westmacott, Investigators 19

In Situ Investigations of Gas-Solid Reactions by Electron Microscopy
James W. Evans, Investigator 37

Local Atomic Configurations in Solid Solutions
Didier de Fontaine, Investigator 39

Alloy Theory
Didier de Fontaine and Leo M. Falicov, Investigators 41

Mechanical Properties

Environmentally Affected Crack Growth in Engineering Materials
Robert O. Ritchie, Investigator 45

Physical Properties

High-Temperature Reactions
Alan W. Searcy, Investigator 52

Structure-Property Relationships in Semiconductor Materials
Jack Washburn, Investigator 56

Fundamental Studies of Chemical Properties and Processing of Advanced Structural Ceramics
Lutgard C. De Jonghe, Investigator 62

Structure and Electrical Properties of Composite Materials
Robert H. Bragg, Investigator 66

Ceramic Interfaces
Andreas M. Glaeser, Investigator 68

Solid-State Physics

Experimental Research

Far-Infrared Spectroscopy
Paul L. Richards, Investigator 71

Experimental Solid-State Physics and Quantum Electronics
Y. Ron Shen, Investigator 76

Excitations in Solids
Carson D. Jeffries, Investigator 81

Time-Resolved Spectroscopies in Solids
Peter Y. Yu, Investigator 84

Superconductivity, Superconducting Devices, and 1/f Noise
John Clarke, Investigator 86

Theoretical Research

Theoretical Studies of the Electronic Properties of Solid Surfaces
Leo M. Falicov, Investigator 91

Theoretical Solid State Physics
Marvin L. Cohen, Investigator 94

Surface, Chemisorption, and Theory of Solids
Steven G. Louie, Investigator 98

Novel High-T_c Superconductors
Alex Zettl, Investigator 102

Materials Chemistry

Chemical Structure

Low-Temperature Properties of Materials
Norman E. Phillips, Investigator 105

Electrochemical Processes
Charles W. Tobias, Investigator 107

High-Temperature and Surface Chemistry

High-Temperature Thermodynamics
Leo Brewer, Investigator 111

Materials Chemistry Problems in Nuclear Technology
Donald R. Olander, Investigator 114

Electrochemical Phase Boundaries
Rolf H. Muller, Investigator 117

Solid State and Surface Reactions
Gabor A. Somorjai, Investigator 121

Nuclear Magnetic Resonance
Alexander Pines, Investigator 131

Synthesis of Novel Solids
Angelica M. Stacy, Investigator 138

CHEMICAL SCIENCES

Fundamental Interactions

Photochemical and Radiation Sciences

Photon-Assisted Surface Reactions, Materials, and Mechanisms
Gabor A. Somorjai, Investigator 141

Photochemistry of Materials in the Stratosphere
Harold S. Johnston, Investigator 143

Chemical Physics

Energy Transfer and Structural Studies of Molecules on Surfaces
Charles B. Harris, Investigator 145

Selective Photochemistry
C. Bradley Moore, Investigator 148

Physical Chemistry with Emphasis on Thermodynamic Properties
Kenneth S. Pitzer, Investigator 151

Molecular Interactions
William A. Lester, Jr., Investigator 155

Spectroscopy and Structures of Reactive Intermediates
Richard J. Saykally, Investigator 160

Theory of Atomic and Molecular Collision Processes
William H. Miller, Investigator 162

Photoelectron Spectroscopy
David A. Shirley, Investigator 165

Crossed Molecular Beams
Yuan T. Lee, Investigator 173

Atomic Physics

High-Energy Atomic Physics
Harvey Gould, Investigator 179

Atomic Physics
Michael H. Prior, Investigator 181

Processes and Techniques

Chemical Energy

Formation of Oxyacids of Sulfur from SO_2
Robert E. Connick, Investigator 184

Catalytic Hydrogenation of CO
Alexis T. Bell, Investigator 185

Potentially Catalytic and Conducting Polyorganometallics
K. Peter C. Vollhardt, Investigator 188

Synthetic and Physical Chemistry
William L. Jolly, Investigator 191

High-Energy Oxidizers and Delocalized-Electron Solids
Neil Bartlett, Investigator 192

Transition Metal–Catalyzed Conversion of CO, NO, H_2, and Organic Molecules to Fuels and Petrochemicals
Robert G. Bergman, Investigator 195

Chemical Engineering Sciences

High-Pressure Phase Equilibria in Hydrocarbon-Water (Brine) Systems
John M. Prausnitz, Investigator 199

NUCLEAR SCIENCES

Low-Energy Nuclear Sciences

Heavy-Element Chemistry

Actinide Chemistry
Norman M. Edelstein, Richard A. Andersen, Neil Bartlett, John G. Conway, Kenneth N. Raymond, Glenn T. Seaborg, Andrew Streitwieser, Jr., David H. Templeton, and Allan Zalkin, Investigators 203

FOSSIL ENERGY

Studies of Materials Erosion in Coal Conversion and Utilization Systems
Alan V. Levy, Investigator 219

Fundamental Studies of Catalytic Gasification
Heinz Heinemann, Investigator, with Gabor A. Somorjai, Investigator, and J. Carrazza 223

ENERGY STORAGE SYSTEMS

Electrochemical Energy Storage
Lutgard C. De Jonghe, James W. Evans, Rolf H. Muller, John Newman, Philip N. Ross, and Charles W. Tobias, Investigators 227

Surface Morphology of Metals in Electrodeposition
Charles W. Tobias, Investigator 227

Engineering Analysis of Electrolytic Gas Evolution
Charles W. Tobias, Investigator 229

Surface Layers on Battery Materials
Rolf H. Muller, Investigator 232

Electrode Kinetics and Electrocatalysis
Philip N. Ross, Investigator 234

Electrical and Electrochemical Behavior of Particulate Electrodes
James W. Evans, Investigator 237

Electrochemical Properties of Solid Electrolytes
Lutgard C. De Jonghe, Investigator 239

Analysis and Simulation of Electrochemical Systems
John Newman, Investigator 243

HEALTH AND ENVIRONMENTAL SCIENCES

Semiconductor Materials and Devices
Eugene E. Haller, Investigator 247

PROGRAM DEVELOPMENT FUNDS

Raman Studies of Surface Processes
Gerd M. Rosenblatt, Investigator 251

Structure Determination at the Metal/Solution Interface
Philip N. Ross, Investigator 254

Novel Properties of Matter at Megabars of Pressure
Marvin L. Cohen, Raymond Jeanloz, and Peter Y. Yu, Investigators 256

Electron Electric Dipole Moment
Eugene Commins and Harvey A. Gould, Investigators 258

WORK FOR OTHERS

United States Office of Naval Research

Quantum Monte Carlo for Molecular Studies
William A. Lester, Jr., Investigator 259

Properties of Superconducting Thin Films; Electron-Phonon and Non-Phonon Coupling
Vladimir Z. Kresin, Investigator 261

United States Air Force

Quantum Monte Carlo Study of Tetrahydrogen
William A. Lester, Jr., Investigator 263

United States Department of Transportation

Materials for Enhanced Heavy Fuel Capability Marine Diesels — Part 1
Alan V. Levy, Investigator 264

Materials for Enhanced Heavy Fuel Capability Marine Diesels — Part 2
Alan V. Levy, Investigator 265

U.S.–Spain Joint Committee for Scientific and Technological Cooperation

Improved Emission Control Catalysts
Heinz Heinemann, Investigator, with J. Odriozola and J. Marti 266

Electric Power Research Institute

Erosion-Corrosion of Materials in Coal-Water Slurries
Alan V. Levy, Investigator 267

A Cold Model Study of Wear on Fluidized Bed Combustor Tubes
Alan V. Levy, Investigator 268

APPENDICES

Appendix A. Division Personnel 269
Appendix B. Division Committees 275
Appendix C. List of Divisional Seminars 276
Appendix D. List of Investigators 281

REMARKS BY THE DIVISION HEAD

The year 1987 saw significant changes in the organization of materials and chemical sciences research at LBL. The major change was the merger of MMRD and CAM to form MCSD, the Materials and Chemical Sciences Division, as the Division is now called. This change followed the recommendation of a task force established by LBL Director David A. Shirley toward the end of 1986, to consider future administrative arrangements for CAM. As of this writing, the merger has been completed. A major principle followed in the merger is that the special nature of CAM programs be preserved. CAM will continue to have its own annual report, separate from this Annual Report.

Sometime after the formation of MCSD, the new Surface Science and Catalysis Laboratory, or SSCL (Building 66), was completed. This new building, adjoining Building 62, was first occupied by the Division Office staff in November 1987. Occupancy of laboratories and research offices was at the 60% level on March 31, 1988, and should be complete by September 30, 1988.

Construction is progressing well on the second new building, the Advanced Materials Laboratory, or AML. The building had been scheduled for completion in March 1989, but completion is now expected by December 1988. This building will be occupied primarily by CAM and other materials research projects.

High-temperature superconductivity developed into a major new focus in the Division in 1987. On July 28, 1987, the President's Superconductivity Initiative was announced by DOE. In the initiative LBL was designated as the Center for Thin Film Applications, one of three Centers for high-temperature superconductivity research. The mission of this Center includes basic research on thin films and devices and dissemination of research and information in these areas throughout the scientific community. The high-T_c research will be administered by CAM.

As in past years, MCSD Investigators received many honors and awards, which include the following:

- Alex Bell was elected to the National Academy of Engineering.
- Robert G. Bergman received the Arthur C. Cope Scholar Award from the American Chemical Society.
- John Clarke was named California Scientist of the Year and shared the Fritz London Memorial Award for low-temperature physics.
- Eugene Commins was elected a member of the National Academy of Sciences and the American Academy of Arts and Sciences.
- Didier de Fontaine received the DOE Outstanding Achievement in Metallurgy and Ceramics for FY 1987 (with P. Turchi, Lawrence Livermore National Laboratory).
- Harold S. Johnston was elected a Fellow of the American Geophysical Union.
- Yuan T. Lee received an honorary Doctor of Science degree from the Chinese Academy of Sciences and honorary professorships from Nanking University and Nankai University, People's Republic of China. He also received the American Academy of Achievement's Golden Plate Award and an achievement award from CEASAC.
- Alexander Pines received the IR 100 Award from *Research and Development* Magazine for his research on nuclear magnetic resonance.
- The University of California Berkeley established an annual Kenneth S. Pitzer lectureship in his honor.
- John Prausnitz received the Carl von Linde Gold Memorial Award from the Deutscher Kaeltetechnischer Verein.
- Robert O. Ritchie was elected a Fellow of the American Society of Metals (ASM International); he also received the Curtis W. McGraw Research Award from the American Society for Engineering Education.
- David A. Shirley received the 1987 Dr. rer. nat. h.c. from the Free University of Berlin, Federal Republic of Germany.

- Gabor Somorjai was the G.N. Lewis Lecturer at the University of California Berkeley; he also delivered the Kolthoff Lectures at the University of Minnesota.
- David H. Templeton and Lieselotte K. Templeton received the A. Lindo Patterson Award from the American Crystallographic Association.
- Gareth Thomas was awarded the 1987–88 Henry Clifton Sorby Award from the International Metallographic Society and the IR 100 Award from *Research and Development* Magazine for his research on dual-phase steels.
- K. Peter C. Vollhardt received the ACS Award in Organometallic Chemistry.

Several new research projects started up in 1987 using LBL Exploratory Research and Development Funds (formerly Program Development Funds). These include Structure Determination at the Metal/Solution Interface, with Philip Ross as the lead Investigator; Matter at Megabars of Pressure, with Peter Yu, Marvin Cohen, and Raymond Jeanloz as Investigators; Electron Electric Dipole Moment, with Harvey Gould and Eugene Commins as Investigators; Film Formation and Dislocation Substructures in Corrosion-Induced Cracking, with Thomas Devine, Ronald Gronsky, and Robert Ritchie as Investigators; and Novel Materials from Nanocrystalline Aggregates, with Ulrich Dahmen and Kenneth Westmacott as Investigators. The High-T_c Superconductivity program is now funded with BES Materials Sciences funds. Although this program is administered by CAM, it will be reported in this Annual Report for 1987.

Fortunately the downward trend in budgets of the past few years has not continued. Although funding for continuing materials sciences programs was constant from FY 1987 to FY 1988, additional funding (k$750) has been received for new programs in Materials Sciences (primarily high-T_c research). The Chemical Sciences budgets were increased by an average of 4.7%.

MCSD staff as of September 30, 1987, totalled 642, of which 103 were Investigators, 30 were other scientists, 25 were postdoctoral associates, 291 were graduate students, 16 were undergraduates, 31 were administrative/clerical, 31 were technical, and 115 were guests. During the calendar year 682 refereed journal articles and LBL reports were published by MCSD investigators (not counting CAM-sponsored publications). Students working with MCSD investigators received 10 M.S. and 31 Ph.D. degrees (again, not counting students sponsored by CAM).

Norman E. Phillips
Division Head
Materials and Chemical Sciences Division

Materials Sciences

METALLURGY AND CERAMICS

STRUCTURE OF MATERIALS

Structure and Properties of Transformation Interfaces*

Ronald Gronsky, Investigator

INTRODUCTION

The modern science of materials devotes increasing attention to the role of solid-state interfaces; these interfaces completely dominate the behavior of thin-film electronic devices, and they strongly influence the behavior of even bulk ceramic and metallic alloys alike. This program seeks a fundamental understanding of the role of interfaces in materials by applications of high-resolution electron microscopy to determine local interfacial structure and composition, by theoretical modeling to relate these parameters to actual atomic structure and composition, and by correlations with interfacial-specific properties, including conductivity, diffusivity, ductility, mobility, and reactivity.

Significant attention has been given this past year to various interfaces in the new high-T_c superconductor materials. Planar defects, twins, and grain boundaries are examples of internal interfaces that act as rather serious obstacles to the commercial implementation of these materials, no matter how high their critical temperatures. The continued emphasis in this program is to understand interfacial atomic structure and transformation behavior.

1. Atomic Mechanisms of Precipitate Plate Growth (Publication 1)

J.M. Howe,† U. Dahmen, and R. Gronsky

In this investigation, the techniques of high-resolution transmission electron microscopy, image simulation, energy-dispersive x-ray spectroscopy, and convergent-beam electron diffraction were used to characterize the atomic structure, chemistry, and growth mechanisms of γ' plate-shaped precipitates in an Al-4.2 at% Ag alloy aged for 30 minutes at 350°C. The results of this study, now complete, show that the γ' precipitates have the composition Ag_2Al and are ordered during the early stages of growth, where the A planes in the h.c.p. precipitates contain nearly pure Ag and the B planes have the composition Al_2Ag (see Figure 1-1). In addition, the precipitate-matrix interphase boundary is largely coherent and faceted along low-energy precipitate-matrix directions, and both the lengthening and the thickening of γ' plates occur by a terrace-ledge-kink mechanism, where the limiting step in the growth process appears to be the substitutional diffusion of Ag atoms across kinks in the Shockley partial dislocation ledges, which terminate in the Ag-rich A planes. The com-

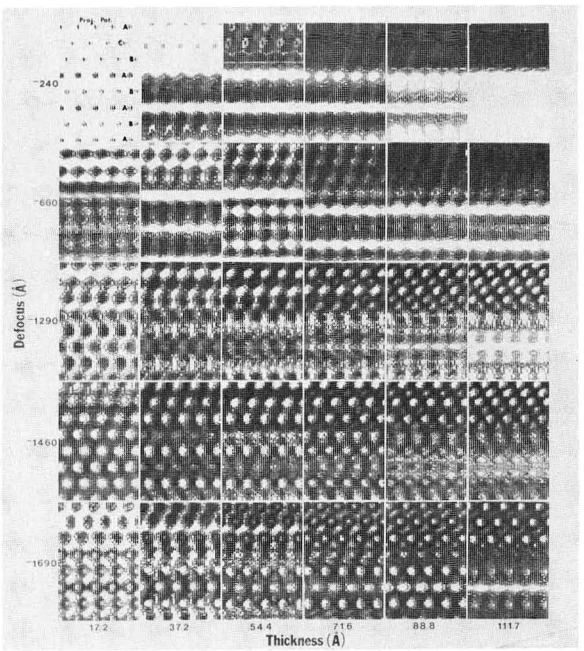

Figure 1-1. Simulated images of a γ' precipitate-matrix interface as a function of objective lens defocus and specimen thickness. The γ' precipitate contains pure Ag on the A planes and 33 at% Ag on the B planes, and the interface is between the last Ag-rich A plane in the precipitate and the first B plane in the Al matrix; JEM 200CX electron microscope. (XBL 852-1378)

*This work was supported by the Director, Office of Energy Research, Office of Basic Energy Sciences, Materials Sciences Division of the U.S. Department of Energy under Contract No. DE-AC03-76SF00098.

plementary information obtained from each of these techniques allows the mechanisms of precipitate plate growth to be explained at the atomic level.

---

†Present address: Department of Metallurgical Engineering and Materials Science, Carnegie-Mellon University, Pittsburgh, PA 15213.

2. High-Resolution Electron Microscopy Study of a Si-Mo X-Ray Mirror (Publication 4)

R. Gronsky and J. Punglia

The science of x-ray optics has undergone rapid growth in recent years, spurred by the availability of high-intensity light sources with tunable optical characteristics[1] in the extreme ultraviolet (XUV) spectral region, which includes soft x-rays and ultraviolet radiation. The development of optical elements for use with XUV radiation has followed a parallel path of development,[2] with most recent emphasis being placed on multilayer coatings that enhance the reflectivity of x-ray mirrors and at the same time provide spectral selectivity. In their simplest form, these coatings consist of alternating thin layers of two materials with different refractive indices that yield both the desired high reflectivity and a relatively broad wavelength bandpass. Additional considerations are based on their materials science: the multilayers must have atomically smooth interfaces and be resistant to interdiffusion or chemical reaction.

The purpose of the present study is to understand the structural nature of the Si-Mo multilayer x-ray mirrors produced in the Center for X-Ray Optics at LBL. The layers were sputtered onto a 3-inch-diameter Si wafer, and for this investigation prepared in cross section by argon ion milling in a cold stage at 5 keV. Microscopy was performed in a JEOL JEM 200CX with ultrahigh-resolution goniometer.

Figure 2-1 is a phase-contrast image of the multilayer in cross section. By employing the known spacing (d = 3.14 Å) of the Si (111) planes imaged in this figure as a calibration, the thickness of the carbon intermediate layer was measured to be 63 ± 3 Å, the Mo layers 25.2 ± 1.1 Å, and the Si layers 4.5 ± 0.5 Å. No evidence of crystallinity was observed within either of the layered components over a relatively wide range of objective lens focus (4500 Å) and thickness (1500 Å). Both layered components appear to be fully amorphous, as found previously for W-Si multilayers. However, even at this

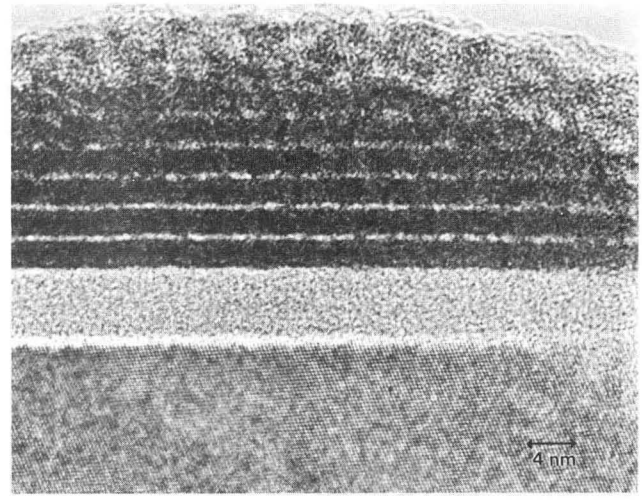

Figure 2-1. Phase-contrast image of Mo-Si multilayer x-ray mirror in cross section. The (111) planes of the Si substrate are clearly visible. (XBB 884-4251)

high magnification and resolution, the layers are remarkably uniform in their overall thickness and flatness despite the fact that the vicinal (111) Si surface on which they were grown has a high ledge density due to its 4.5° deviation from exact (111) crystallography. The fact that these steps are not propagated into the multilayers is attributed to the intermediate amorphous carbon layer, which acts as a structural buffer. Its role is precisely to remove the interfacial irregularities present on the substrate so that the interfacial geometry of the multilayers can be better controlled. From the present results this strategy appears to be successful. Work is continuing on other x-ray mirrors to examine the effects of subsequent thermal processing on interfacial stability and optical performance.

---

1. T. Attwood, K. Halbach, and K.-J. Kim, Science **228**, 1265 (1985).
2. J.H. Underwood, and D.T. Attwood, Physics Today, April 1984, p. 44.

3. Work In Progress

Continuing work is listed by thesis topic, followed by the graduate students responsible for the research: metallic contacts to $YBa_2Cu_3O_7$, M. Tidjani; grain-boundary structure in $YBa_2Cu_3O_7$, L. Yamamoto; the substrate interface in $YBa_2Cu_3O_7$ thin films, K. Atwal; structural transitions in $Bi_2SrCa_2Cu_2O_{8+\delta}$ superconductors, M. Fendorf and K. Fortunati; corrosion susceptibility and grain boundaries in stainless steel, C. Willis; and x-ray mirrors, T. Nguyen.

1987 PUBLICATIONS AND REPORTS

Refereed Journals

1. J.M. Howe, U. Dahmen, and R. Gronsky, "Atomic Mechanisms of Precipitate Plate Growth," *Philos. Mag.* A. **56**, 31 (1987); LBL-21705.
2. T. Sands, V.G. Keramidas, A.J. Yu, K.-M. Yu, R. Gronsky, and J. Washburn, "Ni, Pd, and Pt on GaAs: A Comparative Study of Interfacial Structures, Compositions, and Reacted Film Morphologies," *J. Mater. Res.* **2**, 262 (1987); LBL-21060.

Other Publications

3. R.W. Siegel, H. Hahn, S. Ramasamy, L. Zongquan, L. Ting, and R. Gronsky, "Structure and Properties of Nanophase TiO_2," in *Proc. Interface Science and Engineering '87*, Lake Placid, NY, July 1987.
4. R. Gronsky and J. Punglia, "High Resolution Electron Microscopy Study of a Si-Mo X-ray Mirror," in *Proc. 45th Ann. Meeting Electron Microscopy Soc. America,* G.W. Bailey, Ed., San Francisco Press, 1987, p. 400; LBL-23152.
5. G.F. Holland, R.L. Hoskins, M.A. Dixon, P.D. VerNooy, H.-C. sur Loye, G. Brimhall, D. Sullivan, R. Cormia, H.W. Zandbergen, R. Gronsky, and A.M. Stacy, "The Interplay of Synthesis, Structure and Microstructure and Superconducting Properties of $YBa_2Cu_3O_7$," *A.C.S. Symp. Ser.* **351**, 102 (1987).

LBL Reports

6. C.J. Jou, J. Washburn, Z. Liliental-Weber, and R. Gronsky, "The Morphology and Electrical Properties of the Ag/GaAs Contact," LBL-23033.
7. S. Packer (M.S. Thesis), "A TEM Study of Rhodium on GaAs: Reactions and Morphology," LBL-23536.
8. J. Ding, B. Lee, R. Gronsky, J. Washburn, D. Chin, and T. Van Duzer, "High-Temperature Stability of Nb/GaAs and NbN/GaAs Interfaces," submitted to Appl. Phys. Lett.; LBL-23970.
9. H.W. Zandbergen, R. Gronsky, and G. Thomas, "Surface Decomposition of Superconducting $YBa_2Cu_3O_7$," submitted to Phys. Stat. Sol. (a); LBL-23854.
10. H.W. Zandbergen, G.F. Holland, P. Tejedor, R. Gronsky, and A.M. Stacy, "A Study of Mixed Phase Behavior in the Lanthanide-Substituted Superconducting Oxide $ErBa_2Cu_3O_7$," submitted to Adv. Ceram. Mater.; LBL-23566.
11. H.W. Zandbergen, R. Gronsky, M.Y. Chu, L.C. DeJonghe, G.F. Holland, and A. Stacy, "The Structure and Properties of Twin Boundaries in Superconducting $YBa_2Cu_3O_7$," Proc. Mat. Res. Soc. (in press); LBL-24139.
12. H. W. Zandbergen, R. Gronsky, K. Wang, and G. Thomas, "Simulation and Processing of High Resolution Images of Defects and Interfaces in Superconducting $YBa_2Cu_3O_7$," Proc. Mat. Res. Soc. (in press); LBL-24140.
13. H.W. Zandbergen, C.J.D. Hetherington, and R. Gronsky, "Sample Preparation of $YBa_2Cu_3O_7$ for High Resolution Electron Microscopy," submitted to J. Superconductivity; LBL-24614.
14. H.W. Zandbergen, R. Gronsky, K. Wang, and G. Thomas, "On the Structure of $(CuO)_2$ Double Layers in Superconducting $YBa_2Cu_3O_7$," submitted to Nature; LBL-24671.

Invited Talks

15. R. Gronsky, "Microscopy Characterization of High Temperature Superconductors," DOE Information Meeting on High Temperature Superconductors, Germantown, MD, Feb. 20, 1987.
16. R. Gronsky, "Structure, Morphology, and Evolution of GP Zones in Al-Ag Alloys," TMS/AIME Hume Rothery Memorial Symposium on Guinier-Preston Zones, Denver, Feb. 24–27, 1987.
17. R. Gronsky, "Quasicrystals," Southern California Society for Electron Microscopy, Los Angeles, Mar. 26, 1987.
18. R. Gronsky, "Structural Characterization of High-T_c Superconductors," Leader of Panel Discussion, OBES Information Meeting of High Temperature Superconducting Materials, Germantown, MD, May 14–15, 1987.
19. R. Gronsky, "*Ex-Situ* Techniques for Characterizing Corroded Surfaces," Aqueous Corrosion: Theory and Analysis, University Extension Intensive Course, University of California Berkeley, June 23–26, 1987.
20. R. Gronsky, "Atomic Resolution Imaging of Interfaces," XIIIth Western Regional Meeting for Electron Microscopy and Microbeam Analysis, Concord, CA, June 24–27, 1987.
21. R. Gronsky, "Transformation Interfaces at Atomic Resolution," Phase Transformations '87 (International Conference on Phase Transformations in Solids), University of Cambridge, U.K., July 6–10, 1987.
22. R. Gronsky, "Structure and Strain Determination in the High Resolution Electron Microscope," ASM/MSD Symposium on Structure and Strain Determination at the Sub-Micron Level, Cincinnati, OH, Oct. 12–14, 1987.
23. R. Gronsky, "Structure and Imperfections in Oxide Superconductors—High Resolution Electron Microscope Studies," Special Symposium on High Temperature Superconductors, TMS/ASM Fall Meeting, Cincinnati, OH, Oct. 12–14, 1987.
24. R. Gronsky, Panel Discussion on Materials Science of High Temperature Superconductors, Special Symposium on High Temperature Superconductors, TMS/ASM Fall Meeting, Cincinnati, OH, Oct. 12–14, 1987.

25. R. Gronsky, "High Resolution Electron Microscopy of the Solid-Solid Interface," 34th National Symposium, American Vacuum Society, Anaheim, CA, Nov. 2–6, 1987.

26. R. Gronsky, "Electron Microscopy of High-T_c Superconductors at LBL," DOE Workshops on High-T_c Superconductivity, Oak Ridge National Laboratory, Oak Ridge, TN, Nov. 9–10, 1987; Berkeley, CA, Dec. 14–15, 1987.

Microstructure, Properties, and Alloy Design: Inorganic Materials*

Gareth Thomas, Investigator

INTRODUCTION

This is a multicomponent, interdisciplinary program in advanced inorganic materials involving fundamental quantitative studies of the structure-property relationships in technologically significant materials involved in energy and conservation. All tasks involve characterization of both structure and composition at the highest levels of spatial (transmission electron microscopy) and chemical (spectroscopy) resolutions in order to understand the complexities of structure-composition-processing-property relationships, without which alloy design is impossible. Specific tasks include:

(a) Dual-phase ferrite-martensite steels for rod, bar, and wire: optimization of microstructure and processing: failure analysis of drawn wire; fatigue (with Prof. R. Ritchie); this program terminated in 1987.

(b) Effect of microalloying on structure properties and processing of duplex martensitic-austenite composite steels designed for optimum toughness.

(c) Magnetic materials: ceramics, permanent and hard rare-earth magnets, processing by melt spinning (new program beginning FY 1988).

(d) High-critical-temperature superconducting ceramics (new program beginning FY 1988, representing a redirection of effort).

The overall objectives are to understand structure-property relations so as to design new materials, or to better utilize existing materials and processing routes for industrial practice and to realize materials and energy conservation.

STEELS

The demise of the steel industry in the USA is a reflection of both management and research limitations. The need for improving quality and properties of steels without large capital investment is thus critical. In addition, cost savings by improved processing, minimizing alloying, and reducing or eliminating heat treatments should be a prime factor in the research philosophy. The current purpose of this program has been to optimize the above factors with emphasis on dual-phase low-carbon steels and the medium carbon microcomposite steels already designed under this project. In particular, transferring laboratory techniques to existing hot-mill practice (hot plate, bars, and wire rod are specific examples) has been successfully achieved. Consequently now, the total research effort on steels is being reduced (currently one graduate student and no postdoctorals). The program on fatigue of dual-phase steels with Professor Ritchie was completed in fall 1987.

1. Development of High Strength and Toughness Microcomposite HSLA Fe/Cr/Mn/C Steel With and Without Nb (Publication 34)

G. Thomas, J.K. Kim, D. Manojlovic,† and R. Milovic†

Microcomposite Fe/Cr/Mn/C steels have been designed to consist of fine packet martensite and interlath austenite films in order to attain mechanical and corrosion properties with superior combinations of strength, fracture toughness, and formability

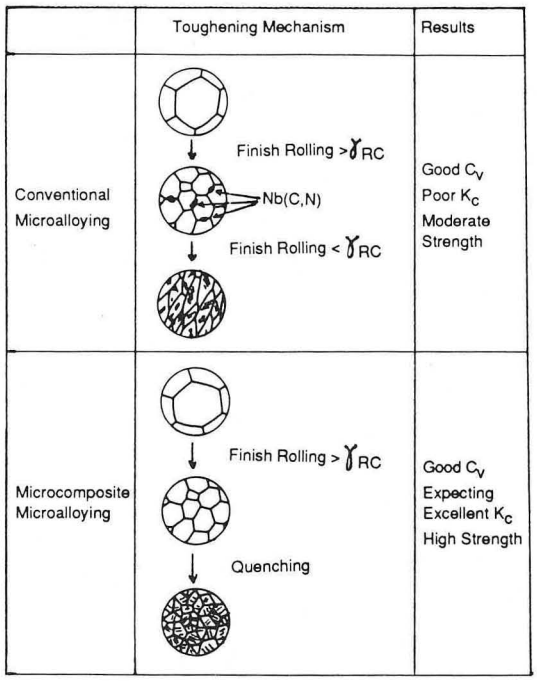

Figure 1-1. Schematic to show processing between conventional and microcomposite microalloying. (XBL 881-213)

*This work was supported by the Director, Office of Energy Research, Office of Basic Energy Sciences, Materials Sciences Division of the U.S. Department of Energy under Contract No. DE-AC03-76SF00098.

in certain conditions. In an effort to improve these properties for on-line production in a hot mill for rounds and plates, modifications with niobium have been investigated and the CCT diagrams determined. The addition of niobium (see Figure 1-1) has achieved grain refinement without destroying the microcomposite morphology of packet martensite and austenite (see Figure 1-2), while yielding higher toughness and strength (see Figures 1-3 and 1-4). New results show excellent cold formability of these steels following short spheroidizing times; and cost savings applications to forgings, fasteners, and chains have been successfully demonstrated. Examples are given in Figures 1-5 and 1-6.

†Permanent address: Boris Kidric Steel Works, Ferrous Metallurgical Institute, Niksic, Yugoslavia.

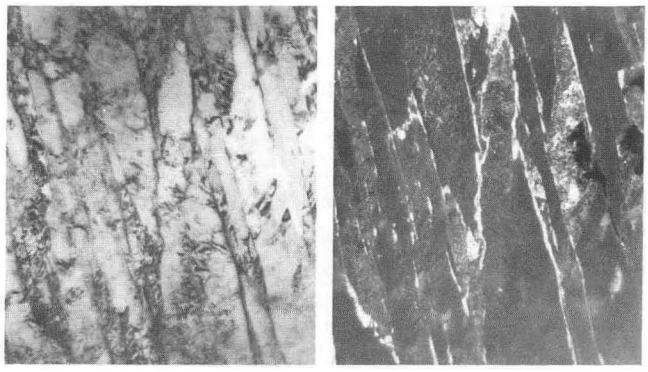

Figure 1-2. Transmission electron micrographs of controlled rolled and as-quenched Nb steel. The dark-field image (on the right) shows interlath retained austenite. (XBB 870-9092)

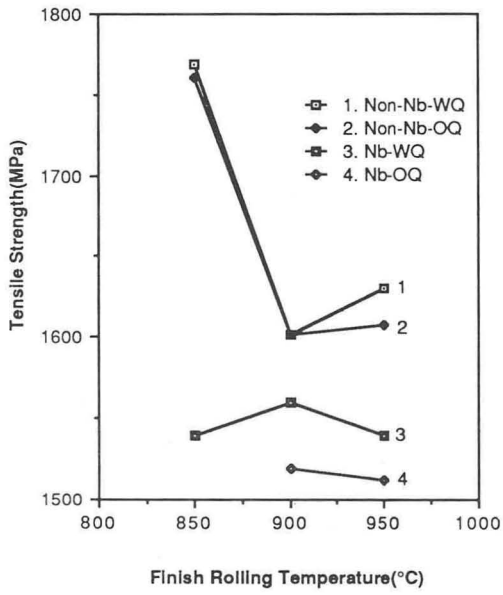

Figure. 1-3. Tensile strength variation vs. finish rolling temperature. (XBL 881-215)

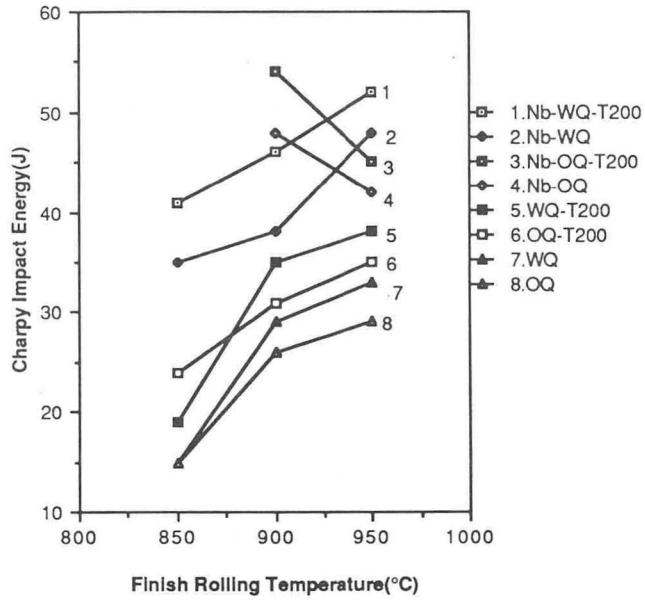

Figure 1-4. Charpy impact energy variation vs. finish rolling temperature. (XBL 881-216)

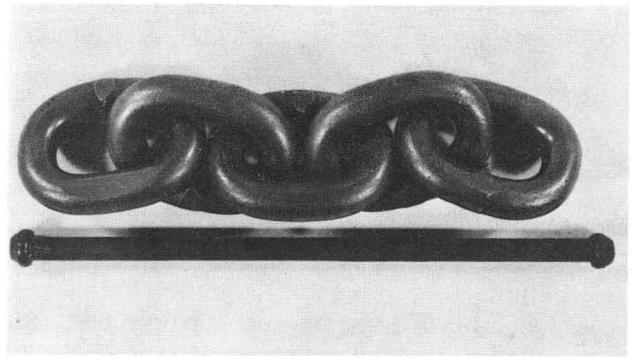

Figure 1-5. Chain made of non-Nb steel after cold forming process. Also shown is a cold headed bar, e.g., for concrete ties. (XBB 870-10666)

2. Fracture Analysis of Drawn Dual-Phase Steel Wires (Publication 18)

L. Sidjanin,† S. Miyasato, and G. Thomas

The high strain-hardening rate and formability of dual-phase composite ferrite–lath martensite steels make them competitive for cold drawing into high-strength wire with no intermediate patenting heat treatments. In this paper, the relationship between the void density in drawn wires and the drawing limit has been studied. Detailed scanning electron microscopy (SEM) metallographic analysis was performed on Fe/2%Si/0.1%C drawn wires, treated dif-

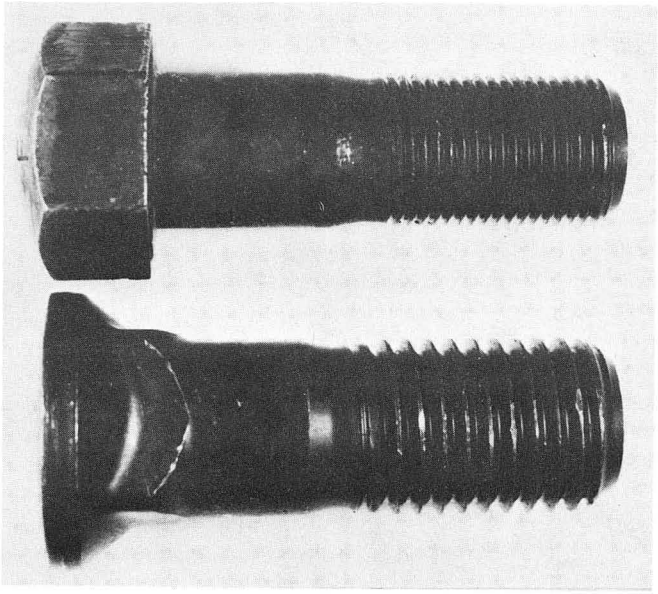

Figure 1-6. Cold-headed screws made of non-Nb steel. (XBB 883-1752)

ferently to give varied martensite morphology but at constant volume fraction. Void formation during wire drawing occurred in all the dual-phase steel microstructures examined. A linear relationship was found between the true strain and void density (see Figures 2-1 and 2-2). The differences between the drawing limits of the differently treated steels are attributed to the differences in morphology of the composite microstructures relating to interface coherency. Void formation was found to begin either by decohesion of the ferrite/martensite interface or by shear cracking of the martensite particles (e.g., Figure 2-3). The fibrous martensite-ferrite composite structures that formed after the intermediate quenching processing appear to be the most promising for high-strength wire, e.g., tire cord.

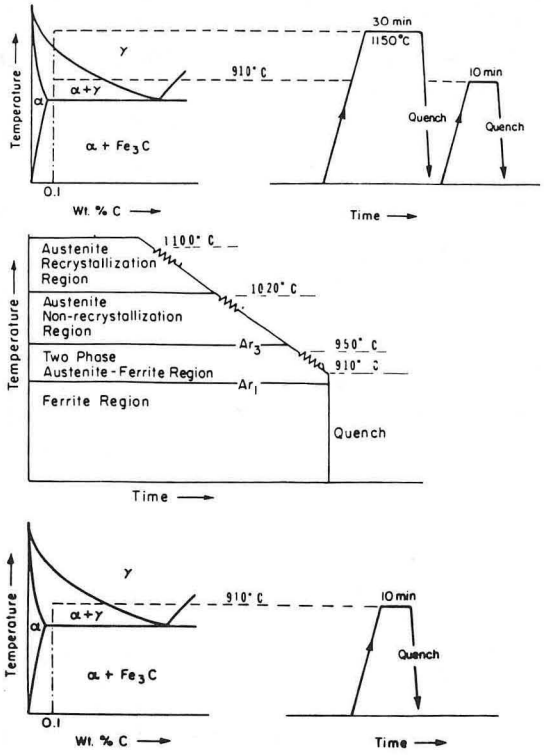

Figure 2-1. Schematic diagram to show the thermal and thermomechanical heat treatments used: intermediate quenching process (top); controlled rolling process (center); intercritical annealing process (bottom). (XBL 878-3479)

†Permanent address: Associate Professor, Univ. of Novom Sadu, Novi Sad, Yugoslavia.

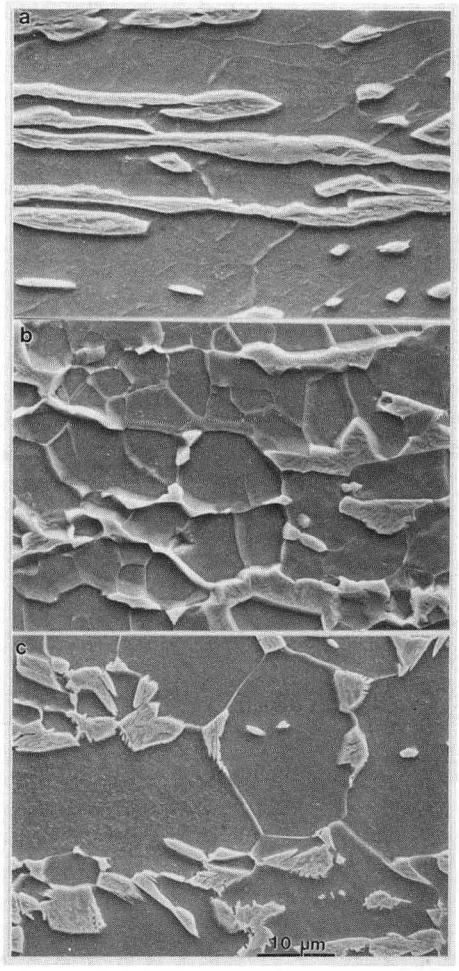

Figure 2-2. Scanning electron micrographs of the dual-phase microstructures obtained after processing: fibrous martensite produced by intermediate quenching (IQ); unidirectionally aligned martensite island produced by controlled rolling (COR); globular martensite particles produced by intermediate annealing (IA). (XBB 876-4847)

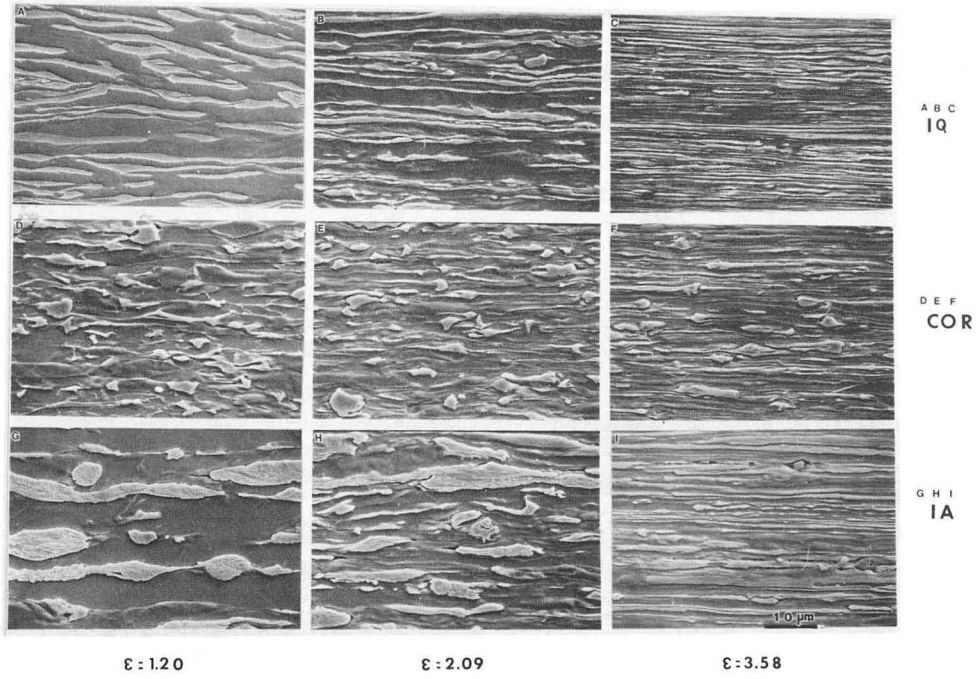

Figure 2-3. Variation of void density with true strain for different martensite morphologies (A, B, and C for IQ; D, E, and F for COR; G, H, and I for IA; with ϵ = 1.20, 2.09, and 3.58). (XBB 875-3834)

3. The Mechanical Properties of Drawn Dual-Phase Steel Wires (Publication 49)

S. Miyasato

In this study, Fe/xC/2Si alloys were heat treated to obtain different ferrite/martensite morphologies and relative volume fractions, and the work-hardening rate at true plastic strain $\epsilon = 0.006$ was determined. Wires were then drawn from 4.2 to 1.4 mm in diameter, which corresponded to a strain of $\epsilon = 2.3$, and tested in tension and fatigue. The early work-hardening rate increased with increased volume fraction of martensite, increased strength of martensite, and decreased ferrite/martensite interface coherency. The wire drawing limit was raised by preventing void formation at ferrite/martensite interfaces and shear cracking through martensite particles (see abstract 2 above). The lowest void density is obtained in a structure of fibrous martensite with coherent ferrite/martensite interfaces (i.e., produced by intermediate quenching). The fatigue limit of drawn dual phase wires is 600 MPa, or 25–30% of the ultimate tensile strength, which appears to be higher than that of similar pearlitic steel wire. There was no superior microstructure for fatigue resistance in wires, as any morphology differences produced in the initial structure are indistinguishable after heavy deformation. Fatigue cracks initiated on the wire surface at inclusions, sites of interface decohesion, and martensite particle cracking, and in the interior of the wire at large cracks that formed during wire drawing.

MAGNETIC MATERIALS

4. On the Grain-Boundary Phase in Iron Rare-Earth Boron Magnets (Publication 1)

R. Ramesh, J.K. Chen, and G. Thomas

Results of structural and microanalytical studies on sintered iron rare-earth boron permanent magnets are presented in this paper. It is shown that the structure of the phase present at the two-grain boundaries is the same as that of the phase at the three-grain junctions (see Figure 4-1); both are fcc with a lattice parameter of 5.24 Å. It is also shown that this fcc phase is stabilized by the presence of significant quantities of oxygen. The possible effects of thin foil preparation by ion-milling techniques in producing the observed bcc phase are also discussed briefly.

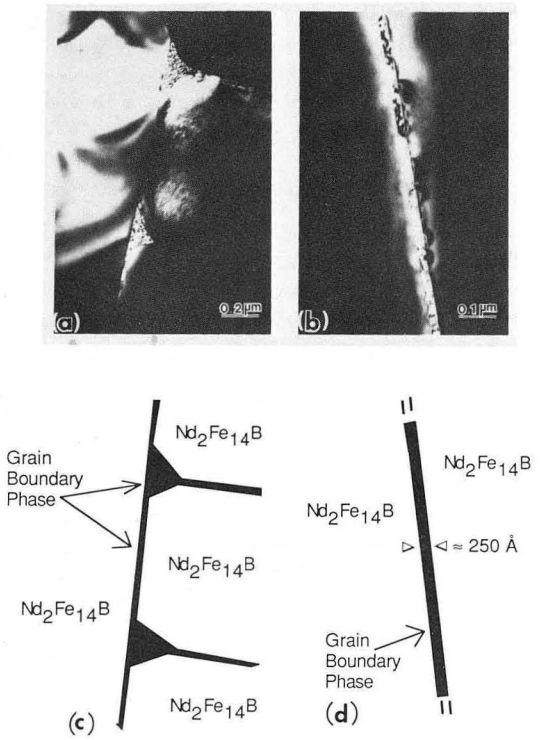

Figure 4-1. General bright-field microstructure of the magnet depicting the grain-boundary phase at the (a) three-grain junction and (b) two-grain boundaries. Parts (c) and (d), respectively, depict (a) and (b) schematically. (XBB 862-1270)

5. Effect of Dy Additions on Microstructure and Magnetic Properties of Fe-Nd-B Magnets (Publication 7)

R. Ramesh, G. Thomas, and B.M. Ma[†]

This paper addresses the effect of Dy addition on the magnetic properties, microstructure, and microcomposition of Fe-Nd-B magnets. It is shown that increasing additions of Dy causes the remanence B_r to decrease linearly. The intrinsic coercivity iHc increases sharply for small additions of Dy, but the increase is not proportional for higher Dy contents. The iHc increases almost linearly with the effective anistropy field of the $RE_2Fe_{14}B$ phase until the Dy content is about 10% of the total rare-earth content. Above this concentration, there is a strong deviation from linearity. Figures 5-1 through 5-3 show these properties. Various types of possible concentration profiles of the substituted rare earth are suggested. It is also argued that preferential segregation of Dy to the interfaces could be beneficial in increasing the nucleation field. Morphologically there is no apparent effect of Dy on the microstructure. However, in the 5-at% Dy sample, Dy-rich oxides were observed. It is shown through energy-dispersive x-ray spectroscopy (EDXS) line profiling that Dy partitions preferentially into the $RE_2Fe_{14}B$ phase in all the cases. No segregation of Dy to the interphase interfaces has been detected.

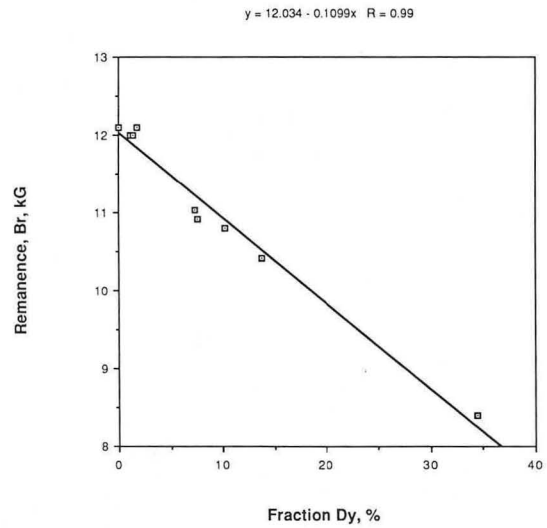

Figure 5-1. Effect of Dy content on the remanence B_r of Fe-Nd-B sintered magnets. The total rare-earth content in all cases is 35.1 wt.%. (XBL 884-1327)

[†]Present address: Crucible Research Center, Pittsburgh, PA 15230.

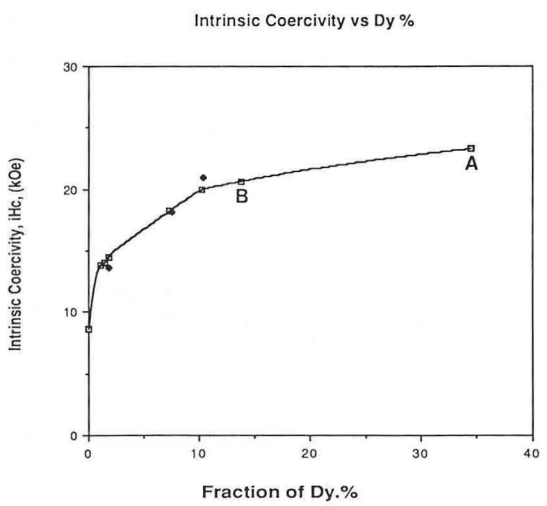

Figure 5-2. Effect of Dy content on the intrinsic coercivity iHc of Fe-Nd-B sintered magnets. The total rare-earth content in all cases is 35.1 wt.%. (XBB 884-1329)

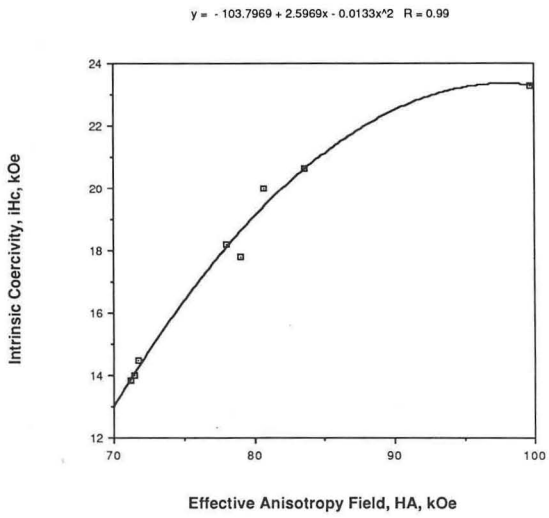

Figure 5-3. Dependence of intrinsic coercivity on the effective anisotropy constant $_{eff}H_A$. The total rare-earth content is constant at 35.1 wt.%. (XBB 884-1328)

6. Effect of Quench Rate on the Intrinsic Coercivity of Iron/Rare Earth/Boron Permanent Magnets (Publication 47)

R. Ramesh and G. Thomas

The effect of post-sintering cooling rate on the microstructure and magnetic properties of Fe-Nd-B–based magnets has been studied. It has been shown that the intrinsic coercivity and energy product vary inversely with the cooling rate. In all cases, the magnet behaves as a nucleation-controlled magnet characterized by a high initial permeability, although nucleation of reverse domains occurs at progressively lower fields as the cooling rate is increased. Samples quenched into water and oil exhibited extensive intergranular quench cracking. Scanning Auger elemental mapping as well as energy dispersive x-ray microanalysis showed the presence of oxygen, along with the rare earths, in the grain-boundary phase. A qualitative argument for the influence of oxygen in reducing the magnetocrystalline anisotropy of the $RE_2Fe_{14}B$ phase is presented. Finally, the effect of cooling rate on the intrinsic coercivity and energy product can be understood in terms of the effect of local strains, at the grain boundaries and interfaces, on the magnetocrystalline anisotropy of the $RE_2Fe_{14}B$ phase.

7. Cross-Sectioning Magnetic Thin Films for TEM (Publication 12)

H.M. Ho, G. Thomas, C.N. Schooley,[†] and J.S. Gau[‡]

Oblique-incidence magnetic thin films are considered the most appropriate recording media for the next generation of videotape applications. In order to study the microstructure of such thin films, a specimen-preparation technique employing ultramicrotomy has been developed. Because oblique-incidence thin films have a porous structure and poor adhesion to the substrate, the problem of splitting of the thin films from the substrate is severe. This problem is reduced considerably by taking the following steps: (1) using an acrylic embedding resin, e.g., LR White (London Resin Co.); (2) degreasing thoroughly with solvents; (3) using a 55° diamond knife; and (4) trimming the block with a microtome before actual sectioning. Best results have been obtained when the area of the block is very small and when the cutting direction is from the thin film side and normal to the film plane.

[†]Present address: Electron Microscope Laboratory, U.C. Berkeley.
[‡]Permanent address: Control Data Co., Minneapolis, MN 55435.

8. Microstructure of Oblique-Incidence CoNi Thin Films (Publication 37)

H.M. Ho and G. Thomas

Because of their application as recording media for high-density recording, oblique-incidence thin films have been studied by many investigators. It is well known that oblique-incidence thin films have a columnar structure; however, localized microstructural information, i.e., information obtained directly from individual columns, has not yet been reported. In this study, the microstructure of CoNi oblique-incidence thin films has been examined by transmission electron microscopy and microdiffraction techniques. Results of thin films prepared with various incident angles indicate that the columns in oblique incidence thin films are single crystals (see Figure 8-1), and the c-axis of the columns does not necessarily coincide with the column axis (see Figure 8-2).

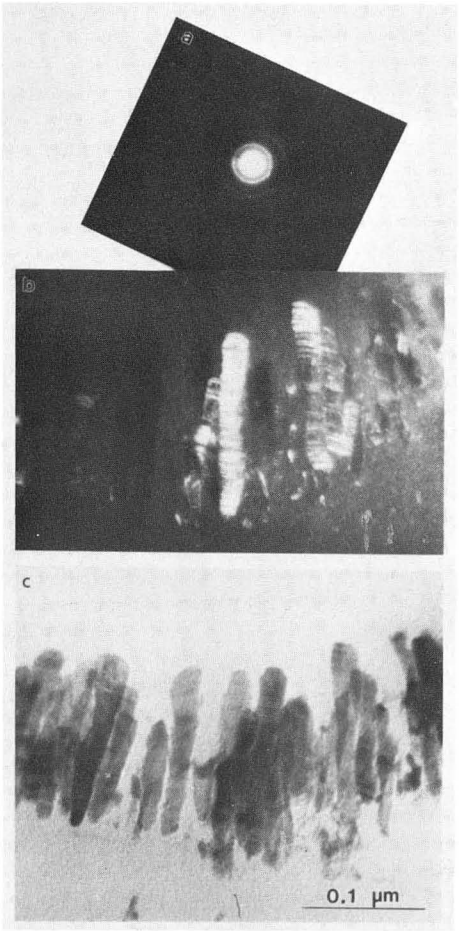

Figure 8-1 (a) Selected-area diffraction, (b) dark-field image, and (c) bright-field image of a sample prepared in a direction perpendicular to the incident direction, showing each column is a single crystal. (XBB 873-2019)

Figure 8-2. (a) Convergent-beam diffraction and (b) dark-field image of an individual column, showing planar faults on (0001). Note that the column axis is not perpendicular to the fault plane. (XBB 873-2027)

9. On the Minimum Grain Size for Domain Formation in Lanthanum-Modified Lead Titanate Ferroelectric Ceramics (Publication 3)

B.G. Demczyk, A.G. Khachaturyan, and G. Thomas

When cubic lead titanate, point group m3m, is cooled below its Curie point, it transforms in <100>, becoming tetragonal, point group 4mm. This is the ferroelectric state. In order to relieve the transformation strain, twins (ferroelectric domains) form, with (101) habit. However, it has been observed previously that twins only form if the grain size exceeds some minimum value. Estimates have been made as to this minimum size from the transformation and twinning strain energies. In the present investigation a critical grain size for twinning has also been found using transmission electron microscopy of tetragonal lanthanum-modified lead titanate. The experimentally observed minimum grain size for twinning ($<0.3\ \mu m$) is consistent with values derived from a balance of the cubic-to-tetragonal elastic strain and twin surface energies.

10. Work in Progress

Characterization of Microstructure in Magnetic Materials for Recording Heads

The microstructural changes that occur during the $B2=DO_3$ transition in an $Fe_3Si_{0.6}Al_{0.4}$ alloy and the interactions between defect structures and magnetic domain walls are being investigated. The ordering of $B2 \rightarrow DO_3$ occurs in a classical manner, developing a two-phase mixture, contrary to Fe_3Al and Fe_3Si alloys, and the two-phase region can be identified by interfacial dislocations of the

a/2<100> type. Lorentz electron microscopy has shown that the strain field due to dislocations interacts with magnetic domain walls; however, thermal antiphase boundaries and slip-produced antiphase boundaries have little effect on the magnetic domain wall. Further studies of these interfaces are under way.

Polycrystalline $Ba_2(Cu_{0.8}Zn_{1.2})Fe_{12}O_{22}$ for high-frequency VTR heads exhibits large anisotropy and high permeability on its c-planes at high frequencies. The ferrite grains have been magnetically oriented during processing. Characterization of grain-boundary structures with TEM and AEM shows that some triple grain junctions have high concentrations of Cu. Ba-deficient second-phase particles have been observed and characterized by CBED. Twins and dislocations have also been observed. The effects of the microstructural defects on the magnetic properties of the materials will now be studied using Lorentz electron microscopy.

Analysis of Strains at Grain-Boundary Interfaces in Fe/Nd/B Magnets

Since magnetostriction in these alloys is very high and since reverse magnetic domain nucleation is associated with the oxygen-stabilized grain-boundary phase, detailed analyses are planned to utilize convergent-beam diffraction for measurement of strains at and near the matrix–grain-boundary interfaces.

High-T_c Ceramic Superconductors [R. Gronsky, C.J.D. Hetherington, G. Thomas, (NCEM), Investigators; H. Zandbergen and R. Ramesh, Guest Scientists]

The overall objectives of our research are to characterize the new generation of warm superconductors based on the orthorhombic rare-earth copper-oxide 1-2-3 ceramics typified by $YBa_2Cu_3O_7$. The characterization is done on samples prepared by Professors Stacy and DeJonghe of MCSD, and Dr. Paul Chu (Houston) using the unique facilities of the ARM at 1.6-A° resolution over 40° of tilt in the National Center for Electron Microscopy.

This research serves as a focal point for understanding these ceramics, e.g., the types of grain boundaries, interfaces, and internal defects that affect superconducting properties, particularly critical currents.

1987 PUBLICATIONS AND REPORTS

Refereed Journals

1. R. Ramesh, J.K. Chen, and G. Thomas, "On the Grain-Boundary Phase in Iron Rare-Earth Boron Magnets," J. Appl. Phys. **61**, 2993 (1987); LBL-20698.
2. J.M. Rincon, T.R. Dinger, G. Thomas, J.S. Moya, and M.I. Osendi, "Microstructure of Mullite/ZrO_2 and Mullite/Al_2O_3/ZrO_2 Tough Ceramic Composites," Acta Metall. **35**, 1175 (1987).†
3. B.G. Demczyk, A.G. Khachaturyan, and G. Thomas, "On a Minimum Grain Size for Domain Formation in Lanthanum Modified Lead Titanate Ferroelectric Ceramics," Scripta Metall. **21**, 967 (1987); LBL-23204.
4. P. Miranzo, P. Pena, S. de Aza, J.S. Moya, J. Rincon, and G. Thomas, "TEM Study of Reaction-Sintered-Zirconia-Mullite Composites with CaO and Mg Additions," J. Mat. Sci. **22**, 2987 (1987).†
5. R.S. Rai, M.A. O'Keefe, and G. Thomas, "Structure Imaging and Defects in Crystallized Oxynitride Glasses," Mat. Res. Soc. Symp. Proc. **82**, 429 (1987); LBL-21754.
6. V. Radmilovic, C. Nelson, and G. Thomas, "Electron Microscopy of TMT Al-Li-Cu Alloys," in *Proc. 45th Annual Meeting EMSA*, Baltimore, MD, G.W. Bailey, Ed., San Francisco Press, p. 230; LBL-23654.‡
7. R. Ramesh, G. Thomas, and B.M. Ma, "Effect of Dy Additions on Microstructure and Magnetic Properties of Fe-Nd-B Magnets," Mat. Res. Soc. Symp. Proc. **96**, 203 (1987); LBL-22477.
8. J.K. Chen and G. Thomas, "Aluminum Substitutions in Nd-Fe-B Sintered Magnets," Mat. Res. Soc. Symp. Proc. **96**, 221 (1987); LBL-22476.
9. V. Radmilovic and G. Thomas, "Atomic Imaging in Al-Li-Cu Alloys," J. de Physique, Coll. C3, **48**, C3-385 (1987); LBL-23558.†
10. J.G. Ulan, E. Kuo, W.F. Maier, R.S. Rai, and G.Thomas, "The Effect of Lead Acetate in the Preparation of the Lindlar Catalyst," J. Org. Chem. **52**, 3126 (1987); LBL-21980.‡
11. B.G. Demczyk, "In-Situ Transmission Electron Microscopy Study of the Paraelectric to Ferroelectric (Cubic to Tetragonal) Phase Transformation in Lanthanum-Modified Lead Titanate Ceramics," in *Proc. 45th Annual Meeting EMSA*, Baltimore, MD, G.W. Bailey, Ed., San Francisco Press, 1987, p. 172; LBL-23117abs.
12. H.M. Ho, G. Thomas, C.M. Schooley, and J.S. Gau, "Cross-sectioning Magnetic Thin Films for TEM," MRS Fall Meeting, Boston, MA, Nov. 30–Dec. 5, 1987; Mat. Res. Soc. Symp. Proc. **115**, 149 (1988); LBL-23565abs.

13. T.R. Dinger, R.S. Rai, and G. Thomas, "Crystallization Behavior of a Glass in the Y_2O_3-SiO_2 AIN System," J. Am. Ceram. Soc. **71**, 236 (1988); LBL-23251.†
14. H.W. Zandbergen, R. Gronsky, and G. Thomas, "Surface Decomposition on Superconducting $YBa_2Cu_3O_7$," Phys. Status Solidi (a) **105**, 207 (1988); LBL-23854.
15. G. Thomas, "High Voltage, High Resolution Electron Microscopy in Materials," J. de Microscopie et de Spectroscopie Electroniques **12**, 535 (1987); LBL-22571.

Other Publications

16. G. Thomas, "Design of Dual Phase Steels for Bars and Rods," in *Fundamentals of Microalloying Steels*, G. Krauss and S.K. Banerji, Eds. TMS/AIME, 1987, p. 505; LBL-21663.
17. K.M. Krishnan and G. Thomas, "Microanalysis of Polytypoid Ceramics by Imaging, Diffraction, and Spectroscopy," in *Microbeam Analysis — 1987, Conf. Proc. Microbeam Analysis Society*, Kona, Hawaii, July 13–17, 1987, R.H. Geiss, Ed., p. 222; LBL-22924.
18. L. Sidjanin, S. Miyasato, and G. Thomas, "Fracture Analysis of Drawn Dual-Phase Steel Wires," in *Conf. Proc. 57th Annual Wire Conf. Interwire '87*, Wire Association Limited, 1987, p. 70; LBL-23250.
19. R. Ramesh and G. Thomas, "High-Voltage Lorentz Electron Microscopy of Fe-Nd-B Magnets," J. Appl. Phys. **61**, 4225 (1987); LBL-21746abs.
20. K. Srikrishna and G. Thomas, "High Resolution Electron Microscopy of Mullite/Zirconia Composites," 89th Annual Meeting ACS, Pittsburgh, PA, Apr. 26–30, 1987.†
21. H.M. Ho, J.S. Gau, and G. Thomas, "Evolution of Oblique-Incidence Co-Ni Thin Films," Proc. 3rd Annual Symposium on Magnetism and Magnetic Materials, Taipei, Taiwan, April 22–24, 1987; LBL-22588.
22. R. Ramesh, G. Thomas, M. Okada, and M. Homma, "Effect of Quench Rate on the iHc of Fe-Re-B Magnets," 1987 Intermag Conf., Tokyo, Japan, April 14–17, 1987; LBL-22592.
23. L.H. Chan, J.S. Gau, and G. Thomas, "Microstructure and Magnetic Properties in Bulk Co-Cr Alloys," 1987 Intermag Conf., Tokyo, Japan, April 14–17, 1987; LBL-22637.
24. M.L.A. Dass and G. Thomas, "Convergent-Beam Electron Diffraction Studies of Domains in Rhombohedral Phase of Lead Zirconate Titanate Ceramics," Microbeam Analysis Society Conf., Kona, HI, July 13–17, 1987, in *Analytical Electron Microscopy*, San Francisco Press, 1987, p. 132; LBL-23055.
25. K.M. Krishnan and G. Thomas, "Microanalysis of Polytypoid Ceramics by Imaging, Diffraction and Spectroscopy," Microbeam Analysis Society Conf., Kona, HI, July 13–17, 1987, in *Micro Beam Analysis*, R.H. Geiss, Ed., 1987, p.222; LBL-22924.
26. M.L.A. Dass and G. Thomas, "Characterization of Microstructure and Domains in Lead Zirconate Titanate Ceramics," 1987 Gordon Research Conf. on Solid State Studies in Ceramics, July 27–31, 1987, Plymouth State College, Plymouth, NH; LBL-23237.
27. T. Yamamoto, K. Okazaki, K. Hisano, M.L.A. Dass, and G. Thomas, "Microstructure and Dielectric Properties at the Morphotropic Phase Boundary (MPB) of $PbTiO_3$-$PbZrO_3$ System," 6th European Meeting of Ferroelectricity, September 1987, Poland; LBL-23436.
28. G. Thomas, "The Contribution of Electron Microscopy of Materials Science to Society," symposium on the Contribution of Electron Microscopy to Society, to honor Nobel Laureate E. Ruska, Eindhoven, The Netherlands, Sept. 24–25, 1987; LBL-24049.
29. J.S. Gau, H.M. Ho, L.H. Chan, and G. Thomas, "Texture in Magnetic Thin-Film Media," International Conference on Textures of Materials, Santa Fe, NM, Sept. 1987; LBL-23726abs.
30. G. Thomas, "Materials Characterization by Modern Electron Microscopy," in *Conf. Proc. U.S.–Japan Seminar on Electron Microscopy*, Honolulu, HI, Sept. 7–12, 1987, Kyoto Univ. Kyoto, Japan, p. 25; LBL-24025.
31. R. Ramesh, J.K. Chen, L.K. Rabenberg, and G. Thomas, "Microstructure and Properties of Rare Earth Magnets," Symposium on Magnetic Materials, Cincinnati, OH, Oct. 11–14, 1987 (in press); LBL-24129.
32. R. Martinez, G. Thomas, M.P. Corral, and J.S. Moya, "TEM Study of the Mullite Formation during Heating of a Kaolinite Single Crystal," Sintering '87 Conf. Nov. 4–6, Tokyo, Japan.†
33. K. Srikrishna, G. Thomas, and J.S. Moya, "Characterization with Alumina in Mullite/Zirconia Composites," First International Conf. on Mullites, Nov. 9–11, Tokyo, Japan.†
34. G. Thomas, J. Kim, D. Manojlovic, and R. Milovic, "Development of High Strength and Toughness Microcomposite HSLA Fe/Cr/Mn/C Steel with and without Nb," International Symposium on Processing, Microstructure and Properties of HSLA Steels, Pittsburgh, PA, Nov. 3–5, 1987; LBL-23968.
35. R. Ramesh and G. Thomas, "Al_2O_3 Additions to Fe-Nd-B Magnets: Can Pinning be Achieved?," MMMI Conference, Chicago, IL, Nov. 9–12, 1987; LBL-23526abs.
36. R. Ramesh, J.K. Chen, and G. Thomas, "Al-Fe-Nd-B Magnets: Where does the Al Go?" MMMI Conference, Chicago, IL, Nov. 9–12, 1987; LBL-23525abs.
37. H.M. Ho and G. Thomas, "Microstructure of Oblique Incidence CoNi Thin Films," MMMI Conference, Chicago, IL, Nov. 9–12, 1987; LBL-23545abs.
38. M.L.A. Dass and G. Thomas, "Study of Microstructure and Domains in Rhombohedral Phase of PZT Ceramic," 40th Pacific Coast Regional Meeting, The American Ceramic Society, Nov. 1–4, 1987; LBL-23552abs.

39. M.L.A. Dass and G. Thomas, "Study of Microstructure and Domains in Tetragonal Phase of PZT Ceramic," 40th Pacific Coast Regional Meeting, The American Ceramic Society, Nov. 1–4, 1987; LBL-23553abs.
40. R. Martinez, M.P. Carrol, D. de Aza, J.S. Moya, T.A. Bielicki, and G. Thomas, "Study of the Kaolinite First Exothermic Reaction using Single Crystals," Conf. Proc. 6th European Clay Meeting, 1987.†
41. G. Thomas, N.J. Kim, and R. Ramesh, "Method of Forming High-Strength, Corrosion-Resistant Steel," U.S. Patent #4,671,827.
42. G. Thomas, "Impact of Electron Microscopy in Materials Sciences," in Proc. of SIME Congress of Electron Microscopy, Bologna, Italy, Oct. 14–17, 1987 *Atti del XVI Congresso di Microscopie Elettronica*, 99, 1987; LBL-23682.
43. D.L. Callahan (M.S. Thesis), "Microstructure of C_2S/CZ Composite Ceramics."

LBL Reports

44. C. Kumai, J. Kusinski, G. Thomas, and T.M. Devine, "Influence of Aging at 200C on the Corrosion Resistance of Al-Li Copper Alloys," J. Corrosion (in press); LBL-23142.‡
45. J.S. Gau, H.M. Ho, and G. Thomas, "Magnetic Properties and Structure of Co-Ni Thin Films Evaporated near the Grazing Angle," LBL-22617.
46. T. Yamamoto, K. Okazaki, M.L.A. Dass, and G. Thomas," Microstructures and Dielectric Properties at the Morphotropic Phase Boundary of $PbTiO_3$-$PbZrO_3$ System," Proc. 6th European Meeting of Ferroelectrics, Poznan, Poland, Sept. 1987, Ferroelectrics (in press); LBL-24209.
47. R. Ramesh and G. Thomas, "Effect of Quench Rate on the Intrinsic Coercivity of Iron–Rare Earth–Boron Permanent Magnets," Acta Metall. (in press); LBL-24218.
48. J.K. Chen (M.S. Thesis), "Structural and Magnetic Characterization of Nd-Fe-B Sintered Permanent Magnets," LBL-24387.
49. S. Miyasato (M.S. Thesis), "The Mechanical Properties of Drawn Dual-Phase Steel Wire," LBL-24388.
50. L.H. Chan (M.S. Thesis), "Microstructure and Magnetic Properties of Cobalt-Chromium Alloys," LBL-24074.
51. R. Ramesh (Ph.D. Thesis), "Microstructure and Magnetization Reversal of Iron-Rare Earth Boron Permanent Magnets," LBL-24552.

Invited Talks

52. G. Thomas, "Steel Research at Berkeley," Workshop on Steels, Army Research Office, Durham, NC, Jan. 12–15, 1987.
53. G. Thomas, "Fundamentals of Structural Alloy Design," "Cold Formable Dual Phase Steel for Wires," "Modern Tough Ceramic Composites," and "New Developments in Al-Li Alloys for Aerospace," Iron and Steel Institute, Boris Kidric, Niksic, Yugoslavia, May 22, 1987.
54. G. Thomas and V. Radmilovic, "Atomic Resolution in Al-Li-Cu Alloys," 4th International Al-Li Conference, Paris, France, June 10–12, 1987.
55. G. Thomas, "Rare Earth Magnets and Ceramics and Warm Super Conductors," Univ. of Technology, Helsinki, Finland, July 14, 1987.
56. G. Thomas, "HREM for Materials Research," Materials Research Laboratories, Hsinchu, Republic of China, July 1987.
57. G. Thomas, "Materials Characterization by Modern Electron Microcopy," U.S.–Japan Seminar on Electron Microscopy, Honolulu, HI, Sept. 7–12, 1987; LBL-24025.
58. G. Thomas, "Electron Microscopy Characterization of Inorganic Materials," SST/MRI Seminar, IBM Almaden Research Center, San Jose, CA, Sept. 29, 1987.
59. G. Thomas, invited speaker covering the field of materials at a special symposium on the Contribution of Electron Microscopy to Society, organized by the Philips Company to honor Nobel Prize Winner, Dr. Ernst Ruska, inventor of the electron microscope (1931) and to dedicate the new Philips Electron Optics Building at Eindhoven, The Netherlands, Sept. 24–25, 1987.
60. G. Thomas, "The Microstructural World of Materials," Department of Materials Science and Engineering, University of California Berkeley, Oct. 1, 1987.
61. G. Thomas "Microstructure-Property Relationships in Hard Magnetic Materials," Joint ASM/TMS(AIME) Fall Meeting, Symposium on Hard and Soft Magnetic Properties of Rare Earth Magnetics, Cincinnati, OH, Oct. 12, 1987.
62. G. Thomas, "Characterization of Magnetic Materials," Joint ASM/TMS(AIME) Fall Meeting, Symposium on Hard and Soft Magnetic Properties of Rare Earth Magnetics, Cincinnati, OH, Oct. 12, 1987.
63. G. Thomas "High Resolution Studies of TMT Al-Li Based Alloys," Symposium on Al-Li Alloys, Joint ASM/TMS(AIME) Fall Meeting, Symposium on Hard and Soft Magnetic Properties of Rare Earth Magnetics, Cincinnati, OH, Oct. 12, 1987.
64. G. Thomas, "Impact of Electron Microscopy in Materials Sciences," Keynote Speaker, XVI SIME Conference on Electron Microscopy, Bologna, Italy, Oct. 14–17, 1987; LBL-23682.
65. G. Thomas, "Effect of Niobium on Microcomposite: Strong, Tough Steels," International Symposium on Processing, Microstructure and Properties of HSLA Steels, Pittsburgh, PA, Nov. 3–5, 1987; LBL-23986.
66. G. Thomas, "Interfaces in Mullite/Zirconia Composites," First International Conference on Mullites, Tokyo, Japan, Nov. 9–11, 1987.†
67. G. Thomas, "Alloy Design of Micro-composite Steels," "Cold Formability of Dual Phase Steels," and "Interfacial Defects in Structural and Superconducting Ceramics," Centro Sviluppo Material, Rome, Italy, Dec. 21–22, 1987.

68. M.L.A. Dass, "Characterization of Microstructure and Domains in PZT Ceramics," American Ceramic Society, Northern California Section, Student Meeting, Berkeley, CA, Apr. 21, 1987.

†This work was supported by the National Science Foundation.

‡This work was partially supported through the Center for Advanced Materials by the Director, Office of Energy Research, Office of Basic Energy Sciences, Materials Sciences Division of the U.S. Department of Energy under Contract No. DE-AC03-76SF00098.

Solid-State Phase Transformation Mechanisms*

Kenneth H. Westmacott, Investigator

INTRODUCTION

This research is directed towards understanding the structural factors that govern phase changes and phase stability. From such knowledge first-principles alloy design for specific service applications is possible. A variety of electron-optical techniques, especially high-voltage electron microscopy (HVEM) and high-resolution electron microscopy, is used to infer the atomic rearrangements that occur when a product phase precipitates from the parent matrix. Since accommodation of a new phase of disparate size or crystal structure must involve deformation, the role of lattice defects in transformations is a focus of this work. This approach has been successful in identifying the specific defects associated with several classes of transformations characterized by different transformation strains. It has been possible to predict precipitate morphologies (growth directions, habit planes, orientation relationships, etc.) from first principles for several model alloy systems.

Extension of the principles to more complex alloys will contribute both to understanding alloy stability in severe operating conditions and to designing improved materials.

1. Factors Determining the Morphology of Precipitation in Aluminum-Germanium and Aluminum-Silicon Alloys (Publication 9)

K.H. Westmacott and U. Dahmen

HVEM *in situ* studies of precipitation in Al-Si and Al-Ge alloys complemented by high-resolution observations have provided a clear picture of the fundamental nucleation and growth processes. A model for the role of vacancies in precipitate growth was in general agreement with a dynamic sequence recording the loss of coherency during plate growth. High-resolution images obtained on NCEM's Atomic Resolution Microscope provided direct information of precipitate/matrix interface structure, internal precipitate structure, and orientation relationships. A striking example showing the wealth of information in such images is given in Figure 1-1. Figure 1-2 is a schematic diagram of a simple twinned Ge nucleus in Al. Based on the observations, simple model nuclei for various morphologies are proposed. These suggest that variations in the absolute and local vacancy supersaturation give rise to the precipitate patterns observed.

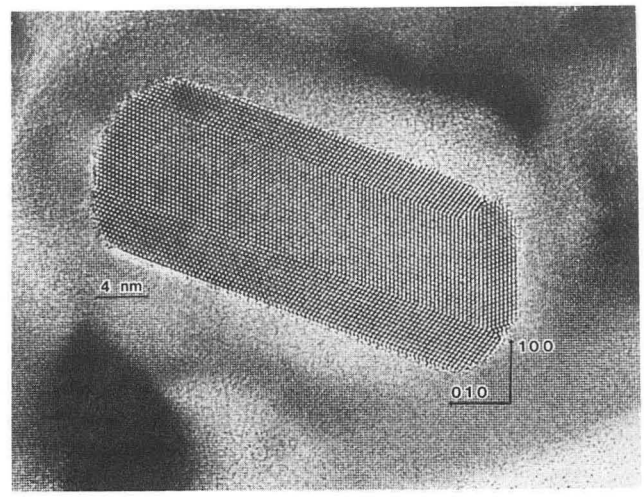

Figure 1-1. High-resolution structure image of a <100> needle of Ge in Al. Several features are noteworthy, e.g., the precision of the orientation relationship along the axis, $<110>_{Ge} || <100>_{Al}$, and in the plane, $\{100\}_{Al} || \{111\}_{Ge}$, the internal twinning, the good accommodation of the precipitate in the matrix, and the interface structure. The observation that the particles are invariably twinned has led to models for the nucleation event. (XBB 860-8555A)

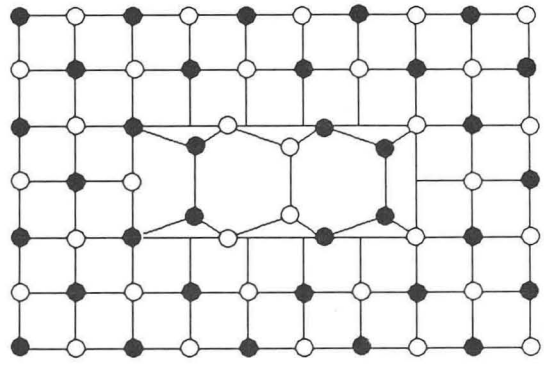

Figure 1-2. Schematic diagram of the simplest plausible twinned Ge nucleus in Al showing the excellent atomic matching and the small vacancy requirement. Open and solid circles represent atoms in alternate layers. (XBL 876-2964)

*This work was supported by the Director, Office of Energy Research, Office of Basic Energy Sciences, Materials Sciences Division of the U.S. Department of Energy under Contract No. DE-AC03-76SF00098.

2. The Accommodation of Precipitate Plates Modeled as a Tensile Test (Publication 10)

U. Dahmen and K.H. Westmacott

Thin plate precipitates in transformations with principal strains of mixed sign are approximately in a state of uniaxial stress if the interface contains an invariant line. This similarity to a tensile test can be used for the prediction of coherent and semicoherent plate habits; to relieve the uniaxial stress, the tensile axis must lie in an elastically soft direction for coherent plates and at approximately 45° to the operative slip system for semicoherent plates. In Figure 2-1 (a) and (b) the two cases are depicted schematically; in Figure 2-2 direct experimental support for the semicoherent model is given. The habit plane is the plane that contains both the invariant line and the tensile axis. Predictions of this simple model are shown to be in excellent agreement with available experimental observations on plate precipitates in several bcc interstitial alloys.

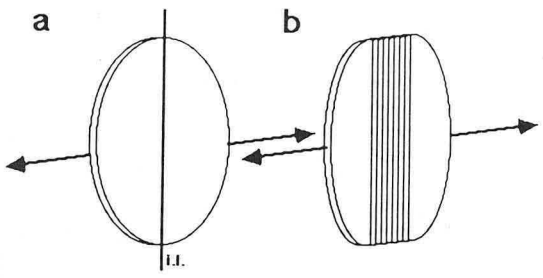

Figure 2-1. Illustration of tensile test analogy showing coherent plate under uniaxial stress in (a) and loss of coherency by plastic yielding in (b). (XBL 885-1586)

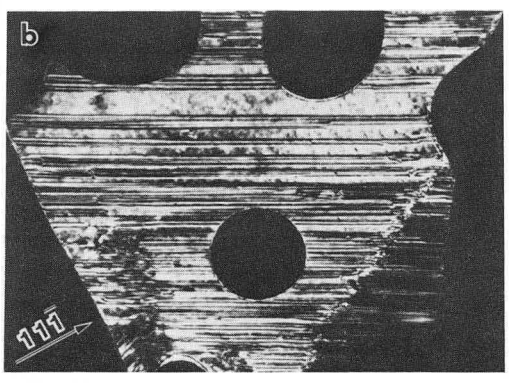

Figure 2-2. Dark-field electron micrograph of extracted semicoherent precipitate plate ($\gamma'Fe_4N$) with shear faults. (XBB 877-6246)

1987 PUBLICATIONS AND REPORTS

Refereed Journals

1. K.H. Westmacott, A.Thorel, D. Broussaud, and J.Y. Laval, "Microstructural Changes in (Mg) PSZ During Aging at 1000°C," Ultramicrosc. **22**, 15 (1987); LBL-21335.
2. U. Dahmen, P. Ferguson, and K.H. Westmacott, "A TEM Study of α''-$Fe_{16}N_2$ and $\gamma'Fe_4N$ Precipitation in Iron-Nitrogen," Acta Metall. **35**, 1037 (1987); LBL-21441.
3. K.H. Westmacott and U. Dahmen, "Recent TEM Studies of Precipitate Growth Mechanism," Rev. Phys. Appl. **21**, 757 (1986); LBL-21504.
4. J.M. Howe, U. Dahmen, and R. Gronsky, "Atomic Mechanisms of Precipitate Plate Growth," Philos. Mag. A **56**, 31 (1987); LBL-21705.
5. U. Dahmen, "Surface Relief and the Mechanism of a Phase Transformation," Scripta Metall. **21**, 1029 (1987); LBL-18405.
6. U. Dahmen and K.H. Westmacott, "Substructure of Needle-Shaped Precipitates in an Al-Ge Alloy," in *Proc. 45th Annual Meeting EMSA*, G.W. Bailey, Ed., 1987, p. 368; LBL-23145abs.

Other Publications

7. U. Dahmen, "Phase Transformations, Crystallographic Aspects," chapter in *Encyclopedia of Physical Science and Technology*, R.A. Meyers, Ed., Academic Press, New York, Vol. 10, p. 319.
8. P. Pirouz, R. Chaim, and U. Dahmen, "Hexagonal Silicon, A Stress Induced Martensitic Transformation," Proc. Fall Meeting MRS, Dec. 1987, in press.

LBL Reports

9. K.H. Westmacott and U. Dahmen, "Factors Determining the Morphology of Precipitation in Aluminum-Germanium and Aluminum-Silicon Alloys," presented at the Phase Transformations '87 Conference, Cambridge, England, July 6–10, 1987; LBL-23810.
10. U. Dahmen and K.H. Westmacott, "The Accommodation of Precipitate Plates Modelled as a Tensile Test," presented at the Phase Transformations '87 Conference, Cambridge, England, July 6–10, 1987; LBL-23811.

Invited Talks

11. K.H. Westmacott, "HVEM *In Situ* Studies of Crack Propagation in Ceramics," UCB/Grandes Ecoles Meeting, Grenoble, France, May 21, 1987.
12. K.H. Westmacott, "High Voltage Electron Microscopy at the National Center for Electron Microscopy," Caltech, Pasadena, CA, May 28, 1987.

13. K.H. Westmacott, "Precipitation Mechanisms," École Nationale Superieure des Mines de Saint-Etienne, France, July 2, 1987.

14. K.H. Westmacott, "Precipitate Morphology in Al-Ge and Al-Si Alloys," Phase Transformations '87, Cambridge, England, July 6–10, 1987.

15. U. Dahmen, "Microstructural Evolution During the Decomposition of Mg $(OH)_2$," Symposium on Chemistry on the Electron Microscope, Wickenburg, AZ, Jan. 1987.

16. U. Dahmen, "The Use of Symmetry in the TEM Analysis of Precipitate Morphologies," Stanford Annual Symposium on Applications of Contemporary Electron Microscopy, Stanford, CA, Feb. 18, 1987.

17. U. Dahmen, "Morphological Analysis of Phase Transformations by TEM," Case Western Reserve University, Cleveland, OH, Mar. 1987.

18. U. Dahmen, "Applications of Symmetry in the TEM Analysis of Precipitates," IBM Research Labs, Yorktown Heights, NY, July 1987.

19. U. Dahmen, "The Symmetry Within — Crystallography of Microstructures Observed by TEM," Raychem Corp., Menlo Park, CA, Dec. 1987.

20. U. Dahmen, "The Accommodation of Precipitate Plates Modelled as a Tensile Test," Phase Transformations '87, Cambridge, England, July 6–10, 1987.

National Center for Electron Microscopy*

Gareth Thomas, Ronald Gronsky, and Kenneth H. Westmacott, Investigators

INTRODUCTION

The National Center for Electron Microscopy (NCEM) provides advanced facilities for electron-optical characterization of materials. Its resident staff operate, maintain, design, and develop equipment and software, making it available to all Center users, and in addition conduct their own forefront research on problems in the materials sciences.

Central to NCEM are two unique high-voltage electron microscopes, a 1.5-MeV machine (the High-Voltage Electron Microscope, or HVEM), which is the most powerful in the U.S., and a 1-MeV machine (the Atomic Resolution Microscope, or ARM), which offers the best resolution in the world (better than 1.6 Å). These instruments are backed by "feeder" microscopes (for specimen screening, preliminary experiments, and complementary microchemical analysis), by specimen-preparation facilities, and by image processing and analysis facilities, all within the same building and exclusively dedicated to electron microscopy.

The 200-keV analytical electron microscope (AEM) is fully utilized in support of Center research. Current projects on the instrument include standard analyses as well as the development and refinement of new techniques (e.g., electron-energy-loss spectroscopy and convergent-beam electron diffraction) and software for quantification. The NCEM computer system is designed to assist interpretation of electron microscope images in three ways: (1) real-time enhancement of live video-rate TV images from the electron microscopes under control of the microscope operator; (2) interactive *a posteriori* processing of stored experimental images at a work station hosted by the computer; and (3) matching experimental images to ones simulated from a proposed model structure at a work station controlled by the host computer, in order to confirm (or reject) the suitability of the model.

Both operations (2) and (3) are running and available for use by users at a two-station Gould IP8500 image processor controlled by the microVAX. For implementation of operation (3), a second microVAX is available to control sets of DataCube modules that will digitize a video image in real time, store it in memory, and average it over a (selected) time interval to improve the signal-to-noise ratio and display the enhanced image on the microscope operator's monitor. A small array processor (MCS ZIP3232) provides background correction and the capability to present the operator with the diffractogram of the image.

Guidance for NCEM is provided by a steering committee, chaired by J.J. Hren (North Carolina State University). Its present members are C.W. Allen (Argonne National Laboratory), J.M. Gibson (A.T.T.), D.G. Howitt (University of California, Davis), F. Ponce (Xerox Palo Alto Research Center), J. Barry (Arizona State University), L.E. Thomas (Westinghouse), T. Hayes (LBL), and the investigators on this project. Meetings are held yearly.

Research projects at the Center cover a wide spectrum, including phase-transformation studies in metals, ceramics, and minerals; high-T_c superconductors, semiconductor devices, and catalyst and amorphous-metal investigations, as well as biological medical-science applications.

Ongoing research projects at NCEM are listed in Table 1-1.

Some examples of recent research at the Center are listed below.

1. Surface Decomposition of Superconducting $YBa_2Cu_3O_7$ (Publication 69)

H.W. Zandbergen, R. Gronsky, and G. Thomas

High-resolution electron microscopy has been performed on a number of samples of $YBa_2Cu_3O_7$ before and after heating at several temperatures between 20° and 450°C, and in three different atmospheres; oxygen, air, and vacuum. By comparison studies of the same crystals, it is shown that in all atmospheres the surface decomposes rapidly at temperatures above approximately 150°C. Below 150°C the rate of decomposition is much lower: crystals exposed to air for one week show several planar defects indicating the onset of the decomposition. The decomposition reaction proceeds by the insertion of extra CuO planes into the original structure resulting in $(CuO)_2$ double layers between BaO planes (see Figures 1-1 and 1-2). This reaction induces large lattice strains at the exposed surfaces, sometimes resulting in fragmentation and spalling.

*This work was supported by the Director, Office of Energy Research, Office of Basic Energy Sciences, Materials Sciences Division of the U.S. Department of Energy under Contract No. DE-AC03-76SF00098.

Table 1-1
NCEM Research Proposals (active during 1987)

Principal Investigator	Affiliation	Title
HVEM		
J. Apps	LBL/UC Berkeley	Characterization of stress-induced defects in minerals in relation to enhanced aqueous dissolution
J. Bastacky	LBL/UC Berkeley	The phagocytic process involved in uptake of coal combustion particulates (fly ash) by pulmonary macrophage cells
R. Beyers	IBM Almaden	*In situ* TEM study of oxygen in $Y_1Ba_2Cu_3O_{9-x}$
G. Brooks	LBL/UC Berkeley	Mitochondrial reticulum of rat skeletal muscle
T. Cass	Hewlett-Packard	Defect structures in semiconductor devices
W.A.T. Clark	Ohio State University	Micromechanisms of polycrystalline strain propagation
B. Constantz	UC Santa Cruz	The microstructure and mineralogy of coral skeleton nuclei
J.A. Cornie	MIT	Tayloring and modeling interfaces in metal-matrix composites
J. Dash	Portland State University	Electrodeposition of chromium and copper in magnetic fields
		Phase transformation induced by high pressures and temperatures in a ballistic compressor
D. deFontaine	LBL/UC Berkeley	*In situ* observation of the Devil's staircase in the long-period superstructures of binary alloys
L. DeJonghe	LBL/UC Berkeley	Structure of Si_3N_4 and SiC whiskers coated with metal oxides or polymers
J.W. Evans	LBL/UC Berkeley	Thermal oxidation of InP; dynamic transmission electron microscopy
L. Eyring	Arizona State University	*In situ* studies of phase reactions in PrO
R. Fisher	LBL/Wolverhampton, U.K.	Critical voltage studies of alloys
D. Frear	Sandia National Laboratory	Microstructural study of Al thin films
		Microstructure of solder interconnections in electronic packaging polymers
R. Geiss	IBM	(Proprietary)
R. Gronsky	LBL/UC Berkeley	*In situ* oxidation study of the Y/Ba/Cu/O superconductors
J. Howe	Carnegie-Mellon University	*In situ* studies of precipitate growth by a terrace-ledge-kink mechanism
D. Howitt	UC Davis	*In situ* studies of the kinetics of transformations in nuclear waste glasses
		In situ environmental studies of the leaching behavior in nuclear waste glasses

Table 1-1 (continued)

Principal Investigator	Affiliation	Title
D. Howitt	UC Davis	Study of electron radiation damage in ICPP nuclear waste ceramics
		Structural study of thin film ceramics
V. Jayaram	UC Santa Barbara	Microstructural study of rapidly solidified powders
C. Lyman	Lehigh University	Reduction of CuO and CuO/ZnO catalysts
D. Mattern	Data General	DC silicide and wafer crystallographic defect study
J.W. Morris, Jr.	LBL/UC Berkeley	Fatigue crack propagation mechanisms of structural alloys at cryogenic temperatures
		Fundamental study of dislocation cell formation and development in formable steel
V. Polito	UC Davis	A high-voltage EM study of the ultrastructure of freeze-substituted pollen tubes in Pyrus communis L
D. Olander	LBL/UC Berkeley	Electron-irradiation induced amorphization of precipitates in Zircaloy
A.W. Searcy	LBL/UC Berkeley	TEM studies of decomposition reactions
G. Shiflet	U. Virginia	HVEM of pearlite in a Fe-C-Mn alloy
W. Stacy	Philips	Transistor pipes
Gareth Thomas	LBL/UC Berkeley	Domain structure of lanthanum modified lead titanate ferroelectric ceramics
		High-voltage Lorentz microscopy of Fe-Nd-B magnets
		In situ studies of plastic deformation in Al-Li base alloys
		A systematic study of Cu-Ni thin films for magnetic recording media
George Thomas	Sandia National Laboratory	*In situ* oxidation studies on stainless steel
		Gases in metals
R. Wenk	LBL/UC Berkeley	Phase transformation in silica minerals
		Dislocation properties of silicate garnets
K.H. Westmacott	LBL/UC Berkeley	Dynamic hot-stage studies of precipitate development in interstitial and substitutional alloys
M.C. Williams	LBL/UC Berkeley	*In situ* study of strain deformation of block copolymer microstructures
F. Wilt	Cal State Hayward	Determining the localization of the endoskeleton of the sea urchin embryo
C. Wong	GM	The effects of oxidation-reduction treatments on the morphology of supported rhodium catalysts

Table 1-1 (continued)

Principal Investigator	Affiliation	Title
ARM		
D. Blake	NASA Ames	HREM observation of interstellar diamonds in meteorites
J. Cornie	MIT	Tayloring and modeling interfaces in metal matrix composites
M. Dollar	Carnegie-Mellon University	Atomic resolution study of nickel base single crystal superalloys
J. Goral	Solar Energy Research Institute	High-resolution structural study of $YBa_2Cu_3O_{7-x}$
		Ordering in GaInP
R. Gronsky	LBL/UC Berkeley	Atomic mechanisms of precipitate plate growth
		Dislocations and grain boundaries in silicon—structure and segregation
		Quasicrystals
		Defects in oxide superconductors
		Study of dislocation loops in arsenic-rich GaAs
J. Howe	Carnegie-Mellon University	Atomic resolution studies of shearable coherent precipitates in Al-Li alloy
		Atomic resolution microscopy of interfaces in intermetallic-matrix composites
		Atomic resolution studies of {225} martensite-austenite interfaces
R. Hull	Hewlett-Packard	Atomic scale structure of epitaxial semiconductor-semiconductor and semiconductor-metal interfaces
J.Y. Laval	CNRS, Paris	Atomic structure of internal interfaces in covalent materials
Z. Liliental	LBL/UC Berkeley	The structure of metal contacts to GaAs
C. Lyman	Lehigh University	ARM of copper crystallites via methanol synthesis Cu/ZnO catalyst
		HREM study of zirconia based eutectics
L. Mardinly	Lockheed	Gallium arsenide–indium gallium arsenide superlattice
N. Otsuka	Purdue University	A study of heteroepitaxial interfaces by ARM
F. Ponce	Xerox	Atomic imaging of binary compound semiconductor metals
G. Shiflet	U. Virginia	HREM growth ledges on T1 (Al_2CuLi) plates
		HR studies of interfacial pearlitic structures in a Fe-C-Mn alloy
L. Tanner	LLNL	HRTEM studies of pretransformation microstructures in metallic alloys

Table 1-1 (continued)

Principal Investigator	Affiliation	Title
Gareth Thomas	LBL/UC Berkeley	HREM on glasses
		Investigation of ordering in tetragonal zirconia polycrystals and in interfaces in zirconia-mullite
		Structure of PFZ in Al-Li alloys
H.L. Wenk	LBL/UC Berkeley	Superstructure identification in carbonate minerals
K.H. Westmacott	LBL/UC Berkeley	Studies of precipitate morphologies and interfaces
AEM		
K. Krishnan	LBL/UC Berkeley	Determination of the composition of the icosahedral phase in Al-Mn alloys at high spatial resolution
		Processing and microstructural characterization of the crystalline phases in the Al_2O_3-AlNd system
		Applications and development of channelling enhanced microanalysis
		Compound semiconductor contact metallizations
K. Krishnan and C. Echer	LBL/UC Berkeley	Experimental determination of UTW K-factors for low atomic number elements
J. Dash	Portland State University	Characterization of hydrides in steels by microdiffraction and EELS
Z. Liliental, J. Washburn, and R. Gronsky	LBL/UC Berkeley	Ohmic and Schottky Au contacts on GaAs
R. Ramesh, J. Chen, and G. Thomas	LBL/UC Berkeley	Role of grain boundary phases in Fe-Nd(B) permanent magnets
M. Sattler, A.T. Bell, and P.N. Ross	LBL/UC Berkeley	EDX characterization and electron microdiffraction of submicron catalyst particles of TiO_2 on SiO_2, Pt and Pt_3Co on C, Rh on La_2O_3 and on SiO_2
J. Kouvetakis, K. Krishnnan, and N. Bartlett	LBL/UC Berkeley	EELS analysis of B-C-N chemically vapor deposited crystallites
		Characterization of new graphite-like materials ($C_xB_yN_z$) by electron energy loss spectroscopy
E. Kamenetzky, L. Tanner, and W. Johnson	LBL/UC Berkeley, LLNL/Caltech	Solid state amorphization reactions; glass formation by particle melting in a Cu-Ti alloy
		Solid state amorphization reactions; nucleation of glass at grain boundaries, Ni on Zr
		Solid state amorphization reactions; kinetics of glass formation in Ni-Zr multilayers
P. Sattler and R. Gronsky	LBL/UC Berkeley	Microstructural characterization of rapidly solidified magnesium alloys and precipitates via EDX, CBED, and microdiffraction for microchemical and structural analysis

Table 1-1 (continued)

Principal Investigator	Affiliation	Title
Gareth Thomas and V. Radmilovic	LBL/UC Berkeley	Structure of PFZ in Al-Li alloys
D. Blake	NASA Ames	Characterization of carbonaceous phases contained in meteorites and interplanetary dust particles
J. Goral and K. Jones	Solar Energy Research Institute	Characterization of interfacial island inclusions formed during CVD deposition of InAs (InP) on GaAs substrate and subsequently capped with GaAs
P. Kuo	U. Utah	Light element characterization of AlN-Al_2OC ceramics
M. Sattler	LBL/UC Berkeley	Characterization of submicron Pt_3Co particles on carbon substrate; these catalyst powders are used in fuel cell applications
M. Sattler and J. Dobson	LBL/Rasor Assoc.	Microchemical characterization of a niobium-sandwiched Al_2O_3–2%Y_2O_3 insulator sheath
V. Radmilovic	LBL/UC Berkeley	Characterization of type 308 stainless steel weldment that showed intergranular stress corrosion cracking in the heat altered zone region
		Characterization of inclusions contained in Al-Li alloys
C. O'Connor	U. New Orleans	Microchemical analysis to determine compositions of amorphous and crystalline phases in Ci-Sm-Te alloys
J. Bastacky	LBL/UC Berkeley	Microchemical analysis of the alveolar walls in the human lung
E. Kamenetzky	LLNL	Characterization of glass nucleation in the grain boundaries of Ni-Zr layers during solid state amorphization reactions
R. Spontak	LBL/UC Berkeley	Characterization of microstructure resulting from microphase-separated block copolymers composed of polysiloxane and polymide
W. Hirt and K. Krishnan	LBL/UC Berkeley	Channelling enhanced microanalysis of a metastable intermediate phase between pure calcite and pure dolomite
K. Srikrishna	LBL/UC Berkeley	Characterization of oxygen content in aluminum oxynitride ceramics
H. Chan	UC Davis	Microstructural characterization of simulated Idaho chemical processing plant nuclear waste material
M. Sattler	LLNL	Characterization of small precipitates in Ce and Nd doped $Gd_3Sc_2Ga_3O_{12}$ single crystals contaminated with Ir and Cr
N. Schryvers	LBL/UC Berkeley	Characterization of bulk mullite chemical composition with standard mullite powder
H. Zandbergen	LBL/U. Leiden, The Netherlands	EDX and EELS characterization of $YBa_2Cu_3O_7$ type superconductors
W. Hirt	LBL/UC Berkeley	EDX and EELS characterization of pyroxene

Table 1-1 (continued)

Principal Investigator	Affiliation	Title
COMPUTER PROJECTS		
K. Wang and H. Zandbergen	LBL/UC Berkeley	Processing of images of defects in high-T_c superconductors
R.S. Rai and M.A. O'Keefe	LBL/UC Berkeley	Processing of images of phases of yttrium disilicate
		Simulation of phases in $Y_2Si_2O_7$
Z. Liliental and M.A. O'Keefe	LBL/UC Berkeley	Processing of images of GaAs antiphase boundaries
M. Sattler and M.A. O'Keefe	LBL/UC Berkeley	Processing of images of catalysts (anatase/rutile on amorphous Si)
I. Chan, R. Csencsits, and M.A. O'Keefe	Chevron/LBL	Processing to detect Pt clusters in Y-zeolite
H. Zandbergen	LBL/U. Leiden	Processing of images of Pt on zeolite; simulation of images of Pt on TiO_2
R. Kilaas, K. Krishnan, and R.S. Rai	LBL/UC Berkeley	Processing and simulation of 32H AlN/Al_2O_3 images
N. Schryvers and M.A. O'Keefe	LBL/LLNL	Simulation of images of mullite
J.Y. Laval and R. Kilaas	LBL/CNRS, Paris	Silicon nitride and interface simulation
H. Zandbergen and R. Kilaas	LBL/UC Berkeley	Simulation of defects in high-T_c superconductors
M. Sattler and M.A. O'Keefe	LBL/LLNL	Simulation of anatase/rutile particles on amorphous SiO_2
N. Schryvers and R. Kilaas	LBL/LLNL	Simulation of "tweed" image of NiAl
U. Dahmen and M.A. O'Keefe	LBL/UC Berkeley	Simulation of metastable phases in zirconia
B. Lee	LBL/UC Berkeley	Simulation of defects in GaAs

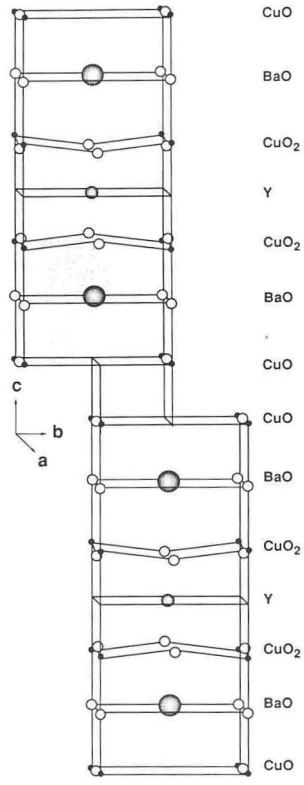

Figure 1-1. Model of the $(CuO)_2$ double layer as observed in $YBa_2Cu_3O_7$ and used for simulating the image shown in Figure 1-2. The model consists of two unit cells of $YBa_2Cu_3O_7$ shifted over half the b axis. The composition of this model, having each second CuO layer replaced by a $(CuO)_2$ double layer, is $YBa_2Cu_3O_{7.5}$. (XBL 877-3399)

2. Grain Boundaries in Sintered $YBa_2Cu_3O_{7-\delta}$ (Publication 73)

H.W. Zandbergen and G. Thomas

High-resolution electron microscopy has been carried out on grain boundaries of 92% dense $YBa_2Cu_3O_{7-\delta}$ in the tetragonal form. Grain boundaries were found to be predominantly parallel to (001) of one of the adjacent grains. No amorphous interlayer was observed at the grain boundaries. At some grain boundaries highly localized strains were detected.

3. Microstructural Evolution during the Decomposition of $Mg(OH)_2$ (Publication 2)

U. Dahmen, M.G. Kim, and A.W. Searcy

The microstructural evolution during the decomposition of $Mg(OH)_4$ is characterized by transmission electron microscopy. The reaction is pseudomorphic and topotactic, with an orientation relationship of parallel close-packed planes and directions. High-resolution micrographs show directly the small size and nearly cubic shape of the resulting MgO crystallites and their oriented stacking (see Figure 3-1). The microstructure is discussed in terms of alternative reaction mechanisms.

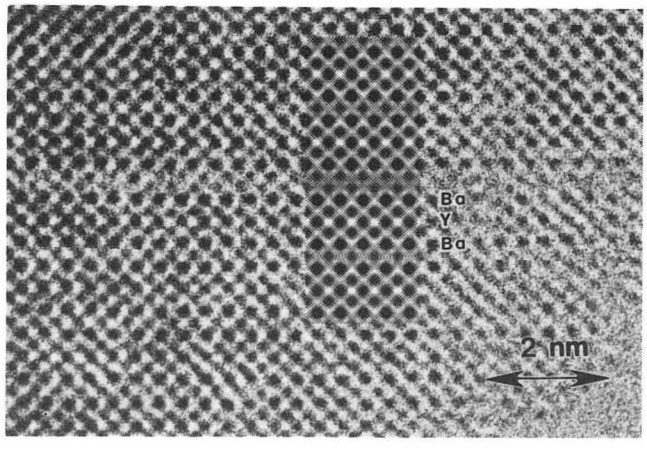

Figure 1-2. Atomic resolution image and inset simulation of the $(CuO)_2$ double layer in the 1-2-3 phase. Agreement is excellent at the atomic scale of the micrograph. (XBB 877-6268)

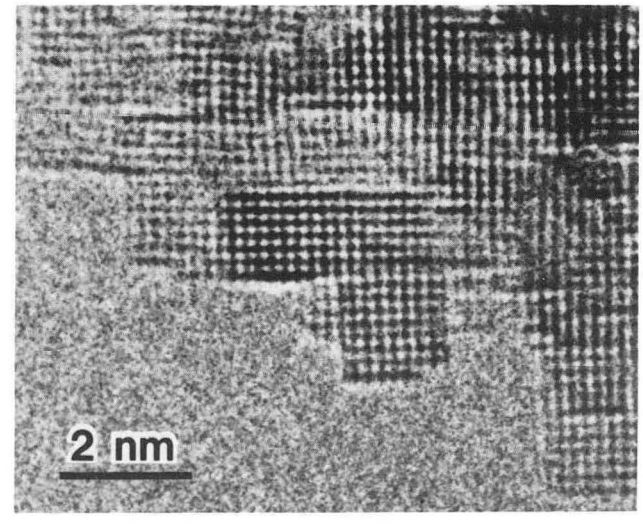

Figure 3-1. High-resolution micrograph showing misorientation and overlap of individual small crystallites of MgO. (XBB 871-62)

4. One-Dimensional Long-Period Superstructures in Cu_3Pd Observed by High-Resolution Electron Microscopy (Publication 68)

S. Takeda,[†] J. Kulik, and D. de Fontaine

One-dimensional long-period superstructures (LPS) in Cu_3Pd have been studied by electron diffraction and high-voltage, high-resolution electron microscopy. Use of a high accelerating potential (800 to 1000 kV) for the electron microscope has resulted in micrographs showing well-defined antiphase boundaries (see Figure 4-1). Boundaries contain frequent jogs in specimens of low Pd content. These observations contrast with previous electron microscopy studies, which failed to resolve sharp boundaries presumably because of dynamical diffraction effects of lower energy (200 kV) electrons.

[†]Present address: Department of Physics, College of General Education, Osaka University, Toyonaka, Osaka 560, Japan

5. TEM Study of GaAs/Si Interfaces (Publication 39)

Z. Liliental-Weber

The growth of GaAs on Si has been recognized as a highly desirable technology goal for a number of years. However, the large misfit between GaAs and Si (4%) and the problem of growing a polar crystal on a nonpolar substrate can result in a high density of lattice defects, including antiphase disorder. Transmission electron microscope studies show that the main defects are misfit and threading dislocations, stacking faults, and microtwin lamellae.

Silicon surface preparation was found to play an essential role on the density of defects formed at the Si/GaAs interface. It was observed that additional defects were nucleated at the Si surface irregularities and impurities. Distribution of the dislocations was not uniform at the interface (see Figure 5-1). Two types of misfit dislocations were found at the interface: one with their Burgers vectors parallel to the interface (~85%) and the second one with inclined Burgers vectors (~15%). This small fraction of dislocations with inclined Burgers vectors (those that climb to the epitaxial GaAs layer) is probably the reason for the substantial decrease in dislocation density of the GaAs layer after the special cleaning procedure of the Si surface.

6. Atomic Resolution Imaging in Al-Li-Cu Alloy (Publication 9)

V. Radmilovic[†] and G. Thomas

The structure of β'/δ' and T1 precipitates in Al-Li-Cu alloys has been investigated using the Atomic Resolution Microscope and computer simulation. Thermal-mechanical processing was done in a program designed to define precipitate nucleation and

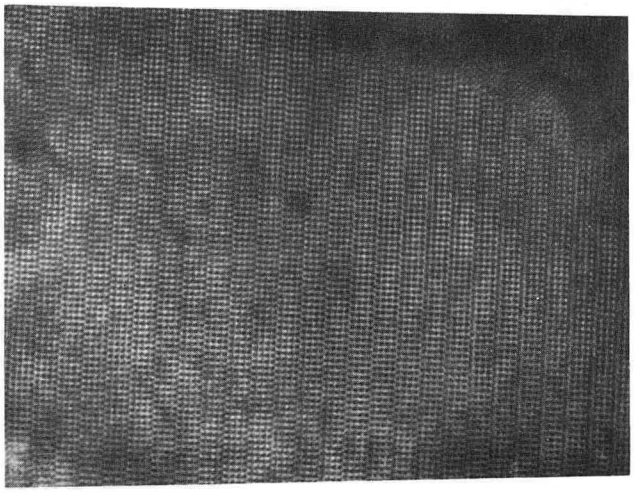

Figure 4-1. A commensurate antiphase boundary structure with a domain size of 4 in a specimen of Cu–25.2 at.% Pd annealed at 424°C. Note the sharpness of the antiphase boundaries. (XBB 863-1715)

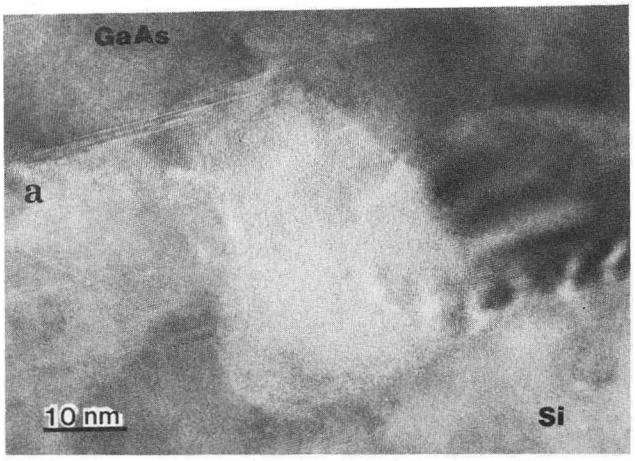

Figure 5-1. Dislocation nets formed due to the mismatch of the Si/GaAs interface. (The dislocations may be seen by viewing the micrograph at a shallow angle along the atomic planes normal to the interface.) Impurities present on the Si surface create additional defects in the form of protrusions. (XBB 872-1471)

growth conditions. The results show that the β'/δ' complexes are misoriented (1°) $L1_2$ ordered particles. The δ' shell develops polygonal facets around a β' core. An example of this effect is shown in Figure 6-1. Figure 6-2 illustrates the good agreement found between the computer-simulated and experimentally observed high-resolution images. The T1 phase density is considerably increased by mechanical processing between aging treatments, and the results are consistent with increased heterogeneous nucleation, especially by slip within δ' particles. The structure of T1 is proposed to be hexagonal with different composition layers ABCDA, but which are faulted during growth.

†Permanent address: Department of Physical Metallurgy, University of Belgrade, Belgrade, Yugoslavia 11001.

7. TEM Investigation of Orthorhombic-Type Phases in Stabilized Zirconias (Publication 54)

T.A. Bielicki,† U. Dahmen, G. Thomas, and K.H. Westmacott

The crystal structures of the thin-foil orthorhombic phases of zirconia have been investigated by microdiffraction and high-resolution transmission electron microscopy in MgO-PSZ and Y_2O_3-TZP. In the latter material, a slight distortion from orthorhombic symmetry was apparent. The structure there is believed to be rhombohedral but with the same layered and shear-faulted character as in MgO-PSZ. Image simulation of the orthorhombic phase with the ~(5 × 5 × 5) Å unit cell was performed, based on a domain structure in which O_1 atoms can occupy either obverse or reverse positions, as suggested in a previous x-ray structure refinement. Simulated and experimental images were in good agreement. A structure is proposed for the orthorhombic phase with the ~(10 × 5 × 5) Å unit cell, consisting of a planar arrangement of obverse and reverse domains in alternation.

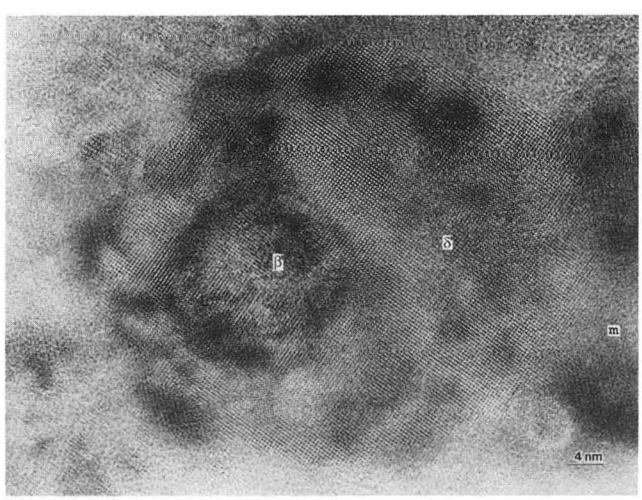

Figure 6-1. Atomic resolution image of d′/b′ particles; polygonal morphology of the d′ shell; overaged condition; zone axis [100]. (XBB 875-3898)

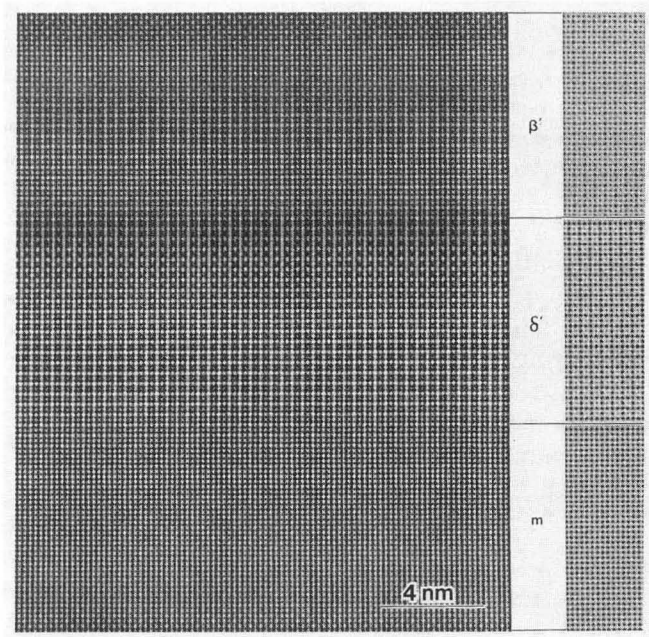

Figure 6-2. Simulated high-resolution TEM image of a d′/b′ complex particle in Al matrix; the white spots represent atom positions. The projected potential for the same particles are shown on the right. Black spots represent atom positions. (XBB 875-3897)

†Present address: 34 Butler Avenue, Harrow, Middlesex, HA1 4EH, U. K.

8. A High-Resolution Electron Microscopy Study of the Martensitic Transformation in Ni-Al: Premartensitic Microstructures (Publication 49)†

D. Schryvers and L.E. Tanner‡

Microstructures of the β_2 (B2, ordered BCC) parent phase in Ni-rich Ni-Al alloys prior to its thermoelastic martensitic transformation to a rhombohedral 7R (52) product phase have been examined by HREM. The images exhibit a diffuse domain

substructure of ~5 nm diameter, and within each domain are microcontrast modulations of ~1.3 nm parallel to {110} planes of β_2 (see Figure 8-1). Diffraction shows diffuse <110>* streaks emanating from Bragg peaks, as well as satellites at ~0.16<110>*; the latter values are inversely proportional to the modulation spacing (see inset to Figure 8-1). The incommensurate modulations can be explained by introducing a small homogeneous {110}<110> shear in conjunction with a transverse sine-wave atomic shuffle of proper periodicity to the β_2 lattice. There are six equivalent variants of these elastic distortions, and each domain contains one of the six to produce a three-dimensional mosaic assembly. The foregoing are consonant with elastic and inelastic neutron-scattering experiments made on the same material by S.M. Shapiro *et al.* of Brookhaven National Laboratory. In particular, they find a temperature-dependent anomalous dip at ~0.16**q**[110] of the transverse acoustic [110] phonon branch, and this lattice "softening" is believed related to the evolution in the incommensurate premartensitic microstructure, which approximates the periodicity of the commensurate 7R martensite to be formed. Accordingly, the parent β_2 is viewed as preparing itself as it approaches eventual transformation.

---

†Work performed under the auspices of the U.S. Department of Energy through Lawrence Livermore National Laboratory (LLNL), Contract No. W-7405-ENG-48.

‡Permanent address: Chemistry and Materials Science Department, LLNL.

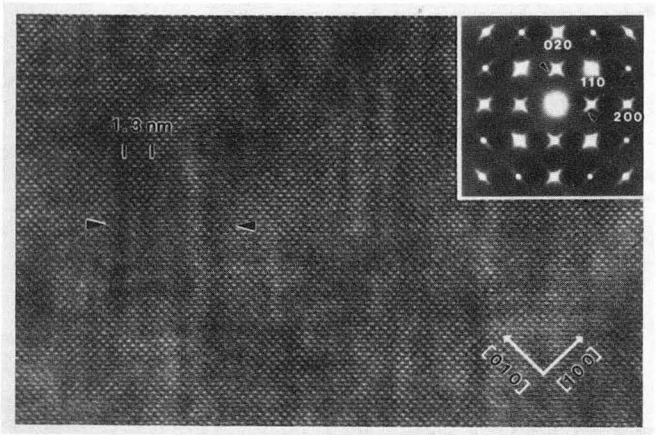

Figure 8-1. Cross-fringe HREM image in an [001] orientation of $b_2(B_2)$ NiAl showing premartensitic domain structure. Inset is associated zone-axis electron-diffraction pattern. (XBB 870-9254A)

9. Factors Determining the Morphology of Precipitation in Aluminum-Germanium and Aluminum-Silicon Alloys (Publication 60)

K.H. Westmacott and U. Dahmen

HVEM *in situ* studies of precipitation in Al-Si and Al-Ge alloys complemented by high-resolution observations have provided a clear picture of the fundamental nucleation and growth processes. A model for the role of vacancies in precipitate growth was in general agreement with a dynamic sequence recording the loss of coherency during plate growth (see Figures 9-1 and 9-2). High-resolution images obtained on NCEM's Atomic Resolution Microscope provided direct information of precipitate/matrix interface structure, internal precipitate structure, and orientation relationships. Based on the observations, simple model nuclei for various morphologies are proposed. These suggest that variations in the absolute and local vacancy supersaturation give rise to the precipitate patterns observed.

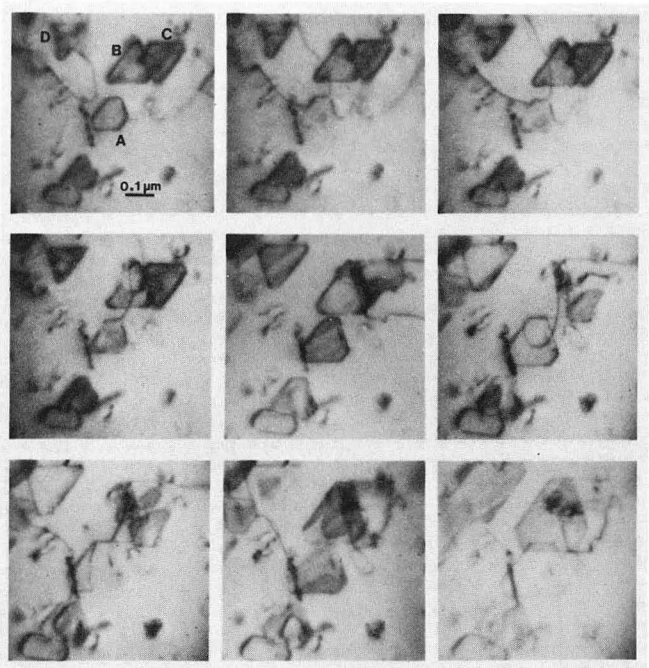

Figure 9-1. Sequence of micrographs taken from a videotape that illustrates the loss of coherency of {111} precipitate plates in Al-1 at% Si resulting from interaction with a matrix glide dislocation. The strong 1/2<110> strain contrast initially exhibited by plate A disappears as the dislocation is incorporated in the interface. Subsequent thickening of the plate is manifested by changes in the displacement contrast in the plate interior as ledges propagate and the progressive development of contrast at the plate periphery as the ledges fully expand across the face. (XBB 876-5375)

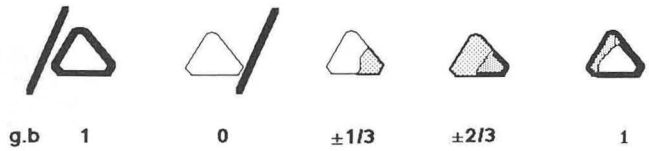

Figure 9-2. Schematic diagram showing the progressive changes in structure and contrast (g.b. and g.R. values) following loss of coherency induced by interaction of the plate with a 1/2<110> dislocation. (XBL 876-2968)

10. Surface Characterization of Silicon Nitride and Silicon Carbide Powders (Publication 10)

M.N. Rahaman, Y. Boiteux, and L.C. DeJonghe

The nature and composition of the surfaces of silicon nitride and silicon carbide powders were investigated using high-voltage and high-resolution transmission electron microscopy (TEM), x-ray photoelectron spectroscopy (XPS), and secondary-ion mass spectrometry (SIMS). An amorphous oxide (or oxygen-rich) layer, ≈3–5 nm thick, present on the powder surfaces forms strong bridges between particles. Both XPS and SIMS show that oxygen is the major impurity on the powder surfaces, but minor impurities, such as chlorine, fluorine, carbon, iron, and sodium, are also revealed. The extent of the oxide layer was reduced substantially by washing the powder in anhydrous hydrofluoric acid or by treatment in an argon/hydrogen gas mixture at ≈1300°C. Surface treatment in the gas mixture did not cause further agglomeration of the powder.

11. A Summary of the Low-Angle X-Ray Atomic Scattering Factors that Have Been Measured by the Critical Voltage Effect in High-Energy Electron Diffraction (HEED) (Publication 28)

A.G. Fox[†] and R.M. Fisher[‡]

A tabulated summary of all the accurate (~0.1%) low-angle x-ray atomic scattering (form) factors that have been determined by the systematic critical-voltage technique in HEED is presented. For low-atomic-number elements ($Z \leqslant 40$), the low-angle form factors can be significantly different to best free-atom values, and so the best band-structure-calculated and/or x-ray-measured form factors consistent with the critical-voltage measurements are also indicated. At intermediate atomic numbers ($Z \simeq 40 \rightarrow 50$), only the very low-angle form factors appear to be different from the best free-atom values, and even then only by a small amount. For heavy elements ($Z \geqslant 70$), the best free-atom form factors appear to agree very closely with the critical-voltage-measured values, and so, in this case, critical-voltage measurements give very accurate measurements of Debye-Waller factors.

[†]Permanent address: School of Engineering, The Polytechnic, Wolverhampton, WV1 1SB, U.K.

[‡]R.M. Fisher is supported by the Center for Advanced Materials.

12. Advances in High-Resolution Image Simulation (Publication 59)

M.A. O'Keefe and R. Kilaas

Since an earlier report, continuing advances in hardware and software have improved both the speed and the range of computations that can be made to simulate HREM images from various structures. Use of image display systems and array processors has made the image-simulation procedure much more interactive, while laser printers provide a fast high-quality hard-copy output.

Use of array processors has enabled the rewriting of electron-scattering algorithms to include convergence effects (previously only considered after the scattered electron beams had emerged from the specimen) and upper-Laue-layer-line effects. With an array processor, it is faster to compute the effects of spatial and temporal coherence in real space than to use the approximations derived from reciprocal space.

With a frame buffer and suitable software, the user has the facility to change parameters and view the results of the change almost immediately. Selected images can then be directed to hard-copy output, in contrast to batch methods, where series of hardcopy images are produced and then selected from. Given a microdensitometer for output of experimental images from plates, or a video camera attached to the electron microscope and a frame buffer, split-screen comparisons between experimental and computed images are possible, including independent control of image contrast, magnification, and orientation.

13. Interactive Software for Simulation of High-Resolution TEM Images (Publication 34)

R. Kilaas

A new highly interactive and user-friendly software package for simulation and processing of high-resolution transmission electron micrographs has been developed at NCEM. Designed to be used by scientific visitors to the Center, the software is completely menu driven from a graphics terminal with a mouse and requires almost no computer knowledge for proper usage. Although the software is written to insure maximum performance with hardware available at the NCEM, hardware-dependent code is kept in separate modules that are easily modified. The new software package combines an unparalleled ease of use with the latest theory in the field of simulation of high-resolution transmission electron micrographs.

14. On the Inclusion of Upper Laue Layers in Computational Methods in High-Resolution Transmission Electron Microscopy (Publication 6)

R. Kilaas, M.A. O'Keefe, and K.M. Krishnan

Three different methods for computing scattering amplitudes in high-resolution transmission electron microscopy (HRTEM) have been investigated as to their ability to include upper Laue layer (ULL) interaction. The conventional first-order multislice method using fast fourier transform (FFT) and second-order multislice method are shown to yield calculated intensities of first-order Laue reflections with the use of slice thicknesses smaller than the crystal periodicity along the incident electron-beam direction. It is argued that the calculated intensities of ULL reflections approach the correct values in the limiting case of vanishing slice thickness and electron wavelength. The third method, the improved phasegrating method (IPG), in principle also includes ULL effects but is severely limited as to choice of slice thickness and sampling interval. A practical way to use slice thicknesses less than the crystal periodicity along the incident beam direction is shown for both the conventional FFT method and the second-order multislice method and tested on a spinel structure. It is also shown that the IPG method does not easily allow for a slice thickness different from the crystal periodicity in the beam direction.

15. Channelling Enhanced Microanalysis: A High-Resolution Analytical Technique for Atomic Site and Species Determinations (Publication 57)

K.M. Krishnan

The formulation, development, and applications of a novel crystallographic technique to determine specific-site occupations of elemental additions in crystalline materials, using the channelling or Borrman effect in electron diffraction, is reviewed. This technique is based on the effect of incident-beam orientations on the intensities of either the characteristic x-ray emissions or the characteristic electron-energy-loss edges. The formulation of the technique under both planar and axial channeling conditions for crystalline materials is presented. In general, this technique can distinguish neighbors in the periodic table; involves no adjustable parameters, external standards, or special specimen preparations; is applicable to trace-elemental concentrations (0.2–0.3 wt% or 10^{25} atoms/m^3); is very accurate; and can be applied routinely at high spatial resolutions (~10–40 nm). In the EELS formulation the technique can also provide specific site-valence information. Finally, applications of this technique to site-occupation studies in a variety of materials is outlined.

16. Determination of Ultrathin Window (UTW) K_{XSi} Factors for Low-Atomic-Number Microanalysis: A Systematic Approach (Publication 36)

K.M. Krishnan and C.J. Echer

A systematic measurement of experimental K_{XSi} factors, with particular emphasis on low-Z microanalysis ($6 \leqslant Z \leqslant 32$), at 200 kV for a KEVEX UTW Si(LI) detector fitted to a JEOL 200CX analytical microscope, using a variety of high-purity standards, has been carried out. Under normal operating conditions using a LaB_6 filament, it is shown that absorption in the specimen is very critical, particularly for heavy-element matrices, and sample thicknesses need to be measured for accurate

microanalysis of low-Z elements (C, N, O). Using these measured K_{XSi} factors, quantitative UTW–energy-dispersive x-ray microanalysis has been routinely extended to carbon.

17. The Nature and Origin of Interstellar Diamond (Publication 20)

D. Blake,[†] F. Freund,[†] K. Krishnan, C. Echer, C. Hetherington, R. Shipp,[†] T. Bunch,[†] A. Tielens,[†] R.J. Lipari,[‡] and S. Chang[†]

Recently, microscopic diamond was discovered in oxidized acid residues from several carbonaceous chondrite meteorites (e.g., the Cδ component of the Allende meteorite). Previous authors have remarked on the results obtained by various techniques—for example, the "sootlike" features noted in IR spectra, the low combustion and gas release temperatures, and the anomalously low density of the material—that appear to conflict with properties expected of diamond. Here we present high-spatial-resolution analytical data that may serve in part to explain such results. The Cδ diamond is single phase, but surface and interfacial carbon atoms, which comprise as much as 25% of the total, impart an "amorphous" feature to some spectral data. Nonporous clumps of diamond, 10–500 nm in size, consist of tightly packed mosaics of 0.5–10 nm crystallites. We propose that Cδ diamond results from high-velocity grain-grain collisions behind a supernova shock front in the interstellar medium, and that other high-pressure mineral phases should also exist in primitive meteorites and cosmic dust as a result of such processes.

[†]Permanent address: NASA/Ames Reseach Center, Moffett Field, CA 94035.

[‡]Permanent address: Surface Science Laboratories, Mountain View, CA 94043.

18. Work in Progress

Short-Range Order in Cu-Pd under Electron Irradiation (J. Kulik and D. de Fontaine)

Restoration of short-range order (SRO) in Cu-Pd alloys has been observed after samples were initially disordered using the electron beam in NCEM's high-voltage (1.5-MeV) electron microscope. Complete disorder under the beam action is observed at 100 K. SRO reappears at temperatures at 150 K and higher due to beam-induced kinetics. In the temperature range of 150 K to about 300 K, such kinetics are likely the result of interstitialcies since vacancies are effectively immobile at such temperatures. Diffuse peaks of SRO-scattered intensity appear at positions [q10] and equivalent in the first Brillouin Zone of the disordered fcc lattice. The value of q is known to depend on Fermi surface effects, but we also observe a temperature dependence in the value of q over the temperature range 150 to 400 K. The estimated displacement rate due to the action of the electron beam is approximately 5×10^{-3} displacements per atom per second. A reirradiation experiment has shown these effects to be repeatable and therefore not a consequence of irradiation damage or a local beam-induced composition change.

1987 PUBLICATIONS AND REPORTS

Refereed Journals

1. R. Csencsits and R. Gronsky, "Damage of Zeolite Y in the TEM and its Effects on TEM Images," Ultramicroscopy **23**, 421 (1987); LBL-22695.
2. U. Dahmen, M.G. Kim, and A.W. Searcy, "Microstructural Evolution During the Decomposition of $Mg(OH)_2$," Ultramicroscopy **23**, 365 (1987); LBL-22899.
3. U. Dahmen and K.H. Westmacott, "Simple Model for the Prediction of Coherent and Semicoherent Plate Precipitate Habit Planes," Acta Metall. **34**, 475 (1986); LBL-21423.
4. A. Fox and R.M. Fisher, "Structure Factors and Debye Temperatures of Al-Li Solid-Solution Alloys," Acta Crystallogr. **A43**, 260 (1987).
5. J.M. Howe, "Metallographic and Diffraction Scanning Calorimetry Analyses of Precipitated and Recrystallization in Al-Mn Alloy," Metall. Trans. **17A**, 593 (1986).
6. R. Kilaas, M.A. O'Keefe, and K.M. Krishnan, "On the Inclusion of Upper Laue Layers in Computational Methods in High Resolution Transmission Electron Microscopy," Ultramicroscopy **21**, 47 (1987); LBL-20836.
7. M.G. Kim, U. Dahmen, and A.W. Searcy, "Structural Transformations in the Decomposition of $Mg(OH)_2$ and $MgCO_3$, J. Am. Ceram. Soc. **70**, 146 (1987); LBL-21587.
8. K.M. Krishnan, "When is 'Parallel' Illumination Best Parallel for ALCHEMI?" Ultramicroscopy **23**, 199 (1987); LBL-22618.
9. V. Radmilovic and G. Thomas, "Atomic Resolution Imaging in Al-Li-Cu Alloy," J. de Physique, Colloque C3, **48**, C3–385 (1987); LBL-23558.
10. M.N. Rahaman, Y. Boiteux, and L.C. De Jonghe, "Surface Characterization of Silicon Nitride and Sili-

con Carbide Powders," Ceram. Bull. **65**, 1171 (1986); LBL-20389.

11. D.K. Sadana, M.H. Norcott, R.G. Wilson, and U. Dahmen, "Transmission Electron Microscopy of Aluminum Implanted and Annealed (100)Si: Direct Evidence of Aluminum Precipitate Formation," Appl. Phys. **49**, 1169 (1986).
12. T. Sands, V.G. Keramidas, J. Washburn, and R. Gronsky, "On the Structures and Composition of Ni_xGaAs," Appl. Phys. Lett. **48**, 402 (1986).
13. T. Sands, V.G. Keramidas, A.J. Yu, K.M. Yu, R. Gronsky, and J. Washburn, "Ni, Pd and Pt on GaAs: a Comparative Study of Reacted Film Morphologies," J. Mater. Res. (March/April 1987); LBL-21060.
14. T. Sands, V. Keramidas, R. Gronsky, and J. Washburn, "Initial Stages of the Pd-GaAs Reaction Formation and Decomposition of Ternary Phases," Thin Solid Films **136**, 105 (1986).
15. M.L. Sattler and P.N. Ross, "The Surface Structure of Pt Crystallites Supported on Carbon Black," Ultramicroscopy **20**, 21 (1986); LBL-20873.
16. S.M. Shapiro, J.Z. Larese, Y. Noda, S.C. Moss, and L.E. Tanner, "Neutron Scattering Study of Premartensitic Behavior in Ni-Al Alloys," Phys. Rev. Lett. **57**, 3199 (1986).
17. J. Turner and K.M. Krishnan, "An Improved Photographic Process for Convergent Beam Electron Diffraction Applications," J. Elec. Microsc. Tech. **5**, 211 (1987); LBL-21581.
18. J.G. Ulan, E. Kuo, W.F. Maier, S.J. Chettle, R.S. Rai, and G. Thomas, "The Effect of Lead Acetate in the Preparation of the Lindlar Catalyst," J. Org. Chem. **52**, 3132 (1987); LBL-21980.

Other Publications

19. N. Bartlett, J. Kouvetakis, R. Kaner, and K.M. Krishnan, "Novel Metallic and Semiconductive Graphites," Science (in press).
20. D. Blake, F. Freund, K. Krishnan, C. Echer, C. Hetherington, R. Shipp, T. Bunch, A. Tielens, R.J. Lipari, and S. Chang, "The Nature and Origin of Interstellar Diamond," submitted to Nature.
21. E.D. Bourret, B.-T. Lee, and J.M. Jaklevic, "Structural Characterization of Undoped and Doped GaAs: a Comparative Study of Four Techniques," in *Proc. Int. Symp. Defect Recognition and Image Processing in Compounds*, Monterey, CA, April 27–29, 1987, p. 95; LBL-22698.
22. U. Dahmen, "Phase Transformations, Crystallographic Aspects," in *Encyclopedia of Physical Science Technology*, Vol. 10, Academic Press, 1987, p. 319.
23. U. Dahmen and K.H. Westmacott, "Substructure of Needle-Shaped Precipitates in an Al-Ge Alloy," in *Proc. 45th Annual Meeting EMSA*, Baltimore, MD, G.W. Bailey, Ed., San Francisco Press, 1987, p. 368; LBL-23145abs.
24. B.G. Demczyk, "In-situ Transmission Electron Microscopy Study of the Paraelectric to Ferroelectric (Cubic to Tetragonal) Phase Transformation in Lanthanum Modified Lead Titanate Ceramics," in *Proc. 45th Annual Meeting EMSA*, G.W. Bailey, Ed., San Francisco Press, 1987, p. 172.
25. V.P. Dravid, M.R. Notis, and C.E. Lyman, "Analytical and High Resolution Electron Microscopy of Interphase Interfaces in Zirconia-Based Eutectics," to be published in *Proc. Phase Transformations 1987*, The Institute of Metals, Cambridge, U.K., July 6–10, 1987.
26. R.M. Fisher, "The Critical Voltage Effect in Metals, Alloys and Compounds," in *Proc. Beijing Conf. Exhibition on Instrumental Analysis*, Vol. 1, Feb. 1987.
27. R.M. Fisher, "Stress Anisotropy and Delamination of Evaporated Chromium Films," in *Proc. 45th Annual Meeting EMSA*," San Francisco Press, 1987.
28. A.G. Fox and R.M. Fisher, "A Summary of the Low Angle X-ray Atomic Scattering Factors Which Have Been Measured by the Critical Voltage Effect in High Energy Electron Diffraction (HEED)," Australian J. Phys. (in press).
29. R. Gronsky, R.L. Hines, and C. Nelson, "Platinum Surface Structures at Atomic Resolution," in *Proc. XIth Int. Cong. Electron Microscopy*, Kyoto, Japan, Aug. 31–Sept. 7, 1986, Vol. II, T. Imura, S. Maruse, and T. Suzuki, Eds., the Japanese Society of Electron Microscopy, Tokyo, Japan 1986, p. 961; J. Electron Microsc. **35**, Supplement (1986).
30. G.F. Holland, R.L. Hoskins, M.A. Dixon, P.D. Ver-Nooy, H.-C. zur Loye, G. Brimhall, D. Sullivan, R. Cormia, H.W. Zandbergen, R. Gronsky, and A.M. Stacy, "The Interplay of Synthesis, Structure and Microstructure and Superconducting Properties of $YBa_2Cu_3O_7$," submitted to J. Am. Chem. Soc.
31. J.M. Howe, R. Gronsky, and H.I. Aaronson, "Nucleation of g' Plates from GP Zones in an Al-Ag Alloy," in *Proc. 44th Annual Meeting EMSA*, G.W. Bailey, Ed., San Francisco Press, 1986, p. 552; submitted to Scripta Metall.
32. J.M. Howe and R. Gronsky, "TEM Studies of Precipitate Growth at the Atomic Level," in *MRS Symp. Proc.* **62**, 241 (1986).
33. R. Hull and S.J. Rosner, "Atomic Structure of the GaAs/Si Interface," submitted to Appl. Phys. Lett.
34. R. Kilaas, "Interactive Software for Simulation of High Resolution TEM Images," presented at MAS Conference, Kona, HI, July 13–17, 1987; in *Microbeam Analysis 1987*, R.H. Geiss, Ed., San Francisco Press, 1987, p. 293; LBL-23259.
35. K.M. Krishnan, "Study of Novel Graphite-Like Materials in the B-C-N System by Electron Energy-Loss Spectroscopy," in *Proc. Microbeam Analysis Soc. Conf.*, Kona, HI, July 13–17, 1987; LBL-22923.
36. K.M. Krishnan and C.J. Echer, "Determination of UTW K_{XSi} Factors for Low Atomic Number Microanalysis: A Systematic Approach," in *Proc.*

Microbeam Analysis Society Conf., Kona, HI, July 12–17, 1987; LBL-23739.

37. K.M. Krishnan and G. Thomas, "Microanalysis of Polytypoid Ceramics by Imaging, Diffraction and Spectroscopy," in *Proc. Microbeam Analysis Society Conf.*, Kona, HI, July 13–17, 1987; LBL-22924.
38. B.-T. Lee, T. Sands, R. Gronsky, and E. Bourret, "A TEM Study of Precipitates in As-Grown Semi-Insulating Indium-Doped GaAs," in *Inst. Phys. Conf. Ser.* No. 83, Chapter 2; presented at International Symposium on GaAs and Related Compounds, Las Vegas, NV, 1986.
39. Z. Liliental-Weber, "The Structure of GaAs-Si (211) Heteroepitaxial Layers," in *Mat. Res. Soc. Symp. Heteroepitaxy in Silicon Technology* **91**, 91 (1987); LBL-23462.
40. C.E. Lyman, P. Schabes-Retchkiman, and D. Ackland, "Controlled Atmosphere Reduction and Beam-Induced Reduction of CuO," in *Proc. 45th Annual Meeting EMSA*, Baltimore, MD, G.W. Bailey, Ed., San Francisco Press, 1987, p. 833.
41. A. Meike, "Specimen Cage Modification for TEM In-Situ Shearing," in *Proc. MRS Meeting*, Fall 1987.
42. A. Meike, H.-R. Wenk, R. Gronsky, and M. O'Keefe, "Atomic Resolution Microscopy of Carbonates. Interpretation of Contrast," in special issue of *Physics and Chemistry of Solids* (NATO-sponsored Advanced Study Institute, Cambridge, England, July 27–Aug. 8, 1987).
43. M.A. O'Keefe, "A Computer System for HREM Image Processing and Simulation," in *Proc. 45th Annual Meeting EMSA*, Baltimore, MD, G.W. Bailey, Ed., San Francisco Press, 1987, p. 364; LBL-23184.
44. D.K. Sadana, G.M. Towner, M.H. Norcott, and R.C. Ellwanger, "Some TEM Observations on Electromigrated Al and Al Alloy Interconnects," in *Interim. Reliability Physics Symp.* **24**, 38 (1986).
45. T. Sands, "Contributions of Electron Microscopy to the Understanding of Reactions on Compound Semiconductor Surfaces," in *Mat. Res. Soc. Symp. Proc.* **62**, 25 (1986).
46. M. Sarikaya, "Characterization of Advanced Materials by High Resolution Transmission Electron Microscopy," in *Proc. MRS*, Seattle, Aug. 29–Sept. 2, 1987 (in press).
47. M.L. Sattler and M.A. O'Keefe, "Atomic Structure Analysis of Small Particles Supported on Amorphous Material," in *Proc. 45th Annual Meeting EMSA*, Baltimore, MD, G.W. Bailey, Ed., San Francisco Press, 1987, p. 104; LBL-23172.
48. D. Schryvers, L.E. Tanner, and G. VanTendeloo, "Premartensitic Microstructures as Seen in the High-Resolution Electron Microscope: A Study of a Ni-Al Alloy," in *NATO/ASI Meeting on Phase Stability*, A. Gonis and M. Stocks, Eds., Martinus Nijhoff Publ., Dordrecht, The Netherlands (in press).
49. D. Schryvers and L.E. Tanner, "A High-Resolution Electron Microscopy Study of the Martensitic Transformation in Ni-Al: I, Premartensitic Microstructures," submitted to Philos. Mag.
50. S. Takeda, J. Kulik, and D. de Fontaine, "Spinodal Ordering Beyond the Lifshitz Point in Cu-Pd Observed in the High Voltage Electron Microscope," in *Proc. XIth Int. Cong. Electron Microscopy*, Kyoto, Japan, 1986, p. 1001; LBL-22035.
51. S. Takeda, J. Kulik, D. de Fontaine, and L.E. Tanner, "Antiphase Boundaries in Cu-Pd Observed by High Resolution and High Voltage Electron Microscopy," in *Proc. XIth Int. Cong. on Electron Microscopy*, Kyoto, Japan, 1986, p. 957.
52. L.E. Tanner, "On the Systematics of Phase Transformations in Metallic Alloys," in *Proc. Symp. Competing Interactions and Microstructures Statics and Dynamics*, Springer Solid State Sciences Series, Springer-Verlag, Berlin (in press).
53. L.E. Tanner, A.R. Pelton, G. VanTendeloo, D. Schryvers, and M. Wall, "Premartensitic Microstructures in Ni-Al Ordered b_2 Phase: I, Effects Induced by Cooling," submitted to Scripta Metall.

LBL Reports

54. T.A. Bielicki, U. Dahmen, G. Thomas, and K.H. Westmacott, "TEM Investigation of Orthorhombic-Type Phases in Stabilized Zirconias," in *Proc. Zirconia '86*, Tokyo, Japan, Sept. 9–11, 1986 (in press); LBL-22367.
55. U. Dahmen and K.H. Westmacott, "The Accommodation of Precipitate Plates Modeled as a Tensile Test," in *Proc. Phase Transformations Conference, 1987*, The Institute of Metals, Cambridge, England (in press); LBL-22949 and LBL-23811.
56. C.J.D. Hetherington, "The Preparation of Semiconductor Cross-Sections by Cleaving," 1987 MRS Fall Meeting, Boston, MA, Nov. 30–Dec. 5, 1987: Workshop on Spec. Prep. for TEM of Materials; LBL-23566.
57. K.M. Krishnan, "Channelling Enhanced Microanalysis: A High Resolution Analytical Technique for Atomic Site and Species Determination," Indo-U.S. Workshop "Advanced Techniques for Microstructural Characterization," Bombay, India, Jan. 11–15, 1988, submitted to Mat. Sci. Forum, Trans. Tech. Pub.; LBL-24317.
58. K.M. Krishnan and G. Thomas, "Determination of Specific Site Occupation in Crystalline Magnetic Materials by Channelling Enhanced Microanalysis: a Review," TMS/AIME Fall Meeting, Orlando, FL, Oct. 5–9, 1986; LBL-21324abs.
59. M.A. O'Keefe and R. Kilaas, "Advances in High Resolution Image Simulation," in *Proc. 6th Pfefferkorn Conf. on Image and Signal Processing*, Niagara Falls, Ontario, April 28–May 2, 1987 (in press); LBL-24727.
60. K.H. Westmacott and U. Dahmen, "Factors Determining the Morphology of Precipitation in Al-Ge and Al-Si Alloys," in *Proc. "Phase Transforma-*

tions," July 6–10, 1987, The Institute of Metals, Cambridge, England (in press); LBL-23810.

61. H.W. Zandbergen, "High Resolution Electron Microscopic Study of the Growth of Denser Phases on Zeolite Y and Zeolite L," in *Proc. MRS Meeting*, Fall 1987, Boston, MA (in press); LBL-24615.
62. R. Csencsits, C. Schooley, and R. Gronsky, "An Improved Method for Thin Sectioning of Particulate Catalysts," J. Electron Microsc. Techn. (in press); LBL-19549.
63. R. Csencsits and R. Gronsky, "Vitrification of Zeolite Y in the TEM," submitted to Zeolites; LBL-22549.
64. R. Gronsky, "Spectroscopic Information from High Resolution Images," special publication of Ultramicroscopy entitled "Limits of Submicron Spectroscopy," J. Hren and M.J. Kersker, Eds. (in press); LBL-22387.
65. R. Kilaas, "New Image Simulation Software Development at the National Center for Electron Microscopy," submitted to Ultramicroscopy; LBL-22683.
66. B.-T. Lee, R. Gronsky, and E.D. Bourret, "Dislocation Loops and Precipitates Associated with Excess Arsenic in GaAs," submitted to J. Appl. Phys.; LBL-24363.
67. M.L. Sattler, M.G. Reichmann, and A.T. Bell, "Identification of Phases and Surfaces in Small TiO_2 Catalyst Particles using High Resolution Electron Microscopy/Spectroscopy Techniques, Part I.," submitted to Ultramicroscopy; LBL-20037.
68. S. Takeda, J. Kulik, and D. de Fontaine, "One-Dimensional Long Period Superstructures in Cu_3Pd Observed by High Resolution Electron Microscopy," submitted to J. Phys. F; LBL-24132.
69. H.W. Zandbergen, R. Gronsky, and G. Thomas, "Surface Decomposition of Superconducting $YBa_2Cu_3O_7$," submitted to Phys. Stat. Sol.; LBL-23854.
70. H.W. Zandbergen, G.F. Holland, P. Tejedor, R. Gronsky, and A.M. Stacy, "A Study of Mixed Phase Behavior in the Lanthanide-Substituted Superconducting Oxide $ErBa_2Cu_3O_7$," to be published in a special issue of "Advanced Ceramic Materials," J. Am. Ceram. Soc.; LBL-23566.
71. H.W. Zandbergen, C.J.D. Hetherington, and R. Gronsky, "Sample Preparation of $YBa_2Cu_3O_{7-d}$ for High Resolution Electron Microscopy," J. Superconductivity (in press); LBL-24614.
72. H.W. Zandbergen, R. Gronsky, K. Wang, and G. Thomas, "On the Structure of $(CuO)_2$ Double Layers in Superconducting $YBa_2Cu_3O_7$," submitted to Nature; LBL-24671.
73. H.W. Zandbergen and G. Thomas, "Grain Boundaries in Sintered $YBa_2Cu_3O_{7-\delta}$," submitted to Acta Crystallogr. B; LBL-24603.

Invited Talks

74. D.A. Ackland and K.H. Westmacott, "Current Performance and Capabilities of the NCEM 1.5 MeV HVEM," XIIth Western Regional Meeting for Electron Microscopy and Microbeam Analysis, Concord, CA, June 24–27, 1987.
75. U. Dahmen, "The Accommodation of Precipitate Plates Modelled as a Tensile Test," Meeting on Phase Transformations '87, Cambridge, England, July 1987.
76. U. Dahmen, "Microstructural Evolution During the Decomposition of $Mg(OH)_2$," Symposium on Chemistry on the Electron Microscope, Wickenburg, AZ, Jan. 1987.
77. U. Dahmen, "Morphological Analysis of Phase Transformations by TEM," Case Western Reserve University, Cleveland, OH, Mar. 1987.
78. U. Dahmen, "The Symmetry Within—Crystallography of Microstructures Observed by TEM," Raychem Corp., Menlo Park, CA, Dec. 1987.
79. U. Dahmen, "The Use of Symmetry in the TEM Analysis of Precipitates," IBM, Yorktown Heights, NY, July 1987.
80. U. Dahmen, "The Use of Symmetry in the TEM Analysis of Precipitate Morphologies," Stanford Annual Symposium on Applications of Contemporary Electron Microscopy, Stanford, CA, Feb. 18, 1987.
81. C.J. Echer, "Capabilities and Applications of the AEM Facility at NCEM," XIIth Western Regional Meeting for Electron Microscopy and Microbeam Analysis, Concord, CA, June 24–27, 1987.
82. R. Gronsky, "Atomic Resolution Microscopy," Centennial Technology Seminar on Physical Metallurgy, Alcoa Laboratories, Brewster, MA, Aug. 23–28, 1987.
83. R. Gronsky, "High Resolution Electron Microscopy of the Solid-Solid Interface," 34th National Symposium and Topical Conference of the American Vacuum Society, Anaheim, CA, Nov. 2–6, 1987.
84. R. Gronsky, "High Resolution Transmission Electron Microscopy," Conference on Emerging Technologies in Materials, U.S. Navy, Minneapolis, MN, Aug. 18–20, 1987.
85. R. Gronsky, "Structure and Strain Determination in the High Resolution Electron Microscope," TMS Fall Meeting, Cincinnati, OH, Oct. 10–16, 1987.
86. K.M. Krishnan, "Novel Graphites in the BCN System: Characterization by Electron Energy Loss Spectroscopy," XIIth Western Regional Meeting for Electron Microscopy and Microbeam Analysis, Concord, CA, June 24–27, 1987.
87. C. Nelson, "A Technical Perspective of the Berkeley ARM," XIIth Western Regional Meeting for Electron Microscopy and Microbeam Analysis, Concord, CA, June 24–27, 1987.

88. M.A. O'Keefe and R. Kilaas, "HREM Image Analysis at the HVEM," XIIth Western Regional Meeting for Electron Microscopy and Microbeam Analysis, Concord, CA, June 24–27, 1987.
89. M.L. Sattler, W.J. Smith, and R. Gronsky, "Microstructural Changes across the Cross-Section of Rapidly Solidified Ribbon Alloys," XIIth Western Regional Meeting for Electron Microscopy and Microbeam Analysis, Concord, CA, June 24–27, 1987.
90. G. Thomas and V. Radmilovic, "Atomic Resolution in Al-Li-Cu Alloys," 4th International Al-Li Conference, Paris, France, June 10–12, 1987; session chairman on Fracture.
91. G. Thomas, "HREM for Materials Research," Materials Research Laboratories, Hsinchu, Republic of China, July 1987.
92. G. Thomas, "Materials Characterization by Modern Electron Microscopy," U.S.-Japan Seminar on Electron Microscopy, Honolulu, HI, Sept. 7–12, 1987.
93. G. Thomas, "Electron Microscopy Characterization of Inorganic Materials," SST/MRI Seminar, IBM Corp., Almaden Research Center, San Jose, CA, Sept. 29, 1987.
94. G. Thomas, "High Resolution Studies of TMT Al-Li Based Alloys," Joint ASM/TMS (AIME) Fall Meeting, Symposium on Hard and Soft Magnetic Properties of Rare Earth Magnetics, Cincinnati, OH, Oct. 12, 1987.
95. G. Thomas, "Impact of Electron Microscopy in Materials Science," Keynote Speaker, XVI SIME Conference on Electron Microscopy, Bologna, Italy, Oct. 14–17, 1987.
96. K.H. Westmacott, "HVEM In-situ Studies of Crack Propagation in Ceramics," University of California Berkeley/Grandes Ecoles Comité Mixte Meeting, Grenoble, France, May 21, 1987.
97. K.H. Westmacott, "What Factors Determine Precipitate Morphology in Al-Ge and Al-Si Alloys?" Phase Transformations '87, Cambridge, England, July 8, 1987.
98. K.H. Westmacott, "High Voltage Electron Microscopy at the National Center for Electron Microscopy," Dedication of the Caltech Materials Research Group Laboratories, Pasadena, CA, May 28, 1987.
99. K.H. Westmacott, "Precipitation Mechanisms," École Nationale Superièure des Mines de Saint-Etienne, France, June 23, 1987.

In Situ Investigation of Gas-Solid Reactions by Electron Microscopy*

James W. Evans, Investigator

INTRODUCTION

This work is concerned with the microstructural changes resulting from gas-solid reactions. Of particular interest is the nucleation and growth of the solid products from the parent phase. The experimental tools used in this investigation are the environmental cells that are placed in the two high-voltage transmission electron microscopes at LBL. These cells enable a solid to be contacted with a gas at elevated temperatures without adversely affecting the vacuum in the microscope column. The evolution of the microstructure as the reaction proceeds can then be observed at high magnification. In addition, the new solid phases that are forming can immediately be identified from the electron diffraction pattern as these phases form. Conventional transmission electron microscopy of cross sectioned reacted samples is used to obtain additional information on the morphology and chemistry of phases occurring at the reaction front. Auxiliary techniques such as secondary-ion mass spectroscopy (SIMS) also play a role in this investigation.

The focus of this investigation is now on the oxidation of III-V compound semiconductor materials, particularly gallium arsenide and indium phosphide. Oxidation is a well-established technique in the processing of silicon, the most widely used semiconductor material; dielectric layers can readily be formed on silicon in this way. This straightforward method of producing dielectric layers has so far eluded the processors of III-V compound semiconductors. An objective of this research is to determine whether conditions can be found for the formation of oxide layers of suitable morphology on III-V compounds.

*This work was supported by the Director, Office of Energy Research, Office of Basic Energy Sciences, Materials Sciences Division of the U.S. Department of Energy under Contract No. DE-AC03-76SF00098.

1. Oxidation of III-V Compound Semiconductor Materials (Publications 2 and 3)

O.R. Monteiro and J.W. Evans

The thermal oxidation of two important III-V compound semiconductor materials, GaAs and InP, between 300 and 600°C has been studied. *In situ* transmission electron microscopy (TEM), cross-sectional TEM (XTEM), and SIMS analyses were used to characterize the reaction products. The first technique allows observation of the reactions at the very moment they are occurring. XTEM provides a clearer picture of the distribution of phases in the oxidized samples. SIMS provides information on dopant distribution after oxidation as well as on enrichment of the group V element at the oxide-semiconductor interface.

At temperatures below 400°C, both compounds produced amorphous oxides. *In situ* experiments at higher temperatures allowed the oxidation of GaAs to be followed and revealed the occurrence of an

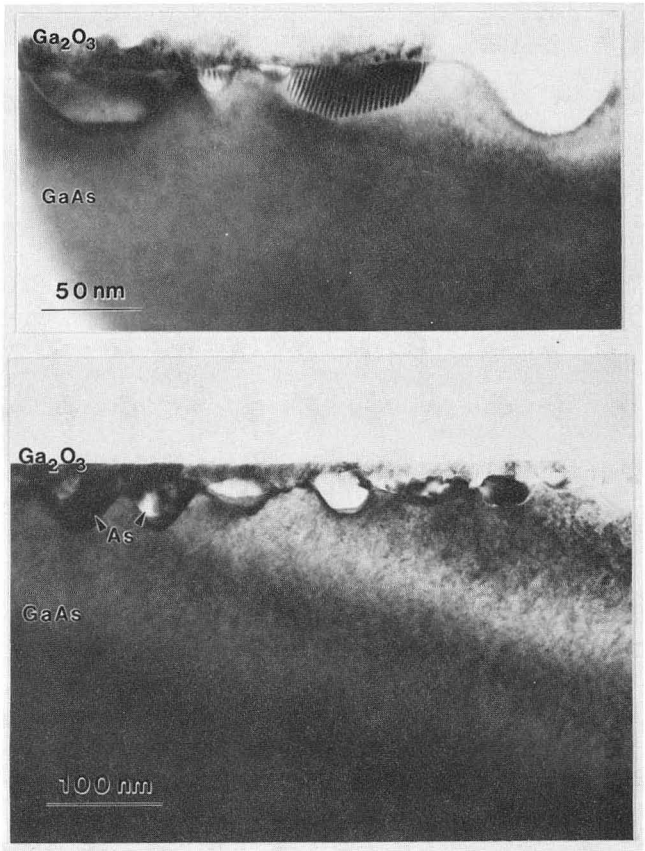

Figure 1-1. Cross-section micrographs of tellurium-doped GaAs oxidized for 2 hours at 600°C (top) and 500°C (bottom). Note Moire fringes occurring in As particles. [XBB 879-7467 (top); XBB 879-7480 (bottom)]

intermediate phase, α-Ga_2O_3, which grows epitaxially on the parent GaAs prior to the final formation of polycrystalline β-Ga_2O_3. Both phases are mixed with small quantities of arsenic oxides (As_2O_3 and As_2O_5). Arsenic enrichment at the oxide-semiconductor interface, which occurs during the reaction, leads to the precipitation of As at the interface, as can be seen in Figure 1-1.

In situ experiments on the oxidation of InP showed that between 400 and 600°C the reaction leads to the formation of $InPO_4$ and In_2O_3, with the former preceding the latter. The electron diffraction patterns show that $InPO_4$ forms with a specific orientation relationship to the parent InP. The orientation relationships are illustrated in Figure 1-2. The four possible positions of the $InPO_4$ lattice (open squares) are at measured angles of 11.7° to the host InP lattice. The O-lattice theory predicts four possible positions with an angle of 9.9° between the lattices. This is thought to represent reasonable agreement between theory and experiment.

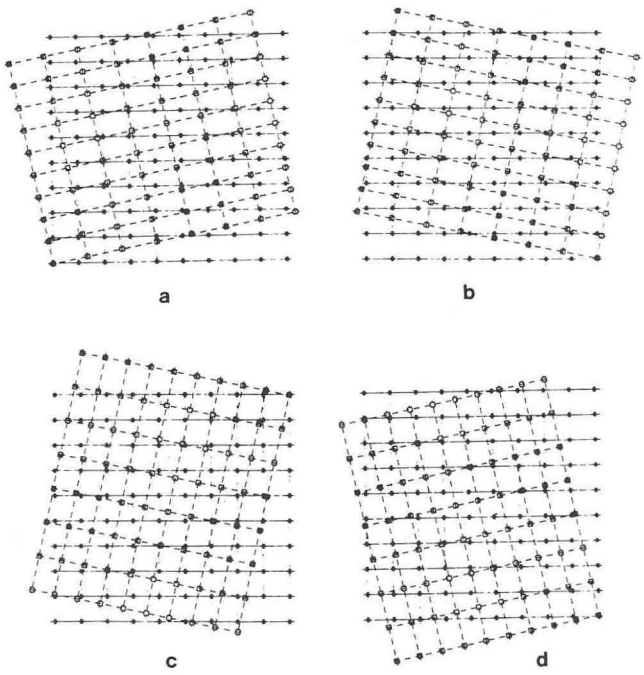

Figure 1-2. Four possible variants of the orientation relationship between epitaxial $InPO_4$ formed by oxidation of InP as determined from *in situ* electron diffraction patterns. (XBL 8712-5310)

2. Work in Progress

Preliminary experiments have been carried out on the reaction of silicon with tungsten hexafluoride (used in depositing tungsten films on silicon during semiconductor processing) and on the oxidation of high-T_c superconductor materials.

1987 PUBLICATIONS AND REPORTS

Refereed Journals

1. M-F. Rau, D. Rieck, and J.W. Evans, "Investigation of Iron Oxide Reduction by TEM," Metall. Trans. **18B**, 257 (1987); LBL-22108.

Other Publications

2. O.R. Monteiro and J.W. Evans, "Thermal Oxidation of III-V Compounds," in *Proc. 172nd Meeting Electrochem. Soc.*, Honolulu, HI, Oct. 1987; LBL-24459.

LBL Reports

3. O.R. Monteiro and J.W. Evans, "Thermal Oxidation of Indium Phosphide," LBL-23467.

Local Atomic Configurations in Solid Solutions*

Didier de Fontaine, Investigator

INTRODUCTION

This investigation is concerned with ordering phenomena in alloys, and the recent emphasis has been on long-period ordered superstructures (modulated structures) in binary fcc alloys. Two systems are currently under study: Cu-Pd and $CePd_3$. Detailed structural observations on the Cu-Pd system have been carried out using the Atomic Resolution Microscope at LBL's National Center for Electron Microscopy (NCEM), and the nature of the periodic antiphase boundaries present in this alloy has been characterized. In addition, a systematic investigation of long and short range order in Cu-Pd has begun using *in situ* variation of temperature and radiation dose in the high-voltage electron microscope at NCEM. Other work on the Cu-Pd system, using standard electron microscopy techniques, is directed toward clarification of the equilibrium phase diagram. Concerning the theoretical aspect of this project, a statistical mechanics model for modulated structures in alloys has been proposed and solved within the mean-field approximation. Results show agreement with some real systems.

Studies of the $CePd_3$ system have just begun in an effort to discover if atomic ordering effects, such as the modulated ordered structures observed at other compositions, are responsible for anomalous resistivity measurements reported in this system.

1. Cu_3Pd Observed by High-Voltage Electron Microscopy (Publication 3)

J. Kulik, S. Takeda,† and D. de Fontaine

Cu-Pd samples of compositions varying from 16 to 26 at% Pd were irradiated *in situ* in a 1.5-MeV electron microscope at various temperatures. Low-temperature (90 K) irradiation produced completely disordered solid solutions. Irradiation at room temperature up to as high as about 500 K produced steady-state short-range order (SRO), which, for specimens of 18% or more Pd, is characterized by diffuse intensity at $[1, \pm q, 0]$ and equivalent positions in reciprocal space (modulated SRO). In general, q is a function of composition, temperature, and irradiation dose. High-temperature irradiation tended to produce the expected equilibrium long-range order — either $L1_2$ or a long-period superstructure, depending on composition and temperature. The 18 and 20% samples irradiated at room temperature exhibited steady-state modulated SRO even though the expected equilibrium structure is one of unmodulated order ($L1_2$). It is suggested that spinodal ordering is responsible for this latter effect. An fcc-based Cu-Pd phase diagram is proposed incorporating ordering stability loci and a mestastable Lifshitz point.

*This work was supported by the Director, Office of Energy Research, Office of Basic Energy Sciences, Materials Sciences Division of the U.S. Department of Energy under Contract No. DE-AC03-76SF00098.

†Present address: Department of Physics, College of General Education, Osaka University, Toyonaka, Osaka 560, Japan.

2. One-Dimensional Long-Period Superstructures in Cu_3Pd Observed by High-Resolution Electron Microscopy (Publication 6)

S. Takeda,† J. Kulik, and D. de Fontaine

One-dimensional long-period superstructures (LPS) in Cu_3Pd have been studied by electron diffraction and high-voltage, high-resolution electron microscopy. Use of a high accelerating potential (800 to 1000 kV) for the electron microscope has resulted in micrographs showing well-defined antiphase boundaries. Boundaries contain frequent jogs in specimens of low Pd content (see Figure 2-1).

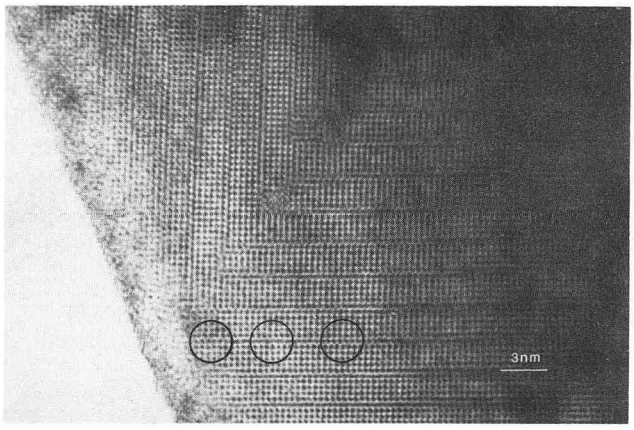

Figure 2-1. A Cu-22 at% Pd alloy annealed at 448°C shows sharp, well-defined antiphase boundaries. Occasional jogs in the boundaries are revealed in this image from the Atomic Resolution Microscope at LBL, as indicated by the circles. (XBB 862-1329)

These observations contrast with previous electron microscopy studies, which failed to resolve sharp boundaries presumably because of dynamical diffraction effects of lower-energy (200 kV) electrons.

---

†Present address: Department of Physics, College of General Education, Osaka University, Toyonaka, Osaka 560, Japan.

3. Mean-Field Theory of Long-Period Superstructures on the fcc Lattice (Publication 5)

J. Kulik and D. de Fontaine

An Ising model with long-range competing interactions on the fcc lattice is examined by mean-field theory. The competition of the interaction parameters is characterized by a parameter k, and a phase diagram in the (T, k) plane is presented. Long-period superstructures are obtained as ordered states. Results are compared with the ordered structures observed in Ag_3Mg.

4. Work in Progress

Investigation of *in situ* evolution of short-range order in Cu-Pd using high-voltage electron microscopy is continuing. Recent experiments have confirmed that the change of the diffraction pattern with irradiation dose is not a consequence of a local beam-induced composition change but appears to be the natural evolution of the (nonequilibrium) short-range order as a consequence of irradiation-enchanced kinetics. The temperature dependence of the evolution is currently being studied. The future should also see further investigation of the behavior of long-range order under irradiation.

Conventional electron-microscopy techniques are currently being used to refine the equilibrium phase diagram of Cu-Pd. Also, equilibrium studies on $CePd_3$ have just begun in order to determine whether this alloy system exhibits modulated structures since reports of electrical-resistivity anomalies have caused speculation about modulated order being the possible origin of these anomalies. Detailed structural information about this alloy is not available in the literature at present.

1987 PUBLICATIONS AND REPORTS

Refereed Journals

1. J. Kulik, S. Takeda, and D. de Fontaine, "Long Period Superstructures in Ag_3Mg," Acta Metall. **35**, 1137 (1987); LBL-21610.
2. S. Takeda, J. Kulik, and D. de Fontaine, "Spinodal Ordering Beyond the Lifshitz Point in Cu_3Pd Observed by High-Voltage Electron Microscopy," Acta Metall. **35**, 2243 (1987); LBL-22035.

Other Publications

3. J. Kulik, S. Takeda, and D. de Fontaine, "Cu_3Pd Observed by High-Voltage Electron Microscopy," in *Proc. Workshop Competing Interactions and Microstructures: Statics and Dynamics*, Center for Materials Science, Los Alamos, NM, May 5–8, 1987, Springer-Verlag; LBL-23757.
4. J. Kulik, K.B. Do, and D. de Fontaine, "Long Period Superlattices in an FCC Ising Model," abstract for TMS-AIME meeting, Denver, CO, Feb. 24, 1987.

LBL Reports

5. J. Kulik and D. de Fontaine, "Mean Field Theory of Long Period Superstructures on the FCC Lattice," submitted to J. Phys. C; LBL-24264.
6. S. Takeda, J. Kulik, and D. de Fontaine, "One-Dimensional Long Period Superstructures in Cu_3Pd Observed by High Resolution Electron Microscopy," accepted by J. Phys. F; LBL-24132.

Invited Talks

7. J. Kulik, "Cu_3-Pd Observed by High-Voltage Electron Microscopy," Los Alamos National Laboratory conference on "Competing Interactions in Microstructures: Statics and Dynamics," May 7, 1987.

Alloy Theory*

Didier de Fontaine and Leo M. Falicov, Investigators

INTRODUCTION

Temperature-composition phase diagrams are of great practical interest as they constitute useful "maps" of thermodynamic systems such as binary, ternary,..., alloys. These diagrams are generally determined experimentally, but the exciting possibility now exists of deriving certain classes of phase diagrams virtually from first principles. This possibility rests on the very significant advances that have been made recently in the two relevant areas of alloy theory — electronic-band-structure calculations and statistical thermodynamics. The purpose of this project is to combine the latest electronic structure and statistical thermodynamic calculations in integrated packages in order to produce phase diagrams from a minimum amount of empirical information and to compare with one another various approximate computational methods. A temperature-composition diagram for the Ti-Rh system has been derived that agrees remarkably well with that determined empirically. The same theoretical techniques are also being applied successfully to vacancy ordering in the high-T_c superconductors. It has also been proved that for some systems, and probably for many, inclusion of many-body effects beyond the mean-field or density-functional approximations should be taken carefully into account.

1. Tight Binding Calculation of Ti-Rh-Type Phase Diagram (Publication 14)

M. Sluiter, P. Turchi,† F. Zezhong,‡ and D. de Fontaine

Canonical tight binding electronic-band-structure calculations were combined with a cluster-variation configurational free energy, the effective-pair interaction parameters of which were evaluated by the generalized perturbation method. Only d-orbitals were included, and the numbers of d electrons per atom were taken to be 3 for the pure A element and 8 for pure B. A phase diagram was constructed incorporating, for the first time, both fcc and bcc lattices and their simple ordered superstructures (see Figure 1-1). The calculated diagram agreed reasonably well with those determined empirically for Ti-Rh or Ti-Ir. This work was given the award for Outstanding Scientific Accomplishments in Metallurgy and Ceramics by the U.S. Department of Energy.

*This work was supported by the Director, Office of Energy Research, Office of Basic Energy Sciences, Materials Sciences Division of the U.S. Department of Energy under Contract No. DE-AC03-76SF00098.

†Present address: Department of Materials Sciences, Lawrence Livermore National Laboratory, Livermore, CA 94550.

‡Present address: California Institute of Technology, Pasadena, CA 91125.

2. Stability Analysis of Special-Point Ordering in the Basal Plane in $YBa_2Cu_2O_{7-d}$ (Publications 2 and 12)

D. de Fontaine, L.T. Wille, and S.C. Moss†

It is shown that the Cu-O basal plane of $YBa_2Cu_3O_{7-d}$ can undergo three types of ordering-wave instabilities at the k points <0,0>, <1/2,0>, or <1/2,1/2>, depending on the values of the effective-pair interactions between filled and empty oxygen sites. The <0,0> instability gives rise to the observed chains of oxygen atoms along either the a or the b axis of the crystals. The <1/2,0> and <1/2, 1/2> instabilities produce doubling and quadrupling of the unit cell, respectively. Ordered superstructures consisting of occupied and empty oxygen sites in the Cu-O basal plane of $YBa_2Cu_3O_z$ have been determined. Pairwise interactions

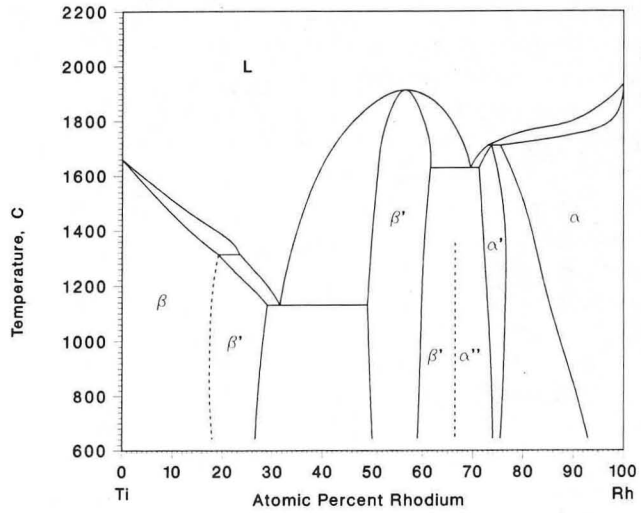

Figure 1-1. Phase diagram calculated with fitted free-energy curve for the liquid phase included. Phases are: L=liquid, α=fcc (disordered), α'=$L1_2$, β'=B2, α''=$L1_0$ (metastable). (XBL 875-2293).

(V_1,V_2,V_3) between nearest and next-nearest neighbor sites are assumed, and ordering maps are plotted as a function of V_2/V_1 and V_3/V_1 (in the ordering case: $V_1 > 0$) (see Figure 2-1). The ground state of this Ising model is determined by a direct enumeration method. The predicted <1/2,0> instability and z = 6.5 have since been confirmed by x-ray and electron diffraction and microscopy.

†Present address: Physics Department, University of Houston, Houston, TX 77004.

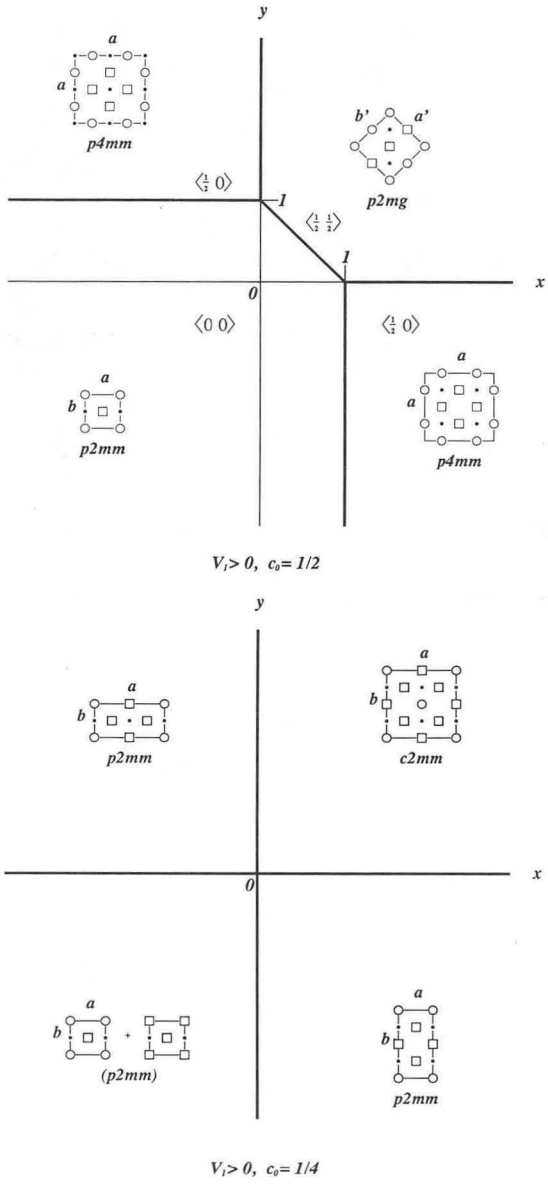

Figure 2-1. Ground states as a function of $x=V_2/V_1$, $y=V_3/V_1$, at oxygen concentration 0.50 (top); 0.25 (bottom). [XBL 878-3718 (top); XBL 878-3717 (bottom)]

3. Oxygen-Vacancy Ordering in the $YBa_2Cu_3O_z$ Basal Plane Studied by the Cluster Variation Method (Publication 11)

A. Berera,† L.T. Wille, and D. de Fontaine

The cluster variation method is used to calculate a phase diagram for a two-dimensional Ising model representing the Cu_2O plane of the high-T_c superconductor $YBa_2Cu_3O_z$. Both first- (V_1) and second-neighbor (V_2) interactions are considered, with $V_2/V_1 = -1/2$. At high temperatures, the transition from the disordered (tetragonal) to the ordered (orthorhombic) phase is second order. A tricritical point is found below which phase separation occurs. Fractional site occupancy and second-neighbor pair correlations are calculated as a function of temperature. The relevance of the model to the thermodynamics of ordering in the high-T_c compound is discussed.

†Present address: Department of Physics, University of California, Berkeley, CA 94720.

4. Many-Body Tetrahedral-Cluster Model for Binary and Ternary Alloys (Publication 3)

A. Reich and L.M. Falicov

An exact solution of a four-site tetrahedral crystal model with periodic boundary conditions, the smallest face-centered-cubic crystal, is presented in the case of binary and ternary alloy systems. The model consists of (a) a single s orbital per site with nearest-neighbor-only hopping, (b) a Coulomb repulsion between electrons on the same site, and (c) a single electron per atom. The model, which represents Cu, Ag, Au, and their alloys, shows all the segregational, solutional, and compound-forming tendencies of the real system. Such characteristics are absent in noninteracting independent-electron approaches. Calculations demonstrate extreme sensitivity to the input one-electron parameters, with minor differences resulting in widely different alloying properties.

5. Phase Stability of Ternary Alloys in the Four-Sublattice Bragg-Williams Approximation (Publication 4)

D.C. Chrzan and L.M. Falicov

A full Bragg-Williams calculation of a four-sublattice face-centered-cubic ternary alloy is presented. It corresponds to elements that, similarly to Cu, Ag, and Au, form disparate binaries: one pair that strongly segregates, one pair that forms strongly ordered compounds, and a third pair that forms only weakly ordered binaries. The obtained diagrams are internally consistent, have a sensible temperature evolution towards disorder, and present a variety of behaviors that include ordered and disordered homogeneous single phases, and regions of heterogeneous two- and three-phase mixtures. Although not realistic, the calculation gives a good starting point for more sophisticated models that may include short-range correlations and a better thermodynamic treatment.

6. Work in Progress

Much progress has been made in Prof. de Fontaine's group in developing a very general set of computer codes based on a completely new theoretical idea: that of computing effective pair interactions (EPI) for disordered alloys by direct configurational averaging in crystal space. Calculation of the band-structure energies is accomplished by the (real-space) recursion technique. Tight-binding electronic-structure parameters are obtained from the extensive tables recently calculated by D. Papacontantopoulos.

The partial ordering in the Cu-O basal plane of $YBa_2Cu_3O_z$ has been investigated as a function of oxygen content and temperature. A phase diagram is calculated by means of the cluster variation method applied to an asymmetric two-dimensional Ising model with interaction parameters so as to guarantee the stability of the experimentally observed double-cell structure around $z = 6.5$. The calculated transition temperatures at various oxygen partial pressures are in excellent agreement with experimental values determined very recently by a research group at the Oak Ridge National Laboratory. The pair probabilities along the Cu-O chains show a plateau with varying oxygen concentration, not unlike the reported dependence of T_c on oxygen content.

The understanding of the various phases of face-centered-cubic binary alloys with ordering structures (e.g., the copper-gold system) is being reexamined. Most of the forces in these phenomena are short range; the formation of antiphase boundaries and long-period superlattices, as well as their thermodynamic behavior, need further studies. The short-range order in these alloys is paramount; the frustration inherent in the face-centered-cubic lattices produces statistical mechanical effects that are being reexamined in great detail.

1987 PUBLICATIONS AND REPORTS

Refereed Journals

1. P. Turchi, M. Sluiter, and D. de Fontaine, "Prototype FCC Based Binary Alloy Phase Diagrams from Tight Binding Electronic Structure Calculations," Phys. Rev. B **36**, 3161 (1987).
2. D. de Fontaine, L.T. Wille, and S.C. Moss, "Stability Analysis of Special-Point Ordering in the Basal Plane of $YBa_2Cu_3O_{7-d}$," Phys. Rev. B: Rapid Commun. **36**, 5709 (1987); LBL-23878.
3. A. Reich and L.M. Falicov, "Many-Body Tetrahedral-Cluster Model for Binary and Ternary Alloys," Phys. Rev. B **36**, 3117 (1987); LBL-23174.
4. D.C. Chrzan and L.M. Falicov, "Phase Stability of Ternary Alloys in the Four-Sublattice Bragg-Williams Approximation," Phys. Rev. B **37**, 3894 (1988); LBL-24227.

Other Publications

5. D. de Fontaine, M. Sluiter, and P. Turchi, "First-Principles Theory of Order-Disorder Phase Equilibria," to be published in *Proc. Phase Transformations '87*, University of Cambridge, England.
6. D. de Fontaine, "Alloy Phase Stability," in *Electronic Band Structure and Its Applications*, Vol. 283 of Lecture Notes Series of Springer Verlag, Heidelberg, 1987, p. 410; LBL-22608.
7. P. Turchi, M. Sluiter, F. Zezhong, and D. de Fontaine, "Tight Binding Cluster Variation Calculations of Prototype FCC and BCC Based Binary Phase Diagrams," abstract, TMS-AIME, Denver, CO (in press).
8. M. Sluiter, P. Turchi, and D. de Fontaine, "Prediction of Ordering Tendencies in Alloys from a Simple Electronic Band Structure Model," abstract, TMS-AIME, Denver, CO (in press).
9. L.T. Wille, D. de Fontaine, and S.C. Moss, "Ordered Superstructures in the Basal Plane of $YBa_2Cu_3O_z$," in *Proc. TMS Topical Symposium, Materials of High Temperature Superconductors*, Cincinnati, OH, 1987.
10. A. Reich and L.M. Falicov, "Many-Body Tetrahedral-Cluster Model for Binary and Ternary Alloys," abstract, Annual Solid State Meeting, Danish Physical Society, Nyborg Denmark, May 22, 1987.

LBL Reports

11. A. Berera, L.T. Wille, and D. de Fontaine, "Oxygen-Vacancy Ordering in the $YBa_2Cu_3O_z$ Basal Plane Studied by the Cluster Variation Method," accepted by J. Stat. Phys.: Short Commun.; LBL-24261.
12. L.T. Wille and D. de Fontaine, "Ground State Analysis of Ordered Superstructures in the Basal Plane of $YBa_2Cu_3O_z$," accepted by Phys. Rev. B; LBL-23900.
13. L.T. Wille, A. Berera, D. de Fontaine, and S.C. Moss, "Vacancy Ordering in the Basal Plane of $YBa_2Cu_3O_z$," in *Proc. Mat. Res. Soc.* (in press); LBL-24263.
14. M. Sluiter, P. Turchi, F. Zezhong, and D. de Fontaine, "Tight Binding Calculations of Ti-Rh-Type Phase Diagram," Phys. Rev. Lett. (in press); LBL-23884.
15. D. de Fontaine, "Electronic Structure and Phase Stability of Alloys," in Materials Science Forum, *Proc. U.S.-Japan Seminar: "Electronic Structure and Lattice Defects in Alloys,"* May 4–7, 1987 (in press); LBL-24262.
16. D. de Fontaine, "Simple Models for the Omega Phase Transformation," Metall. Trans. (in press); LBL-21555.
17. E.C. Sowa and L.M. Falicov, "Many-Body Small Cluster Theory of bcc Fe, Co, and the FeCo Alloy," submitted to Phys. Rev. B; LBL-24124.

Invited Talks

18. D. de Fontaine, "Tight Binding Approach to Transition Metal Alloy Phase Diagrams," Naval Research Laboratory, Washington, D.C., Mar. 11, 1987.
19. D. de Fontaine, "Phase Diagrams from First Principles," Almaden Research Center, IBM San Jose, CA, Mar. 18, 1987.
20. D. de Fontaine, "Electronic Structure and Phase Stability," keynote lecture, U.S.-Japan Seminar on Electronic Structure and Lattice Defects in Alloys, University of Hawaii, Honolulu, May 4, 1987.
21. D. de Fontaine, "First-Principles Calculations of Binary Alloy Phase Diagrams," CALPHAD XVI, Irsee, Federal Republic of Germany, May 25, 1987.
22. D. de Fontaine, "Calculation of Binary Alloy Phase Equilibria," Max-Planck-Institute, Stuttgart, Federal Republic of Germany, May 29, 1987.
23. D. de Fontaine, "The Cluster Variation Method and the Calculation of Alloy Phase Diagrams," series of three lectures, NATO Advanced Study Institute on Alloy Phase Stability, Maleme, Crete, June 18, 1987.
24. D. de Fontaine, "First-Principles Theory of Order-Disorder Phase Equilibria," Phase Transformations '87 Conference, Cambridge, England, July 6, 1987.
25. A. Reich, "Many-Body Cluster Model for Binary and Ternary Alloys," H.C. Orsted Institute, University of Copenhagen, Denmark, April 8, 1987.
26. L.M. Falicov, "Binary and Ternary Alloys: A Many-Body Problem," Physics Department, Autonomous University of Madrid, Spain, April 27, 1987.
27. L.M. Falicov, "Many-Body Cluster Model for Binary and Ternary Noble-Metal Alloys," Physics Department, Technical University of Sweden, Stockholm, May 8, 1987.

MECHANICAL PROPERTIES

Environmentally Affected Crack Growth in Engineering Materials*

Robert O. Ritchie, Investigator

INTRODUCTION

The objective of this program is to examine, from both macroscopic and microscopic perspectives, the mechanics and micromechanisms of the subcritical growth of cracks. Primary studies are currently devoted to (i) the concept of crack-tip shielding in fracture and fatigue, where crack growth is impeded by mechanisms which locally reduce the "crack driving force"; (ii) brittle fracture by transgranular cleavage, where statistical models have been developed to predict fracture toughness behavior; (iii) variable-amplitude fatigue-crack propagation in titanium alloys, where both numerical and experimental studies have been used to determine the mechanistic sequence responsible for observed transient crack-growth behavior; (iv) fatigue in ceramics, where cyclic studies in transformation-toughened partially stabilized zirconia have resulted in the first reported evidence of fatigue crack propagation under tension-tension loading in ceramics; and (v) crack growth along ceramic/metal interfaces [in collaboration with Dr. R.M. Cannon of the Center for Advanced Materials (CAM)], where the roles of interface geometry and environment have been explicitly examined. The highlights of the past year have been the discovery that, contrary to traditional notions, ceramics can be very susceptible to fatigue failure under cyclic tension-tension loading, and that the fracture toughness and subcritical crack-growth resistance of glass/copper interfaces can be markedly enhanced through interface engineering, specifically by incorporating patterned arrays of interfacial microcrack-like voids, emplaced out of plane to the main crack.

*This work was supported by the Director, Office of Energy Research, Office of Basic Energy Sciences, Materials Science Division of the U.S. Department of Energy under Contract No. DE-AC03-76SF00098.

1. Crack-Tip Shielding in Fatigue (Publication 10)

R.O. Ritchie

Crack-tip shielding phenomena, whereby the "effective crack driving force" actually experienced at the crack tip is reduced compared to the far-field value, have been examined with reference to fatigue-crack propagation behavior in metals and ceramics. Sources of shielding have been analyzed in terms of mechanisms relying on the production of elastically constrained zones that envelop the crack (zone shielding), on the generation of wedging, bridging, or sliding forces between the crack surfaces (contact shielding), and on crack-path deflection and meandering (see Figures 1-1 and 1-2). These are applied to the problems of the fatigue behavior of high-strength lithium-containing aluminum alloys

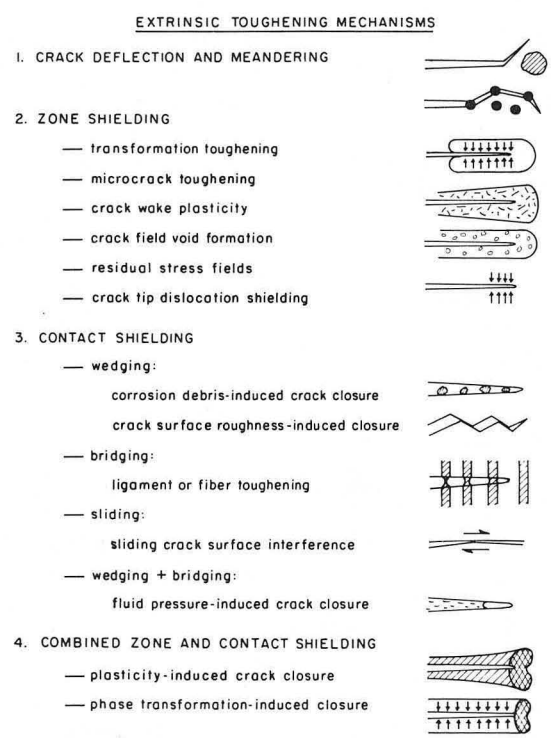

Figure 1-1. Schematic representation of the classes and mechanisms of crack-tip shielding. (XBL 861-7432)

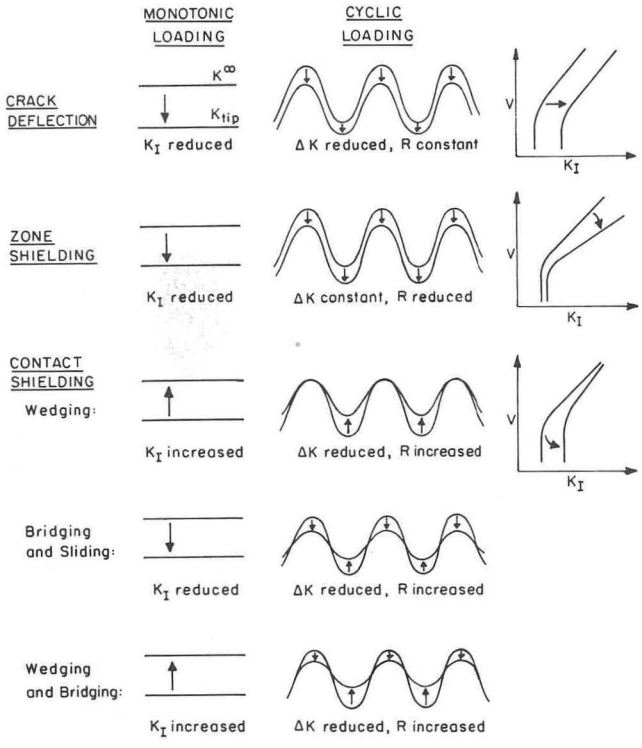

Figure 1-2. Effectiveness of the classes and mechanisms of crack-tip shielding shown in Figure 1-1 on the "crack driving force" (e.g., the stress intensity K) and the crack velocity (v), under monotonic and cyclic loading. (XBL 861-7433)

and the fracture and fatigue behavior of zirconia ceramics. It was found that, whereas crack-tip shielding can provide a potent means to enhance "resistance" to crack growth, such extrinsic toughening mechanisms can result in the apparently anomalous behavior of "small cracks" and the susceptibility of brittle materials to fatigue failure.

2. Statistical Modeling of Cleavage Fracture: Role of Sampling Volume (Publications 1 and 16)

T. Lin and R.O. Ritchie

Reported observations of an experimental variation in the microscopic fracture stress for transgranular cleavage (σ_f*) with specimen geometry and size have been quantitatively examined in terms of a recently proposed weakest-link statistical model for brittle fracture, wherein failure coincides with the critical propagation of a particle microcrack into the matrix (see Figure 2-1). By analyzing the onset of fracture in the "sharp-crack" (K_{Ic}) specimen, the "rounded-notch" (Charpy) specimen, and the uniaxial tensile specimen, it has been shown that values of σ_f* are reduced progressively in the "sharp-crack," notched, and unnotched geometries and with increasing specimen size, consistent with an increase in statistical sampling volume. Quantitative predictions for the magnitude of this variation were derived for a low-strength steel.

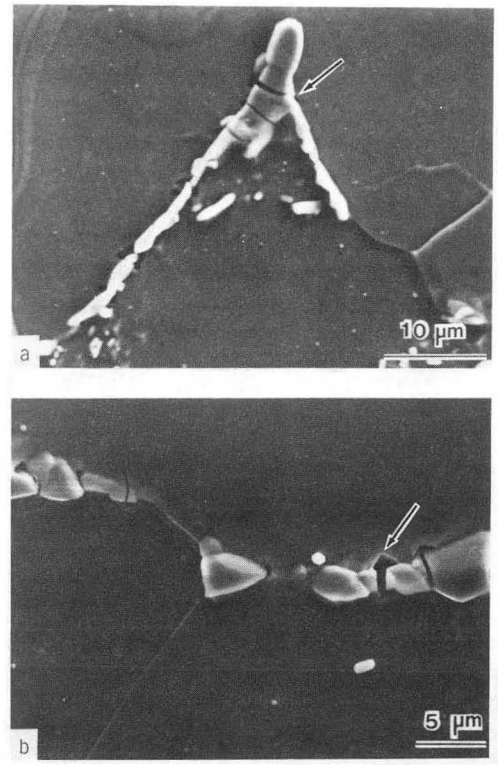

Figure 2-1. Scanning electron micrographs of particle microcracks in AISI 1008 microstructure at lower shelf temperatures. Microcracks are formed in grain-boundary carbides several grains ahead of the unbroken fatigue pre-crack (in a DEN specimen), just prior to the onset of catastrophic cleavage fracture at (a) −120°C, and (b) −100°C. Note how several carbide microcracks have become blunted at the higher temperature. (XBB 852-1105B)

3. Fatigue-Crack Propagation under Variable-Amplitude Loading in Titanium Alloys (Publications 15 and 18)

C.M. Ward-Close and R.O. Ritchie

An experimental and numerical study has been made of the mechanisms of fatigue-crack growth and crack-closure behavior in an α/β titanium alloy Ti-4Al-4Mo-2Sn-0.5Si (IMI 550), following both single and block tensile overloads (see Figure 3-1). Closure immediately behind the crack front (near-tip closure) was found to be the main factor controlling load-

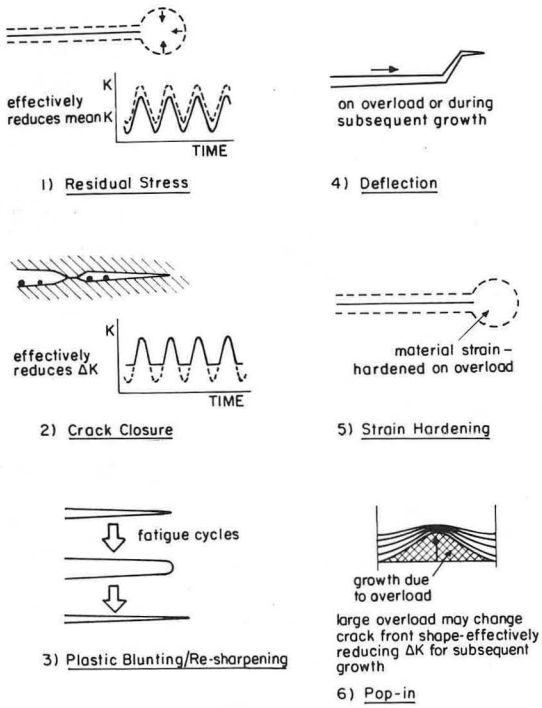

Figure 3-1. Schematic illustration of various proposed mechanisms to account for retardation following a tensile overload. (XBL 864-7618)

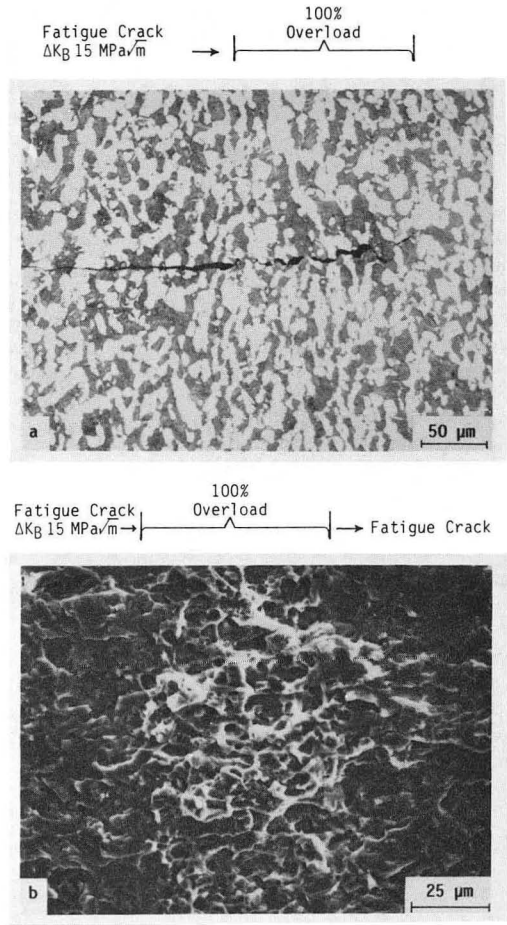

Figure 3-2. (a) Optical micrograph of the crack path profile, at center section, in an α/β-annealed microstructure following 100% tensile overload at ΔK_B = 15 MPa$\sqrt{m}$. Note blunting at the pre-overload crack tip, and asperity contact is in region where crack extension occurred at the overload. (b) Corresponding scanning electron micrograph of the fracture surface. (XBB 864-2939)

interaction effects. Single tensile overloads were found to remove near-tip closure and to slightly reduce far-field closure along the crack length, resulting in an initial acceleration in fatigue-crack growth rates. Subsequent delayed retardation of crack growth rates were accompanied by an increase in the near-tip closure load, due to the enlarged compressive residual stress in the overload plastic zone. High/low block overloads caused greater retardation than single overloads of the same magnitude, and this was attributed to changes in the degree of closure in the wake of the crack. Numerical predictions of such transient behavior, based on a modified Dudgale model, are found to be in close agreement with experimental results, both in terms of observed crack growth rates and crack-opening displacements. Load-interaction effects were found to be most severe when the baseline stress intensity range (ΔK) was close to the fatigue threshold (ΔK_{TH}), or when the overload maximum stress intensity (K_{max}) approached the fracture toughness of the material. At low ΔK levels, the magnitude of the delay was sensitive to microstructure (see Figure 3-2) and found to be enhanced in coarse-grained β-heat-treated microstructures compared to standard fine-grained α/β microstructures. Based on these results, mechanistic sequences are suggested to explain the transient fatigue-crack growth behavior following single and block tensile overload cycles.

4. Fatigue-Crack Propagation in Ceramics (Publication 4)

R.H. Dauskardt, W. Yu, and R.O. Ritchie

Fatigue-crack propagation under tension-tension loading has been observed in a transformation-toughened partially stabilized zirconia (PSZ) ceramic containing 9 mol% MgO. Such subcritical crack-growth behavior has been demonstrated for the first time to be cyclically induced, based on a comparison with behavior under sustained loading (at the maximum load in the fatigue cycle) and at varying cyclic frequencies. Crack-extension rates, measured as a function of the cyclic stress-intensity range ΔK over

the range 10^{-10} to 10^{-6} m/cycle, have been found to be load-ratio and environment dependent and to show evidence of fatigue-crack closure, similar to behavior in metals. Cyclic crack-growth rates are observed at ΔK levels as low as 3 MPa$\sqrt{m}$, and are typically many orders of magnitude faster than reported data on environmentally assisted subcritical crack growth in PSZ under monotonic loading conditions (see Figure 4-1). Such behavior has been rationalized in terms of both crack-tip shielding and fatigue "damage" mechanisms.

5. Subcritical Crack Growth along Ceramic/Metal Interfaces (Publication 5)

T.S. Oh, R.M. Cannon, and R.O. Ritchie

Environmentally assisted subcritical crack growth along glass/copper interfaces has been examined in ambient-temperature gas environments as a function of humidity. Resulting interfacial crack velocities (v), characterized in terms of the crack-extension force (G) and approximate solutions for the linear-elastic stress-intensity factor (K), were found to show v-K curve behavior typical of (bulk) ceramics (see Figure 5-1). Subcritical crack-growth rates were observed to be initially highly sensitive to K (or G) and to show evidence of a threshold stress intensity between 0.1 and 0.25 MPa$\sqrt{m}$ (Region I). At higher crack velocities, typically between $\sim 10^{-5}$ and 10^{-4} m/sec, growth rates displayed a plateau and tended to become K-independent (Region II). Although specimen-to-specimen scatter was large in Region I, interfacial crack velocities in moist environments far exceeded those in dry environments, a phenomenon associated with an environmentally induced weakening of interfacial bonds by adsorbing water molecules. In addition, interfacial growth rates were over 3 orders of magnitude faster (at fixed K) than reported rates for (bulk) soda-lime glass.

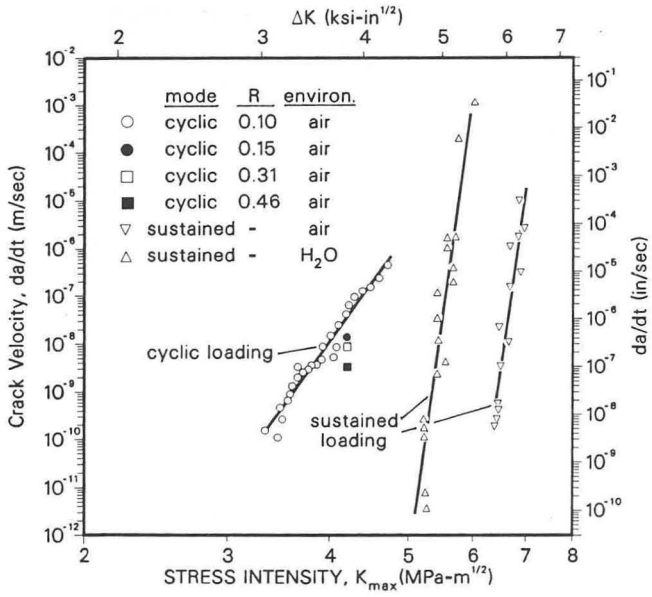

Figure 4-1. Subcritical crack-growth behavior in PSZ (MgO) showing a comparison of cyclic crack velocities, da/dt, from the present study with sustained-load cracking data of Becher for 55% relative humidity air and distilled water. Note how fatigue-induced crack growth is much faster than environmentally assisted crack growth under monotonic loading conditions. (XBL 873-1282)

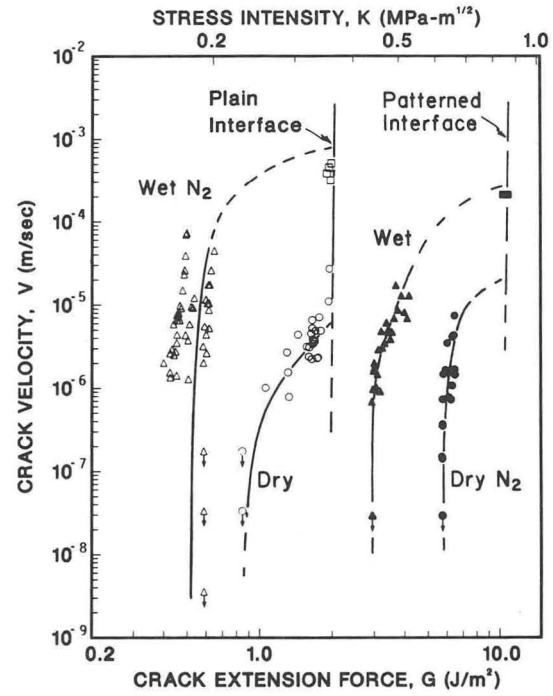

Figure 5-1. Variation in subcritical stress-corrosion crack-growth rates (da/dt) along plain and patterned (chemically etched) glass/copper interfaces as a function of the crack extension force (G) and approximate stress intensity (K) in wet and dry gaseous nitrogen environments. Note how the presence of controlled arrays of "microcracks/voids" near the interface results in far lower crack velocities and a 6- to 7-fold increase in the threshold fracture energy for interfacial crack growth. (XBL 8710-4144)

6. Toughening of Ceramic/Metal Interfaces using Controlled Interfacial Geometries (Publications 17 and 25)

T.S. Oh, J. Rödel, R.M. Cannon, and R.O. Ritchie

Toughening of ceramic/metal interfaces through the use of controlled interfacial geometries and non-coplanar microcrack-like pores was examined with respect to both critical and subcritical crack growth. Patterned uniform arrays of inclined interfacial steps and of "microcracks/voids" (with width 22 μm and spacing 10 μm), out of plane to the main interfacial crack, were produced for glass/copper interfaces by photolithographic techniques combined with evaporation and diffusion-bonding processes (see Figure 6-1). Significant toughening and improved stress corrosion crack-growth resistance was achieved through the promotion of crack-tip shielding primarily from crack bridging. Specifically, plastic void growth within the copper was seen to generate bridged ligaments of metal film between the glass substrates; the resulting mechanical crack bridging led to plastic stretching of the film and provided the dominant toughening mechanism, with a smaller contribution from crack deflection (see Figure 6-1). Correspondingly, subcritical (pre-instability) crack-growth rates with the patterned arrays in "wet" and "dry" gaseous atmospheres were found to be retarded by orders of magnitude compared to rates for plain interfaces (see Figure 5-1). The toughness with the various patterned interfaces was seen to exhibit marked resistance-curve (R-curve) behavior with fracture-toughness values increased by factors of 4 to 9 compared to intrinsic fracture toughness, G_o, values of $\sim$2 J/m^2 for these plain glass/copper interfaces. The surface roughness of the glass substrate was reasoned to be a controlling parameter for the shape and magnitude of such crack-resistance curves.

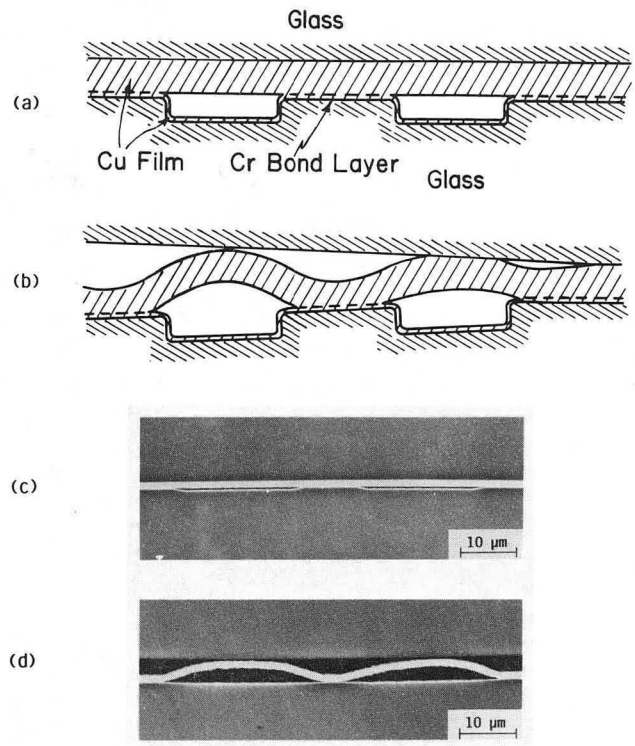

Figure 6-1. Schematic illustrations and scanning electron micrographs of interfacial "microcrack/void" geometry before (a and c) and after (b and d) crack growth for cracking along the plain side of the patterned region. Note how this configuration promotes shielding by crack bridging of plastically stretched ligaments of metal film. (XBB 8712-10272)

1987 PUBLICATIONS AND REPORTS

Refereed Journals

1. T. Lin, A.G. Evans, and R.O. Ritchie, "Stochastic Modelling of the Independent Roles of Particle Size and Grain Size in Transgranular Cleavage Fracture," Metall. Trans. A **18A**, 641 (1987); LBL-21393.
2. J.K. Shang, J.-L. Tzou, and R.O. Ritchie, "Role of Crack Tip Shielding in the Initiation and Growth of Long and Small Fatigue Cracks in Composite Microstructures," Metall. Trans. A **18A**, 1613 (1987); LBL-21895.
3. R.O. Ritchie, "A Comparison of Fatigue Crack Propagation in Modes I and III," in *Fracture Mechanics 18th Symposium*, ASTM STP 945, R.P. Read and D.T. Reed, Eds., American Society for Testing and Materials, Philadelphia, PA, 1987, p. 821; LBL-19828.
4. R.H. Dauskardt, W. Yu, and R.O. Ritchie, "Fatigue Crack Propagation in Transformation-Toughened Zirconia Ceramic," J. Am. Ceram. Soc. **70**, C248 (1987); LBL-23164.
5. T.S. Oh, R.M. Cannon, and R.O. Ritchie, "Subcritical Crack Growth along Ceramic-Metal Interfaces," J. Am. Ceram. Soc. **70**, C352 (1987); LBL-23311.†
6. R.W. Hertzberg, W.A. Herman, and R.O. Ritchie, "Use of a Constant K_{max} Test Procedure to Predict Small Crack Growth Behavior in 2090-T8E41 Aluminum-Lithium Alloy," Scripta Metall. **21**, 1541 (1987); LBL-24508.‡
7. R.H. Dauskardt, R.D. Pendse, and R.O. Ritchie, "Effects of Pre-Existing Grain Boundary Microvoid Distributions on Fracture Toughness and Fatigue Crack Growth in Low Alloy Steel," Acta Metall. **35**, 2227 (1987).§
8. W. Yu and R.O. Ritchie, "Fatigue Crack Propagation in 2090 Aluminum-Lithium Alloy: Effect of Compression Overload Cycles," J. Eng. Mater. Technol., Trans. ASME, Series H **109**, 81 (1987).‖

Other Publications

9. R.O. Ritchie, W. Yu, A.F. Blom, and D.K. Holm, "An Analysis of Crack Tip Shielding in Aluminum Alloy 2124: A Comparison of Large, Small, Through-Thickness and Surface Fatigue Cracks," in *Fatigue and Fracture of Engineering Materials and Structures* **10**, 343 (1987).[‖]
10. R.O. Ritchie, "Crack Tip Shielding in Fatigue," in *Mechanical Behaviour of Materials — V*, M.G. Yan, S.H. Zhang, and Z.M. Zheng, Eds., Pergamon Press, Oxford, U.K., 1987; LBL-22600.
11. J.K. Shang and R.O. Ritchie, "On the Development of Unusually High Fatigue Crack Propagation Resistance in Steels: Crack Tip Shielding in Duplex Microstructures," in *Mechanical Behaviour of Materials — V*, M.G. Yan, S.H. Zhang, and Z.M. Zheng, Eds., Pergamon Press, Oxford, U.K., 1987, p. 511; LBL-22350.
12. K.T.V. Rao, W. Yu, and R.O. Ritchie, "On the Role of Crack Tip Shielding in Influencing the Behavior of Long and Small Fatigue Cracks in Aluminum-Lithium Alloy 2090," in *Fatigue '87*, Proc. Third Int. Conf. on Fatigue and Fatigue Thresholds, Vol. 1, R.O. Ritchie and E.A. Starke, Eds., EMAS Ltd., Warley, U.K., 1987, p. 291; LBL-22842.[‡]
13. R.O. Ritchie, W.W. Gerberich, and J.H. Underwood, "Fracture and Fatigue," in *Encyclopedia of Physical Science and Technology*, Vol. 5, R.A. Meyers, Ed., Academic Press, San Diego, CA, 1987, p. 594; LBL-24521.
14. R.O. Ritchie and E.A. Starke, Eds., *Fatigue '87*, Proc. Third Int. Conf. on Fatigue and Fatigue Thresholds, Charlottesville, VA, June 1987, Vols. 1–4, EMAS Ltd., Warley, U.K., 1987.

LBL Reports

15. C.M. Ward-Close and R.O. Ritchie, "On the Role of Crack Closure Mechanisms in Influencing Fatigue Crack Growth Following Tensile Overloads in Titanium Alloys: Near-Threshold vs. Higher ΔK Behavior," in *Mechanisms of Fatigue Crack Closure*, ASTM STP 982, J.C. Newman, Jr., and W. Elber, Eds., American Society for Testing and Materials, Philadelphia, PA, 1988 (in press); LBL-21485.
16. T. Lin and R.O. Ritchie, "On the Effect of Sampling Volume on the Microscopic Cleavage Fracture Stress," Engineering Fracture Mechanics (1988) (in press); LBL-23466.
17. T.S. Oh, J. Rödel, R.M. Cannon, and R.O. Ritchie, "Ceramic/Metal Interfacial Crack Growth: Toughening by Controlled Microcracks and Interfacial Geometries," Acta Metall. (in press); LBL-24285.[†]
18. C.M. Ward-Close, A.F. Blom, and R.O. Ritchie, "Mechanisms Associated with Transient Fatigue Crack Growth during Variable-Amplitude Loading: An Experimental and Numerical Study," submitted to Engineering Fracture Mechanics; LBL-24267.
19. K.T.V. Rao, W. Yu, and R.O. Ritchie, "Fatigue Crack Propagation in Aluminum-Lithium Alloy 2090: Part I. Long Crack Behavior," Metall. Trans. A (in press); LBL-22178.[‡]
20. K.T.V. Rao, W. Yu, and R.O. Ritchie, "Fatigue Crack Propagation in Aluminum-Lithium Alloy 2090: Part II. Small Crack Behavior," Metall. Trans. A (in press); LBL-22179.[‡]
21. K.T.V. Rao and R.O. Ritchie, "Effect of Prolonged High-Temperature Exposure on the Fatigue and Fracture Behavior of Aluminum-Lithium Alloy 2090," Mater. Sci. Eng. (in press); LBL-23136.[‡]
22. K.T.V. Rao, W. Yu, and R.O. Ritchie, "On the Behavior of Small Fatigue Cracks in Commercial Aluminum-Lithium Alloys," Engineering Fracture Mechanics (in press); LBL-23680.[‡]
23. K.T.V. Rao, H.F. Hayashigatani, W. Yu, and R.O. Ritchie, "On the Fracture Toughness of Aluminum-Lithium Alloy 2090-T8E41 at Ambient and Cryogenic Temperatures," Scripta Metall. (in press); LBL-24081.[‡]
24. K.T.V. Rao and R.O. Ritchie, "Mechanisms for the Retardation of Fatigue Cracks Following Single Tensile Overloads: Behavior in Aluminum-Lithium Alloys," Acta Metall. (in press); LBL-24028.[‡]
25. T.S. Oh, J. Rödel, R.M. Cannon, A.M. Glaeser, and R.O. Ritchie, "Toughening of Ceramic/Metal Interfaces using Patterned Arrays of Near-interfacial Pores," submitted to J. Am. Ceram. Soc.; LBL-24407.[†]

Invited Talks

26. R.O. Ritchie, "Fatigue Crack Growth in Composite Microstructures," Workshop on Composites, University of California, Santa Barbara, Jan. 5–15, 1987.
27. R.O. Ritchie, "Modelling the Ductile-Brittle Transition," Workshop on Composites, University of California, Santa Barbara, Jan. 5–15, 1987.
28. R.O. Ritchie, "Mechanical Analysis of the Monostrut Heart Valve: Procedures for Life Prediction," Monostrut Valve Symposium, Society of Thoracic Surgeons, Dallas, TX, Jan. 23–26, 1987.
29. R.O. Ritchie, "Toughening Mechanisms in Metals, Ceramics, and Composites," Department of Mechanical Engineering, Clemson University, Clemson, SC, Feb. 13, 1987.
30. R.O. Ritchie, A.G. Evans, and T. Lin, "Statistical Analysis of Brittle Fracture in Steels: Local Models for Fracture Toughness Behavior," Symposium of Role of Crack Tip Plasticity on Brittle Fracture, 1987 TMS Annual Meeting, Denver, CO, Feb. 23–26, 1987.
31. K.T.V. Rao and R.O. Ritchie, "Near-Threshold Behavior of Long and Small Fatigue Cracks in 2090 Aluminum-Lithium Alloy: Role of Load Ratio," Symposium on Effect of Load and Thermal Excursions on the Mechanical Behavior of Materials, 1987 TMS Annual Meeting, Denver, CO, Feb. 23–26, 1987.
32. R.O. Ritchie, "Crack-Tip Fields," Department of Materials Science and Mineral Engineering, University of California Berkeley, Mar. 1987.

33. K.T.V. Rao, W. Yu, and R.O. Ritchie, "Fatigue Crack Propagation of Commercial Aluminum-Lithium Alloys," ASM Aluminum-Lithium Symposium, WESTEC '87, Los Angeles, CA, Mar. 25, 1987.
34. R.O. Ritchie, "Design of Steels with Duplex Microstructures for Optimum Fatigue Resistance," Symposium on High Performance Steels, WESTEC '87, Los Angeles, CA, Mar. 25, 1987.
35. R.O. Ritchie, "Fatigue Failures," ASM Course on Principles of Failure Analysis, Pleasanton, CA, Mar. 1987; Oakland, CA, Apr. 1987.
36. R.O. Ritchie, "Physical Modelling of Cleavage Fracture and the Ductile Brittle Transition," Los Alamos National Laboratory, Los Alamos, NM, Apr. 2, 1987.
37. R.O. Ritchie, "Analysis of Life Prediction in Prosthesis Heart Valves," Shiley, Inc., Chicago, IL, Apr. 14, 1987.
38. R.O. Ritchie, "Crack-Tip Shielding," 1987 Materials Research Center Research Review, Lehigh University, Bethlehem, PA, Apr. 7, 1987.
39. R.O. Ritchie, "Statistical Fracture Mechanics," Department of Metallic Materials Engineering, Shaanxi Institute of Mechanical Engineering, Xi'an, People's Republic of China, May 1987.
40. R.O. Ritchie, "Crack-Growth Behavior of Metals and Ceramics," Northwestern Polytechnical University, Xi'an, People's Republic of China, May 1987.
41. R.O. Ritchie, "Recent Studies on the Mechanics and Mechanisms of Subcritical Crack Propagation in Materials," Research Institute for Strength of Metals, Xi'an Jiaotong University, Xi'an, People's Republic of China, May 1987.
42. R.O. Ritchie, "Statistical Models for the Ductile-Brittle Transition," Department of Mechanical Engineering, Tsinghua University, Beijing, People's Republic of China, June 1987.
43. R.O. Ritchie, "Crack-Tip Shielding in Fracture and Fatigue," Fifth International Conference on the Mechanical Behavior of Materials (ICM-5), Beijing, People's Republic of China, June 12, 1987.
44. R.O. Ritchie and R.J. Bucci, "Growth of Small Cracks," ALCOA Centennial Meeting on Mechanics, Hilton Head, SC, June 1987.
45. R.O. Ritchie, "Micromechanical Modelling of Crack Initiation and Crack Growth: Fracture Mechanics and Microstructural Aspects," 20th National Symposium on Fracture Mechanics, Lehigh University, Bethlehem, PA, June 23, 1987.
46. R.O. Ritchie, "Near-Threshold Fatigue and Small Cracks," Third International Conference on Fatigue and Fatigue Thresholds, University of Virginia, Charlottesville, June 1987.
47. R.O. Ritchie, "Micromechanisms of Fracture and the Stochastic Modelling of the Lower Shelf and the Ductile-Brittle Transition," National Bureau of Standards/Materials Property Council Workshop on "Understanding Scatter of Fracture Toughness Data in the Transition Temperature Regime," Boulder, CO, July 1987.
48. R.O. Ritchie, "Fatigue: Mechanisms of Crack Growth," Department of Energy Workshop on "Mechanics and Physics of Crack Growth: Application to Life Prediction," Keystone, CO, Aug. 3–7, 1987.
49. R.O. Ritchie, "Fatigue and Fracture Mechanics of Advanced Materials," Grumman Aerospace Co., Plainview, NY, Sept. 1987.
50. R.O. Ritchie, "Crack-Tip Shielding: A Metallurgist's Perception," Case Western Reserve University, Cleveland, OH, Sept. 15, 1987.
51. R.O. Ritchie, "Toughening Mechanisms in New Materials," Detroit Section, The Metallurgical Society of AIME, Detroit, MI, Oct. 5, 1987.
52. R.O. Ritchie, "Statistics of Fracture," Department of Materials Science and Engineering, University of Michigan, Ann Arbor, Oct. 1987.
53. R.O. Ritchie, "Threshold Fatigue Behavior of Long and Short Cracks," ASM Symposium on Fracture at the ASM Materials Congress, Cincinnati, OH, Oct. 10, 1987.
54. T.S. Oh, R.M. Cannon, and R.O. Ritchie, "Subcritical Crack Growth along Ceramic-Metal Interfaces," Symposium on Metal-Matrix Composites, TMS-AIME Fall Meeting, Cincinnati, OH, Oct. 14, 1987.
55. R.O. Ritchie, "Crack-Tip Shielding and its Relevance to the Fracture Properties of Advanced Materials," General Electric Co., Engine Group, Evandale, OH, Oct. 1987.
56. R.O. Ritchie, "Fatigue Crack Propagation in ARALL Laminates: Models and Experiments," Alcoa Conference on ARALL Laminates, Seven Springs, PA, Oct. 26, 1987.
57. R.H. Dauskardt and R.O. Ritchie, "Fatigue of Ceramics," ASTM E-9 Committee on Fatigue, ASTM Fall Meeting, Orlando, FL, Nov. 1987.
58. R.O. Ritchie, "Damage-Tolerant Life Prediction Procedures for Heart Valve Prostheses," St. Jude Medical, Inc., St. Paul, MN, Nov. 1987.

---

†Work in collaboration with Dr. R.M. Cannon, who is funded through the Center for Advanced Materials (CAM) by the Director, Office of Energy Research, Office of Basic Energy Sciences, Materials Sciences Division of the U.S. Department of Energy under Contract No. DE-AC03-76SF000981.

‡Work supported through CAM.

§Work supported by the Advanced Research and Development, Fossil Energy Materials Program, U.S. Department of Energy, through Subcontract 19X-27429C with Oak Ridge National Laboratory under Martin-Marietta Contract No. DE-AC05-84OR21400.

‖Work supported by the Air Force Office of Scientific Research under Grant No. AFOSR-82-0181.

PHYSICAL PROPERTIES

High-Temperature Reactions*

Alan W. Searcy, Investigator

INTRODUCTION

The central purposes of this program are to develop and to experimentally test thermodynamic and kinetic models of important processes in materials science. A theoretical breakthrough has been the reconciliation of the kinetics to the thermodynamics of equilibria among edge, surface, and bulk molecules in crystalline particles. The new understanding of the thermodynamics in particles makes it possible to evaluate the previously neglected roles of ledge nucleation and growth in sintering of crystalline particles and in exaggerated grain growth. New expressions for sintering and grain growth are consistent with important experimental observations that are inconsistent with predictions of classical surface thermodynamic theory. A theory for sintering in temperature gradients has been obtained as a consequence of extending the new thermodynamic approach to nonisothermal systems. Tests of various theoretical predictions are in progress.

1. The Influence of Temperature Gradients on Sintering: Experimental Tests of a Theory (Publication 12)

D. Beruto,† R. Botter,‡ and A.W. Searcy

Temperature gradients have not been thought to influence densification by condensed phase or surface diffusion. But theoretical considerations of the kind summarized in Abstract 3 led to the prediction that thermal gradients can do so.[1]

In this study the H_2O-catalyzed sintering of MgO in temperature gradients between 1303 K and 1233 K is compared to sintering of isothermal samples. Figure 1-1 shows that sample dimensions in planes normal to the temperature gradients are greater than predicted on the assumption that sintering is a function only of each local temperature in the gradient. Figure 1-2 shows the densities measured for 1-mm sections of a sample heated two hours at a uniform temperature of 1303 ± 2 K. The band on Figure 1-3 shows the range of measured densities expected if a specimen held in a linear gradient densified like an isothermal sample at each local temperature. The measured densities (data points) all lie above the band.

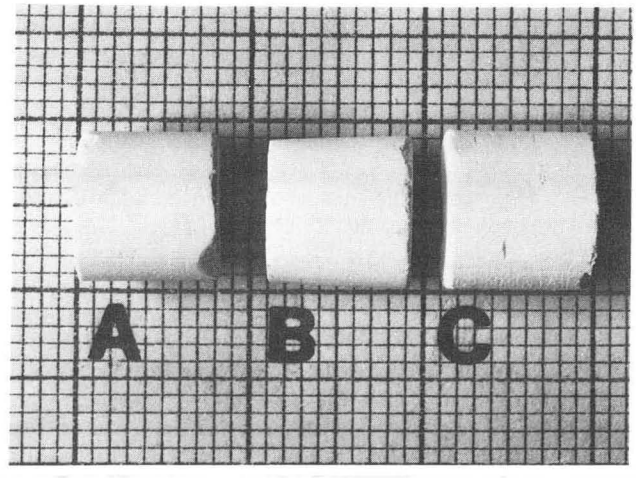

Figure 1-1. (A) Specimen after 2 hr at 1303 K; (B) specimen after 2 hr in gradient from 1303 K at left to 1235 K at right; (C) specimen after 2 hr at 1235 K. (XBB 877-6393)

*This work was supported by the Director, Office of Energy Research, Office of Basic Energy Sciences, Materials Sciences Division of the U.S. Department of Energy under Contract No. DE-AC03-76SF00098.

†Permanent address: LBL and University of Genoa, Italy.

‡Permanent address: University of Genoa, Italy.

1. A.W. Searcy, J. Am. Ceram. Soc. **70**, C-61 (1987).

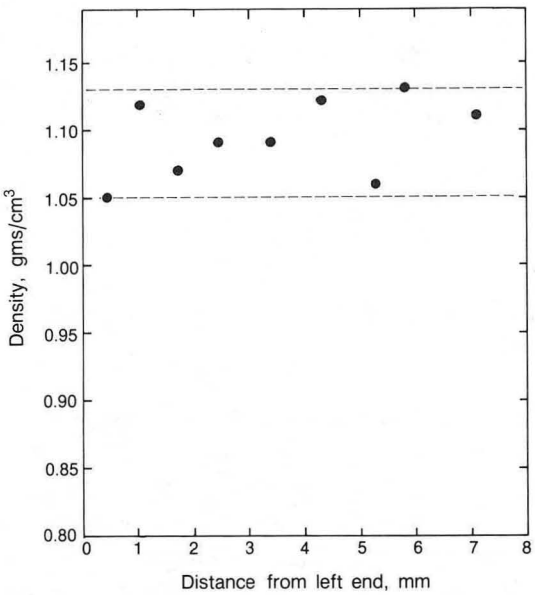

Figure 1-2. Densities measured for slices of a specimen held 2 hr at 1303 K. (XBL 8710-4408A)

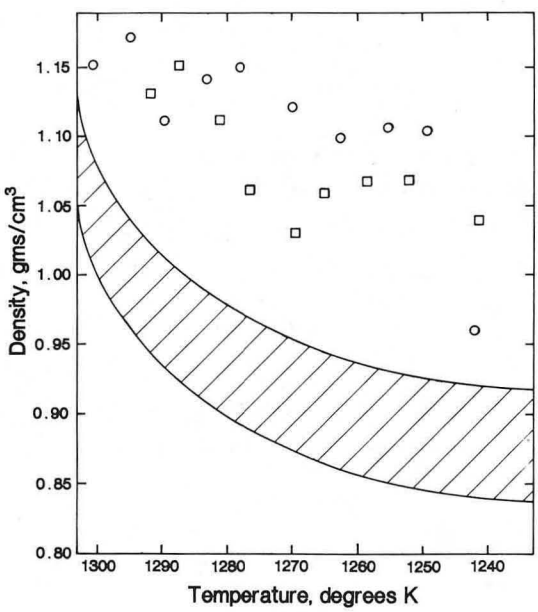

Figure 1-3. Band shows densities predicted from isothermal data for sections of an 8-mm specimen held in a temperature gradient between 1235 and 1303 K. Points show the experimental densities. (XBL 8710-4410)

2. The Influence of Thermal Cycling on Densification: Further Tests of a Theory (Publication 11)

D. Beruto,[†] R. Botter,[‡] and A.W. Searcy

The H_2O-catalyzed densification of MgO specimens that were thermally cycled between 1408 K and temperatures about 70 K lower is compared to the densification in specimens held isothermally. Both temperature gradients and rates of change in temperature were measured during cycling. The cycling produces densities that are marginally higher than expected from isothermal kinetics. The results are consistent with expectations from recent experiments with constant temperature gradients (Abstract 1): the rate of temperature change does not appear to affect the densification rates significantly. Temperature differences are as high as 3 to 5°C between different positions on and in the 12-mm (one-half inch) specimens under nominally isothermal conditions. Such differences in temperature can provide a significant driving force for sintering in what are intended to be isothermal experiments.[1]

[†]Permanent address: LBL and University of Genoa, Italy.
[‡]Permanent address: University of Genoa, Italy.
1. A.W. Searcy, J. Am. Ceram. Soc. **70**, C-61 (1987).

3. Maximum Stability in a Temperature Gradient (Publication 13)

A.W. Searcy

Attempts to describe both directions and rates of diffusion of interstitial solutes in temperature gradients in terms of a single parameter, the heat of transport, have been unsuccessful. It is suggested here that a single-parameter expression is inadequate because interstitial solutions belong to a class of systems in which diffusion is driven by a thermodynamic gradient, which may have a positive or negative temperature dependence, at rates dependent on a positive activation energy barrier. It is taken as an axiom that matter confined in a rigid vessel held in a fixed orientation and subjected to a constant thermal flux will eventually evolve to a state of maximum stability for the imposed constraints. Three

classes of kinetically governed states of maximum stability are illustrated: chaotic, oscillating, and steady states. A fourth class, which includes solid solutions and fluid phases for which cooperative molecular movements are prevented, is characterized by zero net molecular flux exchange between adjacent volume elements. For single-phase solid solutions, the stable distribution of molecules and vacancies between temperatures i and j is found to depend strongly on ratios of their local partial molecular Helmholtz free energies to the local temperature and weakly on temperature-insensitive exchange-attempt frequencies. Stable distributions of ideal gas mixtures in temperature gradients are shown to be governed by the same basic relation, with the attempt frequencies now dominant terms. It is hypothesized that when neither cooperative movements of molecules nor field gradients other than temperature gradients are important, stable state distributions in all constant-volume, single-phase closed systems are governed by the same basic equation. Its quantitative application is illustrated for vacancies in copper and for palladium in copper, and it is shown to predict positive and negative partitioning in interstitial solid solutions.

4. Theory and Experiments for Isothermal and Nonisothermal Sintering (Publication 10)

A.W. Searcy and D. Beruto[†]

This paper uses new formulations of thermodynamics for surfaces and for nonisothermal systems as a basis for analyzing the kinetics of isothermal and nonisothermal sintering. The analysis suggests several conclusions that differ from generally accepted ideas about sintering: (1) Rates of microstructural changes in crystalline aggregates sometimes are limited by layer growth instead of by diffusion. (2) Temperature gradients can drive microstructural changes in a aggregate. (3) Surface diffusion over distances much greater than particle diameters can promote densification and/or coarsening. A fourth conclusion, which is also at variance with generally accepted theory, is suggested by the writers' experiments with aggregates of very small CaO and MgO crystals: coupled pore and grain growth can be a dominant process from the initiation of sintering. Densification studies with isothermal and nonisothermal aggregates confirm a significant effect of temperature gradients. Deductions from the theory and experiments are compared to observations of others.

[†]Permanent address: LBL and the University of Genoa, Italy.

5. Microstructural Evolution During the Decomposition of $Mg(OH)_2$ (Publication 5)

U. Dahmen, M.G. Kim, and A.W. Searcy

The microstructural evolution during the decomposition of $Mg(OH)_2$ is characterized by transmission electron microscopy. The reaction is pseudomorphic and topotactic with an orientation relationship of parallel close-packed planes and directions. High-resolution micrographs show directly the small size and nearly cubic shape of the resulting MgO crystallites and their oriented stacking. Optical diffraction reveals a relatively narrow size distribution of pores and crystallites. The microstructure is discussed in terms of alternative reaction mechanisms.

1987 PUBLICATIONS AND REPORTS

Refereed Journals

1. A.W. Searcy, "Theory for Sintering in Temperature Gradients: The Role of Long Range Mass Transport," J. Am. Ceram. Soc. **70**, C-61 (1987); LBL-21776.
2. M.G. Kim, U. Dahmen, and A.W. Searcy, "Structural Transformations in the Decomposition of $Mg(OH)_2$ and $MgCO_3$," J. Am. Ceram. Soc. **70**, 146 (1987); LBL-21587.
3. D. Beruto, R. Botter, and A.W. Searcy, "H_2O-Catalyzed Sintering of ~2 nm Cross Section Particles of MgO," J. Am. Ceram. Soc. **70**, 155 (1987); LBL-20271.
4. D. Beruto, R. Botter, and A.W. Searcy, "Thermodynamics of Two, Two-Dimensional Phases Formed by CO_2 Chemisorption on MgO," J. Phys. Chem. **91**, 3578 (1987); LBL-22161.
5. U. Dahmen, M.G. Kim, and A.W. Searcy, "Microstructural Evolution During the Decomposition of $Mg(OH)_2$," Ultramicroscopy **23**, 365 (1987); LBL-22899.

Other Publications

6. M.G. Kim, U. Dahmen, and A.W. Searcy, "Origin of Cracking Phenomena Observed in Decomposition Reactions," in *Ceramic Microstructures 86*, J.A. Pask and A.G. Evans, Eds., Plenum, New York, 1987, p. 145; LBL-22160.
7. A.W. Searcy, "Sintering Theory for Crystalline Solids," in *Ceramic Microstructures 86*, J.A. Pask and A.G. Evans, Eds., Plenum, New York, 1987, p. 591; LBL-22162.
8. A.G. Hegedus (Ph.D. Thesis), "The Thermodynamics of Narrow Phase Width Solid Solutions: Dolomite, A Case Study."

LBL Reports

9. D. Beruto, M.G. Kim, and A.W. Searcy, "Microstructural Criteria for Selecting Sorbent Porous Oxides: CaO/CO_2 Systems," accepted by High Temp.–High Pressure; LBL-22158.
10. A.W. Searcy and D. Beruto, "Theory and Experiments for Isothermal and Non-Isothermal Sintering," to appear as opening paper in *Science of Ceramics 14*; LBL-23220.
11. D. Beruto, R. Botter, and A.W. Searcy, "The Influence of Thermal Cycling on Densification: Further Tests of a Theory," to appear in *Proc. First Int. Conf. on Ceramic Powder Processing Science*; LBL-24196.
12. D. Beruto, R. Botter, and A.W. Searcy, "Influence of Temperature Gradients on Sintering: Experimental Tests of a Theory," LBL-24197.
13. A.W. Searcy, "Maximum Stability in a Temperature Gradient," LBL-23229.

Invited Talks

14. U. Dahmen, M.G. Kim, and A.W. Searcy, "Microstructural Evolution during the Decomposition of $Mg(OH)_2$," Tempe, AZ, Jan. 1987.
15. D. Beruto, R. Botter, and A.W. Searcy, "The Influence of Temperature Gradients on Densification: Experimental Tests of a Theory," National Meeting, American Ceramic Society, Pittsburgh, PA, May 1987.
16. A.W. Searcy, "The Influence of Particle Size on Segregation of Solutes to Surfaces of Crystalline Particles," National Meeting, Materials Research Society, Anaheim, CA, Apr. 1987.
17. D. Beruto, M.G. Kim, and A.W. Searcy, "Microstructure Criteria for Selecting Sorbent Porous Oxides: CaO/CO_2 System," 5th International Conference on High Temperature and Related Materials, Rome, Italy, May 25, 1987.
18. A.W. Searcy and D. Beruto, "Theory and Experiments for Isothermal and Non-Isothermal Sintering," Opening Plenary Lecture, Biannual Meeting, Association of European Ceramic Societies, Canterbury, England, Sept. 7, 1987.
19. D. Beruto, R. Botter, and A.W. Searcy, "Influence of Thermal Cycling on Densification: Further Tests of a Theory," First International Conference on Ceramic Powder Processing Science, Orlando, FL, Nov. 2, 1987.
20. J.W. Bierach and A.W. Searcy, "Compositions and Rates of Intermediate Phase Formation in the $BaCO_3$-TiO_2 reactions at 1050°C," 40th Pacific Coast Regional Meeting, American Ceramic Society, San Diego, CA, Nov. 3, 1987.

Structure-Property Relationships in Semiconductor Materials*

Jack Washburn, Investigator

INTRODUCTION

The purpose of this program is to advance the understanding of the effects of structural defects, including the structure of interfaces on the electrical or optical properties of semiconductor materials. Systems chosen for study are those that have interfaces and defects formed during state-of-the-art solid-state device processing, such as ion implantation, oxidation, contact formation, and heteroepitaxial growth.

The approach has lead naturally to areas of basic research interest. Recent results have contributed to (1) improved understanding of the mechanisms of misfit accommodation at heteroepitaxial interfaces, (2) clarification of the mechanism of the crystalline-to-amorphous transformation during light-ion irradiation, (3) identification of factors that affect the type and density of secondary defects resulting from ion implantation, (4) an improved understanding of the mechanism of Schottky barrier formation, and (5) an understanding of the important role of thin native oxide layers in determining interface morphology and stability of the electrical properties of Schottky and ohmic contacts to GaAs.

High-resolution lattice-imaging transmission electron microscopy (TEM), particularly on cross-section samples and, when possible, with computer simulation of images, combined with analytical electron microscopy has proved to be a powerful tool for revealing and identifying fine-scale defects and interface structure. The TEM information is combined with supplementary structural observations on the same specimens by electron paramagnetic resonance (EPR), Rutherford backscattering (RBS), secondary-ion mass spectroscopy (SIMS), x-ray diffraction, or microanalytical electron microscopy. These observations have frequently been made on the same specimens from which electrical measurements such as I-V characteristics were previously measured.

1. Surface Faceting of (110) GaAs: Analysis and Elimination (Publications 1, 6, 7, and 15)

L. Parechanian-Allen, E.R. Weber, Y.C. Pao, A.G. Elliot, and J. Washburn

A systematic study has been made on (110) GaAs grown by molecular beam epitaxy. This work represents the first systematic investigation of commonly observed faceting on the (110) GaAs surface. Faceting of (110) GaAs was analyzed with respect to facet geometry and kinetics of initial facet formation. This approach has, for the first time, allowed facet-free molecular beam epitaxy (MBED) (110) GaAs to be consistently grown. Facet-free growth was ensured by angling the (110) substrates 6° toward the (111) surface. This tilt provided stable Ga-rich ledges needed to promote the two-dimensional growth of the epitaxial layer in the ultrahigh-vacuum (UHV) environment. The epitaxial GaAs layers grown in this way exhibited a room-temperature electron mobility of $\approx 5700\ cm^2/V\text{-}sec$ for $N_{Si} \approx 4 \times 10^{15}$ and a strong exciton photoluminescence emission at 4 K. This breakthrough in MBE growth of III-V compounds allows for fabrication of (110) GaAs devices that will take advantage of the unique properties of this orientation.

2. Amorphization of Silicon by Boron Ion Implantation (Publication 3)

Y. Shih, J. Washburn, R. Gronsky, and E.R. Weber

The amorphization of silicon due to implantation of boron ions (boron is the lightest element used for integrated circuit fabrication processes) has been systematically studied at various temperatures, voltages, and dose rates. A model for formation of amorphous silicon by light-ion implantation was proposed. It was suggested that accumulation of point defects and/or clusters is required at the initial stage of the amorphization process. Diinterstitial-divacancy pairs were suggested to be the embryos of amorphous zones formed during implantation at

*This work was supported by the Director, Office of Energy Research, Office of Basic Energy Sciences, Materials Sciences Division of the U.S. Department of Energy under Contract No. DE-AC03-76SF00098.

room temperature. Out-diffusion of highly mobile interstitials during amorphization is thought to explain differences in the critical energy for amorphization with low- and high-energy implantation at liquid-nitrogen temperature.

3. Formation of Amorphous and Crystalline Ternary Phases (Publications 2 and 13)

T. Sands, C.C. Chang, A.S. Kaplan, V.G. Keramidas, K.M. Krishnan, and J. Washburn

Three ternary phases of the type Ni_xInP have been observed to be the primary reaction products of the Ni/InP reaction. The first phase, amorphous Ni_xInP ($x \cong 2.7$), forms at the Ni/InP interface by a solid-state amorphization process at low temperatures ($T \lesssim 200°C$). Amorphous Ni_xInP crystallizes at ~300°C to form a hexagonal Ni_xInP phase (a_o = 0.412 nm and c_o = 0.483 nm) with a similar composition. A third ternary phase, with nominal composition Ni_2InP (monoclinic, a_o = 0.681 nm, b_o = 0.529 nm, c_o = 1.280 nm, and $\beta = 95°$), nucleates at higher temperatures and is the final reaction product. This final phase is stable at temperatures up to 500°C in samples capped with SiO_2.

4. A Comparative Study of Phase Stability and Film Morphology in Thin-Film Metal/GaAs Systems (Publication 5)

T. Sands, V.G. Keramidas, K.M. Yu, J. Washburn, and K. Krishnan

To attain reproducible and stable contacts to compound semiconductor devices, it is necessary to achieve thermodynamically stable phases after the reaction of metals with the compound semiconductor. In this study, the final phases produced by the reactions between GaAs and thin metal films of Co, Rh, Ir, Ni, Pd, and Pt have been investigated. The phases are identified as MGa for M = Co, Rh, Ni, Pd, and Pt; monoarsenides of Co and Ni; diarsenides of Rh, It, Pd, and Pt; and It_3Ga_5. These phases, if deposited directly on GaAs, will produce thermally stable contacts. In addition to the identification of these stable phases, analyses of the products of thin-film M/GaAs reactions by transmission electron microscopy, x-ray diffraction, and Rutherford backscattering spectrometry reveal the distribution, grain size, and crystallographic texture of these end phases. It was found that (1) Surface and interface contributions to the free energy are sufficient to alter the relative phase stabilities for thin metal films on GaAs (e.g., 12-nm Pd on GaAs). (2) Silica caps are effective in significantly reducing the loss of As from metal films on GaAs at annealing temperature up to 600°C. (3) M/GaAs systems that react to form M-Ga and M-As binary phases exhibit lateral phase separation when the grain size in the reacted film is larger than the reacted film thickness and vertical phase separation (stratification) when it is smaller. (4) For M/GaAs systems annealed under the same conditions, the grain size in the reacted film is larger for deposited metals with smaller heats of vaporization. (5) Under conditions that yield phase stratification in reactive metal/GaAs systems, the arsenide resides at the interface due to the relatively low mobility of As in the reacted layer.

5. The Influence of Residual Impurities on the Orientation Relationship Between Metal Contact Layers and GaAs (Publication 9)

Z. Liliental-Weber

The interface morphology of gold contacts on UHV-cleaved, air-exposed, and chemically prepared GaAs surfaces has been studied by electron microscopy. The morphology of the overlayer was found to depend strongly on annealing and surface treatment. TEM results indicate that the interface is flat and abrupt for all unannealed diodes, as well as for annealed diodes formed on atomically clean surfaces. For annealed diodes formed on the air-exposed surfaces, the metal-semiconductor interface contains large metallic protrusions extending up to several hundred Angstroms into the semiconductor. The interface for commercially prepared samples [chemically cleaned (100) surfaces] is even more complex than interfaces formed on the atomically clean but subsequently air-exposed cleaved (110) surfaces. Evidence was found that Au diffuses through imperfections or gaps in the interfacial native oxide layer, forming islands in intimate contact with the semiconductor.

A difference in the orientation relationship between differently prepared samples occurred after annealing. Three different orientation relationships were discovered. Type I relationships include $[0\bar{1}1]_{GaAs} \parallel [0\bar{1}1]_{Au}$, $[011]_{GaAs} \parallel [011]_{Au}$, and $[1\underline{0}0]_{GaAs} \parallel [1\underline{2}2]_{Au}$. Type IIa relationships include $[0\bar{1}1]_{GaAs} \parallel [0\bar{1}1]_{Au}$, $[011]_{GaAs} \parallel [\bar{4}11]_{Au}$, and $[1\underline{0}0]_{GaAs} \parallel [\underline{1}\underline{2}2]_{Au}$.

Type IIb relationships include $[01\bar{1}]_{GaAs} \parallel [122]_{Au}$, $[011]_{GaAs} \parallel [\bar{4}11]_{Au}$, and $[\bar{1}00]_{GaAs} \parallel [0\bar{1}1]_{Au}$. Type III relationships include $[0\bar{1}1]_{GaAs} \parallel [0\bar{1}1]_{Au}$, $[011]_{GaAs} \parallel [\bar{5}22]_{Au}$, and $[100]_{GaAs} \parallel [455]_{Au}$. The type I and II orientation relationships exist for annealed air-exposed samples. Type I especially is formed because γ-Ga_2O_3 grows epitaxially on GaAs: $(011)_{Ge_2O_3} \parallel (011)_{GaAs}$ with $[100]_{Ge_2O_3} \parallel [100]_{GaAs}$. This oxide provides an excellent lattice match to Au. Our observations suggest that as soon as GaAs is exposed to air, epitaxial γ-Ga_2O_3 is formed, and the deposited metal then epitaxially relates to the oxide already existing at the interface. The oxide on GaAs is not a continuous layer. In the areas where the oxide is not present, twinning takes place, giving a better match at the interface (type II).

The orientation relationship in UHV-cleaved and deposited Au samples annealed *ex situ* in N_2 was completely different (type III). A 10° angle occurred between $(111)_{Au}$ planes and $(111)_{GaAs}$ planes. The same angle was also observed for Al (see Figure 5-1) and Ag when the metal was deposited *in situ* in UHV on cleaved GaAs surfaces. This behavior can be hypothetically explained by As accumulation on the interfaces. The metal probably tries to accommodate to the accumulated As. The best match can be achieved with $[422]_{GaAs} \parallel [030]_{As} \parallel [3\bar{1}1]_{Au}$. The match between $[422]_{GaAs}$ and $[3\bar{1}1]_{Au}$ was observed for many grains and resulted in a 10% angle between $(111)_{Au}$ and $(\bar{1}11)_{GaAs}$.

The special alignment between different metals and GaAs supports the idea that this effect originates from the substrate itself and that As, discovered in our earlier study to accumulate at the interface, can determine the relationship between metals and GaAs.

6. The Influence of Surface Reconstruction on the Al/GaAs Interface Structure (Publication 10)

Z. Liliental-Weber, R. Ludeke, C. Nelson, R. Gronsky, and J. Washburn

A systematic study of Al/GaAs interfaces was performed by high-resolution electron microscopy. The Al layers were deposited in a molecular-beam epitaxy chamber. The GaAs substrate temperature varied during Al deposition from −30°C to 400°C. The mechanism responsible for the final orientation of the Al overlayer is still far from being understood. Our results show that deposition of Al on cold substrates (<25°C) resulted in in epitaxial growth of (001) Al on (001) GaAs. Droplets of Ga were observed in samples with the substrate temperature at −30°C (1×2) and 0°C [c(2×8)]. Postannealing of these samples resulted in formation of the AlGaAs phase. Deposition of Al on hot substrates (150°C and 400°C) resulted in the formation of the AlGaAs phase, which separated (110) oriented Al from (001) GaAs.

7. The Role of Strained-Layer Superlattices on Dislocation Propagation in GaAs/Si Heterostructures (Publication 11)

Z. Liliental-Weber, E.R. Weber, T.Y. Liu, H. Kroemer, and J. Washburn

There has been great interest in GaAs/Si heteroepitaxy technology. The monolithic integration of ultrahigh-speed GaAs with high-density Si

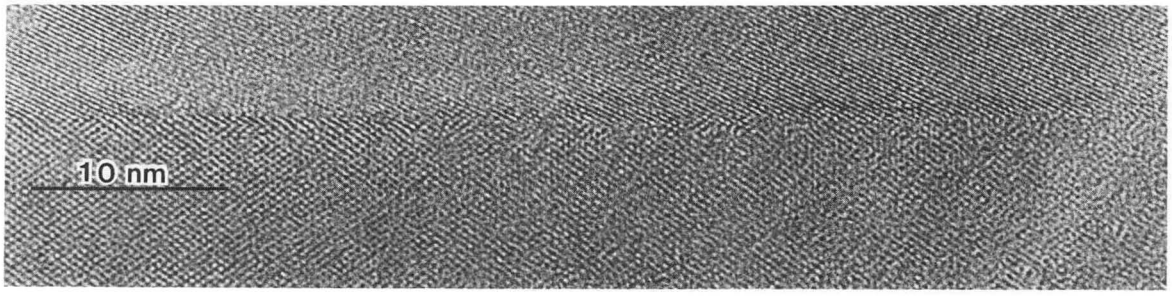

Figure 5-1. High-resolution image of Al/GaAs interface for Al deposited *in situ* on UHV-cleaved GaAs. Note the 10° angle between the $\{111\}_{Al}$ and $\{111\}_{GaAs}$ planes. (XBB 868-6147)

could lead to potential advantages for optical interconnects, optoelectronic integrated circuits, and very large scale integration. However, the problems presented make the technology difficult. These problems include a 4% lattice mismatch, a large thermal expansion coefficient, a polar/non-polar interface with antiphase disorder, cross-doping, and phase segregation. One solution to these problems may be the use of (211) Si substrates to grow GaAs. However, in contrast to GaAs grown on a (100) Si surface, where a large fraction of the dislocations formed at the interface have Burgers vectors parallel to the interface, all misfit dislocations formed at the (211) interface have Burgers vectors inclined to the GaAs layers (see Figure 7-1), making them susceptible to propagation into the GaAs layer. The dislocation density at the interface due to the mismatch between GaAs and Si is expected to be in the range of $10^{11}/cm^2$, and material with such a high dislocation density is not suitable for device application. This work has shown that the dislocation density can be significantly reduced by first growing strained-layer superlattices (SLSLs). Two different types of SLSLs, InGaAs/InGaP and InGaAs/GaAs, were applied either directly to the Si substrate, to a graded layer (GaP-InGaP), or to a GaAs buffer layer to stop the defect propagation into the GaAs film. Growth of InGaAs/GaAs instead of InGaAs/InGaP was found to be more effective in blocking defect propagation. In all SLSLs investigated, dislocation propagation was stopped primarily at the top interface between the superlattice and the GaAs (see Figure 7-2). Graded layers and unstrained AlGaAs/Gas superlattices did not significantly block dislocation propagation from the interface.

By using SLSLs it was possible to obtain a dislocation density in the range of $5\times10^7/cm^2$. This value is comparable to the recently reported density of dislocations in the GaAs layers grown on (100) Si substrates.

8. Quality of GaAs Grown on (100) Si (Publications 8 and 12)

Y.H. Lo, M.N. Charasse, H. Lee, D. Vakhshoori, Y. Huang, P. Yu, and Z. Liliental-Weber

Transmission electron microscopy (TEM) and Raman scattering were employed to investigate the quality of GaAs grown on (100) Si. Raman scattering was measured along a bevel-etched GaAs epitaxial film grown on Si by molecular-beam epitaxy. The strain profile calculated from the Raman peak shift shows that about 0.6% compressive strain exists near the interface because of lattice mismatch. TEM results showed that an ultraclean Si surface is essential for dislocation confinement. The distance between dislocations at the interface was found to be nonuniform, varying from 50 Å to 125 Å, with an average distance of 81 Å. Most of the dislocations

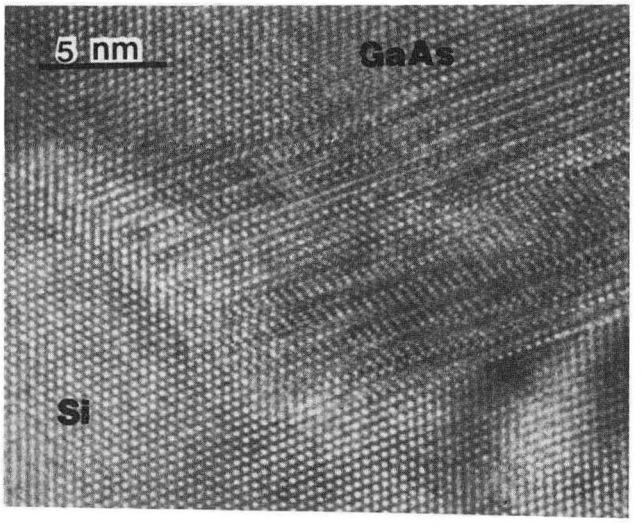

Figure 7-1. Transmission electron micrograph of stacking faults formed at the interface of GaAs epitaxially grown on Si. The formation of dislocations and stacking faults still is a major obstacle in the development of GaAs-on-Si devices. (XBB 872-1474)

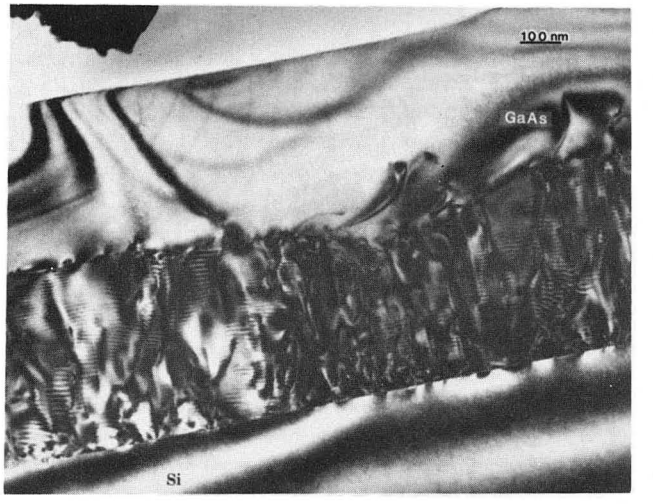

Figure 7-2. High-quality GaAs achieved by growing InGaAs/GaAs strained-layer superlattices on {211}Si. Note the blocking of propagating dislocations at the uppermost interface between the strained-superlattice layers and the GaAs. (XBB 871-46)

formed at the interface with Burgers vector parallel to the interface (beneficial to GaAs quality) are formed at the double steps on the Si surface, which are mainly due to the substrate's being tilted instead of being heated before growth. Based on our study, the (100) Si substrate with double steps along both [110] and [$\bar{1}\bar{1}0$] axes provided the best condition for growing low-defect-density GaAs on Si substrates. A GaAs p-i-n photodetector on a Si substrate was fabricated, but a high dark current (50 nA) and relatively low responsivity (0.01 A/W) showed that the material quality needs to be improved further to make a minority carrier vertical transition device.

1987 PUBLICATIONS AND REPORTS

Refereed Journals

1. L. Parechanian-Allen, E.R. Weber, J. Washburn, and Y.C. Pao, "Surface Faceting of (110) GaAs: Analysis and Elimination," Mat. Res. Soc. Symp. Proc. **82**, 487 (1987).
2. T. Sands, C.C. Chang, V.G. Keramidas, K.M. Krishnan, and J. Washburn, "The Ni-InP Reaction: Formation of Amorphous and Crystalline Ternary Phases," Appl. Phys. Lett. **50**, 1398 (1987).
3. Y. Shih, J. Washburn, R. Gronsky, and E.R. Weber, "Amorphization of Silicon by Boron-Ion Implantation," Mat. Res. Soc. Symp. Proc. **71**, 203 (1986); LBL-21422.
4. I. Brown and J. Washburn, "The MEVVA Ion Source for High Current Metal Ion Implantation," Nucl. Instrum. Meth. in Phys. Res. B **21**, 201 (1987).
5. T. Sands, V.G. Keramidas, K.M. Yu, J. Washburn, and K. Krishnan, "A Comparative Study of Phase Stability and Film Morphology in Thin-Film M/GaAs Systems (M=Co, Rd, Ir, Ni, Pd and Pt)," J. Appl. Phys. **62**, 2070 (1987); LBL-21060.
6. L. Parechanian-Allen, E.R. Weber, and J. Washburn, "Device Quality Growth and Characterization of (110) GaAs Grown by Molecular Beam Epitaxy," Appl. Phys. Lett. **51**, 670 (1987); LBL-22564.
7. L. Parechanian-Allen, E.R. Weber, J. Washburn, Y.C. Pao, and A.G. Elliot, "Characterization of Surface Faceting on (110) GaAs/GaAs Grown by Molecular Beam Epitaxy," J. Crystal Growth, **87**, 193 (1988); LBL-22692.
8. Y.H. Lo, M.N. Charasse, H. Lee, D. Vakhshoori, Y. Huang, P. Yu, Z. Liliental-Weber, M. Werner, and S. Wang, "Raman Scattering Spectrum Along a Bevel Etched GaAs on Si, TEM Study and GaAs p-i-n Photodetector on Si," Mat. Res. Soc. Symp. Proc. **91**, 149 (1987); LBL-23742.
9. Z. Liliental-Weber, "The Structure and Electrical Properties of Metal Contacts on GaAs," J. Vac. Sci. Technol. **B4**, 1007 (1987); LBL-23016.
10. Z. Liliental-Weber, C. Nelson, R. Gronsky, J. Washburn, and R. Ludeke, "The Structure of Al/GaAs Interfaces," Mat. Res. Soc. Symp. Proc. **77**, 229 (1987); LBL-22581.
11. Z. Liliental-Weber, E.R. Weber, J. Washburn, T.Y. Liu, and H. Kroemer, "The Structure of GaAs/Si(211) Heteroepitaxial Layers," Mat. Res. Soc. Symp. Proc. **91**, 91 (1987); LBL-23462.
12. Y.H. Lo, M.C. Wu, H. Lee, S. Wang, and Z. Liliental-Weber, "The Dislocation Microstructures on Flat and Stepped Si Surfaces: Guidance for Growing High Quality GaAs on (100) Si Substrates," Appl. Phys. Lett. **52**, 1386 (1988); LBL-24476.

Other Publications

13. K.M. Krishnan, T. Sands, and R. Caron, "Early Stages of the M-InP(M=Ni,Pd) Reaction: Solid-State Amorphization and Subsequent Crystallization," in *Proc. 45th Annual Meeting Electron Microscopy Society of America*, San Francisco Press, Inc., 1987, p. 330; LBL-23185.

LBL Reports

14. C.J. Jou, J. Washburn, Z. Liliental-Weber, and R. Gronsky, "The Morphology and the Electrical Properties of the Ag/GaAs Contact," LBL-23033.
15. L. Parechanian-Allen (Ph.D. Thesis), "Successful Molecular Beam Epitaxy Growth and Characterization of (110)GaAs/GaAs and (110)AlGaAs/GaAs," LBL-23427.

Invited Talks

16. T. Sands, "Stable Phases at Reactive Metal/Compound Semiconductor Interfaces," Workshop on 3–5 Semiconductors: Metal Interfacial Chemistry and Its Effect on Electrical Properties, Stanford University, Stanford, CA, Nov. 1986.
17. T. Sands, "Stable Phases at Reactive Metal/Compound Semiconductor Interfaces," Department of EECS, University of California, San Diego, Nov. 1986.
18. Z. Liliental-Weber, "The Structure of Au/GaAs and Al/Gas Interfaces," Workshop on 3–5 Semiconductors: Metal Interfacial Chemistry and Its Effect on Electrical Properties, Stanford University, Stanford, CA, Nov. 1986.
19. Z. Liliental-Weber, "The Structure and Electrical Properties of Metal Contacts on GaAs," Conference on Physics and Chemistry of Semiconductor Interfaces, Salt Lake City, UT, Jan. 27–29, 1987.
20. Z. Liliental-Weber, "Structural Characterization of III-V Semiconductors," Continuing Education in Engineering, University Extension, and the College of Engineering, Stanford University, Stanford, CA, Nov. 1986.

21. Z. Liliental-Weber, "Au and Al Contacts to GaAs," IBM, Yorktown Heights, NY, Dec. 1986.
22. Z. Liliental-Weber, "TEM Study of Defects and Interfaces in Semiconductors, Oregon State University, Corvallis, May 1987.
23. Z. Liliental-Weber, "TEM Study of Metal/Semiconductor and Semiconductor/Semiconductor Interfaces," Oregon State University, Corvallis, May 1987.

Fundamental Studies of Chemical Properties and Processing of Advanced Structural Ceramics*

Lutgard C. De Jonghe, Investigator

INTRODUCTION

The key barrier to the exploitation of the properties of ceramics in new technologies has been recognized as the difficulty of fabricating these materials with sufficient reproducibility, reliability, and cost efficiency. Many of the poorly understood aspects of processing are common to a variety of ceramics, including the ceramic matrix particulate composites, and microcomposite electroceramics. The fabrication of reliable ceramics requires the control of the structure of the starting powders as well as of the densification process, to allow for the manipulation of systems, such as microcomposites, at the necessary microscopic scale.

The densification (with and without applied stress), microstructure development, and possible interactions of reaction and densification for such systems is complex and raises a range of processing problems that must be addressed at a fundamental level to provide the basis for a rational approach to processing. Of paramount importance in all the systems is the control of microstructural and microchemical heterogeneities. These must be incorporated in the development of predictive processing models that consider the response of the system to applied stresses during powder compaction and densification. One approach is to consider the transient incompatibility stresses, resulting from differential densification, as the basis of the effects that modify densification and microstructural development during the fabrication of heterogeneous ceramics.

1. Rearrangement During Sintering in Two-Dimensional Arrays (Publication 1)

M. Weiser and L.C. De Jonghe

Densification of two-dimensional arrays of nearly monosized copper spheres was examined by hot-stage optical microscopy. The evolution of the particle arrangement was studied with computer methods, and statistical correlations were sought. Color graphics were found useful for displaying the spatial relationship of the local sintering parameters. It was found that differential densification was the major cause of rearrangement, rather than asymmetric neck formation (see Figure 1-1).

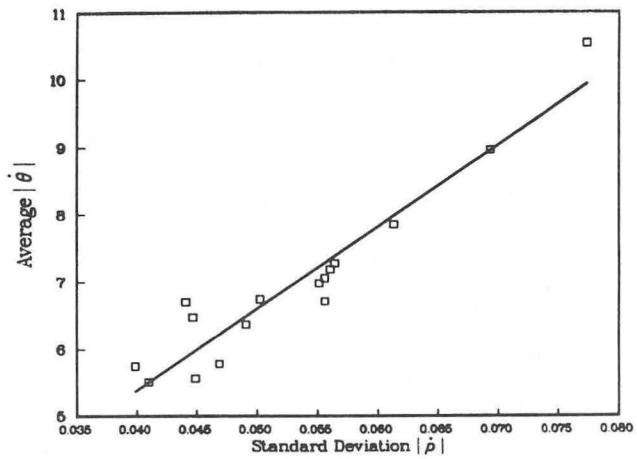

Figure 1-1. Average of the absolute rate of angular change in a two-dimensional raft of copper spheres during sintering, versus the standard deviation of the absolute local densification rate. The angular change refers to the interparticle angles that are defined as the angles between the lines radiating from a particle center to the nearest-neighbor particle centers. The absolute values of the angular changes for all particles in the system of about 100 particles constitute the value for the vertical axis. The local densification rate of a single particle in a two-dimensional raft is defined as the time dependence of the area of projection in the raft. (XBL 8511-4541)

*This work was supported by the Director, Office of Energy Research, Office of Basic Energy Sciences, Materials Sciences Division of the U.S. Department of Energy under Contract No. DE-AC03-76SF00098.

2. Creep and Densification During the Sintering of Glass Powder Compacts (Publication 2)

M.N. Rahaman, L.C. De Jonghe, G. Scherer,[†] and R. Brook[‡]

The simultaneous creep and densification of glass powder compacts was studied as a function of low applied uniaxial stress, temperature, and particle size (see Figure 2-1). The creep rate can be expressed as the sum of the contribution from the applied stress, which varies linearly with stress, and a contribution due to anisotropic densification, which varies linearly with the densification rate. For a constant applied stress, the ratio of the creep rate to the densification rate is almost independent of both temperature and density. While these observations are consistent with the model of Scherer for the viscous sintering of glass, other observations show significant deviations from the model. Both the densification rate and creep viscosity, which has an exponential dependence on porosity, show much stronger dependence on density compared with theoretical predictions.

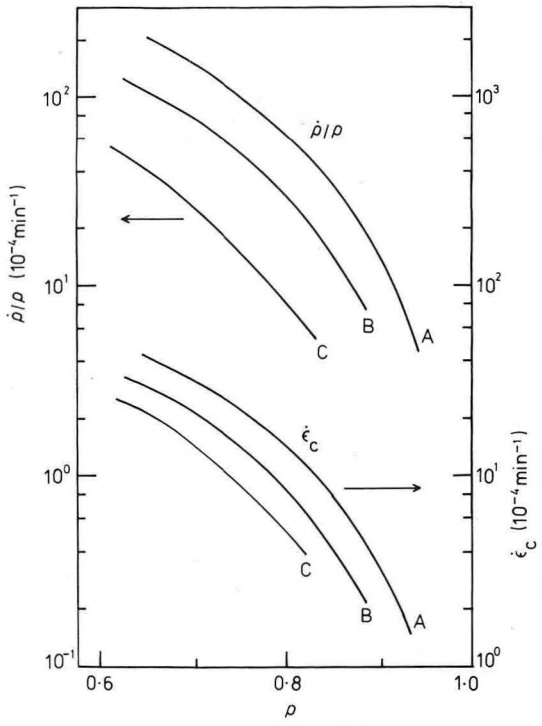

Figure 2-1. Creep rate ($\dot{\epsilon}_C$) and densification rate ($\dot{\rho}/\rho$) versus relative density for glass powders sintered at 783 K. Powders A, B, and C had an average particle size of 4, 8.5, and 33 μm, respectively. (XBL 873-1016)

[†]Present address: Central Research and Development Department, E.I. DuPont de Nemours and Co., Wilmington, DE.

[‡]Present address: Department of Ceramics, University of Leeds, England.

3. Creep-Sintering and Microstructure Development of Heterogeneous MgO Compacts (Publication 4)

M. Lin, M. Rahaman, and L.C. De Jonghe

Simultaneous creep and densification and the microstructure development of magnesium oxide powder compacts were studied at 1250°C and for applied stresses of up to 0.25 MPa. Die-pressing the powder into compacts with a relative green density of ~0.40 led to an approximately bimodal distribution of pores, with one fraction having sizes of the order of 10 times the initial particle size, and the other fraction having pore sizes of the order of the particle size. The presence of the large pores in turn gave rise to rather unusual sintering effects (see Figure 3-1). After first decreasing with relative density (ρ), the densification rate ($d\rho/dt$) and the creep rate ($d\rho/dk$) then increased dramatically for $0.6 < \rho < 0.75$. This range of ρ corresponded to the stage of microstructure development when grain growth and coalescence of the smaller pores have created a more

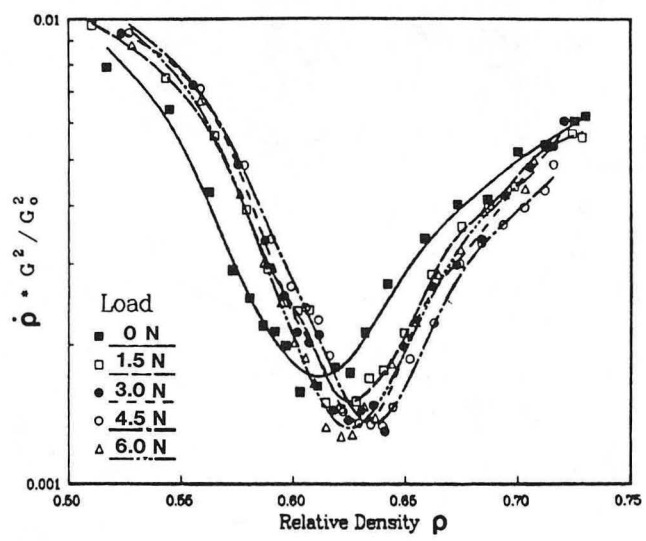

Figure 3-1. Grainsize-compensated densification rates versus relative density for MgO powers sintered at 1523 K at various applied loads. The rise in densification rate after relative densities of 0.62 can be attributed to the closure of pores that have a decreased grain coordination number as a result of grain growth. (XBL 864-1649)

uniform pore distribution. Above $\rho \sim 0.75$, both $d\rho/dt$ and $d\epsilon/dt$ (the creep rate) again decreased with ρ. These trends in the densification behavior are discussed in terms of material parameters such as the equilibrium dihedral angle and the pore coordination number.

4. Intrusion Bonding of Nickel and Zirconia (Publication 8)

I. Reimanis, S. Shinde, and L.C. De Jonghe

Intrusion bonding of nickel to zirconia was achieved by hot pressing the zirconia powder onto an Ni sheet, at pressures of about 55 MN/m^2 and at temperatures of about 1573 K. The intrusion zone can be several hundred micrometers thick, providing a gradual transition from ceramic to metal (see Figure 4-1). The most extensive intrusion occurred when pressure was applied late in the heating cycle, after the zirconia powder had coarsened. The parameters determining the extent of the intrusion bonding are discussed. The intrusion bonds are compared to diffusion bonds for which a discrete metal/ceramic interface was maintained. Vickers microindentation tests in the intrusion bond zone indicated that metal intrusion provided improved bonding.

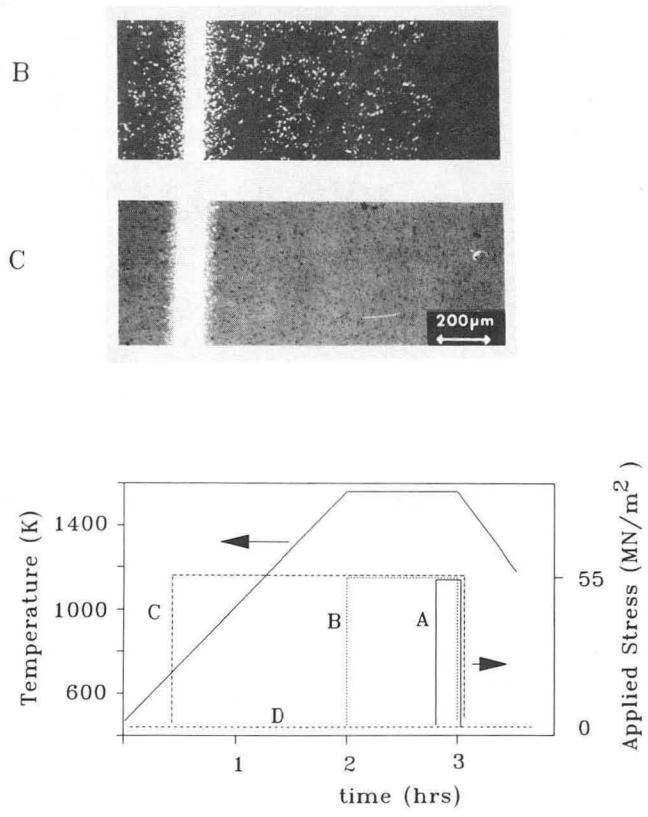

Figure 4-1. Intrusion bonds of specimens A, B, C, and D, and their corresponding temperature-time-pressure histories in the pressure welding operation. (XBB 873-2196A)

5. Degradation in a Thermal Barrier Coating (Publication 5)

S. Shinde, I. Reimanis, and L.C. De Jonghe

The failure of a thermal barrier coating involves cracking and spalling of the ceramic layer, primarily brought about by bond-coat oxidation during operation. The present investigation has focused on the microstructural and microchemical changes in a thermal barrier coating, oxidized in air for 1 and 10 hours at 900°C. The zirconia coating shows a gradual increase in the amount of monoclinic phase with time at temperature. The bond-coat layer shows substantial aluminum depletion in the region adjacent to the ceramic. This aluminum forms an oxide layer (Al_2O_3) at the interface. However, nickel oxide (NiO) is also found to be another important oxidation product. The relevance of these observations to the degradation observed in thermal barrier coatings has been considered.

1987 PUBLICATIONS AND REPORTS

Refereed Journals

1. M. Weiser and L.C. De Jonghe, "Rearrangement During Sintering in Two-Dimensional Arrays," J. Am. Ceram. Soc. **69**, 822 (1986); LBL-19021.
2. M.N. Rahaman, L.C. De Jonghe, G. Scherer, and R.J. Brook, "Creep and Densification During Sintering of Glass Powder Compacts," J. Am. Ceram. Soc. **70**, 766 (1987); LBL-23177.
3. M.N. Rahaman and L.C. De Jonghe, "Angle-Resolved XPS Analysis of Oxidized Polycrystalline SiC Surfaces," Ceram. Soc. Bull. **66**, 782 (1987); LBL-21460.
4. M. Lin, M.N. Rahaman, and L.C. De Jonghe, "Creep-Densification and Microstructure Development of Heterogeneous MgO Compacts," J. Am. Ceram. Soc. **70**, 360 (1987); LBL-21508.
5. S.L. Shinde, I. Reimanis, and L.C. De Jonghe, "Degradation of a Thermal Barrier Coating," Adv. Ceram. Mat. **2**, 60 (1987); LBL-21045.

LBL Reports

6. L. De Jonghe and M. Rahaman, "Sintering Stress of Homogeneous and Heterogeneous Powder Compacts," LBL-21903.
7. M. Rahaman and L. De Jonghe, "Creep-Sintering of Zinc Oxide," LBL-22706.
8. I. Reimanis, S. Shinde, and L. De Jonghe, "Intrusion Bonding of Nickel and Zirconia," LBL-23598.
9. M. Rahaman, L. De Jonghe, S. Shinde, and P. Tewari, "Sintering and Microstructure of Aerogel-Derived Mullite," LBL-23529.
10. M. Weiser and L. De Jonghe, "Inclusion Size and Sintering of Composite Powders," LBL-23670.

Invited Talks

11. L.C. De Jonghe, "Heterogeneities in Ceramics: Benefit or Detriment?" Case Western Reserve University, Cleveland, OH, Oct. 1986.
12. M. Rahaman and L. De Jonghe, "Densification of Heterogeneous Powder Compacts," ACS Meeting, New Orleans, LA, Nov. 1986.
13. L. De Jonghe, "Processing of Ceramic Superconductors," Argonne National Laboratory, Argonne, IL, Sept. 1987.

Structure and Electrical Properties of Composite Materials*

Robert H. Bragg, Investigator

INTRODUCTION

The goal of this work is to understand how the structure-sensitive properties of carbon materials, such as mechanical strength, tensile creep, magnetic susceptibility, and the Hall coefficient, are related to their microstructure. The microstructure undergoes disorder-order phase transformations when soft carbons are annealed in inert atmosphere at temperatures above 2000°C, and ultimately they are converted to graphite. This graphitization is thus energy intensive and the critical step in the manufacture of carbon products, and in predicting property changes at high temperatures, high pressures, or other extreme environments. It is becoming clear that graphitization is a thermally activated process in which carbon interstitials are annihilated in several discrete stages with well-defined activation energies. The annealing induced microstructural changes are characterized by wide-range x-ray and neutron diffraction, and small-angle x-ray scattering measurements at room temperature; and the resulting property changes are obtained from measurements of electrical conductivity, Hall coefficient, and magnetoresistance at temperatures down to 2 K and in magnetic fields to 5 T.

1. Kinetics of Surface Area Changes in Glass-Like Carbon: Reanalysis of the Data (Publication 1)

J. Lachter and R.H. Bragg

In a previous study,[1] measurements were made of the kinetics of the thermally activated decrease in the specific surface area of the pores in annealed glass-like carbon and used to derive an effective activation energy of 64 ± 10 kcal/mole for this process. The pore coarsening was attributed to vacancy migration, but the value of ΔH obtained was only in fair agreement with the literature value 71.5 ± 4.6 kcal/mole. More recently,[2] a value of $\Delta H = 75.0 \pm 3.6$ was obtained from an analysis of the kinetics of increase of the mean pore size during the annealing of glass-like carbon. Since the agreement in this case is considerably better, the results of the surface area study were questioned. A reanalysis of the data revealed that there had been no correction for the transient heat-up time required to bring samples to the appropriate heat-treatment temperature; the functional form of the kinetic equation used in the analysis required modification, and the large statistical error, ± 10 kcal/mole, was caused by the inclusion of data that should have been rejected or given a very low weight. The appropriate corrections were applied and the resulting data were analyzed according to the Lifschitz, Slyozoy, and Wagner theory of pore coarsening, in which the specific surface area was used to obtain an equivalent pore radius. The new result was $\Delta H = 75 \pm 7.2$ kcal/mole, in excellent agreement with the generally accepted value. Thus, the discrepancy has been removed, and it can be taken that the best value for the activation energy for vacancy migration in carbon is 75 ± 3 kcal/mole.

1. S. Bose and R.H. Bragg, Carbon **19**, 289 (1981).
2. J. Lachter, L.G. Henry, and R.H. Bragg, J. Mater. Res. **1**, 832 (1986).

2. A Novel Model for the Kinetics of Graphitization of Pyrocarbon (Publication 4)

R.H. Bragg and J. Lachter

The proposed mechanism of the graphitization of soft carbon, in which the spacing of the layers of fused rings of carbon atoms takes on metastable values of 3.44 Å, 3.40 Å, 3.375 Å, and finally 3.354 Å during annealing, is attributed to annihilation of interstitials and has been extensively tested. The results confirm that the transformations between metastable interstitial configurations are characterized by activation energies of 243 ± 4 kcal/mole, 274 ± 6 kcal/mole, and 330 ± 2 kcal/mole. Figure 2-1 shows the best experimental data available in the literature used to test the model (points) and the curve (solid line) calculated from the model. It appears that the model correctly describes the graphitization behavior of both pyrocarbons and pitch cokes, and the adjustable parameters correlate strongly with known differences in microstructure.

*This work was supported by the Director, Office of Energy Research, Office of Basic Energy Sciences, Materials Sciences Division of the U.S. Department of Energy under Contract No. DE-AC03-76SF00098.

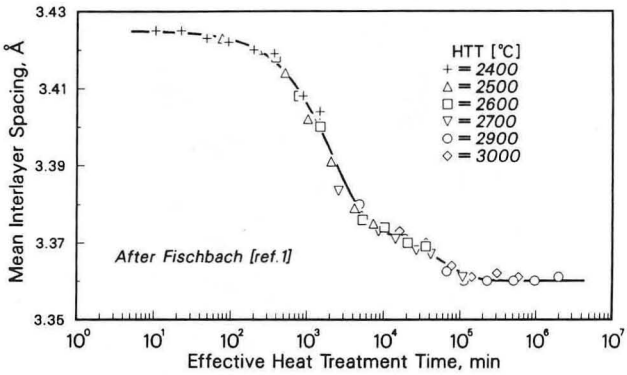

Figure 2-1. Fitting of the data of Fischbach to the four-level model of the mechanism of graphitization. The abscissae have been displaced to refer all data to 2400°C. (XBL 884-1332)

Knowledge that the same metastable states, i.e., carbon interstitial configurations, occur in all graphitizing carbons has enabled an explanation of puzzling features of data obtained in this laboratory.[1] The system of disordered carbon may be considered as a solid solution of interstitial carbon in carbon, with phase boundaries at specific concentrations of carbon interstitials. Thus, the discrete layer spacings correspond to metastable phases, and the spacings are a measure of the concentration and type of carbon interstitials. Since these concentrations are only a few percent by weight, the interstitial concentrations are of the order of 10^{21} cm^{-3}.

1. K. Kawamura and R.H. Bragg, LBL-17982.

3. Work in Progress

Measurements are being made of the electrical conductivity, Hall coefficient, and magnetoresistance of pyrocarbons annealed to achieve the interstitial states discussed in abstract 2, and x-ray measurements are being made to obtain more definitive information on the structure of these phases in order to correlate types of interstitials with electronic properties.

1987 PUBLICATIONS AND REPORTS

Refereed Journals

1. J. Lachter and R.H. Bragg, "Kinetics of Surface Area Changes in Glass-Like Carbon: Reanalysis of the Data," J. Mater. Res. **2**, 846 (1987); LBL-22603.
2. J. Lachter, B.N. Mehrotra, L.G. Henry, and R.H. Bragg, "Non-Kinetic Changes in Heat Treated Glass-Like Carbon," Carbon **25**, 775 (1987); LBL-22358.

LBL Reports

3. J. Lachter, L.G. Henry, and R.H. Bragg, "Indirect Determination of Incoherent Scattering in Disordered Carbon Materials," J. Appl. Cryst. (in press); LBL-15611.
4. R.H. Bragg and J. Lachter, "A Novel Model for the Graphitization Kinetics of Pyrocarbon," LBL-23284.

Ceramic Interfaces*

Andreas M. Glaeser, Investigator

INTRODUCTION

Numerous properties of ceramics depend strongly on microstructure, necessitating control of microstructural characteristics developed during processing. This research program focuses on improving our understanding of processes that dictate the microstructural changes occurring during materials fabrication and utilization. Current efforts are directed at studying microstructure development in model compacts formed from an "ideal," nominally monodispersed, chemically synthesized titania powder. The effects of crystallization, polymorphic phase transformations, and particle substructure on microstructural evolution are being examined by applying transmission electron microscopy to ultramicrotomed sections of heat-treated compacts. In addition, techniques for generating controlled-geometry pore structures at bicrystal and single crystal–polycrystal interfaces are being refined to broaden the range of microdesigned interfacial structures that can be produced, and thus to expand the range of phenomena that can be studied using model experiments. To date, these controlled interfacial pore arrays have been applied primarily to fundamental studies of pore-boundary interactions in doped and undoped alumina.

1. The Role of Particle Substructure in the Sintering and Coarsening of Monosized Titania (Publications 7, 8, and 9)

L.H. Edelson and A.M. Glaeser

The effects of intraparticle substructure on the sintering and coarsening behavior of titania compacts constituted of monosized ($\simeq$0.35-μm diameter) agglomerates of $\simeq$6 nm primary particles (see Figure 1-1) was evaluated. Changes in macroscopic dimensions were correlated with changes in particle microstructure and chemistry. Five contributions to the total shrinkage, and to the temperature ranges for the associated processes, were identified. Firing schedules incorporating low-temperature thermal pretreatments, which crystallize the amorphous as-synthesized powder and induce controlled intra-agglomerate densification, were developed. These anneals had a minimal effect on the apparent particle size distribution, but they modified the subsequent coarsening behavior and the ultimate microstructural characteristics significantly. Porous compacts with controlled, extremely narrow particle size and pore size distributions were produced; these microstructural attributes are desirable for sensor applications.

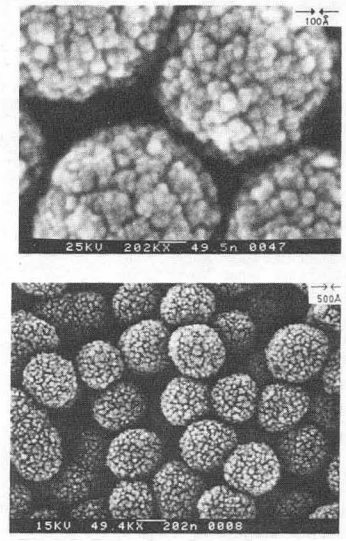

Figure 1-1. High-resolution scanning electron micrographs of monosized, $\simeq$0.35-μm-diameter agglomerates of $\simeq$6-nm primary particles. The evolution of this particle substructure during subsequent annealing has a significant effect on the sintering and coarsening behavior. (XBB 860-9990)

2. The Morphological Stability of Continuous and Finite-Length Phases (Publications 2, 3, 4, and 6)

W.C. Carter and A.M. Glaeser

The morphological stability of finite-length intergranular phases, with coordination numbers (**n**) of 2 and 3, and with dihedral angles ψ ranging from 180° to 0° for **n** = 2 and from 180° to 60° for **n** = 3, has been analyzed. Dihedral angle and coordination number dependent aspect ratios were determined, specifying minimum length/"diameter" ratios necessary for breakup into multiple "particles." This work represents an extension of a previous thermodynamic analysis of the morphological stability of continuous intergranular phases.

*This work was supported by the Director, Office of Energy Research, Office of Basic Energy Sciences, Materials Sciences Division of the U.S. Department of Energy under Contract No. DE-AC03-76SF00098.

3. Production and Application of Microdesigned, Controlled-Morphology, Intergranular Pore Arrays (Publication 5)

J. Rödel and A.M. Glaeser

A technique for generating controlled-geometry pore arrays on single crystal sapphire surfaces, and then "transferring" these arrays to grain boundaries in bicrystals of controlled misorientation, or to single crystal–polycrystal interfaces, has been developed and refined. Arrays of pores having controlled size, size distribution, spacing, and shape can be produced (see Figure 3-1). Model experiments exploiting specimens containing such microdesigned interfacial pore structures have been developed. Phenomena amenable to investigation include pore–grain boundary interactions during sintering (see Figure 3-2), the morphological evolution and stability of high-aspect-ratio intergranular phases (see Figure 3-3), surface energy anisotropy, pore coarsening, pore elimination, high-temperature crack healing, and toughening of ceramic-metal interfaces.

4. Work In Progress

Microstructure development in model compacts formed from an "ideal," monodispersed, chemically synthesized titania powder is under continued investigation. Ultramicrotomed sections of as-settled and heat-treated compacts are being examined using high-resolution transmission electron microscopy. Work on microtomed sections of as-prepared powder has confirmed the particulate substructure deduced from (indirect) measurements of several powder properties and from the sintering characteristics. The general objective of this work is to improve our understanding of how the microstructural characteristics of, and structural evolution within, chemically synthesized ceramic precursors affect the subsequent sintering behavior and microstructural evolution.

Controlled-geometry interfacial pore arrays have been introduced at single crystal–polycrystal (sapphire-alumina) interfaces. The pore size and spacing have been varied to control the magnitude of

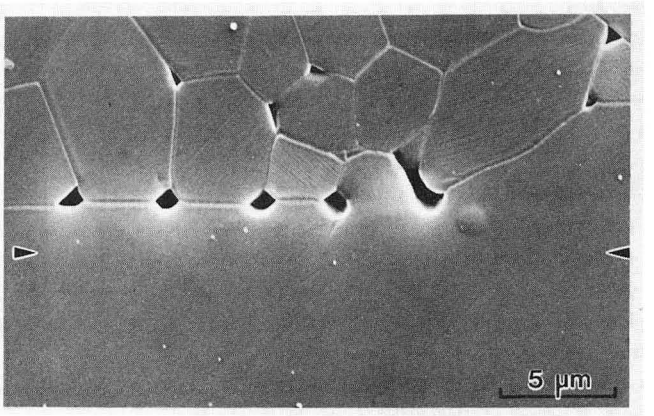

Figure 3-2. Etched single crystal–alumina polycrystal interface following annealing. The arrows indicate the original position of the sapphire-alumina interface. The abrupt decrease in boundary displacement (right to left) is the result of pore drag (left). The ability to systematically change the pore size and spacing is being used to study pore drag effects and pore-boundary separation in alumina. (XBB 8710-9071)

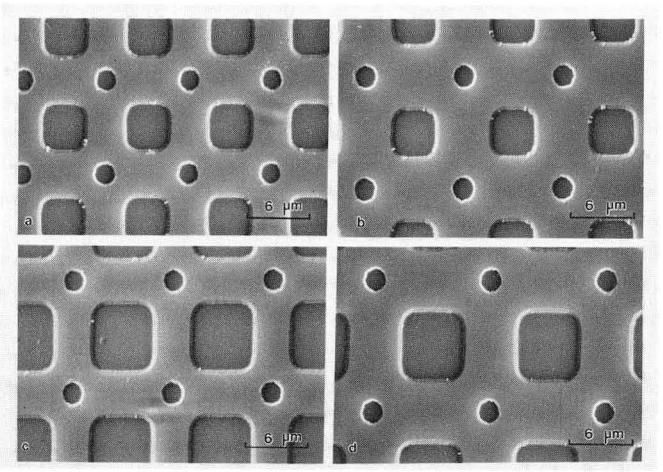

Figure 3-1. Illustration of arrays of surface features having controlled size, size distribution, spacing, and shape. Hot pressing is used to convert these features into internal pores. (XBB 878-6527)

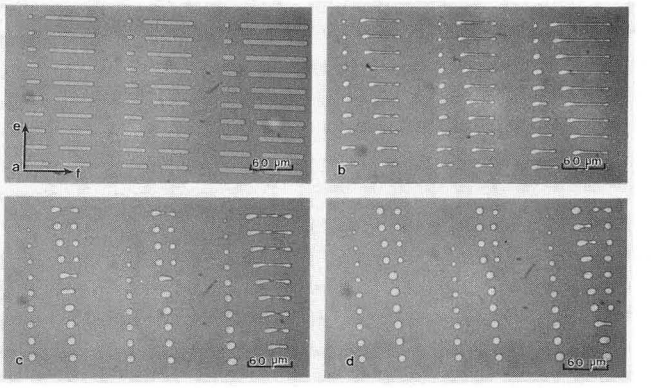

Figure 3-3. Optical micrographs of the morphological evolution of internal, controlled-aspect-ratio pore channels in sapphire at 1600°C after anneals of (a) 0 hr, (b) 30 hr, (c) 120 hr, and (d) 180 hr. Pore arrays were etched into the basal plane. The directions indicated as e and f are $[\bar{1}100]$ and $[11\bar{2}0]$, respectively. Minimum aspect ratios for breakup into multiple particles can be determined. Corresponding anneal times can be used to estimate transport coefficients. (XBB 878-6528)

the pore mobility and the total drag force. Both undoped and Mg-doped alumina polycrystals have been used. During high-temperature annealing, pores either migrate with the boundary or separate from the boundary. The objectives of this work are to determine pore and grain boundary mobilities in both doped and undoped materials, and to identify and "map" the conditions for pore–grain boundary separation and attachment. Avoidance of pore-boundary separation is a requirement for complete densification.

Preliminary studies investigating the feasibility of using controlled-aspect-ratio pore channels to examine the morphological stability of intragranular and intergranular pore channels (in sapphire bicrystals) have been initiated. Pore channel width, sapphire surface orientation, bicrystal misorientation, annealing temperature, and dopant concentration are potential experimental variables. The goals of this work are to improve our understanding of pore structure evolution during sintering and to provide an accurate, reliable, and relatively simple method for measuring surface diffusion coefficients.

1987 PUBLICATIONS AND REPORTS

Refereed Journals

1. L.H. Edelson and A.M. Glaeser, "Method of Removing Surface Porosity on Glassy Carbon Tiles," Carbon **24**, 635 (1986); LBL-20130.
2. W.C. Carter and A.M. Glaeser, "The Morphological Stability of Continuous Intergranular Phases: Thermodynamic Considerations," Acta Metall. **35**, 237 (1987); LBL-20673.
3. W.C. Carter and A.M. Glaeser, "The Effect of Finite Amplitude Perturbations on the Stability of Continuous Phases," Mat. Sci. Eng. **89**, L41 (1987); LBL-21197.
4. A.M. Glaeser, "On the Morphological Stability of Finite-Length Intergranular Phases," Mater. Lett. **5**, 239 (1987); LBL-21326.
5. J. Rödel and A.M. Glaeser, "Production of Controlled Morphology Intergranular Pore Arrays: Implications and Opportunities," J. Am. Ceram. Soc. **70**, C172 (1987); LBL-22717.

LBL Reports

6 W.C. Carter (M.S. Thesis), "The Morphological Stability of Continuous Intergranular Phases: Thermodynamic Considerations," LBL-24695.

7. L.H. Edelson and A.M. Glaeser, "Effects of Thermal Pretreatment on Coarsening of Nominally Monodispersed Titania," J. Am. Ceram. Soc. (in press); LBL-23567.
8. L.H. Edelson and A.M. Glaeser, "The Role of Particle Substructure in the Sintering of Monosized Titania" J. Am. Ceram. Soc. (in press); LBL-23358.
9. L.H. Edelson (M.S. Thesis), "The Role of Particle Substructure in the Sintering of Monosized Titania," LBL-22752.
10. W.C. Carter, "On the Behavior of Fluids in Contact with Solids," submitted to Acta Metall.; LBL-24694.

Invited Talks:

11. J. Rödel, "Production of Controlled Morphology Pore Intergranular Pore Structures in Alumina: Implications and Opportunities," Annual Meeting, American Ceramic Society, Pittsburgh, PA, Apr. 27–30, 1987.
12. W.C. Carter, "Stability of Pores for Ceramics with Dihedral Angle Distributions," Annual Meeting, American Ceramic Society, Pittsburgh, PA, Apr. 27–30, 1987.
13. W.C. Carter, "Two-Dimensional Grain Growth," Annual Meeting, American Ceramic Society, Pittsburgh, PA, Apr. 27–30, 1987.
14. L.H. Edelson, "Role of Particle Substructure in the Sintering of Monosized Titania," Annual Meeting, American Ceramic Society, Pittsburgh, PA, Apr. 27–30, 1987.

SOLID-STATE PHYSICS

EXPERIMENTAL RESEARCH

Far-Infrared Spectroscopy*

Paul L. Richards, Investigator

INTRODUCTION

Improvements in infrared technology are making possible increases in the sensitivity of many types of infrared measurements. In this project, improved types of infrared sources, spectrometers, and detectors are being developed. Improved infrared techniques are being used to do experiments in areas of fundamental and applied infrared physics where their impact is expected to be large.

Progress in infrared technology includes (a) development of a new source for broadly tuned far-infrared spectroscopy based on harmonic generation from microwave oscillators, (b) studies of the voltage-dependent nonlinearity in neutron transmutation doped Ge bolometers and thermometers over the temperature range from 0.1 to 4.2 K, and (c) development of ultrasensitive photoconductive detectors for the 50–1000 μm range. In addition, (d) the bolometric detector previously developed for far-infrared spectroscopy is being reconfigured as a microcalorimeter to measure the heat capacity of monolayers deposited on metal surfaces.

Infrared experiments in progress include (a) measurements of the far-infrared reflectivity of the new high-T_c superconductors, (b) measurements of the infrared emission spectra of molecules chemically adsorbed on metal surfaces, (c) measurements of the infrared spectra of one-dimensional conductors, (d) measurements of the heat capacity of monolayer films on metal surfaces, and (e) an experimental test with unprecedented accuracy of the Planck theory for the shape of the spectral emissivity curve of a blackbody.

*This work was supported by the Director, Office of Energy Research, Office of Basic Energy Sciences, Materials Sciences Division of the U.S. Department of Energy under Contract No. DE-AC03-76SF00098.

1. Energy Gap in the High-T_c Superconductor $La_{1.85}Sr_{0.15}CuO_4$ (Publication 7)

U. Walter, M.S. Sherwin, A. Stacy, P.L. Richards, and A. Zettl†

The far-infrared (FIR) reflectance of the high-T_c superconductor $La_{1.85}Sr_{0.15}CuO_4$ has been measured in the frequency range 15 to 400 cm^{-1}. Below the superconducting onset temperature T = 36 K, absorption features in the FIR spectrum indicate an energy gap with a functional form similar to the BCS gap, but with a smaller magnitude.

†This is a collaborative project with Prof. A. Zettl. Prof. Zettl's research is supported in part by the National Science Foundation.

2. Temperature-Dependent Far-Infrared Reflectance of La-(Sr,Ca)-Cu-O: BCS Electrodynamics—but What is the Energy Gap? (Publication 21)

M.S. Sherwin, P.L. Richards, and A. Zettl†

The available far-infrared data for polycrystalline La-(Sr,Ca)-Cu-O show a reflectance edge with energy near 2.5 k_BT_c. This edge has been variously interpreted as the onset of absorption due to an energy gap, and as a low-frequency plasma edge caused by strong far-infrared resonances. Our measured temperature dependence of the reflectance edge closely fits the temperature dependence of the order parameter in a mean-field theory, and hence is consistent with the energy-gap hypothesis (see Figures 2-1, 2-2, and 2-3). In this paper, we construct a model dielectric function for $La_{1.85}Sr_{0.15}CuO_4$ that is consistent with mean-field theory and the hypothesis of a plasma edge. We find that the temperature dependence of the plasma frequency in this model also closely fits the measured temperature dependence of the reflectance edge. Furthermore, both hypotheses accurately predict the experimentally observed temperature dependence of the absorption at frequencies much less than the reflectance edge. This observation has significant implications for the construction

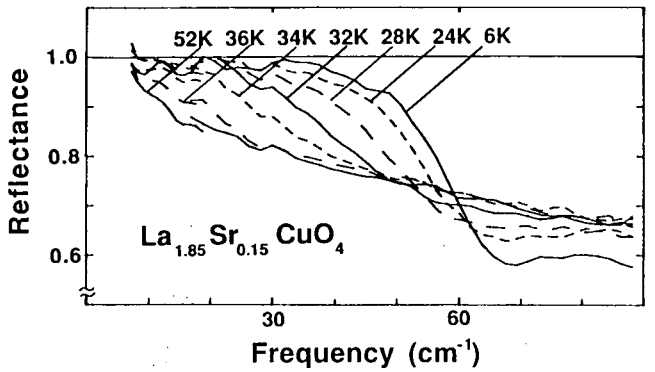

Figure 2-1. Reflectance of polycrystalline $La_{1.85}Sr_{0.15}CuO_4$ at selected temperatures above and below T_{co}. The temperature-dependent reflectance edge has been interpreted both as an energy gap and as a plasma edge. (XBL 881-1)

of fast low-loss superconducting devices. We conclude that the electrodynamics of the superconducting transition in $La_{1.85}Sr_{0.15}CuO_4$ are well described by a BCS-like mean-field theory. However, given the identical predictions of the energy-gap and plasma-edge hypotheses, it is premature to deduce a precise value for the magnitude of the energy gap from the infrared data.

†This is a collaborative project with Prof. A. Zettl. Prof. Zettl's research is supported in part by the National Science Foundation.

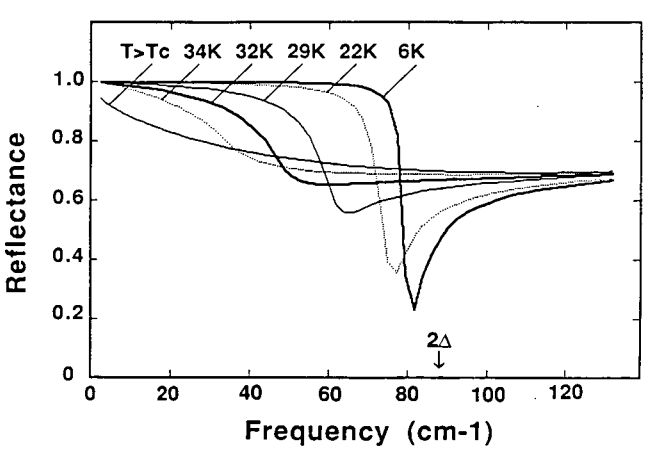

Figure 2-2. Reflectance of polycrystalline $La_{1.85}Sr_{0.15}CuO_4$ calculated at selected temperatures from a model that contains free carriers and a strong phonon, and treats the reflectance edge as a plasma edge. The model qualitatively reproduces the experimental data of Figure 2-1. The position of the energy gap $2\Delta(T=0)$ used in this calculation is marked with an arrow. There is no obvious feature in the calculated reflectance at this frequency. (XBL 881-2)

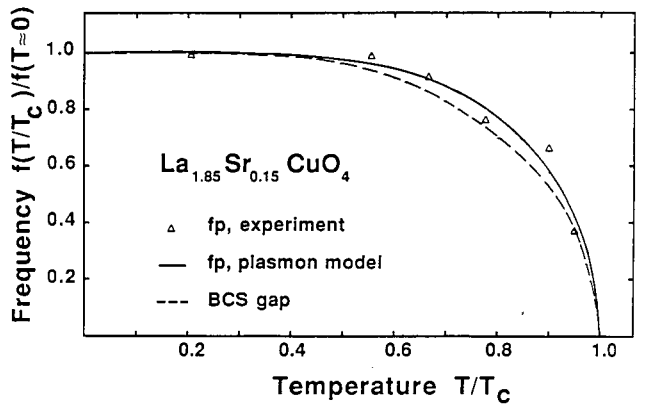

Figure 2-3. Frequency of the reflectance edge vs. reduced temperature for experiment (triangles) and for the plasmon model (solid line). The BCS gap is also plotted (dashed line). We conclude from this modeling exercise that no strong feature marking the energy gap is expected in the far-infrared reflectivity of polycrystalline $La_{1.85}Sr_{0.15}CuO_4$ (and probably also in $YB_2C_3O_7$). Despite the claims of some groups, the presence of a BCS gap-like feature with the BCS temperature dependence in polycrystalline samples cannot be used as evidence that a gap has been observed. (XBL 881-3)

3. A Stressed Photoconductive Detector for Far-Infrared Space Applications (Publication 12)

J.-Q. Wang, P.L. Richards, J.W. Beeman, and E.E. Haller†

An optimized leaf-spring apparatus for applying uniaxial stress to a Ge:Ga far-infrared photoconductor has been designed and tested. This design has significant advantages for space applications that require high quantum efficiency and stable operation over long periods of time. The important features include adequate spring deflection with relatively small overall size, torque-free stress, easy measurement of applied stress, and a detector configuration with high responsivity. One-dimensional arrays of stressed photoconductors can be constructed using this design (see Figure 3-1). A peak responsivity of 38 A/W is achieved in a detector with a cutoff wavelength of 200 μm, which was operated at a temperature of 2.0 K and a bias voltage equal to one half of the breakdown voltage.

†Samples for this study were provided by the group led by Prof. E.E. Haller. Prof. Haller's work is supported by the Engineering Division of LBL.

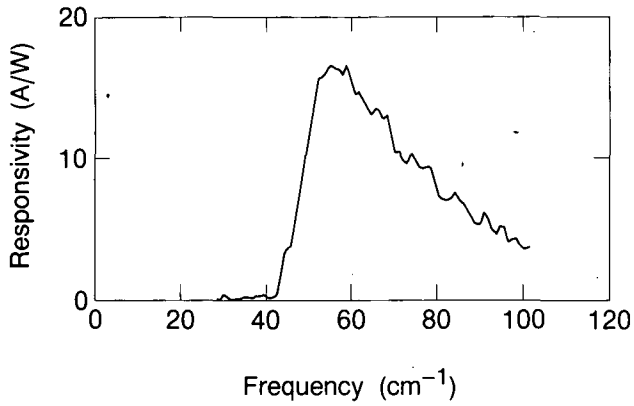

Figure 3-1. Absolute spectral responsivity of a Ge:Ga endfire photoconductor with large stress showing an onset of photoconductivity at 45 cm^{-1}. Without stress, the onset is at 85 cm^{-1} in Ge:Ga. (XBL 8611-6482)

4. An Infrared Emission Study of the Molecule-Substrate Mode of CO on Pt(111) (Publication 3)

R.G. Tobin and P.L. Richards

We have used infrared emission spectroscopy to study the molecule-substrate vibrational mode of on-top CO on Pt(111), as a function of coverage and of temperature, in the range from 210 to 400 K. Little change in the line is observed as a function of coverage, except for an abrupt shift, of ~6 cm^{-1}, to lower frequency, at coverages >0.5. The line shape is asymmetric, and the linewidth varies much more slowly with temperature than is predicted by theories of lifetime broadening by phonon emission. Based on these observations, our conclusion is that the line is inhomogeneously broadened (see Figure 4-1). Our measurements place an upper limit on the homogeneous linewidth for this mode. The conclusion that the line is inhomogeneously broadened is in contrast to suggestions that the corresponding mode of CO on Ni(100) is lifetime broadened by a two-phonon decay process. We also report the observation of the atom-substrate mode of O on Pt(111).

5. Work in Progress

Measurements are being carried out of the far-infrared transmittance and reflectance of a-b plane films of $YBa_2Cu_3O_7$ on $SrTiO_3$ substrates.

Measurements of the far-infrared absorptance of a-b plane single-crystal samples are also in progress. These measurements will be analyzed in terms of energy-gap models.

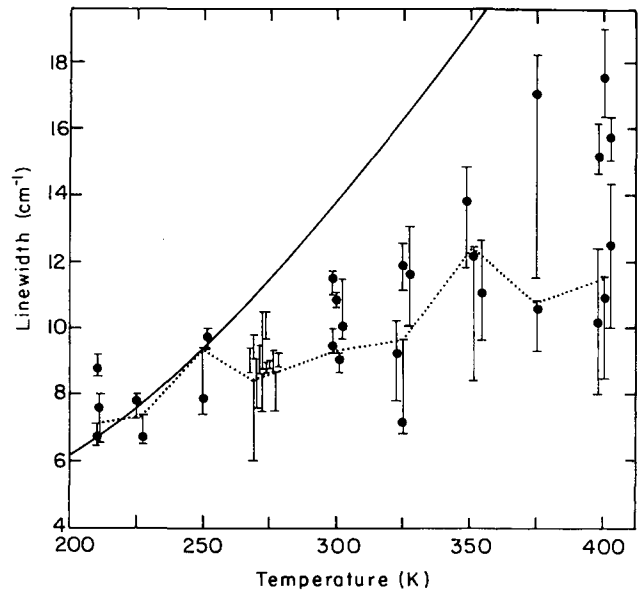

Figure 4-1. Linewidth of the C-Pt stretch band as a function of temperature. The solid line represents the predicted temperature dependence of the linewidth due to either three-phonon decay or dephasing, calculated within the Persson model and normalized to the experimentally determined linewidth at 210 K. The dotted line represents an upper limit on the natural linewidth of the mode, which appears to be inhomogeneously broadened. (XBL 863-7592)

Measurements of the temperature dependence of the linewidth of the molecule-substrate mode of CO on Ni(100) are being made to distinguish between different theoretical predictions for the effects of multiple phonon relaxation.

Our new technique for measuring the heat capacity of monolayer overlayers on solid surfaces is being used to measure the melting transition of monolayers of ^{4}He on metal films.

Measurements of the spectral shape of the emission from a blackbody as a function of temperature and far-infrared frequency are in progress.

Construction has begun on a new source for broadly tuned far-infrared spectroscopy based on harmonic generation from microwave oscillators.

1987 PUBLICATIONS AND REPORTS

Refereed Journals

1. J.L. Bonomo, J.B. Peterson, P.L. Richards, and T. Timusk, "Calibration of a Photometer for Measurement of the Cosmic Microwave Background," Gamow Cosmology **LXXXVI**, 341 (1986); LBL-14739.†
2. D.G. Crété, W.R. McGrath, P.L. Richards, and F.L. Lloyd, "Performance of Arrays of SIS Junctions in

Heterodyne Mixers," IEEE Trans. Microwave Theory Tech. **MTT-35**, 435 (1987).‡

3. R.G. Tobin and P.L. Richards, "An Infrared Emission Study of the Molecule-Substrate Mode of CO on Pt(111)," Surf. Sci. **179**, 387 (1987); LBL-21506.
4. A.E. Lange, S. Hayakawa, T. Matsumoto, H. Matsuo, H. Murakami, P.L. Richards, and S. Sato, "A Rocket-Borne Submillimeter Radiometer," Appl. Opt. **26**, 401 (1987).§
5. S. Sato, S. Hayakawa, A.E. Lange, T. Matsumoto, H. Matsuo, H. Murakami, and P.L. Richards, "Horn Antenna with Low Sidelobe Response for Observations of Diffuse Celestial Radiation," Appl. Opt. **26**, 410 (1987).§
6. R.G. Tobin, R.B. Phelps, and P.L. Richards, "An Infrared Emission Study of the C=O Stretch Vibration of Bridge-Bonded CO on Pt(111)," Surf. Sci. **183**, 427 (1987); LBL-22229.
7. U. Walter, M.S. Sherwin, A. Stacy, P.L. Richards, and A. Zettl, "Energy Gap in the High-T_c Superconductor $La_{1.85}Sr_{0.15}CuO_4$," Phys. Rev. B Rapid Commun. **B35**, 5327 (1987); LBL-22989.‖
8. R.G. Tobin, "Vibrational Linewidths of Adsorbed Molecules: Experimental Considerations and Results," Surf. Sci. **183**, 226 (1987); LBL-21912.
9. P.L. Richards, "Progress in the Development of SIS Quasiparticle Mixers," IEEE Trans. Magn. **MAG-23**, 1247 (1987).‡
10. G.-J. Cui, D.W. Face, E.K. Track, D.E. Prober, A.V. Räisänen, D.G. Crété, and P.L. Richards, "High Quality Ta/PbBi Tunnel Junctions for 85–110 GHz SIS Mixer Experiments," IEEE Trans. Magn. **MAG-23**, 688 (1987).‡
11. M.S. Sherwin, A. Zettl, and P.L. Richards, "Complete Excitation Spectrum for a Charge Density Wave System," Phys. Rev. B Rapid Commun. **B36**, 6708 (1987); LBL-22624.‖
12. J.-Q. Wang, P.L. Richards, J.W. Beeman, and E.E. Haller, "A Stressed Photoconductive Detector for Far-Infrared Space Applications," Appl. Opt. **26**, 4767 (1987); LBL-23222.**
13. R.G. Tobin and P.L. Richards, "The Vibrational Line Shapes of CO on Pt(111) Studied by Infrared Emission Spectroscopy," J. Vac. Sci. Technol. **A5**, 454 (1987); LBL-21505.

Other Publications

14. P.L. Richards and R.G. Tobin, "Infrared Spectroscopy of Adsorbates on Metals: Direct Absorption and Emission," in *Vibrational Spectroscopy of Molecules on Surfaces*, Vol. 1 of *Methods of Surface Characterization*, J.T. Yates, Jr., and T.E. Madey, Eds., Plenum Publ. Corp., New York, 1987, p. 417; LBL-20228.
15. A.E. Lange (Ph.D. Thesis), "An Attempt to Measure the Diffuse Brightness of the Sky at Submillimeter Wavelengths.†
16. P.L. Richards, "Measuring the Temperature of the Universe," Bull. Am. Phys. Soc. **32**, 33 (1987).†
17. T.W. Kenny and P.L. Richards, "Heat Capacity Measurements of Multilayers Adsorbed on Evaporated Metal Films," Bull. Am. Phys. Soc. **32**, 434 (1987); LBL-22625abs.
18. R.B. Phelps, R.G. Tobin, and P.L. Richards, "The C=O Stretch Mode of Bridge-Bonded CO on Pt(111) Studied by Infrared Emission Spectroscopy," Bull. Am. Phys. Soc. **32**, 863 (1987); LBL-22626abs.
19. A.V. Räisänen, D.G. Crété, P.L. Richards, and F.L. Lloyd, "A 100 GHz SIS Quasiparticle Mixer with 10 dB Coupled Gain," IEEE Microwave Theory Tech. MTT-S Digest **II**, 929 (1987).‡
20. M.S. Sherwin, A. Zettl, and P.L. Richards, "Far Infrared Response of $(TaSe_4)_2I$: Observation of the Charge Density Wave Optical Phason," Bull. Am. Phys. Soc. **32**, 521 (1987): LBL-23059abs.‖

LBL Reports

21. M.S. Sherwin, P.L. Richards, and A. Zettl, "Temperature Dependent Far Infrared Reflectance of La-(Sr,Ca)-Cu-O: BCS Electrodynamics—But What is the Energy Gap?" Phys. Rev. B1 (in press); LBL-24160.‖
22. M.S. Sherwin, P.L. Richards, and A. Zettl, "Far Infrared Reflectance of La-(Sr,Ca)-Cu-O: BCS Electrodynamics but Uncertain Energy Gap," Bull. Am. Phys. Soc. (in press); LBL-24502abs.‖
23. T.W. Kenny and P.L. Richards, "Heat Capacity Measurements of Gas Phase ^4He Adsorbed on Evaporated Silver Films," Bull. Am. Phys. Soc. (in press); LBL-24504abs.

Invited Talks

24. P.L. Richards, "Measuring the Temperature of the Universe," Joint Meeting, American Physical Society and American Association of Physics Teachers, San Francisco, CA, Jan. 28–31, 1987.
25. P.L. Richards, "SIRTF Detectors," Department of Physics Seminar, Nagoya University, Japan, Feb. 25, 1987.
26. P.L. Richards, "RF Impedance Matching Structures for Planar SIS Mixers," Submillimeter (Terahertz) Receiver Technology Conference, Lake Arrowhead, CA, Apr. 7–8, 1987.
27. P.L. Richards, "Rocket Measurement of the Submillimeter Background," Alvarez Group Seminar, Lawrence Berkeley Laboratory, Berkeley, CA, Apr. 13, 1987.
28. A.E. Lange, "A Measurement of the Submillimeter Background," Delta T Over Tea Workshop, University of Toronto, Ontario, May 1, 1987.
29. P.L. Richards, "Measuring the Temperature of the Universe," General Motors Research Laboratories, Eclectic Lecture Series, Warren, MI, May 13, 1987.
30. P.L. Richards, "Superconducting Detectors," Santa Barbara Research Center, Goleta, CA, May 28, 1987.
31. P.L. Richards, "Spectrum of the Microwave Background," Third International IRAS Conference,

"Comets to Cosmology," London, England, July 6–10, 1987.

32. P.L. Richards, "Superconducting Detectors for Infrared and Microwaves," Rockwell International Science Center, Thousand Oaks, CA, July 20, 1987.
33. P.L. Richards, "Superconducting Detectors for Infrared and Microwaves," Hughes Aircraft Co., Space and Communcations Group, El Segundo, CA, July 21, 1987.
34. P.L. Richards, "The Submillimeter Spectrum of the Cosmic Background Radiation," Miller Institute for Basic Research in Science, Berkeley, CA, Dec. 8, 1987.
35. P.L. Richards, "Far Infrared Properties of New High T_c Superconductors," 12th International Conference on Infrared and Millimeter Waves, Walt Disney World Village, FL, Dec. 14–18, 1987.
36. P.L. Richards, "Rocket Measurement of the Cosmic Background at Submillimeter Wavelengths," 12th International Conference on Infrared and Millimeter Waves, Walt Disney World Village, FL, Dec. 14–18, 1987.

---

†Supported in part by the U.S. National Aeronautics and Space Administration.

‡Supported in part by the U.S. Air Force Office of Scientific Research.

§Supported by the National Science Foundation and the California Space Institute.

‖Collaboration with Prof. A. Zettl, whose research is supported by the National Science Foundation.

**Collaboration with Prof. E. E. Haller, whose research is supported by the Engineering Division of Lawrence Berkeley Laboratory.

Experimental Solid State Physics and Quantum Electronics*

Y.R. Shen, Investigator

INTRODUCTION

The object of this program is to further basic understanding of laser interaction with matter and to develop modern optical techniques for material studies. Both theoretical and experimental research on various aspects of nonlinear interaction of light with matter are being carried out. Newly developed techniques are being used to study problems of current interest.

Current research projects include (1) search for a basic understanding of surface nonlinearities at interfaces, (2) evaluation of the possibility of using optical second-harmonic generation to study surface magnetization, (3) development of the infrared (IR)-visible sum-frequency generation technique for surface vibrational spectroscopy, (4) use of nonlinear optical spectroscopic techniques to study local modes of molecules and vibrational predissociation of molecular clusters in molecular beams, and (5) development of coherent tunable light sources in the vacuum ultraviolet range.

1. Highly Resolved Spectra of Local Modes of Benzene (Publication 6)

R.H. Page, Y.R. Shen, and Y.T. Lee

The familiar normal-mode (NM) picture describes well the small-amplitude molecular vibrations at low vibrational excitations. But as the vibrational energy is raised, the density of vibrational states increases rapidly, and anharmonic couplings between normal modes become important; the normal-mode picture then ceases to provide a good description of the vibrational motion. It was found that for some molecules even at relatively high vibrational energies (10,000–25,000 cm^{-1}), there still exist well-defined peaks in the vibrational spectrum. They were identified as overtone vibrations confined largely to single bonds — for example, a C-H stretch. Such vibrations localized to single bonds are often known as local modes (LM).

Couplings between the LM and other modes, however, add fine structure to the LM spectrum. For a better understanding of high excited molecular vibrations, we would like to know how the vibrational spectrum changes from the NM to the LM picture as the vibrational energy increases. Reported measurements on the C-H stretches of benzene showed that even in the transformation from NM to LM, the successive overtones seem to be always fairly broad, with widths in the tens of inverse centimeters. We wonder whether the observed widths were the results of poor spectral resolution or actual lifetime broadening.

With the help of supersonic cooling of molecules and the nonlinear-labeling spectroscopic technique, we were able to obtain high-resolution spectra for the C-H stretches of benzene from $\nu = 1$ to $\nu = 3$. Rich fine structure in the spectra has been observed (see Figure 1-1). Transformation from the NM picture to the LM picture seems to occur between $\nu = 2$ and $\nu = 3$. Vibrational lifetimes in local-mode bands exceed ~0.5 psec.

2. Surface Vibrational Spectroscopy by Infrared-Visible Sum-Frequency Generation (Publication 1)

X.D. Zhu, H. Suhr, and Y.R. Shen

We report here the first successful observation of a vibrational spectrum of a monolayer adsorbed by the technique. To see that the technique could be applied to surface vibrational spectroscopy in the mid-IR region, we chose to study modes between 920 and 1100 cm^{-1} using a discretely tunable CO_2 laser. The results pave the way for future dynamic studies of surface phonons and molecular vibrations.

Surface vibrational spectroscopy is important for *in-situ* identification of adsorbates on surfaces and for understanding of interactions between adsorbates and between adsorbates and surfaces. This has led to the development of a number of surface spectroscopic techniques. However, none of these techniques are suitable for studies of fast surface molecular dynamics. We have now developed a new optical probe based on infrared-visible sum-frequency generation (SFG) that is also capable of following surface modification with a subpicosecond time resolution.

*This work was supported by the Director, Office of Energy Research, Office of Basic Energy Sciences, Materials Sciences Division of the U.S. Department of Energy under Contract No. DE-AC03-76SF00098.

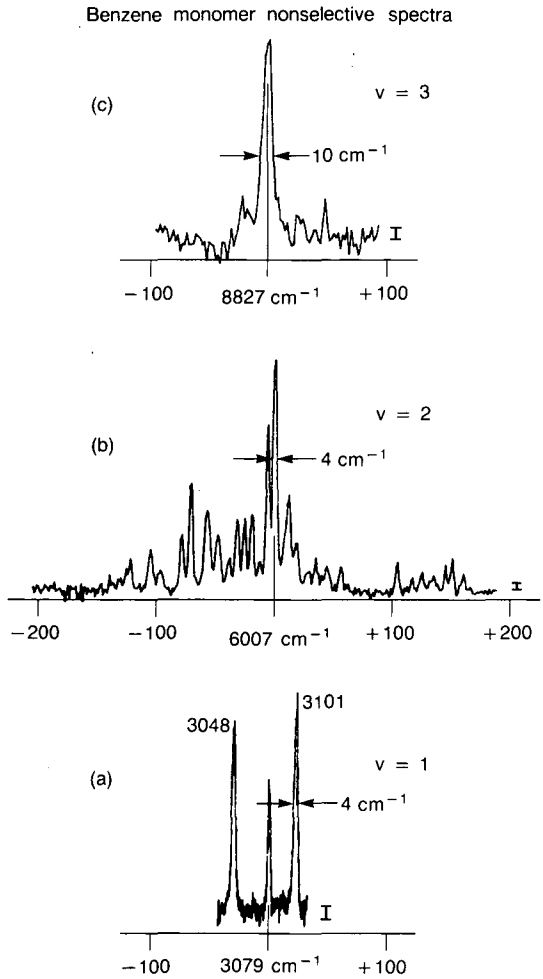

Figure 1-1. Nonselective (Q-branch probe) spectra of v = 1, 2, and 3 bands of CH stretches of benzene. Absorption is in arbitrary units; error bars indicate the noise level. Band centers are marked at 3079, 6007, and 8827 cm^{-1}. "Localization" is evident in the spectra as v increases from 1 to 3. (XBL 872-6146)

3. Observation of C-H Stretch Vibrations of Monolayers of Molecules Using Optical Sum-Frequency Generation: Study of Molecular Orientation in a Langmuir Film (Publications 7 and 18)

J.H. Hunt, P. Guyot-Sionnest, and Y.R. Shen

We report the observation of the C-H stretch modes of monolayers of a number of molecules adsorbed on glass and water using sum-frequency generation. For this measurement we used a picosecond optical parametric amplifier tuned around 3.5 μm together with a picosecond frequency-doubled Nd:YAG laser. The results are most interesting and exciting. They show that surface vibrational spectroscopy can be carried out with picosecond or femtosecond laser pulses. The technique, therefore, is potentially a very powerful tool for *in situ* studies of surface molecular dynamics and surface reactions.

We have applied this technique to obtain the vibrational spectrum of a monolayer of pentadecanoic acid on water in the CH stretch region. From the polarization dependence, we were able to deduce the average orientation of the CH_3 group on the molecules. We have monitored the molecular orientation at different surface densities (see Figure 3-1). It was found that the molecules in the liquid condensed phase have their alkane chains extended and oriented nearly normal to the surface, while in the liquid expanded phase the chains are highly disordered.

4. Local and Nonlocal Surface Nonlinearities for Surface Optical Second-Harmonic Generation (Publication 9)

P. Guyot-Sionnest and Y.R. Shen

We investigated the physical origins of the surface nonlinear susceptibility responsible for surface optical second-harmonic generation (SHG). The SH signal generated in reflection from an interface

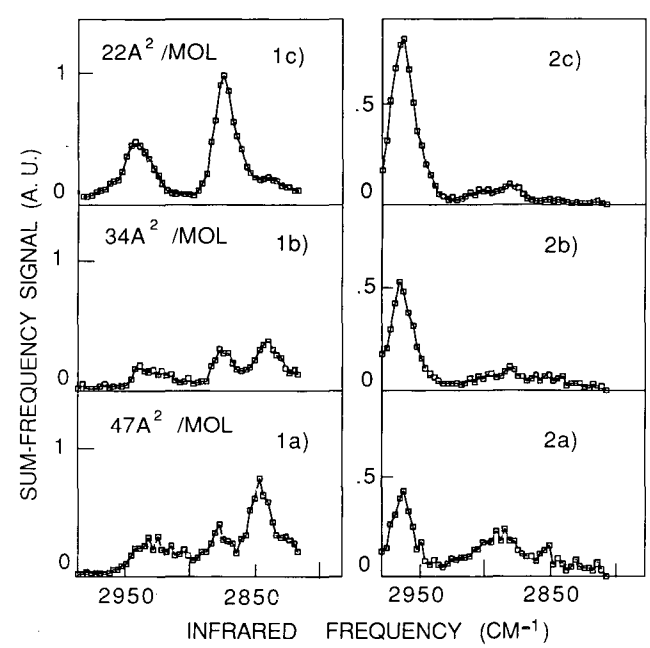

Figure 3-1. SFG spectra of pentadecanoic acid at different surface coverages normalized per molecule. (1a)-(1c) were taken with the s-visible, p-IR polarization combination. (2a)-(2c) were taken with p-visible, s-IR combination. (XBL 877-3072)

between two centrosymmetric media comes partly from the interfacial layer with electric-dipole contribution and partly from the bulk with electric-quadrupole and magnetic-dipole contributions; the former part often dominates or is at least comparable to the latter. While it is easy to see that the strong surface nonlinearity arises from the broken symmetry at the interface, the more detailed physical origin of the surface nonlinearity is still a subject of confusion. Is the field discontinuity or the structural discontinuity, or both, at the interface responsible for the nonlinearity? Is the nonlinearity dominated by local or nonlocal response of the interfacial layer to the applied field?

Experiments performed on simple covalent systems were designed to distinguish between the nonlocal electric-quadrupole-type nonlinearity induced by field discontinuity and the local intrinsic, electric-dipole-type nonlinearity of a surface or interface. We find that both mechanisms could operate: the latter usually dominates when the surface layer has a strong structural asymmetry with the fundamental or the second-harmonic frequency at resonance with a dipole-allowed transition.

5. Optical Second-Harmonic Generation as a Probe for Surface Magnetization (Publication 4)

R.P. Pan and Y.R. Shen

Surface magnetization is a subject of great current interest. We suggest here that optical second-harmonic generation could be used as an effective tool to probe surface magnetization. The idea is based on the fact that the normally vanishing tensor components of the second-order nonlinear optical susceptibility of a surface may become nonvanishing in the presence of a surface magnetization. The experimental feasibility is supported by a numerical estimate.

6. Infrared Vibrational Predissociation Spectra of Large Water Clusters (Publication 8)

R.H. Page, M.F. Vernon, Y.R. Shen, and Y.T. Lee

The infrared absorption spectrum in the O-H stretching region of $(H_2O)_{19}$ clusters formed in a supersonic molecular beam is reported. It was obtained with mass-spectrometric detection and is compared with a similarly obtained spectrum of $(H_2O)_6$ and a large-cluster spectrum obtained with bolometric detection.

The mass-resolved spectra show a broad absorption band between $\sim$3200 and 3600 cm^{-1}, reminiscent of the H-bonding feature in a condensed-phase spectrum. The spectrum obtained with a bolometer is peaked in the blue of this region, suggesting that the level of H-bonding is much lower. It must be dominated by small and/or warm clusters such as dimers. Mass resolution is clearly advantageous in selectively obtaining spectra of large clusters, free of interference from smaller ones.

7. Frequency Tripling into the 720–1025 Å Region with Pulsed Free Jets (Publication 5)

R.H. Page, R.J. Larkin, A.H. Kung, Y.R. Shen, and Y.T. Lee

We have developed a coherent source of extreme ultraviolet (XUV) light, which is continuously tunable between 904 and 1024 Å, and line tunable to 720 Å. It employs the technique of frequency tripling in a pulsed free jet of gas and requires a single tunable laser system. Spectra of the relative XUV output vs wavelength in the 904–1024 Å range are obtained for the tripling gases Ar, Kr, Xe, CO, and N_2. Relative outputs obtained by tripling at resonantly enhanced lines between 720 and 900 Å in Kr, Xe, and CO are also measured.

8. Work in Progress

The possibility of using optical SHG to study monolayer adsorption on substrates without inversion symmetry is being explored. With the help of polarization discrimination, the bulk contribution to the second-harmonic signal could be largely suppressed. The success of this experiment would eliminate the widely believed limitation of SHG as a surface probe that can only be applied to media with inversion symmetry.

Laser desorption, mass spectroscopy, and SHG are being used together to study thermal desorption with an exceptionally fast heating rate. The preexponential factor and the desorption energy barrier could be determined from the results.

Surface diffusion, plasma deposition, and metal deposition on polymers are being probed by SHG. An ultrahigh-vacuum chamber for such experiments has been constructed.

Collaboration with Y.T. Lee on the studies of local modes of benzene, vibrational structure of electronically excited benzene, and photoionization spectra of water cluster is being brought to an end. The technique developed in these experiments combines nonlinear optical spectroscopy with supersonic molecular beams; it is generally applicable to other molecular spectroscopic problems.

1987 PUBLICATIONS AND REPORTS

Refereed Journals

1. X.D. Zhu, H. Suhr, and Y.R. Shen, "Surface Vibrational Spectroscopy by Infrared-Visible Sum-Frequency Generation," Phys. Rev. B Rapid Commun. **35**, 3047 (1987); LBL-21636.
2. P. Guyot-Sionnest, T.F. Heinz, and Y.R. Shen, "Comments on 'Determination of the Nonlinear Optical Susceptibility $\chi^{(2)}$ of Surface Layers' by B. Dick *et al.*," Appl. Phys. B **42**, 237 (1987); LBL-21637.
3. D.H. Auston, T.K. Gustafson, A.E. Kaplan, P.L. Kelley, and Y.B. Shen, "Limits on Nonlinear Optical Interactions," Appl. Opt. **26**, 231 (1987).
4. R.-P. Pan and Y.R. Shen, "Optical Second Harmonic Generation as a Probe for Surface Magnetization," Chin. J. Phys. **25**, 175 (1987); LBL-22569.
5. R.H. Page, R.J. Larkin, A.H. Kung, Y.R. Shen, and Y.T. Lee, "Frequency Tripling into the 720–1025 Å Region with Pulsed Free Jets," Rev. Sci. Instrum. **58**, 1616 (1987); LBL-23306.
6. R.H. Page, Y.R. Shen, and Y.T. Lee, "Highly-Resolved Spectra of Local Modes of Benzene," Phys. Rev. Lett. **59**, 1293 (1987); LBL-23768.
7. P. Guyot-Sionnest, J.H. Hunt, and Y.R. Shen, "Sum-Frequency Vibrational Spectroscopy of a Langmuir Film: Study of Molecular Orientation of a Two-Dimensional System," Phys. Rev. Lett. **59**, 1597 (1987); LBL-23771.†
8. R.H. Page, M.F. Vernon, Y.R. Shen, and Y.T. Lee, "Infrared Vibrational Predissociation Spectra of Large Water Clusters," Chem. Phys. Lett. **141**, 1 (1987); LBL-24006.
9. P. Guyot-Sionnest and Y.R. Shen, "Local and Nonlocal Surface Nonlinearities for Surface Optical Second-Harmonic Generation," Phys. Rev. B **35**, 4420 (1987); LBL-22490.

Other Publications

10. Y.R. Shen, "Surface Studies by Nonlinear Optics," in *Proc. IVth Int. School on Laser Spectroscopy and Applications*, Vilnius, USSR, August 1987.
11. J.H. Hunt, P. Guyot-Sionnest, and Y.R. Shen, "Second-Harmonic and Sum-Frequency Generation for Surface Studies," in *Laser Spectroscopy VIII*, W. Persson and S. Svanberg, Eds., Springer-Verlag, Berlin, 1987, p. 253; LBL-23676.†
12. E.W. Plummer, T. Gustafsson, D.R. Hamann, I. Lindau, D.L. Mills, C.F. Quate, and Y.R. Shen, "New Ways of Looking at Surfaces," in *Advancing Materials Research*, P.A. Psaras and H.D. Langford, Eds., National Academy Press, Washington, D.C., 1987, p. 283.

LBL Reports

13. R.H. Page (Ph.D. Thesis), "Nonlinear-Spectroscopic Studies of Highly Excited States of Molecules in Supersonic Beams," LBL-23307.
14. R.H. Page, Y.R. Shen, and Y.T. Lee, "Infrared-Ultraviolet Double Resonance Studies of Benzene Molecules in a Supersonic Beam," accepted by J. Chem. Phys.; LBL-23769.
15. R.H. Page, Y.R. Shen, and Y.T. Lee, "Local Modes of Benzene and Benzene Dimer, Studied by Infrared-Ultraviolet Double Resonance in a Supersonic Beam," accepted by J. Chem. Phys.; LBL-24007.
16. T. Stehlin, M. Feller, P. Guyot-Sionnest, and Y.R. Shen, "Optical Second Harmonic Generation as a Surface Probe for Non-Centrosymmetric Media," submitted to Opt. Lett.; LBL-24365.
17. R.H. Page, R.J. Larkin, Y.R. Shen, and Y.T. Lee, "High Resolution Photoionization Spectrum of Water Molecules in a Supersonic Beam," accepted by J. Chem. Phys.; LBL-24158.
18. P. Guyot-Sionnest, R. Superfine, J.H. Hunt, and Y.R. Shen, "Vibrational Spectroscopy of a Silane Monolayer at Air/Solid and Liquid/Solid Interfaces using Sum-Frequency Generation," accepted by Chem. Phys. Lett.; LBL-24365.†
19. P. Guyot-Sionnest (Ph.D. Thesis), "Optical Second Harmonic Generation and Infrared Visible Sum Frequency Generation as a Surface Probe."
20. R. Superfine, P. Guyot-Sionnest, J.H. Hunt, C.T. Kao, and Y.R. Shen, "Surface Vibrational Spectroscopy of Molecular Adsorbates on Metals and Semiconductors by Infrared-Visible Sum-Frequency Generation," submitted to Surf. Sci.; LBL-24434.†

Invited Talks

21. Y.R. Shen, "Optical Probing of Surfaces, Interfaces, and Films," Western Spectroscopy Association, 34th Annual Conference on Modern Spectroscopy, Asilomar, CA, Jan. 28–30, 1987.
22. Y.R. Shen, "Nonlinear Optical Probing of Adsorbates at Interfaces," General Motors Research Laboratories, Warren, MI, Feb. 16, 1987.
23. Y.R. Shen, "Nonlinear Optical Experiments on Interfaces," Modern Optics and Spectroscopy Seminar, MIT, Cambridge, MA, Feb. 17, 1987.
24. Y.R. Shen, "Nonlinear Optical Probing of Adsorbates at Interfaces," Seminar, JILA, Boulder, CO, Feb. 24, 1987.

25. Y.R. Shen, "Recent Experiments on Nonlinear Optical Studies of Adsorbates at Interfaces," Department of Chemistry, Caltech, Pasadena, CA, Mar. 10, 1987.
26. Y.R. Shen, "Surface and Interface Studies by Second Harmonic and Sum-Frequency Generation," Laser Spectroscopy Workshop, Lake Arrowhead, CA, Mar. 14–15, 1987.
27. M.S. Wartak, L.H. Yang, C.Y. Fong, and Y.R. Shen, "Localization in Multivibrational Coherent Excitations," March Meeting of the American Physical Society, New York, Mar. 16–20, 1987.
28. Y.R. Shen, "Nonlinear Optical Probing of Molecules at Interfaces," 193rd National American Chemical Society Meeting, Denver, CO, Apr. 5–10, 1987.
29. J.H. Hunt, P. Guyot-Sionnest, and Y.R. Shen, "Sum-Frequency Generation for Surface Vibrational Spectroscopy," XV International Conference on Quantum Electronics, Baltimore, MD, Apr. 1987.
30. P. Guyot-Sionnest, "Surface Vibrational Spectroscopy by Sum-Frequency Generation," Exxon Research and Engineering Co., Annandale, NJ, Apr. 30, 1987.
31. J.H. Hunt, P. Guyot-Sionnest, and Y.R. Shen, "Second-Harmonic and Sum-Frequency Generation for Surface Studies," 8th International Conference on Laser Spectroscopy, Åre, Sweden, June 22–26, 1987.
32. Y.R. Shen, "Surface Studies by SHG," 3M Central Research Laboratories, St. Paul, MN, July 9, 1987.
33. Y.R. Shen, "Surface Studies by Nonlinear Optics," IVth International School on Laser Spectroscopy and Applications, Vilnius, USSR, Aug. 1987.
34. Y.R. Shen, "Probing Molecular Adsorbates by Surface Nonlinear Optics," XIIIth International Conference on Photochemistry, Budapest, Hungary, Aug. 9–14, 1987.
35. Y.R. Shen, "Recent Advances in Surface Studies by Nonlinear Optics," Max-Planck-Institute, Göttingen, Federal Republic of Germany, Sept. 30, 1987.
36. Y.R. Shen, "Nonlinear Optical Probing of Surfaces and Interfaces," Kernforschungsanlage, Jülich, Federal Republic of Germany, Oct. 8, 1987.
37. G. Yang and Y.R. Shen, "Self-Phase Modulation and Spectral Broadening of Ultrashort Pulses in a Nonlinear Medium," 1987 Annual Meeting of the Optical Society of America, Rochester, NY, Oct. 19–23, 1987.
38. P. Guyot-Sionnest, J.H. Hunt, R. Superfine, and Y.R. Shen, "IR-Visible Sum Frequency Generation as a Surface Vibrational Spectroscopic Probe," 3rd International Laser Science Conference, Atlantic City, NJ, Nov. 1–5, 1987.
39. P. Guyot-Sionnest, "Surface Vibrational Spectroscopy by Sum-Frequency Generation," du Pont Research Laboratories, Wilmington, DE, Nov. 5, 1987; AT&T Bell Laboratories, Holmdel, NJ, Nov. 9, 1987.
40. Y.R. Shen, "Nonlinear Optics on Surfaces," Free University of Berlin, Federal Republic of Germany, Nov. 17, 1987.
41. Y.R. Shen, "Surface Studies by Nonlinear Optics," University of Aachen, Federal Republic of Germany, Dec. 8, 1987.
42. Y.R. Shen, "Nonlinear Optics and Surface Science," Max-Planck-Institute for Polymer Science, Mainz, Federal Republic of Germany, Dec. 14, 1987.

---

*This work was initially under the sponsorship of MCSD and completed under support through the Center for Advanced Materials by the Director, Office of Energy Research, Office of Basic Energy Sciences, Materials Sciences Division of the U.S. Department of Energy under Contract No. DE-AC03-76SF00098.

Excitations in Solids*

Carson D. Jeffries, Investigator

INTRODUCTION

Many phenomena in solid state systems display nonlinear behavior under suitable excitation, and instabilities may arise. These instabilities can be advantageously studied experimentally from the viewpoint of nonlinear dynamical systems theory, which recognizes that a wide class of phenomena display qualitatively similar behavior that, in some sense, must be universal. Examples of such phenomena are hydrodynamic instabilities; electrical and mechanical oscillations; chemical reaction oscillations; and spinwaves, acoustic waves, plasma waves, and charge-density waves in solids. The general objectives of this program are (1) to study experimentally nonlinear behavior in solid state systems and (2) to develop theoretical models to interpret observed behavior. This report describes work on two specific systems: spinwaves in ferrite spheres and nonlinear behavior in superconducting systems. In the spinwave studies one measures the microwave ac susceptibility of a ferrite sphere in a dc field and finds induced self-oscillations, period doubling, quasiperiodicity, and chaos, all of which can be understood from a numerical iteration of a model based on first principles. For superconductor systems, studies are reported on (1) the theoretical nonlinear effects of noise on Josephson junction parametric amplifiers, and (2) the microwave ac susceptibility observed in low magnetic fields in high-temperature ceramic superconductors, arising from the intergranular Josephson junction currents in these materials.

The results of this program have a bearing on a wide class of solid state systems of practical importance and on devices of technological interest.

*This work was supported by the Director, Office of Energy Research, Office of Basic Energy Sciences, Materials Sciences Division of the U.S. Department of Energy under Contract No. DE-AC03-76SF00098.

1. Nonlinear Dynamics of Spinwaves in a Yttrium Iron Garnet (YIG) Sphere (Publications 5, 6, and 7)

C.D. Jeffries, P.H. Bryant, and K. Nakamura

Ferromagnetic resonance in a small YIG sphere in a dc magnetic field is excited by pumping with an ac magnetic field at 10^{10} Hz. As the microwave pump power is increased, the uniformly precessing magnetization couples to a manifold of spinwaves in the sphere, one of which becomes abruptly excited at the Suhl threshold. Figure 1-1 is a parameter-space diagram of the regions and boundaries of observed dynamics, showing novel behavior. When two modes become excited, the system displays collective oscillations at a frequency of the order of 10^5 Hz; these oscillations undergo a period-doubling route to chaos; but this cascade is sometimes interrupted by the excitation of a third mode and the onset of quasiperiodicity, frequency entrainment, and a different route to chaos. In other regions of parameter space are found hysteresis and abrupt onset of chaos; high-level wide-band chaos; and aperiodic relaxation oscillations, with no resolved spectral features. This wide variety of behavior can be systematically accounted for by a first-principles theoretical model of coupled nonlinear oscillators, which can be numerically iterated. Figure 1-2 shows the computed behavior for two modes: asymmetric and symmetric modes of collective oscillations, both of which undergo period doubling and symmetry-breaking bifurcations and proceed ultimately to chaotic behavior. Starting from the viewpoint of microscopic scattering processes of spinwaves, this model

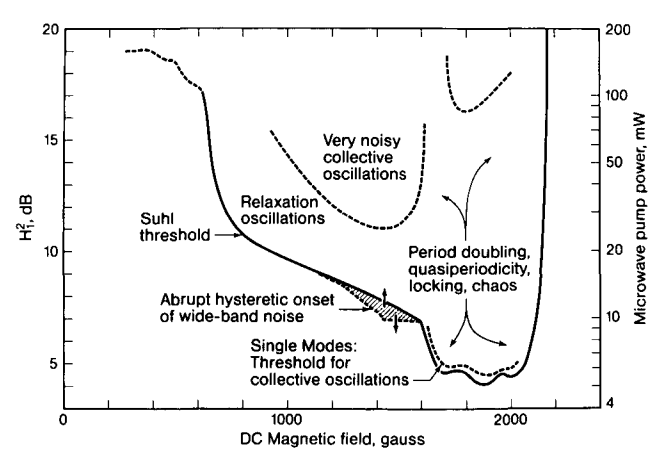

Figure 1-1. Regions and boundaries of observed spinwave instability behavior in a 0.06 cm yttrium iron garnet sphere pumped at 9.2 GHz. (XBL 873-652)

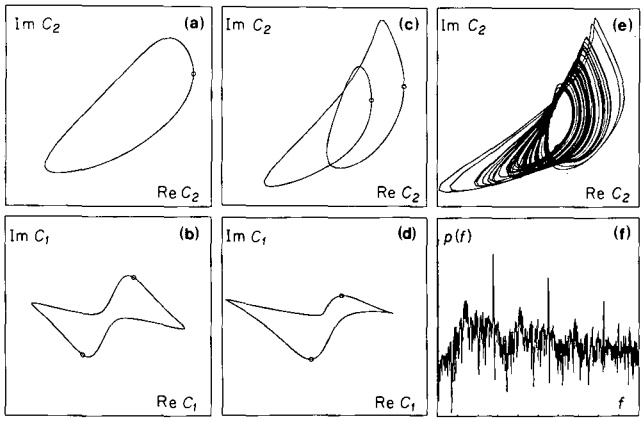

Figure 1-2. Computed nonlinear behavior for two spinwave modes: (a) phase portrait for collective oscillations, asymmetric mode; (b) symmetric mode; (c) period doubling; (d) symmetry breaking; (e) chaotic portrait; (f) power spectrum of (e). (XBL 873-651)

makes a connection to the theoretical framework of nonlinear dynamics and elucidates the observed behavior.

2. Nonlinear Effects of Noise on Josephson Junction Parametric Amplifiers (Publications 2 and 3)†

P. Bryant, K. Wiesenfeld, and B. McNamara

An old problem is reexamined: the observed "noise rise" in superconducting Josephson junction parametric amplifiers. By exploring recent insights from dynamical systems theory, it is shown how the interplay of random noise and (nonchaotic) deterministic dynamics can result in a noise rise like that observed in experiments. The analysis leads to a universal first-order equation that applies to all similar systems in the high-gain regime. Several predictions are proposed that can be tested experimentally, including the prediction that a similar noise rise should occur in modulated semiconductor injection lasers. Also analyzed is a previously unknown mode of operation—a "six-photon" mode associated with a symmetry-breaking bifurcation; its potential advantages over the previously studied three- and four-photon modes is discussed.

†Research in collaboration with K. Wiesenfeld, whose work was supported by DOE Contract No. DE-AC02-76CH00016, and in collaboration with B. McNamara, whose work was supported by the U.S. Office of Naval Research under Contract No. N00014-86-K-0154.

3. Work in Progress

Detailed experiments are in progress to study the linear and nonlinear parts of the complex ac susceptibility of high-temperature ceramic superconductors in low-dc magnetic fields. These studies reveal novel electrodynamic properties of these materials, owing to their granular structure. A large differential susceptibility in samples of $YBa_2Cu_3O_7$, provided by Professor A. Zettl, was discovered at 10^{10} Hz and 77 K using a spin resonance spectrometer with magnetic field modulation. The field derivative of the susceptibility has a typical maximum at a dc field of a few Gauss. This differential susceptibility is believed to originate from the granular character of the material and the existence of Josephson tunnel junctions or weak links between grains. In zero field the sample displays a large diamagnetic susceptibility due to bulk shielding currents. However, the intergranular loop currents reach criticality when the intergranular space is penetrated by the external field, which can occur for a few Gauss for loop areas of a few square microns. For a number of samples, this phenomenon was observed in the temperature range from 4 to 90 K, with the penetration field in the range of 5 to 40 Gauss, somewhat dependent on sample. The susceptibility also displays flux jumping and hysteresis as the dc field is scanned symmetrically through zero, with a hysteresis diagram of shape and symmetry similar to that found in Type II superconductors in much higher fields. The continuation of these studies is expected to provide detailed information on the electromagnetic properties of these and related granular superconductors.

1987 PUBLICATIONS AND REPORTS

Refereed Journals

1. P. Bryant and C.D. Jeffries, "The Dynamics of Phase Locking and Points of Resonance in a Forced Magnetic Oscillator," Physica **25D**, 196 (1987); LBL-21133.
2. B.S. McNamara,† P.H. Bryant, and K. Wiesenfeld,‡ "Noise Rise in Parametric Amplifiers," Phys. Rev. B **36**, 752 (1987); LBL-22128.
3. B.S. McNamara,† P.H. Bryant, and K. Wiesenfeld,‡ "The Nonlinear Effects of Noise on Parametric Amplification: An Analysis of Noise Rise in Josephson Junctions and Other Systems," J. Appl. Phys. **62**, 2898 (1987).

Other Publications

4. P.H. Bryant, C.D. Jeffries, and K. Nakamura, "Dynamical Interaction Between Spin Wave Modes

in Garnet Spheres," Bull. Am. Phys. Soc. **32**, 599 (1987).

LBL Reports

5. P. Bryant, C. Jeffries, and K. Nakamura, "Spin Wave Turbulence," in *The Physics of Chaos and Systems Far From Equilibrium*, M. Duong-van and B. Nichols, Eds., Nucl. Phys. B (in press); LBL-23041.
6. P. Bryant, C. Jeffries, and K. Nakamura, "Spinwave Nonlinear Dynamics in a Yttrium Iron Garnet Sphere," LBL-24471.
7. P.H. Bryant (Ph.D. Thesis), "Studies of Nonlinear and Chaotic Phenomena in Solid State Systems," LBL-23975.

Invited Talks

8. C.D. Jeffries, "Spin Wave Turbulence," International Conference on the Physics of Chaos and Systems Far From Equilibrium, Monterey, CA, Jan. 11–14, 1987.
9. C.D. Jeffries, "Turbulence in Solids," Technical Seminar, Varian Associates, Palo Alto, CA, May 4, 1987.

---

†Supported by the U.S. Office of Naval Research under Contract N00014-86-K-0154.

‡Supported by the U.S. Department of Energy under Contract DE-AC02-76CH00016.

Time-Resolved Spectroscopies in Solids*

Peter Y. Yu, Investigator

INTRODUCTION

The purpose of this project is to use picosecond and subpicosecond laser pulses generated by modelocked dye lasers to study ultrafast interactions between elementary excitations in solids. An understanding of these interactions, such as interactions between electrons and phonons and among electrons, is important in the design of the new generation of fast electronic devices. Nonequilibrium phonons and electron-hole plasmas are excited in semiconductors such as GaAs by picosecond laser pulses. Their subsequent expansion and cooling are monitored as a function of time by techniques such as photoluminescence and Raman scattering. The influence of defects, impurities, carrier confinement, and external perturbations such as strain are also investigated.

The effect of pressure on the electrical and optical properties of solids is also studied. Insulator-to-metal transitions induced by pressure are monitored by measuring sample resistance as a function of pressure inside diamond anvil high-pressure cells. Electron-phonon interactions and superconductivity in the high-pressure metallic phases are studied by measuring the temperature dependence of the electrical resistance. The effect of pressure on impurity levels in semiconductors has been studied by capacitance techniques such as deep-level transient spectroscopy (DLTS) and photocapacitance techniques.

1. Electrical Properties of the New High-T_c Superconductors Under High Pressure (Publications 4 and 9)†

D. Erskine,‡ E. Hess, A.M. Stacy, A. Zettl, and P.Y. Yu

Using a gasketed diamond anvil cell, the electrical resistance and superconducting transition temperature of the new high-T_c superconductors YBaCuO, LaSrCuO, and LaBaCuO have been studied up to 20 GPa. The highly nonlinear dependence of T_c in LaSrCuO on pressure has been compared with existing theories of superconductivity in these materials.

*This work was supported by the Director, Office of Energy Research, Office of Basic Energy Sciences, Materials Sciences Division of the U.S. Department of Energy under Contract No. DE-AC03-76SF00098.

†Supported in part by the LBL Director's Program Development Funds under Contract No. DE-AC03-76SF00098.

‡Present address: Lawrence Livermore National Laboratory, Livermore, CA 94550.

2. Study of Lattice Relaxation in the DX Center in $Ga_{1-x}Al_xAs$ Alloys and in the Related Pressure-Induced Deep Donors in GaAs (Publications 5 and 11)

M. Li,† W. Shan,‡ W.L. Hansen, E.R. Weber, and P.Y. Yu

Recently there has been much interest in whether deep centers in semiconductors, such as the DX center in GaAlAs alloys, have large or small lattice relaxations. To resolve this controversy, Li and Yu have proposed a model based on the determination of the pressure coefficients of the relevant defect energies. Using DLTS the pressure coefficients of defect energies in the DX center in $Ga_{1-x}Al_xAs$:Te and in GaAs:Si have been measured using a diamond anvil cell. From these results it is concluded that both the DX center in the GaAlAs alloys and the pressure-induced deep donors in GaAs:Si have large lattice relaxations associated with them.

†Present address: Graduate School of the University of Science and Technology of China, Beijing, People's Republic of China.

‡On leave of absence from the Shanghai Institute of Technical Physics, Academia Sinica, Shanghai, People's Republic of China.

3. Characterization of GaAs Films Grown on Si by Raman Scattering (Publications 3 and 8)

Y. Huang, Y. Lo,† M.-N. Charasse,† H. Lee,† S. Wang,† and P.Y. Yu

Raman scattering has been used to determine the strain and crystallinity of GaAs films grown on Si substrates. The GaAs sample has been angle-etched into a bevel to reveal the interface between GaAs and Si. From an analysis of the longitudinal optical phonon lineshape and peak positions, the strain and dislocation density in GaAs have been determined as a function of distance from the interface.

†Supported by the Joint Services Electronic Program, Grant No. AFOSR F49620-84-C-0057.

4. Work in Progress

The cooling rate of photoexcited hot electron-hole plasmas is being studied with subpicosecond time-resolved Raman scattering using a colliding-pulse modelocked dye laser.

The pressure dependence of electrical resistance and superconducting transition temperature in the new family of high-T_c superconductors will continue to be investigated. Pressure-induced insulator-to-metal transitions in various compounds, such as semiconductor alloys, superlattices, and oxides of Cu, will also be studied.

In collaboration with materials scientists at LBL's Center for Advanced Materials, the effects of boron implanted into GaAlAs alloys and GaAs on the DX center are being studied. Since boron can change the local environment of the deep centers, it can potentially reduce the lattice relaxation associated with these deep centers and hence remove the undesirable effects these centers have on devices. The effect of pressure on Schottky barrier heights formed by different metals on GaAs is also being investigated.

In collaboration with scientists in the Department of Electrical Engineering at U.C. Berkeley, the quality of GaAs epitaxial films grown on Si substrates is being studied by optical techniques such as Raman scattering and photoluminescence. The magnitude of thermally induced stress and minority carrier lifetimes in GaAs films will be studied as a function of growth conditions.

1987 PUBLICATIONS AND REPORTS

Refereed Journals

1. D. Erskine, P.Y. Yu, and G. Martinez, "A New Technique for Making Electrical Measurements in a Diamond Anvil Cell at Cryogenic Temperatures," Rev. Sci. Instrum. **58**, 406 (1987); LBL-22485.†
2. Y. Huang and P.Y. Yu, "Femtosecond Collision Times of Hot Electrons in GaAs Determined by Picosecond Time-Resolved Light Scattering," Solid State Commun. **63**, 109 (1987); LBL-23345.
3. Y. Huang, P.Y. Yu, M.-N. Charasse,‡ Y. Lo,‡ and S. Wang,‡ "Raman Study of an Epitaxial GaAs Layer on a Si [100] Substrate," Appl. Phys. Lett. **51**, 192 (1987); LBL-23471.
4. D. Erskine, E. Hess, P.Y. Yu, and A.M. Stacy, "Pressure Dependence of the Superconducting Transition Temperature in $La_{1.85}Sr_{0.15}CuO_4$ to 8 GPa," J. Mater. Res. **2**, 783 (1987); LBL-23808.†
5. M.F. Li, P.Y. Yu, E.R. Weber, and W.L. Hansen, "Photocapacitance Study of Pressure Induced Deep Donors in GaAs:Si," Phys. Rev. B **36**, 4531 (1987); LBL-23756.†

Other Publications

6. Y. Huang and P.Y. Yu, "Picosecond Time-Resolved Raman Scattering from Photoexcited Electron-Hole Plasma in GaAs," in *18th Int. Conf. Physics of Semiconductors*, O. Engstrom, Ed., World Scientific, Singapore, 1987, p. 1457; LBL-21989.
7. D. Erskine, P.Y. Yu, K.J. Chang, and M.L. Cohen, "Stability of the Si Lattice: Electron-Phonon Interactions and Superconductivity in Hexagonal Si," in *18th Int. Conf. Physics of Semiconductors*, O. Engstrom, Ed., World Scientific, Singapore, 1987, p. 1217; LBL-21990.†
8. Y.H. Lo,‡ M.-N. Charasse,‡ H. Lee,‡ D. Vakhshoon,‡ Y. Huang, P.Y. Yu, Z. Liliental-Weber, M. Werner,‡ and S. Wang,‡ "Raman Scattering Spectrum along a Bevel Etched GaAs on Si, TEM Study and GaAs P-I-N Photodetector on Si," in *Heteroepitaxy on Si II, Mater. Res. Soc. Symp. Proc.*, Vol. 91, J.C.C. Fan, J.M. Phillips, and B.-Y. Tsaur, Eds., MRS, Pittsburg, PA, 1987, p.149.

LBL Reports

9. D. Erskine, E. Hess, P.Y. Yu, A.M. Stacy, A. Zettl, and M.L. Cohen, "Electrical Properties of High T_c Superconductors under High Pressures," LBL-23692.†
10. Y. Huang and P.Y. Yu, "A Variable Band Pass Filter with High Rejection Ratio for Raman Scattering," LBL-23957.

Invited Talks

11. M.F. Li, W. Shan, P.Y. Yu, W.L. Hanson, E.R. Weber, and E. Bauser, "Lattice Relaxation of the DX Centers in $Ga_{1-x}Al_xAs$ and of the Pressure-induced Deep Donors in GaAs," Symposium on Defects in Semiconductors, 1987 Fall Meeting, Materials Research Society, Boston, MA; LBL-24523.†
12. P.Y. Yu, "DX Center in GaAs under High Pressure," Service National des Champs Intenses, Grenoble, France, Mar. 26, 1987.
13. P.Y. Yu, "Characterization of GaAs Epitaxial Films on Si by Raman Scattering and Photoluminescence," General Telephone and Electronic Research Laboratories, Waltham, MA, Dec. 4, 1987.
14. P.Y. Yu, "Femtosecond Hot Carrier Relaxation Times in GaAs by Time-resolved Raman Scattering," Workshop on Femtosecond Physics in Semiconductors, Phoenix, AZ, Dec. 9, 1987.

†Supported in part by the LBL Director's Program Development Funds under Contract No. DE-AC03-76SF00098.

‡Supported by the Joint Services Electronic Program, Grant No. AFOSR F49620-84-C-0057.

Superconductivity, Superconducting Devices, and 1/f Noise*

John Clarke, Investigator

INTRODUCTION

DC Superconducting QUantum Interference Devices (SQUIDs) are being used in a wide variety of applications, including geophysical measurements, noise thermometry, the investigation of high-T_c superconductors, and nuclear and quadrupole magnetic resonance in the frequency range from a few kHz to 100 MHz. SQUIDs are being operated at temperatures down to 20 mK to investigate their ultimate noise limitations for such applications as transducers for gravity-wave antennas. The dependence of the low-frequency flicker (1/f) noise on the materials from which the SQUIDs are fabricated is being studied. The lifetime of current-biased Josephson tunnel junctions against macroscopic quantum tunneling is being measured, with particular emphasis on the effects of dissipation. Very small tunnel junctions are being studied at low temperatures in an attempt to observe the so-called "Bloch oscillations"; the observation of this phenomenon would lead to the development of a new current standard. A detailed study is being made of the excess low-frequency noise induced in metal films by electron and ion bombardment; in addition to providing valuable information on the origin of the noise, these measurements constitute a new technique for the investigation of mobile defects in metals.

1. Upper Limit on the Resistivity of $La_{1.85}Sr_{0.15}CuO_4$ (Publication 3)

F.C. Wellstood, M.J. Ferrari, J. Clarke, A.M. Stacy, A. Zettl, and M.L. Cohen

During the early stages of research on the new class of superconducting oxides, measurements of the resistive transition showed a drop of several orders of magnitude in the resistivity to a value of 10^{-8} Ω cm or higher. This value is comparable with the low-temperature resistivity of copper with a residual resistivity ratio of about 100. We therefore decided to carry out an experiment to impose a much lower upper limit on the resistivity of an oxide superconductor.

The experimental configuration is shown in Figure 1-1. A superconducting solenoid is attached to a silicon chip on the reverse side of which is a thin-film planar dc SQUID. A hollow cylinder of the material under investigation can be inserted coaxially into the coil form. In the absence of any sample, we measure the mutual inductance between the coil and the SQUID; we repeat this measurement in the presence of a Pb cylinder to determine the reduction in the mutual inductance. By monitoring the stability of the magnetic flux in the SQUID in the presence of a current in the solenoid, one can infer the stability of the screening current in the superconducting cylinder.

We repeated the measurement on a hollow cylinder of LaSrCuO. From the observed lack of decay of flux in the SQUID, we inferred that the time constant for the decay of the screening current was greater than 3×10^6 sec. Estimating the inductance of the cylinder to be about 2 nH, we deduce a resistance of less than 6×10^{-16} Ω. To estimate the resistivity of the material, we assume that the currents flow uniformly throughout the sample: this assumption neglects skin depth effects, and provides a conservative upper limit on the resistivity of 3×10^{-17} Ω cm.

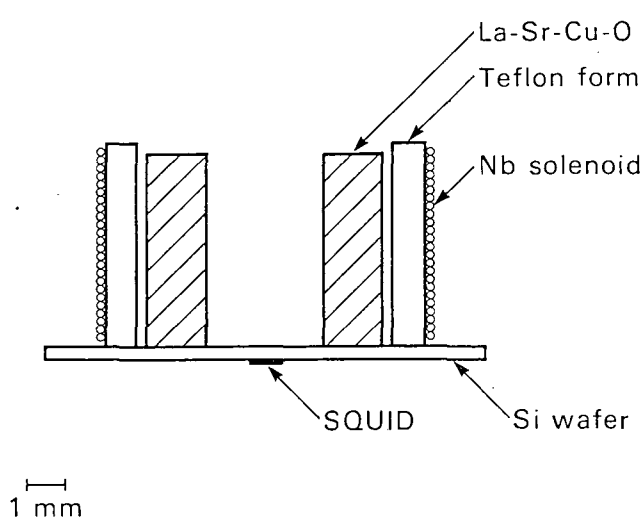

Figure 1-1. Experimental configuration for determination of upper limit of resistivity of LaSrCuO. (XBL 873-7617)

*This work was supported by the Director, Office of Energy Research, Office of Basic Energy Sciences, Materials Sciences Division of the U.S. Department of Energy under Contract No. DE-AC03-76SF00098.

2. Measurement of the Effect of Moderate Dissipation on Macroscopic Quantum Tunneling (Publication 19)

A.N. Cleland, J.M. Martinis, and J. Clarke

The current-biased Josephson tunnel junction provides an ideal device for measuring the effects of temperature and dissipation on macroscopic quantum tunneling (MQT). One can model the junction as a particle moving on a tilted washboard potential. The zero voltage state of the junction corresponds to the confinement of the particle in one of the wells, whereas the voltage state corresponds to the particle running down the washboard. The escape of the particle from the well is manifested by the sudden onset of a voltage across the junction. In MQT, the particle escapes from the well by tunneling through the potential barrier: this process is closely analogous to the escape of an α-particle from a radioactive nucleus. The theory of Caldeira and Leggett makes a precise prediction for the reduction of the escape rate in the presence of dissipation, and it is this prediction that we test.

Junctions were fabricated with a resistive shunt to provide accurately known dissipation, and cooled to low temperatures in a dilution refrigerator. We determined the escape rate by ramping the current through the junction and measuring the value at which a voltage appeared; this process was repeated typically 10^5 times at each temperature. The escape rate Γ is conveniently expressed as an escape temperature T_{esc}, defined through the relation $\Gamma = (\omega_p/2\pi)\exp(-\Delta U/k_B T_{esc})$; here ω_p is the plasma frequency and ΔU is the barrier height. Figure 2-1 shows T_{esc} vs T, together with the theoretical prediction. No parameters have been fitted in this comparison. The very good agreement establishes the correctness of the Caldeira-Leggett theory.

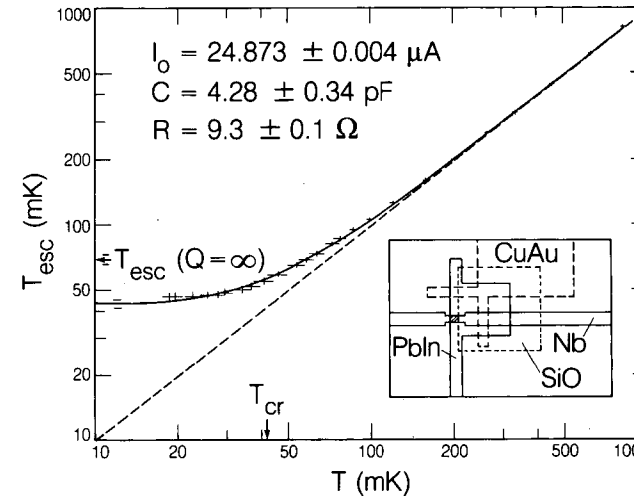

Figure 2-1. T_{esc} vs T for the shunted junction shown in the inset: horizontal and vertical error bars are indicated. Solid curve is theory. Crossover temperature (T_{cr}) between classical and quantum regimes and T_{esc} for undamped junction are shown. Dashed line is classical prediction. (XBL 874-9266D)

3. Signal and Noise in Measurements of Low-Frequency Geomagnetic Fields (Publication 21)†

E. Nichols, H.F. Morrison, and J. Clarke

In certain geophysical prospecting techniques, one applies a low-frequency electrical pulse to the ground and measures the resulting magnetic field at an array of sites. The accuracy of the detection of the magnetic field is reduced by two classes of noise: geomagnetic noise, and noise due to movement of the magnetic field sensors in the earth's static field, for example, because of seismic motion. The purpose of this experiment was to determine the reduction that could be achieved in the apparent noise level by means of an array of magnetometers together with appropriate cross-correlation techniques.

An array of four 3-axis SQUID magnetometers was fielded near Leach Hot Springs, Nevada. The magnetometers were instrumented with tilt-meters to enable us to correct for apparent noise due to the motion of the magnetometers. All the outputs were connected to a microcomputer for in-field data processing. A least-squares fitting program was used to predict the magnetic field at a given site from data at a remote site. Figure 3-1 shows the results of a typical experiment. In (a), the local magnetic field varies by about ±5 nT over a period of 1.8 hours. After the cancellation provided by the remote site, the variation is reduced to about ±0.001 nT, a reduction in amplitude of 5,000. This cancellation of spurious fields down to ±1 pT is quite unprecedented and opens up new possibilities for active electromagnetic surveying techniques for natural resources.

†Work supported in part by the Gas Research Institute.

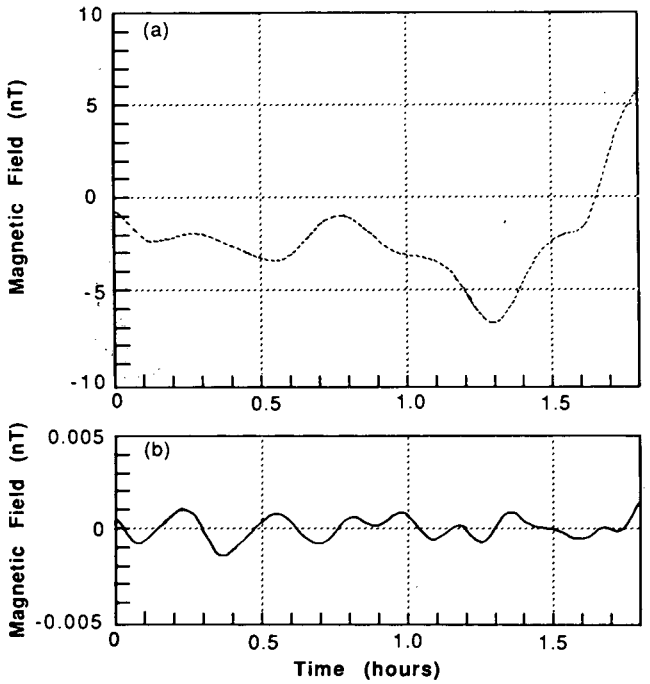

Figure 3-1. (a) Observed magnetic signal and (b) residual magnetic signal of an array of SQUID magnetometers located near Leach Hot Springs, Nevada. Data have been low-pass filtered at 0.1 Hz. (XBL 8711-4972)

4. Flicker (1/f) Noise in Cu Films Due to High-Energy Electron and Ion Irradiation (Publication 18)†

J. Pelz and J. Clarke

We have studied the effects of electron and ion irradiation on thin Cu films and found that it increases the level of 1/f noise in a predictable way. The increase is attributed to the creation of defects, some of which are mobile, and all of which can be annealed out with a corresponding reduction in the noise.

The films, evaporated on silicon chips, were irradiated with 1.2-MeV electrons while maintained at 90 K in a transmission electron microscope. One can determine the approximate number of Frenkel pairs (vacancy-interstitial pairs) so created by measuring the change in resistivity. In Figure 4-1, we show the variation in the spectral density of the resistivity fluctuations, $S\rho(f_o)$ at $f_o = 5$ Hz vs the change in resistivity, $\Delta\rho$, at 80 K; N is the number of atoms in the sample. We observe that the noise (open circles) increases linearly with $\Delta\rho$. Also shown is the increase $S_\rho(f_o)$ after irradiation with 1-MeV Kr^+ ions. We note that $S_\rho(f_o)$ increases with $\Delta\rho$ with the same slope as for the electron irradiation, but

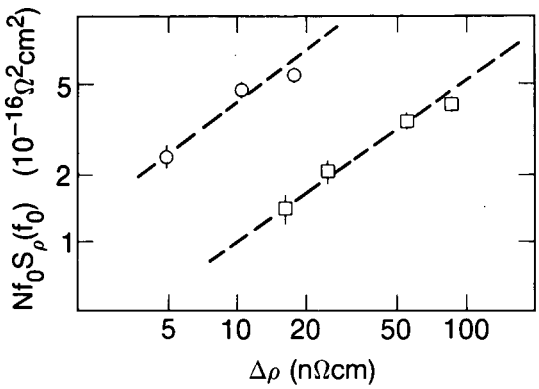

Figure 4-1. Change in noise magnitude vs. change in resistivity for irradiated Cu film. Open circles were measured after 1.1 MeV electron radiation, open squares after 1 MeV Kr^+ irradiation. (XBL 884-1326)

that the overall magnitude is reduced by a factor of about 8. This result is consistent with the notion that the ion irradiation creates large numbers of spatially correlated defects, or clusters. These clusters create a substantial change in resistivity, but, because they are largely immobile at 80 K, contribute very little to the noise. Thus only the relatively small fraction of defects that are isolated and not in clusters contributes to the noise.

These results, together with detailed studies of the effects of annealing, establish mobile defects as a major source of 1/f noise in metals.

†This work was done in collaboration with Dr. Wayne King at Argonne National Laboratory. Part of this work was performed at Argonne.

5. Quantitative "Local Interference" Model for 1/f Noise in Metal Films (Publication 8)

J. Pelz and J. Clarke

For many years there has been much interest in the origin of low-frequency flicker (1/f) noise in metal films. Recent experiments have provided very strong evidence that the noise arises from the motion of defects, which modifies the resistance of the film in a random manner and thus causes the voltage to fluctuate in the presence of a steady bias current. We have developed a model that accounts for this defect motion in a quantitative way.

The model leads to the following expression for the mean square resistivity fluctuations $<(\delta_\rho)^2>$, normalized to the square of the resistivity ρ^2:

$$N \frac{<(\delta\rho)^2>}{\rho^2} = (n\ell\delta\sigma)^2 \frac{n_m}{n} \quad .$$

Here, N is the number of atoms in the sample of volume V, n = N/V, ℓ is the electron mean free path, $\delta\sigma$ is the average change in cross section of a defect when it rotates, and n_m is the concentration of mobile defects. The measured 1/f noise is often expressed as $NS_\rho(f)/\rho_2 = \alpha/f$, where $S_\rho(f)$ is the spectral density of the resistivity fluctuations. Integrating this expression over an appropriate bandwidth, we obtain $N<(\delta\rho)^2>/\rho^2 \sim 5.5\alpha$. For typical metals at room temperature, $\alpha \sim 10^{-3}$, and one can account for the 1/f noise with $n_m/n \sim 10^{-5}$, a very reasonable value. The theory also accounts for the noise added by electron irradiation (see abstract 4) if one assumes that about 5% of the added defects are mobile. This model is the first to explain 1/f noise quantitatively and accounts for the observed 1/f noise in a very satisfactory way.

1987 PUBLICATIONS AND REPORTS

Refereed Journals

1. F.C. Wellstood, C. Urbina, and J. Clarke, "Low-Frequency Noise in dc Superconducting Quantum Interference Devices Below 1 K," Appl. Phys. Lett. **50**, 771 (1987); LBL-22907.
2. J.M. Martinis, M.H. Devoret, and J. Clarke, "Experimental Tests for the Quantum Behavior of a Macroscopic Degree of Freedom: The Phase Difference Across a Josephson Junction," Phys. Rev. B **35**, 4682 (1987); LBL-21936.
3. F.C. Wellstood, M.J. Ferrari, J. Clarke, A.M. Stacy, A. Zettl, and M.L. Cohen, "Upper Limit on the Resistivity of $La_{1.85}Sr_{0.15}CuO_4$," Phys. Lett. A **122**, 61 (1987); LBL-23261.
4. B. Savo, F.C. Wellstood, and J. Clarke, "Low-Frequency Excess Noise in Nb-Al_2O_3-Nb Josephson Tunnel Junctions," Appl. Phys. Lett. **50**, 1757 (1987); LBL-22744.
5. J. Pelz and J. Clarke, "Comment on 'Sensitivity of the Conductance of a Disordered Metal to the Motion of a Single Atom: Implications for 1/f Noise'," Phys. Rev. Lett. **59**, 1061 (1987); LBL-21937.
6. T. Sleator, E.L. Hahn, C. Hilbert, and J. Clarke, "Nuclear-Spin Noise and Spontaneous Emission," Phys. Rev. B **36**, 1969 (1987); LBL-23120.
7. A.N. Cleland, J.M. Martinis, and J. Clarke, "Effect of Dissipation on Macroscopic Quantum Tunneling," Jap. J. Appl. Phys. **26**, 1427 (1987); LBL-23121.
8. J. Pelz and J. Clarke, "A Qualitative 'Local Interference' Model for 1/f Noise in Metal Films," Phys. Rev. B Rapid Commun. **36**, 4479 (1987); LBL-23677.
9. F.C. Wellstood, C. Urbina, and J. Clarke, "Excess Noise in dc SQUIDs from 4.2 K to 0.022 K," IEEE Trans. Magn. **MAG-23**, 1662 (1987); LBL-22328.
10. J. Mygind, J. Bindslev-Hansen, J. Clarke, G.A. Ovsyannikov, and H. Svensmark, "Period Three Generation on Microwave-Induced Constant-Voltage Steps of Josephson Tunnel Junction," IEEE Trans. Magn. **MAG-23**, 1061 (1987); LBL-22431.
11. M.H. Devoret, D. Esteve, J.M. Martinis, A. Cleland, and J. Clarke, "Resonant Activation of a Brownian Particle From a Potential Well: Microwave-Enhanced Escape From the Zero Voltage State of a Josephson Junction," Phys. Rev. B **36**, 58 (1987); LBL-23118.

Other Publications

12. F.C. Wellstood, B. Savo, and J. Clarke, "Excess Noise in Nb-Al_2O_3-Nb Superconducting Tunnel Junctions," Bull. Am. Phys. Soc. **32**, 481 (1987); LBL-22726abs.
13. T. Sleator, E.L. Hahn, M.B. Heaney, C. Hilbert, and J. Clarke, "Nuclear Electric Quadrupole Induction of Atomic Polarization," Bull. Am. Phys. Soc. **32**, 528 (1987).
14. A. Cleland, J. Martinis, and J. Clarke, "Macroscopic Quantum Tunneling and Dissipation in the Current-Biased Josephson Junction," Bull. Am. Phys. Soc. **32**, 482 (1987); LBL-22728abs.
15. J. Pelz, "1/f Noise Induced by Defects in Irradiated Copper Films," Bull. Am. Phys. Soc. **32**, 543 (1987); LBL-22730abs.

LBL Reports

16. M.H. Devoret, J.M. Martinis, D. Esteve, and J. Clarke, "Experimental Observation of the Quantum Behavior of a Macroscopic Degree of Freedom," accepted by Chance and Matter; LBL-23119.
17. J. Clarke, A.N. Cleland, M.H. Devoret, D. Esteve, and J. Martinis, "Macroscopic Quantum Effects in a Josephson Tunnel Junction," LBL-23679.
18. J. Pelz, J. Clarke, and W. King, "Flicker (1/f) Noise in Cu and Dilute Alloy Films Due to High Energy Electron and Ion Irradiation," LBL-23789.
19. A.N. Cleland, J.M. Martinis, and J. Clarke, "Measurement of the Effect of Moderate Dissipation on Macroscopic Quantum Tunneling," submitted to Phys. Rev. Lett.; LBL-23877.
20. J. Clarke, A.N. Cleland, M.H. Devoret, D. Esteve, and J.M. Martinis, "Quantum Mechanics of a Macroscopic Degree of Freedom: The Phase Difference Across a Josephson Tunnel Junction," accepted by Science; LBL-24144.
21. E. Nichols, H.F. Morrison, and J. Clarke, "Signals and Noise in Measurements of Low Frequency Geomagnetic Fields," submitted to J. Geophys. Res.; LBL-24325.

Invited Talks

22. J. Clarke, "Macroscopic Quantum Tunneling and Quantized Energy Levels in a Josephson Junction," Colloquium, University of Texas, Austin, Feb. 18, 1987.
23. T. Sleator, E.L. Hahn, M.B. Heaney, C. Hilbert, and J. Clarke, "Nuclear Electric Quadrupole Induction of Atomic Polarization," March Meeting, American Physical Society, New York, Mar. 16–20, 1987.
24. A. Cleland, J. Martinis, and J. Clarke, "Macroscopic Quantum Tunneling and Dissipation in the Current-Biased Josephson Junction," March Meeting, American Physical Society, New York, Mar. 16–20, 1987.
25. J. Pelz, "1/f Noise Induced by Defects in Irradiated Copper Films," March Meeting, American Physical Society, New York, Mar. 16–20, 1987.
26. J. Clarke, "California Scientist of the Year," acceptance speech, Museum of Science and Industry, Los Angeles, Apr. 24, 1987.
27. J. Clarke, "Macroscopic Quantum Tunneling and Quantized Energy Levels in a Josephson Junction," Colloquium, University of California, Irvine, Apr. 30, 1987.
28. J. Clarke, "Quantum Noise and Macroscopic Quantum Tunneling in Josephson Tunnel Junctions," Plenary Lecture, Ninth International Conference on Noise in Physical Systems, Montreal, Quebec, May 1987.
29. J. Pelz, "Flicker (1/f) Noise in Cu and Dilute Alloy Films due to High Energy Electron and Ion Irradiation," Plenary Lecture, Ninth International Conference on Noise in Physical Systems, Montreal, Quebec, May 1987.
30. B. Savo, F.C. Wellstood, and J. Clarke, "Investigation of Low Frequency Excess Noise in Nb-Al_2O_3-Nb Josephson Tunnel Junctions," Soviet-Italian Symposium on Weak Superconductivity, Naples, Italy, May 5–7, 1987.
31. J. Clarke, "Macroscopic Quantum Tunneling and Quantized Energy Levels in Josephson Tunnel Junctions," Conference on Condensed Matter on the Submicron Scale, University of California, Santa Barbara, June 1987.
32. J. Clarke, "Quantum Phenomena in Superconductors," Fritz London Memorial Award acceptance talk, Eighteenth International Conference on Low Temperature Physics, Kyoto, Japan, Aug. 20–26, 1987.
33. A.N. Cleland, J.M. Martinis, and J. Clarke, "Effect of Dissipation on Macroscopic Quantum Tunneling," Eighteenth International Conference on Low Temperature Physics, Kyoto, Japan, Aug. 20–26, 1987.
34. J. Clarke, "Quantum Behavior of a Macroscopic Variable: The Phase Difference across a Josephson Tunnel Junction," Colloquium, Michigan State University, E. Lansing, MI, Oct. 13, 1987.
35. J. Clarke, "Effects of Dissipation on Macroscopic Quantum Tunneling and Quantized Energy Levels," Workshop on Quantum Mechanics of Macroscopic Variables, Spring Hill Conference Center, Wayzata, MN, Oct. 29–31, 1987.
36. J. Clarke, "Small-Scale Analog Applications of High Temperature Superconductors," Perspectives in the New Superconductivity, Boston, MA, Nov. 9–11, 1987.
37. J. Clarke, "Prospects for High-T_c SQUIDs," Electrical Engineering and Computer Science Department, University of California Berkeley, Nov. 17, 1987.
38. J. Clarke, "SQUIDs," Society of Engineering Students, University of California Berkeley, Nov. 24, 1987.

THEORETICAL RESEARCH

Theoretical Studies of the Electronic Properties of Solid Surfaces*

L.M. Falicov, Investigator

INTRODUCTION

The purpose of this research is to further basic understanding of the physical properties of materials and materials systems, in particular their surfaces and interfaces. The emphasis is on carrying out quantum-mechanical calculations on realistic systems so that a microscopic understanding may be obtained from first principles. Studies include bulk materials, surfaces and chemisorbed systems, interfaces, defects in solids, and clusters. Comparisons with experiment show that the calculations are accurate and of predictive power. Bulk materials research is focused on electronic, magnetic, structural, and vibrational properties; crystal structure determination; solid-solid phase transformations at high pressure; and defect properties. Surface and interface research is focused on atomic, electronic, and magnetic structures.

During 1987 Professor L.M. Falicov was on sabbatical leave based in Copenhagen, Denmark. He kept constant contact with his students and collaborators both in Berkeley and Copenhagen, as well as with outside coworkers at the University of Virginia. He also established new collaborations with scientists in Denmark and Spain.

During his stay in Europe Professor Falicov was a frequently invited speaker at conferences and colloquia as well as a visitor to a variety of institutions throughout Europe.

*This work was supported by the Director, Office of Energy Research, Office of Basic Energy Sciences, Materials Sciences Division of the U.S. Department of Energy under Contract No. DE-AC03-76SF00098.

1. Magnetoquantum Oscillations, Magnetic Breakdown, and Fermi-Surface Modifications in $NbSe_3$ (Publication 2)

M.P. Everson,† A. Johnson,† H.-A. Lu,† R.V. Coleman,† and L.M. Falicov

The magnetoquantum oscillations in $NbSe_3$ show frequency shifts and beat structures due to interaction between the pinned charge-density-wave (CDW) configuration and the normal Fermi surface (FS). Spatial variations in the phase deformation of the CDW pinned at impurities can result in changes in the local Fermi level and CDW gap, giving rise to a distribution of extremal FS areas. Magnetic breakdown (MB) between these small FS sections and the open nested sheets of FS can have striking effects on the amplitude and frequency of the quantum oscillations due to modulation of the transmission and reflection of coefficients at the MB junctions. A model using a one-dimensional open-orbit network and a rectangular distribution of FS areas has been used to fit the data in the range 0–225 kG. Good fits to the beat periods and frequency shifts are obtained and provide an accurate measure of the width of the frequency distribution for different CDW configurations. The existence of these MB mechanisms also provides an explanation for hysteresis and asymmetry observed in the magnetoresistance as the CDW configuration is manipulated in electric and magnetic fields.

†Permanent address: Department of Physics, University of Virginia, Charlottesville, VA 22901.

2. Delocalization and Correlation Effects in Atomic Systems: Solution of the Hubbard Model for General Spin (Publication 4)

K.B. Whaley† and L.M. Falicov

The effects of quantum statistics and atomic correlations on motion in two-dimensional periodic potentials is studied within a Hubbard model for

both Bose-Einstein and Fermi-Dirac statistics. Exact eigenstates are obtained for finite clusters with periodic boundary conditions, and the extent of ground-state delocalization evaluated for both statistics.

†Permanent address: Department of Chemistry, University of California, Berkeley, CA 94720.

3. Extended One-Dimensional Hubbard Model: A Small-Cluster Approach (Publication 13)

L.M. del Bosch† and L.M. Falicov

The one-dimensional Hubbard model with nearest-neighbor hopping, first- and second-nearest-neighbor particle interaction, and one particle per site is re-examined by means of a small-crystal approach — an exact solution of a four-site cluster with periodic-boundary conditions. Lines of symmetry crossing as well as singular lines and points are found. Analysis of correlation functions indicates that although there are smooth, strong changes as the parameters approach the values of the charge-to-spin-density-wave transition (a suggestion of an incipient second-order transition), the actual change involves a crossover between unrelated symmetries (a clear indication of a first-order transition). The relatively simple calculation and its results agree well with previous Monte Carlo numerical simulations and settles the unresolved question of the order of the spin- to charge-density-wave transition.

†Permanent address: Departamento de Fisica de la Materia Condensada, Universidad Autonoma de Madrid, E-28049 Madrid, Spain.

4. A Heavy-Fermion System: An Exact Many-Body Solution to a Periodic-Cluster Hubbard Model (Publication 14)

A. Reich and L.M. Falicov

An exact solution of an eight-site crystal model with periodic boundary conditions, a small face-centered cubic crystal, is presented for the case of a heavy-fermion system. The model consists of: (a) a single, fully symmetric orbital per site, with nearest-neighbor and second nearest-neighbor hopping; (b) an infinite Coulomb repulsion between electrons on the same site; (c) antiferromagnetic superexchange interactions; and (d) a nearly half-filled band (7/8 electron per site). Application of group-theoretical techniques yields a set of energies that are at most (analytic) solutions of quadratic equations. Depending on the sign of the nearest-neighbor hopping parameter, the ground state exhibits either a huge accidental degeneracy (the heavy-fermion case), or simple, uniform, saturated itinerant ferromagnetism. The model is, at once, easy to handle and yet rich in structure. Fermi surface, spin-wave, and electron transport properties are investigated, and consequences for real systems are discussed.

1987 PUBLICATIONS AND REPORTS

Refereed Journals

1. E.C. Sowa and L.M. Falicov, "Photoemission, Inverse Photoemission, and Fluctuations in an Exactly Soluble Many-Body Cluster Model of bcc Iron," Phys. Rev. B **35**, 3765 (1987); LBL-22297.
2. M.P. Everson, A. Johnson, H.-A. Lu, R.V. Coleman, and L.M. Falicov, "Magnetoquantum Oscillations, Magnetic Breakdown, and Fermi-Surface Modifications in $NbSe_3$," Phys. Rev. B **36**, 6953 (1987); LBL-23491.
3. J.M. Kahn, R.E. McMurray, Jr., E.E. Haller, and L.M. Falicov, "Trigonal Hydrogen-Related Acceptor Complexes in Germanium," Phys. Rev. B **36**, 8001 (1987); LBL-23305.
4. K.B. Whaley and L.M. Falicov, "Delocalization and Correlation Effects in Atomic Systems: Solution of the Hubbard Model for General Spin," J. Chem. Phys. **87**, 7160 (1987); LBL-23703.

Other Publications

5. J.M. Kahn, E.E. Haller, and L.M. Falicov, "Copper-Dihydrogen Acceptors in High-Purity Germanium," in *The Physics of Semiconductors* (Proc. 18th Int. Conf., Stockholm, Sweden, Aug. 11–15, 1986), O. Engstrom, Ed., World Scientific, Singapore, 1987, p. 1003; LBL-21183.
6. E.E. Haller and L.M. Falicov, "Hydrogen-Related Impurity Complexes in Germanium and Silicon," in *Semiconductor Physics* (Proc. Third Brazilian School, University of Campinas, Brazil, Feb. 16–26, 1987), C.E.T. Goncalves da Silva, L.E. Oliveira, and J.R. Leite, Eds., World Scientific, Singapore, 1987, p. 132; LBL-22976.
7. R.V. Coleman, M.P. Everson, H.-A. Lu, A. Johnson, and L.M. Falicov, "Fermi Surface Modifications and Magnetic Breakdown Connected to Charge-Density Waves in $NbSe_3$," in *Proc. 18th Conf. Low-Temperature Physics, Kyoto, Japan, 1987*, Jap. J. Appl. Phys **26**, Supplement 26-3, 615 (1987); LBL-23493.

LBL Reports

8. L.E. Oliveira and L.M. Falicov, "Energy Spectra of Shallow Donors and Acceptors in GaAs-$Ga_{1-x}Al_xAs$ Superlattices," in *Proc. Third Escola Brasileira de Fisica de Semicondutores*, Campinas, Brazil, Feb. 16–26, 1987 (in press); LBL-23492.
9. L.M. Falicov, "A Periodic Small-Cluster Approach to Many-Body Problems," in *Recent Progress in Many-Body Theories*, Vol. 1, E. Pajanne and R.F. Bishop, Eds., Plenum, New York (in press); LBL-23894.
10. L.M. Falicov, "Electronic Band Structure and Photoemission: A Review and Projection," in J. de Physique (Paris), *Proc. 14th Int. Conf. X-ray and Inner Shell Processes*, Paris, Sept. 14–18, 1987 (in press); LBL-23976.
11. L.M. Falicov, "An Overview of Recent Developments in High-Temperature Superconductivity," Annual European ICASE Seminar, Oct. 9, 1987; in *Proc. ICASE Seminar*, Bulletin of the Danish Physics-Chemistry-Math High School Teachers Organization (in press); LBL-24323.
12. C.R. Proetto and L.M. Falicov, "Exact Solution of a Periodic-Cluster Hubbard Model with an Electron-Lattice Interaction," submitted to Phys. Rev. B; LBL-24642.
13. L. Milans del Bosch and L.M. Falicov, "Extended One-Dimensional Hubbard Model: a Small Cluster Approach," accepted by Phys. Rev. B; LBL-23704.
14. A. Reich and L.M. Falicov, "Heavy-Fermion System: an Exact Many-Body Solution to a Periodic-Cluster Hubbard Model," accepted by Phys. Rev. B; LBL-24099.

Invited Talks

15. L.M. Falicov, "Correlation Effects in Transition Metals and Rare Earth Compounds," Annual Hund-Klemm Lecture, Max-Planck-Institut for Solid State Physics, Stuttgart, Federal Republic of Germany, Jan. 19, 1987; NORDITA, Copenhagen, Denmark, Feb. 4, 1987; University of Dortmund, Federal Republic of Germany, June 16, 1987.
16. L.M. Falicov, "Fluctuations and Photoemission in Highly Correlated Metals," Atomic Energy Establishment, Risø, Denmark, Feb. 23, 1987; University of Uppsala, Sweden, May 7, 1987; University of Lund, Sweden, May 25, 1987; Jülich Center for Research, Federal Republic of Germany, May 29, 1987.
17. L.M. Falicov, "Open Problems in Condensed Matter Physics," AFI Institute, University of Stockholm, Sweden, May 6, 1987; Annual Solid State Meeting of the Danish Physical Society, Nyborg, Denmark, May 21, 1987; Physics Department, University of Aarhus, Denmark, Oct. 28, 1987.
18. L.M. Falicov, "Theory of High-Temperature Superconductivity," Workshop on High-Temperature Superconductivity, NORDITA, Copenhagen, Denmark, May 14, 1987; Properties of Highly Correlated Systems, Stavenden, Holland, June 4, 1987; Joint meeting, Danish Physics-Math-Chemistry High School Teachers Association and the European Society of Science High School Teachers, Lyngby, Denmark, Oct. 9, 1987; The Danish Physical Society, Lyngby, Denmark, Dec. 9, 1987.
19. L.M. Falicov, "A Periodic Small-Cluster Approach to Many-Body Problems," Oulu Conference on Recent Progress in Many-Body Problems, Oulu, Finland, Aug. 6, 1987.
20. L.M. Falicov, "Superconductivity: a Brief Survey and Assessment," the Danish Academy of Technical Sciences, Lyngby, Denmark, Sept. 10, 1987.
21. L.M. Falicov, "Electronic Band Structure and Photoemission: Review and Projection," 14th International Conference on X-Ray and Inner Shell Processes, Paris, France, Sept. 17, 1987.
22. L.M. Falicov, "Superconductivity and the Hubbard Model," H.C. Ørsted Institute, University of Copenhagen, Denmark, Sept. 29, 1987.
23. L.M. Falicov, "Highly Correlated Metals: a Small-Cluster Approach to Heavy Fermions and Superconductivity," NORDITA Symposium on Recent Progress in Condensed Matter Physics, Copenhagen, Denmark, Oct. 7, 1987; Catholic University of Rio de Janeiro, Brazil, Oct. 23, 1987; ETH, Technical University of Switzerland, Zürich, Nov. 5, 1987; Physics Department, Göteborg Institute of Technology, Göteborg, Sweden, Nov. 24, 1987; Trondheim Institute of Technology, Trondheim, Norway, Dec. 4, 1987.
24. L.M. Falicov, "A Survey of Condensed Matter Physics," Third Symposium on Pan American Collaboration, Rio de Janeiro, Brazil, Oct. 20, 1987.
25. L.M. Falicov, Participant in the Round Table on "Collaboration in Physics between the United States and Latin America," Third Symposium on Pan American Collaboration, Rio de Janeiro, Brazil, Oct. 22, 1987.
26. L.M. Falicov, "Electronic and Magnetic Properties of Transition-Metal Surfaces and Overlayers," Göteborg Institute of Technology, Göteborg, Sweden, Nov. 25, 1987; Physics Department, Free University of Berlin, Berlin, Germany, Dec. 11, 1987.
27. L.M. Falicov (with A. Reich), "Superconducting Correlations in a Small-Cluster Hubbard Model," Danish Physical Society, Lyngby, Denmark, Dec. 9, 1987.

Theoretical Solid State Physics*

Marvin L. Cohen, Investigator

INTRODUCTION

The emphasis of the theoretical work is on the properties of real materials. A significant effort is made to interact with experimental groups at Berkeley and elsewhere. In the area of high-temperature superconductivity, the collaboration has already resulted in a series of studies of the new high-temperature superconducting oxides. The other theoretical work focuses on the properties of solids and clusters. High-pressure studies of semiconductors and insulators reveal the possibility of new solid-solid phase transitions. Much of the work relies only on first-principles approaches, which require only input about the constituent atoms. The information about the solid state is obtained in most cases from only a knowledge of the atomic number and atomic mass of the atoms making up the solid.

HIGH-TEMPERATURE SUPERCONDUCTIVITY

A series of studies of the high-temperature superconducting oxides resulted in a series of important studies. The first observation of superconductivity above the boiling of liquid nitrogen was made by Chu and Wu. An independent but subsequent observation of superconductivity in Y-Ba-Cu-O was made at Berkeley through a collaboration between theory and experiment. Other experiments in this area include the observation of a near-zero isotope effect in Y-Ba-Cu-O and a finite but small isotope effect in La-Ba-Cu-O. Other experiments include studies of the elasticity, transport properties, tunneling properties, and a nonreproducible observation of superconductivity around room temperature. The theoretical component of this work consisted of suggestions for experiments and analysis of the results once the experiment was done.

SUPERCONDUCTIVITY AND ELECTRON-PHONON INTERACTIONS

The pseudopotential total-energy method was applied to examine electron-phonon scattering in semiconducting silicon to obtain intervalley electron-phonon matrix elements. This work was analogous to the work that was done earlier to compute electron-phonon matrix elements to study the superconducting properties of highly compressed silicon. The results were consistent with Raman scattering experiments, but this work is in a primitive stage and will require refinement before accurate determinations of the electron-phonon matrix elements are made.

HIGH PRESSURE AND STRUCTURAL PROPERTIES OF SOLIDS

1. Pressure Coefficients of Band Gaps of Diamond (Publication 5)

S. Fahy, K.J. Chang, S.G. Louie, and M.L. Cohen

Ab initio pseudopotential calculations of the pressure dependence of the direct and indirect band gaps in diamond using a plane-wave and a local-orbital method are presented. The pressure derivative of the fundamental gap is found to be positive, in contrast with the negative derivative usually observed near the X point in the diamond and zinc-blende-structure semiconductors. Its value is found to be 0.53 meV/kbar for the local-orbital method and 0.58 meV/kbar for the plane-wave method, as compared to the measured value of 0.5 meV/kbar. The anomalous sign of the pressure derivative of the fundamental gap is understood in terms of the absence of d states with the same principal quantum number as the low-lying s and p valence states of the carbon atom.

2. High-Pressure Phases of III-V Zincblende Semiconductors (Publication 7)

S.B. Zhang and M.L. Cohen

With the use of the pseudopotential total-energy approach, the stability of two likely high-pressure structures, the A5 (β-Sn) and rocksalt structure, for the III-V compounds AlP, AlAs, AlSb, GaP, GaAs, GaSb, InP, InAs, and InSb are investigated. We present the calculated pressure for the phase transformations and compare them with the experimental values. As previously reported for AlP, there are discrepancies in the transition pressures between theory and experiment for Al compounds, and these

*This work was supported jointly by the Director, Office of Energy Research, Office of Basic Energy Sciences, Materials Sciences Division of the U.S. Department of Energy under Contract No. DE-AC03-76SF00098, and by the National Science Foundation under Grant No. DMR8319024.

are discussed. A new high-pressure phase of GaSb is analogous to the simple hexagonal phase at a pressure of 528 kbar. Using the measured and calculated results for the high-pressure phases of the zincblende compounds, we conclude that the rocksalt phase is stabilized relative to the A5 phase by the averaged optical energy gap (both homopolar and heteropolar contributions) of the material.

3. Theoretical Total-Energy Study of the Transformation of Graphite into Hexagonal Diamond (Publication 8)

S. Fahy, S.G. Louie, and M.L. Cohen

Variations in the structural energy of solid carbon along a transformation path from a graphitic structure with ...[AA]... stacking to hexagonal diamond are calculated using the first-principles pseudopotential local-orbital total-energy method. The transformation path is that defined in an earlier study of the transformation of rhombohedral graphite into cubic diamond. The energy barrier along the transformation path is found to be only slightly higher than that of the corresponding path in the earlier study. Thus, the major features of the energetics of the transformation are found to be relatively insensitive to the stacking of the graphite. However, it is found that in the region of metastability of graphite, the ...[AA]... stacking never has lower energy than the rhombohedral stacking, and so we do not expect a transition from rhombohedral to ...[AA]... stacking under static pressure. While the energy of hexagonal diamond is higher than that of cubic diamond in their final formation, nevertheless, as the sp^3 bonds are forming during the transition from graphite, it is found that the hexagonal diamond has approximately the same energy as cubic diamond. The implications of these results for the synthesis of diamond from graphite are discussed.

4. *Ab initio* Pseudopotential Study of Structural and High-Pressure Properties of SiC (Publication 9)

K.J. Chang and M.L. Cohen

An *ab initio* pseudopotential method is used to study the structural properties of SiC at low and high pressures. For cubic SiC, the calculated ground-state properties, such as the equilibrium lattice constant, bulk modulus, and cohesive energy, are in good agreement with experiment. The indirect band gap of cubic SiC is predicted to decrease with increasing pressure; this behavior is similar to Si but not to C. To study the structural phase stability at high pressures, the rocksalt and tetragonal β-Sn phases are considered. Our calculations suggest that the zincblende structure of SiC transforms into the rocksalt phase under a hydrostatic pressure of 660 ± 50 kbar. The calculated value should be regarded as an upper bound for the pressure of a structural phase transition from the zincblende. The valence-charge distribution for cubic SiC resembles those for other zincblende semiconductors.

5. Analytic Relation Between Bulk Moduli and Lattice Constants (Publication 15)

P.K. Lam, M.L. Cohen, and G. Martinez

An analytic relation between the bulk modulus of a solid and its equilibrium lattice constant is sought by examining how the various components of the total structural energy scale with distance. Simple formulas are obtained for the bulk modulus and its pressure derivative. A comparison is made with an empirical scaling approach for diamond and zincblende materials.

1987 PUBLICATIONS AND REPORTS

Refereed Journals

1. G. Martinez, J.M. Mignot, G. Chouteau, K.J. Chang, M.M. Dacorogna, and M.L. Cohen, "Superconductivity of Silicon," Phys. Scripta **T13**, 226 (1986).
2. S.L. Richardson and M.L. Cohen, "Conduction-Band-Edge Charge Densities in Elemental and Compound Semiconductors," Phys. Rev. B **35**, 1388 (19B7); Erratum: Phys. Rev. B **36**, 1275 (1987).†
3. W.D. Knight, W.A. de Heer, W.A. Saunders, K. Clemenger, M.Y. Chou, and M.L. Cohen, "Alkali Metal Clusters and the Jellium Model," Chem. Phys. Lett. **134**, 1 (1987).
4. L.C. Bourne, M.L. Cohen, W.N. Creager, M.F. Crommie, A.M. Stacy, and A. Zettl, "Onset of Superconductivity in Y-Ba-Cu-O at 100 K," Phys. Lett. **A120**, 494 (1987).
5. S. Fahy, K.J. Chang, S.G. Louie, and M.L. Cohen, "Pressure Coefficients of Band Gaps of Diamond," Phys. Rev. B **35**, 5856 (1987).
6. F.C. Wellstood, M.J. Ferrari, J.Clarke, A.M. Stacy, A. Zettl, and M.L. Cohen, "Upper Limit on the

Resistivity of $La_{1.85}Sr_{0.15}CuO_4$," Phys. Lett. **A122**, 61 (1987).
7. S.B. Zhang and M.L. Cohen, "High-Pressure Phases of III-V Zinc-Blende Semiconductors," Phys. Rev. B **235**, 7604 (1987).‡
8. S. Fahy, S.G. Louie, and M.L. Cohen, "Theoretical Total-energy Study of the Transformation of Graphite into Hexagonal Diamond," Phys. Rev. B **35**, 7623 (1987).
9. K.J. Chang and M.L. Cohen, "*Ab initio* Pseudopotential Study of Structural and High-Pressure Properties of SiC," Phys. Rev. B **35**, 8196 (1987).
10. M.L. Cohen, M.Y. Chou, W.D. Knight, and W.A. de Heer, "Physics of Metal Clusters," J. Phys. Chem. **91**, 3141 (1987).
11. L.C. Bourne, M.F. Crommie, A. Zettl, H.-C. zur Loye, S.W. Keller, K.L. Leary, A.M. Stacy, K.J. Chang, M.L. Cohen, and D.E. Morris, "Search for Isotope Effect in Superconducting Y-Ba-Cu-O," Phys. Rev. Lett. **58**, 2337 (1987); Erratum: Phys. Rev. Lett. **59**, 1492 (1987).
12. L.C. Bourne, A. Zettl, K.J. Chang, M.L. Cohen, A.M. Stacy, and W.K. Ham, "Elasticity Studies of $La_{2-x}Sr_xCuO_4$," Phys. Rev. B **35**, 8785 (1987).
13. M.F. Hundley, A. Zettl, M.L. Cohen, and A.M. Stacy, "Transport Properties of the Superconducting Oxide $La_{1.85}Sr_{0.15}CuO_4$," Phys. Rev. B **35**, 8800 (1987).
14. M.F. Crommie, L.C. Bourne, A. Zettl, M.L. Cohen, and A.M. Stacy, "Tunneling Measurement of the Energy Gap in Y-Ba-Cu-O," Phys. Rev. B **35**, 8853 (1987).
15. P.K. Lam, M.L. Cohen, and G. Martinez, "Analytic Relation Between Bulk Moduli and Lattice Constants," Phys. Rev. B **35**, 9190 (1987).†
16. L.C. Bourne, M.L. Cohen, W.N. Creager, M.F. Crommie, and A. Zettl, "Compositionally Dependent Superconducting Transition Temperature of Y-Ba-Cu Oxides," Phys. Lett. **A123**, 34 (1987).
17. T.A. Faltens, W.K. Ham, S.W. Keller, K.J. Leary, J.N. Michaels, A.M. Stacy, H.-C. zur Loye, D.E. Morris, T.W. Barbee, III, L.C. Bourne, M.L. Cohen, S. Hoen, and A. Zettl, "Observation of an Oxygen Isotope Shift in the Superconducting Transition Temperature of $La_{1.85}Sr_{0.15}CuO_4$," Phys. Rev. Lett. **59**, 915 (1987).
18. S.B. Zhang, M.L. Cohen, and M.Y. Chou, "Electronic Shell Structure of Simple Metal Heteroclusters," Phys. Rev. B **36**, 3455 (1987).‡
19. L.C. Bourne, A. Zettl, T.W. Barbee, III, and M.L. Cohen, "Complete Absence of Isotope Effect in $YBa_2Cu_3O_7$: Consequences for Phonon Mediated Superconductivity," Phys. Rev. B **36**, 3990 (1987).
20. S.B. Zhang, M.L. Cohen, and J.C. Phillips, "Relativistic Screened Orbital Radii," Phys. Rev. B **36**, 5861 (1987).
21. R.M. Wentzcovitch, M.L. Cohen, and P.K. Lam, "Theoretical Study of BN, BP, and BAs at High Pressures," Phys. Rev. B **36**, 6058 (1987).

Other Publications

22. W.A. de Heer, W.D. Knight, M.Y. Chou, and M.L. Cohen, "Electronic Shell Structure and Metal Clusters," in *Solid State Physics*, Vol. 40, H. Ehrenreich and D. Turnbull, Eds., Academic Press, New York, p. 93.
23. D.Erskine, P.Y. Yu, K.J. Chang, and M.L. Cohen, "Stability of the Si Lattice: Electron-Phonon Interactions and Superconductivity in Hexagonal Si," in *Proc. 18th Int. Conf. Physics of Semiconductors, 1986*, World Scientific, Singapore, 1987, p. 1217.
24. S.L. Richardson, M.M. Dacorogna, F.H. Pollak, M.L. Cohen, and O.J. Glembocki, "First-Principles Calculation of the Γ-X Electron (Hole)-Phonon Matrix Elements in Silicon," in *Proc. 18th Int. Conf. Physics of Semiconductors, 1986*, World Scientific, Singapore, 1987, p. 1353.
25. M.L. Cohen, "Shell Structure in Clusters," in *Microclusters*, Proceedings of the First NEC Symposium, Springer-Verlag, Berlin, 1987, p. 2.
26. M.L. Cohen, "New Directions in Calculating Electron-Phonon Interactions," in *Condensed Matter Physics: The Theodore D. Holstein Symposium*, R.L. Orbach, Ed., Springer-Verlag, New York, 1987, p. 116.
27. M.L. Cohen, "My First Meeting with Ted Holstein," in *Condensed Matter Physics: The Theodore D. Holstein Symposium*. R.L. Orbach, Ed., Springer-Verlag, New York, 1987, p. 178.
28. M.L. Cohen, A.M. Stacy, and A. Zettl, "A Status Report on the Berkeley Research on High T_c Superconductors," in *High Temperature Superconductors*, D.U. Gubser and M. Schluter, Eds., MRS Society, Pittsburgh, PA, 1987, p. 93.
29. D.E. Morris, U.M. Scheven, L.C. Bourne, M.L. Cohen, M.F. Crommie, and A. Zettl, "Mobile Oxygen and Isotope Effect in the High Temperature Superconductor $YBa_2Cu_3O_{7-\delta}$," in *High Temperature Superconductors*, D.U. Gubser and M. Schluter, Eds., MRS Society, Pittsburgh, PA, 1987, p. 209.
30. M.L. Cohen, D.E. Morris, A. Stacy, and A. Zettl, "Oxygen Isotope Effect in the High Temperature Superconductors $YBa_2Cu_3O_{7-\delta}$ and $La_{1.85}Sr_{0.15}CuO_4$, with ^{18}O Substituted by Diffusion," in *Novel Superconductivity*, S.A. Wolf and V.Z. Kresin, Eds., Plenum, New York, 1987, p. 733.
31. M.L. Cohen, "Trends and Future: Theory," in *Novel Superconductivity*, S.A. Wolf and V.Z. Kresin, Eds., Plenum, New York, 1987, p. 1095.
32. S.L. Richardson and M.L. Cohen, "Conduction Band Edge Charge Densities in Elemental and Compound Semiconductors," Bull. A.P.S. **32**, 462 (1987).
33. J.L. Martins, K.J. Chang, and M.L. Cohen, "Superconductivity of the High Pressure Simple Hexagonal Phase of Ge," Bull. A.P.S., **32**, 523 (1987).
34. M.L. Cohen, "*Ab initio* Calculations of Properties of Matter at High Pressures," Bull. A.P.S. **32**, 855 (1987).

35. S. Fahy, K.J. Chang, S.G. Louie, and M.L. Cohen, "Pressure Dependence of the Band Gaps in Diamond," Bull. A.P.S. **32**, 855 (1987).
36. S.L. Richardson, M.M. Dacorogna, M.L. Cohen, and F.H. Pollak, "First-Principles Calculation of the Γ-X Electron (Hole)-Phonon Matrix Elements in Silicon," Bull. A.P.S. **32**, 933 (1987).

Invited Talks

37. M.L. Cohen, "Predicting New Solids and Superconductors," MMRD Annual Review, Lawrence Berkeley Laboratory, Berkeley, CA, Mar. 5, 1987.
38. M.L. Cohen, "Theoretical Models of Solids and Clusters," Joint UCLA–Caltech.–USC Solid State Seminar, Department of Physics, UCLA, Los Angeles, CA, Mar. 6, 1987.
39. M.L. Cohen, "*Ab initio* Calculations of Properties of Matter at High Pressures," March American Physical Society Meeting, New York, NY, Mar. 20, 1987.
40. M.L. Cohen, "Superconductivity Above 100 K," Hydrogen Photo-Production Workshop, Pacific International Center for High Technology Research, Kona, HI, Mar. 26, 1987.
41. M.L. Cohen, "Superconductivity Above 100 K," Monday Night Seminar Series, Luis Alvarez' home, Berkeley, CA, Mar. 30, 1987.
42. M.L. Cohen, "High Temperature Superconductivity," Society of Physics Students, Department of Physics, University of California Berkeley, Apr. 3, 1987.
43. M.L. Cohen, "The New High Temperature Superconductors," Department of Physics, University of California Berkeley, Apr. 15, 1987.
44. M.L. Cohen, "A Status Report on the Berkeley Research on High T_c Superconductivity," Spring Meeting, Materials Research Society, Anaheim, CA, Apr. 23, 1987.
45. M.L. Cohen, "The New Superconductors at High Temperatures," Sigma Xi, University of California Berkeley, Apr. 30, 1987.
46. M.L. Cohen, "Latest Developments in High Temperature Superconductivity," LURE, Universitaire Paris-Sud, Orsay, France, June 9, 1987.
47. M.L. Cohen, "Theoretical Models of Solids and Clusters," LURE, Universitaire Paris-Sud, Orsay, France, June 11, 1987.
48. M.L. Cohen, "Trends and Future: Theory," International Workshop on Novel Mechanisms of Superconductivity, Berkeley, CA, June 26, 1987.
49. M.L. Cohen, "The New High Temperature Superconductors," Hughes Aircraft Company, Space and Communications Group, Los Angeles, CA, June 30, 1987.
50. M.L. Cohen, "Electronic Structure of Semiconductors," Workshop on Fundamental Aspects of the Physics of Semiconductors, Santander, Spain, July 13, 1987.
51. M.L. Cohen, "Superconductors Calientes," Workshop on Fundamental Aspects of the Physics of Semiconductors, Santander, Spain, July 16, 1987.
52. M.L. Cohen, "The New Superconductors," Commonwealth Club, San Francisco, CA, Aug. 6, 1987.
53. M.L. Cohen, "Recent Results on High Temperature Superconductors," Xerox Palo Alto Research Center, Palo Alto, CA, Sept. 4, 1987.
54. M.L. Cohen, "Latest Berkeley Results on High T_c Superconductivity: Theory and Experiment," Symposium in Honor of Morrel H. Cohen's 60th Birthday, Exxon Research and Engineering Laboratories, Annandale, NJ, Sept. 11, 1987.
55. M.L. Cohen, "Introduction to Superconductivity," TV Broadcast for Continuing Education for Engineers, Hewlett-Packard, Palo Alto, CA, Sept. 15, 1987.
56. M.L. Cohen, "LBL Superconducting Materials Development," University of California Regents' Oversight Committee of the Department of Energy Laboratories, Lawrence Berkeley Laboratory, Berkeley, CA, Sept. 28, 1987.
57. M.L. Cohen, "The New High Temperature Superconductors," Opening Plenary Paper, IEEE Nuclear Science Symposium, San Francisco, CA, Oct. 21, 1987.
58. M.L. Cohen, "The New High Temperature Superconductors," Lunch Seminar, Center for Pure and Applied Mathematics, University of California Berkeley, Oct. 29, 1987.
59. M.L. Cohen, "The New High Temperature Superconductors," Department of Materials Science and Engineering, Stanford University, Stanford, CA, Oct. 30, 1987.
60. M.L. Cohen, "The New High Temperature Superconductors," After Dinner Speaker, Miller Institute for Basic Research in Science, University of California Berkeley, Nov. 2, 1987.
61. M.L. Cohen, "Theory of Bulk Moduli of Hard Solids," Third International Conference on the Science of Hard Materials, Nassau, Bahamas, Nov. 9, 1987.
62. M.L. Cohen, "Superconducting Ceramics," Third International Conference on the Science of Hard Materials, Nassau, Bahamas, Nov. 10, 1987.
63. M.L. Cohen, "The New High Temperature Superconductors," Opening Lecture, Annual Meeting of the County Supervisors Association of California, Monterey, Nov. 19, 1987.
64. M.L. Cohen, "The New High Temperature Superconductors," American Electronics Association Meeting, Hotel Sofitel, Redwood City, CA, Dec. 1, 1987.

---

†Supported through the Center for Advanced Materials by the Director, Office of Energy Research, Office of Basic Energy Sciences, Materials Sciences Division of the U.S. Department of Energy under Contract No. DE-AC03-76SF00098.

‡Supported by NSF Grant No. DMR8319024.

Surface, Chemisorption, and Theory of Solids*

Steven G. Louie, Investigator

INTRODUCTION

The purpose of this work is to further basic understanding of the electronic and structural properties of solids and materials systems such as surfaces and interfaces. First-principles quantum mechanical calculations are carried out to obtain a microscopic understanding of realistic systems. The research effort encompasses the study of bulk materials, surfaces, chemisorption systems, and interfaces, and the formulation and development of new theoretical techniques for calculating ground-state and excited-state properties. Current projects include work on surface atomic and electronic structures, structural and vibrational properties of solids, electronic excitation spectra of solids, and solid-solid structural phase transformations.

1. Theory of Quasiparticle Energies in Alkali Metals (Publication 10)†

J.E. Northrup, M.S. Hybertsen, and S.G. Louie

The quasiparticle band structures of Na and Li are calculated by evaluation of the electron self-energy to first order in the dynamically screened Coulomb interaction. For Na, our results explain quantitatively the large bandwidth reduction observed in recent angle-resolved photoemission experiments. The inclusion of exchange-correlation effects in the dielectric screening and the requirement that the energy dependence of the electron Green's function be treated self-consistently are found to be important in our obtaining the correct bandwidths.

†Supported in part (graduate student salary) by NSF Grant No. DMR8319024.

2. Many-Body Calculation of Surface States: As on Ge(111) and Si(111) (Publications 3 and 14)†

M.S. Hybertsen and S.G. Louie

A first-principles theory of the quasiparticle surface-state energies is given. The electron self-energy operator is evaluated with inclusion of both local fields and dynamical screening effects in a surface calculation using a repeated slab geometry. The results for the prototypical Ge(111):As and Si(111):As surfaces are in excellent agreement with recent angle-resolved photoemission data and show a substantially larger gap between the empty and occupied surface states in comparison to local-density functional calculations. Implications for local-density-functional calculations of surface-state energies in semiconductors are discussed.

†Supported in part (graduate student salary) by NSF Grant No. DMR8319024.

3. Potential Fluctuations and Density of Gap States in Amorphous Semiconductors (Publication 2)

C.T. Chan,† S.G. Louie, and J.C. Phillips

The exponential-band-tail (Urbach-tail) problem for structurally disordered material is treated by a simple model in which quantum wells (used to model the effects of local disorder) trap states in the gap. The density of states in the gap is calculated and is shown to have approximately exponential behavior over a range of energy of physical interest. A direct relation is established between the Urbach-tail slope and the glass transition temperature. Agreement with experimentally determined Urbach-tail slopes is obtained for the Ge-Sn-Se glasses for reasonable parameters employed in the present model.

†C.T. Chan was supported in part (graduate student salary) by NSF Grant No. DMR8319024.

*This work was supported by the Director, Office of Energy Research, Office of Basic Energy Sciences, Materials Sciences Division of the U.S. Department of Energy under Contact No. DE-AC03-76SF00098.

4. Pressure Coefficients of Band Maps of Diamond (Publication 6)

S. Fahy,† K.J. Chang, S.G. Louie, and M.L. Cohen

Ab initio pseudopotential calculations of the pressure dependence of the direct and indirect band gaps in diamond using a plane-wave and a local-orbital method are presented. The pressure derivative of the fundamental gap is found to be positive, in contrast with the negative derivative usually observed near the X point in the diamond and zinc-blende-structure semiconductors. Its value is found to be 0.53 meV/kbar for the local-orbital method and 0.58 meV/kbar for the plane-wave method, as compared to the measured value of 0.5 meV/kbar. The anomalous sign of the pressure derivative of the fundamental gap is understood in terms of the absence of d states with the same principal quantum number as the low-lying s and p valence states of the carbon atom.

†S. Fahy was supported in part (graduate student salary) by NSF Grant No. DMR8319024.

5. High-Pressure Structural and Electronic Properties of Carbon (Publication 9)

S. Fahy† and S.G. Louie

The high-pressure properties of carbon in eight different structures are calculated using an *ab initio* pseudopotential local-orbital method. In particular, the structural properties of hexagonal diamond and variation of its fundamental band gap with pressure are calculated for the first time. The variation of the fundamental gap in hexagonal diamond is found to have the opposite sign to that in cubic diamond, although the cubic and hexagonal forms have almost identical structural properties. Among the structures examined, diamond is found to transform under hydrostatic pressure first to the fourfold coordinated bc-8 (or Si-III) structure. The bc-8 form is favored at pressures greater than 11.1 Mbar. This is a slightly lower transformation pressure than that recently calculated using the pseudopotential plane-wave method. The sixfold coordinated structures, simple cubic and β-tin, are found at low pressure to be kinetically unstable, transforming spontaneously without an energy barrier into the cubic diamond structure. This result suggests that sixfold coordination of liquid carbon will be unlikely to occur at moderate pressure and temperature. Similarly, sixfold coordination is not expected in carbon clusters.

†S. Fahy was supported in part (graduate student salary) by NSF Grant No. DMR8319024.

6. Theoretical Total-Energy Study of the Transformation of Graphite into Hexagonal Diamond (Publication 8)

S. Fahy,† S.G. Louie, and M.L. Cohen

Variations in the structural energy of solid carbon along a transformation path from a graphitic structure with ...[AA]... stacking to hexagonal diamond are calculated using the first-principles pseudopotential local-orbital method. The transformation path is that defined in an earlier study of the transformation of rhombohedral graphite into cubic diamond. The energy barrier along the transformation path is found to be only slightly higher than that of the corresponding path in the earlier study. Thus, the major features of the energetics of the transformation are found to be relatively insensitive to the stacking of the graphite. However, it is found that in the region of metastability of graphite, the ...[AA]... stacking never has lower energy than the rhombohedral stacking, and so we do not expect a transition from rhombohedral to ...[AA]... stacking under static pressure. While the energy of hexagonal diamond is higher than that of cubic diamond in their final formation, nevertheless, as the sp^3 bonds are forming during the transition from graphite, it is found that the hexagonal diamond has approximately the same energy as cubic diamond. The implications of these results for the synthesis of diamond from graphite are discussed.

†S. Fahy was supported in part (graduate student salary) by NSF Grant No. DMR8319024.

7. Probing Electronic Density of States and Magnetic Interactions at the Rare-Earth Site (Publication 12)

U. Walter, S. Fahy,† A. Zettl, S.G. Louie, M.L. Cohen, P. Tejedor, and A.M. Stacy

By exploiting the 4f-shell properties of Er in the high-T_c superconductor $ErBa_2Cu_3O_7$, we find by inelastic magnetic neutron scattering that the electro-

static field around the rare earth site is anomalously large. Above T_c there exists considerable magnetic interaction between the conduction electrons and the rare earth's 4f shell: $N(E_F)J_{ex} = 0.025$. This interaction is lost in the superconducting state. The ground-state magnetic moment of Er in the host lattice is $\mu_{eff} = 5.3$ B.

---

†S. Fahy was supported in part (graduate student salary) by NSF Grant No. DMR8319024.

1987 PUBLICATIONS AND REPORTS

Refereed Journals

1. S.G. Louie, "Quasiparticle Energies in Semiconductors and Insulators," in *Proc. 18th Conf. Phys. of Semiconductors*, D. Engstrom, Ed., World Scientific, Singapore, 1987, p. 1095.†
2. C.T. Chan, S.G. Louie, and J.C. Phillips, "Potential Fluctuations and Density of Gap States in Amorphous Semiconductors," Phys. Rev. B **35**, 2744 (1987); LBL-21868.‡
3. M.S. Hybertsen and S.G. Louie, "Many-Body Calculation of Surface States: As on Ge(111)," Phys. Rev. Lett. **58**, 1551 (1987); LBL-22665.‡
4. M.S. Hybertsen and S.G. Louie, "*Ab initio* Static Dielectric Matrices from the Density Functional Approach 1: Formulation and Application to Semiconductors and Insulators," Phys. Rev. B **35**, 5585 (1987).†
5. M.S. Hybertsen and S.G. Louie, "*Ab initio* Static Dielectric Matrices from the Density Functional Approach II: Calculation of the Screening Response in Diamond, Si, Ge, and LiCl," Phys. Rev. B **35**, 5602 (1987).†
6. S. Fahy, K.J. Chang, S.G. Louie, and M.L. Cohen, "Pressure Coefficients of Band Gaps of Diamond," Phys. Rev. B **35**, 5856 (1987); LBL-22307.‡
7. D. Tomanek, S.G. Louie, H.J. Mamin, D.W. Abraham, R.E. Thomson, E. Ganz, and J. Clarke, "Theory and Observation of Highly Asymmetric Atomic Structure in Scanning Tunneling Microscopy Images of Graphite," Phys. Rev. B **35**, 7790 (1987); LBL-22338.§
8. S. Fahy, S.G. Louie, and M.L. Cohen, "Theoretical Total Energy Study of the Transformation of Graphite into Hexagonal Diamond," Phys. Rev. B **35**, 7623 (1987); LBL-22755.‡
9. S. Fahy and S.G. Louie, "High Pressure Structural and Electronic Properties of Carbon," Phys. Rev. B **36**, 3373 (1987); LBL-22653.‡
10. J.E. Northrup, M.S. Hybertsen, and S.G. Louie, "Theory of Quasiparticle Energies in Alkali Metals," Phys. Rev. Lett. **59**, 819 (1987); LBL-23256.‡
11. S.G. Louie and M.S. Hybertsen, "Theory of Quasiparticle Energies: Band Gaps and Excitation Spectra in Solids," Int. J. Quant. Chem.: Quant. Chem. Symp. **21**, 31 (1987); LBL-23257.‡
12. U. Walter, S. Fahy, A. Zettl, S.G. Louie, M.L. Cohen, P. Tejedor, and A.M. Stacy, "Probing Electronic Density of States and Magnetic Interactions at the Rare Earth Site in $ErBa_2Cu_3O_7$," Phys. Rev. B **36**, 8899 (1987).

Other Publications

13. S.G. Louie, "Theory of Quasiparticle Energies and Excitation Spectra of Semiconductors and Insulators," in *Electronic Band Structure and Its Applications*, Springer Verlag Lecture Notes Series, Vol. 283, M. Yussouf, Ed., Springer-Verlag, Heidelberg, 1987, p. 93.†
14. S.G. Louie, "*Ab initio* Calculation of Ground- and Excited-State Properties of Surfaces," in *Proc. Asia-Pacific Symp. Surf. Phys.*, Xie Xide, Ed., World Scientific, Singapore, 1987, p. 140; LBL-23258.‡
15. J.E. Northrup, M.S. Hybertsen, and S.G. Louie, "Quasiparticle Band Structure of Na and Li," Bull. A.P.S. **32**, 461 (1987).‡
16. D. Tomanek, C.T. Chan, and S.G. Louie, "Coverage-Dependent Adsorption Properties from a First-Principles Calculation: H/Pd(001)," Bull. A.P.S. **32**, 477 (1987).§
17. D. Tomanek, S.G. Louie, H.J. Mamin, D.W. Abraham, R.E. Thomson, E. Ganz, and J. Clarke, "Theory and Observation of Highly Asymmetric Atomic Structure in Scanning Tunneling Images of Graphite," Bull. A.P.S. **32**, 648 (1987).§
18. S. Fahy, K.J. Chang, S.G. Louie, and M.L. Cohen, "Pressure Dependence of the Band Gaps in Diamond," Bull. A.P.S. **32**, 855 (1987).‡
19. S. Fahy and S.G. Louie, "Calculated High Pressure Properties of Solid Carbon," Bull. A.P.S. **32**, 857 (1987).‡
20. M.S. Hybertsen and S.G. Louie, "Local Fields and Exchange-Correlation Effects in the Static Screening Response of Diamond, Si, Ge, and LiCl," Bull. A.P.S. **32**, 1398 (1987).†

LBL Reports

21. D. Tomanek and S.G. Louie, "First Principles Calculation of Highly Asymmetric Structure in Scanning Tunneling Microscopy Images of Graphite," Phys. Rev. B (in press); LBL-23746.§
22. R.S. Becker, B.S. Swartzentruber, J.S. Vickers, M.S. Hybertsen, and S.G. Louie, "Geometric and Local Electronic Structure of Si(111)-As," Phys. Rev. Lett. (in press); LBL-24343.‡
23. M.S. Hybertsen and S.G. Louie, "Theory of Quasiparticle Surface States in Semiconductor Surfaces," LBL-24517.‡
24. S.B. Zhang, D. Tomanek, S.G. Louie, M.L. Cohen, and M.S. Hybertsen, "Quasiparticle Calculation of Valence Band Offset of AlAs-GaAs(001)," LBL-24598.‡

25. S. Fahy and S.G. Louie, "Variation Monte Carlo Sampling of the Superconducting Ground State," LBL-24318.‡
26. D. Tomanek, R. Wentzcovitch, S.G. Louie, and M.L. Cohen, "Calculation of Electronic and Structural Properties of BC_3," LBL-24507.§
27. S.G. Louie, "First-Principles Calculation of Quasiparticle Energies at Surfaces and Interfaces: Semiconductor Surface-State Spectra and Band Offsets," LBL-24467.‡

Invited Talks

28. S.G. Louie, "Electron Correlation and Quasiparticle Energies in Crystals," Third International Workshop on Total Energy and Force Methods, Trieste, Italy, Jan. 26, 1987.
29. S.G. Louie, "Predicting the Properties of Solids from Atoms," Miller Institute, University of California Berkeley, Mar. 10, 1987.
30. S.G. Louie, "Theory of Quasiparticle Energies and Band Gaps in Solids," International Symposium on Atomic, Molecular, and Solid-State Theory, Scattering Problems, Many-Body Phenomena, and Computational Methods, St. Augustine, FL, Mar. 21, 1987.
31. S.G. Louie, "*Ab initio* Calculation of Ground- and Excited-State Properties of Surfaces," Asia-Pacific Symposium on Surface Physics, Shanghai, People's Republic of China, Apr. 16, 1987.
32. S.G. Louie, "Electron Correlation and Quasiparticle Energies in Solids," Institute of Physics, Academia Sinica, Beijing, People's Republic of China, Apr. 24, 1987.
33. S.G. Louie, "Predicting the Structures and Properties of Solids," Physics Department, General Motors Research Laboratories, Warren, MI, June 17, 1987.
34. S.G. Louie, "Predicting the Structures and Properties of Solids from Atoms," Physical Sciences Colloquium, IBM Almaden Research Center, San Jose, CA, Dec. 3, 1987.
35. S.G. Louie, "First-Principles Calculations of Quasiparticle Energies of Surfaces and Interfaces: Semiconductor Surface-State Spectra and Band Offsets," Solvay Conference on Surface Science, Austin, TX, Dec. 17, 1987.

---

†Supported by the National Science Foundation.

‡Supported in part by NSF Grant No. DMR8319024.

§Supported through the Center for Advanced Materials by the Director, Office of Energy Research, Office of Basic Energy Sciences, Materials Sciences Division of the U.S. Department of Energy under Contract No. DE-AC03-76SF00098.

Novel High-T_c Superconductors*

Alex Zettl, Investigator

INTRODUCTION

The purpose of this work is to synthesize and understand the properties of new classes of superconducting oxides such as La-Sr-Cu-O and Y-Ba-Cu-O. These materials have superconducting transition temperatures (T_c) greatly exceeding those of conventional superconducting materials. In order to understand how the new oxide superconductors work, normal-state and superconducting properties have been tested by Hall effect, thermoelectric power, resistivity, infrared reflectivity, tunneling, and elasticity measurements. Isotope substitutions, which allow direct tests of theories of superconductivity, have been performed. The results suggest that superconductivity in the high-T_c oxides may arise from nonphonon mechanisms.

1. Onset of Superconductivity in Y-Ba-Cu-O at 100 K (Publication 1)

L.C. Bourne, M.L. Cohen, W.N. Creager, M.F. Crommie, A.M. Stacy, and A. Zettl

A metallic oxide has been synthesized with a superconducting transition temperature above the boiling point of nitrogen. Resistive and magnetic measurements indicate transitions to the superconducting state beginning near 100 K with transition widths typically around 15 K (see Figure 1-1).

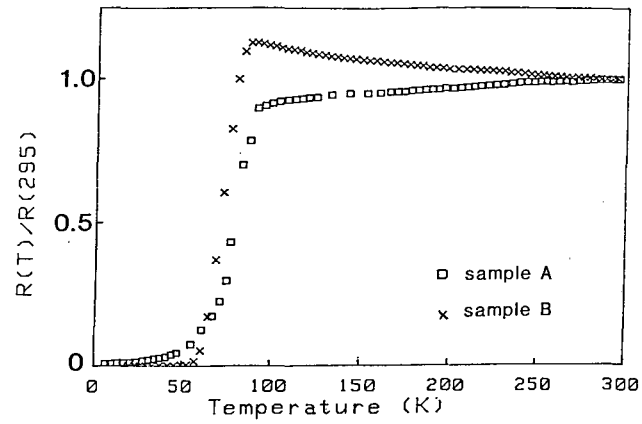

Figure 1-1 Electrical resistance versus temperature for two samples of $Y_{1.2}Ba_{0.8}CuO_4$. The onset of superconductivity is near 100 K. (XBL 884-1322)

2. Temperature-Dependent Far-Infrared Reflectance of La-(Sr,Ca)-Cu-O (Publications 2 and 11)

M.S. Sherwin, P.L. Richards, U. Walter, and A. Zettl

Far-infrared reflectance data for polycrystalline La-(Sr,Ca)-Cu-O show a reflectance edge with energy near 2.5 k_BT_c. This edge is interpreted as the onset of absorption due to an energy gap, or as a low-frequency plasma edge caused by strong far-infrared resonances. The measured temperature dependence of the reflectance edge closely fits the temperature dependence of the order parameter in a mean-field theory and hence is consistent with the energy-gap hypothesis. A model dielectric function for $La_{1.85}Sr_{0.15}CuO_4$ has also been constructed that is consistent with mean-field theory and the hypothesis of a plasma edge. It is found that the temperature dependence of the plasma frequency in this model also closely fits the measured temperature dependence of the reflectance edge. Furthermore, both hypotheses accurately predict the experimentally observed temperature dependence of the absorption at frequencies much less than the reflectance edge. This observation has significant implications for the construction of fast low-loss superconducting devices. However, given the identical predictions of the energy-gap and plasma-edge hypotheses, it is premature to deduce a precise value for the magnitude of the energy gap from the infrared data.

3. Tunneling Measurement of the Energy Gap in Y-Ba-Cu-O (Publication 5)

M.F. Crommie, L.C. Bourne, A. Zettl, M.L. Cohen, and A. Stacy

Superconductor-insulator-normal tunneling measurements have been performed on the high-T_c superconductor $YBa_2Cu_3O_7$ at 4.2 and 77 K. The results indicate an energy gap of magnitude 3.9 k_BT_c, with a temperature dependence consistent with the Bardeen-Cooper-Schrieffer theory of superconductivity.

*This work was supported by the Director's Program Development Funds of the Lawrence Berkeley Laboratory under Contract No. DE-AC03-76SF00098.

4. Elasticity Studies of $La_{2-x}Sr_xCuO_4$ (Publication 9)

L.C. Bourne, A. Zettl, K.J. Chang, M.L. Cohen, A.M. Stacy, and W.K. Ham

The Young's modulus and internal friction of $La_{2-x}Sr_xCuO_4$ have been measured as a function of temperature and x. For x = 0.15, anomalies in the Young's modulus and internal friction at T_c = 40 K are preceded by a dramatic decrease in the modulus, indicative of a soft phonon mode beginning near 200 K. For x = 0.30, the softening is absent. The magnetic-field dependence of the elastic constants are investigated, and predictions are made for specific heat anomalies and temperature derivatives of the critical field.

5. Transport Properties of $La_{1.85}Sr_{0.15}CuO_4$ (Publication 4)

M.F. Hundley, A. Zettl, A. Stacy, and M.L. Cohen

Electrical resistivity, Hall effect, and thermoelectric power (TEP) measurements have been performed on $La_{1.85}Sr_{0.15}CuO_4$ in the normal and superconducting states. The transport properties indicate that in the normal state the material conducts via holes with a carrier concentration of 6.0×10^{21} cm^{-3}. Evidence is found for unusual phonon-drag effects above T_c and granular or inhomogeneous superconductivity in the vicinity of T_c. Below T_c the resistivity, Hall constant, and TEP all drop to zero, as expected for a superconducting ground state.

6. Isotope Studies on High-T_c Superconducting Oxides (Publications 3, 7, 8, 12, and 14)

L.C. Bourne, M.F. Crommie, A. Zettl, S. Hoen, T.W. Barbee III, K.J. Chang, M.L. Cohen, H.C. zur Loye, S.W. Keller, K.L. Leary, T.A. Faltens, W.K. Ham, A. Stacy, and D.E. Morris

An oxygen-isotope effect has been searched for in $YBa_2Cu_3O_7$ and $La_{1.85}Sr_{0.15}CuO_4$ through substitution of ^{18}O for ^{16}O. In $YBa_2Cu_3O_7$, no shift in T_c is observed by electrical resistivity or magnetic susceptibility measurements, within the experimental accuracy of 0.3 K. With $T_c = M^{-k}$ with M the ion mass, k = 0 ± 0.027 for $YBa_2Cu_3O_7$. For $La_{1.85}Sr_{0.15}CuO_4$, a finite shift is observed, on the order of 0.3–0.4 K. This implies that for $La_{1.85}Sr_{0.15}CuO_4$, k = 0.15 ± 0.03. For $YBa_2Cu_3O_7$, Ba and Cu isotope substitutions have also been performed, with no detectable isotope shifts. For Ba, k = 0 ± 0.1, while for Cu, k = 0 ± 0.07. These results are examined within the framework of phonon-mediated electron pairing. For $YBa_2Cu_3O_7$, the null isotope shifts appear incompatible with phonon-mediated pairing alone. A similar result is obtained for $La_{1.85}Sr_{0.15}CuO_4$, using the small observed value of k.

7. Work in Progress

Tunneling and isotope studies are under way for a series of superconducting oxides.

1987 PUBLICATIONS AND REPORTS

Refereed Journals

1. L.C. Bourne, M.L. Cohen, W.N. Creager, M.F. Crommie, A.M. Stacy, and A. Zettl, "Onset of Superconductivity in Y-Ba-Cu-O at 100 K," Phys. Lett. A **120**, 494 (1987).
2. U. Walter, M.S. Sherwin, A. Stacy, P.L. Richards, and A. Zettl, "Energy Gap in the High T_c Superconductor $La_{1.85}Sr_{0.15}CuO_4$," Phys. Rev. B **35**, 5327 (1987).
3. L.C. Bourne, M.F. Crommie, A. Zettl, H.C. zur Loye, S.W. Keller, K.L. Leary, A.M. Stacy, K.J. Chang, M.L. Cohen, and D.E. Morris, "Search for Isotope Effect in Superconducting Y-Ba-Cu-O," Phys. Rev. Lett. **58**, 2337 (1987).
4. M.F. Hundley, A. Zettl, A. Stacy, and M.L. Cohen, "Transport Properties of the Superconducting Oxide $La_{1.85}Sr_{0.15}CuO_4$," Phys. Rev. B **35**, 8800 (1987).
5. M.F. Crommie, L.C. Bourne, A. Zettl, M.L. Cohen, and A. Stacy, "Tunneling Measurements of the Energy Gap in Y-Ba-Cu-O," Phys. Rev. B **35**, 8853 (1987).
6. F.C. Wellstood, M.J. Ferrari, J. Clarke, A.M. Stacy, A. Zettl, and M.L. Cohen, "Upper Limit on the Resistivity of $La_{1.85}Sr_{0.15}CuO_4$," Phys. Lett. A **122**, 61 (1987).
7. L.C. Bourne, A. Zettl, T.W. Barbee III, and M.L. Cohen, "Complete Absence of Isotope Effect in $YBa_2Cu_3O_7$: Consequences for Phonon-Mediated Superconductivity," Phys. Rev. B **36**, 3990 (1987).
8. T.A. Faltens, W.K. Ham, S.W. Keller, K.J. Leary, J.N. Michaels, A.M. Stacy, H.C. zur Loye, D.E. Morris, T.W. Barbee III, L.C. Bourne, M.L. Cohen, S. Hoen, and A. Zettl, "Observation of an Oxygen Isotope Shift in the Superconducting Transition Temperature of $La_{1.85}Sr_{0.15}CuO_4$," Phys. Rev. Lett. **59**, 915 (1987).

9. L.C. Bourne, K.J. Chang, M.L. Cohen, A.M. Stacy, and W.K. Ham, "Elasticity Studies of $La_{2-x}Sr_xCuO_4$," Phys. Rev. B **35**, 8785 (1987).
10. U. Walter, S. Fahy, A. Zettl, S.G. Louie, M.L. Cohen, P. Tejedor, and A.M. Stacy, "Probing Density of States and Interactions at the Rare Earth Site in Superconducting $ErBa_2Cu_3O_7$," Phys. Rev. B **36**, 8899 (1987).
11. M.S. Sherwin, P.L. Richards, and A. Zettl, "Temperature Dependent Far Infrared Reflectance of La-(Sr,Ca)-Cu-O: BCS Electrodynamics—but Uncertain Energy Gap?" Phys. Rev. B **37**, 1587 (1988).

Other Publications

12. D.E. Morris, U.M. Scheven, L.C. Bourne, M.L. Cohen, M.F. Crommie, and A. Zettl, "Mobile Oxygen and Isotope Effect in the High Temperature Superconductor $YBa_2Cu_3O_{7-d}$," in *Proc. Symp. S 1987 Spring Meeting Mat. Res. Soc.*, April 21–25, Anaheim, CA, 1987, D. Gubser and M. Schluter, Eds., p. 209.
13. M.L. Cohen, A. Stacy, and A. Zettl, "A Status Report on the Berkeley Research on High T_c Superconductors," in *Proc. Symp. S 1987 Spring Meeting Mat. Res. Soc.*, April 21–25, Anaheim, CA, D. Gubser and M. Schluter, Eds., 1987, p. 93.
14. M.L. Cohen, D.E. Morris, A. Stacy, and A. Zettl, "Oxygen Isotope Effect in the High Temperature Superconductors $YBa_2Cu_3O_{7-d}$ and $La_{1.85}Sr_{0.15}CuO_4$, with ^{18}O Substituted by Diffusion," in *Proc. Workshop on Novel Mechanisms of Superconductivity*, Berkeley, CA June 22–26, 1987, V. Kresin and S. Wolf, Eds., 1987, p. 733.

Invited Talks

15. A. Zettl, "Current Status of High-T_c Research at Berkeley," DOE Workshop on High-T_c Research, Germantown, MD, Feb. 20, 1987.
16. A. Zettl, "High-T_c Research at Berkeley," March Meeting, American Physical Society, Superconductivity Symposium, New York, Mar. 18, 1987.
17. A. Zettl, "Collective-Mode Transport in Low-Dimensional Conductors," Naval Research Laboratory, Washington, D.C., Mar. 31, 1987.
18. A. Zettl, "Advances in High-T_c Superconductivity," University of California, Santa Cruz, Apr. 28, 1987.
19. A. Zettl, "High-T_c Superconductivity," University of California, Davis, June 9, 1987.
20. A. Zettl, "High-T_c Superconductivity—Why All the Excitement?" Walnut Creek Rotary Club, Walnut Creek, CA, June 16, 1987.
21. A. Zettl, "Transport and Elastic Properties of High-T_c Superconductors," Workshop on Novel Superconductivity, Berkeley, CA, June 23, 1987.
22. A. Zettl, "High-T_c Superconductivity," LBL Summer Lecture Series, Berkeley, CA, July 22, 1987.
23. A. Zettl, "Transport, Magnetic, and Elastic Properties of High-T_c Superconductors," LBL/Industrial Panel, Berkeley, CA, Aug. 5, 1987.
24. A. Zettl, "High Temperature Superconductivity: Fascinating Physics," Physics Department Colloquium, University of California Berkeley, Sept. 23, 1987.
25. A. Zettl, "Transport, Optical, Mechanical, and Isotope Studies of High-T_c Superconductors," Institute for Theoretical Physics, Santa Barbara, CA, Oct. 21, 1987.
26. A. Zettl, "Transport, Tunneling, Mechanical, and Isotope Studies of High-T_c Superconductors," LBL/Oak Ridge/Los Alamos High-T_c Meeting, Oak Ridge National Laboratory, Oak Ridge, TN, Nov. 9, 1987.
27. A. Zettl, "High Temperature Superconductors—Theoretical Implications," Engineers Honor Society Lecture Series, University of California Berkeley, Nov. 17, 1987.
28. A. Zettl, "High Temperature Superconductors: Materials, Methods, and Mechanism," University of Kentucky, Lexington, Dec. 11, 1987.

MATERIALS CHEMISTRY

CHEMICAL STRUCTURE

Low-Temperature Properties of Materials*

Norman E. Phillips, Investigator

INTRODUCTION

The major objective of this program is to obtain information that contributes to an understanding of the behavior of materials by the measurement of their low-temperature properties, particularly specific heats. There are numerous special cases in which specific-heat data provide either a test of theoretical models or values of important parameters that could not otherwise be obtained. Much of the work is in the region below 1 K, where the temperature scale is not well established. Because accurate temperature determinations are important for specific-heat measurements, research is also conducted on methods of temperature measurement, and an accurate temperature scale has been developed to 5 mK. The interest in high-T_c superconductors has led to an extension of the measurement capabilities to ~100 K. Recent specific-heat measurements include measurements on He in the Fermi-liquid region that have established the correct values of important parameters; measurements on a number of heavy-fermion compounds, including UPt_3 and UBe_{13}—two of the three heavy-fermion superconductors—and $CeCu_6$, $(Ce,Gd)Al_3$, $CeRu_2Si_2$, and $(U,Th)Be_{13}$; and measurements on high-T_c superconductors that have demonstrated the reality of bulk superconductivity, given estimates of the electronic density of states, and suggested the existence of an intrinsic linear term in the zero-field specific heat. Future objectives include studies on high-T_c superconductors, and specific-heat measurements at pressures to 20 kbar and in magnetic fields to 9T on other heavy-fermion compounds.

*This work was supported by the Director, Office of Energy Research, Office of Basic Energy Sciences, Materials Sciences Division of the U.S. Department of Energy under Contract No. DE-AC03-76SF00098.

1. Specific Heat of High-Temperature Superconductors (Publications 3, 7, and 8)

N.E. Phillips, R.A. Fisher, S.E. Lacy, C. Marcenat, J.A. Olsen, W.K. Ham, A.M. Stacy, J.E. Gordon, and M.L. Tan

The specific heat (C) has been measured for one or two samples of each of the La-Cu oxides, with formulas of the type $La_{1.85}M_{0.15}CuO_4$, with M = Ca, Ba, or Sr; and for five samples of "YBCO," $YBa_2Cu_3O_7$, several of which were "doped" with low concentrations of Cr that substitute on the Cu sites. The measurements extend from ~ 0.4 K to above T_c in almost all cases and were also made in fields to 7 T. A striking feature of these results is the occurrence of a linear term in C, $\gamma(0)T$, in zero magnetic field. The other quantities determined by the measurements are the field dependence of the linear term, $d\gamma/dH$; the lattice specific heat, C_l; the "discontinuity" in C at T_c, $\Delta C(T_c)$; the hyperfine specific heat, C_h; and an impurity contribution C_i, associated with magnetic impurities.

2. Work in Progress

High-T_c Superconductors

The origin of the nonzero value of $\gamma(0)$ remains a major fundamental question related to an understanding of the mechanism for superconductivity in these materials. Studies related to this question will be a major part of the program in 1988 and 1989. They will be based on modification of the electronic density of states by substituting other metals on the Cu sites in YBCO and determining the values of $\gamma(0)$, $d\gamma/dH$, and $\Delta C(T_c)$. The measurements will be made in samples for which the oxygen content is reliably determined and corresponds to the stoichiometry $YBa_2Cu_3O_7$.

Development of an apparatus for measurements on small samples will be initiated. Such an apparatus is important for measurements on high-T_c materials because certain sample qualities can be obtained more easily in smaller samples. It is also important for other materials to be studied in this program in the longer term.

Heavy-Fermion Compounds

Work will be resumed on heavy-fermion compounds in 1988 and 1989. Although high-T_c superconductors will be given a higher priority because of their technical importance, the heavy-fermion compounds remain an important source of information on the mechanism(s) of superconductivity and on other materials properties.

The heavy-fermion compound $U_{1-x}Th_xBe_{13}$ has attracted a great deal of attention because, for $0 < x < 4$, there is a complicated dependence of T_c on x, and a region of x in which there are two successive transitions that occur with decreasing temperature, as might be expected for a triplet-pairing superconductor (and as observed in ^3He). However, the real nature of the second transition is still an open question. Preliminary specific-heat measurements, on a sample with relatively broad transitions and a linear term in C_s, have shown that both transitions are sharply depressed by an applied pressure of 8 kbar. The measurements will be extended to intermediate pressures to follow the course of the transitions as a function of pressure and, later, to new samples, with sharper transitions, that are currently being prepared at Los Alamos National Laboratory (LANL). The results will give insight into the nature of the second transition that cannot be obtained by other measurements.

A new sample of UBe_{13} with a relatively sharp transition temperature has been prepared at LANL. Measurements of C_s and the normal-state specific heat (C_n) have already been made at zero pressure. The measurements will be extended to high pressure to investigate the pressure dependence of the interesting structure in the temperature dependence of C_n and C_s at zero pressure (a continued increase in C_n/T with decreasing temperature, and a change in the coefficient of the T^3 term in C_s). The results will give information about the interactions between the heavy fermions in the normal state and, possibly, about the nature of the superconducting state.

1987 PUBLICATIONS AND REPORTS

Refereed Journals

1. A.S. Edelstein, R.A. Fisher, and N.E. Phillips, "The Temperature Dependence of the Specific Heat and Entropy of $CeAl_3$," J. Appl. Phys. **61**, 3177 (1987); LBL-22444.
2. R.A. Fisher, N.E Phillips, and M. Seto, "Magnetic Susceptibility of AuFe: T_g and Curie-Weiss Parameters," J. Appl. Phys. (Japan) **26**, 779 (1987); LBL-23530.
3. N.E. Phillips, R.A. Fisher, S.E. Lacy, C. Marcenat, J.A. Olsen, W.K. Ham, and A.M. Stacy, "Magnetic Field Dependence of the Specific Heat of Some High-T_c Superconductors," J. Appl. Phys. (Japan) **26**, 1115 (1987); LBL-23531.
4. R.A. Fisher, S.E. Lacy, C. Marcenat, J.A. Olsen, N.E. Phillips, J. Flouquet, A. Amato, and D. Jaccard, "Specific Heat of Heavy-Fermion $CeCu_6$: Effect of Pressure and Magnetic Field," J. Appl. Phys. (Japan) **26**, 1257 (1987); LBL-23532.
5. R.A. Fisher, S.E. Lacy, C. Marcenat, J.A. Olsen, N.E. Phillips, Z. Fisk, and J.L. Smith, "Specific Heat of $(U_{0.97}Th_{0.03})Be_{13}$ Under Pressure," J. Appl. Phys. (Japan) **26**, 1219 (1987); LBL-23533.
6. A. Amato, D. Jaccard, J. Flouquet, F. Lapierre, J.L. Tholence, R.A. Fisher, S.E. Lacy, J.A. Olsen, and N.E. Phillips, "Thermodynamic and Transport Properties of $CeCu_6$," J. Low Temp. Phys. **68**, 371 (1987); LBL-22942.
7. N.E. Phillips, R.A. Fisher, S.E. Lacy, C. Marcenat, J.A. Olsen, W.K. Ham, A.M. Stacy, J.E. Gordon, and M.L. Tan, "Specific Heat of the High T_c Superconductors $(La,M)_2CuO_4$ and $YBa_2Cu_3O_7$ in Magnetic Fields," Physica **148B**, 360 (1987); LBL-23872.

Other Publications

8. N.E. Phillips, R.A. Fisher, S.E. Lacy, C. Marcenat, J.A. Olsen, W.K Ham, and A.M. Stacy, "Magnetic Field Dependence of the Specific Heat of Some High-T_c Superconductors," in *Novel Superconductivity*, S. Wolf and V.Z. Kresin, Eds., Plenum, New York, 1987, p. 739; LBL-23531rev.
9. A.S. Edelstein, R.L. Holtz, M. Rubinstein, J. Tyson, R.A. Fisher, and N.E. Phillips, "Heavy-Fermion, Spin Glass, and Antiferromagnetic Behavior in $(Ce,Gd)Al_3$," Bull. Am. Phys. Soc. **31**, 344 (1986); LBL-23101.
10. R.A. Fisher, J.R. Gordon, and N.E. Phillips, "Specific Heat Clues for Theory," Nature **330**, 601 (1987); LBL-24374.

Invited Talks

11. N.E. Phillips, "Pressure Dependence of the Specific Heat of Heavy Fermion Compounds," CRTBT/CNRS, Grenoble, France, Jan. 1987; March meeting, American Physical Society, New York, Mar. 1987.
12. N.E. Phillips, "Specific Heat of High-T_c Superconductors," Yamada Conference on Superconductivity, Sendai, Japan, Sept. 1987.

Electrochemical Processes*

Charles W. Tobias, Investigator

INTRODUCTION

This program is designed to advance the scientific foundations of electrochemical engineering and to broaden the range of useful applications of electrochemical transformations. Electrolysis processes have inherent advantages over thermochemical methods with respect to material yield and energy efficiency. However, in spite of their long history of economically significant applications, cell processes have not achieved their potential with respect to performance and range of applications in chemical synthesis, nor in energy conversion or storage. A major reason for this condition is the complex nature of transport phenomena in ionic media, as they are coupled to charge-transfer processes at the electrode surface.

- A model has been established for the precise control of composition in the electrodeposition, under pulsed-current conditions, of binary and ternary alloys. Emphasis has been placed on magnetic and photoelectric materials.
- In projects jointly directed with Dr. R.H. Muller, novel methods are explored for the reduction of mass-transfer resistance in high-rate applications, including in electroforming of metals, and in electroorganic synthesis. The effects of suspended inert solid particles in flowing electrolytes, on transport rates, and on electrocrystallization are determined and correlated.

Applied research on the "Surface Morphology of Metals in Electrodeposition," on "Engineering Analysis of Electrolytic Gas Evolution," and on "Metal Couples in Non-Aqueous Electrolytes" is supported by the Assistant Secretary of Conservation and Renewable Energy, Office of Energy Storage and Distribution of the U.S. Department of Energy under Contract No. DE-AC03-76SF00098. Results are presented in this Annual Report in the Energy Storage Systems Section.

*This work was supported by the Director, Office of Energy Research, Office of Basic Energy Sciences, Materials Sciences Division of the U.S. Department of Energy under Contract No. DE-AC03-76SF00098.

1. Enhancement of Mass Transfer to a Rotating Disk by Suspended Solids (Publication 9)

P.K. Andersen, R.H. Muller, and C.W. Tobias

The enhancement of mass-transfer rates by suspended, inert solid particles was studied using a rotating-disk electrode (RDE). The effects of solids concentration, particle size, and shear rate on limiting currents were measured for the reduction of ferrocyanide ion. The suspensions contained glass or polymer particles of various sizes (1–200 μm) and concentrations (0–40% by volume). To minimize sedimentation of the solid phase, the RDE was placed close to the cell bottom, where the rotation of the disk could keep the solids in suspension.

The data show clear evidence of two different transport mechanisms, both of which depend on particle size. Particles the same size as, or smaller than, the thickness of the mass-transfer boundary layer create small-scale "microconvective" vortices that increase the dispersion of solutes and the dissipation of energy. In such cases, the Sherwood number Sh is found to be a function of a Peclet number Pe:

$$Sh = \alpha Pe^m \quad ,$$

where α and m are experimentally determined functions of the solids volume fraction (see Figures 1-1 and 1-2). The Peclet number involves the particle

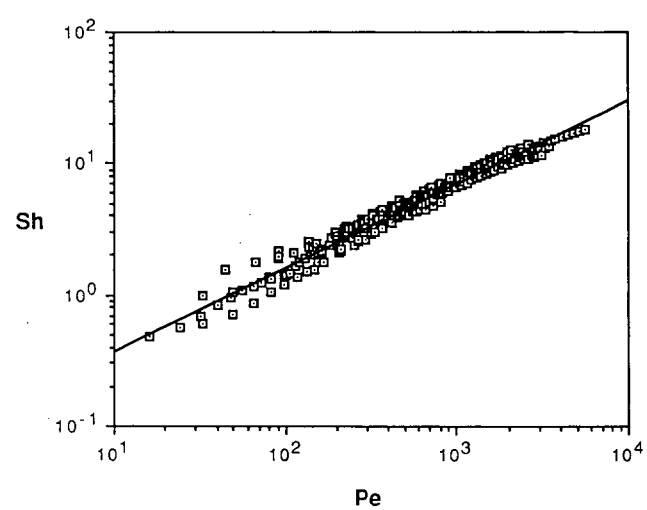

Figure 1-1. Sherwood number as a function of Peclet number for various 40% suspensions of glass beads. The data were obtained using six different electrodes, ranging in area from 0.123 to 5 cm^2, and four different bead samples, ranging from 2.5 to 9.0 μm. The line represents a least-squares fit to the data. (XBL 884-1324)

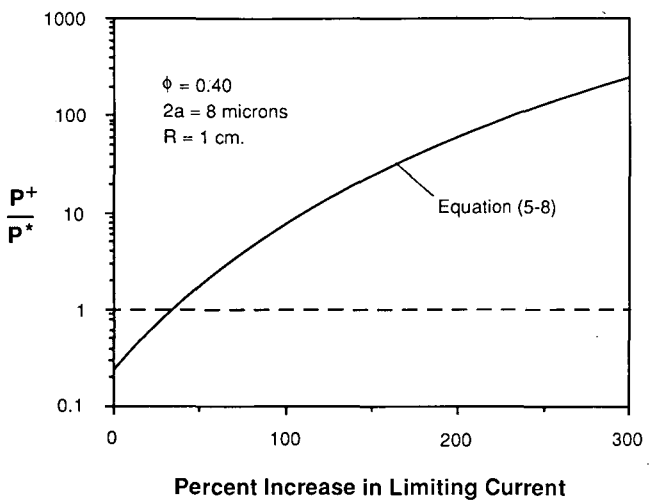

Figure 1-2. Relative power requirements to achieve the same increase in limiting current shown in Figure 1-1. The term p^* is the power requirement when using a 40% suspension of glass beads; p^+ is the power required by a higher disk speed in the absence of solids. (XBL 8711-4900)

diameter 2a, the thickness of the mass-transfer boundary layer δ_{mt}, and the bulk shear rate γ:

$$Pe = \frac{2a\delta_{mt}\gamma}{(D^2\nu)^{1/3}} ,$$

where D is the molecular diffusivity and ν is the kinematic viscosity of the liquid phase.

To determine α and m using the RDE system, it was necessary first to solve the transport equations assuming that the diffusivity varies with radial position on the disk. The analysis yields

$$\frac{I_L^*}{I_L} \propto \left[\alpha Pe_R^m\right]^{2/3} ,$$

where I^*_L/I_L is the ratio of limiting current obtained with particles to the limiting current without, and Pe_R is the Peclet number evaluated at the outer radius of the electrode (r = R).

For particles much larger than the thickness of the mass-transfer boundary layer, transport enhancement results from the formation of a particle-depleted "slip" layer at the electrode surface. The shear rate is higher inside the slip layer than would be the case in a homogeneous suspension; this has the effect of thinning the mass-transfer boundary layer. If it is assumed that this layer is of constant thickness, and that the r- and θ-velocity gradients are increased by the same factor, it can be shown that the limiting current is related to the torque required to turn the disk:

$$\frac{I_L^*}{I_L} = \left(\frac{T^*}{T}\right)^{1/3} ,$$

where T* and T are the torques on the disk with and without particles, respectively. Measurements of the torque show that this equation underestimates the limiting current by as much as 60%, while failing to account for the observed increase in current density with electrode size.

The torque measurements were also useful in estimating the mixing-power requirements. In most cases, the use of suspended solids requires significantly less power to achieve a given increase in limiting current than would an increase in the disk rotation rate.

2. Some Experimental Aspects of the Cadmium-Tellurium Electrochemical Codeposition Process (Publication 4)

M.W. Verbrugge and C.W. Tobias

The cathodic codeposition of Cd and Te represents an intriguing problem with unique chemistry. As is the case in the present study, most Cd-Te codeposition processes make use of an aqueous cadmium sulfate, tellurium dioxide, sulfuric acid electrolyte. Since the Cd-electrodeposit morphology is known to be strongly influenced by the frequency of the cell-current source, we were motivated to study the effect of a pulse-current source on the Cd-Te electrodeposit characteristics. In addition, steady-state and variable frequency illumination was employed to examine the photovoltaic properties of electrodepositing Cd-Te thin films.

A low-frequency triangular current source with a minimum cathodic current density of 0 and a maximum cathodic current density of 5.1 mA/cm^2 is shown in the upper plot of Figure 2-1; in the lower part the potential response is given for varying intensities. At the beginning of the current ramp, the deposit is mostly Te. As the cell-current density approaches 1.5 times $i_{HTeO_2^+,lim}$, the diffusion-limited current density of the $HTeO_2^+$ species, the deposit composition nears the 1:1 mole ratio of Cd to Te (1:1 CdTe), and a photoresponse is seen. The light, which generates minority carriers (electrons) in the p-semiconductor, displaces the electrode potential to more-positive values around the peak cathodic current density. Near zero current, the deposit surface is mostly metallic Te and no longer a semiconductor. It is apparent from Figure 2-1, however, that

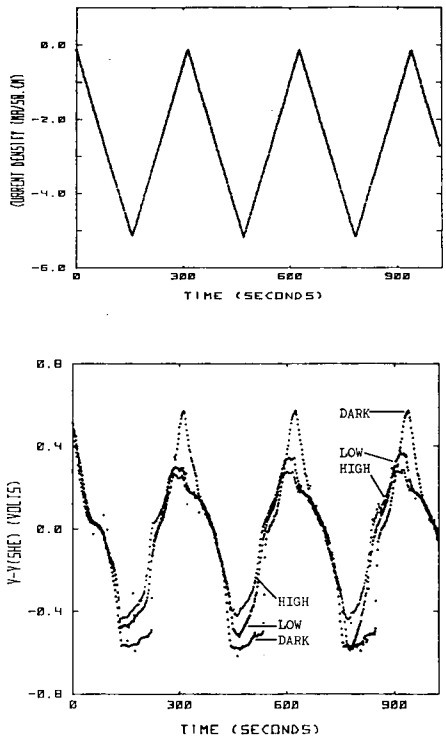

Figure 2-1. Photoresponse of electrodepositing cadmium-tellurium material. Upper plot: cell-current density. Lower plot: potential response for varying illumination intensities. The illumination intensities (DARK, LOW, HIGH) are indicated for each curve. (XBL 884-1325)

the open-circuit potential (at 300, 600, and 900 sec) is a function of the illumination intensity. This is due to the different deposit compositions, which have been altered by the incident light source during the deposition process. For higher illumination intensities, more Cd is incorporated into the electrodeposit, and a more cathodic potential is observed at zero current.

The photoresponse of deposits obtained with pulsed square-wave current over the range of 0.1 to 1,000 Hz was highest at 100 Hz. Although a dependence of surface morphology of the Cd-Te deposits on pulse frequency has been detected by means of optical and electron microscopy, the reasons for optimal photoresponse at 100 Hz are yet to be correlated with subtle changes in composition and in surface morphology.

3. Work in Progress

Work continues in this laboratory on the periodic electrodeposition of alloys, notably of cadmium-telluride. A study of the deposition of nickel and iron alloy, a soft magnetic material, has been initiated. In addition to its practical applications, this system is of interest because it exhibits anomalous behavior; i.e., iron, the less noble metal, deposits preferentially in the presence of nickel ions. This phenomenon is not unique to Ni/Fe systems; anomalous deposition occurs in the codeposition of nickel with a number of other metals (e.g., cobalt) and has also been observed in some alloys of metals as different in electrochemical behavior as zinc and palladium.

1987 PUBLICATIONS AND REPORTS

Refereed Journals

1. M.W. Verbrugge and C.W. Tobias, "The Periodic Electrochemical Codeposition of Cadmium and Tellurium," AIChE J. **33**, 628 (1987); LBL-21013.
2. R.T. Atanasoski, H.H. Law, R.C. McIntosh, and C.W. Tobias, "Electrochemical Analysis of Trace Amounts of Water in Propylene Carbonate Electrolytes," Electrochim. Acta **32**, 887 (1987); LBL-22467.
3. M.W. Verbrugge and C.W. Tobias, "The Transient and Periodic Illumination of a Semiconductor-Electrolyte Interface," J. Electrochem. Soc. **134**, 1437 (1987); LBL-21795.
4. M.W. Verbrugge and C.W. Tobias, "Some Experimental Aspects of the Codeposition of Cadmium and Tellurium," J. Electrochem. Soc. **134**, 3104 (1987); LBL-22519.

Other Publications

5. P.K. Andersen, R.H. Muller, and C.W. Tobias, "The Effect of Suspended Solids on Mass Transport to a Rotating Disk," in *Ext. Abs. The Electrochem. Soc.*, Vol. 87-1, No. 366, May 1987; based on LBL-24522.
6. D.P. Barkey, R.H. Muller, and C.W. Tobias, "Limiting Currents of High-Rate Metal Deposition on a Rotating Cylinder," Ext. Abs., No. 3.1, 38th International Meeting of the International Society of Electrochemistry, Maastricht, The Netherlands, Sept. 13–18, 1987; based on LBL-23880.

LBL Reports

7. D.P. Barkey (Ph.D. Thesis), with R.H. Muller and C.W. Tobias, "Studies on High-Speed Electroforming," LBL-23880.
8. P.K. Andersen (Ph.D. Thesis), with R.H. Muller and C.W. Tobias, "The Effect of Suspended Solids on Mass Transport to a Rotating Disk," LBL-24522.
9. P.K. Andersen, R.H. Muller, and C.W. Tobias, "The Effect of Suspended Solids on Mass Transport to a Rotating Disk," submitted to J. Electrochem. Soc.; LBL-24425.

Invited Talks

10. P.K. Andersen, R.H. Muller, and C.W. Tobias, "The Effect of Suspended Solids on Mass Transport to a Rotating Disk," 171st National Meeting, The Electrochemical Society, Philadelphia, PA, May 10–15, 1987.
11. D.P. Barkey, R.H. Muller, and C.W. Tobias, "Limiting Current of High Rate Metal Deposition on a Rotating Cylinder," 38th Annual Meeting, International Society of Electrochemistry, Maastricht, The Netherlands, Sept. 13–18, 1987.
12. M.W. Verbrugge, "Electrochemical Co-deposition of Cadmium and Tellurium," The Lindsay Lectures of 1987–1988, Department of Chemical Engineering, Texas A&M University, College Station, Dec. 4, 1987.

HIGH-TEMPERATURE AND SURFACE CHEMISTRY

High-Temperature Thermodynamics*

Leo Brewer, Investigator

INTRODUCTION

The understanding of high-temperature chemistry is not only important for processes carried out at high temperatures, such as those of fusion and fission reactors and fossil-fuel power generators, but it is important for the preparation and fabrication of ceramics, metals, semiconductors, superconductors, and many other materials. The understanding of high-temperature behavior is complicated by the occurrence of unusual species and phases that are often unstable at conventional temperatures. It is difficult to carry out measurements to obtain the data needed for design of high-temperature systems. Thus, it is most important to develop broad predictive models that provide reliable prediction of high-temperature behavior. The experiments in progress are aimed at the testing or development of such predictive models.

Previous research of this program has led to the development of a variety of successful models of predictive capability for the behavior of gases, refractory containment materials, and of many metallic systems. At the present time the main thrust of the research is aimed at providing quantitative predictive models for the strongly interacting transition-metal alloys exhibiting generalized Lewis acid-base behavior. A variety of experimental methods are being used to characterize the thermodynamics of these systems.

*This work was supported by the Director, Office of Energy Research, Office of Basic Energy Sciences, Materials Sciences Division of the U.S. Department of Energy under Contract No. DE-AC03-76SF00098.

1. The Thermodynamics and Vaporization Behavior of Oxides (Publications 1, 6, and 10)

R.H. Lamoreaux,† D.L. Hildenbrand,† B.B. Ebbinghaus, and L. Brewer

Oxide phases and species play an important role in many high-temperature systems. The thermodynamic properties are necessary to be able to predict the behavior over a wide range of conditions. In recognition of the need to have tabulations of thermodynamic data available, an extensive compilation was prepared during the Manhattan Project days and has been updated and expanded a number of times since then. In connection with the determination of the thermodynamic properties of intermetallic phases through oxide equilibration, the number of oxide phases covered has been considerably expanded and the tabulation has been used in a variety of ways. Analytical equations have been derived for the Gibbs energy function $-(G^\circ - H^\circ_{298})/RT$ as a function of temperature from 298 to 3000 K and higher for many of the oxides. These equations, together with values of $\Delta H^\circ_{298}/R$, allow the calculation of high-temperature equilibria.

Publication 1 illustrates one application. The partial pressures of the various elemental and oxide species in equilibrium with the condensed oxide phases have been calculated for congruent vaporization, vaporization under highly reducing conditions, and vaporization under highly oxidizing conditions. The results are plotted so that a reader can see at a glance the nature of the oxide vaporization behavior. The elements covered were the second-group elements from Be to Ba and from Zn to Hg, the third-group metals B, Al, Ga, In, and Tl, and the fourth-group elements Si to Pb. Publication 10 presents the procedure used to characterize the thermodynamic properties of all the high-temperature oxides of vanadium that are being used in our acid-base titrations of metallic systems. Publication 6 is the first draft that is being distributed for review of the thermodynamic data for all of the elements and all of their solid, liquid, and gaseous oxides.

†Present address: SRI International, Menlo Park, CA 94025.

2. Bonding Models for Actinide Metal Systems (Publications 2 and 6)

L. Brewer

The prediction of properties of actinide systems is important because their radioactivity makes them difficult to study. They are particularly challenging because the availability of 5f, 6d, 7p, and 7s orbitals considerably complicates their behavior. Fortunately, bonding models that have been tested for lighter elements can be extended to the actinides. Extensive spectroscopic data are available for the actinides, and predictive models can provide the remainder of the promotion energies of the various electronic configurations, so that the bonding contributions of the various types of electrons can be assigned. It is possible to understand the occurrence of complex crystal structures of the actinide metals in that atoms with different electronic configurations and size will occupy nonequivalent lattice positions. Bonding models using the effects of internal pressure and size differences as well as electronic interactions can provide predictions of thermodynamic properties that can be used to calculate many of the phase diagrams of the actinides with reasonable accuracy. However, the very strong generalized Lewis acid-base interactions between actinide metal acids and platinum-group bases are difficult to characterize with sufficient accuracy. The experimental data that have been accumulating for acid-base interactions involving 3d, 4d, and 5d orbitals should improve the ability to predict the interactions involving 6d and 5f orbitals.

3. Acid-Base Reactions of Transition Metal Alloys (Publication 8)

J. Bularzik

The determination of the thermodynamics of the strongly interacting combinations of left-hand transition metals with the platinum-group metals is difficult to carry out reliably. The phases formed are among the most stable compounds of any kind known. Because of their strong bonding, diffusion is slow and they can be difficult to equilibrate. Results obtained using solid-electrolyte cells must be checked by other means to ensure that all systematic errors have been recognized. One of the techniques used has been equilibration with pairs of oxides that fix the metal activity. This is particularly useful for Ti, V, and Nb because of the large number of oxides, but it would not be useful for Zr, Hf, or Ta, which have only a single oxide phase. Vapor pressure measurements are usually a straightforward method of obtaining thermodynamic data. However, vapor pressures are greatly reduced in these strongly interacting systems. One must go to very high temperatures and use sensitive methods of determining vapor pressures. In previous studies, some results have been obtained using a mass spectrometer with a Knudsen cell. However, the creep of the liquid up the walls of the cell is difficult to control.

In the present study, vapor pressures of palladium and rhodium have been determined for Ti, V, and Nb alloys by measurement of thermally induced atomic emission spectra for liquids from 2000 to 2300 K in a graphite King furnace. Measurements could be taken from very low concentrations of Ti, V, and Nb up to the concentration at which reaction with graphite to form the carbide takes place. The measurements of the concentration at which carbide formation takes place allow the use of the thermodynamics of the carbide to provide an independent measure of the activity of the metal. Although the measurements are not as reproducible as the lower-temperature cell and oxide measurements, extrapolation of the thermodynamic values to the lower temperatures confirms the measurements by the other methods within experimental error.

4. Work in Progress

The titration of Nb with Pd and Rh using oxide equilibration, solid-electrolyte-cell measurements, and vapor pressure measurements is being extended to Ti and V on the left-hand side of the Periodic Table and to Ir and Pt on the right-hand side. The critical evaluation of thermodynamic data for the oxides of niobium has been extended to vanadium and titanium to allow use of oxide equilibration. The data obtained from cell measurements and oxide equilibration to date are fitting in with the niobium data in a consistent manner. It should be possible to accurately characterize the acid and base bonding characteristics of the 3d, 4d, and 5d orbitals to develop a predictive model of practical accuracy. It should be possible to extend this model to predict the behavior of the 4f, 5f, and 6d orbitals of the lanthanides and actinides and to the prediction of a large number of multicomponent phase diagrams. The strong interactions of platinum-group metals with transition metals of the third to eighth groups and the lanthanides and actinides have not been

widely recognized. This lack of recognition has caused difficulties in the use of platinum-group metals. The ability to quantitatively predict the degree of interaction should greatly improve the utilization of these metals and should provide unusual combinations with unique properties.

1987 PUBLICATIONS AND REPORTS

Refereed Journals

1. R.H. Lamoreaux, D.L. Hildenbrand, and L. Brewer, "High Temperature Vaporization of Oxides II. Oxides of Be, Mg, Ca, Sr, Ba, B, Al, Ga, In, Tl, Si, Ge, Sn, Pb, Zn, Cd and Hg," J. Phys. Chem. Ref. Data **16**, 419 (1987); LBL-23030.
2. L. Brewer, "The Unusual Bonding of Actinide Systems," J. Less-Common Metals **133**, 15 (1987); LBL-22481.

Other Publications

3. L. Brewer, "Gases (A) Spectroscopy of Interest to High-Temperature Chemistry, and (B) Reactions Between Gases and Condensed Phases," in *Bibliography on the High-temperature Chemistry and Physics of Materials*, Vol. 31, Part 2, M.B. Hocking and V. Vasantasree, Eds., IUPAC Commission on High Temperatures and Refractory Materials, London, 1987; LBL-23644.
4. J. Perepezko, L. Brewer, and R. Schaefer, "Principles Underlying Coatings and Surface Modification Science," Mat. Sci. Eng. **70**, 9 (1985); LBL-23615.
5. L. Brewer and R.H. Lamoreaux, in *Binary Alloy Phase Diagrams*, T.B. Massalski, Ed., American Society for Metals, Metals Park, OH, 1986; LBL-23020. Binary phase diagrams of molybdenum with the 24 elements from Ac to Ga are presented in Vol. 1, pp. 3, 44, 133–35, 191, 208, 211–12, 366–67, 419, 461–62, 517, 554, 576, 621, 667, 725, 754, 758, 777, 896, 933, 935, 998, 1026, 1046, 1053, 1142, and 1145. Binary phase diagrams of molybdenum with the 56 elements from Gd to Zr are presented in Vol. 2, pp. 1191–92, 1271-72, 1295, 1297, 1330, 1362, 1373, 1381, 1417, 1422, 1443, 1463, 1488, 1513, 1515, 1522, 1568–69, 1607–10, 1612–13, 1633–34, 1636–39, 1641–44, and 1646–49. The Mo-Au phase diagram is presented by T.B. Massalski, H. Okamoto, and L. Brewer in Vol. 1, pp. 283–84.

LBL Reports

6. L. Brewer, "High Temperature Thermodynamic Properties of Elements and Their Oxides," LBL-22481.
7. M.J. Cima and L. Brewer, "Generalized Lewis Acid-Base Titration of Palladium and Niobium," submitted to Metall. Trans. B; LBL-23613.
8. J. Bularzik (Ph.D. Thesis), "Acid-Base Reactions of Transition Metal Alloys: Thermochemistry of the Base-Rich End," LBL-23665.
9. L. Brewer, "Chemical Bonding Theory Applied to Metals," American Society of Metals (in press); LBL-23612.
10. L. Brewer and B. Ebbinghaus, "The Thermodynamics of Solid Oxides of Vanadium," Thermochim. Acta (in press); LBL-24468.

Invited Talks

11. L. Brewer, "A Bonding Model for Strong Generalized Lewis Acid-Base Interactions in Intermetallics," Plenary Lecture, Fifth International Conference on High Temperature and Energy-Related Materials, Rome, Italy, May 25–29, 1987; LBL-23614.
12. L. Brewer, "Use of Oxide Equilibria to Determine Thermodynamic Properties," 42nd Annual Calorimetry Conference, Boulder, CO, July 26–29, 1987.
13. L. Brewer, "High Temperature Electrolyte Cells," Research Assistance Task Force Meeting on the Role of Interfaces in Fuel Cells and Metal Air Battery Electrochemical Reactions, Reaction Dynamics in Metal Air Batteries and Fuel Cells Working Group, Lake Geneva, WI, Sept. 23–24, 1987.
14. L. Brewer, "Methods of Obtaining Thermodynamic Data," National Research Council Workshop on Chemical Processes and Products in Severe Reactor Accidents, South Seas Plantation, Captiva Island, FL, Dec. 9–12, 1987; LBL-24469.

Materials Chemistry Problems in Nuclear Technology*

Donald R. Olander, Investigator

INTRODUCTION

This experimental research program has two principal objectives. The first is concerned with the chemical and physical behavior of materials of nuclear reactor systems, both fission and fusion. The experiments are designed to explore the fundamental processes that underlie the performance of these materials in their service environments, which are characterized by combinations of high temperature, intense radiation fields, and reactive gases or liquids.

The second direction of the project is the study of gas-solid chemical reactions such as corrosion or etching by the method of molecular beams coupled with mass spectrometry. The objective of these studies is to understand the kinetics and mechanisms of such reactions in clean, well-characterized systems.

1. Collimator Efficiency in Laser Vaporization Systems Using Mass Spectrometric Detection (Publication 1)

H. Ohashi, S.K. Yagnik, and D.R. Olander

High-temperature vaporization characteristics of refractory solids are often investigated using laser pulse heating and mass spectrometric detection. The geometry of the vaporizing surface, collimator, and the detector is an important consideration in interpreting such experimental results. The mass spectrometer signal depends on the radial dependence both in the laser beam power density and of the relative effectiveness of off-center radial positions on the surface in contributing to the total signal. The function characterizing the latter effect is called the collimator function. Its measurement and application to a typical laser evaporation experimental system has been described.

*This work was supported by the Director, Office of Energy Research, Office of Basic Energy Sciences, Materials Sciences Division of the U.S. Department of Energy under Contract No. DE-AC03-76SF00098.

2. Lattice and Grain Boundary Diffusion in Polycrystalline Thoria-Urania (Publication 2)

D.R. Olander

Recently measured uranium-concentration distributions in air-annealed mixed uranium-thorium oxides were analyzed by a model incorporating simultaneous direct volume diffusion and grain boundary diffusion. The diffusivities for these two processes were strongly affected by the uranium content of the mixed oxide; mobility increased with the cation fraction of uranium. This effect is attributed to the increase in hyperstoichiometry that accompanies replacement of thorium by uranium. Porosity that developed as a result of loss of uranium from the solid did not appear to have a significant effect on grain boundary diffusion.

3. The Transition from Free Molecule to Collisional Flow During Vaporization Into Vacuum by the Test-Particle Method (Publication 3)

C.-H. Tsai and D.R. Olander

A test-particle method was developed to estimate the conditions that lead to collision-dominated evaporation during pulse heating of a solid surface in vacuum. The method consists of calculating the number density of evaporated molecules above the surface, neglecting collisions, and then sending a test particle through this cloud. The probability that the test particle escapes from the cloud without making a collision is the measure of the importance of intermolecular collisions during the blowoff. The method is applied to the heating of a ~1-cm-diameter spot on the surface with a heat pulse of ~1 msec duration. These conditions characterize laboratory laser vaporization experiments intended to measure the vapor pressures of refractory solids at very high temperatures. The principal variable that determines the escape probability is the maximum surface temperature during the transient. When applied to laser heating of uranium dioxide, collisional effects in the vapor are predicted to begin at a maximum surface temperature between 2600 and 2800 K.

4. Reaction of Water and Oxygen with Liquid Uranium (Publication 4)

M. Balooch, D.R. Olander, and W.J. Siekhaus

The reactions of water vapor and oxygen with liquid uranium were studied by modulated-molecular-beam mass-spectrometric methods. Equivalent pressures of the reactant fluxes on the surface ranged from 6×10^{-6} to 2×10^{-4} Torr. Temperatures up to 1570 K were investigated. The metal surface was kept clean during reaction by mechanically removing the oxide formed with a tungsten needle. For the clean liquid uranium surface, the water reaction probability of ~0.4 was deduced both from measurement of the reaction-product hydrogen signal and by the temperature dependence of the scattered reactant signal. Based solely on the latter measure, a reaction probability of 0.6 was estimated for oxygen. The reaction probabilities on the clean surface were temperature-independent. They decreased as the coverage of the surface by islands of oxide increased and, for water, appeared to approach a value of 0.08 for a surface completely covered with an oxide estimated to be 500 Å thick. Bombardment of the surface during reaction with argon ions produced an increase in the reactivity of solid uranium but had a negligible effect on the reaction probability of the liquid.

5. Ceramics in Fission and Fusion Technology (Publication 5)

D.R. Olander

The role of ceramic components in fission and fusion reactors is described. Almost all of the functions normally performed by ceramics, except mechanical, are required of nuclear ceramics. The oxides of uranium and plutonium are of predominant importance in nuclear applications, but a number of other ceramics play peripheral roles. The unique service conditions under which nuclear ceramics must operate include intense radiation fields, high temperatures and large temperature gradients, and aggressive chemical environments. Examples of laboratory research designed to broaden understanding of the behavior of uranium dioxide in such conditions are given. The programs described include high-temperature vaporization, diffusional processes, and interaction with hydrogen.

6. Work in Progress

Molecular-beam studies of the kinetics of the reaction of the fluorine-containing gases F_2, F, and XeF_2 with single-crystal silicon are continuing.

The reaction of chlorine with refractory metals is being investigated by the molecular-beam method.

The amorphization of intermetallic precipitates in Zircaloy is being studied by irradiation by high-energy electrons in the High-Voltage Electron Microscope (HVEM) at LBL's National Center for Electron Microscopy and by proton irradiation using a small cyclotron.

The high-temperature corrosion of Zircaloy by steam in the presence of hydrogen is being studied by a gravimetric technique. The solubility of hydrogen in Zircaloy is also being investigated.

Oxygen self-diffusion in the tetragonal high-temperature form of zirconia is being measured gravimetrically using the oxygen isotope exchange method.

The interaction of iodine vapor with oxidized steel is being studied in a flow system with mass-spectrometric sampling.

The effect of grain size of UO_2 on the release of fission products is being investigated.

A simple mathematical technique for incorporating the heat effect of a phase change on moving-boundary heat-conduction problems is under investigation.

The combined effects of moving grain boundaries and solute diffusion into the lattice on solute transport by grain boundary diffusion are being analyzed theoretically.

1987 PUBLICATIONS AND REPORTS

Refereed Journals

1. H. Ohashi, S. Yagnik, and D. Olander, "Collimator Efficiency in Laser Vaporization Systems Using Mass Spectrometric Detection," Int. J. Mass Spec. Ion Proc. **73**, 313 (1986); LBL-21513.
2. D.R. Olander, "Lattice and Grain Boundary Diffusion in Polycrystalline Thoria-Urania," J. Nucl. Mater. **144**, 105 (1986); LBL-20880.
3. C-H. Tsai and D.R. Olander, "The Transition from Free Molecule to Collisional Flow During Vaporization Into Vacuum by the Test-Particle Method," Phys. Fluids **30**, 386 (1987); LBL-21404.
4. M. Balooch, D.R. Olander, and W. J. Siekhaus, "Reaction of Water and Oxygen with Liquid Uranium," Oxidation of Metals **28**, 195 (1987); LBL-22468.

Other Publications

5. D.R. Olander, "Ceramics in Fission and Fusion Technology," in *High Tech Ceramics*, P. Vincenzini, Ed., Elsevier Science Publishers, Amsterdam, 1987, p. 173; LBL-21481.

LBL Reports

6. D.F. Sherman (Ph.D. Thesis), "Hydrogen Retention and Release from Uranium Dioxide," LBL-24030.
7. F. Tehranian, "A Gasdynamic Model of Rapid Evaporation of a Solid Into a Vacuum," LBL-24109.
8. D.R. Olander, M. Balooch, and J. Abrefah, "Modulated Molecular Beam Studies of the Surface Chemistry of Silicon Reaction with Reactive Gases," LBL-23205.
9. S. Yagnik and D.R. Olander, "Surface Temperature Transients from Pulsed Laser Heating of UO_2," LBL-24022.
10. K.T. Kim and D.R. Olander, "Dissolution of Uranium Dioxide by Molten Zircaloy, I: Diffusion-Controlled Reaction," LBL-23778.
11. S. Yagnik and D.R. Olander, "Dissolution of Uranium Dioxide by Molten Zircaloy, II: Convection-Controlled Reaction," LBL-23802.
12. S.G. Prussin, D.R. Olander, W. Klau, and L. Hansson, "Release of Fission Product Xe, I, Te, Mo, and Tc from UO_2," LBL-23786.
13. K.T. Kim (Ph.D. Thesis), "Interaction of Uranium Dioxide with Molten Zircaloy," LBL-23310.
14. S.K. Yagnik and D.R. Olander, "Laser-Induced Vaporization of Uranium Dioxide," LBL-23391.
15. R. Allred (M.S. Thesis), "Determination of Laser-Evaporated Uranium by Neutron Activation Analysis," LBL-23630.
16. D.R. Olander, S.K. Yagnik, and C.H. Tsai, "Laser-Pulse Vaporization of Uranium Dioxide and Other Refractory Materials," LBL-24405.
17. J. Abrefah, "The Reaction of Silicon with Atomic Hydrogen by Modulated Beam Mass Spectrometry," LBL-24382.
18. M. Balooch, D.S. Fischl, D.R. Olander, and W.J. Siekhaus, "The Kinetics of Tungsten Etching by Atomic and Molecular Chlorine," LBL-24255.

Invited Talks

19. D.R. Olander, "Molecular Beam Studies of the Surface Chemistry of Silicon Reaction with Reactive Gases," Second Topical Meeting on Microphysics of Surfaces, Beams, and Adsorbates, Santa Fe, NM, Feb. 16–18, 1987.
20. D.R. Olander, "UO_2 Dissolution by Molten Zircaloy," Bay Area High Temperature Science and Technology Symposium, Davis, CA, Mar. 12, 1987.
21. D.R. Olander, "UO_2 Dissolution by Liquid Zircaloy," Annual Meeting, American Ceramic Society, Pittsburgh, PA, Apr. 29, 1987.
22. D.R. Olander, "Nuclear Reactor Fuel Under Severe Accident Conditions," Joint Meeting of the Hokkaido Sections of the Atomic Energy Society of Japan and the Japan Institute of Metals, Sapporo, June 4, 1987.
23. D.R. Olander, "Post-Irradiation Annealing Studies of Fission Product Release from UO_2," US-Japan Seminar on the High-Temperature Chemistry of Light-Water Reactors, Tokyo, June 8, 1987.
24. D.R. Olander, "Effect of UO_2 Morphology on the Transient Release of Volatile Fission Products from Severely-Damaged LWR Fuels," US-Japan Seminar on the High-Temperature Chemistry of Light-Water Reactors, Tokyo, June 9, 1987.
25. D.R. Olander, "Dissolution of Uranium Dioxide by Molten Zircaloy," US-Japan Seminar on High-Temperature Chemistry of Light-Water Reactors, Tokyo, June 10, 1987; Conference on Materials for Nuclear Applications, University of Missouri, Rolla, Oct. 26, 1987.
26. D.R. Olander, "High-Temperature Chemistry in Severe-Fuel-Damage Accidents in Nuclear Reactors," Department of Nuclear Engineering Colloquium, University of California Berkeley, Sept. 21, 1987; Institute of Nuclear Energy Research, Taipei, Taiwan, Oct. 14, 1987; Conference on Materials for Nuclear Applications, University of Missouri, Rolla, Oct. 27, 1987; Annual Meeting, Israel Nuclear Society, Haifa, Dec. 21, 1987.
27. D.R. Olander, "Post-Irradiation Annealing Studies of Fission-Product Release from UO_2," Institute of Nuclear Energy Research, Taipei, Taiwan, Oct. 13, 1987.
28. D.R. Olander, "Hydrogen Retention and Release from UO_2," Department of Nuclear Engineering, Tsing Hua University, Taipei, Taiwan, Oct. 14, 1987.
29. D.R. Olander, "Modulated Molecular Beam Studies of GaAs Etching," Materials Research Laboratory, Hsinchu, Taiwan, Oct. 15, 1987.
30. D.R. Olander, "Laser-Induced Vaporization of Uranium Dioxide," Electrochemical Society Meeting, Honolulu, HI, Oct. 21, 1987.
31. D.R. Olander, "Molecular Beam Studies of Silicon Etching by F_2," Electrochemical Society Meeting, Honolulu, HI, Oct. 22, 1987.
32. D.R. Olander, "The Role of Grain Boundaries in the Liquefaction of UO_2 by Molten Zircaloy," Electrochemical Society Meeting, Honolulu, HI Oct. 22, 1987.

Electrochemical Phase Boundaries*

Rolf H. Muller, Investigator

INTRODUCTION

New experimental techniques are used to determine the effect of adsorbed organic molecules on the initial stages in the electrocrystallization of metals and on the properties of thin-film metal deposits. Although adsorbed materials have long been used as leveling and brightening agents in the electrodeposition of metals, it is still not clear how important the supply, reaction, and incorporation of adsorbed molecules is for their effect. Factors that limit the rate of metal deposition, which is of great practical importance, and fundamentals of electrochemical mass transfer are investigated in collaboration with C.W. Tobias. Some of this work is reported under "Electrochemical Processes." Studies of surface layers on battery electrode materials are reported under "Electrochemical Energy Storage."

1. Ellipsometry as an *in situ* Probe for the Study of Electrode Processes (Publication 3)

R.H. Muller

Ellipsometry involves the measurement of the change in the state of polarization caused by the reflection of polarized light from a surface under study. Changes in the state of polarization are often sensitive to the presence of surface layers of fractional monolayer coverage. Since ellipsometer measurements can be conducted on surfaces immersed in liquids, the technique is particularly attractive for electrochemical surface studies.

Spectroscopic ellipsometer measurements in the near-visible spectral range have been used to derive chemical composition and electronic structure of surfaces as well as to derive multiple unknown parameters of the reflecting surface. Combinations of physical parameters that provide best agreement with measurements are determined by least-squares regression analysis. Multiple, porous, and island films have thus been determined (see Figure 1-1).

Recent applications of ellipsometry include anodic oxide formation, cathodic metal deposition, electrochromic conversions, the physical and chemical adsorption of atoms and molecules on metals and semiconductors, the cleaning and ion implantation of surfaces, and the structure of liquid surfaces.

2. Optimum Angle of Incidence for Observing Thin-Film Interference Colors (Publication 4)

R.H. Muller and M.L. Sand

A colorimetric analysis of white-light interference colors for transparent films on absorbing (metal) substrates has shown that specific angles of incidence exist for which the purity of thin-film interference colors is predicted to be greatest for s- or p-polarized light. These optimal angles of incidence depend primarily on the optical constants of the substrate, and

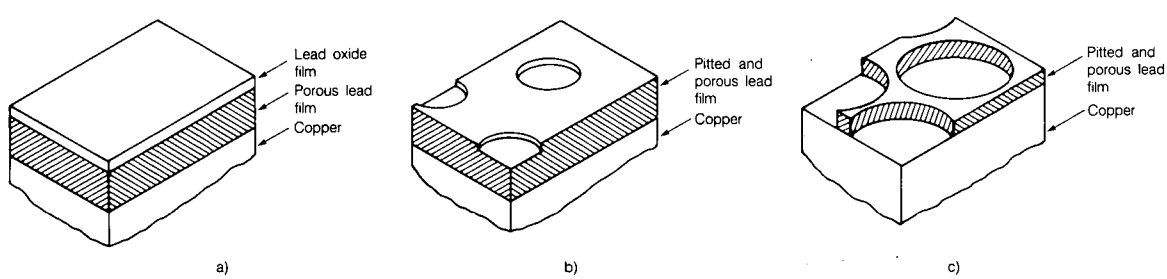

Figure 1-1. Two-layer island-film model for the nonuniform removal of an oxide-covered thin lead film on a copper substrate (a). After removal of the oxide layer, the growth of pits (b) and the gradual exposure of the substrate (c) are represented by an island-film optical model. (XBL 879-11166)

*This work was supported by the Director, Office of Energy Research, Office of Basic Energy Sciences, Materials Sciences Division of the U.S. Department of Energy under Contract No. DE-AC03-76SF00098.

they decrease from the first to the third order of interference. They provide the best conditions for the determination of film thicknesses from interference colors, and their use is essential for making interference colors visible with highly reflective substrates. As an alternate measure of the observability of interference colors, a polychromatic fringe visibility has been introduced. Its use provided similar predictions of optimum angles. The computations are in good agreement with experimental observations.

3. The Role of Long-Range Forces in the Formation of Thin Liquid Films on Metals (Publication 5)

J.R. Gyory and R.H. Muller

The drainage of different liquids from smooth, vertical metal surfaces has been observed experimentally to result in liquid films with thickness profiles that become time-independent after drainage periods of a few days. Several equilibrium and dynamic models have been investigated to explain this behavior. Van der Waals interactions, which result in a repulsive force between the two film surfaces, have been shown to predict the correct shape of the film profiles and, for dilute electrolytes, the correct film thickness. The model also predicts the observed increase in film thickness with increasing electrolyte concentration. The magnitude of this interaction is characterized by the Hamaker constant, which has been calculated from the dielectric functions of film and substrate materials at imaginary frequencies by use of the general theory of van der Waals interactions due to Lifshitz. Hamaker constants thus calculated agree well with those derived from measured film profiles (see Table 3-1).

Table 3-1
Hamaker constant A, derived from film profile measurements and predicted from dielectric functions.

System	A (from film profile) ergs	A (calculated) ergs
3M KOH on platinum	-2.1×10^{-11}	-1.6×10^{-12}
2M KOH on platinum	-1.7×10^{-11}	-1.5×10^{-12}
1M KOH on platinum	-1.0×10^{-11}	-1.4×10^{-11}
0.5M KOH on platinum	-8.2×10^{-12}	-1.2×10^{-12}
0.01M KOH on platinum	-1.0×10^{-12}	-1.1×10^{-12}
1M H_3PO_4 on platinum	-3.4×10^{-11}	-2.3×10^{-12}
1M KOH on gold	-2.0×10^{-12}	-1.3×10^{-12}
0.5M KOH on gold	-1.4×10^{-12}	-1.1×10^{-12}
0.1M KOH on gold	-0.9×10^{-12}	-1.0×10^{-12}

4. High-Speed Electroforming of Copper (Publication 6)

D.P. Barkey, with R.H. Muller and C.W. Tobias

Factors that limit the rate at which metallic objects can be produced by electrodeposition (electroforming) have been investigated for the deposition of copper from sulfate solutions. Rotating cylinder electrodes, for which extensive mass transfer studies have been conducted earlier, and on which turbulent flow conditions can be established readily (boundary layer thickness 50–300 μm), have been chosen for these studies.

Coherent deposits have been obtained at current densities of up to 5 A/cm^2 (0.11 mm/min). The deposition rate is limited by ionic mass transfer in the solution; surface roughness of the deposit represents another limitation. The development of surface textures has been followed by the Fourier analysis of digitized surface profiles. Deposits have also been characterized by microhardness, tensile strength, and density measurements. Surface roughness is observed to increase with deposit thickness (see Figure 4-1) and fraction of limiting current density (see Figure 4-2), but to decrease with increasing absolute current density (see Figure 4-3). Thus, thinning of the boundary layer results in a substantially improved deposit surface. A stability analysis that includes kinetic, mass transfer, and ohmic overpo-

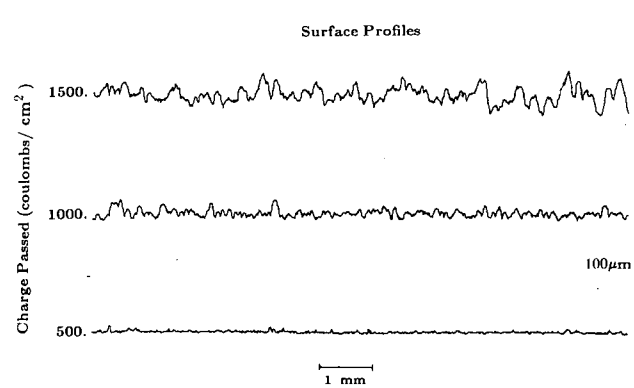

Figure 4-1. Surface profiles of electroformed copper showing increased roughness with increasing deposit thickness (0.8 A/cm^2, 20% of limiting current, 1M $CuSO_4$ + 1M H_2SO_4, 50°C). (XBL 877-3268)

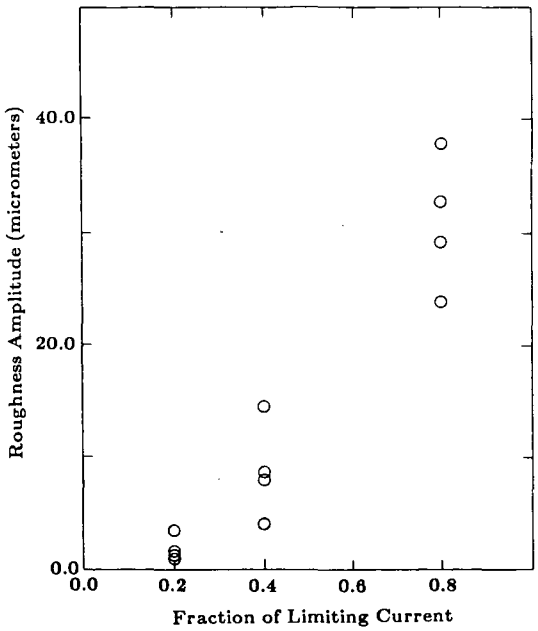

Figure 4-2. Increase in the roughness of electroformed copper deposited at increasing fractions of limiting current density (500 coul/cm^2, 0.8 A/cm^2 1M $CuSO_4$ + 1M H_2SO_4, 50°C). (XBL 877-3260)

tentials has been conducted for deposition on sinusoidal surface profiles of different spatial frequencies. The analysis predicts, in agreement with experiment, a decrease in the spatial period of the roughness with current density at constant fraction of limiting current, but the predicted values are about half of those observed.

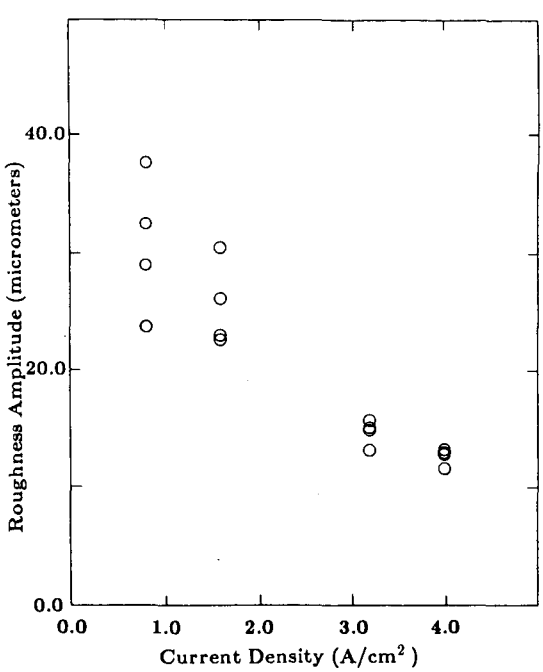

Figure 4-3. Decrease in deposit roughness with increasing absolute current density at fixed (80%) fraction of limiting current (500 coul/cm^2, 1M $CuSO_4$ + 1M H_2SO_4, 50°C). (XBL 877-3262)

5. Work in Progress

Brightening of Copper Electrodeposits (M.T. Armstrong and R.H. Muller)

The mechanism by which additives reduce the microroughness of metal deposits is investigated for the deposition of copper. Fifteen compounds have been explored as brightening agents, and two, benzotriazole and fluorescein, were chosen for detailed study. Nucleation and growth of crystallites is altered by these agents to result in a smaller grain size. In a theoretical model of deposition into a triangular groove, the effect of local potential and composition of the solution on current distribution is analyzed. The use of experimentally determined kinetic data in this model has shown that the inhibitor, even if it is not reacting or being incorporated in the deposit, causes a more uniform current distribution between peaks and valleys of the electrode.

1987 PUBLICATIONS AND REPORTS

Other Publications

1. P.K. Andersen, R.H. Muller, and C.W. Tobias, "The Effect of Suspended Solids on Mass Transport to a Rotating Disk," *Ext. Abs., The Electrochem. Soc.*, Vol. 87-1, No. 366, May 1987.
2. D.P. Barkey, R.H. Muller, and C.W. Tobias, "Limiting Currents of High Rate Metal Deposition on a Rotating Cylinder," *Ext. Abs.*, No. 3.1, 38th International Meeting of the International Society of Electrochemistry, Maastricht, The Netherlands, Sept. 13–18, 1987.

LBL Reports

3. R.H. Muller, "Ellipsometry as an *in situ* Probe for the Study of Electrode Processes," submitted as a chapter in *Techniques for Characterization of Electrodes and Electrochemical Processes,* Wiley, New York; LBL-23916.
4. R.H. Muller and M.L. Sand, "Optimum Angle of Incidence for Observing Thin-Film Interference Colors," submitted to Appl. Opt.; LBL-23697.
5. J.R. Gyory (Ph.D. Thesis), with R.H. Muller, "The Role of Long-Range Forces in the Formation of Thin Liquid Films on Metals," LBL-23698.

6. D.P. Barkey (Ph.D. Thesis), with R.H. Muller and C.W. Tobias, "Studies on High-Speed Electroforming," LBL-23880.

7. P.K. Andersen (Ph.D. Thesis), with R.H. Muller and C.W. Tobias, "The Effect of Suspended Solids on Mass Transport to a Rotating Disk, LBL-24522.

8. P.K. Andersen, R.H. Muller, and C.W. Tobias, "The Effect of Suspended Solids on Mass Transport to a Rotating Disk," submitted to the J. Electrochem. Soc.; LBL-24425.

Invited Talks

9. P.K. Andersen, R.H. Muller, and C.W. Tobias, "The Effect of Suspended Solids on Mass Transport to a Rotating Disk," 171st National Meeting, The Electrochemical Society, Philadelphia, PA, May 10–15, 1987.

10. D.P. Barkey, R.H. Muller, and C.W. Tobias, "Limiting Current of High Rate Metal Deposition on a Rotating Cylinder," 38th Annual Meeting, International Society of Electrochemistry, Maastricht, The Netherlands, Sept. 13–18, 1987.

Solid State and Surface Reactions*

Gabor A. Somorjai, Investigator

INTRODUCTION

The research program is centered on studies of the atomic structure of solid surfaces and adsorbed monolayers and on investigations of the surface science of catalyzed reactions. Well-characterized crystal surfaces are used at low and high pressures. The macroscopic catalytic properties are correlated with the atomic structure, chemical bonding, and composition at the surface and in the near-surface region.

The materials that are the focus of our studies are transition metals and their oxides or sulfides. These include iron, molybdenum, cobalt, rhenium, vanadium, rhodium, and platinum, and bimetallic layers of these. The adsorbates are mostly organic molecules, oxygen, nitrogen, hydrogen, ammonia, and water.

The investigations are directed toward atomic-scale understanding of the catalytic behavior of solid surfaces.

THE STRUCTURE OF SOLID SURFACES AND OF ADSORBED MOLECULES. THE SURFACE CHEMICAL BOND

1. LEED Intensity Analysis of the Surface Structures of Pd(111) and of CO Adsorbed on Pd(111) in a $(\sqrt{3} \times \sqrt{3})R30°$ Arrangement (Publication 18)

H. Ohtani, M.A. Van Hove, and G.A. Somorjai

The surface structures of clean Pd(111) and of CO adsorbed on Pd(111) with a $(\sqrt{3} \times \sqrt{3})R30°$ periodicity at one-third monolayer coverage were investigated by dynamical low-energy electron-diffraction (LEED) intensity analyses of measured I-V curves. The clean Pd(111) structure was confirmed to be close to the ideal bulk structure. Slight, possibly hydrogen-induced deviations were obtained for the interlayer spacings down to the fifth layer: $\Delta d_{12} = +0.03 \pm 0.03$ Å, $\Delta d_{23} = -0.03 \pm 0.03$ Å, and $\Delta d_{34} = \Delta d_{45} = +0.05 \pm 0.03$ Å (positive values indicate expansion from the bulk spacing value). The CO molecules are favored to adsorb at fcc-type hollow sites with the C-O axis perpendicular to the surface. The optimal carbon-oxygen and metal-carbon bond lengths are 1.15 ± 0.05 Å and 2.05 ± 0.04 Å, respectively. This is the first LEED structure analysis of CO adsorbed at a hollow site on clean metal surfaces without coadsorbates.

2. The Molecular Structure of Benzene Coadsorbed with CO on Pd(111): A Dynamical LEED Analysis (Publications 48 and 50)

H. Ohtani, M.A. Van Hove, and G.A. Somorjai

The molecular structure of the ordered (3×3) superlattice of coadsorbed C_6H_6 and CO on the Pd(111) crystal face was analyzed by dynamical calculations of LEED intensities.

The benzene molecules were found to be oriented with their carbon rings parallel to the surface, centered over fcc-type threefold hollow sites. The C-C bond lengths in the benzene ring skeleton were found to be either 1.40 ± 0.10 Å or 1.46 ± 0.10 Å, depending on the position of the C-C bonds relative to the underlying Pd atoms. These bond lengths are very close to the corresponding gas-phase value of 1.397 Å. This contrasts with similar coadsorbate systems of benzene and CO on Rh(111) or Pt(111), where significant in-plane distortions and enlargements of the benzene rings have been detected. A trend toward more distortion and increasing average C-C bond length has been found in changing substrates from Pd to Rh and Pt, while the metal-carbon bond lengths decrease in that same sequence. This is interpreted to indicate that the metal-carbon bond becomes shorter, while C-C bonds weaken from Pd to Rh and Pt, which is further supported by high-resolution electron-energy-loss spectroscopy (HREELS) data.

Coadsorbed CO molecules are necessary to form an ordered benzene overlayer on Pd(111). They occupy fcc-hollow sites surrounding the benzene molecules. The C-O axis is perpendicular to the surface, and the carbon-oxygen and palladium-carbon bond lengths are found to be 1.17 ± 0.05 Å and 2.05 ± 0.07 Å, respectively.

*This work was supported by the Director, Office of Energy Research, Office of Basic Energy Sciences, Materials Sciences Division of the U.S. Department of Energy under Contract No. DE-AC03-76SF00098.

3. The Missing-Row Model for the Reconstructed Pt(110)-(1 × 2) Surface: A LEED Intensity Analysis Showing Multilayer Distortions (Publication 52)

E.C. Sowa, M.A. Van Hove, and D.L. Adams

The (1 × 2) missing-row reconstruction of clean Pt(110) was studied with a new LEED intensity analysis. In order to obtain theoretical intensity-voltage curves in good agreement with experiment, it was necessary to consider distortions from the basic missing-row model in the theoretical treatment. In our calculations, alternating row-pairing and vertical-buckling distortions down to the fourth layer were allowed for the first time.

Large contractions were seen in the first three layer spacings, and significant distortions were found even in the fourth layer. The distortions are similar to those seen in Ir and Au LEED results as well as those predicted by the Embedded Atom Method (EAM) for Pt. In the optimum geometry, the top-layer spacing contracts by 18%. The atoms in the second layer pair towards the missing rows, in agreement with LEED on Ir and Au but in the direction opposite to that predicted by EAM. The R-factors are especially sensitive to the third-layer buckling. The fourth-layer pairing is also towards the missing rows, in agreement with the EAM prediction.

It is shown that full dynamical LEED calculations of this kind can be realistically run on a personal computer with suitable coprocessor board.

4. A Tabulation and Classification of the Structures of Clean Solid Surfaces and of Adsorbed Atomic and Molecular Monolayers as Determined from Low Energy Electron Diffraction Patterns (Publication 27)

H. Ohtani, C.-T. Kao, M.A. Van Hove, and G.A. Somorjai

A tabulation was compiled of the ordering characteristics of clean and adsorbate-covered single-crystal surfaces based on diffraction patterns observed with LEED. Over 3000 structures are classified by rotational symmetry of the substrate surfaces, and by important sub-classes that reflect recent directions of LEED studies. These include metallic monolayers, alloy surfaces, organic overlayers, coadsorbed overlayers, physisorbed overlayers, and high-Miller-index (stepped) surfaces.

5. Coadsorbate-Induced Ordering on Rh(111) and Rh(100) Surfaces: Structural and Chemical Effects (Publication 47)

C.-T. Kao, G.S. Blackman, M.A. Van Hove, and G.A. Somorjai

Carbon monoxide (CO) induced ordering of atomic and molecular coadsorbates on Rh(111) and Pt(111) surfaces was first observed in this laboratory. To further understand the interaction between coadsorbates in an ordered overlayer, the study has been extended to various pairwise combinations of coadsorbates on Rh(111) and Rh(100) surfaces. The experiments were performed in three different ultrahigh-vacuum (UHV) chambers with a base pressure of 2×10^{-10} torr. Several experimental techniques, including work-function measurement, HREELS, and dynamical LEED structural analysis, were utilized in these studies. It emerges that ordering only occurs when a donor adsorbate and an acceptor adsorbate are combined, indicating attractive interactions between them and repulsive interactions between adsorbates of like type.

6. The Surface Structure and Thermal Decomposition of Acetylene on the Rh(111) Single Crystal Surface and the Effect of Coadsorbed Carbon Monoxide (Publication 45)

C.M. Mate, C.-T. Kao, B.E. Bent, and G.A. Somorjai

The surface structure and thermal chemistry of acetylene on the Rh(111) crystal surface have been studied from 30 to 800 K using HREELS, LEED, and thermal desorption spectroscopy (TDS). Adsorbed acetylene on the Rh(111) is disordered at 30 K, but orders into a (2 × 2) LEED structure at 60 K; this is the lowest ordering temperature that has been reported for chemisorbed acetylene on a metal surface. HREEL spectra of C_2H_2 and C_2D_2 ordered in the (2 × 2) structure at 77 K on Rh(111) indicate that the carbon-carbon bond of chemisorbed acetylene rehybridizes between sp^2 and sp^3. At 270 K, chemisorbed molecular acetylene decomposes predominantly to CCH_2 species. Above 400 K, further decomposition to a mixture of CCH and CH species is observed. When CO and molecular acetylene are coadsorbed at 220 K, we observe a c(4 × 2) LEED structure rather than the (2 × 2) LEED structures observed for acetylene or CO adsorbed alone on Rh(111). Also, chemisorbed ace-

tylene, when coadsorbed with CO, decomposes at 270 K to a mixture of CCH_3 (ethylidyne) and CCH (acetylide) species rather than the CCH_2 species.

7. Molecular Ethylene Adsorption on Rh(111) and Rh(100): Estimation of the C-C Stretching Force Constant from the Surface Vibrational Frequencies (Publication 40)

B.E. Bent, C.M. Mate, C.-T. Kao, A.L. Slavin, and G.A. Somorjai

Molecular ethylene adsorption on Rh(111) and Rh(100) between 90 and 200 K has been studied by TDS, LEED, and HREELS. The HREEL vibrational spectra for molecularly adsorbed ethylene on these surfaces are interpreted using the Dewar-Chatt-Duncanson model for ethylene coordination to metal atom(s); gas-phase ethylene and gauche 1,2-dibromoethane are used to model the coordination extremes. It is shown that the traditional CH_2 functional-group modes are coupled in adsorbed ethylene and do not adequately describe the normal modes of vibration. However, the C-C stretching force constant in adsorbed ethylene can be estimated from the deuterated ethylene vibrational frequencies, and a general correlation between deuterated vibrational frequency and adsorbed C-C force constant is proposed. Using this correlation together with empirical correlations between force constant and bond length derived for gas-phase molecules, we estimate C-C bond orders of 1.5 and 1.2 for ethylene adsorbed on Rh(111) and Rh(100), respectively. These results indicate that on both surfaces, chemisorbed ethylene is strongly distorted from its gas-phase geometry.

8. Vibrational and Electronic Spectroscopy of Pyridine and Benzene Adsorbed on the Rh(111) Crystal Surface (Publication 25)

C.M. Mate, G.A. Somorjai, H.W.K. Tom, X.D. Zhu, and Y.R. Shen

The vibrational and electronic spectra for pyridine and benzene adsorbed on the Rh(111) crystal surface have been obtained by HREELS. LEED, TDS, and optical second-harmonic generation (SHG) have also been used to provide complementary information. Pyridine adsorption on Rh(111) was studied over the 77 to 450 K temperature range. At 77 K, multilayers of pyridine are observed with a vibrational spectrum similar to that of liquid pyridine. Between 185 to 230 K, HREELS and TDS indicate that both physisorbed and chemisorbed pyridine species are present on the surface. The physisorbed species desorbs at 295 K, while the chemisorbed species is stable until it decomposes on the surface at 400 K. We propose that the chemisorbed species is an α-pyridyl complex, as TDS indicates partial dehydrogenation of this pyridine surface species. Electronic-energy-loss spectra for both benzene and pyridine adsorbed at 310 K show only a weak transition centered at $\sim$4 eV. The absence of prominent $\pi \rightarrow \pi^*$ transitions, which are readily observed for multilayers of benzene adsorbed on Rh(111), implies that the π orbitals are strongly involved in the chemisorption bond of these molecules with the Rh(111) surface.

9. Organic Monolayers on Transition Metal Surfaces. The Catalytically Important Sites (Publication 23)

G.A. Somorjai, M.A. Van Hove, and B.E. Bent

The structure and bonding of organic monolayers have been explored by combined LEED and HREELS studies. Unusual bonding arrangements for adsorbed ethylene and benzene have been found. There is a temperature-induced sequential fragmentation of molecules that is a unique feature of the surface chemical bond. All the surface species appear very similar to multinuclear organometallic clusters, revealing that the surface chemical bond is similar to that found in these clusters. The strongly bound organic surface species are not reaction intermediates during ethylene hydrogenation at 300 K but are spectators that play only secondary roles in this catalytic reaction. The coadsorption of electron acceptor molecules (CO or NO) facilitates the ordering of benzene and other organic molecules that are electron donors to the transition-metal substrates. This ordering indicates the importance of adsorbate-adsorbate interactions in forming surface structures.

10. The Preparation and Characterization of Rhenium-Modified Pt(111) and Pt(100), and Platinum-Modified Re(0001) Single-Crystal Surfaces (Publication 46)

D.J. Godbey and G.A. Somorjai

Rhenium metal grows epitaxially on Pt(111) and Pt(100) in a layer-by-layer mode, as shown by Auger electron spectroscopy (AES) and LEED. Platinum metal on Re(0001) was also found to grow layer by layer. Rhenium evaporated onto Pt(111) grows with a hexagonal close-packed structure exposing the (0001) face, while on Pt(100) it grows with a face-centered-cubic structure exposing the (100) face. The surface composition of the bimetallic Re-Pt surface can be determined from the Auger spectrum when the coverage of rhenium is less than three monolayers.

Following rhenium deposition on platinum, chemical shifts were detected in the 4f levels of both adsorbate and substrate using x-ray photoelectron spectroscopy (XPS), and this is indicative of the formation of a surface alloy between the two metals. Annealing the bimetallic surface to 1150 K caused further shifts to higher binding energies for both the platinum and the rhenium 4f lines.

The presence of platinum on a partially oxidized Re(0001) surface was found to catalyze the decomposition of rhenium oxides under UHV and at a temperature as low as 400°C.

11. The Conversion of Acetylene to Benzene Over Palladium Single-Crystal Surfaces. II. The Effect of Additives (Publication 2)

M.A. Logan, T.G. Rucker, T.M. Gentle,[†] E.L. Muetterties,[‡] and G.A. Somorjai

The conversion of acetylene to benzene has been studied over palladium single-crystal surfaces [(111), (100), and (110)] modified with submonolayer quantities of silicon, phosphorus, sulfur, chlorine, and potassium under both UHV and atmospheric pressure conditions. At atmospheric pressures electron-donating additives enhance the rate of benzene formation, and electron-accepting additives reduce the rate. Potassium and silicon reduce the amount of surface carbon that accumulates during the reaction and thereby increase the rate of benzene formation relative to the undoped surface. The general trends of the (111), (100), and (110) faces indicate that at low pressures potassium suppresses, silicon and phosphorus enhance, and sulfur and chlorine leave unchanged the benzene yield. Silicon on the (100) face showed the greatest enhancement in the benzene yield, possibly due to surface compound formation.

[†]Present address: Dow Corning Corp., Midland, MI 48640.
[‡]Deceased

12. An XPS Study of the Oxidation and Reduction of the Rhenium-Platinum System Under Atmospheric Conditions (Publication 19)

W.T. Tysoe, F. Zaera, and G.A. Somorjai

The oxidation and reduction of the platinum-rhenium system has been studied by using XPS. Rhenium was deposited on a platinum foil under vacuum until a film of about 10 monolayers was formed. This sample was sequentially exposed to 1 atm of oxygen at different temperatures and then reduced with 1 atm of H_2. XP spectra were taken after each high-pressure experiment. A mixture of rhenium oxides was formed after oxidation at above 475 K, and depletion of the surface rhenium was observed after treatments above 575 K due to the formation of the volatile Re_2O_7. Hydrogen treatment did not completely reduce these oxides, and a low-oxidation rhenium state could be detected by XPS, perhaps ReO. The behavior of platinum-rhenium alloys after similar treatments was also studied. Extensive oxidation was also seen for this system, even more than for the rhenium overlayer case. Subsequent hydrogen treatment, however, did reduce all the rhenium to its metallic state, indicating that platinum intermixed with the rhenium catalyzed its reduction.

13. The Chemisorption and Surface Reactions of D_2 and Hydrocarbons on the Re(0001) Single-Crystal Surface: When Clean and in the Presence of CO-Adsorbed Sulfur or Carbon (Publication 20)

D.G. Kelly, J.A. Odriozola, and G.A. Somorjai

The chemisorption and surface reactions of thiophene, D_2, and the hydrodesulfurization products (1,3-butadiene and butenes) have been studied on Re(0001) at low ambient pressure (10^{-9} torr)

using TDS, LEED, and AES. D_2 adsorption was found to be blocked by sulfur or carbon overlayers. Sulfur preadsorption induced small changes in the D_2 desorption energy, and adsorption was completely blocked above 0.4 monolayer of sulfur ($\theta_x = 0.4$). Carbon readsorption lowered the temperature of the desorption maxima (380 K to 290 K) and blocked D_2 adsorption nonlinearly. Sequential dehydrogenation of the adsorbed unsaturated hydrocarbons leading to complete decomposition at high temperature (>700 K) was observed on the clean Re(0001) surface. Addition of sulfur or carbon blocked dehydrogenation. No changes in the dehydrogenation (yielding H_2) TDS peak temperatures were observed for both sulfur or carbon preadsorption. However, selective blocking of dehydrogenation states was observed for both sulfur or carbon pre-adsorption. In addition, carbon adsorption did allow hydrogenation of butadiene to occur. It is concluded that, for all systems, preadsorbed sulfur acts as a site-blocker for adsorption and dissociation with only small effects on bonding of adsorbed molecules on Re(0001). Although this also seems to be true for preadsorbed carbon as well, other subtle effects are observed that can change the surface chemistry of adsorbed molecules, as exemplified by the hydrogenation of butadiene.

THE SURFACE SCIENCE OF HETEROGENEOUS CATALYSIS

14. The Effects of Potassium on the Ammonia Synthesis Over Iron Single-Crystal Surfaces (Publication 22)

D.R. Strongin and G.A. Somorjai

The effects of potassium on ammonia synthesis over model iron single-crystal catalysts of (111), (100), and (110) orientation have been studied under high-pressure reaction conditions (20 atm reactant pressure of nitrogen and hydrogen). Under these conditions, no more than 0.15 monolayer (ML) of potassium can be stabilized on the iron surfaces.

The Fe(110) surface showed no activity for ammonia synthesis in this study with or without adsorbed potassium. The presence of potassium on the Fe(111) and Fe(100) surfaces increased the rate of ammonia synthesis markedly. At a low reaction conversion of 0.5%, the rate over Fe(111) and Fe(100) was enhanced by a factor of two in the presence of potassium. The effect of potassium on Fe(111) and Fe(100) was enhanced as higher reaction conversions (i.e., increasing ammonia partial pressures) are achieved, because potassium induces changes in the reaction orders for both ammonia and hydrogen. This is the first study showing that the activity of the clean Fe(111) surface can be improved upon. No change in the activation energy for the reaction was observed with potassium, suggesting that the reaction mechanism has not been altered. Temperature-programmed desorption showed that the adsorption energy of ammonia is significantly reduced when coadsorbed with potassium.

A model is proposed whereby the decrease of the ammonia adsorption energy, induced by potassium, reduces the concentration of ammonia on the iron surface. This effect decreases the number of active sites blocked by the ammonia product, thereby increasing the rate of ammonia synthesis. The model also suggests that an additional effect of potassium is to increase the rate of nitrogen dissociative chemisorption by about 30% over Fe(111) and Fe(100) under ammonia-synthesis conditions.

15. On the Rate Enhancement of Ammonia Synthesis Over Iron Single Crystals by Coadsorption of Aluminum Oxide with Potassium (Publication 44)

D.R. Strongin and G.A. Somorjai

The iron ammonia-synthesis catalyst that is utilized in industry is usually mixed with potassium oxide and aluminum oxide additives that further increase the rate of ammonia synthesis. It is found that aluminum oxide additives alone increase the rate of ammonia synthesis by increasing the active surface area of the iron. Potassium addition decreases the iron surface area but still increases the rate by a factor of three to ten. The doubly "promoted" iron catalyst surface consists of regions where potassium oxide resides alone and areas where it interacts with aluminum oxide. Combined high-pressure and UHV studies in our laboratory have elucidated the mechanisms by which aluminum oxide or potassium adsorbed alone increases the rates of ammonia synthesis over Fe(111), Fe(100), and Fe(110) single-crystal surfaces. In this study we have investigated the combined effects of coadsorbed potassium and aluminum oxides commonly used in preparing the industrial iron catalyst.

16. Thiophene Hydrodesulfurization Over Transition-Metal Surfaces: Structure-Insensitive Over Molybdenum and Structure-Sensitive Over Rhenium (Publication 49)

M.E. Bussell, A.J. Gellman, and G.A. Somorjai

We have performed thiophene hydrodesulfurization (HDS) experiments over molybdenum and rhenium single crystals. Thiophene HDS activities were measured for three low-Miller-index single-crystal planes of molybdenum and four of rhenium. Surfaces of comparable openness and corrugation were studied for the two metals, yet thiophene HDS was found to be structure-insensitive over molybdenum and structure-sensitive over rhenium. The rhenium surfaces showed a sixfold variation of HDS activities in the order $(0001)<(11\bar{2}1)<(11\bar{2}0)<(10\bar{1}0)$, while the three molybdenum surfaces studied [(110), (100), and (111)] exhibited almost uniform activities. Comparing the activities of the rhenium and molybdenum surfaces, the least active rhenium surface [Re(0001)] has an activity similar to those of the molybdenum surfaces, while the most active rhenium surface $[Re(10\bar{1}0)]$ is six times more active than the molybdenum surfaces. We suggest that the active catalytic surface of the Mo single crystals studied is covered with adsorbed carbon and that this overlayer blocks the influence of the metal's surface structure on the catalyst's activity.

17. A Novel High-Pressure Isolation Cell Capable of Reaching 120 Atm Mounted in an Ultrahigh-Vacuum Chamber (Publication 43)

T.G. Rucker, K. Franck, D. Colomb, M.A. Logan, and G.A. Somorjai

A high-pressure cell and manipulator mounted inside a UHV surface analysis chamber has been built that can reach 1800 psi. With this apparatus, catalytic reactions on small-surface-area (~ 1 cm^2) single crystals and polycrystalline surfaces can be monitored, and the effect of reactant pressure, surface composition, and surface structure can be correlated with catalytic activity.

18. Work in Progress

A digital LEED system is being applied to determine the surface structures of disordered monolayers of small molecules (CO, C_2H_2, H_2O) on metal crystal surfaces and for studies of surfaces of insulating materials (LiF, ice) that up to now were not accessible to surface studies.

Surface structures of organic monolayers are being obtained by both LEED and scanning tunneling microscopy, and the results are being correlated.

The surface science and catalytic behavior of copper single crystals are being explored for producing alcohols from CO and H_2.

The addition of cobalt to molybdenum crystals is being studied to explore the formation of the superior Mo-Co catalysts for hydrodesulfurization, an important chemical energy-conversion reaction.

The platinum-rhenium and cobalt-molybdenum alloy systems are being studied using single crystals to elucidate the catalytic behavior of alloys for hydrocarbon conversion reactions.

Potassium and alumina additives to iron greatly accelerate the rate of ammonia synthesis. Their role is being verified by combined surface science and catalytic studies. Their possible role in ammonia synthesis over rhenium surfaces is being explored.

The copper-zinc oxide system is being explored to understand the surface science of methanol production from CO and H_2 over this important catalyst.

1987 PUBLICATIONS AND REPORTS

Refereed Journals

1. J.E. Crowell, W.T. Tysoe, and G.A. Somorjai, "Potassium Coadsorption Induced Dissociation of CO on the Rh(111) Surface: An Isotope Mixing Study," J. Phys. Chem. **89**, 1598 (1986); LBL-18123.
2. M.A. Logan, T.G. Rucker, T.M. Gentle, E.L. Muetterties, and G.A. Somorjai, "The Conversion of Acetylene to Benzene Over Palladium Single Crystal Surfaces II: The Effect of Additives," J. Phys. Chem. **90**, 2709 (1986); LBL-19760.
3. M.E. Levin, M. Salmeron, A.T. Bell, and G.A. Somorjai, "The Effects of Titania and Alumina Overlayers on the Hydrogenation of CO over Rhodium," J. Chem. Soc., Faraday Trans. I. **83**, 2061 (1987); LBL-21607.

4. D.G. Kelly, M. Salmeron, and G.A. Somorjai, "The Adsorption and Reactions of Hydrocarbons on Molybdenum Single Crystal Surfaces; When Clean and in the Presence of Co-adsorbed Sulfur and Carbon," Surf. Sci. **175**, 465 (1986); LBL-21251.
5. C.M. Mate and G.A. Somorjai, "The Delocalized Quantum Nature of Hydrogen Adsorbed on the Rh(111) Crystal Surface," Solid State Commun. **34**, 7417 (1986); LBL-21545.
6. D.R. Strongin, J. Carrazza, S.R. Bare, and G.A. Somorjai, "The Importance of C_7 Sites and Surface Roughness in the Ammonia Synthesis Reaction over Iron," J. Catal. **103**, 213 (1987); LBL-21500.
7. D.F. Ogletree, M.A. Van Hove, and G.A. Somorjai, "Benzene and Carbon Monoxide Adsorbed on Pt(111): A LEED Intensity Analysis," Surf. Sci. **183**, 1 (1987); LBL-21502.
8. Hu Zi-lu, D.E. Ogletree, M.A. Van Hove, and G.A. Somorjai, "LEED Theory for Incommensurate Overlayers: Application to Graphite on Pt(111)," Surf. Sci. **180**, 433 (1987); LBL-21511.
9. B.E. Bent, C.M. Mate, J.E. Crowell, B.E. Koel, and G.A. Somorjai, "Bonding and Thermal Decomposition of Propylene, Propadiene and Methylacetylene on the Rh(111) Single Crystal Surface," J. Phys. Chem. **91**, 1493 (1987); LBL-21504.
10. D.R. Strongin, S.R. Bare, and G.A. Somorjai, "The Effects of Aluminum Oxide in Restructuring Iron Single Crystal Surfaces for Ammonia Synthesis," J. Catal. **103**, 289 (1987); LBL-21836.
11. M.E. Bussell and G.A. Somorjai, "A Radiotracer (^{14}C) and Catalytic Study of Thiophene Hydrodesulfurization on the Clean and Carbided Mo(100) Single Crystal Surface," J. Catal. **106**, 93 (1987); LBL-22141.
12. M.A. Van Hove, R.F. Lin, D.F. Ogletree, G.S. Blackman, C.M. Mate, and G.A. Somorjai, "Coadsorption Structures of Benzene and Carbon Monoxide on Rh(111) And Pt(111) By HREELS and LEED," J. Vac. Sci. Technol. A **5**, 692 (1987); LBL-22079.
13. M.A. Van Hove, R.F. Lin, G.S. Blackman, and G.A. Somorjai, "LEED Intensity Analysis of the Structure of Coadsorbed Benzene and CO on Rh(111)," Acta Crystallogr. **B43**, 368 (1987); LBL-21501.
14. M.I. Ban, M.A. Van Hove, and G.A. Somorjai, "The Tilting of CO Molecules Chemisorbed on a Pt(110) Surface—A Molecular Orbital Study," Surf. Sci. **185**, 355 (1987); LBL-21554.
15. S. Bare and G.A. Somorjai, "Surface Chemistry," Encyclopedia of Physical Science and Technology **13**, 524 (1987); LBL-20904.
16. A.J. Gellman, D. Neiman, and G.A. Somorjai, "Catalytic Hydrodesulfurization Over The Mo(100) Single Crystal Surface I: Kinetics and Overall Mechanism," J. Catal. **107**, 92 (1987); LBL-20356
17. A.J. Gellman, M.E. Bussell, and G.A. Somorjai, "Catalytic Hydrodesulfurization Over The Mo(100) Single Crystal Surface II: The Role of Adsorbed Sulfur and Mechanism of the Desulfurization," J. Catal. **107**, 103 (1987); LBL-21891.
18. H. Ohtani, M.A. Van Hove, and G.A. Somorjai, "LEED Intensity Analysis of the Surface Structures of Pd(111) and of CO Adsorbed on Pd(111) in a $(\sqrt{3} \times \sqrt{3})R30°$ Arrangement," Surf. Sci. **187**, 372 (1987); LBL-23004.
19. W.T. Tysoe, F. Zaera, and G.A. Somorjai, "An XPS Study of the Oxidation and Reduction of the Rhenium-Platinum System Under Atmospheric Conditions," Surf. Sci. **191**, 271 (1987); LBL-23032.
20. D.G. Kelly, J.A. Odriozola, and G.A. Somorjai, "The Chemisorption and Surface Reaction of D_2 and Hydrocarbons on the Re(0001) Single Crystal Surface; When Clean and In the Presence of Co-Adsorbed Sulfur or Carbon," J. Phys. Chem. **91**, 5695 (1987); LBL-23242.
21. A.J. Gellman, W.T. Tysoe, and G.A. Somorjai, "An XPS/UPS Investigation of the Adsorption of Sulfur to the Mo(100) Surface: Adsorption Site and Lateral Interactions," Surf. Sci. **191**, 271 (1987); LBL-20357.
22. D.R. Strongin and G.A. Somorjai, "The Effects of Potassium on the Ammonia Synthesis Over Iron Single Crystal Surfaces," J. Catal. **109**, 51 (1988); LBL-23403.
23. M.A. Van Hove, B.E. Bent, and G.A. Somorjai, "Organic Monolayers on Transition Metal Surfaces. The Catalytically Important Sites," J. Phys. Chem. **92**, 973 (1988); LBL-23627.
24. R. Prins and G.A. Somorjai, "Contributions of Gas Chromatography to the Development of Heterogeneous Catalysis," J. Chromatography **406**, 151 (1987); LBL-23626.
25. C.M. Mate, H.W.K. Tom, X.D. Zhu, Y.R. Shen, and G.A. Somorjai, "Vibrational and Electronic Spectroscopy of Pyridine and Benzene Adsorbed on the Rh(111) Crystal Surface," J. Chem. Phys. **88**, 441 (1988); LBL-23628.

Other Publications

26. G.A. Somorjai, "The Building of Catalysts: A Molecular Surface Science Approach, Chapter 2 in *Catalyst Design, Progress and Perspectives*, John Wiley & Sons, New York, 1987, p. 11; LBL-21763.
27. H. Ohtani, C.T. Kao, M.A. Van Hove, and G.A. Somorjai, "A Tabulation and Classification of the Structures of Clean Solid Surfaces and of Adsorbed Atomic and Molecular Monolayers as Determined from Low Energy Electron Diffraction Patterns," in *Progress in Surface Science*, Vol. 23, 1987, p. 155; LBL-23106.
28. H. Ohtani, M.A. Van Hove, and G.A. Somorjai, "The Structures of CO, NO and Benzene on Various Transition Metal Surfaces: Overview of LEED and HREELS Results," in *The Structure of Surfaces-II, Proc. ICSOS-II*, J.F. van der Veen and M.A. Van Hove, Eds., Springer-Verlag, Heidelberg and Berlin, 1987, p. 219.
29. M.A. Van Hove, W.H. Weinberg, and C.-M. Chan, *Low-Energy Electron Diffraction: Experiment,*

Theory and Structural Determination, Vol. 6 in Springer Series in Surface Sciences, Springer-Verlag, Berlin, 1986.

30. M.A. Van Hove and G.A. Somorjai, "Molecular Structures at Surfaces of Metal Single Crystals," in *Proc. Sci. Conf. Chem. Def. Res.*, CRDEC-SP-87008, 1986.
31. J.M. McLaren, J.B. Pendry, P.J. Rous, D.K. Saldin, G.A. Somorjai, M.A. Van Hove, and D.D. Vvedensky, *Surface Crystallographic Information Service: A Handbook of Surface Structures,* Reidel, Dordrecht, 1987.
32. J.F. van der Veen and M.A. Van Hove, Eds., *The Structure of Surfaces-II, Proc. ICSOS-II,* Springer-Verlag, Heidelberg and Berlin, 1987.
33. M.A. Van Hove, "Solving Complex and Disordered Surface Structures with Electron Diffraction," in *Proc. ISISS-8,* Milwaukee, Aug. 1987, Springer-Verlag, Heidelberg and Berlin (in press).

LBL Reports

34. D.R. Strongin and G.A. Somorjai, "A Surface Science and Catalytic Study of the Effects of Aluminum Oxide and Potassium on the Ammonia Synthesis Over Iron Single Crystal Surfaces," in *Catalytic Ammonia Synthesis: Fundamentals and Practice* by J.R. Jennings, Plenum Pub. Co. (in press); LBL-23752.
35. G.A. Somorjai, "Classification of Catalytic Reactions Based on Molecular Surface Science," in *Proc. Boreskov Memorial Conference,* special issue of J. Reaction Kinetics Catal. Lett. (in press); LBL-23799.
36. H. Ohtani, B.E. Bent, C.M. Mate, M.A. Van Hove, and G.A. Somorjai, "Structure Determination with HREELS and LEED: The Molecular Structure of Chemisorbed Benzene on Pd(111)," 4th ICSFS, Hamamatsu, Japan, Aug. 23–27, 1987, to be published in Appl. Surf. Sci.; LBL-23881.
37. M.A. Van Hove, "Recent Progress in Structure Determination by LEED," in *Proc. 4th Int. Symp. Surface Phys.*, Bechyne, Czechoslovakia, Sept. 7–11, 1987, J. Koukal, Ed., Elsevier, Amsterdam (in press); LBL-23927.
38. C.M. Mate, B.E. Bent, and G.A. Somorjai, "Vibrational Spectroscopy of Hydrogen Adsorbed on Metal Surfaces," chapter in *Hydrogen in Catalysis,* Z. Paal, Ed. (in press); LBL-20361.
39. F. Zaera and G.A. Somorjai, "The Role of Hydrogen in Low and High Pressure Hydrocarbon Reactions Over Metal Single Crystal Surfaces," chapter in *Hydrogen in Catalysis,* Z. Paal, Ed. (in press); LBL-19932.
40. B.E. Bent, C.M. Mate, C.T. Kao, A.L. Slavin, and G.A. Somorjai, "Molecular Ethylene Adsorption on Rh(111) and Rh(100): Estimation of the C-C Stretching Force Constant from the Surface Vibrational Frequencies," J. Phys. Chem. (in press); LBL-24240.
41. D.F. Ogletree, K. Frank, and G.A. Somorjai, "An Ultra-High Vacuum Sample Manipulator for Angle-Resolved Electron Spectroscopy," J. Vac. Sci. Tech. (in press); LBL-21694.
42. S.W. Wang, D.F. Ogletree, M.A. Van Hove, and G.A. Somorjai, "The State of Surface Structural Chemistry: Theory and Experiment," Adv. Quantum Chem. (in press); LBL-18030.
43. T.G. Rucker, K. Franck, D. Colomb, M.A. Logan, and G.A. Somorjai, "A Novel High Pressure Isolation Cell Capable of Reaching 120 atm Mounted in an Ultra-High Vacuum Chamber," Rev. Sci. Instrum. (in press); LBL-23277.
44. D.R. Strongin and G.A. Somorjai, "The Effects of Coadsorbed Potassium and Aluminum Oxide on the Rate of Ammonia Synthesis Over Iron Single Crystal Surfaces," submitted to J. Catal.; LBL-23291.
45. C.M. Mate, C.-T. Kao, B.E. Bent, and G.A. Somorjai, "The Surface Structure and Thermal Decomposition of Acetylene on the Rh(111) Single Crystal Surface and the Effect of Coadsorbed Carbon Monoxide," Surf. Sci. (in press); LBL-23736.
46. D.J. Godbey and G.A. Somorjai, "The Preparation and Characterization of Rhenium Modified Pt(111) and Pt(100) Single Crystal Surfaces," Surf. Sci. (in press); LBL-23058.
47. C-T. Kao, G.S. Blackman, M.A. Van Hove, and G.A. Somorjai, "Coadsorbate Induced Ordering on Rh(111) and Rh(100) Surfaces: Structural and Chemical Effects," J. Vac. Sci. Technol. A (in press); LBL-23999.
48. H. Ohtani, M.A. Van Hove, and G.A. Somorjai, "The Structures of Benzene Adsorbed on Pd(111): A Dynamical LEED Study," J. Vac. Sci. Technol. B (in press); LBL-23537.
49. M.E. Bussell, A.J. Gellman, and G.A. Somorjai, "Thiophene Hydrodesulfurization over Transition Metal Surfaces: Structure Insensitive over Molybdenum and Structure Sensitive over Rhenium," J. Catal. (in press); LBL-23953.
50. H. Ohtani, M.A. Van Hove, and G.A. Somorjai, "The Molecular Structure of Benzene Coadsorbed with CO on Pd(111); A Dynamical LEED Analysis," submitted to J. Phys. Chem.; LBL-24011.
51. A.J. Gellman, W.T. Tysoe, and G.A. Somorjai, "Photoelectron Spectroscopy Studies of Thiophene Chemisorption and Decomposition on the Mo(100) Surface," submitted to Surf. Sci.; LBL-24241.
52. E. Sowa, M.A. Van Hove, and D.L. Adams, "The Missing-Row Model for the Reconstructed Pt(110)–(1×2) Surface: A LEED Intensity Analysis Showing Multilayer Distortions," Surf. Sci. (in press); LBL-24284.

Invited Talks

53. G.A. Somorjai, "Surfaces: Chemistry and Structure in Two Dimensions," TMS Fall Meeting Physical, Metallurgy and Materials, Orlando, FL, Oct. 6, 1986.
54. G.A. Somorjai, "The Surface Chemistry of Catalytic Ammonia Synthesis and the Hydrogenation of Organic Molecules Emerging New Concepts of

Research," University of California, Riverside, Oct. 15, 1986.

55. G.A. Somorjai, "New Development in the Surface Science of Catalysis," Three-Site Catalyst Meeting, Charleston, WV, Dec. 5, 1986.
56. G.A. Somorjai, "The Atomic Structure and Composition at Metal-Oxide-Organic Interfaces and the Near Interface Region. A Status Report," International Symposium on "Micronics," Fall 1986, Stockholm, Sweden, Dec. 15–16, 1986.
57. G.A. Somorjai, "Surface Science and Heterogeneous Catalysis," Lezioni Lincee, Politecnico di Milano, Italy, Jan. 5–7, 1987.
58. G.A. Somorjai, "The Structure and Bonding of Organic Monolayers on Metal Single Crystal Surfaces," Progress in Molecular Structure Analysis, a Meeting in Honor of Massimo Simonetta, University of Milan, Italy, Jan. 8–9, 1987.
59. G.A. Somorjai, "Surface Science of Heterogeneous Catalysis," Boston University, Boston, MA, Jan. 26, 1987.
60. G.A. Somorjai, "The Surface Science of Catalytic Nitrogen Fixation and Ethylene Hydrogenation. Emerging New Concepts of Research," California Institute of Technology, Pasadena, CA, Feb. 3, 1987.
61. G.A. Somorjai and D. Godbey, "A Study of the Platinum-Rhenium Reforming Catalyst Using Model Single Crystal Catalysts" California Catalysis Society Spring Meeting, University of California Berkeley, Mar. 26, 1987.
62. G.A. Somorjai, D. Strongin, and S. Bare, "The Effects of Aluminium Oxide in Restructuring Iron Single Crystal Surfaces for Ammonia Synthesis," California Catalysis Society Spring Meeting, University of California Berkeley, Mar. 26, 1987.
63. G.A. Somorjai and T. Rucker, "The Effect of Morphology on the Selectivity and Reaction Properties of Porous Catalysts," California Catalysis Society Spring Meeting, University of California Berkeley, Mar. 27, 1987.
64. G.A. Somorjai, "Surface Chemistry and Heterogeneous Catalysis," Technical Chemistry Department, ETH Zurich, Switzerland, Apr. 22, 1987.
65. G.A. Somorjai, "The Molecular Surface Science of Heterogeneous Catalysis," Baker Institute, Copenhagen, Denmark, May 4, 1987.
66. G.A. Somorjai, "The Surface Science of Catalytic Nitrogen Fixation. Emerging New Concepts of Research," Fritz-Haber Institute, Berlin, Federal Republic of Germany, May 11, 1987.
67. G.A. Somorjai, "The Surface Chemical Bond," University of Leyden, The Netherlands, May 18, 1987.
68. G.A. Somorjai, "Frontiers of Heterogeneous Catalysis," Shell Research Laboratory, Amsterdam, The Netherlands, May 19, 1987.
69. G.A. Somorjai, "Catalyzed Hydrocarbon Conversion Reactions on Metal Single Crystal Surfaces," Third Annual Meeting of the University of California, Berkeley—Conference des Grandes Ecoles, Grenoble and Paris, France, May 21–25, 1987.
70. G.A. Somorjai, "Recent Surface Science Studies of Metal Catalysis," University of Paris, France, May 25, 1987.
71. G.A. Somorjai, "The Surface Chemical Bonds of Organic Monolayers," lectures at Imperial College, London, June 4, 1987.
72. G.A. Somorjai, "The Molecular Surface Science of Metal Catalysis," Boreskov Memorial Conference, Catalysis Institute, Novosibirsk, USSR, June 22, 1987.
73. G.A. Somorjai, "Surface Science of Heterogeneous Catalysis," Solid State Physics Department, ETH, Zurich, Switzerland, June 29, 1987.
74. G.A. Somorjai, "The Surface Science of Chemical Energy Conversion," University of Zurich, Switzerland, June 30, 1987.
75. G.A. Somorjai, "The Surface Chemical Bond of Organic Monolayers," University of Bern, Switzerland, July 2, 1987.
76. G.A. Somorjai, "Frontiers of Heterogeneous Catalysis," University of Pisa, Italy, July 3, 1987.
77. G.A. Somorjai, "Surface Science of Heterogeneous Catalysis," University of Lausanne, Switzerland, July 7, 1987.
78. G.A. Somorjai, "Frontiers of Surface Science," Institute for Vacuum Physics, Julich, Federal Republic of Germany, July 9, 1987.
79. G.A. Somorjai, "The Surface Science of Technologically Important Catalysts," Hoffmann La Roche Co., Basel, Switzerland, July 13, 1987.
80. G.A. Somorjai, "Frontiers of Organic Surface Chemistry," Physical Chemistry Department, ETH, Zurich, Switzerland, July 14, 1987.
81. G.A. Somorjai, "New Directions of Catalysis Research," ACS Conference on the Future of Catalysis, Berkeley, CA, July 21–22, 1987.
82. G.A. Somorjai, "New Conceptions in Surface Science and Heterogeneous Catalysis," The Hungarian Chemical Society, Szeged, Hungary, Aug. 17, 1987.
83. G.A. Somorjai, "Modern Tools of Surface Crystallography: the Dynamical Behavior of Surface Morphology during Catalytic Activity," The Summer School, Bern, Switzerland, Sept. 18, 1987.
84. G.A. Somorjai, "Frontiers of Surface Science," The CERN Colloquium, Geneva, Switzerland, Sept. 18, 1987.
85 M.A. Van Hove, "Surface Structure Determination of Metal Surfaces and Molecular Adsorbates," University of Missouri, Columbia, Oct. 22, 1986.
86. M.A. Van Hove, "Benzene and Carbon Monoxide Coadsorption Structures on Rh(111) and Pt(111) by HREELS and LEED," 10th International Conference on Surface Science, 33rd National Symposium, American Vacuum Society, Baltimore, MD, Oct. 31, 1986.
87. M.A. Van Hove, "Progress in Surface Crystallography, Metal Reconstructions and Molecular Adsorp-

tion Structures," University of Washington, Seattle, Nov. 10, 1986.

88. M.A. Van Hove, "Solving Complex and Disordered Surface Structures with Electron Diffraction," IBM, Almaden, CA, Nov. 12, 1986.
89. M.A. Van Hove, "Molecular Structures at Surfaces of Metal Single Crystals," 1986 Chemical Research, Development and Engingeering Center Science Conference on Chemical Defense Research, Aberdeen, MD, Nov. 18, 1986.
90. M.A. Van Hove, "Molecular Structures at Metal Surfaces," Lawrence Berkeley Laboratory, Berkeley, CA, Mar. 5, 1987.
91. M.A. Van Hove, "Structural Effects Between Coadsorbates on Metal Surfaces Detected by LEED and HREELS," APS Meeting, New York, NY, Mar. 17, 1987.
92. M.A. Van Hove, "Structural Effects Between Coadsorbates on Metal Surfaces Detected by LEED and HREELS," 9th European Conference on Surface Science, Lucern, Switzerland, Apr. 13, 1987.
93. M.A. Van Hove, "Forward Focusing Effects Calculated for Spectroscopies that Use Electron Diffraction," 2nd International Conference on the Structure of Surfaces, Amsterdam, The Netherlands, June 22, 1987.
94. M.A. Van Hove, "Solving Complex and Disordered Surface Structures with Electron Diffraction," 8th International Summer Institute on Surface Science, Milwaukee, WI, Aug. 20, 1987.
95. M.A. Van Hove, "Molecular Distortion, Decomposition and Interaction at Metal Surfaces, Studied by LEED and HREELS," 194th ACS Meeting, New Orleans, LA, Sept. 3, 1987.
96. M.A. Van Hove, "Recent Progress in Surface Structure Determination by LEED," 4th International Symposium on Surface Physics, Bechyne, Czechoslovakia, Sept. 7, 1987.
97. M.A. Van Hove, "Recent Structure Determinations with LEED, Metal Reconstructions, Molecular Overlayers," Technische Universität, Clausthal-Zellerfeld, Federal Republic of Germany, Sept. 14, 1987.
98. M.A. Van Hove, "Organic Adsorbates," Imperial College, London, Sept. 17, 1987.
99. H. Ohtani, M.A. Van Hove, B.E. Bent, C.M. Mate, and G.A. Somorjai, "Coadsorption of Benzene and CO on Pd(111): A Dynamical LEED and HREELS Study," ICSFS-4, Hamamatsu, Japan, Aug. 23–27, 1987.
100. C.-T. Kao, C.M. Mate, B.E. Bent, and G.A. Somorjai, "The Surface Structure and Thermal Decomposition of Acetylene and Coadsorbed Acetylene with CO on the Rh(111) Single Crystal Surface," 192nd ACS National Meeting, Denver, CO, Apr. 7, 1987.
101. G.S. Blackman, C.M. Mate, C.-T. Kao, B.E. Bent, D.F. Ogletree, M.A. Van Hove, and G.A. Somorjai, "Colloid and Surface Science Coadsorbate Induced Ordering," 192nd ACS National Meeting, Denver, CO, Apr. 7, 1987.
102. M.E. Bussell and G.A. Somorjai, "A Surface Science and Catalytic Study of Thiophene Hydrodesulfurization Over Transition Metal Foils and Single Crystals," American Chemical Society Meeting, New Orleans, LA, Sept. 1987.
103. D.R. Strongin, S.R. Bare, and G.A. Somorjai, "The Effects of Aluminum Oxide and Potassium on Ammonia Synthesis Over Iron Single Crystal Surfaces," American Chemical Society Meeting, New Orleans, LA, Sept. 1987.

Nuclear Magnetic Resonance*

A. Pines, Investigator
G. Chingas, Staff Scientist

INTRODUCTION

The nuclear magnetic resonance (NMR) program has two complementary directions. The first is the development of new concepts and techniques in NMR in order to extend the applicability of the spectroscopy to a wider range of problems and materials. Such a program demands a study of the interaction of nuclear spins with each other, with other degrees of freedom such as molecular rotations, and with external excitations such as radiofrequency pulses and light. It also requires the development of new theoretical tools and the design and implementation of novel experimental methods. Such methods entail a substantial effort in the design and fabrication of next-generation NMR equipment. Some developments currently under way in this direction are multiple-quantum NMR and clustering, zero-field NMR, solid-state materials imaging, spatially selective NMR with surface coils, superconducting quantum interference device (SQUID) detectors in high-sensitivity two-dimensional NMR of dipolar couplings, high-temperature NMR, multiple-pulse and iterative schemes, optical polarization of gases, selective polarization of surfaces, and development of high-resolution quadrupolar techniques. The second direction is the application of novel NMR methods and instrumentation to materials research problems in collaboration with other programs at LBL as well as with outside laboratories. Some of the materials and problems currently under investigation in this direction are the structure of doped semiconductors, organic and organometallic solids, ordering and phase transitions in liquid crystals, dynamics of oriented and constrained molecules, structure and motion in silicate glasses, and clustering in zeolite cavities and solid-gas interfaces. This program addresses a national need for a model effort to implement the rapid development and transfer of NMR technology to laboratories in industry and other organizations.

1. Iterative Maps

H. Cho,[†] J. Guckenheimer,[‡] K. Mueller, and A.J. Shaka[§]

Iterative maps on SO(3) have been designed and implemented for broadband and narrowband excitation as well as for bilinear couplings. Maps with multiple fixed points have been used for bistable excitation.

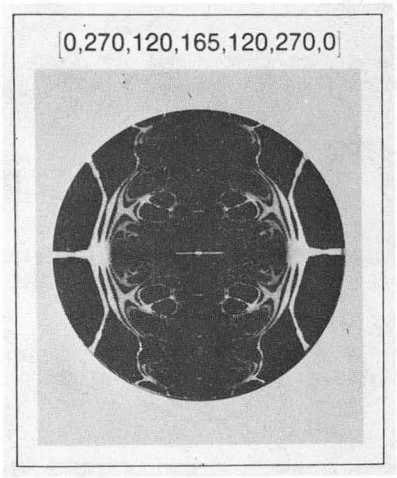

(All figures taken from CBB 885-5690)

[†]Present address: Laboratorium für Physikalische Chemie, E.T.H., CH-8092 Zürich, Switzerland.

[‡]Permanent address: Department of Mathematics, Cornell University, Ithaca, NY 14853.

[§]Miller Fellow, University of California, Berkeley, CA 94720.

*This work was supported by the Director, Office of Energy Research, Office of Basic Energy Sciences, Materials Sciences Division of the U.S. Department of Energy under Contract No. DE-AC03-76SF00098.

2. Geometrical Quantum Phases

R.Y. Chaio,[†] R.A. Harris,[‡] K. Mueller, and D. Suter[§]

The quantum geometrical phases of Berry and Aharonov-Anandan have been studied by NMR interferometry. The relationship between quantum phases in optics and magnetic resonance has been elucidated.

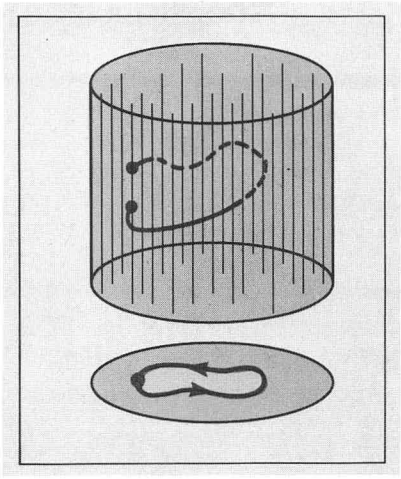

[†]Permanent address: Department of Physics, University of California, Berkeley, CA 94720.

[‡]Permanent address: Department of Chemistry, University of California, Berkeley, CA 94720.

[§]Present address: Laboratorium für Quantenoptik, ETH Hönggerberg (HPT), CH-8093 Zürich, Switzerland.

3. Multiple-Quantum Spectroscopy and Clusters

J. Baum,[†] J. Pearson, D. Shykind, M. Trecoske, and U. Werner

Multiple-quantum spectroscopy has been used to study clustering in solids. The time dependence of the multiple-quantum transitions has been modeled as a directed walk in Liouville space.

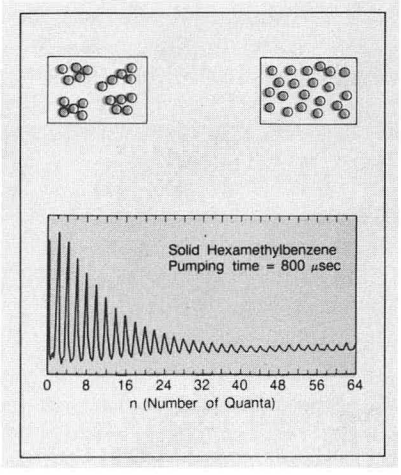

[†]Present address: Inorganic Chemistry Laboratory, Oxford University, Oxford OX1 3QR, England.

4. Conformations of Oriented Hydrocarbon Chains

M. Gochin,[†] M. Rosen, S. Rucker, C. Schmidt, and A.J. Shaka[‡]

The conformational probabilities of partially oriented chains have been determined by two-dimensional NMR and statistical mechanics models in liquid crystals.

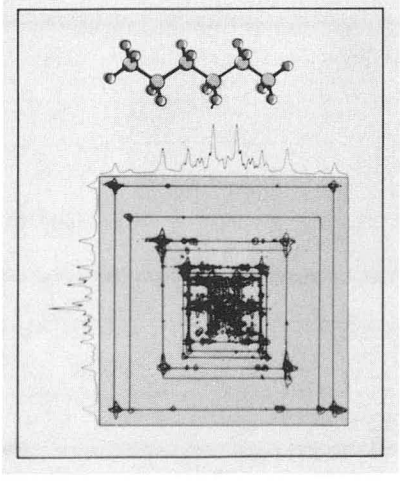

[†]Present address: Department of Pharmaceutical Chemistry, University of California, San Francisco, CA 94143.

[‡]Miller Fellow, University of California, Berkeley, CA 94720.

5. Spin Decoupling and Second Order Spinning

C.J. Lee,[†] K. Mueller, A. Samoson,[‡] B.Q. Sun, D. Suter,[§] and T. Terao

New schemes have been developed for spin decoupling in solids. Magic angle spinning (MAS) has been extended to Second Order Spinning and Second Order Spectroscopy (SOS) to remove second-order broadening.

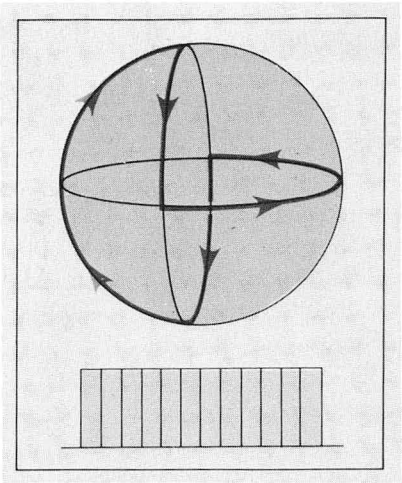

[†]Present address: Department of Chemistry, Princeton University, Princeton, NJ 08544.

[‡]Permanent address: Institute of Chemical and Biological Physics, Estonian Academy of Sciences, Tallinn, U.S.S.R. 200001.

[§]Present address: Laboratorium für Quantenoptik, ETH Hoñggerberg (HPT), CH-8093 Zürich, Switzerland.

6. Zero-Field NMR

D. Caplan, S. Matsui, B.Q. Sun, C. Schmidt, T. Jarvie, and U. Werner

Zero-field NMR has been extended to chemical exchange and to the study of spin diffusion. Short-range order and local symmetry have been investigated in disordered materials.

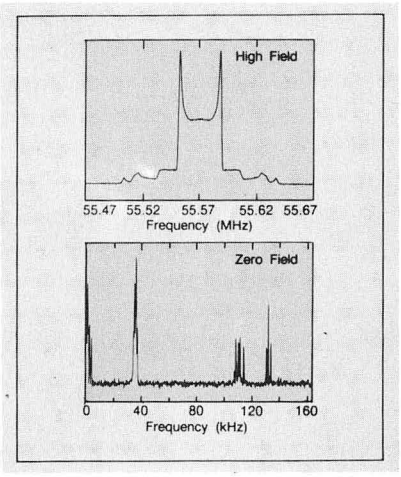

7. Zeolites and High-Temperature Silicates

B. Chmelka,[†] L.C. deMenorval,[‡] S.-B. Liu,[§] A. McCormick,[‖] E.E. Petersen, C.J. Radke, R. Ryoo,[**] J. Stebbins,[††] and M. Trecoske

Xenon and metal clusters have been observed in zeolite cavities. The structure and dynamics of silicate glasses and liquids have been investigated by NMR at high temperatures.

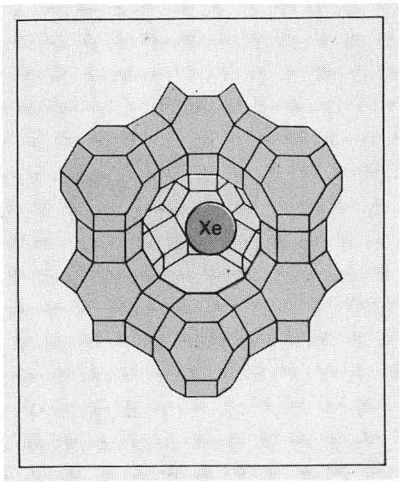

[†]Permanent address: Department of Chemical Engineering, University of California, Berkeley, CA 94720.

[‡]Present address: Academie de Montpellier, Université des Sciences et Techniques du Languedoc, 34060 Montpellier Cedex, France.

[§]Present address: Institute of Atomic and Molecular Sciences, Academia Sinica, Taipei, Republic of China.

[‖]Present address: Department of Chemical Engineering, University of Minnesota, Minneapolis, MN 55455.

[**]Permanent address: Korea Institute of Technology, Choong-gu, Taejon, 300-31, Republic of Korea.

[††]Permanent address: Department of Geology, Stanford University, Stanford, CA 94305.

8. Optical Pumping and SQUID Detectors

J. Clarke,[†] J. Chang, C. Connor, N. Fan,[†] D. Raftery, D. Shykind, and E. Hahn[†]

Optical pumping can produce high-nuclear-spin polarization. Zero-field quadrupole resonance of aluminum-27 has been detected by a SQUID detector at low temperature with circularly polarized radio-frequency excitation.

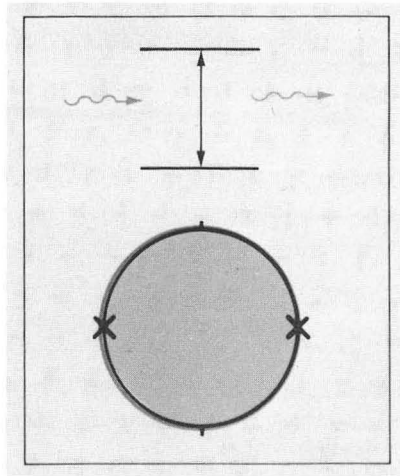

[†]Permanent address: Department of Physics, University of California, Berkeley, CA 94720.

1987 PUBLICATIONS AND REPORTS

Refereed Journals

1. A. Thayer and A. Pines, "Zero Field NMR," Acct. Chem. Res. **20**, 47 (1987); LBL-21458.
2. M. Gochin, D. Hugi-Cleary, H. Zimmermann, and A. Pines, "Two-Dimensional Multiple-Quantum NMR of Isotopic Mixtures in Liquid Crystals," Mol. Phys. **60**, 205 (1987); LBL-21815.
3. A.J. Shaka and A. Pines, "Symmetric Phase Alternating Composite Pulses," J. Magn. Reson. **71**, 495 (1987); LBL-22031.
4. E. Schneider, J.F. Stebbins, and A. Pines, "Speciation and Local Structure in Alkali and Alkaline Earth Silicate Glasses: Constraints from Si-29 NMR Spectroscopy," J. Noncryst. Solids **89**, 371 (1987); LBL-22391.
5. H. Cho, J. Baum, and A. Pines, "Iterative Maps with Multiple Fixed Points for Excitation of Two Level Systems," J. Chem. Phys. **86**, 3089 (1987); LBL-22390.
6. M. Luzar, A.M. Thayer, and A. Pines, "Quenching of Residual Fields by Nonaxially Symmetric Dipolar Coupling in Zero Field NMR," J. Magn. Reson. **73**, 459 (1987); LBL-22435.
7. D. Suter, S.B. Liu, J. Baum, and A. Pines, "Multiple Quantum NMR Excitation with a One Quantum Hamiltonian," Chem. Phys. **114**, 103 (1987); LBL-22438.
8. D. Suter, K.V. Schenker, and A. Pines, "Theory of Broadband Heteronuclear Decoupling in Multispin Systems," J. Magn. Reson. **73**, 90 (1987); LBL-22439.
9. K.V. Schenker, D. Suter, and A. Pines, "Broadband Heteronuclear Decoupling in the Presence of Homonuclear Dipolar and Quadrupolar Interactions," J. Magn. Reson. **73**, 99 (1987); LBL-22440.
10. A.M. Thayer, M. Luzar, and A. Pines, "Zero Field NMR Study of the Biaxial Smectic E Phase," Liquid Crystals **2**, 241 (1987); LBL-22441.
11. M. Munowitz, M. Mehring, and A. Pines, "Multiple Quantum Dynamics: A Directed Walk through Liouville Space," J. Chem. Phys. **86**, 3172 (1987); LBL-22443.
12. A.M. Thayer, M. Luzar, and A. Pines, "Zero Field NMR of Nematic Liquid Crystals with Positive and Negative Magnetic Susceptibility Anisotropies," J. Phys. Chem. **91**, 2194 (1987); LBL-22436.
13. M. Gochin, H. Zimmermann, and A. Pines, "Assignment of Dipolar Couplings and Estimation of Conformational Probabilities in Partially Oriented Hexane," Chem. Phys. Lett. **137**, 51 (1987); LBL-22434.
14. A.M. Thayer, M. Luzar, and A. Pines, "Heteronuclear Zero Field NMR of Liquid Crystals," J. Magn. Reson. **72**, 567 (1987); LBL-22671.
15. M. Luzar, A.M. Thayer, and A. Pines, "Zero Field NMR of Uniaxial and Biaxial Smectic Liquid Crystals," Mol. Phys. **62**, 573 (1987); LBL-22677.
16. T. Jarvie, A.M. Thayer, J. Millar, and A. Pines, "Effect of Correlated Proton Jumps on the Zero Field NMR Spectrum of Solid p-Toluic Acid," J. Phys. Chem. **91**, 2240 (1987); LBL-22437.
17. H. Cho and A. Pines, "Iterative Maps for Broadband Excitation of Transverse Coherence in Two Level Systems," J. Chem. Phys. **86**, 6591 (1987); LBL-22680.
18. C. Lee, D. Suter and A. Pines, "Theory of Multiple Pulse NMR at Low and Zero Fields," J. Magn. Reson. **75**, 110 (1987); LBL-22442.
19. D. Suter, G. Chingas, R.A. Harris, and A. Pines, "Berry's Phase in Magnetic Resonance," Mol. Phys. **61**, 1327 (1987); LBL-22995.
20. A. Bielecki and A. Pines, "Pake Patterns from Zero to High Field," J. Magn. Reson. **74**, 381 (1987); LBL-23091.

21. D. Suter, T.P. Jarvie, B. Sun, and A. Pines, "Observation of Spin Diffusion in Zero Field Magnetic Resonance," Phys. Rev. Lett. **59**, 106 (1987); LBL-23411.
22. P. Meier, G. Kothe, P. Jonsen, M. Trecoske, and A. Pines, "Theory of Lineshapes for Zero Field NMR in the Presence of Molecular Motion," J. Chem. Phys. **87**, 6867 (1987); LBL-22994.
23. S.-B. Liu, A. Pines, M. Brandriss, and J.F. Stebbins, "Relaxation Mechanisms and Effects of Motion in Albite ($NaAlSi_3O_8$) Liquid and Glass: A High Temperature NMR Study," Phys. Chem. Minerals **15**, 155 (1987); LBL-22999.
24. R. Ryoo, S.-B. Liu, L.C. de Menorval, K. Takegoshi, B. Chmelka, M. Trecoske, and A. Pines, "Distribution of Hexamethylbenzene in a Zeolite Studied by Xenon-129 and Multiple-Quantum NMR," J. Phys. Chem. **91**, 6575 (1987); LBL-24182.
25. D. Suter and A. Pines, "Recursive Evaluation of Interaction Pictures," J. Magn. Reson. **75**, 509 (1987); LBL-23489.

Other Publications

26. A. Pines, D.P. Weitekamp, A. Bielecki, D.B. Zax, and K.W. Zilm, U.S. Patent 4,710,714—Method and Apparatus for Measuring Nuclear Magnetic Resonance.

LBL Reports

27. J.B. Murdoch, J.F. Stebbins, I.S.E. Carmichael, and A. Pines, "A Silicon-29 Nuclear Magnetic Resonance Study of Silicon-Aluminum Ordering in Leucite and Analcite," Phys. Chem. Minerals (in press); LBL-22552.
28. A. Pines, "Lectures on Pulsed NMR," in *Proc. Fermi School on Physics of NMR in Biology and Medicine*, B. Maraviglia, Ed. (in press); LBL-22326.
29. A.J. Shaka, D.N. Shykind, G.C. Chingas, and A. Pines, "Multiple-Pulse Sequences for Precise Transmitter Phase Alignment," J. Magn. Reson. (in press); LBL-24027.
30. D. Suter, A. Pines, J.H. Lee, and G. Drobny, "Broadband Heteronuclear Spin Decoupling in Solids," Chem. Phys. Lett. (in press); LBL-24170.
31. S.-B. Liu, J.F. Stebbins, E. Schneider, and A. Pines, "Diffusive Motion in Alkali Silicate Melts: an NMR Study at High Temperature," submitted to Geochim. et Cosmochim. Acta; LBL-23806.
32. A.J. Shaka, C.J. Lee, and A. Pines, "Iterative Schemes for Bilinear Operators: Applications to Spin Decoupling," J. Magn. Reson. (in press); LBL-23797.
33. D.N. Shykind, J. Baum, S.-B. Liu, A. Pines, and A.N. Garroway, "Phase-Incremented MQ-NMR Experiments," J. Magn. Reson. (in press); LBL-23696.
34. R.J. Wittebort, M.G. Usha, D.J. Ruben, D.E. Wemmer, and A. Pines, "Observation of Molecular Reorientation in Ice by Proton and Deuterium Magnetic Resonance," submitted to J. Phys. Chem.; LBL-24890.
35. D. Suter, K. Mueller, and A. Pines, "Study of the Aharanov-Anandan Phase by NMR Interferometry," Phys. Rev. Lett. (in press); LBL-24428.
36. K. Takegoshi, T.P. Jarvie, D. Suter, D.B. Zax, and A. Pines, "Suppression of The Zero-Frequency Peak in Time-Domain Zero-Field NMR," submitted to Chem. Phys. Lett.; LBL-24429.
37. J. Anandan, R.Y. Chaio, G. Ghingas, K.M. Ganga, R.A. Harris, H. Jiao, A.S. Landsberg, A. Pines, and D. Suter, "Nonadiabatic Geometrical Phase in NMR and Optics," submitted to Phys. Rev. Lett.; LBL-23410.
38. K. Takegoshi, T.P. Jarvie, D. Suter, and A. Pines, "Spin-Echo Phenomena in Zero-Field NMR," submitted to Chem. Phys.; LBL-24426.
39. S.-B. Liu, L.C. de Menorval, K. Takegoshi, R. Ryoo, M. Trecoske, and A. Pines, "Xenon-129 and Multiple-Quantum NMR Studies of Molecular Sorption in Na-Y Zeolite: The Effect of Thermal Treatment," submitted to J. Phys. Chem.; LBL-24425.
40. D. Suter and J.G. Pearson, "Experimental Classification of Multi-Spin Coherence Under the Full Rotation Group," submitted to Phys. Rev. Lett.; LBL-24034.
41. A.J. Shaka, S. Rucker, and A. Pines, "Iterative Carr-Purcell Trains," J. Magn. Reson. (in press); LBL-24424.
42. M. Gochin, K. Schenker, P. Neidig, and A. Pines, "Two Dimensional NMR of Oriented Hexane," LBL-24423.
43. A. Pines and M.V. Berry, "Holonomy of Photons and Deuterons," LBL-24422.
44. D. Suter and A. Pines, "Manifestation of the Wilczek-Zee Gauge in Magnetic Resonance," LBL-24421.
45. C.J. Lee, A. Samoson, B. Sun, D. Suter, T. Terao, and A. Pines, "Removal of Second Order Quadrupole Broadening," LBL-24420.
46. B.F. Chmelka, L.C. de Menorval, S.-B. Liu, E.E. Petersen, C.J. Radke, R. Ryoo, and A. Pines, "Mechanisms of Metal Cluster Formation in Zeolites," submitted to J. Am. Chem. Soc.; LBL-24419.
47. A. Bielecki (Ph.D. Thesis), "Development and Applications of NMR in Low and Zero Fields," LBL-23508.
48. C.J. Lee (Ph.D. Thesis), "NMR with Generalized Dynamics of Spin and Spatial Coordinates," LBL-24418.
49. J. Baum (Ph.D. Thesis), "NMR Studies of Selective Population Inversion and Spin Clustering," LBL-21259.
50. M. Gochin (Ph.D. Thesis), "Two-Dimensional NMR in Liquids and Oriented Molecules," LBL-22992.

Invited Talks

51. A. Pines, "Magnetic Moments," AT&T Bell Laboratories, Murray Hill, NJ, Jan. 20, 1987.
52. A. Pines, "NMR Studies of Clustering in Solids," IBM Solid State Physics Division, Yorktown Heights, NY, Jan. 21, 1987.
53. A. Pines, "Clusters in Zeolites," DuPont Central Research Division Research, Wilmington, DE, Jan. 22, 1987.
54. A. Pines, "Does NMR Count?" Chemistry Department, West Virginia University, Morgantown, Feb. 26, 1987.
55. A. Pines, "Some Magnetic Moments," Chemistry Department, University of California, Irvine, Mar. 3, 1987.
56. A. Pines "New Techniques in Solid State NMR," Materials and Molecular Research Division Review, Lawrence Berkeley Laboratory, Mar. 4, 1987.
57. A. Pines, "Some Magnetic Moments," Department of Chemistry, University of California, Berkeley, Mar. 17, 1987.
58. A. Pines, "Magnetic Moments in Solids," Chemistry Department, Cornell University, Ithica, NY, Mar. 20, 1987.
59. A. Pines, "New Angles in NMR," Princeton University, Princeton, NJ, Mar. 23, 1987.
60. A. Pines, "Multiple-Quantum and Zero-Field Spectroscopy," Department of Chemistry, University of Queensland, Australia, Mar. 30, 1987.
61. A. Pines, "NMR Studies of Clusters in Solids," Australian National University, Canberra, Mar. 31, 1987.
62. A. Pines, "Iterative Maps," University of Melbourne, Australia, Apr. 3, 1987.
63. A. Pines, "Zero Field NMR," University of Sydney and CSIRO, Australia, Apr. 4, 1987.
64. A. Pines, "Pulsed NMR in Solids," Department of Physics, Massey University, Palmerston, New Zealand, Apr. 7, 1987.
65. A. Pines, "NMR Studies of Conformations of Liquid Crystals," Department of Chemistry, Auckland University, Auckland, New Zealand, Apr. 8, 1987.
66. D. Suter, "Diffusion of Spin Order in Resolved Solid State NMR Spectra," 28th Experimental NMR Conference, Asilomar, CA, Apr. 1987.
67. R. Ryoo, S.-B. Liu, L.C. de Menorval, and A. Pines, "Multiple-Quantum and Xenon-129 NMR Studies of the Distribution of Molecules in a Zeolite," 28th Experimental NMR Conference, Asilomar, CA, Apr. 1987.
68. S.-B. Liu, A. Pines, and J.F. Stebbins, "Relaxation Mechanisms and Effects of Motion in $NaAlSiO_3O_8$ Liquid and Glass: A High Temperature NMR Study," 28th Experimental NMR Conference, Asilomar, CA, Apr. 1987
69. T. Jarvie, M. Luzar, J. Millar, A. Thayer, D.B. Zax, and A. Pines, "Zero-Field NMR Studies of Local Symmetry," 28th Experimental NMR Conference, Asilomar, CA, Apr. 1987
70. D. Suter, "Berry's Phase in Magnetic Resonance," Chemistry Department, University of California Berkeley, Apr. 1987.
71. A. Pines, "Some Magnetic Moments," Isotope Department, Weizmann Institute of Science, Rehovot, Israel, Apr. 22, 1987.
72. A. Pines, "New Techniques in Solid State NMR," Department of Chemistry, Tel Aviv University, Israel, Apr. 23, 1987.
73. A. Pines, "NMR with Regular and Irregular Irradiation," Department of Chemistry, Hebrew University of Jerusalem, Israel, Apr. 24, 1987.
74. A. Pines, "Echoes of the Future," Physical Chemistry Seminar, Oxford University, England, May 18, 1987.
75. A. Pines, "Quantum Adabatic Phase in Magnetic Resonance," University of Bristol, England, May 19, 1987.
76. A. Pines, "On Multiple Quantum NMR and Its Applications," Waterloo Nuclear Magnetic Resonance Summer Institute, University of Waterloo, Ontario, June 4–12, 1987 (3 lectures).
77. A. Pines, "Berry's Phase in Magnetic Resonance," Gordon Conference on Magnetic Resonance, Wolfeboro, NH, June 15–19, 1987.
78. D. Suter, "Broadband Heteronuclear Decoupling in the Presence of Strong Homonuclear Interactions," Francis Bitter National Magnet Laboratory, Cambridge, MA, June 1987.
79. A. Pines, eight lectures on modern NMR research, École Superieure de Physique et Chimie, Paris, France, May–June, 1987.
80. A. Pines, "Counting Clusters in Semiconductors by Multiple Quantum NMR," Ecole Polytechnique, Paris, France, July 2, 1987.
81. A. Pines, "Quantum Geometrical Phase in Optics and Magnetic Resonance," Quantum Physics Laboratory, E.S.P.C.I., Paris, France, July 9, 1987.
82. A. Pines, "Making NMR Count," Chemistry Department, Lausanne University, Lausanne, Switzerland, July 27, 1987.
83. B. Chmelka, "Xenon-129 NMR Applications to Platinum-Zeolite Catalyst Characterization," Physics Department, Universidad de Nacional Autonoma de Mexico, Mexico City, Aug. 20, 1987.
84. B. Chmelka, "NMR Techniques for Probing Metabolic Processes in Immobilized Cells," Biochemistry Department, Universidad de Nacional Autonoma de Mexico, Mexico City, Aug. 20, 1987.
85. A. Pines, "Order and Disorder in Solids Studied by Pulsed NMR," C.E.N., Grenoble, France, Aug. 31, 1987.
86. A. Pines, six-lecture series on modern NMR, Les Houches Summer School on Solid-State NMR, Les Houches, France, Sept. 3–15, 1987.
87. A. Pines, "Multiple Quantum and Zero Field NMR Studies of Liquid Crystals," 8th Specialized Colloque Ampere on Liquid Crystals and Liquid Crystalline Polymers, Lisbon, Portugal, Sept. 14–18, 1987.

88. A. Pines, "Quantum Phase in Magnetic Resonance," Nonintegrable Phases in Dynamical Systems Workshop, Theoretical Physics Institute, University of Minnesota–Minneapolis, Sept. 30–Oct. 2, 1987.
89. A. Pines, "New NMR Techniques of Possible Applicability in Biology," Biophysics/Stanford Magnetic Resonance Laboratory, Stanford University, Stanford, CA, Oct. 8, 1987.
90. A. Pines, "Some Magnetic Moments," Chemistry Department, University of California at Los Angeles, Oct. 12, 1987.
91. A. Pines, "Counting Clusters by Multiple Quantum NMR," Chemistry Department Symposium on Resonance in Perspective, Washington University, St. Louis, MO, Oct. 15, 1987.
92. A.J. Shaka, "Topics in Modern NMR," Second Beijing Conference and Exhibition on Instrumental Analysis, Beijing, People's Republic of China, Oct. 20–23, 1987.
93. A. Pines, "Some Magnetic Moments," Chemistry Department, Texas A&M University, College Station, Oct. 29, 1987.
94. A. Pines, "Xenon and Multiple Quantum NMR Studies of Molecular Distributions in Zeolites," Shell Development Company Catalysis and Analytical Departments, Houston, TX, Oct. 30, 1987.
95. A. Pines, "Some Magnetic Moments," Joint Harvard-MIT Physical Chemistry Seminar, Cambridge, MA, Nov. 5, 1987.
96. B. Chmelka, "Mechanisms of Platinum Cluster Formation in NaY Zeolite," National Meeting, American Institute of Chemical Engineers, New York, Nov. 19, 1987.
97. A. Pines, "Are Photons Really That Different From Deuterons?" Opening Lecture, Weizmann Institute of Science, Rehovot, Israel, Dec. 1987.
98. A. Pines, "Zero Field NMR," Fritz Haber Workshop on Modern Techniques in Magnetic Resonance, Tiberias, Israel, Dec. 13–17, 1987.
99. A. Pines, "Multiple-Quantum NMR," Fritz Haber Workshop on Modern Techniques in Magnetic Resonance, Tiberias, Israel, Dec. 13–17, 1987.

Synthesis of Novel Solids*

Angelica M. Stacy, Investigator

INTRODUCTION

The goal of this research is to synthesize advanced materials with novel properties. Current work is focused on rare-earth transition-metal phosphides. Rare-earth compounds have attracted attention because they exhibit cooperative phenomena, including valence fluctuations, heavy-fermion superconductivity, and unusual types of magnetic ordering. These cooperative phenomena are difficult to model and remain a challenge to our understanding of condensed matter. The goals are to synthesize and characterize new classes of rare-earth transition-metal phosphides that exhibit cooperative phenomena (especially superconductivity). Such synthetic studies will lead to numerous new classes of materials with novel magnetic and electronic properties.

1. Magnetic Phase Transitions in $EuNi_5P_3$: Unusual Steps in the Magnetization with Field (Publication 1)

J.V. Badding and A.M. Stacy

In order to understand the unusual macroscopic behavior of $EuNi_5P_3$ on a microscopic level, preliminary powder neutron diffraction experiments were performed. Scans were obtained at a wavelength of 2.371 Å at 6 K (below the Neel temperature of 8 K). Several magnetic peaks were observed. The two lowest-angle peaks can be indexed in terms of a doubling along either the b or c axis; the data are not good enough to distinguish between these possibilities. What is significant is that there appears to be no cell doubling along the a axis; i.e., the Eu chains are ferromagnetic. Since the easy axis for magnetization is the a axis, the moments are nearly parallel to the a axis.

In addition to measurements made on pure $EuNi_5P_3$, doped materials were prepared with the stoichiometry $(Eu_{0.9}M_{0.1})Ni_5P_3$, where M = Ca and Sr. The new compound $SrNi_5P_3$ was also synthesized and found to be isostructural with $EuNi_5P_3$. Fewer steps are observed in the magnetization vs. field curves for the doped compounds. As the field increases, the magnetization jumps to 1/4 the saturation magnetization, then 1/2, and finally to saturation. The first step occurs at a lower field than in the undoped compound, suggesting that the Ca/Sr substitution has weakened the magnetic interaction between Eu^{+2} ions.

The data described above suggest ferromagnetic Eu chains aligned antiferromagnetically, with a cell doubling either along the b or c axis. As the magnetic field applied along the a axis is increased, it is probable that entire chains of Eu atoms are flipping, but not all at once. A series of intermediate phases is formed with various spin configurations; this gives rise to steps in the magnetization and magnetoresistance. Although many questions remain about the magnetic behavior, we are applying ideas about commensurate-incommensurate phase transitions and the "Devil's Staircase."

2. Probing Electronic Density of States and Magnetic Interactions at the Rare-Earth Site (Publication 10)

U. Walter, S. Fahy, A. Zettl, S.G. Louie, M.L. Cohen, P. Tejedor, and A.M. Stacy

By exploiting the 4f-shell properties of Er in the high-T_c superconductor $ErBa_2Cu_3O_7$, we find by inelastic magnetic neutron scattering that the electrostatic field around the rare earth site is anomalously large. Above T_c there exists considerable magnetic interaction between the conduction electrons and the rare earth's 4f shell: $N(E_F)J_{ex} = 0.025$. This interaction is lost in the superconducting state. The ground-state magnetic moment of Er in the host lattice is $\mu_{eff} = 5.3$ B.

3. Work in Progress

Since only a few rare-earth intermetallics have been reported to show complex magnetization with a series of steps, the novel magnetic behavior of $EuNi_5P_3$ is being investigated further. Studies on large single crystals are planned, including polarized neutron diffraction experiments with Dr. D. Cox at Brookhaven National Laboratory and low-temperature heat-capacity studies with Prof. N. Phillips of LBL. With these measurements, it will

*This work was supported by the Director, Office of Energy Research, Office of Basic Energy Sciences, Materials Sciences Division of the U.S. Department of Energy under Contract No. DE-AC03-76SF00098.

be possible to examine the coupling between the spins on the Eu^{+2} ions with the conduction electrons and to determine the mechanism of the interaction.

1987 PUBLICATIONS AND REPORTS

Refereed Journals

1. J.V. Badding and A.M. Stacy, "Magnetic Phase Transitions in $EuNi_5P_3$: Unusual Steps in the Magnetization with Field," Phys. Rev. B **35**, 8880 (1987).
2. L.C. Bourne, M.L. Cohen, W.N. Creager, M.F. Crommie, A.M. Stacy, and A. Zettl, "Onset of Superconductivity in Y-Ba-Cu-O at 100 K," Phys. Lett. A **120**, 494 (1987).
3. U. Walter, M.S. Sherwin, A. Stacy, P.L. Richards, and A. Zettl, "Energy Gap in the High T_c Superconductor $La_{1.85}Sr_{0.15}CuO_4$," Phys. Rev. B **35**, 5327 (1987).
4. L.C. Bourne, M.F. Crommie, A. Zettl, H.C. zur Loye, S.W. Keller, K.L. Leary, A.M. Stacy, K.J. Chang, M.L. Cohen, and D.E. Morris, "Search for Isotope Effect in Superconducting Y-Ba-Cu-O," Phys. Rev. Lett. **58**, 2337 (1987).
5. M.F. Hundley, A. Zettl, A. Stacy, and M.L. Cohen, "Transport Properties of the Superconducting Oxide $La_{1.85}Sr_{0.15}CuO_4$," Phys. Rev. B **35**, 8800 (1987).
6. M.F. Crommie, L.C. Bourne, A. Zettl, M.L. Cohen, and A. Stacy, "Tunneling Measurements of the Energy Gap in Y-Ba-Cu-O," Phys. Rev. B **35**, 8853 (1987).
7. F.C. Wellstood, M.J. Ferrari, J. Clarke, A.M. Stacy, A. Zettl, and M.L. Cohen, "Upper Limit on the Resistivity of $La_{1.85}Sr_{0.15}CuO_4$," Phys. Lett. A **122**, 61 (1987).
8. T.A. Faltens, W.K. Ham, S.W. Keller, K.J. Leary, J.N. Michaels, A.M. Stacy, H.C. zur Loye, D.E. Morris, T.W. Barbee III, L.C. Bourne, M.L. Cohen, S. Hoen, and A. Zettl, "Observation of an Oxygen Isotope Shift in the Superconducting Transition Temperature of $La_{1.85}Sr_{0.15}CuO_4$," Phys. Rev. Lett. **59**, 915 (1987).
9. L.C. Bourne, K.J. Chang, M.L. Cohen, A.M. Stacy, and W.K. Ham, "Elasticity Studies of $La_{2-x}Sr_xCuO_4$," Phys. Rev. B **35**, 8785 (1987).
10. U. Walter, S. Fahy, A. Zettl, S.G. Louie, M.L. Cohen, P. Tejedor, and A.M. Stacy, "Probing Density of States and Interactions at the Rare Earth Site in Superconducting $ErBa_2Cu_3O_7$," Phys. Rev. B **36**, 8899 (1987).

Other Publications

11. M.L. Cohen, A. Stacy, and A. Zettl, "A Status Report on the Berkeley Research on High T_c Superconductors," in *Proc. Symp. S 1987 Spring Meeting Mat. Res. Soc.*, April 21–25, Anaheim, CA, D. Gubser and M. Schluter, Eds., 1987, p. 93.
12. M.L. Cohen, D.E. Morris, A. Stacy, and A. Zettl, "Oxygen Isotope Effect in the High Temperature Superconductors $YBa_2Cu_3O_{7-d}$ and $La_{1.85}Sr_{0.15}CuO_4$, with ^{18}O Substituted by Diffusion," in *Proc. Workshop on Novel Mechanisms of Superconductivity*, Berkeley, CA June 22–26, 1987, V. Kresin and S. Wolf, Eds., 1987, p. 733.

Chemical Sciences

FUNDAMENTAL INTERACTIONS

PHOTOCHEMICAL AND RADIATION SCIENCES

Photon-Assisted Surface Reactions, Materials, and Mechanisms*

Gabor A. Somorjai, Investigator

INTRODUCTION

This project explores the surface science of photocatalyzed chemical reactions that take place at the solid-vapor and solid-liquid interfaces. We focus on processes that thermodynamically could not occur without the presence of light as the energy source. The photodissociation of water to produce hydrogen and oxygen, of nitrogen to form ammonia, and of carbon dioxide to produce formic acid are investigated. The catalysts are semiconductor surfaces that absorb and convert light to separated, excited electron-electron vacancy pairs that initiate the reduction and oxidation of adsorbed species. The materials that are being used include iron oxides, silicates, and silicon carbide. The purpose of these studies is to explore the elementary steps of the photon-assisted surface reaction by a combination of modern surface science techniques and then to establish the optimum conditions (of surface structure, composition, temperature, and reactant mixture) to maximize the rate of production of desired chemicals.

1. Photoassisted Catalytic Dissociation of H_2O To Produce Hydrogen on Partially Reduced α-Fe_2O_3 (Publication 2)

M.M. Khader, G.H. Vurens, I.-K. Kim, M. Salmeron, and G.A. Somorjai

The photodissociation of H_2O on partially reduced Fe_2O_3 powders and pellets is shown to be a catalytic process if the semiconductor is illuminated by visible light of energy greater than 2.2 eV. Activation of the Fe_2O_3 catalysts involved reduction in a mixture of H_2 and H_2O followed by oxidation. Up to 380 μmol of H_2 were produced with 190 μmol of Fe_2O_3 powder. The rate was 40 μmol $hr^{-1}g^{-1}$ for the first 200 hr and started to decay thereafter. O_2 was also produced, as shown by using $H_2{}^{18}O$ in amounts of up to 40 ± 15% of the amount of H_2 detected in the same experiment. In photoelectrochemical experiments with the use of a three-compartment cell, the active pellets produced photocurrents of approximately 4 $\mu A\ cm^{-2}mW^{-1}$ at +0.5 V bias (SCE, pH = 13). Simultaneously, H_2 was produced at a rate of 0.06 μmol hr^{-1} mW^{-1}. A lower limit to the conversion efficiency of approximately 10^{-3} H_2 molecules per photon was obtained.

2. Photocatalysis (Publication 3)

G.A. Somorjai

The photocatalyzed processes may be divided into two classes: (1) Thermodynamically uphill reactions that could not occur without light. In this circumstance light is a reactant. The photodissociation of water, nitrogen, or CO_2 belongs to this class. (2) Photon-assisted reactions that are thermodynamically feasible but occur at accelerated rates or with altered selectivity in the presence of light. Photodecomposition or photooxidation of organic molecules are examples of this class.

Through discussions of selected subjects, the progress in these areas was reviewed using single crystals, small and larger size colloids, and small particles as photocatalysts.

*This work was supported by the Director, Office of Energy Research, Office of Basic Energy Sciences, Chemical Sciences Division of the U.S. Department of Energy under Contract No. DE-AC03-76SF00098.

3. Structure, Composition, and Chemisorption Studies of Thin Ordered Iron Oxide Films on Platinum(111) (Publication 4)

G.H. Vurens, M. Salmeron, and G.A. Somorjai

The epitaxial growth of iron oxide overlayers has been investigated on a platinum(111) single crystal, in the monolayer and the multilayer regimes. Different LEED structures have been observed for each of these regimes. At one-monolayer coverage, iron oxide forms an incommensurate overlayer with 10% longer unit cell vectors than those of clean platinum. At coverages of 3 to 10 monolayers, iron oxide forms a new structure, which is (2×2) with respect to that formed at one monolayer. AES and XPS studies show that the iron in the oxide overlayer is in the 2+ oxidation state, and from ISS studies it was determined that both iron and oxygen are present in the outermost atomic layer in about equal amounts. Water adsorption on the iron oxide films was studied by TPD. It was found that the desorption spectrum is very sensitive to the presence of various types of defects on the oxide.

4. Work in Progress

Silicon carbide single crystals, both in the hexagonal and cubic forms, have been obtained, and their surface properties are being explored by a combination of surface science techniques. Photochemical properties of these materials are under intensive study.

Iron oxide monolayers and thin films are being epitaxially grown on platinum single-crystal surfaces, and their structure, ordering, composition, and photochemical properties are being studied by surface science techniques. The chemisorption and photodesorption of small molecules (CO, NH_3, H_2, O_2, and H_2O) are being explored on these surfaces.

1987 PUBLICATIONS AND REPORTS

Refereed Journals

1. M. Khader, N. Lichtin, G. Vurens, M. Salmeron, and G.A. Somorjai, "Photoassisted Catalytic Dissociation of H_2O and Reduction of N_2 to NH_3 on Partially Reduced α-Fe_2O_3," Langmuir **3**, 303 (1987); LBL-21759.
2. M. Khader, I.-K. Kim, G. Vurens, M. Salmeron, and G.A. Somorjai, "Photoassisted Catalytic Dissociation of H_2O to Produce Hydrogen on Partially Reduced α-Fe_2O_3," J. Am. Chem. Soc. **109**, 3581 (1987); LBL-22380.
3. G.A. Somorjai, "Photocatalysis," Nouveau J. De Chimie **11**, 197 (1987).

LBL Reports

4. G.H. Vurens, M. Salmeron, and G.A. Somorjai, "Structure, Composition and Chemisorption Studies of Thin Ordered Iron Oxide Films on Platinum(111)," Surf. Sci. (in press); LBL-24328.

Invited Talks

5. G. Vurens, M. Salmeron, and G.A. Somorjai, "Surface Science Studies of Iron Oxide Thin Films," NCCAVS 9th Surface/Interface Research Meeting, IBM Almaden Research Center, San Jose, CA, Feb. 25, 1987.
6. G.A. Somorjai, "The Production of Hydrogen by the Photocatalytic Dissociation of Water in the Solar Energy Range," Hydrogen from Renewable Energy Symposia, Honolulu, HI, Mar. 23–27,1987.
7. G.A. Somorjai, "New Directions of Chemical Energy Conversion and Surface Science Research," Kolthoff Lectures, University of Minnesota, Minneapolis, Apr. 13–16, 1987.
8. G.A. Somorjai, "The Surface Science of Photocatalytically Active Iron Oxides," 11th DOE Solar Photochemistry Research Conference, Granlibakken Conference Center, Tahoe City, CA, June 8–11, 1987.
9. G.A. Somorjai, "Surface Chemistry Related to Photocatalysis," NATO Photoelectrochemistry Conference, Erice, Sicily, Sept. 6–9, 1987.

Photochemistry of Materials in the Stratosphere*

Harold S. Johnston, Investigator

INTRODUCTION

This research is concerned with fundamental gas-phase photochemistry and with global atmospheric photochemical modeling. One goal is to measure the distribution of excess energy in the fragments produced after a molecule is broken apart by an energetic pulse of light. Another goal is to obtain optical and kinetic data in the laboratory that are needed by modelers of the atmosphere. The experimental methods include laser flash photolysis, laser resonance absorption, resonance fluorescence, dispersed chemiluminescence from photolysis products, and infrared diode lasers. In collaboration with others, quantum mechanical studies are made of the molecular structure of certain atmospheric molecules, and other theoretical model studies are made of global atmospheric photochemistry. This research has applications to molecular dynamics, to problems of atmospheric ozone, and to problems of global change of trace gases in the atmosphere.

1. Quantum Mechanical Energy and Structural Calculations on the Nitrate Free Radical (Publication 1)

B. Kim, H.S. Johnston, D.A. Clabo,† and H.F. Schaefer III†

Ab initio molecular quantum mechanics has been used to study the four lowest electronic states of the nitrate free radical at the D_{3h} geometry deduced by Ishiwata, Tanaka, Kawaguchi, and Hirota. Basis sets of double zeta (9s5p/4s2p) and double zeta plus polarization (DZ + P) quality were used. Both self-consistent-field (SCF) and configuration interaction (CI) functions were employed, with molecular orbitals determined for the various electronic states of NO_3 and for the ground-state nitrate anion. The CI wave functions included single (S), double (D), and in some cases triple (T) excitations. The CISDT wave functions included as many as 511,474 configurations in C_{2v} point group symmetry. The predicted energetic position of the $^2E'$ state agrees well with the known T_0, 15,100 cm^{-1}. The $^2E''$ state, not yet observed, is predicted to lie at a vertical excitation energy of about 3600 cm^{-1}. On the basis of these theoretical calculations, an experiment has been designed to observe and precisely locate the lowest excited state of NO_3.

†Present address: University of Georgia, Athens, GA.

2. Primary and Secondary NO_3 Quantum Yields from Photolysis of $ClONO_2$ (Publication 2)

D. Oh, W. Sisk, and H.S. Johnston

The quantum yields of primary photofragments NO_3 and Cl from $ClONO_2$ photolysis were investigated by laser flash photolysis followed by resonance absorption of NO_3 $\{A(0,0,0,0) \leftarrow X(0,0,0,0)\}$ at 661.9 nm. Using 1.9×10^{-17} cm^2 for the NO_3 absorption cross section at 661.9 nm, the primary NO_3 quantum yield was found to be 0.97 ± 0.09 (1σ), and the secondary NO_3 quantum yield (presumably following reaction of $ClONO_2$ with Cl) is 0.87 ± 0.09 (1σ), approaching unity at high gas pressure. There was a fast initial rise in the NO_3 X(0,0,0,0) concentration, which was dependent on carrier gas pressure. This initial rise was interpreted as the deactivation of vibrationally excited NO_3 molecules produced by laser photolysis, and analysis of this initial rise yielded the quenching rate constant k for the deactivation step:

$$NO_3\,(v > 0) + M \rightarrow NO_3\,(0,0,0,0) + M \ ,$$

where $k(N_2,O_2)$ is equal to $(4.04 \pm 0.02) \times 10^{-13}$ cm^3 $molecule^{-1}$ s^{-1}. The NO_3 X(0,0,0,1) level was probed via the transition, $A(0,0,0,0) \leftarrow X(0,0,0,1)$, at 679 nm.

*This work was supported by the Director, Office of Energy Research, Office of Basic Energy Sciences, Chemical Sciences Division of the U.S. Department of Energy under Contract No. DE-AC03-76SF00098.

3. Ozone Calculations Including Large Perturbations of Chlorine and Nitrous Oxide (Publication 3)

D. Kinnison, H.S. Johnston, and D. Wuebbles[†]

By bracketing realistic conditions and possible perturbations in a one-dimensional atmospheric model with unrealistic conditions and unlikely degrees of perturbation, this study identifies and graphically presents several interactions between the chlorine system and the oxides of nitrogen in the stratosphere. A contour plot of percentage ozone-column reduction is given as a joint function of stratospheric NOX and ClX, each varying from zero to a large value (see Figure 3-1). A zone is identified wherein increasing NOX increases the ozone column. When the maximum mixing ratio of stratospheric ClX exceeds about one-third the maximum mixing ratio of stratospheric NOX, the ozone reduction by ClX becomes nonlinear with an increasingly negative slope. In this case ClX, instead of NOX, dominates the destruction of stratospheric ozone. In the hypothetical absence of all HOX and NOX in the stratosphere, even 1 ppb of ClX (approximately the 1960 value) would dominate ozone destruction from the bottom to the top of the stratosphere and reduce the ozone column to a value less than that presently observed in the present atmosphere.

[†]Permanent address: Lawrence Livermore National Laboratory, Livermore, CA 94550.

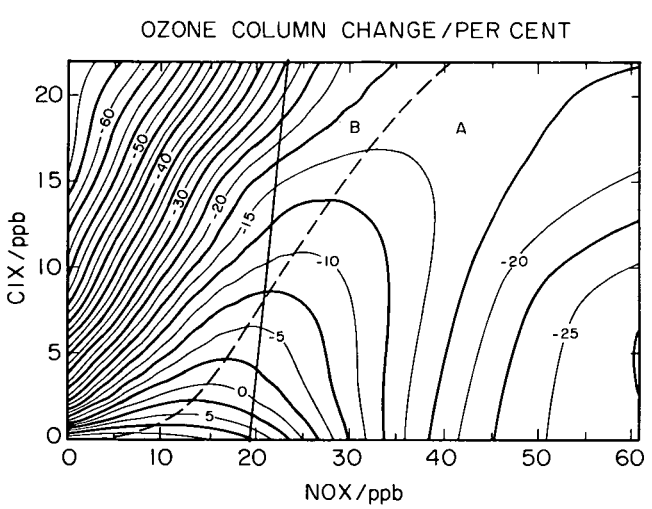

Figure 3-1. Contour plot of percentage ozone-column reduction as a function of stratospheric NOX and ClX. (XBL 885-1751)

4. Work in Progress

Collision-free nitrogen dioxide fluorescence is induced by fast (15 ns) excimer-laser photolysis of RNO_2 compounds at low pressure (5 mtorr). A large amount of such data was taken this year with variation of the photolyzed molecules (named above), ultraviolet wavelength through Raman shifting of the excimer laser pulse, and delay time between photolysis and observation. The dispersed spectra give information about the internal energy distribution (first two moments) of the photolysis products, if one knows the fluorescence lifetime as a function of wavelength. Extrapolated literature values of fluorescence lifetimes were used in the previous studies here, but these values are very sparse and uncertain at wavelengths above 600 nm. A project is under way to measure the collision-free NO_2 fluorescence lifetimes, especially at wavelengths above 600 nm. After these measurements are completed (early 1988), it will be possible to carry through the calculation of internal energy distribution from the observed photolysis induced fluorescence spectra for the cases studied here and to prepare articles for publication. (D. Kinnison, C. Miller, D. Oh, K. Patten, W. Sisk, and H.S. Johnston)

In collaboration with Y.T. Lee and his graduate students, these molecules have been photolyzed in a molecular beam to obtain the translational energies of the product fragments. The internal energy distribution given by the photolysis induced fluorescence is supplementary information to the translational energy distribution given by the molecular beam experiment. By these methods, a fairly complete accounting will be obtained of the nascent energy of the photolysis products for this series of similar reactants with 4, 5, and 7 atoms.

1987 PUBLICATIONS AND REPORTS

LBL Reports

1. B. Kim, H. Johnston, D.A. Clabo, and H.F. Schaefer III, "The Vertical Electronic Spectrum of NO_3: $^2A_2'$, $^2E''$ ($^2A_2$, $^2B_1$) and $^2E'$ States," submitted to the J. Chem. Phys.; LBL-24204.
2. D. Oh, W. Sisk, and H. Johnston, "Primary and Secondary NO_3 Quantum Yields from Photolysis of $ClONO_2$," LBL-24586.
3. D. Kinnison, H. Johnston, and D. Wuebbles, "Ozone Calculations Including Large Perturbations of Chlorine and Nitrous Oxide," LBL-24573.
4. H. Johnston (Chairman), "Trends in Vertical Ozone Measurements," Chapter in NASA Report of the Ozone Trends Panel (in press); LBL-24574.

CHEMICAL PHYSICS

Energy Transfer and Structural Studies of Molecules on Surfaces*

Charles B. Harris, Investigator

INTRODUCTION

The goal of this research is to study the mechanisms that are responsible for the transfer of energy from the excited states of molecules to metal surfaces and to develop new laser techniques for probing molecule-surface interactions. The research program is both theoretical and experimental in character, and includes nonlinear optical and picosecond laser techniques in addition to a variety of standard surface science tools for characterizing molecule-surface interactions. Recent work has centered on the development of picosecond infrared lasers, the elucidation of the mechanism of surface-enhanced photochemistry, surface-enhanced photoelectron emission, and the breakdown of classical dielectric response theory for explaining energy transfer from molecules to noble metal surfaces. The latter studies have resulted in a classification scheme in which molecular excited states that produce intraband electronic excitations transfer energy to electrons localized near the metal surface, while those excited states that can access direct interband excitations transfer energy to electrons throughout the bulk of the metal. The results of this program have a direct bearing on high-speed technological devices and materials, and on other problems of general interest such as the dynamics of electrical transmission in conductors on ultrafast timescales and the optical properties of thin films.

*This work was supported by the Director, Office of Energy Research, Office of Basic Energy Sciences, Chemical Sciences Division of the U.S. Department of Energy under Contract No. DE-AC03-76SF00098.

1. Electronic Energy Transfer at Interfaces (Publication 4)

C.B. Harris

The fluorescence decays from submonolayers of pyrene separated from various interfaces by Xe spacer layers have been measured as a function of spacer layer thickness (17–200 Å), pyrene coverage, and emission wavelength. The results are explained in terms of two decay channels: energy transfer and trapping among the molecules in the two-dimensional pyrene overlayer, and excitation of electrons at the interface. The intralayer energy transfer was modeled using the Kohlrausch equation $N(t) = N_0 \exp(-t/\gamma)^a$, in which a is related to the distribution of pyrene molecules in energy

2. Photoemission at Metal Interfaces (Publication 9)

C.A. Parsons

Three different pathways have been studied for the relaxation of an optically excited adsorbate/surface system. The first of these, photoemission, is characterized via the molecular coverage dependence and time response of the total photoyield. The observed increase in the yield for the initial adsorbed monolayer is attributed to a lowering of the work function of the Ag(111) surface, while the monatomic decrease in the photoyield upon further adsorption is interpreted as attenuation of the metal photoelectrons by the multilayers. Evidence of the structural phase transition for pyridine on Ag(111) is seen in both the coverage dependence and photoyield thermal-desorption spectra. Long (100 nsec) photoyield decay times are observed for multilayer films. Models that account for the effects of trapping and diffusion of electrons in the molecular film under the influence of the image potential have been considered. Radiative emission as a relaxation mechanism for an excited molecule is difficult to observe when adsorbed on a noninsulator surface because of damping by efficient energy

transfer to the solid. Photochemistry is a third path by which an excited adsorbate may relax, although its reactivity is also expected to be severely limited by competition with nonradiative energy transfer. Photodecomposition for a variety of aromatic molecules adsorbed on roughened Ag surfaces is reported here using continuous radiation in the near-uv/visible. The enhanced fields at the surface provide the driving force for the reaction and also allow it to be monitored via the Raman spectrum of the graphitic carbon product. A two-photon initial absorption step is implicated by the intensity dependence of the decomposition rate for most cases. Energy-transfer considerations and possible decomposition mechanisms following absorption are discussed.

3. Chemical Reaction Dynamics in Condensed Phase (Publications 1–3)†

D. Ben-Amotz, R. Jeanloz, and C.B. Harris

The nonradiative decay dynamics of crystal violet, and other triphenyl-methane dyes, dissolved in a variety of solvents, have been studied as a function of temperature and pressure. A linear viscosity dependence of the excited-state absorption decay time in n-alcohol solvents is found at several constant temperatures. The theoretical predictions of three theories for large-amplitude dynamics on a barrierless excited-state potential were tested. The predicted forms for the time-dependent integrated excited-state population are compared with experimentally measured excited-state absorption decays of crystal violet in various solvents. The overall viscosity dependence of the excited-state decay time is linear. Differences between the viscosity dependence observed when varying pressure, temperature, or solvent type at low viscosities are tentatively ascribed to pressure- and temperature-induced conformational changes. In addition, results were obtained that clarified the time scales for predissociation and geminate recombination in the iodine photodissociation/recombination reaction. Direct comparison of absorption features following A-state excitation with those following B-state excitation suggests that predissociation may be much more rapid ($\leq$1 psec) than previously thought, and that geminate recombination is also very rapid ($\leq$2 psec). Both of these results lead to the conclusion that curve crossing in solution is extremely facile and not the rate-limiting step in recombination.

†National Science Foundation program using DOE equipment.

4. Work in Progress

Picosecond Techniques for Electron Emission Studies at Surfaces

In order to study the dynamics of electron emission at a metal surface, we are developing time-correlated single-electron counting as a means for studying surface dynamics. This apparatus relies on a synchronously pumped dye laser system as a source of uv light pulses of 1–3 picoseconds duration. A portion of the ultrashort light pulse is used to generate electrons via photoemission and set the start pulse of an electronic clock. The electrons that are emitted from the surface are scattered by surface states or from molecular adsorbates on the surface. This causes a change in the electron's momentum. The momentum distribution can be measured by time of flight. In particular, the electrons are detected by a channel plate and stop the electronic clock at a time that is proportional to the electron's momentum. This is represented as a voltage, which is stored in a computer. In this manner a histogram of the electron's dynamics is created. This apparatus possesses a dynamic range of 10^5–10^6 and is very sensitive to low quantum yields. The time resolution of this system is <50 picoseconds and has an upper limit of a few hundred microseconds. These unique capabilities will allow us to sensitively probe the electron dynamics at metal surfaces, with the time resolution necessary to elucidate the dynamics directly. In addition, by using femtosecond pump-probe techniques, one can in principle get 50 fsec time resolution.

1987 PUBLICATIONS AND REPORTS

Refereed Journals

1. D. Ben-Amotz and C.B. Harris, "Torsional Dynamics of Molecules on Barrierless Potentials in Liquids: I. Temperature and Wavelength Dependent Picosecond Studies of Triphenyl-methane Dyes," J. Chem. Phys. **86**, 4856 (1987); LBL-22673.
2. D. Ben-Amotz and C.B. Harris, "Torsional Dynamics of Molecules on Barrierless Potentials in Liquids.

II. Test of Theoretical Models," J. Chem. Phys. **86**, 5433 (1987); LBL-22674.

3. D. Ben-Amotz, R. Jeanloz, and C.B. Harris, "Torsional Dynamics of Molecules on Barrierless Potentials in Liquids. III. Pressure Dependent Picosecond Studies of Triphenyl-methane Dye Solutions in a Diamond Anvil Cell," J. Chem. Phys. **86**, 6119 (1987); LBL-22675.
4. A.P. Alivisatos, M.F. Arndt, S. Efrima, D.H. Waldeck, and C.B. Harris, "Electronic Energy Transfer at Semiconductor Interfaces: I. Energy Transfer From Two Dimensional Molecular Films to Si(111)," J. Chem. Phys. **86**, 6540 (1987); LBL-22672.
5. D.E. Smith and C.B. Harris, "Studies of Chemical Reactivity in the Condensed Phase. III. Direct Measurement of Predissociation and Geminate Recombination Times for Iodine in Solution," J. Chem. Phys. **87**, 2709 (1987).

Other Publications

6. D. Ben-Amotz and C.B. Harris, "Test of Theoretical Models for the Barrierless Non-Radiative Relaxation of Triphenyl-methane Dyes," in *Proc. IQEC'87*, Baltimore, MD, Optical Society of America Publishers, 1987.
7. D. Ben-Amotz and C.B. Harris, "Picosecond Studies of the Non-Radiative Decay Dynamics of Triphenyl-methane Dyes in a Diamond Anvil Pressure Cell," in *Proc. IQEC'87*, Baltimore, MD, Optical Society of America Publishers, 1987.
8. J.K. Brown, D.J. Russell, D.E. Smith, and C.B. Harris, "Theoretical Studies of Vibrational Relaxation of Iodine in Low Density Liquid Xenon," Revue de Physique Applique (France) **22**, 1787 (1987).

LBL Reports

9. C.A. Parsons (Ph.D. Thesis), "Photoemission, Fluorescence and Photochemical Studies of Molecular Adsorbates on Metal and Semiconductor Surfaces," LBL-23201.
10. J.K. Brown (Ph.D. Thesis), "Molecular Dynamics Simulations of Simple Liquid Phase Chemical Reactions," LBL-24353.

Invited Talks

11. C.B. Harris, "Fundamental Studies of Chemical Reactivity in Solutions," Department of Chemistry Colloquium, University of Minnesota, Minneapolis, Oct. 6, 1986.
12. C.B. Harris, "The Nature of Dynamical Processes in Condensed Phase on the Femtosecond Timescale," Joint Chemistry-Physics Colloquium, University of Rochester, Rochester, NY, Oct. 8, 1986.
13. C.B. Harris. "The Nature of Chemical Reactions in Liquids on the Femtosecond Timescale," Department of Chemistry Colloquium, Stanford University, Stanford, CA, Oct. 16, 1986.
14. C.B. Harris, "The Nature of Chemical Reactions in Liquids on the Femtosecond Timescale," Department of Chemistry Colloquium, Northwestern University, Evanston, IL, Nov. 7, 1986.
15. C.B. Harris. "The Nature of Chemical Reactions in Liquids on the Femtosecond Timescale," Chemical Physics Colloquium, University of Southern California, Los Angeles, Nov. 10, 1986.
16. C.B. Harris, "The Nature of Chemical Reactions in Liquids on the Femtosecond Timescale," Ultrafast Laser Spectroscopy and Molecular Lineshapes Symposium, Denver, CO, Apr. 5–10, 1987.
17. C.B. Harris, "The Nature of Chemical Reactions in Liquids on the Femtosecond Timescale," Chemistry Department seminar, University of San Diego, La Jolla, Apr. 14, 1987.
18. C.B. Harris, "The Dynamics of Chemical Reactions in Liquids on Ultrafast Timescales," "Symposium on Lasers in Chemistry and Biology" session, XV IQEC'87 Conference, Baltimore, MD, Apr. 27–May 1, 1987.
19. C.B. Harris and D. Ben-Amotz, "Test of Theoretical Models for the Barrierless Non-Radiative Relaxation of Triphenyl-methane Dyes," IQEC'87 Conference, Baltimore, MD, Apr. 27–May 1, 1987.
20. C.B. Harris and D. Ben-Amotz, "Picosecond Studies of the Non-Radiative Decay Dynamics of Triphenyl-methane Dyes in a Diamond Anvil Pressure Cell," IQEC'87 Conference, Baltimore, MD, Apr. 27–May 1, 1987.
21. C.B. Harris, "Energy Transfer and Photochemistry on Metal and Semiconductor Surfaces," Gordon Research Conference on Dynamics of Gas-Surface Interactions, Andover, NH, Aug. 10–14, 1987.

Selective Photochemistry*

C. Bradley Moore, Investigator

INTRODUCTION

The fundamental goals of this program are to understand the photophysics and photochemistry that occur following selective excitation of molecules. Of particular interest are the chemical reactions of specifically excited states and the dynamics of energy transfer, both within a molecule and to surrounding molecules.

Molecules produced in bound excited singlet states may fragment following the conversion of electronic excitation energy into vibrational energy. Intersystem crossing to triplet states is often in competition with internal conversion to singlet states. In this work the dynamics of intersystem crossing and reaction of the triplet state are studied for both unimolecular and bimolecular systems.

For low levels of vibrational excitation in small molecules, individual quantum states may be excited, enabling the measurement of reaction and energy-transfer rate constants for each quantum state. For larger or more highly excited molecules, it is usually not possible to excite single eigenstates. Instead, a number of eigenstates are excited simultaneously, and a redistribution of the initial vibrational excitation occurs. This process, known as intramolecular vibrational energy redistribution (IVR), is extremely rapid and severely limits the realization of truly mode-specific unimolecular reactions

Advances in mode-specific chemistry will come from a more complete understanding of the IVR process and the parameters that control its efficiency. By being able to predict the rates of IVR and the path of vibrational energy flow through a molecule, experiments can be designed utilizing molecular systems that maximize the possibilities for mode-specific effects. Studies designed to elucidate the coupling mechanisms and dominant pathways for IVR are currently under way on a number of model systems.

The rates and mechanisms of free-radical reactions, such as are important in combustion, are often best studied by flash kinetic spectroscopy using lasers for thermal heating, for photolyzing, and for spectroscopic probing. Reactions can be studied as a function of individual quantum states. A fundamental understanding of these reactions is sought to serve as a basis for modeling combustion processes.

*This work was supported by the Director, Office of Energy Research, Office of Basic Energy Sciences, Chemical Sciences Division of the U.S. Department of Energy under Contract No. DE-AC03-76SF00098.

1. T_1 Barrier Height, S_1–T_1 Intersystem Crossing Rate, and S_0 Radical Dissociation Threshold for H_2CO, D_2CO, and HDCO (Publication 3)

M.-C. Chuang, M.F. Foltz, and C.B. Moore

Vacuum uv laser-induced fluorescence has been used to detect the atomic products in the photofragmentation of H_2CO, D_2CO, and HDCO. The dissociation is shown to occur on both the ground (S_0) and the first triplet (T_1) potential surfaces (see Figure 1-1). The T_1 exit barrier height (2.9–6.0 kcal/mol) and the $S_1 \rightarrow T_1$ intersystem crossing rate near the T_1 barrier top (4×10^7 sec^{-1}) have been determined experimentally. The threshold energy for the radical dissociation channel on the S_0 surface, 86.57 ± 0.16 kcal/mol, has also been measured accurately by rovibronically resolved photolysis. The best values for the heat of formation (9.99 ± 0.19 kcal/mol) and

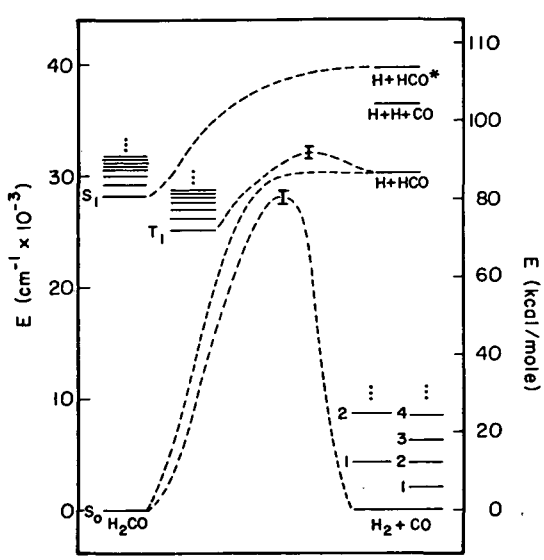

Figure 1-1. Potential curves for formaldehyde photochemistry. A monochromatic uv laser produces molecules in a single rovibronic state of S_1. For energies above the barrier to dissociation on the T_1 surface, intersystem crossing competes effectively with internal conversion to the ground state, S_0. The repulsive force between fragments on the triplet surface pushes the H atom away at a much higher velocity than on the singlet surface. (XBL 884-1337)

the C-H bond enthalpy (15.69 ± 0.19 kcal/mol) of HCO radical have been derived from the measured threshold energies as well.

2. Infrared Flash Kinetic Spectroscopy of HCO (Publication 5)

C.B. Dane,† D.R. Lander,† R.F. Curl,† F.K. Tittle,† Y. Guo, M.I F. Ochsner,‡ and C.B. Moore

The high-resolution infrared spectrum of the CH stretching fundamental of the formyl radical (HCO) has been observed by means of infrared kinetic spectroscopy using 308-nm (XeCl) excimer laser flash photolysis of formaldehyde or acetaldehyde followed by difference-frequency and diode laser probing of the transient absorption (see Figure 2-1). The high-resolution spectra obtained were assigned and fitted with rotational, spin-rotational, and centrifugal distortion constants. The ν_1 band origin is 2434.48 cm^{-1}. New ground-state constants are reported from a least-squares fit combining this ν_1 data with previous microwave and far-infrared laser magnetic resonance measurements.

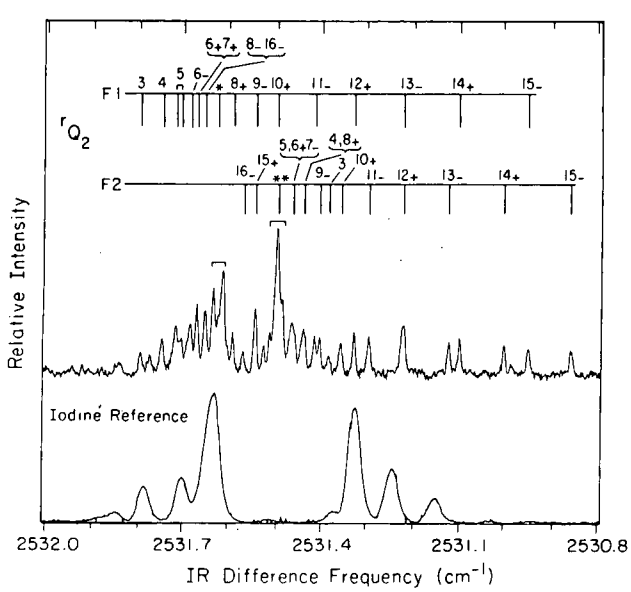

Figure 2-1. A small portion of the CH stretching fundamental spectrum of the HCO free radical. The K = 3 ← 2 perpendicular Q-branches are recorded with the difference-frequency infrared laser. The resolution is Doppler-limited. A 35-mJ pulse of 308-nm radiation is used to photolyze 2.5 Torr of acetaldehyde. (XBL 884-1338)

More accurate equilibrium rotational constants are defined using the rotational constants of the vibrationally excited state. The unusually low vibrational frequency is to be expected from the very low bond enthalpy measured in abstract 1. The frequency is in excellent agreement with the theoretical value (0.6% higher than experiment) calculated by Bowman, Bittman, and Harding.[1] The relative intensities of the parallel and perpendicular components of the transition show that the C-H stretching transition dipole moment direction is tipped 22° away from the C→H bond direction toward the O→C direction. Thus significant displacement of charge in the C-O bond must occur as the C-H bond vibrates.

---

†Permanent address: Chemistry and Electrical Engineering Departments, and Rice Quantum Institute, Rice University, Houston, TX 77251.

‡Present address: CIBA-GEIGY A.G., Analytische Forschung FO3.2, CH-4002 Basel, Switzerland.

1. J.M. Bowman, J.S. Bittman, and L.B. Harding, J. Chem. Phys. **85**, 911 (1986).

3. Work in Progress

Energy transfer and chemical reaction rates are being studied for HCO and triplet CH_2 radicals. A diode laser infrared flash kinetic spectrometer has been constructed to extend this work beyond the 2–4 micron range available with our current difference-frequency spectrometer. Reaction rates of $^3CH_2$ with O_2 and NO have already been measured together with H.S. Johnston. Bending spectra of triplet CH_2 will be recorded. Spectroscopy of radical-radical and radical-molecule reaction complexes is planned.

Unimolecular reaction dynamics are being studied by photofragment spectroscopy. A molecular beam system has been constructed to use with the new VUV laser system being developed together with Y.T. Lee and A.H. Kung. The fragmentation of ketene on its triplet potential energy surface will be studied by detection of CO using a tunable photolysis laser below the threshold for singlet fragmentation.

Infrared spectra of intermediates in organometallic photochemistry in gas and liquid phase are being studied jointly with R.G. Bergman. Emphasis is on CH activation chemistry. A study of the reactions of coordinatively unsaturated CpCo(CO) in liquid and gas phase has been carried out by flash photolysis of $CpCo(CO)_2$ and time-resolved infrared spectroscopy of the CO stretching spectra.

1987 PUBLICATIONS AND REPORTS

Refereed Journals

1. J.S. Wong. W.H. Green. Jr., C.-K. Cheng, and C.B. Moore, "Coupling of CH Stretching and Bending Vibrations in Trihalomethanes," J. Chem. Phys. **86**, 5994 (1987); LBL-20825.
2. W.H. Green, Jr., W.D. Lawrance, and C.B. Moore, "Kinetic Anharmonic Coupling in the Trihalomethanes: A Mechanism for Rapid Intramolecular Redistribution of CH Stretching Vibrational Energy," J. Chem. Phys. **86**, 6000 (1987); LBL-22694.
3. M.-C. Chuang, M.F. Foltz, and C.B. Moore, "T_1 Barrier Height, S_1–T_1 Intersystem Crossing Rate and S_0 Radical Dissociation Threshold for H_2CO, D_2CO and HDCO," J. Chem. Phys. **87**, 3855 (1987); LBL-23653.

LBL Reports

4. M.R. Berman and C.B. Moore, "The Small Molecule Limit of Infrared Multiphoton Dissociation: Collisional Effects in D_2CO," accepted by Laser Chem.; LBL-24761.
5. C.B. Dane, D.R. Lander, R.F. Curl, F.K. Tittle, Y. Guo, M.I.F. Ochsner, and C.B. Moore, "Infrared Flash Kinetic Spectroscopy of HCO," accepted by J. Chem. Phys.; LBL-24278.

Invited Talks

6. C.B. Moore, "Laser Photochemistry," Department of Chemistry, Harvey Mudd College, Claremont, CA, Feb. 26, 1987.
7. C.B. Moore, "Unimolecular Reaction Dynamics — Quantum State by Quantum State," Physical Chemistry Seminar, Department of Chemistry, University of California Berkeley, Mar. 3, 1987; Department of Chemistry, Rice University, Mar. 4, 1987; Department of Chemistry, University of Texas, Austin, Mar. 5, 1987; Department of Chemistry, Texas A&M University, College Station, Mar. 6, 1987.
8. C.B. Moore, "Energy Transfer and Disposition in Unimolecular Reactions," Department of Chemistry, California Institute of Technology, Mar. 24, 1987.
9. C.-K. Cheng, W.H. Green, Jr., D.R. Guyer, W.D. Lawrance, W.F. Polik, and C.B. Moore, "Vibrational Spectroscopy of Chemically Reacting Molecules," American Chemical Society 192nd National Spring Meeting. Denver, CO, Apr. 6–8, 1987.
10. W.H. Green, Jr., W.D. Lawrance, J.S. Wong, C.-K. Cheng, and C.B. Moore, "Coupling of CH Stretching and Bending Vibrations in Trihalomethanes: A Mechanism for Rapid Intramolecular Vibrational Energy Transfer," Department of Energy, Division of Chemical Sciences, Ninth Combustion Research Meeting, Mills College, Oakland, CA, June 3–5, 1987.
11. C.B. Moore, "The Spectroscopy of Free Radicals and the Dynamics of Their Formation," XIIIth International Conference on Photochemistry, Budapest, Hungary, Aug. 9–14, 1987.
12. C.B. Moore, "The Dynamics of Unimolecular Reactions near Threshold," Department of Chemistry, University of Wisconsin, Madison, and The Wisconsin Section of the American Chemical Society, Sept. 15, 1987.
13. C.B. Moore "Unimolecular Dynamics near Reaction Threshold," Chemistry and Photophysics of Energetic Species Symposium, University of Southern California, Los Angeles, Sept. 11, 1987.
14. C.B. Moore, "Breaking Chemical Bonds," Miller Professor Lecture, Miller Institute for Basic Research in Science, University of California Berkeley, Sept. 22, 1987.
15. C.B. Moore, "The Spectroscopy of Chemical Bond Breaking — a High Resolution Look at Unimolecular Reactions," Department of Chemistry, University of Rochester, Oct. 21, 1987.
16. C.B Moore, "The Spectroscopy and Reactions of Formyl and Methylene Radicals," General Motors Research Laboratories, Warren, MI, Oct. 22, 1987.
17. C.B. Moore, "State-to-State Dynamics of Unimolecular Reactions," Oesper Symposium honoring George C. Pimentel, University of Cincinnati, OH, Oct. 23, 1987.
18. C.B. Moore, "Laser Photochemistry and Reaction Dynamics," Department of Chemistry, National Taiwan University, Taipei, Taiwan, Nov. 10, 1987.
19. C.B. Moore, "Overtone Spectroscopy and Photochemistry," Atomic and Molecular Sciences Workshop on Laser Chemistry and Spectroscopy, Lectures on Unimolecular Reactions, Academia Sinica, Taipei, Taiwan, Nov. 12, 1987.
20. C.B. Moore, "Molecular Eigenstate Spectra and Statistics and Rates," Atomic and Molecular Sciences Workshop on Laser Chemistry and Spectroscopy, Lectures on Unimolecular Reactions, Academia Sinica, Taipei, Taiwan, Nov. 12, 1987.
21. C.B. Moore, "Product Energy Distributions — Photofragment Spectroscopy," Atomic and Molecular Sciences Workshop on Laser Chemistry and Spectroscopy, Lectures on Unimolecular Reactions, Academia Sinica, Taipei, Taiwan, Nov. 13, 1987.

Physical Chemistry with Emphasis on Thermodynamic Properties*

Kenneth S. Pitzer, Investigator

INTRODUCTION

The purpose of this program is the discovery and development of methods of calculation of thermodynamic and related properties of important chemical systems by the use of quantum and statistical mechanics together with experimental measurements for key systems. Current emphasis is on novel ionic systems and on properties close to the critical point. Systems comprising fused salts mixed in any proportion with water or other polar solvents are being studied experimentally and with theory. Current studies also include (1) dilute ionic solutions very close to the critical point of the solvent where anomalous properties are observed and (2) the representation of near-critical properties in an equation of state valid over the full range of temperature and density. Recent theoretical advances include treatments of the dielectric constant of H_2O, the thermodynamics of ionic solutions in H_2O above its critical temperature, and the critical properties of pure ionic fluids such as NaCl. Earlier advances yielded improved equations for electrolyte solutions. These various equations are now being applied to a wide variety of systems of industrial or geological interest, including geothermal brines. Other recent research involved the relativistic quantum chemistry of molecules containing very heavy atoms. This research is reviewed in Publication 10.

1. The Electrical Conductivity, Viscosity, and Density of a Two-Component Ionic System at its Critical Point (Publication 8)

D.R. Schreiber, M.C.P. de Lima,† and K.S. Pitzer

The density, viscosity, and electrical conductivity of a system composed of a fused salt in a low-dielectric-constant solvent were examined at a temperature just above the liquid-liquid critical point. The system examined was tetra-n-butylammonium picrate (TNBAP) in 1-chloroheptane. The viscosity data showed no anomalously high values in the region of the critical point, in contrast to reports on systems with neutral molecules. The conductivity decreased to a minimum near 0.001 mol/dm^3 and then increased rapidly through the region of the critical concentration. The data in the region of the minimum were fit using the method of Fuoss and Kraus to determine the ion-pair and triplet ion dissociation constants. The expression obtained was extrapolated to indicate the speciation of the TNBAP in the critical region. The speciation diagram indicated the increasing importance of the ions and ion triplets at the expense of the neutral ion pair. The conductivity results were also compared (see Figure 1-1) to a recent treatment (Publication 6) of the restrictive primitive model (RPM). The fraction of ions calculated by the RPM also shows an increasing importance of the ions and charged clusters, at the expense of neutral clusters, in the region of the critical point. The dielectric constant of 1-chloroheptane was also measured over a range of temperature.

*This work was supported by the Director, Office of Energy Research, Office of Basic Energy Sciences, Chemical Sciences Division of the U.S. Department of Energy under Contract No. DE-AC03-76SF00098.

†Permanent address: Department of Chemistry, University of Coimbra, 3000 Coimbra, Portugal.

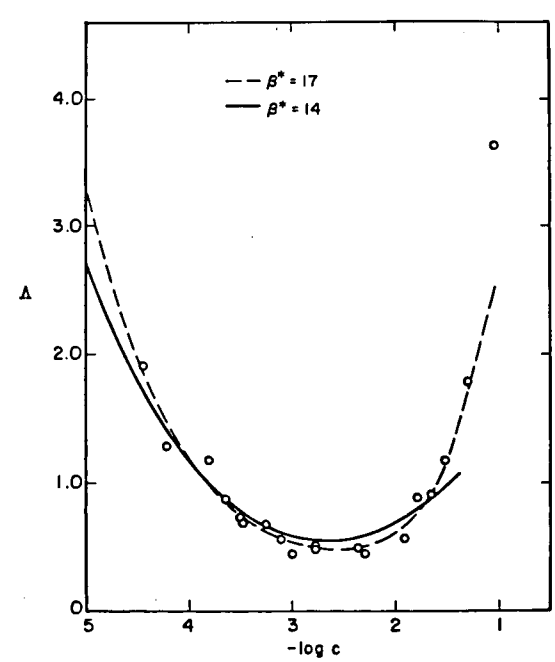

Figure 1-1. Comparison of conductivity data to predictions of the Restrictive Primitive Model, for a reciprocal temperature $\beta^* = 14$ (—) and $\beta^* = 17$ (---). The comparison assumes the same equivalent conductance for all charged species at all concentrations. (XBL 884-1341)

2. Improving Equation-of-State Accuracy in the Critical Region; Equations for Carbon Dioxide and Neopentane as Examples (Publication 13)

K.S. Pitzer and D.R. Schreiber

Typical equations of state fail to accurately represent properties close to the critical point for reasons that are now understood. It is shown that the addition of a specially designed three-term function solves this problem for practical purposes. Although the limiting behavior at the critical point is still not correct, the remaining deviations are negligible for more general applications. This method is related to work on H_2O by Haar, Gallagher, and Kell[1] (HGK) and is tested here for CO_2 and neopentane, for which equations are presented. Figure 2-1 shows that one avoids distortion of near-critical isotherms by adding this special function, which is negligible outside the range 0.99 to 1.01 in reduced temperature.

1. L. Haar, J.S. Gallagher, and G.S. Kell, *NBS-NRC Steam Tables*, Hemisphere, Washington, 1984.

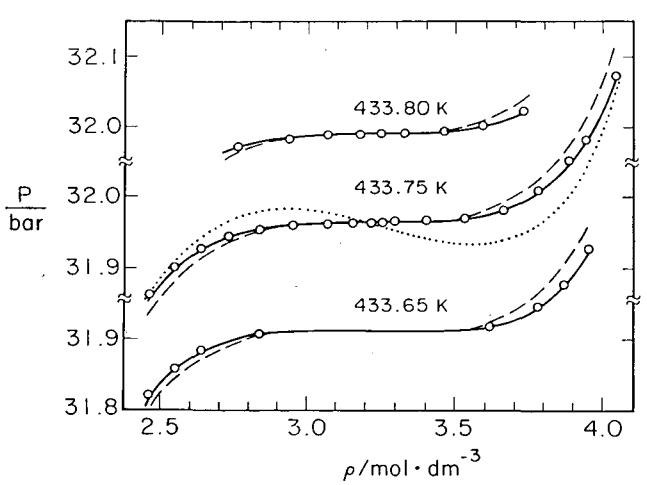

Figure 2-1. Near-critical isotherms for neopentane. Solid lines show the complete equation including the HGK function; dotted line, same without HGK function; dashed line, far-field equation without HGK function refitted and constrained to the critical point. Note the absence of any distortion of the isotherms when the HGK function is included. (XBL 884-1342)

3. The Critical Behavior of Ionic Fluids and the Role of Long-Range Fluctuations (Publication 15)

K.S. Pitzer

The general theory of the critical region for one- and two-component fluids is reviewed briefly, including the exponents that describe the behavior close to the critical point. In contrast to the nonclassical exponents experimentally displayed by nonionic systems and derived from theory for short-range forces, several ionic systems are found to show classical exponents within experimental uncertainty. The nonclassical exponents arise from theories that give special recognition to fluctuations in density or composition of very long range, of longer range than the short-range interparticle forces. Alternate theories are considered that assume longer-range forces that yield classical critical exponents as well as the correspondence between the assumptions of these theories and the expected forces in the ionic fluids. The experimental properties of several systems are reviewed in comparison with these theories. Ionic systems appear to be classical within the uncertainty of the experimental data. Special attention is given to the system H_2O-NaCl under conditions close to the critical point of H_2O, for which a new equation of state is presented.

Figure 3-1 shows two isotherms for NaCl-H_2O, one just below T_c for pure H_2O and the other just above. The calculated curves reproduce very well the remarkable properties measured[1] in the near-critical region. The concentration of NaCl in the vapor phase is extremely small, and the differences are probably within experimental uncertainty.

1. J.L. Bischoff, R.J. Rosenbauer, and K.S. Pitzer, Geochim. et Cosmochim. Acta **50**, 1437 (1986).

4. Work in Progress

Research continues on the near-critical properties of nonionic fluids and on the practically important and very interesting system NaCl-H_2O. Similar methods are being extended to two-component neutral-molecule systems showing liquid-liquid critical points.

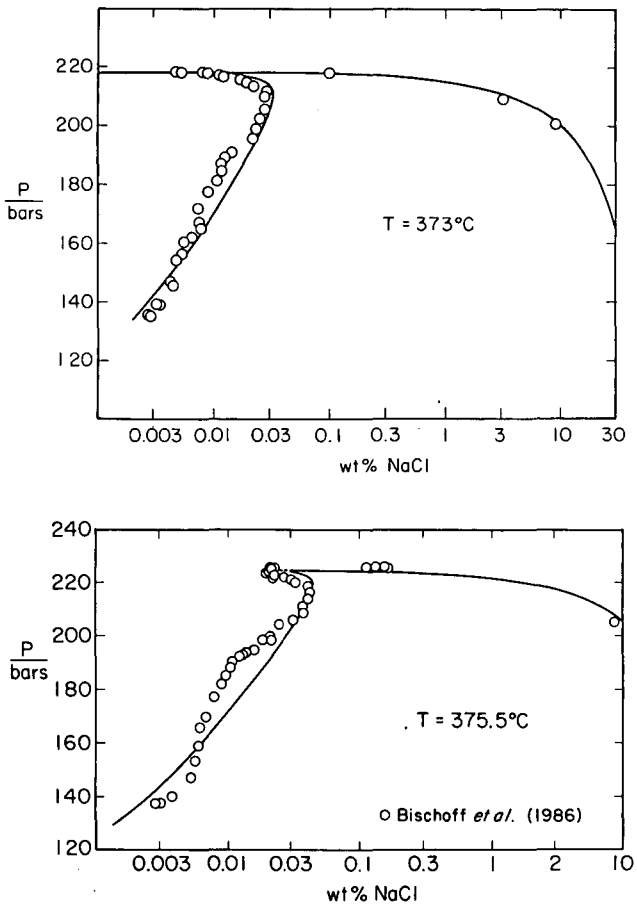

Figure 3-1. Phase diagram for NaCl-H_2O: (top) at 373°C, just below T_c for H_2O (374°C); (bottom) at 375.5°C, just above T_c for H_2O. The curves are calculated from the new equation of state. (top: XBL 884-1343; bottom: XBL 884-1344)

1987 PUBLICATIONS AND REPORTS

Refereed Journals

1. K.S. Pitzer, "Theoretical Considerations of Solubility with Emphasis on Mixed Aqueous Electrolytes," Pure Appl. Chem. **58**, 1599 (1986); LBL-21961.†
2. K.S. Pitzer, "Thermodynamic Properties of Ionic Fluids over Wide Ranges of Temperature," Pure Appl. Chem. **59**, 1 (1987); LBL-21799.
3. R.C. Phutela, K.S. Pitzer, and P.P.S. Saluja, "Thermodynamics of Aqueous Magnesium Chloride, Calcium Chloride, and Strontium Chloride at Elevated Temperatures," J. Chem. Eng. Data **32**, 76 (1987); LBL-21304.†
4. R.P. Neisler and K.S. Pitzer, "The Dipositive Dimeric Ion Hg_2^{2+}: A Theoretical Study," J. Phys. Chem. **91**, 1084 (1987); LBL-22064.
5. K.S. Pitzer, J.L. Bischoff, and R.J. Rosenbauer, "Critical Behavior of Dilute NaCl in H_2O," Chem. Phys. Lett. **134**, 60 (1987); LBL-22309.
6. K.S. Pitzer and D.R. Schreiber, "The Restricted Primitive Model for Ionic Fluids. Properties of the Vapour and the Critical Region," Mol. Phys. **60**, 1067 (1987); LBL-22171.
7. R.T. Pabalan and K.S. Pitzer, "Thermodynamics of NaOH(aq) in Hydrothermal Solutions," Geochim. Cosmochim. Acta **51**, 829 (1987); LBL-21631.†
8. D.R. Schreiber, M.C.P. de Lima, and K.S. Pitzer, "Electrical Conductivity, Viscosity, and Density of a Two-Component Ionic System at its Critical Point," J. Phys. Chem. **91**, 4087 (1987); LBL-22500.
9. R.T. Pabalan and K.S. Pitzer, "Thermodynamics of Concentrated Electrolyte Mixtures and the Prediction of Mineral Solubilities to High Temperatures for Mixtures in the System Na-K-Mg-Cl-SO_4-OH-H_2O," Geochim. Cosmochim. Acta **51**, 2429 (1987); LBL-22790.†

Other Publications

10. K. Balasubramanian and K.S. Pitzer, "Relativistic Quantum Chemistry," Adv. Chem. Phys. **67**, 287 (1987); LBL-20991.
11. K.S. Pitzer, "A Thermodynamic Model for Aqueous Solutions of Liquid-Like Density," Rev. Mineralogy **17**, 97 (1987); LBL-23554.†
12. K.S. Pitzer, "Of Physical Chemistry and Other Activities," Ann. Rev. Phys. Chem. **38**, 1 (1987).

LBL Reports

13. K.S. Pitzer and D.R. Schreiber, "Improving Equation-of-State Accuracy in the Critical Region; Equations for Carbon Dioxide and Neopentane as Examples," accepted by Fluid Phase Equilib.; LBL-24079.
14. R.T. Pabalan and K.S. Pitzer, "Apparent Molar Heat Capacity and Other Thermodynamic Properties of Aqueous KCl Solutions to High Temperatures and Pressures," submitted to J. Chem. Eng. Data; LBL-24085.†
15. K.S. Pitzer, "The Critical Behavior of Ionic Fluids and the Role of Long-Range Fluctuations," chapter in *Thermodynamics of Aqueous Systems*, N. Scrivner, Ed., Hemisphere Publishing Corp., Washington, D.C. (in press); presented at International Conference on Thermodynamics of Aqueous Systems with Industrial Application, Warrenton, VA, May 10–14, 1987; LBL-24191.

Invited Talks

16. K.S. Pitzer, "Critical Phenomena in Ionic Fluids," J.L. Franklin Memorial Lecture, Rice University, Houston, TX, Feb. 4, 1987.
17. K.S. Pitzer, "Theory and Empirical Modeling for Fluid Properties," banquet speech, International Conference on Thermodynamics of Aqueous Systems with Industrial Applications, Warrenton, VA, May 10–14, 1987.

18. K.S. Pitzer, "Critical Behavior of Ionic Fluids," National Bureau of Standards, Washington, D.C., May 15, 1987.

19. K.S. Pitzer, "Critical Behavior of Ionic Fluids with Implications for Nonionic Fluids," first lecture of the newly established annual Kenneth S. Pitzer Lectureship, University of California Berkeley, Aug. 25, 1987.

†This work was supported by the Director, Office of Energy Research, Office of Basic Energy Sciences, Division of Engineering and Geosciences of the U.S. Department of Energy under Contract No. DE-AC03-76SF00098.

Molecular Interactions*

William A. Lester, Jr., Investigator

INTRODUCTION

This research program is directed at extending fundamental knowledge of atoms and molecules, including their electronic structure, mutual interaction, collision dynamics, and interaction with radiation. The approach combines the use of *ab initio* methods — multiconfiguration Hartree-Fock (MCHF), configuration interaction (CI), and the recently developed quantum Monte Carlo (QMC) — to describe electronic structure, intermolecular interactions, and other properties, with various methods for characterizing inelastic and reactive collision processes, and photodissociation dynamics. Current efforts are focused on (1) the development of efficient methods of generating optimum importance functions in QMC, (2) the introduction and application of effective-core- and model-potential methods in QMC, and (3) an adiabatic treatment of single-photon indirect polyatomic photodissociation with emphasis on product rovibrational photofragment distributions.

1. Valence Quantum Monte Carlo for Many Valence-Electron Systems (Publications 5 and 11)

B.L. Hammond,† P.J. Reynolds, and W.A. Lester, Jr.†

A great deal of attention has been focused recently on valence-only methods for QMC. The reason for this interest is the desire to compute reliably molecular properties of large molecules containing heavy atoms, and further, the realization of the steep Z (nuclear charge) dependence of the CPU time required in QMC to achieve a given accuracy. This Z dependence has been estimated to be approximately $Z^{6.5}$. When treating the valence electrons only, however, this dependence becomes $(Z^{eff})^{4.1}$, where Z^{eff} is the screened nuclear charge.

The use of pseudopotentials is long established in solid-state physics and quantum chemistry for large-scale computations involving heavy atoms. Two methods in common use in quantum chemistry are the *ab initio* effective-core potentials (ECP) of Kahn *et al.*[1] and others, and the *ab initio* model potentials (MP) of Huzinaga *et al.*[2] ECP's have been incorporated into QMC recently by Hurley and Christiansen[3] as well as the present authors[4]; however, these studies involve systems of only one- and two-valence electron systems. Such systems are a special case in QMC since they have no nodes and can yield the exact ground-state energy for a given Hamiltonian.

Extension of the ECP-QMC method to systems beyond two electrons should be straightforward, but in fact the nodes can introduce large negative singularities in the local energy that can bias the QMC random walk significantly. Such singularities have the effect of collapsing the QMC distribution into the core. In severe cases the distribution reduces to a single point when a walker becomes trapped in a region of large negative energy and branches until it constitutes the entire ensemble. Procedures investigated here to alleviate this difficulty include use of MP's, improvement of the trial function Ψ_T to smooth out the local potential surface, use of a different local pseudopotential, and introduction of a "frozen core" approximation to prevent unregulated branching. The latter involves a modification of the short-time Green's function, which restricts the QMC distribution in the core to be Ψ_T^2 and smoothly connects to the usual fixed-node distribution in the valence region.

*This work was supported by the Director, Office of Energy Research, Office of Basic Energy Sciences, Chemical Sciences Division of the U.S. Department of Energy under Contract No. DE-AC03-76SF00098.

†Also at Department of Chemistry, University of California, Berkeley, CA 94720.

1. L.R. Kahn, P. Baybutt, and D.G. Truhlar, J. Chem. Phys. **65**, 3826 (1976).

2. S. Huzinaga, L. Seijo, Z. Barandiaran, and M. Klobukowski, J. Chem. Phys. **86**, 2132 (1987).

3. M.M. Hurley and P.A. Christiansen, J. Chem. Phys. **86**, 1069 (1987).

4. B.L. Hammond, P.J. Reynolds, and W.A. Lester, Jr., J. Chem. Phys. **87**, 1130 (1987).

2. One-Electron Property from MCHF Wavefunction: the Dipole Moment of Ozone (Publication 1)

M. Dupuis† and W.A. Lester, Jr.

A systematic study of electron correlation contributions to the dipole moment of ozone is presented. Generalized valence bond (GVB) and MCHF

wavefunctions have been designed and calculated that point to the key role played by a charge-transfer configuration (CTC) in providing an accurate description of the charge separation in ozone. Although this CTC is a primary determiner of the dipole moment, its contribution to the structure determination is minor. A similar analysis should also apply to other molecules.

†Present address: IBM Corp., Kingston, NY 12401.

3. Enforcing Fixed-Node Boundary Conditions in Diffusion Quantum Monte Carlo: Rejection versus Deletion of Random Walks (Publication 8)

P.J. Reynolds, D.M. Ceperley,† R.N. Barnett,‡ and W.A. Lester, Jr.‡

This study addresses a new method of enforcing fixed-node boundary conditions in diffusion QMC. We first note that these boundary conditions do not have to be enforced to maintain the required antisymmetry of fermion systems. Unfortunately, the alternative, sometimes known as "released-node" QMC, is numerically unstable and results in a "transient estimator." Released-node QMC has been quite successful for H_3 but has been generally difficult to converge for larger systems. For most molecular species there has been more success with the fixed-node approach.

In fixed-node QMC, the boundary conditions have been traditionally enforced through the deletion ("killing") of any walker that attempts to cross a node. We have shown that deletion leads to a time-step bias and results in a "growth estimator" of the energy whose mean is different from the local-energy estimator. The usual procedure of extrapolation to zero time step, which is necessary in the diffusion QMC approach due to the short-time approximation to the Green's function, eliminates this bias. Thus the deletion of random walkers on node crossing simply modifies the short-time bias in the diffusion approach. We have shown that an alternative way of enforcing the fixed-node boundary condition by rejecting moves that attempt to cross a node does not introduce this additional bias and numerically leads to a more readily extrapolated energy estimator. This is most readily found when the trial wave function is exact. In this case the local energy estimator of the energy is also exact and has zero variance; however, the growth estimator for the energy has a nonvanishing time-step bias for the case of walker deletion, and possibly more significantly, has finite variance. Using rejection rather than deletion results in an unbiased energy for all time-step sizes and zero variance.

†Present address: Department of Physics, University of Illinois, Urbana.

‡Also at Department of Chemistry, University of California, Berkeley, CA 94720.

4. Direct Calculation of the Correlation Energy with Diffusion QMC (Publication 10)

P.J. Reynolds, R.N. Barnett,† and W.A. Lester, Jr.†

A method has been developed for diffusion QMC in which a single random walk is used to compute both the variational energy associated with the trial wave function and the fixed-node QMC energy. Because the two energies are correlated through their common random walk, the statistical uncertainty of their difference can be considerably smaller than the corresponding uncertainty of the difference of the two separately computed energies. Thus QMC can be used to obtain correlation energies directly and with lower variance than QMC total energies. Furthermore, knowledge of the variational energy, e.g., from self-consistent field methods, allows one also to obtain a low-variance QMC estimator of the total energy. However, in order to maintain a single random walk for both quantities, it has been necessary to introduce a weighting scheme in which the weights become unstable with increased length of the random walk. This causes the variance to rise as the walk progresses. The method is thus in the class of "transient estimator" approaches. To be useful it is necessary that the fixed-node walk reaches equilibrium sufficiently quickly that the weights remain small. We find that for molecular systems such as H_2O, the weights remain sufficiently small until equilibrium is attained. An overall gain of a factor of 2–4 in speed of computation has been obtained.

†Also at Department of Chemistry, University of California, Berkeley, CA 94720.

5. The Role of Cusp Conditions in Atomic and Molecular Quantum Simulations (Publication 9)

P.J. Reynolds, R.N. Barnett,[†] and W.A. Lester, Jr.[†]

In diffusion QMC one uses an approximate "short-time" Green's function to propagate random walks. These walks stochastically solve the Schrödinger equation. However, a time-step bias arises in the computed quantities. Generally this bias may be removed by extrapolation to zero time step $\tau = 0$. It is desirable, however, to minimize the magnitude of the bias for a fixed value of τ. This would enable one to use larger τ's, and also possibly to have a more reliable extrapolation. In this way one can expect to reduce the computational time. We note that a more accurate description of the QMC trial wave function reduces time-step bias. This results from the detailed-balance step in the algorithm, which guarantees that the exact wave function will give zero time-step bias for all values of τ. A side benefit of a more accurate description of the wave function is lower variance in the energy even when all other parameters are fixed. This zero-variance character of QMC is a property of the local energy estimator.

From the above discussion it is clear that one desires a better description of the wave function. In most molecular QMC work a self-consistent field (SCF) wave function is used as a starting point. To improve the wave function, first some correlation is built in through an electron-electron Jastrow function. This function, however, distorts the charge distribution and necessitates an electron-nuclear Jastrow function to restore the average size of the charge density. Usually the parameters in the electron-nuclear function are chosen to minimize the variational energy. In this work we have shown that by satisfying the electron-nuclear cusp condition rather than minimizing the variational energy, one obtains an improved wave function, i.e., one with smaller time-step biases. We demonstrate this by comparing conventional trial wave functions with trial functions that have been constructed to satisfy the electron-nuclear cusp condition on average [Slater-type orbital (STO) basis sets] and with trial functions that satisfy the electron-nuclear cusp condition exactly (Gaussian-type orbital basis sets). Thus correctly describing the wave function at even one point can be significant.

[†]Also at Department of Chemistry, University of California, Berkeley, CA 94720.

6. *Ab Initio* Studies of the Linear Complex $HC_3N...HC_3N$ (Publication 13)

C.A. Taft,[†] J.C. Azevedo,[†] J.G.R. Tostes,[‡] M.N. Ramos,[§] and W.A. Lester, Jr.[‖]

Ab initio calculations using a STO-3G basis set have been performed to obtain the optimized geometry of the complex $HC_3N...HC_3N$. A 6-31G basis set is then used at the STO-3G optimized geometry to estimate hydrogen bond energies, dipole moments, charge-transfer effects, and rotational and vibrational spectroscopic constants, and to analyze the perturbation of the N...H interaction on the intensity parameters of these atoms due to $C{\equiv}N$ and $C{-}H$ stretches using atomic polar tensors and the charge-charge flux-overlap model. These results support the conclusions of our previous work, using a smaller basis set and partially optimized geometry, that the deformation modes are practically unaltered due to the formation of H-bonds, and that the elements associated with the $C{\equiv}N$ and $H{-}C$ stretching modes increase substantially mainly due to a charge-flux term in which charge-transfer and polarization effects make important contributions.

It is interesting that for cyanopolyacetylenes, smaller basis sets and experimental monomer geometries yield similar trends as results obtained using larger basis sets and completely optimized geometries. The 4-31G results using the monomer experimental geometry show, however, better agreement with 6-31G results using a completely optimized geometry than with STO-3G values using the monomer experimental geometry.

[†]Permanent address: Centro Brasileiro de Pesquisas Fisicas, Rio de Janeiro, Brazil.

[‡]Permanent address: Departamento de Fisico-Quimica, Universidade Federal Fluminense, Niteroi, Brazil. Present address: Chemistry Department, UNICAMP, Campinas, Sao Paulo, Brazil.

[§]Also at Departamento de Quimica Fundamental, Universidade Federal de Permambuco, Recife, Brazil, and Departamento de Chimica Industriale, Politeonica de Milano, Milan, Italy.

[‖]Also at Department of Chemistry, University of California, Berkeley, CA 94720.

7. An *Ab Initio* Spectroscopic Study of the HCN...HCN and HCN...HNC Polar Complexes (Publication 12)

M.N. Ramos,[†] *C.A. Taft,*[‡] *J.G.R. Tostes,*[§] *and W.A. Lester, Jr.*[‖]

Ab initio 4-31G calculations with geometry optimization have been performed on the HCN...HCN and HCN...HNC complexes to determine both (i) the vibrational ground-state rotational spectroscopic constants and (ii) the changes in the infrared intensity parameters of HCN and HNC due to complex formation. The spectroscopic constants obtained for HCN...HCN are in good agreement with the experimental values from Buxton *et al.*[1]

The infrared intensity parameters analyzed in terms of atomic polar tensors (APT's) reveal that (i) the APT elements associated with the bending modes are practically insensitive to formation of the H-bond and (ii) the largest changes in the APT elements associated with the stretching modes are observed for the atoms participating in the H-bond resulting in a factor-of-two increase. According to the King and Mast[2] model, this increase is mainly due to the charge-flux term.

[†]Also at Departamento de Quimica Fundamental, Universidade Federal de Permambuco, Recife, Brazil, and Departamento de Chimica Industriale, Politeonica de Milano, Milan, Italy.

[‡]Permanent address: Centro Brasileiro de Pesquisas Fisicas, Rio de Janeiro, Brazil.

[§]Permanent address: Departamento de Fisico-Quimica, Universidade Federal Fluminense, Niteroi, Brazil. Present address: Chemistry Department, UNICAMP, Campinas, Brazil.

[‖]Also at Department of Chemistry, University of California, Berkeley, CA 94720.

1. Buxton *et al.*, Chem. Phys. **56**, 399 (1981).
2. W.T. King and G.B. Mast, J. Phys. Chem. **80**, 2521 (1976).

1987 PUBLICATIONS AND REPORTS

Refereed Journals

1. M. Dupuis and W.A. Lester, Jr., "One-Electron Property from MCHF Wavefunction: The Dipole Moment of Ozone," Theor. Chim. Acta. **71**, 255, (1987); LBL-21708.
2. C.E. Dateo, V.Z. Kresin, M. Dupuis, and W.A. Lester, Jr. "Photodissociation As a Quantum Transition: Photofragment Vibrational Distributions of $C_2N_2(\tilde{C}\,^1\Pi_u)$ Predissociation," J. Chem. Phys. **86**, 2639 (1987); LBL-22681.
3. P.J. Reynolds, R.K. Owen, and W.A. Lester, Jr., "Is There a Zeroth Order Time-Step Error in Diffusion Quantum Monte Carlo?" J. Chem. Phys. **87**, 1905 (1987); LBL-22681.
4. V.Z. Kresin and W.A. Lester, Jr., "On the Mechanism of Singlet-Triplet Transitions," Chem. Phys. Lett. **138**, 59 (1987); LBL-22829.
5. B.L. Hammond, P.J. Reynolds, and W.A. Lester, Jr., "Valence Quantum Monte Carlo with *Ab Initio* Effective Core Potentials," J. Chem. Phys. **87**, 1130 (1987); LBL-22745.

LBL Reports

6. R.M. Grimes (Ph.D. Thesis), "Theoretical Study of Intermolecular Energy Transfer Involving Electronically Excited Molecules," LBL-22466.
7. C.E. Dateo (Ph.D. Thesis), "Theoretical Study of Indirect Photodissociation: Electronic Structure and Product Rovibrational Distributions of $C_2N_2(\tilde{C}\,^1\Pi_u)$," LBL-23944.
8. P.J. Reynolds, D.M. Ceperley, R.N. Barnett, and W.A. Lester, Jr., "Enforcing Fixed-Node Boundary Conditions in Diffusion Quantum Monte Carlo: Rejection versus Deletion of Random Walks," submitted to J. Chem. Phys.; LBL-24677.
9. P.J. Reynolds, R.N. Barnett, and W.A. Lester, Jr., "The Role of Cusp Conditions in Atomic and Molecular Quantum Simulations," submitted to Phys. Rev. A; LBL-24678.
10. P.J. Reynolds, R.N. Barnett, and W.A. Lester, Jr., "Direct Calculation of the Correlation Energy with Diffusion Quantum Monte Carlo," submitted to Chem. Phys. Lett.; LBL-24679.
11. B.L. Hammond, P.J. Reynolds, and W.A. Lester, Jr., "Valence Quantum Monte Carlo for Many Valence-Electron Systems," submitted to J. Chem. Phys.; LBL-24680.
12. M.N. Ramos, C.A. Taft, J.G.R. Tostes, and W.A. Lester, Jr., "An *Ab Initio* Spectroscopic Study of the HCH...HCN and HCN...HNC Linear Complexes," J. Mol. Struct. (in press); LBL-24681.
13. C.A. Taft, J.C. Azevedo, J.G.R. Tostes, M.N. Ramos, and W.A. Lester, Jr., "*Ab Initio* Studies of the Linear Complex $HC_3N \cdots HC_3N$," J. Mol. Struct. (in press); LBL-24682.
14. J.G.R. Tostes, C.A. Taft, M.N. Ramos, and W.A. Lester, Jr., "Role of Polarization Functions on the Bridge Hydrogen Atom in HCN...HCN," Int. J. Quant. Chem. (in press); LBL-24683.

Invited Talks

15. W.A. Lester, Jr., "Theoretical Studies of Molecular Interactions," Combustion Research Contractors Meeting, Mills College, Oakland, CA, June 3–5, 1987.

16. W.A. Lester, Jr., "Quantum Monte Carlo for Molecules," Los Alamos National Laboratory, Los Alamos, NM, June 25, 1987; Department of Chemistry, University of Georgia, Athens, Nov. 16, 1987; Department of Chemistry, Morehouse College, Atlanta, GA, Nov. 19, 1987; Dolphus E. Milligan Science Research Institute, Atlanta, GA, Nov. 20, 1987; Department of Physics, Georgia Institute of Technology, Atlanta, Nov. 23, 1987; Atlanta Athens Chemical Physics Discussion Group, Department of Chemistry, Emory University, Atlanta, GA, Dec. 7, 1987.

Spectroscopy and Structures of Reactive Intermediates*

Richard J. Saykally, Investigator

INTRODUCTION

The objective of this research is to develop new techniques for the detection of unstable forms of molecules, and to use these techniques to carry out detailed measurements of the structures, properties, and dynamics of these species with the goal of improving our large-scale understanding of chemical reactions and energy transfer.

Reactive molecules, including neutral-free radicals and molecular ions, play extremely important roles as reaction intermediates in combustion processes, reactive plasmas, in the terrestrial atmosphere, and in interstellar space. The transient nature of these reactive species has made their detection and characterization a very difficult task, and comparatively few of these important reactive molecules have been studied in detail.

"Van der Waals complexes"—molecules held together at low temperatures only by very weak dispersion or induction forces or by hydrogen bonds—constitute excellent prototypes of these same weak interactions that dominate the condensed phases. One of the chemical physicist's great dreams has been to bridge the gap from the gas phase, where detailed measurements of isolated species are possible, to the condensed phases, where this is clearly impossible, through the investigation of successively more complex van der Waals aggregates in the gas phase. This dream is still a long way from being realized, as these species, like the reaction intermediates, are extremely difficult to detect and characterize. Nevertheless, a new level of understanding of van der Waals forces is emerging from studies of the vibrational motions of the weak bonds.

The primary goal of this research is to carry out detailed investigations of those reaction intermediates that are critical species in the combustion of important fuels. Exactly the same experimental and theoretical techniques employed to study reaction intermediates can be applied to van der Waals molecules; hence, studies of these two crucially important classes of molecules will be undertaken as well, with the long-range objective of correlating the measured properties of these species as a means of understanding condensed phases in more detail.

*This work was supported by the Director, Office of Energy Research, Office of Basic Energy Sciences, Chemical Sciences Division of the U.S. Department of Energy under Contract No. DE-AC03-76SF00098.

1. An Extended Study of the Lowest Π Bending Vibration-Rotation Spectrum of Ar-HCl by Intracavity Far Infrared Laser/Microwave Double Resonance Spectroscopy (Publication 1)

R.L. Robinson,† D. Ray,† Dz.-H. Gwo, and R.J. Saykally

The lowest Π bending state in Ar-HCl has been more completely characterized through the use of far infrared laser/microwave double resonance spectroscopy. This extended analysis includes a partial reassignment of the far infrared spectra of Ar-$H^{35}Cl$ previously reported by Ray *et al.*, as well as an analysis of the Ar-$H^{37}Cl$ spectra. Improved molecular constants have been determined. The value of the rotational constant is now in good agreement with that calculated from the M5 double minimum potential surface. Along with the recently reported spectrum of the Σ bending vibration, this extended analysis provides strong evidence for the existence of two-minima character in the intermolecular potential surface of Ar-HCl.

†Present address: Joint Institute for Laboratory Astrophysics and Department of Chemistry, University of Colorado, Boulder, CO 80309.

2. The High-Resolution Far Infrared Spectrum of a van der Waals Stretching Vibration: The ν_3 Band of Ar-HCl (Publication 2)

R.L. Robinson,† Dz.-H. Gwo, and R.J. Saykally

The first high-resolution measurement of a van der Waals stretching vibration is reported. The ν_3 fundamental stretching vibration in Ar-HCl has been measured by intracavity far infrared laser/microwave double resonance spectroscopy of a supersonic free jet. Coupling between the stretching state and the nearby bending states gives the spectrum an intensity that is greater than predicted. The molecular constants for the stretching state are in close agreement with calculations for the M5 potential surface.

†Present address: Joint Institute for Laboratory Astrophysics and Department of Chemistry, University of Colorado, Boulder, CO 80309.

3. Tunable Far Infrared Laser Spectroscopy in a Planar Supersonic Jet: The Σ Bending Vibration of Ar-$H^{35}Cl$ (Publication 3)

K.L. Busarow, G.A. Blake,† K.B. Laughlin, R.C. Cohen, Y.T. Lee, and R.J. Saykally

The lowest Σ bending vibration (02^00) of Ar-$H^{35}Cl$ has been observed near 23.6 cm^{-1} from P(23) to R(17), in a continuous planar jet expansion using a tunable far infrared laser. A least-squares analysis has been performed to determine the centrifugal distortion constants for the ground and excited states, which will greatly facilitate the determination of an accurate intermolecular potential surface.

†Present address: Center for Cosmochemistry and Geochemistry, Division of Geology and Planetary Sciences, California Institute of Technology, Pasadena, CA 91125.

4. Work in Progress

We are now developing tunable far infrared laser techniques for studying reactive molecules generated by excimer laser photolysis and van der Waals complexes. Ultimately these will possess extremely high sensitivity and resolution such that subtle effects on hydrogen tunneling migration effects can be explored in fluxional radicals like vinylidene and vinyl radical.

1987 PUBLICATIONS AND REPORTS

Refereed Journals

1. R.L. Robinson, D. Ray, Dz.-H. Gwo, and R.J. Saykally, "An Extended Study of the Lowest Π Bending Vibration-Rotation Spectrum of Ar-HCl by Intracavity Far Infrared Laser/Microwave Double Resonance Spectroscopy," J. Chem. Phys. **87**, 5149 (1987); LBL-23559.
2. R.L. Robinson, Dz-H. Gwo, and R.J. Saykally, "The High Resolution Far Infrared Spectrum of a van der Waals Stretching Vibration: The ν_3 Band of Ar-HCl," J. Chem. Phys. **87**, 5156 (1987); LBL-23560.
3. K.L. Busarow, G.A. Blake, K.B. Laughlin, R.C. Cohen, Y.T. Lee, and R.J. Saykally, "Tunable Far Infrared Laser Spectroscopy in a Planar Supersonic Jet: The Σ Bending Vibration of Ar-$H^{35}Cl$," Chem. Phys. Lett. **141**, 289 (1987); LBL-23868.

LBL Reports

4. R.L. Robinson, Dz.-H. Gwo, and R.J. Saykally, "Far Infrared Laser Stark Spectroscopy of the Σ Bending Vibration of ArHCl: Strong Evidence for a Double Minimum Potential Surface," accepted by Mol. Phys.; LBL-24806.
5. K.L. Busarow, G.A. Blake, K.B. Laughlin, R.C. Cohen, Y.T. Lee, and R.J. Saykally, "Tunable Far Infrared Laser Spectroscopy of van der Waals Bonds: The Σ Bend of ArHCl," LBL-24859.

Invited Talks

6. R.J. Saykally, "Velocity Modulation Infrared Laser Spectroscopy of Molecular Anions," Royal Society Meeting, London, England, Mar. 25, 1987; University of Southern California–Loker Hydrocarbon Research Institute, Los Angeles, Apr. 2, 1987.
7. R.J. Saykally, "Infrared Laser Spectroscopy of Negative Ions," American Chemical Society Annual Meeting, New Orleans, LA, Aug. 31–Sept. 4, 1987; 18th International Symposium on Free Radicals, Oxford, England, Sept. 10, 1987.
8. R.J. Saykally, "Anisotropic Intermolecular Potentials from Far Infrared Laser Spectroscopy of van der Waals Bonds," Tenth Colloquium on High Resolution Molecular Spectroscopy, Dijon, France, Sept. 16, 1987.
9. R.J. Saykally, "Infrared Laser Spectroscopy of Molecular Ions," Sixth Asilomar Conference on Mass Spectrometry, Asilomar, CA, Oct. 13, 1987; University of Arizona, Tucson, Oct. 29, 1987.
10. R.J. Saykally, "Far Infrared Laser Spectroscopy of Carbon Clusters," Carbon in the Galaxy: Studies from Earth and Space, NASA Ames Research Laboratory, Moffett Field, CA, Nov. 6, 1987.
11. R.J. Saykally, "Some New Directions in Infrared Laser Spectroscopy," Boston University, Boston, MA, Nov. 9, 1987; Yale University, New Haven, CT, Nov. 11, 1987; University of Pennsylvania, Philadelphia, Nov. 12, 1987.
12. R.J. Saykally, "Velocity Modulation Laser Spectroscopy of Cations and Anions," AT&T Bell Labs, Murray Hill, NJ, Nov. 13, 1987.
13. R.J. Saykally, "Color Center Laser Spectroscopy of Molecular Ions," Burleigh Instruments, Rochester, NY, Nov. 17, 1987.
14. R.J. Saykally, "Far Infrared Laser Spectroscopy of van der Waals Bonds: A New Probe of Intermolecular Forces," University of Rochester, Rochester, NY, Nov. 18, 1987; Pennsylvania State University, University Park, Nov. 19, 1987; Joint Colloquium, Sandia Combustion Facility and LBL Chemical Dynamics Group, Berkeley, CA, Feb. 5, 1988.

Theory of Atomic and Molecular Collision Processes*

William H. Miller, Investigator

INTRODUCTION

This research is primarily involved with the development and application of theoretical methods and models for describing atomic and molecular collision processes and chemical reaction dynamics. Specific topics of interest have included the theory of inelastic and reactive scattering, collision processes involving electronically excited atoms or molecules, collisional ionization phenomena, statistical theories of chemical reactions, scattering of atoms and molecules from surfaces, and the interactions of molecular systems with high-power laser radiation.

Most recently, research has focused on the development of theoretical methods for a first-principles treatment of dynamics in polyatomic molecular systems. The goal is to develop approaches that can utilize *ab initio* quantum chemical calculations of the potential energy surface (in the Born-Oppenheimer approximation) as direct input into the dynamical treatment, and thus, to as great an extent as possible, have a truly predictive theory.

The potential application of these methods is almost without limit. In this group hydrogen atom transfer processes have been studied in a variety of systems. Other research groups have used these approaches to describe a variety of reactions that are relevant to the primary steps in combustion.

1. Tunneling and State-Specificity in Unimolecular Reactions (Publication 1)†

W.H. Miller

The role of tunneling in unimolecular reactions is described. Very much related to this is the state-specific character of unimolecular reaction rates, which is also discussed. It is emphasized that statistical approximations, e.g., the well-known RRKM theory, are approximations to the average unimolecular rate constant for a molecule of energy E (and angular momentum J). Simple models for including the effects of tunneling in these statistical approximations are reviewed. State-specificity of unimolecular reaction rates is defined as significant variation in the rate constants for individual quantum states of the reactant molecule about the average rate at that energy (and angular momentum). Tunneling effects and state-specificity are illustrated by model calculations and by experimental results for the unimolecular decomposition of formaldehyde, $H_2CO \rightarrow H_2 + CO$, in its ground electronic state.

*This work was supported by the Director, Office of Energy Research, Office of Basic Energy Sciences, Chemical Sciences Division of the U.S. Department of Energy under Contract No. DE-AC03-76SF00098.

†Calculations were performed on the Berkeley Theoretical Chemistry computing facility, supported by the National Science Foundation Grant No. CHE84-16345.

2. Basis-Set Methods for Describing the Quantum Mechanics of a "System" Interacting with a Harmonic Bath (Publication 2)†

N. Makri and W.H. Miller

The case of a "system" (e.g., a one-dimensional reaction coordinate) coupled to a "bath" of many harmonic oscillators is treated by quantum mechanical basis-set methods. By choosing the basis set for the "bath" to incorporate the coupling explicitly, it is shown how the "bath" can then be eliminated to obtain an effective Hamiltonian matrix for only the "system." Numerical calculations are carried out that show that, even in the zeroth version of the approach, the effect on the "system" (e.g., the tunneling splitting in a double-well potential) of coupling to the "bath" is described well, even when the effect is extremely large.

This methodology is proving very effective in application of reaction-path models to dynamical treatments in polyatomic molecular systems.

†Calculations were performed on the Berkeley Theoretical Chemistry computing facility, supported by the National Science Foundation Grant No. CHE84-16345.

3. Monte Carlo Path Integration in Real Time via Complex Coordinates (Publication 4)†

J. Chang and W.H. Miller

A method is described for Monte Carlo path integration that is valid for real time propagation. More specifically, it is shown how matrix elements of the complex-time propagator

$e^{-\beta_c H}$, $\beta_c = \beta/2 + it/\hbar$, can be evaluated by straightforward Monte Carlo for values $t >> \beta\hbar/2$. The key feature is that one distorts the path of the integration variables so that the kinetic energy part of the integrand is real. This in turn means that the paths are complex-valued, but it is shown that, at least for barrier-type potentials, this causes no difficulties.

Path integral methods are the most powerful way to incorporate the effect of a "bath" on the dynamics of a "system," so that the extent to which they can be applied has enormous practical implications.

†Calculations were performed on the Berkeley Theoretical Chemistry computing facility, supported by the National Science Foundation Grant No. CHE84-16345.

4. Time-Dependent Self-Consistent-Field (TDSCF) Approximation for a Reaction Coordinate Coupled to a Harmonic Bath: Single and Multiple Configuration Treatments (Publication 11)†

N. Makri and W.H. Miller

This paper explores the usefulness of the time-dependent self-consistent-field (TDSCF) approximation for treating the dynamics of a reaction coordinate coupled to a bath of harmonic degrees of freedom. The reaction coordinate is a one-dimensional double-well potential, typical of a hydrogen atom isomerization process. The standard (i.e., one configuration) TDSCF approximation is found to provide a very poor description of the effect of coupling to the bath on the isomerization rate. A multiconfiguration TDSCF treatment is thus developed and found to provide a much improved description.

†Calculations were performed on the Berkeley Theoretical Chemistry computing facility, supported by the National Science Foundation Grant No. CHE84-16345.

5. An Analysis of the Infrared and Raman Spectra of the Formic Acid Dimer $(HCOOH)_2$ (Publication 10)†

Y-T. Chang, Y. Yamaguchi,‡ W.H. Miller, and H.F. Schaefer‡

Ab initio molecular quantum mechanical methods have been used to study the formic acid dimer and several isotopomers. Structures and harmonic vibrational frequencies have been predicted for the monomer, the equilibrium dimer, and the transition state for simultaneous hydrogen transfer. In an attempt to systematize results obtained at various levels of theory, three different basis sets were used: minimum, double zeta (DZ), and double zeta plus polarization (DZ+P). The predicted self-consistent-field (SCF) dissociation energies D_e are 15.1 (minimum basis), 19.3 (DZ), and 14.3 (DZ+P) kcal/mole. Further consideration of zero-point vibrational energies and finite temperature effects allows a comparison with several experimental values for ΔH_{300}. The infrared and Raman intensities (as well as the vibrational frequencies themselves) are compared with available experimental results. Where comparison is possible, the agreement is generally good. An exception occurs for ν_{18}, the O-D stretch of the $(HCOOD)_2$ molecule, where it is concluded that the experimental analysis may be incorrect.

†Calculations were performed on the Berkeley Theoretical Chemistry computing facility, supported by the National Science Foundation Grant No. CHE84-16345.

‡Permanent address: Center for Computational Quantum Chemistry, School of Chemical Sciences, University of Georgia, Athens, GA 30602.

6. Work in Progress

A new approach for describing reaction dynamics in polyatomic molecular systems is being devised, one that is based on a totally Cartesian representation of the Hamiltonian. This avoids some of the problems encountered by our earlier approaches (reaction path models) and is significantly easier to apply than the reaction surface model that we have recently developed.

A number of new ideas are also being pursued for evaluating Feynman path integral expressions for reactive flux correlation functions. These will be used in conjunction with the above Cartesian reaction Hamiltonian to treat various dynamics processes in complex systems.

1987 PUBLICATIONS AND REPORTS

Refereed Journals

1. W.H. Miller, "Tunneling and State-Specificity in Unimolecular Reactions," Chem. Rev. **87**, 19 (1987); LBL-21203.

2. N. Makri and W.H. Miller, "Basis Set Methods for Describing the Quantum Mechanics of a 'System' Interacting with a Harmonic 'Bath'," J. Chem. Phys. **86**, 1451 (1987); LBL-22366.
3. W.H. Miller and B.M.D.D. Jansen op de Haar, "A New Basis Set Method for Quantum Scattering Calculations," J. Chem. Phys. **86**, 6213 (1987).
4. J. Chang and W.H. Miller, "Monte Carlo Path Integration in Real Time via Complex Coordinates," J. Chem. Phys. **87**, 1648 (1987); LBL-23223.
5. N. Makri and W.H. Miller, "Monte Carlo Integration with Oscillatory Integrands, with Implications for Feynman Path Integration in Real Time," Chem. Phys. Lett. **139**, 10 (1987).
6. J.Z.H. Zhang and W.H. Miller, "New Method for Quantum Reactive Scattering, with Applications to the 3-D $H+H_2$ Reaction," Chem. Phys. Lett. **140**, 329 (1987).

Other Publications

7. W.H. Miller, "Reaction Paths and Surfaces for Hydrogen Atom Transfer Reactions in Polyatomic Molecules," in *Tunneling*, J. Jortner and B. Pullman, Eds., D. Reidel, Boston, 1986, p. 91; LBL-21662.
8. W.H. Miller, "A Schrödinger Equation Analog to the Generalized Langevin Equation of Classical Mechanics, with Application to Reactive Flux Correlation Functions," in *Stochasticity and Intramolecular Redistribution of Energy*, R. Lefebvre and S. Mukamel, Eds., D. Reidel, Boston, 1987, p. 263.

LBL Reports

9. W.H. Miller, "Reactive Flux Correlation Functions and Monte Carlo Evaluation of Real Time Path Integrals," in AIP Conf. Proc. (in press); LBL-23585.
10. Y.-T. Chang, Y. Yamaguchi, W.H. Miller, and H.F. Schaefer, "An Analysis of the Infrared and Raman Spectra of the Formic Acid Dimer $(HCOOH)_2$," J. Am. Chem. Soc. (in press); LBL-23576.
11. N. Makri and W.H. Miller, "Time-Dependent Self Consistent Field (TDSCF) Approximation for a Reaction Coordinate Coupled to a Harmonic Bath—Single and Multi-Configuration Treatments," J. Chem. Phys. (in press); LBL-23646.

Invited Talks

12. W.H. Miller, "Recent Developments in Quantum Mechanical Reactive Scattering," 14th Symposium on Quantum Chemistry of the Academy of Sciences of the German Democratic Republic, Kühlungsborn, German Democratic Republic, Mar. 16–20, 1987.
13. W.H. Miller, W. Albert Noyes Memorial Lectures, Department of Chemistry, University of Rochester, Mar. 23–27, 1987.
14. W.H. Miller, Symposium on Few-Body Systems and Multiparticle Dynamics, American Physical Society, Crystal City, VA, Apr. 20–24, 1987.
15. W.H. Miller, Distinguished Summer Lecturer, Department of Chemistry, Northwestern University, Evanston, IL, June 24–26, 1987.
16. W.H. Miller, "New Techniques in Time Dependent Dynamics," American Conference on Theoretical Chemistry, Gull Lake, MN, July 26–31, 1987.
17. W.H. Miller, "Hydrogen Atom Transfer in Polyatomic Molecules—a New Approach," 10th International Conference on Molecular Energy Transfer, Emmetten, Switzerland, Aug. 23–28, 1987.
18. W.H. Miller, "The Reactive Flux Correlation Function for Collinear Reactions: $H + H_2$, $C\ell + HC\ell$, and $F + H_2$," Faraday Discussion on Dynamics of Elementary Gas Phase Reactions, Birmingham, England, Sept. 14–16, 1987.
19. W.H. Miller, "Lectures on Reactive Scattering," NATO Advanced Study Institute on Collision Theory for Atoms and Molecules, Cortona, Italy, Sept. 14–26, 1987.
20. W.H. Miller, Arthur D. Little Lectures, Massachusetts Institute of Technology, Cambridge, Nov. 9–13, 1987.
21. W.H. Miller, "A New (Cartesian) Reaction Path Model for Dynamics in Polyatomic Systems," Faraday Discussion on Molecular Vibrations, Reading, England, Dec. 15–16, 1987.

Photoelectron Spectroscopy*

David A. Shirley, Investigator

INTRODUCTION

This program addresses both experimental and theoretical aspects of electron spectroscopy for the investigation of electronic structure of matter in the gaseous and condensed phases. Research is conducted using both laboratory sources at LBL and synchrotron radiation in the 5–5000 eV energy range available at the Stanford Synchrotron Radiation Laboratory, where there is participation in developing the spectroscopy of this newly accessible range of the electromagnetic spectrum. Time-of-flight measurements with synchrotron radiation are used to measure angular distributions of photoelectrons and resonant photoemission phenomena in the gas phase. Ultrahigh-resolution photoelectron spectroscopy based on molecular beams is yielding new information about small molecules and about the transition from single metal atoms to behavior characteristic of a three-dimensional solid. Employing angle-resolved, variable-energy photoemission and electron-energy-loss spectroscopy, this program examines the electronic structure of solids. The program also studies the geometric and electronic structure of surface-adsorbate systems using photoelectron diffraction, angle-resolved photoemission extended fine structure (ARPEFS), and surface extended x-ray absorption fine structure (SEXAFS).

1. Complete Photoemission Study of the He $1s^2 \rightarrow 3s3p$ Autoionizing Resonance (Publication 14)

D.W. Lindle,† T.A. Ferrett,† P.A. Heimann,‡ and D.A. Shirley

The total absorption cross section of He (as shown in Figure 1-1) and the He+(1s) partial cross section have been measured using photoelectron spectroscopy and synchrotron radiation in the photon-energy region of the $1s^2 \rightarrow 3s3p$ resonance.

*This work was supported by the Director, Office of Energy Research, Office of Basic Energy Sciences, Chemical Sciences Division of the U.S. Department of Energy under Contract No. DE-AC03-76SF00098. It was performed at the Stanford Synchrotron Radiation Laboratory, which is supported by the Department of Energy's Office of Basic Energy Sciences.

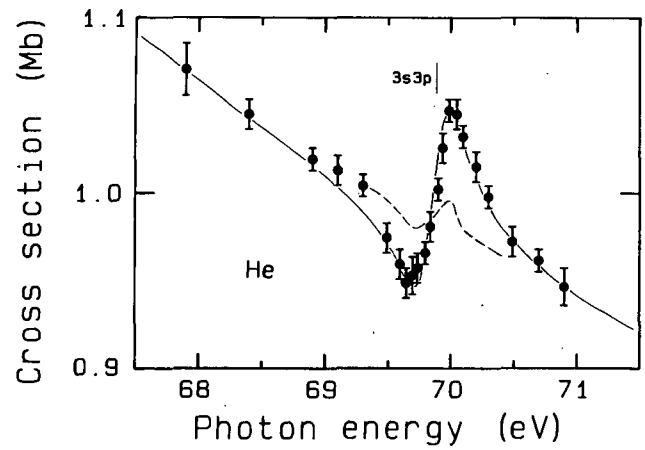

Figure 1-1. Total cross section of He in the vicinity of the $1s^2 \rightarrow 3s3p$ resonance scaled to Marr and West[1] at 68.9 eV. The solid curve is a fit to the data using the Fano formula convoluted with a Gaussian function of 0.19 eV (0.48 Å) full width half maximum to account for monochromator broadening. The dashed curve is an absorption measurement from Ref. 2. (XBL 872-556)

The effects of autoionization are relatively small, causing deviations of 5–10% from the nonresonant cross sections. These new measurements, along with a previous study of the 3s3p resonance behavior of the He+(n = 2) satellite cross section, branching ratio, and angular-distribution parameter, allow the complete determination of all the parameters governing the $1s^2 \rightarrow 3s3p$ resonance. From these experimentally determined parameters, we have derived all of the relevant oscillator strengths and individual dipole and Coulomb matrix elements that describe He photoionization in the vicinity of the 3s3p doubly excited state.

†Present address: National Bureau of Standards, Gaithersburg, MD 20899.

‡Present address: Technische Universität München, Federal Republic of Germany.

1. G.V. Marr and J.B. West, At. Data Nucl. Data Tables **18**, 497 (1976).
2. P. Dhez and D.L. Ederer, J. Phys. B **6**, L59 (1973).

2. Lithium 1s Main-Line and Satellite Photoemission: Resonant and Nonresonant Behavior (Publication 15)

*T.A. Ferrett,† D.W. Lindle,† P.A. Heimann,‡ W.D. Brewer,§ U. Becker,‖ H.G. Kerkhoff,** and D.A. Shirley*

We present experimental results on core-level photoemission of atomic lithium (see spectrum in Figure 2-1), leading to both main-line and satellite

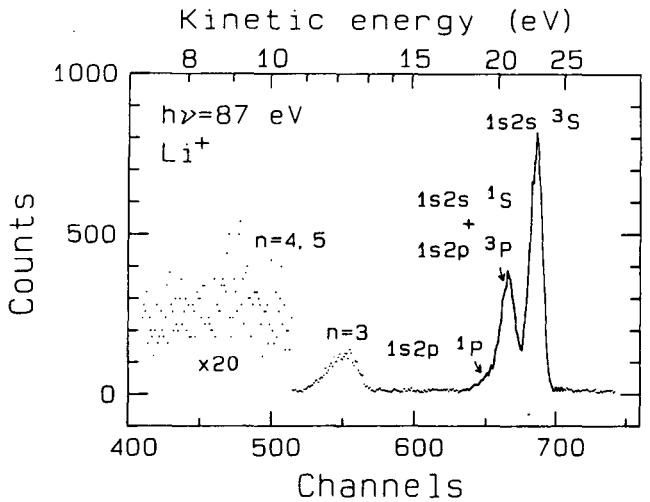

Figure 2-1. Time-of-flight photoelectron spectrum taken at $h\nu = 87$ eV and $\theta = 54.7°$. The 1s2s main-line photoemission is split into ^3S and ^1S components, with the 1s2p $^{1,3}P$ satellites unresolved at slightly higher binding energy. The relatively intense n = 3 satellites (1s3l) have a binding energy of about 75 eV.[1] The very weak higher n satellites are shown also on an expanded scale (x 20). (XBL 8611-4238)

states of the Li^+ ion (1snl where n = 2–5). We have compared the measured 1s2s $^{1,3}S$ main-line cross sections with recent relaxed Hartree-Fock calculations and with previous experimental results, finding reasonable agreement in both cases. For the n = 3 satellite, our results disagree with earlier photoemission work that was complicated by additional peaks at 52 eV kinetic energy. We discuss possible explanations for these extra peaks. For the doubly excited state 1s(3s3p) at 71.14 eV, we present total cross-section results in good agreement with previous photoabsorption measurements. The qualitative differences among our partial cross-section profiles are discussed, and the phase for the total cross section is rationalized by estimating the signs of pertinent matrix elements.

---

†Present address: National Bureau of Standards, Gaithersburg, MD 20899.

‡Present address: Technische Universität München, Federal Republic of Germany.

§Permanent address: Institut für Atom- und Festkorperphysik, Freie Universität Berlin, Federal Republic of Germany.

‖Present address: Physikalisches Institut, Universität Würzburg, Federal Republic of Germany.

**Permanent address: Institut für Strahlungs- und Kernphysik, Technische Universität Berlin, Federal Republic of Germany.

1. C. Moore, Atomic Energy Levels, NSRDS-NBS 35 (U.S. GPO, Washington, D.C., 1971), Vol. 1.

3. Observation of Many New Argon Valence Satellites Near Threshold (Publication 18)

U. Becker,† B. Langer,‡ H.G. Kerkhoff,‡ M. Kupsch,‡ D. Szostak,‡ R. Wehlitz,‡ P.A. Heimann,§ S.H. Liu, D.W. Lindle,‖ T.A. Ferrett,‖ and D.A. Shirley

High-resolution photoelectron spectra and zero-volt electron scans were measured following synchrotron radiation excitation of argon, to elucidate the photon energy range between threshold and the Cooper minimum region of the Ar 3s photoline. A number of the "correlation satellite" lines show a dramatic increase of fractional intensity toward threshold, yielding a total of about 40 observed photolines at threshold, of which more than half were not previously observed in photoemission (see Figure 3-1). This effect is interpreted as arising from inelastic scattering of the outgoing photoelectron by

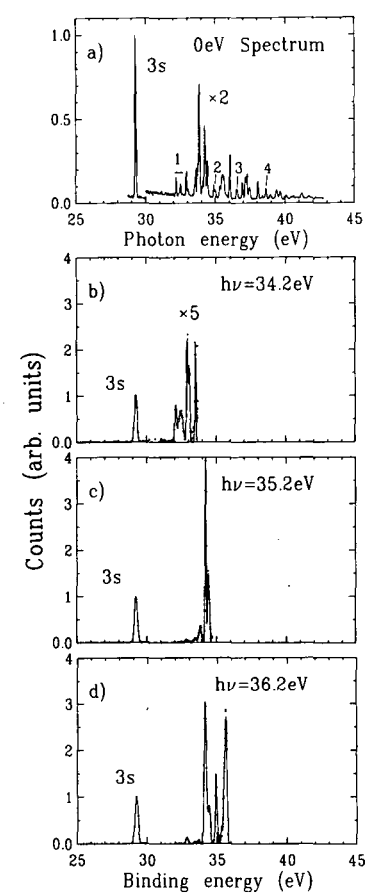

Figure 3-1. Photoelectron spectra (b–d) taken in the near-threshold region of the satellites with lower binding energy together with a zero-volt electron scan (a) between 29 and 43 eV. (XBL 877-3286)

the residual ion, yielding high-angular-momentum ionic states otherwise inaccessible by photoemission.

†Present address: Physikalisches Institut, Universität Würzburg, Federal Republic of Germany.

‡Permanent address: Institut für Strahlungs- und Kernphysik, Technische Universität Berlin, Federal Republic of Germany.

§Present address: Physik-Department E20, Technische Universität München, Federal Republic of Germany.

‖Present address: National Bureau of Standards, Gaithersburg, MD 20899.

4. Photoemission Study of Kr 3d → Np Autoionization Resonances (Publication 9)

D.W. Lindle,† P.A. Heimann,‡ T.A. Ferrett,† M.N. Piancastelli,§ and D.A. Shirley

Resonant photoelectron spectra of Kr have been taken in the photon-energy ranges of the $3d_{5/2} \rightarrow 5p,6p$ and $3d_{3/2} \rightarrow 5p$ excitations. The spectra shown in Figure 4-1, which closely resemble normal Kr^+ $3d^{-1}$ Auger spectra, illustrate the importance of "spectator" Auger-like decay for inner-shell resonances, in which the initially excited electron does not participate in the core-hole deexcitation process, except to respond to the change in the atomic potential. Possible assignments for some of the spectator decay channels are made based on photoemission intensity measurements at the different 3d resonances. These assignments suggest that shake-up (e.g., 5p → 6p) of the "spectator" electron during the decay process is not quite as important as previously suspected. The resonance profiles of some of the more intense satellites have been determined over the 3d → np resonances. Very small resonance effects were also observed in the partial cross section for 4p subshell ionization, which produced asymmetric Fano-type profiles. The 4p angular distribution, in contrast, exhibits a pronounced effect in the resonance energy range. The 4p results demonstrate that nonspectator autoionization also is present.

†Present address: National Bureau of Standards, Gaithersburg, MD 20899.

‡Present address: Technische Universität München, Federal Republic of Germany.

§Permanent address: Department of Chemistry, University of Rome "La Sapienza," 00100 Rome, Italy.

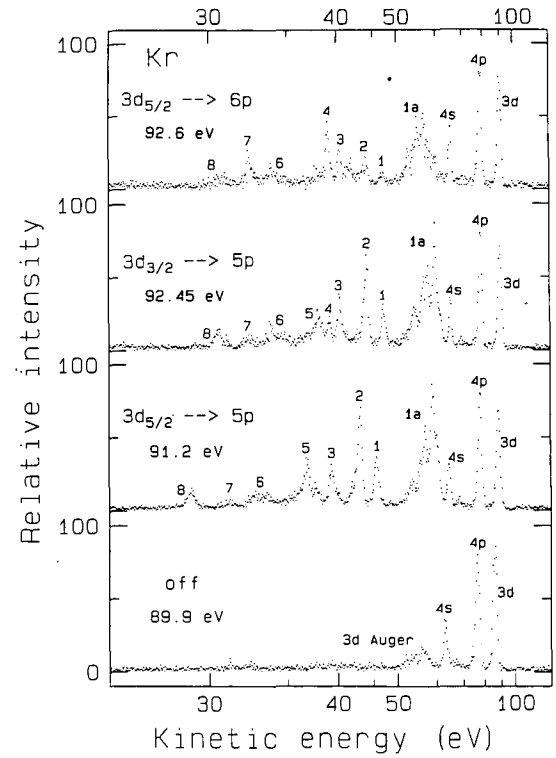

Figure 4-1. Resonant time-of-flight photoelectron spectra of Kr at 89.9 eV, 91.2 eV, 92.45 eV, and 92.6 eV photon energy, which correspond to off-resonance excitation, and excitation of the $3d_{5/2} \rightarrow 5p$, $3d_{3/2} \rightarrow 5p$, and $3d_{5/2} \rightarrow 6p$ resonances, respectively. The spectra are not corrected for analyzer transmission, which varies monotonically from 0.5 to 1 between 30 and 70 eV kinetic energy. The spectra have been scaled so that relative peak intensities in different spectra can be compared. The numbered peaks in the resonant spectra correspond to Kr^+ satellite configurations. The 3d peak is produced by second-order radiation, and the 3d Auger peak in the 89.9 eV spectrum is the $M_{4,5}N_{2,3}N_{2,3}$ Auger from the decay of these "second-order" 3d-hole states. The 3d Auger peak also has a small contribution from valence satellites. (XBL 8612-4889)

5. Photoemission From Xe in the Vicinity of the 4d Cooper Minimum (Publication 24)

D.W. Lindle,† T.A. Ferrett,† P.A. Heimann,‡ and D.A. Shirley

Partial photoionization cross sections and angular-distribution asymmetry parameters have been determined for the Xe 4d (as shown in Figure 5-1) and "4p" subshells in the photon-energy region of the 4d Cooper minimum (160 eV to 270 eV, to

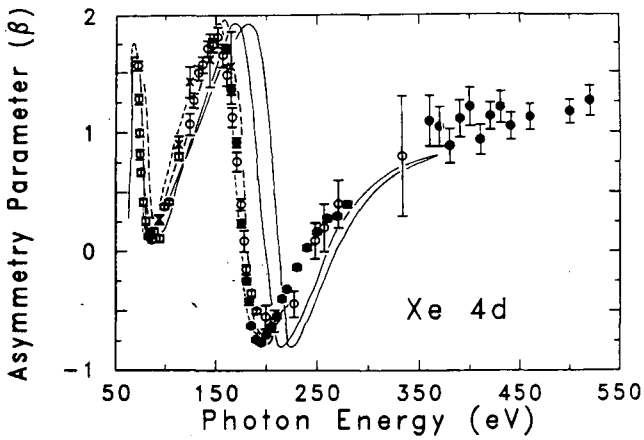

Figure 5-1. Asymmetry parameter of the Xe 4d subshell. The experimental measurements are from the present work (closed circles), Southworth *et al.*[1] (open circles), and Torop *et al.*[2] (X). The theortical curves are from Ong and Manson[3] (DF), Huang *et al.*[4] (RRPA), and Kennedy and Manson[5] (HF-V, HF-L). (XBL 8710-4407)

520 eV for the 4d asymmetry parameter). The Cooper minimum is observed as a distinct cross-section minimum in the 4d photoionization channel. The 4d angular-distribution results are in excellent agreement with Dirac-Fock and relativistic random-phase approximation calculations and with previous measurements. Effects of interchannel coupling are evident in the "4p" results. Both the partial cross section and the angular distribution for the "4p" photoelectron peak track the 4d cross section and angular distribution as functions of photon energy. A similar result is observed for the summed intensity and the angular distribution of the $4d^{-1}5p^{-1}np$ satellites of the 4d main line, which is probably due to the effects of electron correlation between the 4d and the satellite photoionization channels.

†Present address: National Bureau of Standards, Gaithersburg, MD 20899.

‡Present address: Physik-Department E20, Technische Universität München, Federal Republic of Germany.

1. S.H. Southworth, P.H. Kobrin, C.M. Truesdale, D.W. Lindle, S. Owaki, and D.A. Shirley, Phys. Rev. A **24**, 2257 (1981).
2. L. Torop, J. Morton, and J.B. West, J. Phys. B **9**, 2035 (1976).
3. W. Ong and S.T. Manson, unpublished.
4. W.R. Johnson and K.-N. Huang, unpublished.
5. D.J. Kennedy and S.T. Manson, Phys. Rev. A **5**, 227 (1972).

6. Photoelectron Asymmetry Parameter for the S 2p Level of SO_2 (Publication 11)

T.A. Ferrett,† P.A. Heimann,‡ H.G. Kerkhoff,§ U. Becker,‖ D.W. Lindle,† and D.A. Shirley

We present a measurement of the asymmetry parameter (β) for S 2p core-level photoionization of SO_2 in the vicinity of several continuum resonances (see Figure 6-1). Results are contrasted with β(2p) for the central atoms of the molecules SF_6 and SiF_4. Atomic calculations for β(S 2p) appear to reproduce qualitatively the molecular curve for SO_2 aside from a shift to lower β-values for the molecular case.

†Present address: National Bureau of Standards, Gaithersburg, MD 20899.

‡Present address: Physik-Department E20, Technische Universität München, Federal Republic of Germany.

§Permanent address: Institut für Strahlungs- und Kernphysik, Technische Universität Berlin, Federal Republic of Germany.

‖Present address: Physikalisches Institut, Universität Würzburg, Federal Republic of Germany.

1. T.A. Ferrett, D.W. Lindle, P.A. Heimann, M.N. Piancastelli, P.H. Kobrin, H.G. Kerkhoff, U. Becker, W.D. Brewer, and D.A. Shirley, unpublished results.
2. S.T. Manson, private communication.

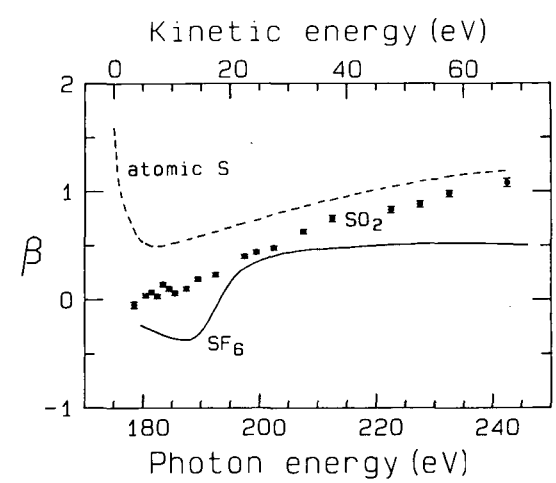

Figure 6-1. The S 2p symmetry parameter (β) for SO_2 as a function of photon energy (bottom scale) and kinetic energy (top scale). The solid curve represents experimental data for β(S 2p) of SF_6,[1] plotted as a function of kinetic energy. Hartree-Slater theory curve[2] for the atomic β(2p) of sulfur is also shown (dashed), as a function of kinetic energy. (XBL 8611-4572)

7. High-Resolution UV Photoelectron Spectroscopy of CO_2^+, COS^+, and CS_2^+ Using Supersonic Molecular Beams (Publication 20)

L.S. Wang, J.E. Reutt,[†] Y.T. Lee, and D.A. Shirley

Very high resolution HeI (584 Å) photoelectron spectra of CO_2^+, COS^+, and CS_2^+ are presented (see Figure 7-1). The spectra were obtained by using supersonic molecular beams to eliminate the rotational and Doppler broadenings. The spin-orbit split components in the Π bands are all explicitly resolved. The removal of the inelastic scattering peaks, due to the use of molecular beams, allowed new features to be observed in the $\tilde{B}$ and $\tilde{C}$ bands of CS_2^+, and new spectroscopic constants were derived.

[†]Present address: AT&T Bell Laboratories, Murray Hill, NJ 07974.

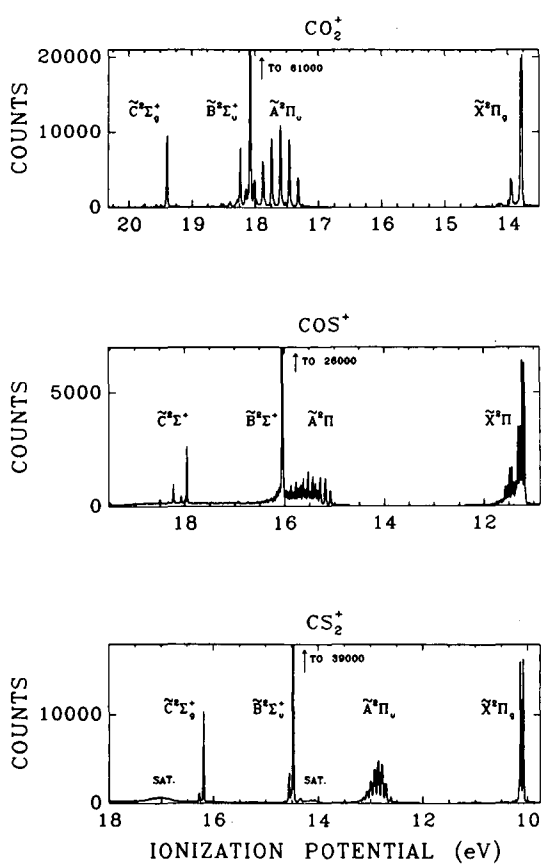

Figure 7-1. HeI photoelectron spectra of CO_2^+, COS^+, and CS_2^+ using supersonic molecular beams. The spectra are plotted to the full scale of the $\tilde{X}$ bands. The full scale of the most prominent peak is indicated in each spectrum. (XBL 878-3608)

8. Si 2p and 2s Resonant Excitation and Photoionization in SiF (Publication 21)

T.A. Ferrett,[†] M.N. Piancastelli,[‡] D.W. Lindle,[†] P.A. Heimann,[§] and D.A. Shirley

We have obtained partial cross-section results for Si 2p and valence photoionization of SiF_4 for photon energies in the vicinity of the Si 2p and 2s thresholds. The continuum shape resonances decay only to the Si 2p main line (see Figure 8-1), in accord with one-electron theory predictions. The Si $L_{2,3}VV$ Auger spectrum was also measured and found to agree with earlier work. We propose that variations in hole-interaction energies are important in assigning the Auger final states. For the Si 2p discrete excitations, spectra obtained on the $\sigma^*(a_1)$ resonances compare well with previous results and the above-threshold Si $L_{2,3}VV$ Auger spectrum. Our results help to quantify the relative enhancement of satellites and main lines, emphasizing the dominance of spectator decay. Spectra obtained at several higher-

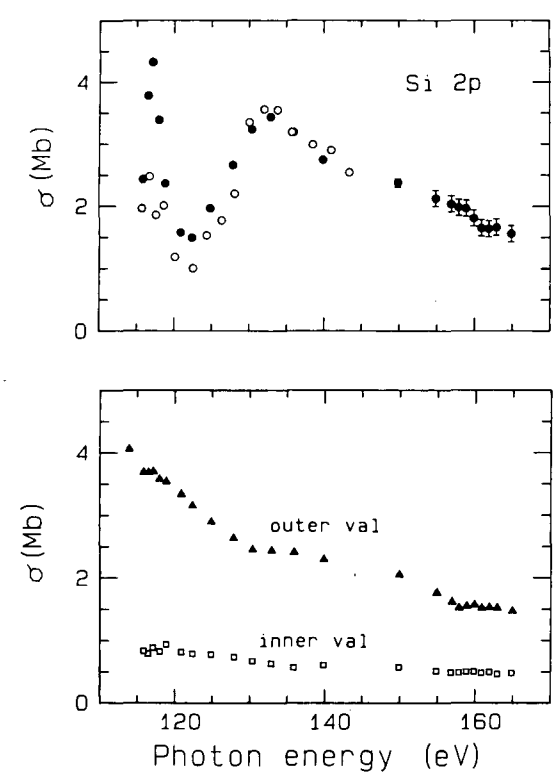

Figure 8-1. Top panel: partial cross sections for Si 2p photoionization (filled circles), compared with the results of Bancroft *et al.*[1] (open circles). Our relative cross sections have been scaled to the absolute values of Bancroft *et al.* at $h\nu$ = 136 eV. Bottom panel: summed outer-valence (solid triangles) and inner-valence (open squares) partial cross sections were calculated using the scaling of the Si 2p values. In both panels, statistical error bars are either shown or are smaller than the symbol size. (XBL 8611-4367)

energy Si 2p and Si 2s excitations also generally support spectator decay as an important mode of relaxation for these discrete states.

---

†Present address: National Bureau of Standards, Gaithersburg, MD 20899.

‡Permanent address: Department of Chemical Sciences and Technologies, II University of Rome, Italy.

§Present address: Physik-Department E20, Technische Universität München, Federal Republic of Germany.

1. G.M. Bancroft, S. Aksela, H. Aksela, K.H. Tan, B.W. Yates, L.L. Coatsworth, and J.S. Tse, J. Chem. Phys. **84**, 5 (1986).

9. C(2×2)S/Cr(001) Surface and Near-Surface Structure Determined Using ARPEFS (Publication 23)

L.J. Terminello, X.S. Zhang,† Z.Q. Huang, S. Kim, A.E. Schach von Wittenau, and D.A. Shirley

We report the surface and near-surface structure of c(2×2)S/Cr(001) determined from ARPEFS. The sulfur 1s photoemission partial cross section was measured in the [001] and [011] emission directions, which yielded fine-structure amplitudes up to 50–70%. Qualitative results are obtained from Fourier transforms of the ARPEFS revealing geometrical information beyond the 10-Å path-length difference from the photoemitter. Structural parameters are determined with greater precision by comparing the Fourier filtered data to multiple-scattering spherical-wave (MSSW) calculations giving statistically tractable results (as shown in Figure 9-1). The directional sensitivity of ARPEFS is demonstrated through the analysis of normal [001] and off-normal [011] emission-direction data. We show that sulfur adsorbs in the fourfold hollow site 1.17 Å above the first chromium layer and that the first-to-second-layer chromium distance contracts to 1.31 Å, 8% less than the 1.44-Å bulk value. Analysis of the near-surface contribution to ARPEFS showed that deeper layers essentially retain the bulk separation.

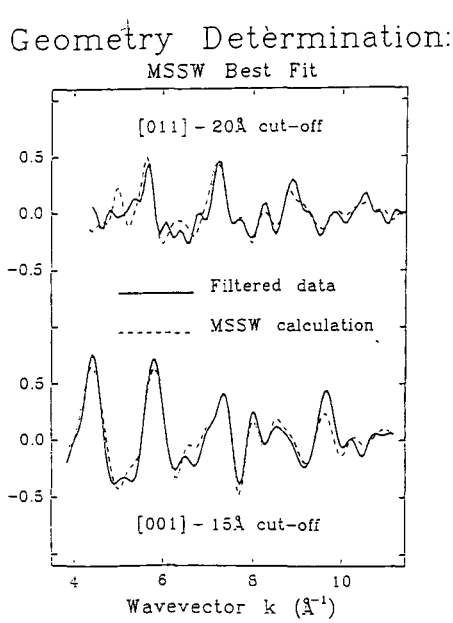

Figure 9-1. Best-fit MSSW calculations compared to experimental curves. Each experimental curve (solid line) has been Fourier filtered and is compared to the MSSW calculated data (dashed line) that gives an absolute r-factor minimum. (XBL 881-109)

---

†Permanent address: Department of Physics, Zhejiang University, Hangzhou, Zhejiang, People's Republic of China.

10. Chemisorption Structure of c(2×2)S/Fe(001) Determined by ARPEFS (Publication 22)

X.S. Zhang,† L.J. Terminello, S. Kim, Z.Q. Huang, A.E. Schach von Wittenau, and D.A. Shirley

ARPEFS spectroscopy is a very effective method to determine surface structures. In this work, ARPEFS has been studied to measure the chemisorption geometries of c(2×2)S/Fe(001) directions for the two adsorbate systems. We have analyzed the normal and off-normal data of both experiments in two ways. One is direct Fourier transform of the experimental data; another is using multiple-scattering spherical-wave calculations to compare with the experiments, which give the structure in detail. Multiple-scattering calculations were done with a cluster size that included path lengths > 15 Å. These long path-length differences were necessary to model the contributions to the ARPEFS signal from near-surface atoms.

The result indicates adsorption in a fourfold hollow site for both systems, and 1.10 ± 0.03 Å distance above the Fe surface indicates a S-Fe bond length of 2.30 ± 0.01 Å. The first-to-second-layer iron distance of 1.40 ± 0.02 Å indicates a slight contraction from the bulk value. This result is also in agreement with self-consistent field (SCF) Xα scattered-wave calculations.

---

†Permanent address: Department of Physics, Zhejiang University, Hangzhou, Zhejiang, People's Republic of China.

1987 PUBLICATIONS AND REPORTS

Refereed Journals

1. J.J. Barton, Z. Hussain, and D.A. Shirley, "Generalized Ramsauer-Townsend Resonance in Angle-Resolved Photoemission Extended Fine-Structure Oscillations," Phys. Rev. B **35**, 933 (1987); LBL-19325.
2. S.W. Robey, J.J. Barton, C.C. Bahr, G. Liu, and D.A. Shirley, "Angle-Resolved-Photoemission Extended-Fine-Structure Spectroscopy Investigation of c(2×2)S/Ni(011)," Phys. Rev. B **35**, 1108 (1987); LBL-18831.
3. D.W. Lindle, P.A. Heimann, T.A. Ferrett, and D.A. Shirley, "Helium Photoelectron Satellites: Low-Energy Behavior of the n = 3–5 Lines," Phys. Rev. A **35**, 1128 (1987); LBL-21651.
4. M.N. Piancastelli, D.W. Lindle, T.A. Ferrett, and D.A. Shirley, "The Relationship Between Shape Resonances and Bond Lengths," J. Chem. Phys. **86**, 2765 (1987); LBL-20027.
5. T.A. Ferrett, M.N. Piancastelli, D.W. Lindle, P.A. Heimann, L.J. Medhurst, S.H. Liu, and D.A. Shirley, "Resonance Effects on the Inner-Valence Levels of SF_6 in the Photon-Energy Range 52–72 eV," Chem. Phys. Lett. **134**, 146 (1987); LBL-18638.
6. C.C. Bahr, J.J. Barton, Z. Hussain, S.W. Robey, J.G. Tobin, and D.A. Shirley, "Geometry of (2×2)S/Cu(001) Determined with Use of Angle-Resolved-Photoemission Extended Fine Structure," Phys. Rev. B **35**, 3773 (1987); LBL-20567.
7. L.S. Wang, J.E. Pollard, Y.T. Lee, and D.A. Shirley, "Molecular Beam Photoelectron Spectroscopy: The $C_2D_4^+$ ($\tilde{X}\ ^2B_3$) Ground State," J. Chem. Phys **86**, 3216 (1987); LBL-21997.
8. S.W. Robey, C.C. Bahr, Z. Hussain, J.J. Barton, K.T. Leung, J. Lou, A.E. Schach von Wittenau, and D.A. Shirley, "Surface Structure of (2×2)S/Ge(111) Determined by Angle-Resolved Photoemission Fine Structure," Phys. Rev. B **35**, 5657 (1987); LBL-20572.
9. D.W. Lindle, P.A. Heimann, T.A. Ferrett, M.N. Piancastelli, and D.A. Shirley, "Photoemission Study of Kr 3d → np Autoionization Resonances," Phys. Rev. A **35**, 4605 (1987); LBL-22065.
10. J.G. Tobin, S.W. Robey, L.E. Klebanoff, and D.A. Shirley, "Development of a Three-Dimensional Valence-Band Structure in Ag Overlayers on Cu(001)," Phys. Rev. B **35**, 9056 (1987); LBL-15134.
11. T.A. Ferrett, P.A. Heimann, H.G. Kerkhoff, U. Becker, D.W. Lindle, and D.A. Shirley, "Photoelectron Asymmetry Parameter for the S 2p Level of SO_2," Chem. Phys. Lett. **138**, 607 (1987); LBL-22400.
12. M.N. Piancastelli, D.W. Lindle, T.A. Ferrett, and D.A. Shirley, 'Reply to the "Comment on 'The Relationship Between Shape Resonances and Bond Lengths' ",' J. Chem. Phys. **87**, 3255 (1987); LBL-23290.
13. L.S. Wang, Y.T. Lee, and D.A. Shirley, "Molecular Beam Photoelectron Spectroscopy of SO_2: Geometry, Spectroscopy, and Dynamics of SO_2^+," J. Chem. Phys. **87**, 2489 (1987); LBL-22413.
14. D.W. Lindle, T.A. Ferrett, P.A. Heimann, and D.A. Shirley, "Complete Photoemission Study of the He $1s^2 \rightarrow 3s3p$ Autoionizing Resonance," Phys. Rev. A **36**, 2112 (1987); LBL-21995.
15. T.A. Ferrett, D.W. Lindle, P.A. Heimann, W.D. Brewer, U. Becker, H.G. Kerkhoff, and D.A. Shirley, "Lithium 1s Main-Line and Satellite Photoemission: Resonant and Nonresonant Behavior," Phys. Rev. A **36**, 3172 (1987); LBL-22068.
16. P.A. Heimann, D.W. Lindle, T.A. Ferrett, S.H. Liu, L.J. Medhurst, M.N. Piancastelli, D.A. Shirley, U. Becker, H.G. Kerkhoff, B. Langer, D. Szostak, and R. Wehlitz, "Shake-Off on Inner-Shell Resonances of Ar, Kr, and Xe," J. Phys. B **20**, 5005 (1987); LBL-22412.

LBL Reports

17. D.A. Shirley, U. Becker, P.A. Heimann, and B. Langer, "Near Threshold Behavior of Photoelectron Satellite Intensities," submitted to J. Phys. (Paris); LBL-23989.
18. U. Becker, B. Langer, H.G. Kerkhoff, M. Kupsch, D. Szostak, R. Wehlitz, P.A. Heimann, S.H. Liu, D.W. Lindle, T.A. Ferrett, and D.A. Shirley, "Observation of Many New Argon Valence Satellites Near Threshold," submitted to Phys. Rev. Lett.; LBL-22464.
19. M.N. Piancastelli, T.A. Ferrett, D.W. Lindle, L.J. Medhurst, P.A. Heimann, S.H. Liu, and D.A. Shirley, "Resonant Processes Above the Carbon 1s Ionization Threshold in Benzene and Ethylene," LBL-22548.
20. L.S. Wang, J.E. Reutt, Y.T. Lee, and D.A. Shirley, "High Resolution UV Photoelectron Spectroscopy of CO_2^+, COS^+, and CS_2^+ using Supersonic Molecular Beams," J. Electron Spectrosc. Rel. Phenom. (in press); LBL-23936.
21. X.S. Zhang, L.J. Terminello, S. Kim, Z.Q. Huang, A.E. Schach von Wittenau, and D.A. Shirley, "Chemisorption Structure of c(2×2)S/Fe(001) Determined by ARPEFS," LBL-24248.
22. L.J. Terminello, X.S. Zhang, Z.Q. Huang, S. Kim, A.E. Schach von Wittenau, and D.A. Shirley, "C(2×2)S/Cr(001) Surface and Near-Surface Structure Determined Using Angle-Resolved Photoemission Extended Fine Structure," LBL-24247.
23. K.T. Leung, L.J. Terminello, Z. Hussain, X.S. Zhang, T. Hayashi, and D.A. Shirley, "Surface Bonding Geometry of (2×1)S/Ge(001) by Normal Emission Angle-Resolved Photoemission Extended Fine Structure," LBL-24616.

Invited Talks

24. D.A. Shirley, "Surface and Adsorbate Effects on Electronic and Atomic Structure: Some New Results," Physical Chemistry Seminar, University of California Berkeley, Jan. 20, 1987.
25. D.A. Shirley, "Gas-Phase Photoemission: Some New Directions in Electron-Correlation Phenomena," Workshop on New Directions in Soft X-Ray Near-Threshold Phenomena, Asilomar, CA, Mar. 1, 1987.
26. D.A. Shirley, "Commencement 1987: A Very Good Year for Science," Commencement Exercises, College of Chemistry, University of California Berkeley, May 23, 1987.
27. D.A. Shirley, "Photoelectron Diffraction: A Deep Surface Probe," Department of Physics, Free University Berlin, Federal Republic of Germany, June 11, 1987.
28. D.A. Shirley, "Multiple Excitations of Atoms," 1987 Atomic Physics Gordon Research Conference, Brewster Academy, Wolfeboro, NH, July 7, 1987.
29. D.A. Shirley, "Near-Threshold Behavior of Photoelectron Satellite Intensities," 14th International Conference on X-Ray and Inner-Shell Processes (X87), Paris, France, Sept. 14–18, 1987.
30. D.A. Shirley, "New Opportunities in Chemistry: An International Symposium on the Uses of Synchrotron Radiation in Chemistry: A Summary," New Opportunities in Chemistry: An International Symposium on the Uses of Synchrotron Radiation in Chemistry, Brookhaven National Laboratory, Upton, NY, Nov. 4–6, 1987.
31. D.A. Shirley, "Photoelectron Diffraction: A Precise Surface Structural Technique," American Chemical Society Analytical Chemistry Seminar for the Wisconsin Section, University of Wisconsin, Madison, Nov. 12–13, 1987.
32. L.J. Terminello, "Surface Structure Determination Using ARPEFS: S/Cr(001)," Applied Physics Division, Stanford University, Palo Alto, CA, May 13, 1987.
33. L.J. Terminello, "An ARPEFS Investigation of c(2×2) S/Fe(001), P/Fe(001), S/Cr(001): A Sensitive Surface and Near-Surface Probe," National Bureau of Standards, Gaithersburg, MD, July 9, 1987.
34. L.J. Terminello, "ARPEFS Studies at SSRL," 14th Annual SSRL User's Meeting, Stanford, CA, Oct. 22–23, 1987.

Crossed Molecular Beams*

Yuan T. Lee, Investigator

INTRODUCTION

The major thrust of this research project is to elucidate detailed dynamics of simple elementary reactions that are theoretically important and to unravel the mechanism of complex chemical reactions or photochemical processes that play important roles in many macroscopic processes. Molecular beams of reactants are used to study individual reactive encounters between molecules or to monitor photodissociation events in a collision-free environment. Most of the information is derived from measurement of the product fragment energy and angular distributions. Recent activities are centered on the mechanisms of elementary chemical reactions involving oxygen atoms with unsaturated hydrocarbons, the dynamics of endothermic substitution reactions, the dependence of the chemical reactivity of electronically excited atoms on the alignment of excited orbitals, the primary photochemical processes of polyatomic molecules, intramolecular energy transfer of chemically activated and locally excited molecules, the energetics of free radicals that are important to combustion processes, the infrared-absorption spectra of carbonium ions and hydrated hydronium ions, and the bond-selective photodissociation through electronic excitation.

1. Infrared Spectra of the Cluster Ions $H_7O_3^+ \cdot H_2$ and $H_9O_4^+ \cdot H_2$ (Publication 1)

M. Okumura, L.I. Yeh, J.D. Myers, and Y.T. Lee

Infrared spectra of the hydrated hydronium ions $H_3O \cdot (H_2O)_n^+$(n = 2,3), with a hydrogen molecule weakly bound to them, have been obtained. The assumption is that the H_2 would bind weakly, resulting in small perturbations of the vibrations of the hydrated hydronium cluster. The H_2 acts as a "messenger"; detection of the water cluster/H_2 complex predissociation allows indirect observation of the absorption by the hydrated hydronium ion itself. The ions are created in a corona discharge of hydrogen, then mass selected, and trapped in a radio frequency ion trap. There they are interrogated spectroscopically in the O-H stretch region. Through vibrational predissociation, the H_2 molecule separates from the parent, leaving the bare hydrated hydronium ion. These $H_3O \cdot (H_2O)_n^+$(n = 2,3) ions are then detected with a quadrupole mass spectrometer.

The tetramer spectrum consists of two doublets centered at 3640 and 3730 cm^{-1}. They lie close to the vibrational origins of the free H_2O symmetric and antisymmetric stretches at 3657 and 3756 cm^{-1}, respectively, and are probably O-H stretches of the three solvating H_2O ligands. In the trimer spectrum, two corresponding bands appear along with a third peak shifted to the red at 3590 cm^{-1}. This last band is assigned to the free O-H stretch of the H_3O^+.

2. Frequency Tripling into the 720–1025 Å Region with Pulsed Free Jets (Publication 11)

R.H. Page, R.J. Larkin, A.H. Kung, Y.R. Shen, and Y.T. Lee

We have developed a coherent source of XUV light, which is continuously tuneable between 904 and 1024 Å, and line tuneable to 720 Å. It employs the technique of frequency tripling in a pulsed free jet of gas and requires a single tuneable laser system. Spectra of the relative XUV output versus wavelength in the 904–1024 Å range are presented for the tripling gases Ar, Kr, Xe, CO, and N_2. Also listed are relative outputs obtained by tripling at resonantly enhanced lines between 720 and 900 Å in Kr, Xe, and CO. Possible improvements to the source are discussed, and examples of its application are given.

3. Highly Resolved Spectra of Local Modes of Benzene (Publication 12)

R.H. Page, Y.R. Shen, and Y.T. Lee

Rotational cooling by supersonic expansion and laser-labeling spectroscopy were used to obtain high-resolution fundamental and first- and second-overtone spectra of C-H stretches of benzene in a molecular beam. Rich fine structure in the spectra has been observed. Transformation from the "normal-mode" picture to the "local-mode" picture seems to occur between $\nu = 2$ and $\nu = 3$. Vibrational lifetimes in local-mode bands exceed ~0.5 psec.

*This work was supported by the Director, Office of Energy Research, Office of Basic Energy Sciences, Chemical Sciences Division of the U.S. Department of Energy under Contract No. DE-AC03-76SF00098.

4. Reactive Scattering of Electronically Excited Alkali Atoms with Molecules (Publication 14)

J.M. Mestdagh, B.A. Balko, M.H. Covinsky, P.S. Weiss, M.F. Vernon, H. Schmidt, and Y.T. Lee

Representative families of excited alkali atom reactions have been studied using a crossed-beam apparatus. For those alkali-molecule systems in which reactions are also known for ground-state alkali and involve an early electron-transfer step, no large differences are observed in the reactivity as Na is excited. More interesting are the reactions with hydrogen halides (HCl): it was found that adding electronic energy into Na changes the reaction mechanism. Early electron transfer is responsible for Na(5S, 4D) reactions, but not for Na(3P) reactions. Moreover, the NaCl product scattering is dominated by the HCl^- repulsion in Na(5S, 4D) reactions, and by the NaCl-H repulsion in the case of Na(3P). The reaction of Na with O_2 is of particular interest since it was found to be state specific. Only Na(4D) reacts, and the reaction requires restrictive constraints on the impact parameter and the reactants' relative orientation. The reaction with NO_2 is even more complex since Na(4D) leads to the formation of NaO by two different pathways. It must be mentioned, however, that the identification of NaO product in these reactions has yet to be confirmed.

5. Dynamics of Endoergic Aromatic Substitution Reactions (Publication 15)

G.N. Robinson, R.E. Continetti, and Y.T. Lee

The endoergic substitution reactions Br + o-, m-,p-$CH_3C_6H_4Cl \rightarrow$ o-,m-,p-$CH_3C_6H_4Br$ + Cl ($\Delta H^\circ_0 \sim 15$ kcal/mol) have been studied using the crossed-beams method in the collision energy range 20–30 kcal/mol. The molecule o-chlorotoluene was found to be more reactive than p-chlorotoluene at the highest collision energy, but the reverse was true below 25 kcal/mol. No reaction was observed for the meta isomer. An explanation for the lower reactivity of m-chlorotoluene is offered in terms of possible features of the potential energy surface.

In all of the reactions observed, the products are forward scattered, indicating that the majority of collision complexes survive for less than one rotational period. This is understandable in light of the ~2 kcal/mol endoergicity to Br addition that results from the loss in resonance stabilization energy. Little of the energy available to the products of these reactions is channeled into translation. The experimental product translational energy distributions and excitation functions suggest that, in those complexes that decompose through Cl elimination, only a few vibrational degrees of freedom in the vicinity of the collision are involved in energy redistribution.

6. Infrared-Ultraviolet Double Resonance Studies of Benzene Molecules in a Supersonic Beam (Publication 17)

R.H. Page, Y.R. Shen, and Y.T. Lee

We have used IR excitation to selectively create populations in admixtures of the zeroth-order states comprising the ~3000 cm^{-1} "C-H stretching Fermi triad" of benzene. UV spectra of the 260-nm $\tilde{A}$ ($^1B_{2u}$) $\leftarrow$ $\tilde{X}$ ($^1A_{1g}$) transition in the IR-excited molecules show several new bands, which we have assigned. Final states in the UV transitions are some vibrational levels that have not been detected before, allowing us to find several excited-state vibrational frequencies. We have determined $\nu_3' = 1327 \pm 3$ cm^{-1}, $\nu_{19}' = 1405 \pm 3$ cm^{-1}, and $\nu_{20}' = 3084 \pm 5$ cm^{-1}. Also, vibrational structure that was unresolved in IR spectra of the "Fermi triad" was resolved in the UV double-resonance spectra, confirming that the C-H stretching admixture is really a tetrad. The 3048, 3079, and 3101 cm^{-1} states had formerly been given the labels ν_{20}'', $\nu_8'' + \nu_{19}''$, and $\nu_1'' + \nu_6'' + \nu_{19}''$, respectively. Actually, the middle level most nearly resembles $\nu_1'' + \nu_5'' + \nu_{19}''$, and the 3101 cm^{-1} level is strongly mixed with $\nu_3'' + \nu_6'' + \nu_{15}''$.

As predicted by molecular orbital theory, excited-state C-H bending and stretching frequencies are not very different from those in the ground state. Furthermore, we suggest that the four C-H stretching frequencies increase uniformly by ~20 cm^{-1} in the excited state; reexamination of the Atkinson and Parmenter 260-nm $\tilde{A} \leftarrow \tilde{X}$ spectrum leads us to reassign ν_2' from 3130 to ~3093 cm^{-1}, which is 19 cm^{-1} above ν_2''.

There is a Fermi resonance between the $\nu_5' + \nu_{20}'$ level and another level ~13 cm^{-1} lower in energy; the strength of the perturbation is ~18 cm^{-1}. Possibilities for the perturbing vibrational state are $\nu_6' + \nu_6' + \nu_{14}'$ and $\nu_5' + \nu_{13}'$.

7. Infrared Spectroscopy of the Cluster Ions $H_3^+\cdot(H_2)_n$ (Publication 18)

M. Okumura, L.I. Yeh, and Y.T. Lee

The vibrational spectra of the clusters $H_3^+(H_2)_n$ were observed near 4000 cm^{-1} by vibrational predissociation spectroscopy. Spectra of mass-selected clusters were obtained by trapping the ions in a radio frequency ion trap, exciting vibrational transitions of the cluster ions to predissociating levels, and detecting the fragment ions with a mass spectrometer. Low-resolution bands of the solvent H_2 stretches were observed for the clusters of one to six H_2 coordinated to an H_3^+ ion. The red-shift of these vibrations relative to the monomer H_2 frequency supported the model of H_9^+ as an H_3^+ with a complete inner solvation shell of three H_2, one bound to each corner of the ion. Two additional bands of H_5^+ were observed, one assigned as the H_3^+ symmetric stretch, and the other as a combination or overtone band. High-resolution scans (0.5 and 0.08 cm^{-1}) of H_n^+, n = 5, 7, and 9, yielded no observable rotational structure, a result of either spectral congestion or rapid cluster dissociation. The band contour of the H_5^+ band changed upon cooling of the internal degrees of freedom, but the peaks remained featureless. The observed frequencies of H_7^+ and H_9^+ agree well with *ab initio* predictions, but those of H_5^+ did not. This deviation is discussed in terms of the large expected anharmonicity of the proton bound dimer H_5^+.

8. Infrared Vibrational Predissociation Spectra of Large Water Clusters (Publication 19)

R.H. Page, M.F. Vernon, Y.R. Shen, and Y.T. Lee

The infrared absorption spectrum in the O-H stretching region of $(H_2O)_{19}$ clusters formed in a supersonic molecular beam is reported. It was obtained with mass-spectrometric detection and is compared with a similarly obtained spectrum of $(H_2O)_6$ and a large-cluster spectrum obtained with bolometric detection.

The mass-resolved spectra show a broad absorption band between ~3200 and 3600 cm^{-1}, reminiscent of the H-bonding feature in a condensed phase spectrum. The spectrum obtained with the bolometer is peaked in the blue of this region, suggesting that the level of H-bonding is much lower. It must be dominated by small and/or warm clusters such as dimers. Mass resolution is clearly advantageous in selectively obtaining spectra of large clusters, free of interference from smaller ones.

9. Local Modes of Benzene and Benzene Dimer Studied by Infrared-Ultraviolet Double Resonance in a Supersonic Beam (Publication 20)

R.H. Page, Y.R. Shen, and Y.T. Lee

We used rotational cooling of molecules to ~5 K by supersonic expansion and state-selective, multilevel saturation spectroscopy to obtain high-resolution spectra of the fundamental and first and second overtone transitions of C-H stretching modes in benzene and its dimer. Greatly reduced linewidths (<3 cm^{-1} full width half maximum) in the rich spectra show that previously reported spectra have suffered from inhomogeneous congestion. Our observed spectral widths indicate that the vibrational lifetimes of the C-H stretches are at least a few psec, even at the energy of the second overtone (8800 cm^{-1}). The "local mode" picture appears to apply when at least 3 quanta of C-H stretching motion are present. Spectra of the dimer are similar to those of the monomer but show a red shift of a few cm^{-1}, the appearance of combination bands involving van der Waals vibrational modes, some intensity changes, and a broadening of spectral features that increases with the vibrational energy. The dimer's predissociation lifetime at ~3000 cm^{-1} vibrational energy exceeds ~3 psec.

10. High-Resolution UV Photoelectron Spectroscopy of CO_2^+, COS^+, and CS_2^+ Using Supersonic Molecular Beams (Publication 21)

L. Wang, J.E. Reutt, Y.T. Lee, and D.A. Shirley

Very high resolution HeI (584 Å) photoelectron spectra of CO_2^+, COS^+, and CS_3^+ are presented. The spectra were obtained by using supersonic molecular beams to eliminate the rotational and Doppler broadenings. The spin-orbit split components in the Π bands are all explicitly resolved. The removal of the inelastic scattering peaks, due to the use of molecular beams, allowed new features to be observed in the $\tilde{B}$ and $\tilde{C}$ bands of CS_2^+, and new spectroscopic constants were derived.

11. Work in Progress

In the area of chemical reaction dynamics, three important investigations are taking place at present. Using oxygen-18 isotopes, the reaction mechanism of oxygen atoms with unsaturated hydrocarbons is starting to become clear. Recent results indicate that theoretical efforts on the understanding of the mechanism of these reactions should now concentrate on the efficiency of the intersystem crossing from triplet to singlet in the reaction complexes. The investigation on the dynamics of endothermic substitution reactions has been centered on the systems of bromine atoms with 1, 1-, and 1,2-dichloroethylene. These studies should further provide some information on the extent of intramolecular energy transfer in substitution reactions. The experiment on $D + H_2 \rightarrow DH + H$ has also started to provide good results on product angular and velocity distributions at high resolutions. A very sophisticated experimental arrangement combining a universal crossed molecular beams apparatus with a laser dissociation pulsed atomic beam source was perfected for this purpose.

In the area of photodissociation dynamics, there have been several exciting advances. The improved experimental apparatus can now provide better information on C-H bond dissociation channels. The improved resolution also allows one to resolve both bending and stretching vibrational excitations of CH_3 radicals in the photofragmentation translation spectroscopy of CH_3I. All the data necessary to understand the photodissociation processes of benzene have been obtained, and the competitive decay channels are rather complicated.

The recently developed spectroscopic technique for ion clusters has been successfully applied to carbonium ions. The spectra of $C_2H_7^+$ and $C_4H_{11}^+$ were obtained recently and solvated ammonium ions, etc., are being explored.

1987 PUBLICATIONS AND REPORTS

Refereed Journals

1. M. Okumura, L.I. Yeh, J.D. Myers, and Y.T. Lee, "Infrared Spectra of the Cluster Ions $H_7O_3^+ \cdot H_2$ and $H_9O_4^+ \cdot H_2$," J. Chem. Phys. **85**, 2328 (1986); LBL-21484.
2. H. Shiromaru, Y. Achiba, K. Kimura, and Y.T. Lee, "Determination of the C-H Bond Dissociation Energies of Ethylene and Acetylene by Observation of the Threshold Energies of H^+ Formation by Synchrotron Radiation," J. Phys. Chem. **91**, 17 (1986).
3. S.W. Bustamente, M. Okumura, D. Gerlich, H.S. Kwok, L.R. Carlson, and Y.T. Lee, "Spin-Forbidden Radiative Decay of the $a^4\Pi^u$ State of O_2^+," J. Chem. Phys. **86**, 508 (1987); LBL-22097.
4. T.K. Minton, G.N. Nathanson, and Y.T. Lee, "Photodissociation of CF_2BrCH_2I at 248, 266, and 308 nm," J. Chem. Phys. **86**, 1991 (1987); LBL-22098.
5. L.J. Butler, E.J. Hintsa, S.F. Shane, and Y.T. Lee, "The Electronic State-Selective Photodissociation of CH_2BrI at 248, 210, and 193 nm," J. Chem. Phys. **86**, 2051 (1987); LBL-21896.
6. L. Wang, J.E. Pollard, Y.T. Lee, and D.A. Shirley, "Molecular Beam Photoelectron Spectroscopy: The $C_2D_4^+$ ($\tilde{X}\ ^2B_3$) Ground State," J. Chem. Phys. **86**, 3216 (1987); LBL-21997.
7. M. Okumura, L.I. Yeh, D. Normand, J.J.H. van den Biesen, S.W. Bustamente, Y.T. Lee, T.J. Lee, N.C. Handy, and H.F. Schaefer III, "Radiative Decay Lifetimes of CH_2^+," J. Chem. Phys. **86**, 3807 (1987); LBL-22428.
8. Y.T. Lee, "Molecular Beam Studies of Elementary Chemical Processes," Nobel Lecture, Chem. Scripta **27**, 2489 (1987); LBL-22621; Science **236**, 793 (1987); LBL-22982.
9. T.K. Minton, G.N. Nathanson, and Y.T. Lee, "Photodissociation of CH_2ClCH_2I at 308 nm," Laser Chem. **7**, 297 (1987); LBL-22099.
10. L. Wang, Y.T. Lee, and D.A. Shirley, "Molecular Beam Photoelectron Spectroscopy of SO_2: Geometry, Spectroscopy, and Dynamics of SO_2^+," J. Chem. Phys. **87**, 2489 (1987); LBL-22413.
11. R.H. Page, R.J. Larkin, A.H. Kung, Y.R. Shen, and Y.T. Lee, "Frequency Tripling into the 720–1025 Å Region with Pulsed Free Jets," Rev. Sci. Instrum. **58**, 1616 (1987); LBL-23306.
12. R.H. Page, Y.R. Shen, and Y.T. Lee, "Highly-Resolved Spectra of Local Modes of Benzene," Phys. Rev. Lett. **59**, 1293 (1987); LBL-23768.

LBL Reports

13. A.M. Wodkte and Y.T. Lee, "High-Resolution Photofragmentation-Translational Spectroscopy," to appear in *Advances in Gas Phase Photochemistry and Kinetics* (1986); LBL-22264.
14. J.M. Mestdagh, B.A. Balko, M.H. Covinsky, P.S. Weiss, M.F. Vernon, H. Schmidt, and Y.T. Lee, "Reactive Scattering of Electronically Excited Alkali Atoms with Molecules," Faraday Discussion No. 84 (in press); LBL-23588.
15. G.N. Robinson, R.E. Continetti, and Y.T. Lee, "Dynamics of Endoergic Aromatic Substitution Reactions," Faraday Discussion No. 84 (in press); LBL-23701.
16. L.I. Yeh, M. Okumura, J.D. Myers, and Y.T. Lee, *Vibrational Spectroscopy of Cluster Ions: Two Novel Methods. Molecular and Cluster Beam Science*, National Research Council, 1987; LBL-23842.
17. R.H. Page, Y.R. Shen, and Y.T. Lee, "Infrared-Ultraviolet Double Resonance Studies of Benzene

Molecules in a Supersonic Beam," submitted to J. Chem. Phys.; LBL-23769.

18. M. Okumura, L.I. Yeh, and Y.T. Lee, "Infrared Spectroscopy of the Cluster Ions $H_3^+ \cdot (H_2)_n$," submitted to J. Chem. Phys.; LBL-23995.
19. R.H. Page, M.F. Vernon, Y.R. Shen, and Y.T. Lee, "Infrared Vibrational Predissociation Spectra of Large Water Clusters," submitted to Chem. Phys. Lett.; LBL-24006.
20. R.H. Page, Y.R. Shen, and Y.T. Lee, "Local Model of Benzene and Benzene Dimer; Studied by Infrared-Ultraviolet Double Resonance in a Supersonic Beam," submitted to J. Chem. Phys.; LBL-24007.
21. L. Wang, J.E. Reutt, Y.T. Lee, and D.A. Shirley, "High Resolution UV Photoelectron Spectroscopy of CO_2^+, COS^+, and CS_2^+ Using Supersonic Molecular Beams," submitted to J. Electron Spectrosc.; LBL-23936.
22. R.J. Brudzynski, Jr. (Ph.D. Thesis), "Molecular Beam Studies of Unimolecular Decomposition of Substituted Benzene Compounds," LBL-23667.
23. R.H. Page (Ph.D. Thesis), "Nonlinear-Spectroscopic Studies of Highly Excited States of Molecules in Supersonic Beams," LBL-23307.

Invited Talks

24. Y.T. Lee, "Dynamics of Molecular Collisions," Lawrence Berkeley Laboratory, Physics Division, Jan. 22, 1987.
25. Y.T. Lee, "Infrared Absorption Spectroscopy of Hydrated Hydronium Ions," Chemistry Department, University of Southern California, Los Angeles, Feb. 25, 1987.
26. Y.T. Lee, "Energetics of Radical Molecules," Sandia National Laboratory Combustion Facilities, Livermore, CA, Mar. 13, 1987.
27. Y.T. Lee, "Crossed Molecular Beam Studies on Elementary Atomic and Molecular Processes," Stanford Linear Accelerator Center, Stanford, CA, Mar. 16, 1987.
28. Y.T. Lee, "Dynamics of Elementary Chemical Reactions," Arthur Davidson Lecture, Department of Chemistry, University of Kansas, Kansas City, Mar. 24, 1987.
29. Y.T. Lee, "Molecular Beam Studies on Chemical Reaction Dynamics," Department of Chemistry, Arizona State University, Tempe, Mar. 27. 1987.
30. L.I. Yeh, "Infrared Spectra of the Hydrated Hydronium Ions, $H_3O(H_2O)_n^+$(n = 1,2,3)," 193rd American Chemical Society Meeting, Denver, CO, Apr. 8, 1987.
31. Y.T. Lee, "Molecular Beam Studies on Dynamics of Chemical Reactions," Sir Run Run Shaw Lecture, State University of New York, Stony Brook, Apr. 22, 1987.
32. Y.T. Lee, "Infrared Absorption Spectroscopy of Ionic Clusters by Ion Trapping Technique," Committee on Atomic and Molecular Science (CASS) Workshop, National Research Council, Washington, D.C., Apr. 27, 1987.
33. Y.T. Lee, "Molecular Beam Studies on Photochemical Processes," Plenary Lecture, International Conference on Quantum Electronics, Baltimore, MD, Apr. 29, 1987.
34. Y.T. Lee, "Dynamics of Elementary Chemical Reactions," Chinese Academy of Sciences, Beijing, People's Republic of China, May 13, 1987.
35. Y.T. Lee, "Laser Chemistry and Laser Spectroscopy," Institute of Chemistry, Academia Sinica, Beijing, People's Republic of China, May 18, 1987.
36. Y.T. Lee, "Crossed Molecular Beam Studies on Elementary Chemical Reactions," Nankai University, Nanking University, Fudan University, and Institute of Chemical Physics, People's Republic of China, May 16–26, 1987.
37. Y.T. Lee, "Molecular Beams Studies on Hot Atom Chemical Reactions," Plenary Lecture, XIII International Hot Atom Chemistry Symposium, Mt. Fuji, Japan, May 24–29, 1987.
38. Y.T. Lee, "Two Way Street Between Dynamics and Spectroscopy," Plenary Lecture, Symposium on Reaction Dynamics, University of Tokyo, Japan, June 3, 1987.
39. Y.T. Lee, "Reactions of Electronically Excited Sodium Atoms," 1987 Conference on Dynamics of Molecular Collisions, Oglebay Park, Wheeling, WV, July 13, 1987.
40. Y.T. Lee, "Molecular Beams Studies of the Primary Photodissociation Processes of Polyatomic Molecules," Plenary Lecture, XIIIth International Conference on Photochemistry, Budapest, Hungary, Aug. 10, 1987.
41. G.N. Robinson, "Dynamics of Endoergic Aromatic Substitution Reactions," Faraday Discussion, University of Birmingham, England, Sept. 15, 1987.
42. Y.T. Lee, "Crossed Molecular Beams Studies of Elementary Chemical Reactions," Selman A. Waksman Lecturer, Rutgers University, New Brunswick, NJ, Oct. 7, 1987.
43. Y.T. Lee, "Molecular Beam Studies of Elementary Chemical Reactions," Nobel Lecture Series, Clark Kerr Campus, University of California, Berkeley, Oct. 13, 1987; Aerospace Corporation, Los Angeles, CA, Oct. 22, 1987; Convocation Lecture, MacAlester College, Minneapolis, MN, Oct. 28, 1987.
44. Y.T. Lee, "Deriving Correct Conclusions from Experimental Observations," Department of Chemistry, MacAlester College, Minneapolis, MN, Oct. 29, 1987.
45. Y.T. Lee, "Molecular Dissociations and Molecular Spectroscopy Using Lasers and Molecular Beams," MacAlester College, Minneapolis, MN, Oct. 30, 1987.
46. Y.T. Lee, "Molecular Beams Studies on Photophysical and Photochemical Processes," Plenary Lecture, International Laser Symposium-III, Atlantic City, NJ, Nov. 2, 1987.

47. Y.T. Lee, "Dynamics of Molecular Dissociations and Photochemical Processes by the Molecular Beams Methods," Distinguished Lecture Series, Office of Naval Research, Washington, D.C., Nov. 3, 1987.

48. Y.T. Lee, "Investigation of Reaction Dynamics by the Molecular Beams Method," Plenary Lecture, Annual Meeting, American Vacuum Society, Anaheim, CA, Nov. 4, 1987.

49. Y.T. Lee, "Disposal of Angular Momentum in Elementary Chemical Reactions," Laser Chemistry Symposium, Kenting, Republic of China, November 12, 1987.

50. Y.T. Lee, "Dependence of Molecular Orientation and Orbital Alignment in the Reactions of Electronically Excited Sodium Atoms," Laser Chemistry Workshop, Kenting, Republic of China, Nov. 13, 1987.

51. Y.T. Lee, "Unimolecular Dissociation of the RDX Molecule by Molecular Beam Photofragmentation Translational Spectroscopy," Laser Chemistry Workshop, Kenting, Republic of China, Nov. 14, 1987.

ATOMIC PHYSICS

High-Energy Atomic Physics*

Harvey Gould, Investigator

INTRODUCTION

The goal of this program is to understand atomic collisions of relativistic ions and to test quantum electrodynamics (QED) in very high atomic number (Z) atoms. These are new areas of research that involve physics that is not accessible at lower energies or with ions of lower atomic number. This research is conducted at the Lawrence Berkeley Laboratory's Bevalac, the world's only relativistic heavy-ion accelerator. Recent results include measurements of the cross sections for multiple ionization of relativistic uranium ions and the channeling of relativistic uranium through silicon single crystals. These and earlier experiments in this program have led to an understanding of relativistic heavy-ion–atom collisions, which in most cases is now more complete than for nonrelativistic collisions. Present activities include measurement of electron-impact ionization cross sections for few-electron uranium, measurement of a state-dependent capture cross section for one-electron uranium, and a precision (0.1%) measurement of the Lamb shift in uranium. Future experiments will attempt to measure polarization in relativistic heavy-ion collisions and a new electron-capture mechanism in ultrarelativistic-ion–atom collisions.

*This work was supported by the Director, Office of Energy Research, Office of Basic Energy Sciences, Chemical Sciences Division of the U.S. Department of Energy under Contract No. DE-AC03-76SF00098.

1. Multiple Ionization in Relativistic Heavy-Ion–Atom Collisions (Publication 1)

W.E. Meyerhof, R. Anholt, X.-Y. Xu, H. Gould, B. Feinberg, R.J. McDonald, H.E. Wegner, and P. Thieberger

We have found that, in relativistic heavy-ion collisions, the independent-particle model (IPM) can be used to predict cross sections for multiple ionization in a single collision with good accuracy. According to the IPM, multiple ionization should follow a binomial distribution. Previously the distribution has been observed in satellite K x-ray spectra, hypersatellite spectra, multiple ionization and multiple capture, and recoil-ion measurements. In the past, detailed comparisons between calculated and measured multiple-ionization cross sections have been hampered by various side effects.

However, at relativistic energies, charge-changing collisions can be accurately described by relatively simple theories for which one should be able to compute multiple-ionization cross sections with a high degree of accuracy.

In an experiment done at the LBL's Bevalac, charge distributions of 430- and 955-MeV/nucleon U^{90+}, U^{89+}, U^{83+}, and U^{68+} beams emerging from solid targets were used to obtain single- and multiple-electron stripping cross sections. The probabilities of stripping electrons from the K, L, or M shells were calculated using the semiclassical approximation and Dirac hydrogenic wave functions. The data generally agree with theory, and comparisons are shown in Figures 1-1 and 1-2.

2. Work in Progress

Experiments to measure the electron-impact ionization cross section for relativistic few-electron uranium ions have been completed, and the data are being analyzed. The experiments were performed by channeling relativistic uranium through the <110> axis of silicon single crystals. These will be the first electron-impact ionization cross sections for a highly ionized ion.

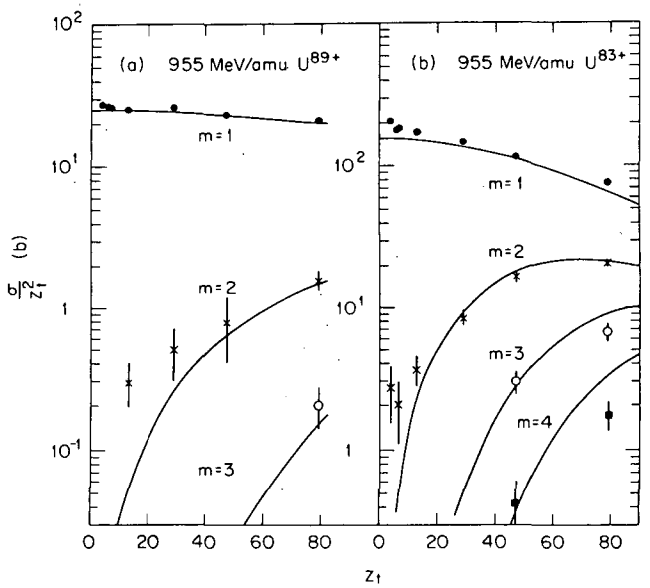

Figure 1-1. Single and multiple stripping cross sections for 955-MeV/nucleon U^{89+} (one L-shell electron) and U^{83+} (seven L-shell electrons) projectiles passing through targets as a function of the target atomic number (Z_t). The cross sections (in barns) have been divided by Z_t^2. On each curve, m indicates the multiplicity of the stripping process. The solid curves show the independent-electron approximation results.

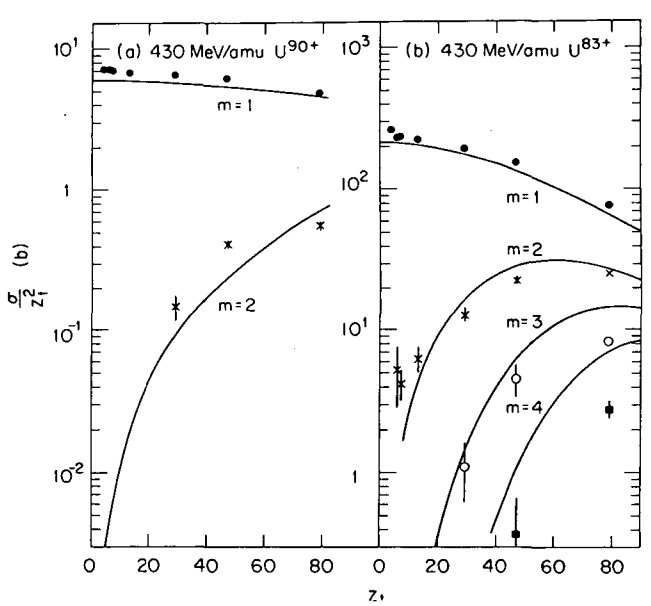

Figure 1-2. Same as Figure 1-1, for 430-MeV/nucleon U^{90+} and U^{83+} projectiles.

1987 PUBLICATIONS AND REPORTS

Refereed Journals

1. W.E. Meyerhof, R. Anholt, X.-Y. Xu, H. Gould, B. Feinberg, R.J. McDonald, H.E. Wegner, and P. Thieberger, "Multiple Ionization in Relativistic Heavy-Ion–Atom Collisions," Phys. Rev. (Rapid Commun.) A **35**, 1967 (1987); LBL-22186.
2. R. Anholt, W.E. Meyerhof, X.-Y. Xu, H. Gould, B. Feinberg, R.J. McDonald, H.E. Wegner, and P. Thieberger, "Atomic Collisions with Relativistic Heavy Ions VIII. Charge-State Studies of Relativistic Uranium Ions," Phys. Rev. A **36**, 1586 (1987); LBL-22699.
3. H. Gould and C. Munger, "Tests of Quantum Electrodynamics in Few-Electron Very High-Z Ions," Phys. Scripta **36**, 476 (1987); LBL-21856.
4. W.E. Meyerhof, R. Anholt, X.-Y. Xu, H. Gould, B. Feinberg, R.J. McDonald, H.E. Wegner, and P. Thieberger, "Multiple Ionization and Capture in Relativistic Heavy-Ion–Atom Collisions," presented at the U.S.-Japan Seminar on Interactions of Highly Ionized Atoms produced in Heavy-Ion Collisions, Kobe, Japan, Mar. 1987; Nucl. Instrum. Meth. A **262**, 10 (1987); LBL-23170.

Other Publications

5. H. Gould, N. Claytor, B. Feinberg, C.E. Bemis, Jr., J. Gomez Del Campo, C.A. Ludemann, and C.R. Vane, "Channeling of Relativistic Uranium," abstract, Annual Meeting, Division of Atomic, Molecular, and Optical Physics, Cambridge, MA, May 18–20, 1987; Bull. Am. Phys. Soc. **32**, 1244 (1987); LBL-22890abs.
6. H. Gould and C. Munger, "Experiments on Few-Electron Very High-Z Ions," in *Physics of Strong Fields,* W. Greiner, Ed., Plenum, New York, 1987, p. 645; LBL-21855.
7. H. Gould and C. Munger, "Measurement of the Lamb Shift in Heliumlike Uranium (Z = 92)," in *Atomic Physics 10,* H. Narumi and I. Shimamura, Eds., North-Holland, Amsterdam, 1987, p. 95–104; LBL-22096.

LBL Reports

8. C.T. Munger, Jr. (Ph.D. Thesis), "The Lamb Shift in Heliumlike Uranium," LBL-22640.

Atomic Physics*

Michael H. Prior, Investigator

INTRODUCTION

This program utilizes the intense multiply charged ion beams available from the LBL ECR (Electron Cyclotron Resonance) ion source for studies of atomic structure, collision dynamics, and radiative processes. Emphasis is placed on topics that have relevance to applied areas such as CTR plasma diagnostics and advanced laser concepts and/or that strongly challenge the current state of atomic theory, and require the unique capabilities of the ECR source.

Presently, efforts are under way that yield metastable energy-level structures of highly charged ions; reveal details of multiple electron-transfer processes, Auger electron, and x-ray emission spectra from ion-atom collisions; and determine cross sections for excitation of multiply charged ion states by electron impact. The latter studies are collaborative efforts with groups from other laboratories.

1. Angular Dependence of Multiple Electron Capture in 90 keV Ne^{7+}–Ne Collisions (Publications 2 and 7)†

*H. Schmidt-Böcking,‡ M.H. Prior, R. Dörner,‡ H. Berg,‡ J.O.K. Pedersen,§ C.L. Cocke,‖ M. Stockli,‖ and A.S. Schlachter***

Electron-capture processes in collisions between slow, highly charged ions and atomic targets continue to attract interest as fundamentally challenging and as important ingredients in the understanding of applied problems in plasma research. Many experimental and theoretical investigations have addressed total electron-capture cross sections, and it has been established by high-resolution Auger electron spectroscopy, x-ray spectroscopy, and projectile energy-gain spectroscopy, that single-electron transfer from the atom to the projectile ion is very final-state selective. However, only a few experimental studies to date have been performed that measure the angular dependence of the single- and multiple-electron capture processes.

This work reports a study of multiple capture as a function of the projectile scattering angle in 90-keV Ne^{7+} collisions with Ne atoms. The experiment was performed at the Lawrence Berkeley Laboratory using the Electron Cyclotron Resonance (ECR) ion source and the atomic physics beam line facilities at the 88-inch cyclotron. A beam of Ne^{7+} ions was collimated to near circular cross section of 0.1 mm^2, and it struck a Neon gas jet target. A weak electric field in the target region transverse to the beam extracted target product ions (recoil ions) into a drift tube, after which they were detected by a channel electron multiplier (CEM). Projectile product ions proceeding in the forward direction were deflected an amount proportional to their charge by a transverse uniform electric field. The deflected projectile product ions were detected by a position-sensitive channel-plate detector with a 4-cm-diameter active area. A fast time signal from the target recoil-ion detector was used to start a time-to-amplitude converter, which was stopped by a delayed time signal from the projectile detector. Because the recoil ions had low initial velocities and were extracted by an electric field, their time of flight into the CEM detector was proportional to $1/\sqrt{k}$, (k = recoil-ion charge). Thus we obtained, for each true kinematic recoil-ion projectile coincidence, a well-resolved time peak, allowing the determination of k. The x-y position information from the projectile detector identified the projectile product charge and scattering angle for each such coincidence. Figure 1-1 summarizes the scattering angle data derived from this experiment.

We have observed capture of up to 6 electrons per encounter by the projectile, and from the scattering measurements we have inferred that capture occurs predominantly into multiply excited states and is thus nearly always followed by autoionization. For scattering angles greater than about 8 milliradians, the projectile and recoil-ion L electron shells form a quasi-molecular system, completely sharing these electrons, which leads to nearly identical product charge-state distributions. A single electron-capture probability is extracted from our data, which, using binomial statistics, provides a fairly good description of the measured recoil-ion charge-state distributions for scattering angles less than 8 milliradians. A parameter-free theoretical description is not available, in part because, at this velocity in the multielectron system, electron screening has a very strong influence on the capture and scattering process. Finally, a simple transformation of the angular scattering data (Figure 1-1) yields the recoil-

*This work was supported by the Director, Office of Energy Research, Office of Basic Energy Sciences, Chemical Sciences Division of the U.S. Department of Energy under Contract No. DE-AC03-76SF00098.

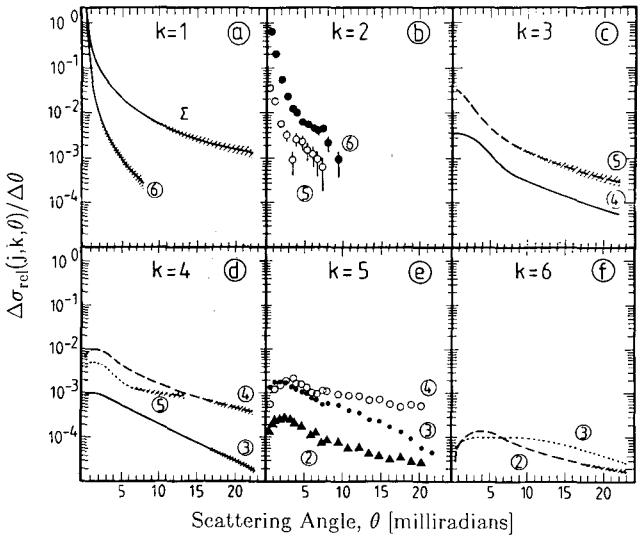

Figure 1-1. Relative differential cross-sections $\Delta\sigma_{rel}(j,k,\theta)/\Delta\theta$ for 90 keV Ne^{7+} + Ne collisions. j = final projectile charge state after the collision; k = final recoil charge state after collision. Values of j are circled. For most cases lines have been drawn through the experimental data points. The hatched areas along the curves indicate the statistical spread of the data where it is significant. Sample data is shown for cases k = 2 and k = 5. (XBL 8712-5205)

ion transverse-energy distributions. We observed, from such a treatment, that the mean recoil-ion energy increases with approximately the 2.6 power of the recoil-ion charge and is nearly independent of the number of electrons lost to autoionization. These results are summarized in Figure 1-2. Direct measurement of such low recoil-ion energies is very difficult and rare in the literature.

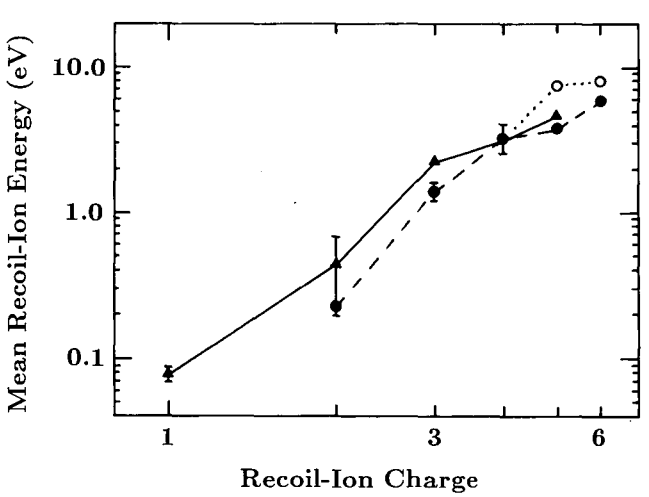

Figure 1-2. Mean recoil-ion energies versus recoil-ion charge. Triangles, solid circles, and open circles are for collisions followed by zero-, one-, and two-electron loss (autoionization), respectively. (XBL 8712-5204).

†Additional support has been received from Kansas State University (H.S.-B., C.L.C., M.S.), the Deutsche Forshungsgemeinshaft (H.S.-B., R.D., H.B.), the NATO Science Fellowships Program (J.O.K.P.), Friedrich Ebert Stiftung (R.D.), and NATO Research Grant #0501/85 (H.B.). Important parts of the apparatus were transported from Frankfurt to San Francisco through the generosity of Lufthansa.

‡Permanent address: Institut für Kernphysik, University of Frankfurt, Federal Republic of Germany.

§Permanent address: Institute of Physics, University of Aarhus, Aarhus, Denmark.

‖Permanent address: Department of Physics, Kansas State University, Manhattan, KS.

**Permanent address: LBL Accelerator and Fusion Research Division.

2. Work in Progress

Study of the spectra of weak, forbidden (magnetic dipole) emission lines from metastable ions produced by the LBL ECR ion source continues with emphasis on obtaining wavelength measurements for transitions among levels in ions with ground $3d^n$ electron configurations. In particular, two new lines were observed from levels of $3d^8$ in Nb^{15+} (Z = 41, 26 electrons, Fe sequence). In 1986, when this observational technique was established, two lines from this ion were measured; they are reported in Publication 1. The immediate goal of this work is to obtain measurements of enough lines from transitions among the $3d^8$ levels, to determine the atomic parameters in the model Hamiltonian used to describe the level structure in this configuration. This would be a unique achievement in the history of the spectroscopic analysis of atomic energy levels, which are commonly derived from observation of much more intense allowed transitions. There are large improvements in accuracy to be gained through use forbidden wavelengths since they determine directly the level structure within a single configuration. In addition to Nb^{15+}, forbidden lines were observed from Nb^{10+} (Ga sequence) and Nb^{11+} (Zn sequence). These and other measurements following in this project will appear in a subsequent publication.

In collaboration with groups from the University of Frankfurt and Kansas State University, further studies are under way of highly charged projectile ion scattering following electron-capture collisions with atomic targets. This work will study 90-keV Ne^{9+} scattering over wider angles (out to 125 milliradians) than measured to date. Scattering to larger angles results from closer approach of the two atomic systems. In this case, penetration will be sufficient to yield detectable probabilities for transfer of the K-vacancy in the one-electron projectile to the target.

A collaborative effort with Dr. D. Schneider of the V-division at Lawrence Livermore National Laboratory is being mounted at the LBL ECR atomic physics facility to study forward emitted electron-energy spectra following collisions of multiply charged ions with gas targets. Initial emphasis will be placed on examining cases similar to those where double electron capture has been observed and recently attributed to correlated behavior of the two active electrons at quasimolecular curve crossings.

1987 PUBLICATIONS AND REPORTS

Refereed Journals

1. M.H. Prior, "Forbidden Lines from Highly Charged, Metastable Ion Beams," J. Opt. Soc. Am. B **4**, 144 (1987); LBL-21922.

Other Publications

2. R. Dörner, H. Berg, J.O.K. Pedersen, H. Schmidt-Böcking, M.H. Prior, A.S. Schlachter, C.L. Cocke, and M. Stockli, "Scattering-Angle Dependence of Multi-Electron Transfer in Ne^{q+} + Noble Gas Collisions," abstract of contributed paper to the annual meeting of the American Physical Society, Division of Atomic, Molecular and Optical Physics, Cambridge, MA, May 18–20, 1987; LBL-24713.
3. S. Chantrenne, P.O. Egan, D.J. Clark, C.M. Lyneis, and M.H. Prior, "An Atomic Physics Beam-Line at the LBL ECR Ion Source," Bull. Am. Phys. Soc. **32**, 1269 (1987).
4. H. Berg, H.J. Crawford, R. Dörner, J.M. Engelage, I. Flores, S. Hagmann, C. Kelbch, S. Kelbsh, D.H. Loyd, J. Pedersen, M. Prior, P. Richard, A.S. Schlachter, H. Schmidt-Böcking, and J. Ullrich, "Multiple Ionization of Noble Gas Atoms by 120 MeV/u U^{91+} Impact," in *Abstract of XV Int. Conf. Physics of Electron and Atomic Collisions*, Brighton, England, July 22–28, 1987, J. Geddes, H.B. Gilbody, A.E. Kingston, C.J. Latimer, and H.J.R. Walters, Eds., Queens University, Belfast, 1987, p. 440.
5. M.H. Prior, "Research with Low Energy Multiply Charged Ions from the LBL ECR Source," Program and Abstracts, VIII-th Atomic Physics Program Workshop, Harvard Smithsonian Center for Astrophysics, Cambridge, MA, May 21–22, 1987, p. 95; LBL-24712.
6. M.H. Prior, "Atomic Physics at the LBL ECR Ion Source," in *Proc. Workshop on Opportunities for Atomic Physics using Slow, Highly-Charged Ions*, Argonne National Laboratory, Jan. 12–13, 1987; ANL-PHY-87-1, p. 149; LBL-24711.

LBL Reports

7. H. Schmidt-Böcking, M.H. Prior, R. Dörner, H. Berg, J.O.K. Pedersen, C.L. Cocke, M. Stockli, and A.S. Schlachter, "Angular Dependence of Multiple Electron Capture in 90 keV Ne^{7+}–Ne Collisions," accepted by Phys. Rev. A; LBL-24446.
8. M.H. Prior, "Studies of Atomic Ions with Traps at Lawrence Berkeley Laboratory," contributed presentation, Workshop and Symposium on the Physics of Low-Energy Stored and Trapped Particles, Stockholm, Sweden, June 14–18, 1987; LBL-24714.

PROCESSES AND TECHNIQUES

CHEMICAL ENERGY

Formation of Oxyacids of Sulfur from SO_2*

Robert E. Connick, Investigator

INTRODUCTION

The primary focus of the research is the fundamental chemistry of sulfur species formed from sulfur dioxide in aqueous solution and the reactions of these species. The chemistry of these species is of particular importance in the problems associated with atmospheric pollution by sulfur dioxide and the resulting formation of acid rain. One of the most important reactions is the oxidation of S(IV) by oxygen in aqueous solution, as this reaction plays a key role in both wet flue-gas desulfurization processes and in the formation of acid rain in aquated aerosols. Work has been concentrated on this reaction, but additional oxidation-reduction chemistry of S(IV) should be investigated, particularly reactions involving two or more oxidation states, e.g., reactions involving HSO_3^-, H_2S, S_8, and the polythionates. A secondary and not closely related goal is to determine the factors controlling the rate of substitution reactions in the first coordination sphere of metal ions. Computer modeling has been extended from two dimensions to three dimensions. Interesting preliminary results are being obtained for configurations of the activated complex.

1. Work in Progress

Rate Law and Mechanism of the Oxidation of Bisulfite Ion by Oxygen

Research is continuing on the mechanism of this important chain reaction. Efforts to separate the three steps of the reaction—initiation, propagation, and termination—have been partially successful. The initiation step appears to be autocatalytic with respect to some intermediate formed in the reaction. The termination step seems to switch from chain carriers that do not react with oxygen in a propagation step to the opposite case as the oxygen concentration becomes very small.

Modeling of Displacement Reactions of Solvent in the First Coordination Sphere of Metal Ions

Computer simulations are being run on the simple displacement of a solvent molecule from the first coordination sphere of a metal ion surrounded by six solvent molecules attracted to it by charge-dipole forces. The model serves as a simple example of a reaction occurring in a condensed liquid phase; and aside from its intrinsic interest in such solvent-exchange processes on metal ions, it clearly illustrates the limitation on reaction rates arising from the nearly complete occupancy of space by molecules in a condensed phase. Any appreciable movement of a molecule requires the simultaneous movement of a number of others.

*This work was supported by the Director, Office of Energy Research, Office of Basic Energy Sciences, Chemical Sciences Division of the U.S. Department of Energy under Contract No. DE-AC03-76SF00098.

Catalytic Hydrogenation of CO*

Alexis T. Bell, Investigator

INTRODUCTION

The purpose of this program is to develop an understanding of the fundamental processes involved in catalytic conversion of carbon monoxide and hydrogen to gaseous and liquid fuels. Attention is focused on defining the factors that limit catalyst activity, selectivity, and resistance to poisoning, and the relationship between catalyst composition/structure and performance. To meet these objectives, a variety of surface diagnostic techniques [low-energy electron diffraction (LEED), Auger electron spectroscopy (AES), x-ray photoelectron spectroscopy (XPS), electron-energy-loss spectroscopy (EELS), nuclear magnetic resonance (NMR), infrared spectroscopy (IRS), and temperature-programmed desorption (TPD)] is used to characterize supported and unsupported catalysts before, during, and after reaction. The information thus obtained is combined with detailed studies of reaction kinetics to elucidate reaction mechanisms and the influence of modifications in catalyst composition and/or structure on the elementary reactions involved in carbon monoxide hydrogenation.

1. Analysis of CO Hydrogenation Pathways Using the Bond-Order Conservation Method (Publication 17)

E. Shustorovich and A.T. Bell

The Bond-Order Conservation (BOC) method has been used to identify the energetics associated with the hydrogenation of CO over (111) surfaces of Ni, Pd, and Pt. In the formation of CH_4, the C-O bond of CO is cleaved. BOC calculations for Ni indicate that cleavage of the C-O bond occurs primarily by direct dissociation of molecularly adsorbed CO. The activation energy for direct dissociation of CO on Pd and Pt is significantly greater than that for hydrogen-assisted dissociation, and hence the latter process is more significant. The BOC calculations indicate that for these metals the species from which C-O bond cleavage occurs is CH_3O_s. Because the activation barriers for CH_3O_s dissociation and hydrogenation to form CH_3OH are close for Pd and Pt, these metals are effective catalysts for both CH_4 and CH_3OH synthesis. By contrast, the BOC method predicts that CH_4 should be the principal product formed over Ni.

2. Lanthana-Promoted Rh/SiO_2: I. Studies of CO and H_2 Adsorption; II. Studies of CO Hydrogenation (Publications 15 and 16)

R.P Underwood and A.T. Bell

Promotion of a Rh/SiO_2 catalyst with lanthana results in a partial coverage of the supported Rh crystallites with LaO_x islands. These moieties reduce the capacity of Rh to adsorb CO but have little effect on the chemisorption of H_2 due to spillover of H atoms from the exposed Rh sites onto the surface of the LaO_x islands. At elevated temperatures, the LaO_x islands promote the dissociation of CO. It is proposed that this process occurs preferentially at Rh sites located along the perimeter of the LaO_x islands. Support for this interpretation is provided by infrared spectra of CO adsorbed on lanthana promoted Rh/SiO_2.

Lanthana-promoted Rh/SiO_2 exhibits higher turnover frequencies for the synthesis of CH_4, C_2-C_4 hydrocarbons, CH_3OH, and C_2-oxygenates than unpromoted Rh/SiO_2. The turnover frequency for each product goes through a maximum with increasing lanthana addition. Lanthana promotion is also found to increase the selectivity for the formation of CH_3OH, C_2-oxygenates, and C_2-C_4 hydrocarbons, and to decrease the selectivity for CH_4. The selectivity for C_2-oxygenates is optimized at low levels of lanthana addition. *In situ* infrared observations show that lanthana promotion blocks the chemisorption of CO onto surface Rh sites. Of particular interest is the observation of a band at 1725 cm^{-1}. This feature is assigned to CO adsorbed on a Rh site immediately adjacent to an LaO_x island. The low frequency of this vibration is attributed to a weakening of the C-O bond caused by the interaction of lanthana cations with the oxygen end of the adsorbed CO. It is postulated that the interaction of the lanthana with the CO is responsible for the enhanced rates of CO dissociation and the formation CH_4 and C_{2+} products. Infrared spectroscopy also provides evidence for acyl, formate, and acetate groups on the

*This work was supported by the Director, Office of Energy Research, Office of Basic Energy Sciences, Chemical Sciences Division of the U.S. Department of Energy under Contract No. DE-AC03-76SF00098.

surface of lanthana-promoted Rh/SiO_2. The possible role of these species in the synthesis of products is discussed.

3. Alumina and Titania Overlayers on Rhodium: A Comparison of the Chemisorption and Catalytic Properties (Publication 19)

M.E. Levin, J.J. Williams, M. Salmeron, A.T. Bell, and G.A. Somorjai

The effects of submonolayer deposits of AlO_x on the adsorption and hydrogenation of CO on a Rh foil have been investigated and compared with the earlier studied effects of TiO_x deposits. AlO_x is found to suppress CO chemisorption in direct proportion to AlO_x coverage without affecting the energy of adsorption, indicating that the only function of AlO_x is site blockage. CO hydrogenation activity of Rh decreases in proportion to AlO_x coverage, but no change is observed in product selectivity or rate parameters for methane synthesis. By contrast, TiO_x suppresses CO chemisorption to an extent greater than that expected for simple site blockage. With increasing TiO_x coverage, the CO hydrogenation activity of Rh passes through a maximum at $\theta_{TiO_x} = 0.15$ ML. The rate parameters for methane synthesis are affected by TiO_x coverage. Relative to clean Rh, the activation energy is lower and the partial pressure dependencies on H_2 and CO are both larger. The unusual effects of TiO_x are attributed to the formation of Ti^{3+} cationic centers at the perimeter of TiO_x islands present on the Rh surface.

4. The Influence of Butene on CO Hydrogenation Over Ruthenium (Publication 18)

D.S. Jordan and A.T. Bell

Reactions of 1-C_4H_8 with H_2 and CO were investigated over Ru/SiO_2. To identify the sources of carbon in the products, ^{13}C-labeled CO and unlabeled 1-C_4H_8 were used, and product analysis was carried out by isotope-ratio gas chromatography–mass spectrometry. Butene undergoes extensive hydrogenation and isomerization in the absence of CO. The production of small quantities of C_1-C_3 and C_{5+} paraffins is also observed, indicating hydrogenolysis and homologation of C_4H_8. The observed product distribution is described by a chain growth scheme involving C_1 and C_4 monomer units. Butene added to synthesis gas strongly influences the reactions of CO while undergoing reaction itself. With increasing C_4H_8 partial pressure, hydrocarbon formation from CO is suppressed, but the production of pentanal and pentanol via hydroformylation is enhanced. The rate of C_4H_8 homologation increases with increasing C_4H_8 pressure, resulting in higher overall rates of production of C_{5+} hydrocarbons in the $C_4H_8/H_2/CO$ reaction than in the H_2/CO reaction. Implications of these results on the chain growth mechanism are discussed. Comparisons are made between the reactions of C_4H_8, C_2H_4, and C_3H_6 with synthesis gas. It is concluded that the efficiency of the olefin in producing monomers that are active in chain growth decreases in the order $C_2H_4 > C_3H_6 >$ 1-C_4H_8.

1987 PUBLICATIONS AND REPORTS

Refereed Journals

1. J.S. Rieck and A.T. Bell, "The Influence of Dispersion on the Interactions of H_2 and CO with Pd/SiO_2," J. Catal. **103**, 46 (1987); LBL-20197.
2. M.E. Levin, M. Salmeron, A.T. Bell, and G.A. Somorjai, "The Effects of Titania and Alumina Overlayers on the Hydrogenation of CO over Rhodium," J. Chem. Soc., Faraday Trans. I **83**, 2061 (1987); LBL-21607.
3. M. DePontes, G.H. Yokomizo, and A.T. Bell, "A Novel Method for Analyzing Transient Response Data Obtained in Isotopic Tracer Studies of CO Hydrogenation," J. Catal. **104**, 147 (1987); LBL-21853.
4. M.G. Reichmann and A.T. Bell, "A Raman Study of the Preparation of SiO_2-Supported TiO_2 from $TiCl_4$ and HCl," Langmuir **3**, 111 (1987); LBL-21902.
5. M.G. Reichmann, F.J. Hollander, and A.T. Bell, "Structure of $[Ti_8O_{12}(H_2O)_{24}]Cl_8 \cdot HCl \cdot 7H_2O$," Acta Crystallogr. C **43**, 1681 (1987); LBL-22344.
6. M. Reichmann and A.T. Bell, "A Raman Study of the Preparation of SiO_2- and Al_2O_3-Supported TiO_2 from $Ti(OCH_3)_4$ and HNO_3," Langmuir **3**, 563 (1987); LBL-22345.
7. M.G. Reichmann and A.T. Bell, "The Influence of Preparation Chemistry on the Phase Distribution of Silica-Supported Titania," Appl. Catal. **32**, 315 (1987); LBL-22515.
8. D.S. Jordan and A.T. Bell, "The Influence of Propylene on CO Hydrogenation over Silica-Supported Ruthenium," J. Catal. **107**, 338 (1987); LBL-22703.
9. R.P. Underwood and A.T. Bell, "The Influence of Particle Size on the Activity and Selectivity of Silica- and Lanthana-Supported Rhodium," Appl. Catal. **34**, 289 (1987); LBL-22742.

10. M.E. Levin, M. Salmeron, A.T. Bell, and G.A. Somorjai, "The Enhancement of CO Hydrogenation on Rhodium by TiO_x Overlayers," J. Catal. **106**, 401 (1987); LBL-22812.
11. A.T. Bell, "CO Hydrogenation Over Group VIII Metals: New Insights into Factors Controlling Catalyst Activity and Selectivity," React. Kinet. Catal. Lett. **35**, 107 (1987).

Other Publications

12. A.T. Bell, "Infrared Spectroscopy of High-Area Catalytic Surfaces" in *Vibrational Spectroscopy of Molecules on Surfaces*, J.T. Yates, Jr., and T.E. Madey, Eds., Plenum, New York, 1987; LBL-18556.
13. A.T. Bell, "Supports and Metal-Support Interactions in Catalyst Design," Chapter 4 in *Catalyst Design—Progress and Perspectives*, L.L. Hegedus, Ed., Wiley, New York, 1987; LBL-20642.
14. A.T. Bell, "Characterization of Carbonaceous Residues on Catalysts," Chapter 9 in *Catalyst Deactivation*, E.E. Petersen and A.T. Bell, Eds., Marcel Dekker, New York, 1987; LBL-21309.

LBL Reports

15. R.P. Underwood and A.T. Bell, "Lanthana-Promoted Rh/SiO_2: I. Studies of CO and H_2 Adsorption and Desorption," J. Catal. (in press); LBL-22656.
16. R.P. Underwood and A.T. Bell, "Lanthana-Promoted Rh/SiO_2: II. Studies of CO Hydrogenation," J. Catal. (in press); LBL-22657.
17. E. Shustorovich and A.T. Bell, "Analysis of CO Hydrogenation Pathways Using the Bond-Order Conservation Method," submitted to J. Catal.; LBL-23010.
18. D.S. Jordan and A.T. Bell, "The Influence of Butene on CO Hydrogenation over Ruthenium," J. Catal. (in press); LBL-23011.
19. M.E. Levin, J.J. Williams, M. Salmeron, A.T. Bell, and G.A. Somorjai, "Alumina and Titania Overlayers on Rhodium: A Comparison of the Chemisorption and Catalytic Properties," Surf. Sci. (in press); LBL-23052.
20. G.H. Yokomizo, K. Krishna, and A.T. Bell, "A Commentary on the Direct Calculation of Propagation and Termination Rates from Steady-State Fischer-Tropsch Synthesis Rate Data," submitted to C_1 Molecule Chem.; LBL-23807.

Invited Talks

21. A.T. Bell, "The Influence of Metal Oxide Promoters on the Reduction of CO and NO," Ford Research Laboratories, Dearborn, MI, Feb. 1987.
22. A.T. Bell, "Monte Carlo Simulation of Temperature-Programmed Desorption from fcc(1111) and (100) Surfaces," California Catalysis Society Meeting, Berkeley, CA, Mar. 1987.
23. A.T. Bell, "AES and XPS Characterization of TiO_x-Promoted Rh," ACS Meeting, Denver, CO, Apr. 1987.
24. A.T. Bell, "Applications of Multiple Analytical Techniques for the Characterization of Catalysts," Shell Development Corp., Houston, TX, May 1987.
25. A.T. Bell, "Advances in Understanding the Chemistry of CO Hydrogenation," 10th North American Catalysis Society Meeting, San Diego, CA, May 1987.
26. A.T. Bell, "CO Hydrogenation over Group VIII Metals: New Insights into Factors Controlling Catalyst Activity and Selectivity," International G.K. Boreskov Memorial Conference, Novosibirsk, USSR, June 1987.
27. A.T. Bell, "Application of the Bond-Order Conservation Method to Calculations of Surface Reaction Rates," Industrial Affiliates Program, Stanford University, Stanford, CA, July 1987.
28. A.T. Bell, "Analysis of Reaction Pathways Using the Bond-Order Conservation Method," ACS Meeting, New Orleans, LA, Sept. 1987.
29. A.T. Bell, "Investigation of Dynamic Processes at Electrode Surfaces Using Vibrational Spectroscopies," ACS Meeting, New Orleans, LA, Sept. 1987.
30. A.T. Bell, "Studies of Elementary Reactions at Surfaces by Means of Temperature-Programmed Desorption Spectroscopy," Department of Chemical Engineering, University of Southern California, Los Angeles, Nov. 1987.
31. A.T. Bell, "Monte Carlo Simulation of Temperature Programmed Desorption from fcc(111) and (100) Surfaces," AIChE Meeting, New York, NY, Nov. 1987.
32. A.T. Bell, Infrared Isotopic Tracer Studies of CO Hydrogenation Over Ru/SiO_2 and Ru/TiO_2," AIChE Meeting, New York, NY, Nov. 1987.

Potentially Catalytic and Conducting Polyorganometallics*

K. Peter C. Vollhardt, Investigator

INTRODUCTION

The purpose of this program is to combine synthetic organic and organometallic methodology in the construction of novel organometallic materials that have potential in catalysis and materials science. In particular, iterative approaches to the synthesis of linked cyclopentadienyl ligands are being studied. Subsequent attachment of a variety of metal centers with control of their binding sequence is giving rise to linear and angular oligometallic arrays in which the metals are held in an unnatural configuration. Such materials hold promise in potential applications as catalysts in a variety of processes of current fundamental and industrial interest, such as coal hydrogenation and conversion to liquid fuels, small-molecule activation, new reaction chemistry, photocatalysis and photochemical energy storage, water splitting, and others. Moreover, the methods to be developed are anticipated to provide access to structures containing alternating organic and metallic layers with potential conducting behavior. Thus, in the long run, successful execution of the proposed work should furnish unique catalytic and potentially conducting materials.

1. Hydrogenation of Arenes by a Homogeneous Rhodium Catalyst (Publications 1, 2, and 3)†

H. Amer,‡ I. Amer,‡ R. Ascher,‡ J. Blum,‡ G. Höhne,§ Y. Sasson,‡ H. Schwarz,§ and K.P.C. Vollhardt

In model studies aimed at developing novel coal hydrogenation catalysts, acenaphthylene, fluorene, anthracene, phenanthrene, benz[a]anthracene, pyrene, fluoranthene, benzo[c]phenanthrene, and some of their derivatives were shown to undergo partial hydrogenation in the presence of a $RhCl_3$-Aliquat 336 catalyst in a highly selective manner. Olefinic double bonds were found to be hydrogenated prior to aromatic moieties. In linear aromatic molecules, only the terminal rings are reduced. In phenanthrene, the C_9-C_{10} bond, and in pyrene, the C_4-C_5 linkage, are the only ones to be affected. Benz[a]anthracene is converted exclusively into 7,8,9,10-tetrahydrobenz[a]anthracene. Benzo[c]phenanthrene is hydrogenated to give primarily the 5,6-dihydro derivative. Chlorine and bromine substituents were found to undergo hydrogenolysis when attached to the reacting moieties, but they usually remain unaffected when located on nonreacting aromatic rings.

The ion pair generated by $RhCl_3$ and Aliquat 336 in an aqueous-organic two-phase medium was shown to catalyze the hydrogenation and deuteration of arenes at 30°C and 0.9 atm under apparently homogeneous conditions. The kinetics of the reductions incorporated characteristic induction periods. Substrates with electron-attracting groups proved to have shorter induction periods and higher reaction rates than those with electron-donating substituents. Sterically hindered benzenes yielded both cyclohexane and cyclohexene derivatives. Hydrogenation of deuterated arenes and deuteration of unlabeled benzenes were found, by mass spectral analysis, to be associated with both side-chain and ring-proton H-D exchange. Recovered starting materials underwent hydrogen exchange as well, but only if the substrate had an α proton in the side chain. The water proved essential for the reduction and played an important part in the H-D exchange. Comparative experiments were carried out with the labile η^3-$C_3H_5Co[P(OCH_3)_3]_3$ arene hydrogenation catalyst precursor. The cobalt- and rhodium-promoted processes were found to have several common features and were assumed to follow similar mechanisms.

The ion pair formed from aqueous rhodium trichloride and Aliquat 336 catalyzed the selective hydrogenation of olefinic C-C bonds of a variety of unsaturated nitro compounds in a two-liquid-phase system at 30°C. Nitrobenzene gave, under these conditions, a mixture of aniline and nitrocyclohexane.

*This work was supported by the Director, Office of Energy Research, Office of Basic Energy Sciences, Chemical Sciences Division of the U.S. Department of Energy under Contract No. DE-AC03-76SF00098.

†Collaborative effort supported by the U.S.-Israel Binational Science Foundation.

‡Permanent address: Department of Organic Chemistry and Casali Institute of Applied Chemistry, The Hebrew University, Jerusalem 91904, Israel.

§Permanent address: Institute of Organic Chemistry, The Technical University, D-1000 Berlin 12, Federal Republic of Germany.

2. Photochemistry and Ligand Substitution Reactions of (Fulvalene)diruthenium-(tetracarbonyl) (Publication 4)

W.B. Tolman† and K.P.C. Vollhardt

Studies of the scope and mechanism of the photoisomerization of (fulvalene)diruthenium(tetracarbonyl) $[FvRu_2(CO)_4]$ to $(\mu_2\text{-}\eta^1:\eta^5\text{-cyclopentadienyl})_2Ru_2(CO)_4$ and of the thermal reversal of the latter were performed ($\Delta\underline{H}^{\ddagger} = 29.9 \pm 0.02$ kcal mol^{-1} and $\Delta\underline{S}^{\ddagger} = 17.2 \pm 2.0$ eu). A rate acceleration and external ligand incorporation was observed when the thermal reversion was performed under CO. Treatment of $FvRu_2(CO)_4$ with PR_3 (R = CH_2CH_3, CH_3, and OCH_3) yielded $FvRu_2(CO)_3(PR_3)$, the ^1H and ^{13}C NMR spectra of which indicated the presence of fluxional behavior in solution, probably by a process involving intramolecular-terminal to bridging-carbonyl exchange. These trialkylphosphine species failed to detectably photoisomerize when R = CH_2CH_3 or CH_3, while that in which R = OCH_3 rapidly and reversibly afforded $(\mu_2\text{-}\eta^1:\eta^5\text{-cyclopentadienyl})_2Ru_2(CO)_3[P(OCH_3)_3]$ upon irradiation with uv light. Heating $FvRu_2(CO)_3[P(CH_2CH_3)_3]$ in the presence of CCl_4 regiospecifically generated a novel adduct containing a CCl_3 moiety instead of the expected dichloride complex.

Treatment of E-2,2′,4,4,-tetra-tert-butylfulvalene with $Ru_3(CO)_{12}$ provided the tetra-tert-butyl-substituted analog of $FvRu_2(CO)_4$, which did not photoisomerize. When irradiated in the presence of CCl_4, the dichloride derivative was rapidly formed. The diastereomers (S*, S*- and S*, R*-3,3′-di-tert-butylfulvalene)$Ru_2(CO)_4$ were prepared by exposing 3,3′-di-tert-butyldihydrofulvalene to $Ru_3(CO)_{12}$. Each of these stereospecifically and reversibly transformed upon uv irradiation to different photoisomers. Derivatives of $FvRu_2(CO)_4$ containing one tert-butyl and one $P(OCH_3)_3$ substituent were synthesized by treatment of (3-tert-butylfulvalene)$Ru_2(CO)_4$ with $P(OCH_3)_3$. These complexes reversibly generated separate regioisomeric photoisomers upon uv irradiation, one of which was characterized by x-ray crystallography. The structure of its precursor was determined using NMR techniques.

Exposure of $FvRu_2(CO)_4$ to an excess of $P(CH_3)_3$ at 120°C afforded trans-$Ru[P(CH_3)_3]_2(CO)_3$ and the novel "ring-slipped" $FvRu[P(CH_3)_3]_2(CO)$, which was characterized by an x-ray structural analysis. A variety of heterodi- and trinuclear complexes incorporating ruthenium were synthesized by exposure of this compound to mononuclear early (Ti, Zr) and late (Cr, Mo, W, Fe) transition-metal reagents. Preliminary studies of the reactions of some of these compounds with various organic substrates were performed.

†W.B. Tolman received support as a W.R. Grace Fellow.

3. Work in Progress

Hetero- and Homonuclear Oligocyclopentadienyl Transition-Metal Complexes (D.A. Newman and K.P.C. Vollhardt)

The synthesis of novel homo- and heterometallic complexes bridged by cyclopentadienyl oligomers has been achieved. The major feature of most of these syntheses involves the use of oxocyclopentenyl as a masked cyclopentadienyl fragment.

The complexes [(3-oxo-1-cyclopentenyl)-η^5-cyclopentadienyl]ML_x [ML_x = $Mo(CO)_3CH_3$, $W(CO)_3CH_3$, or $Mn(CO)_3$] were prepared in low to good yields by combining synthetic organic and organometallic strategies. Those in which M = Mo or W were converted to the monometallic fulvalene (Fv) derivatives [(cyclopentadienyl)-η^5-cyclopentadienyl][$M(CO)_3CH_3$], intermediates on the route to the heterobimetallic systems $FvWMo(CO)_6$, $FvWCr(CO)_6$, and $FvMoCr(CO)_6$, available in adequate yields (29–48%) by this approach. The latter were formed via $Fv[M(CO)_3CH_3][M(CO)_3H]$ intermediates.

The reaction of fulvalene dianion with 3-chloro-2-cyclopentenone followed by treatment with $W(NCCH_3)_3(CO)_3$ led to the preparation of 1- and 2-(3-oxo-1-cyclopentenyl)(η^5:η^5-fulvalene)$(WL_x)_2$ [L_x = $(CO)_3$ or $(CO)_3CH_3$]. The oxocyclopentenyl substituent was converted to the required cyclopentadienyl, which was then complexed to tungsten. An x-ray structural analysis was performed on the novel (η^5:η^5:η^5-1,1′:3′,1″-tercyclopentadienyl)[$W(CO)_3$][$W(CO)_3$]′[$W(CO)_3CH_3$]″. Its most notable feature is the short metal-metal bond (3.266 Å).

The tritungsten complexes of tercyclopentadienyl have been shown to undergo the intermetallic transfer of σ-bound ligands. Crossover labeling experiments revealed that methyl transfer in (η^5:η^5:η^5-1,1′:2′,1″-tercyclopentadienyl)[$W(CO)_3CH_3$]$^-$[$W(CO)_3$]$^-$ is largely intramolecular.

An iterative approach has led to the preparation of the heterotrimetallic complex (η^5:η^5:η^5-1,1′:2′,1″-tercyclopentadienyl)[$W(CO)_3CH_3$][$Re(CO)_3$]′[$Mo(CO)_3CH_3$]″. The synthetic strategy has been modified to

prepare tetratungsten complexes of quatercyclopentadienyl.

Several (fulvalene)diiridium complexes have been synthesized and shown to effect the double activation of benzene C-H bonds. A (fulvalene)ruthenium molybdenum mixed metal system exhibits unique reactivity on exposure to small organic molecules.

1987 PUBLICATIONS AND REPORTS

Refereed Journals

1. I. Amer, H. Amer, R. Ascher, J. Blum, Y. Sasson, and K.P.C. Vollhardt, "Hydrogenation of Arenes by the $RhCl_3$-Aliquat 336 Catalyst. Part 3. Selective Reduction of Polycyclic Compounds," J. Mol. Catal. **39**, 185 (1987).
2. J. Blum, I. Amer, K.P.C. Vollhardt, H. Schwarz, and G. Höhne, "Hydrogenation of Arenes by the $RhCl_3$-Aliquat 336 Catalyst. 4. Hydrogen-Deuterium Exchange and Other Mechanistic Features," J. Org. Chem. **52**, 2804 (1987).
3. I. Amer, T. Bravdo, J. Blum, and K.P.C. Vollhardt, "Selective C-C Bond Hydrogenation in Unsaturated Nitro Compounds in the Presence of the $RhCl_3$-Aliquat 336 Catalyst System," Tetrahedron Lett. **28**, 1321 (1987).

LBL Reports

4. W.B. Tolman (Ph.D. Thesis), "Photochemistry and Ligand Substitution Chemistry of (Fulvalene)-diruthenium(Tetracarbonyl)," LBL-24482.
5. D.A. Newman (Ph.D. Thesis), "Hetero- and Homonuclear Oligocyclopentadienyl Transition Metal Complexes," LBL-24483.

Invited Talks

6. K.P.C. Vollhardt, "From Cyclopentadienylmetals to Polyorganometallics: Remarkable Organometallic Materials," University of Jerusalem, Israel, Mar. 25, 1987; Technion, Haifa, Israel, Mar. 26, 1987; University of Chicago, IL, Mar. 30, 1987; Conference des Grandes Ecoles, Paris, France, May 25, 1987; University of Bordeaux, France, June 1, 1987; University of California Berkeley, Aug. 4, 1987; Stanford University, Stanford, CA, Nov. 25, 1987.
7. K.P.C. Vollhardt, "Novel Organotransition Metal Complexes in Catalysis," University of Lyon I, France, June 10, 1987.

Synthetic and Physical Chemistry*

William L. Jolly, Investigator

INTRODUCTION

The purpose of this project is to use photoelectron spectroscopy to determine the nature of the bonding in significant inorganic and organometallic compounds. By measuring core-electron binding energies of appropriate transition-metal compounds, it is possible to study the interaction of metal d electrons with various ligands and to identify various modes of ligand-metal bonding that have analogues in the intermediates of catalyzed organic reactions. Core binding energies can also be used in conjunction with valence-shell ionization potentials to quantify the bonding or antibonding character of molecular orbitals.

1. Estimated Core-Electron Binding Energies and Their Application in the Interpretation of Valence Ionization Potentials (Publication 1)

W.L. Jolly

Empirical group shifts for estimation of the core-electron binding energies of compounds of 14 elements are evaluated. It is shown, for elements of the first row of the periodic table,. that simple one-parameter group shifts are inadequate for estimating core binding energies of highly positively charged atoms with polarizable ligands. In the case of carbon 1s binding energies, a method involving two parameters — an "electronegativity" parameter and a "polarizability" parameter — is devised that significantly improves the accuracy of the predictions. The nitrogen 1s binding energies of the aminoboranes, NH_2BH_2, $N(CH_3)_2BF_2$, $NH(CH_3)BF_2$, and NH_2BF_2, are estimated. These data, when combined with the nitrogen $p\pi$ ionization potentials, lead to the conclusion that there is an important degree of N-B π bonding in all of these molecules.

1987 PUBLICATIONS AND REPORTS

Refereed Journals

1. W.L. Jolly, "Estimated Core Electron Binding Energies and Their Application in the Interpretation of Valence Ionization Potentials," J. Phys. Chem. **90**, 6790 (1986); LBL-22355.
2. W.L. Jolly, "A Lecture Demonstration: The Induction by Iron(II) of the Oxidation of Iodide by Dichromate," J. Chem. Education **64**, 444 (1987).
3. W.L. Jolly, "B&W Sabatier Print Solarization. What Is It; and How Does It Work?" Darkroom Photography **9**, 30 (1987).

*This work was supported by the Director, Office of Energy Research, Office of Basic Energy Sciences, Chemical Sciences Division of the U.S. Department of Energy under Contract No. DE-AC03-76SF00098.

High-Energy Oxidizers and Delocalized-Electron Solids*

Neil Bartlett, Investigator

INTRODUCTION

The main aim of this program is the synthesis and characterization of new materials that may have value in electrochemical applications or in the efficient conversion of light to electrical energy. The synthetic work tests models and theories that correlate physical properties (such as electrical conductivity) with chemical composition and structure. Major aims in the synthetic strategies are (1) to tailor make the band gap in semiconductor materials and (2) to achieve high carrier concentration and mobility in the conductive materials. The present emphasis is on two-dimensional networks, such as those related to graphite. Electron oxidation of such materials (with accompanying intercalation to form salts) generates durable and conductive materials (some conducting better than aluminum). The layered materials can often be oxidized (and intercalated) electrochemically in reversible processes, and some may find use in high-energy electrodes. Physical and chemical studies are being applied to such materials to determine the structure and bonding changes that accompany oxidation and reduction. Salts that are either proton conductors or fluoride-ion conductors, and that are resistant to oxidation but are not metallic, are being sought as solid electrolytes for use with the metallic layer-material salts.

1. Novel Synthesis of Graphite Fluorometallates with Chlorine-Assisted Oxidation by Lewis-Acid Fluorides (Publication 4)

R. Hagiwara, M. Lerner, and N. Bartlett

Graphite intercalation compounds of main-group metal fluorides are being prepared for the first time utilizing Cl_2 as an oxidizing agent. Graphite does not react at ambient temperatures with Cl_2 or HF. The metal fluorides GeF_4, PF_5, and BF_3 by themselves are also unreactive towards graphite. However, when graphite is brought into interaction with a mixture of one of these fluorides and either Cl_2 or Cl_2 + HF at ambient temperatures, a vacuum-stable fluoride intercalation compound is obtained. Thus, with these oxidizing combinations, it is now possible to produce such fluorometallate salts without the use of elemental fluorine. Table 1-1 shows the enthalpy changes for the formation of metal-fluoride intercalants in some of these reactions. The previously reported[1,2] thermodynamic requirement of ~120 kcal/mol for the formation of first-stage metal-fluoride intercalation compounds in fluorine-assisted reactions can now be expanded. A quantitative relationship between half-reaction enthalpy and higher stage formation is now proposed, which should hold for any fluoro-guest species with effective thickness of a hexafluorospecies oriented along a threefold axis of the octahedron. The reaction of graphite with excess GeF_4 (2 atm) in the presence of 2 atm Cl_2 is observed, on brief evacuation of volatiles, to produce a blue second-stage salt and, eventually, a stable, third-stage material. The GeF_4 + Cl_2 + graphite reaction requires photochemical activation to proceed to a low-stage product. IR spectra of the residual gases reveal the presence of mixed chlorofluorogermanes, which are not produced by reaction of GeF_4 with Cl_2 in the absence of graphite. The reaction of graphite with PF_5 + Cl_2 does not appear to proceed unless HF is present as a reactant; in these reactions HCl is produced. The PF_5 + Cl_2 + HF reaction yields a third-stage salt that becomes fourth-stage after long evacuation. Interaction of graphite with BF_3 + Cl_2 is only observed to

Table 1-1
Enthalpy changes for the formation of some metal fluoride intercalants and the corresponding lowest stages obtained.

Half-reaction	ΔH_{calc}[a] (kcal/mol)	Stage[b]
$e^- + GeF_4 + 1/2F_2 \rightarrow GeF_5^-$	−162	1st
$e^- + 2GeF_4 + 1/2Cl_2 \rightarrow GeF_5^- + GeF_3Cl$	−116[c]	3rd
$e^- + PF_5 + HF + 1/2CL_2 \rightarrow PF_6^- + HCl$	−114	4th
$e^- + BF_3 + HF + 1/2Cl_2 \rightarrow BF_4^- + HCl$	−95	6th

a. ΔH_{calc} are for gas-phase reactions. Fluoride ion affinities have been previously reported [ΔH = −100(8) kcal/mol for GeF_4, ΔH = −92(6) kcal/mol for BF_3, ΔH = −101(8) kcal/mol for PF_5].
b. As determined by x-ray powder diffraction data for the vacuum-stable product.
c. The Ge-F and Ge-Cl bonding energies in GeF_3Cl were approximated by diatomic bond strengths [ΔH = 116(5) kcal/mol for GeF and ΔH = 82(5) kcal/mol for Ge-Cl].

*This work was supported by the Director, Office of Energy Research, Office of Basic Energy Sciences, Chemical Sciences Division of the U.S. Department of Energy under Contract No. DE-AC03-76SF00098.

occur in the presence of HF, yielding a sixth-stage material. The vacuum-stable products in all cases appear to be intercalation salts of metal-fluoroanions. Elemental analyses do not indicate a significant presence of Cl. Powder diffraction data from the new compounds show gallery heights similar to those obtained previously[2] with acid-fluoride/fluorine combinations and are compatible with EF_x species close packed between the carbon layers.

1. N. Bartlett, in *The Chemical Industry*, D.H. Sharp and T.F. West, Eds., Ellis Horwood Ltd., London, Chichester, 1982, p. 292.

2. G.L. Rosenthal, T.E. Mallouk, and N. Bartlett, *Syn. Met.* **9**, 433 (1984).

2. Preparation and Characterization of a New Graphite Relative of Composition BC_2N (Publication 5)

T. Sasaki† and N. Bartlett

Previous syntheses[1,2] of B-C-N graphite-like materials have employed three or more reagents, with the consequence that the product has been a composite, with microscopic homogeneity not guaranteed. To ensure a one-phase product, with homogeneity down to "molecular dimensions," a two-reactant synthetic scheme was sought that had only a one-product path. Such a scheme has been realized in the interaction of acetonitrile and boron trichloride at 850°C or above:

$$BCl_3 + CH_3CN \xrightarrow{\geq 850^\circ} 3HCl + BC_2N$$

The product exhibits the *hk* and *l* reflections typical of an unregistered-layer solid, prominent *d* spacings being similar to those of graphite as follows (all spacings in Å; graphite indexing given in parentheses): 3.40 (002 = 3.35); 2.11 (100 = 2.11); 1.70 (004 = 1.68); 1.22 (110 = 1.22).

Electron microscopic examination shows that the material, as prepared, exhibits a preferred orientation of the microscopic plates, which are stacked parallel to one another. It has also established homogeneity of the solid at least to the 50-Å dimension level, and electron-energy-loss spectroscopy[3] has confirmed the composition BC_2N. The K-edge spectra of the B, C, and N closely resemble those of the same elements in hexagonal BN and graphite. These spectra establish that each element resides in a graphite-like network, the $1s \rightarrow \pi^*$ and $1s \rightarrow \sigma^*$ features being clearly resolved and not significantly shifted from their energy values in graphite and hexagonal BN.

The jet-black solid absorbs light throughout the visible range and into the near infrared. Electrical conductivity measurements give a specific conductivity σ = 18 ohm^{-1} cm^{-1} and have established its semiconductive nature, with log σ being linearly dependent upon the reciprocal temperature; the thermal band gap is 0.03 eV.

A survey of the intercalation chemistry of BC_2N has shown that it more closely resembles graphite than hexagonal BN. It is less easily oxidatively intercalated than is graphite. Thus it does not interact with Br_2 but (like graphite and BN) is intercalated by $S_2O_6F_2$, the dimensions and composition of the first-stage product being similar to those of the graphite relative, as indicated in Table 2-1. Reductive intercalation with Li, Na, and K, to yield first-stage products, has been achieved. The lithium was introduced via the naphthalide in THF, whereas the Na and K compounds were obtained by direct attack of the alkali vapor upon the BC_2N, all in a sealed quartz ampoule (Na, 280°C; K, 260°C). As may be seen from Table 2-1, the interlayer spacing of each first-stage alkali compound compares closely with that of its graphite relative.

†Present address: Mukizaishitsu Kenkyusho, National Institute for Research in Inorganic Materials, 1-1 Namiki, Sakura-Mura, Niihari-Gun, Ibaraki, 305 Japan.

1. A. Badyan, T. Niemski, S. Oppenheimer, and E. Olkusuik, Khim. Svyaz. Popuprov. Polumetallakh., 362 (1972).

2. R.B. Kaner, J. Kouvetakis, C.E. Warble, M.L. Sattler, and N. Bartlett, Mat. Res. Bull. **22**, 399 (1987).

3. Obtained in collaboration with Dr. K. Krishnan, National Center for Electron Microscopy, Lawrence Berkeley Laboratory.

Table 2-1

Comparison of first-stage intercalation compounds of BC_2N with those of graphite relatives.

Composition[a]	Gallery hght (Å)	Composition	Gallery hght (Å)
$(BC_2N)_xSO_3F$	7.7	$Li(BC_2N)_{1.5}$	3.70
x = 2.0−2.5			
C_7SO_3F	7.6[b]	LiC_6	3.70[c]
Composition[a]	**Gallery hght (Å)**	**Composition**	**Gallery hght (Å)**
$Na(BC_2N)_2$	4.20	$K(BC_2N)_2$	5.42
unknown	--	KC_8	5.40[c]

a. The composition of $(BC_2N)_xSO_3F$ was determined by gravimetry. The compositions given for the alkali compounds are those that provided the best agreement for the calculated 00*l* x-ray diffraction line intensities.

b. N. Bartlett, R.N. Biagioni, B.W. McQuillan, A.S. Robertson, and A.E. Thompson, J. Chem. Soc., Chem. Commun., 200 (1978).

c. Yu, N. Novikov and M.E. Vol'pin, Russ. Chem. Rev., **40**, 733 (1971).

3. Work in Progress

Further characterization of the products of the interaction of BCl_3 and benzene has shown that the carbon content increases beyond that required for BC_3 as the temperature is raised above 800°C. At 1000°C the composition is $\sim BC_8$. This carbon supplement derives from the dehydrogenation of benzene ($C_6H_6 \rightarrow 6C + 3H_2$). The composition of the 800°C reaction product is close to BC_3, and four-probe conductivity measurements indicate a specific conductivity for that composition of 1.2×10^3 $ohm^{-1}cm^{-1}$ at 298 K.

An important step forward has been made in the application of salts of the O_2^+ ion in oxidative chemistry. Those studies have been hampered because a noninteractive solvent has not been known. It has been found that $O_2^+SbF_6^-$ (and other O_2^+ salts) dissolve in anhydrous hydrogen fluoride (AHF) and can be recovered quantitatively from it. An associated finding is that O_2F dissolved in AHF is comparable in basicity to alkali fluorides such as KF, dissolved in that solvent.

1987 PUBLICATIONS AND REPORTS

Refereed Journals

1. H. Takenaka, M. Kawaguchi, M. Lerner, and N. Bartlett, "Synthesis and Characterization of Graphite Fluorides by Electrochemical Fluorination in Aqueous and Anhydrous Hydrogen Fluoride," J. Chem. Soc., Chem. Commun., 1431 (1987); LBL-23061.
2. B. Zemva, A. Jesih, D.H. Templeton, A. Zalkin, A.K. Cheetham, and N. Bartlett, "Phases in the System XeF_2/XeF_5AsF_6 and Structural and Vibrational Evidence for the Ionization Pathway: $XeF_2 \rightarrow XeF^+ + F^-$," J. Am. Chem. Soc. **109**, 7420 (1987); LBL-10232.

Other Publications

3. T.J. Richardson, F.L. Tanzella, and N. Bartlett, "Comparison of Polynuclear Aromatic Hydrocarbon Cation Salts with Salts of Simple Fluoroaromatic Cations," in *ACS Advances in Chemistry* Series No. 217, "Chemistry of Polynuclear Aromatics," L. Ebert, Ed., 1987, p. 169; LBL-22089.

LBL Reports

4. R. Hagiwara, M. Lerner, and N. Bartlett, "Novel Synthesis of Graphite Fluorometallates with Chlorine-Assisted Oxidation by Lewis-Acid Fluorides," LBL-24605.
5. T. Sasaki and N. Bartlett, "Preparation and Characterization of a New Graphite Relative of Composition BC_2N," LBL-24606.
6. K. Kourtakis (Ph.D. Thesis), with N. Bartlett, "Energetic and Structural Relationships Involved in the Intercalation of Graphite by Fluorospecies," LBL-23329.

Invited Talks

7. N. Bartlett, "Synthesis and Characterization of New Metals, Semiconductors and Insulators having Graphite-Like Structures," Inorganic Chemistry Colloquium, University of California, Los Angeles, Jan. 14, 1987.
8. N. Bartlett, "The Interplay of Chemistry, Structure and Resistivity in the Graphite Fluoroarsenates and Graphite Fluorides," American Crystallographic Association, University of Texas, Austin, Mar. 19, 1987.
9. N. Bartlett, "New Metallic and Semiconductive Materials based on B/C; C/N; and B/C/N Systems with the Graphite Structure," and "Concerning the Synthesis of Salts of Cations derived from Aromatic Molecules and the Products of F^- attack on those Cations," University of Idaho, Moscow, Mar. 26–27, 1987.
10. N. Bartlett, "Carbon-Boron-Nitrogen Hybrids with the Graphite Structure — Semiconductive Systems," Materials Research Society, Anaheim, CA, Apr. 21, 1987.
11. N. Bartlett, "Novel Metallic and Semiconductive B-C-N Materials having Graphite-Like Structures," Institut Jozef Stefan, Ljubljana, Yugoslavia, June 18, 1987.
12. N. Bartlett, "The Novel Cation $[(XeF)_2CN]^+$ and an Appraisal of the Practical Limits to Noble-Gas Chemistry," Noble Gas Symposium, New Orleans, LA, Aug. 30, 1987.
13. N. Bartlett, "New Metallic and Semiconductors based on the Graphite Structure," Frontiers in Chemistry Series Lecture, Arizona State University, Phoenix, Oct. 2, 1987.
14. N. Bartlett, "New Metallic and Semiconductive Relatives of Graphite: BC_3; C_5N; BCN; and BC_2N," College of the Pacific, Stockton, CA, Oct. 9, 1987.

Transition Metal–Catalyzed Conversion of CO, NO, H_2, and Organic Molecules to Fuels and Petrochemicals*

Robert G. Bergman, Investigator

INTRODUCTION

The goal of this program is the development of new chemical reactions in which transition metals interact with organic materials, and the understanding of how these reactions work. A recent discovery on this project was the finding that certain hydridoiridium and -rhodium complexes undergo oxidative addition into the carbon-hydrogen bonds of completely saturated hydrocarbons (M + R-H → R-M-H). Since this finding was the first example of this long-sought "alkane C-H activation" reaction, research is now being directed at examining the scope, selectivity, and mechanism of the process. During the current year, extensive mechanistic studies were carried out on the first rhodium-based alkane activation system. In this work, strong evidence was obtained that a weak alkane-metal complex is formed on the reaction pathway leading to the final C-H inserted product. In addition, the first quantitative metal-hydrogen and metal-carbon bond dissociation energies were determined for the iridium C-H activating system. These results demonstrated that insertion of iridium into the C-H bonds of alkanes is very exothermic; an even more powerful thermodynamic driving force exists for insertion of the metal into the C-H bonds of arenes.

1. Isomerization of the Hydrido(Alkyl)Rhodium Complexes Formed on Oxidative Addition of Rhodium to Alkane C-H Bonds. Evidence for the Intermediacy of η^2-Alkane Complexes (Publication 1)

R.A. Periana and R.G. Bergman

The products of insertion of the coordinatively unsaturated fragment Cp*RhL (Cp* = η^5-C_5Me_5; L = PMe_3) into alkane C-H bonds are generated by irradiation of Cp*(L)RhH_2, or thermal decomposition of Cp*(L)Rh(neopentyl)(H), at temperatures below −30°C in alkane solvents. The hydrido(alkyl)rhodium products can be converted into the corresponding bromo(alkyl)rhodium complexes, which are stable and can be fully characterized. The structure of the bromo(cyclopropyl) complex has been determined by x-ray diffraction; an ORTEP diagram is illustrated in Figure 1-1. The hydrides can be synthesized independently, also at low temperature, from the corresponding halo(alkyl) complexes by lithiation with t-BuLi followed by protonation. Alternatively, the highly nucleophilic complex Li[Cp*(L)RhH], prepared by deprotonation of Cp*(L)RhH_2, leads to the alkyl(hydrido)rhodium complexes upon treatment with alkyl tosylates R-OTs.

When Cp*RhL is generated in mixtures of linear alkanes, only the products of insertion into primary C-H bonds are observed, even at −100°C. The relative rate constants for the formation of these products correlate directly with the number of secondary C-H bonds in the alkane. This suggests that insertion occurs initially into all the C-H bonds of the alkane, but that even at very low temperatures the secondary insertion products rearrange quickly, and intramolecularly, to the primary products. We suggest that this rearrangement occurs through the intermediacy of η^2–C-H alkane "sigma complexes."

The synthetic procedures summarized above can be used to prepare regiospecifically ^2H and ^{13}C

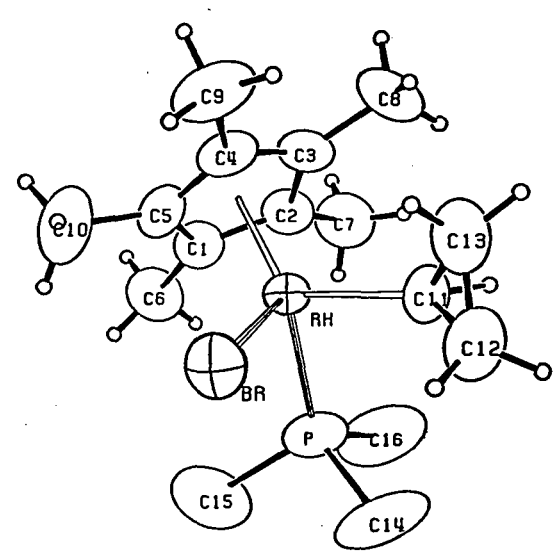

Figure 1-1. ORTEP diagram illustrating the structure of (η^5-C_5Me_5)(PMe_3)(Br)Rh($CH_2CH_2CH_2$). (XBL 884-1334)

*This work was supported by the Director, Office of Energy Research, Office of Basic Energy Sciences, Chemical Sciences Division of the U.S. Department of Energy under Contract No. DE-AC03-76SF00098.

labeled alkyl hydrides at low temperatures. Warming these complexes to temperatures above −80°C in aromatic solvent analysis of the reaction mixture by ^{1}H and ^{13}C NMR spectrometry reveals isotope rearrangements that confirm that the alkyl(hydrido)rhodium complexes are capable of interconverting with one another intramolecularly at rates competitive with, or in some cases faster than, they undergo reductive elimination. For example, rearrangement of the ^{13}C, ^{2}H-labeled ethyl(hydrido)rhodium and the (1-methylcyclopropyl)methyl(hydrido)rhodium complexes has been used to show (Figure 1-2) that the Cp*(L)Rh fragment migrates and inserts most rapidly into the α position of the alkyl group followed by migration to the β and γ positions; reductive elimination is the slowest process that occurs. These results provide further support for the existence of intermediate η^2–C-H alkane complexes.

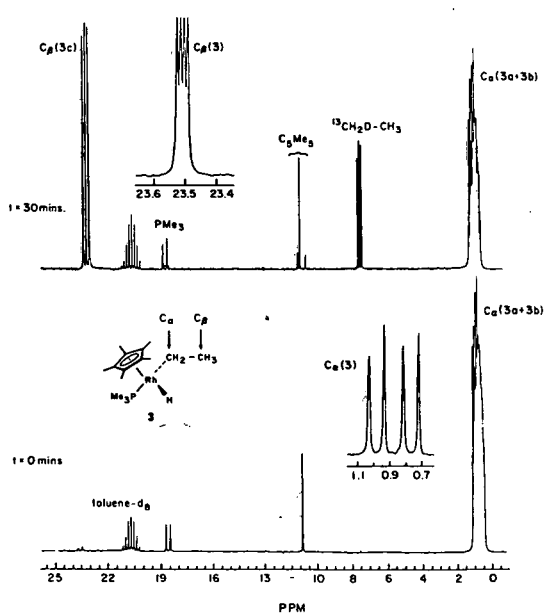

Figure 1-2. The lower half shows the ^{13}C{^{1}H}NMR spectrum (taken in toluene-d$_8$ solution at −60°C) of complex **3** (see insert for drawing of the structure of this compound) labeled with ^{13}C in the α position of the ethyl group and deuterium in the hydride position (**3a**), mixed with a similar amount of the compound labeled with both ^{13}C and deuterium in the α position (**3b**). The upper spectrum shows how the ^{13}C and deuterium isotopes in these molecules have rearranged, and the other products that have formed, after a reaction time of 30 minutes. The new components are β−^{13}C, 2-d-ethyl rhodium complex **3c**, 1-^{13}C,-1-d-ethane (triplet at 8 ppm), and small amounts of toluene C-H activation products (small resonances near 11 ppm). Inset spectra show C$_\alpha$ and C$_\beta$ resonances for the undeuterated ^{13}C labeled complex **3**. (XBL 884-1335)

2. C-C Activation of Organic Small-Ring Compounds by Rearrangement of Cycloalkyl(Hydrido)Rhodium Complexes to Rhodacycloalkanes. Synthesis of Metallacyclobutanes, Including One with a Tertiary M-C Bond, by Nucleophilic Addition to π-Allyl Complexes (Publication 2)

R.A. Periana and R.G. Bergman

Generation of the coordinatively unsaturated fragment [Cp*RhL] (Cp* = η^5-C$_5$Me$_5$; L = PMe$_3$) at −60°C in cyclopropane both by photolysis of Cp*(L)RhH$_2$ and thermal decomposition of Cp*(L)Rh(neopentyl)(H) results only in C-H bond insertion to yield Cp*(L)Rh(cyclopropyl)(H). This complex rearranges at −20°C in arene solvents to the rhodacyclobutane Cp*$\overline{\text{Rh-CH}_2\text{-CH}_2\text{-C}}H_2$ in 65% yield. The structure of this material has been determined by x-ray diffraction; an ORTEP diagram is shown in Figure 2-1. Mechanistic studies of regiospecifically ^{13}C-labeled cyclopropyl(hydrido)rhodium complexes indicate that the rearrangement is intramolecular and occurs by insertion of Cp*RhL into the α-carbon-carbon bond of the cyclopropyl ring. Similarly, C-C activation of 1,1-dimethylcyclopropane is observed to occur by intramolecular rearrangement of Cp*(L)Rh(2,2-dimethylcyclopropyl)(H). This rearrangement occurs with complete regiospecificity yielding only the β,β-dimethylrhodacyclobutane, Cp*(L)$\overline{\text{Rh-CH}_2\text{-CMe}_2\text{-C}}H_2$. The

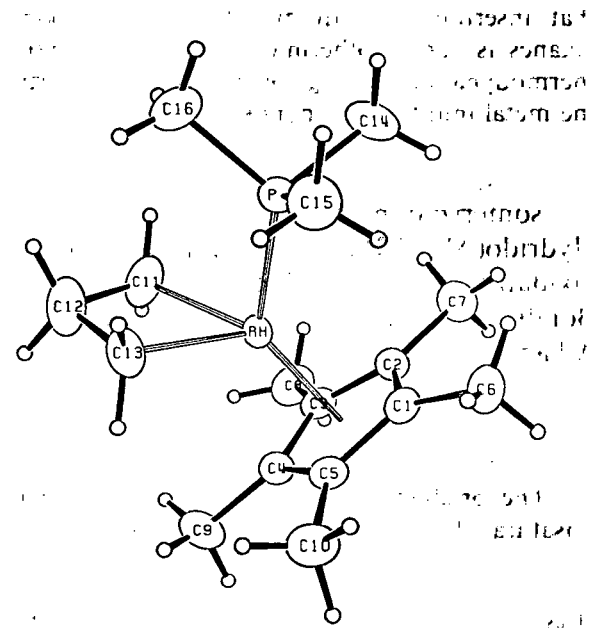

Figure 2-1. ORTEP diagram illustrating the structure of (η^5-C$_5$Me$_5$)(PMe$_3$)$\overline{\text{Rh-(CH}_2\text{CH}_2\text{C}}H_2$). (XBL 884-1336)

possible intermediate formation of the isomeric α,α-dimethyl rhodacyclobutane was ruled out by independent synthesis of this isomer and the demonstration of its stability under the conditions used for isomerization of the cyclopropyl(hydrido)-rhodium complex.

Treatment of $Cp^*(L)Rh(\text{-}\overline{CH\text{-}CR_2\text{-}C}H_2)(X)$ (R = H, Me; X = I) with $AgBF_4$ results in the formation of the catonic π-allyl complexes $[Cp^*(L)Rh(\eta^3\text{-}CR_2\text{-}CH\text{-}CH_2)]^+BF_4^-$ (R = H, Me). Subsequent treatment of these cations with $LiEt_3BH$ results in the clean formation of neutral rhodacyclobutanes $Cp^*(L)\overline{Rh\text{-}CR_2CH_2\text{-}C}H_2$ (R = H, Me). In the case where R = H, the use of $LiEt_3BD$ indicates that the addition of hydride is completely regio- as well as stereospecific, the hydride adding to the β-carbon syn to Cp* ligand.

3. The Heats of Reaction of $Cp^*(PMe_3)Ir(R)(H)$ [R = C_6H_5, C_6H_{11} and H] with HCl, CCl_4, CBr_4, and CH_3I. A Solution Thermochemical Study of Alkane Activation (Publication 3)

S.P. Nolan,[†] C.D. Hoff,[†] P.O. Stoutland, L.J. Newman, J.M. Buchanan, R.G. Bergman, G.K. Yang,[‡] and K.S. Peters[‡]

In reactions where a metal insert into the C-H bonds of alkanes (M + R-H → R-M-H), the sum of the M-H and M-C bond dissociation energies in R-M-H must be comparable to, or larger than, the energy of the alkane C-H bond that is broken. Although this principle is well accepted, little quantitative bond-energy information has been available for third-row metals, which are most often observed to participate in C-H insertion reactions. In this work, using a combination of conventional and photoacoustic calorimetric techniques, the first absolute metal-hydrogen and metal-carbon bond energies have been determined for the iridium-based C-H inserting system $(\eta^5\text{-}C_5Me_5)(PMe_3)Ir + R\text{-}H \rightarrow (\eta^5\text{-}C_5Me_5)(PMe_3)Ir(R)(H)$. Examples of these bond energies are: Ir-H: 74; Ir-cyclohexyl: 51; Ir-phenyl: 81 (all values in kcal/mole). Using these values and the well-known C-H bond energies for alkanes and arenes, it can now be calculated that the insertion of iridium into a C-H bond in cyclohexane is 30 kcal/mole exothermic; insertion into a benzene C-H bond is 45 kcal/mole exothermic. These energies are surprisingly large and demonstrate that it is the possibility of forming strong Ir-H and Ir-C bonds that provides the driving force for C-H insertion in this system.

[†]Present address: Department of Chemistry, University of Miami, Coral Gables, FL.

[‡]Present address: Department of Chemistry, University of Colorado, Boulder, CO.

4. Work in Progress

Projects currently under way are aimed at: (a) studies of insertion of iridium into the C-H bonds of olefins, to determine whether weak complexes different from π-complexes can be detected in the reaction; (b) further studies of the thermodynamics of C-H activation reactions; (c) investigation of the reaction of allyliridium complexes with arenes and alkanes, to determine whether the allyl group can be utilized as a "trap" for the hydride ligand, and the system applied to alkane homologation reactions; (d) development of new dinuclear C-H activation systems.

1987 PUBLICATIONS AND REPORTS

Refereed Journals

1. R.A. Periana and R.G. Bergman, "Isomerization of the Hydrido(Alkyl)Rhodium Complexes Formed on Oxidative Addition of Rhodium to Alkane C-H Bonds. Evidence for the Intermediacy of η^2-Alkane Complexes," J. Am. Chem. Soc. **108**, 7332 (1986); LBL-21317.
2. R.A. Periana and R.G. Bergman, "C-C Activation of Organic Small Ring Compounds by Rearrangement of Cycloalkyl(Hydrido)Rhodium Complexes to Rhodacycloalkanes. Synthesis of Metallacyclobutanes, Including One with a Tertiary M-C Bond, by Nucleophilic Addition to π-Allyl Complexes," J. Am. Chem. Soc. **108**, 7436 (1986); LBL-21316.
3. S.P. Nolan, C.D. Hoff, P.O. Stoutland, L.J. Newman, J.M. Buchanan, R.G. Bergman, G.K. Yang, and K.S. Peters, "The Heats of Reaction of $Cp^*(PMe_3)Ir(R)(H)$ [R = C_6H_5, C_6H_{11} and H] With HCl, CCl_4, CBr_4 and CH_3I. A Solution Thermochemical Study of Alkane Activation," J. Am. Chem. Soc. **109**, 3143 (1987); LBL-24541.

LBL Reports

4. P.O. Stoutland, R.G. Bergman, S.P. Nolan, and C.D. Hoff, "The Thermodynamic Driving Force for C-H Activation at Iridium," submitted to *Polyhedron*, "Symposium-in-Print" on "Metal-Ligand Bonding Energetics in Organotransition Metal Compounds," LBL-24357.

5. P.O. Stoutland and R.G. Bergman, "C-H Insertion and π-Complex Formation of $(\eta^5\text{-}C_5Me_5)(PMe_3)Ir$ with Ethylene: An Intra- and Intermolecular Isotope Effect Study," submitted to J. Am. Chem. Soc.; LBL-24358.
6. W.D. McGhee and R.G. Bergman, "Synthesis of an $(\eta^3$-Allyl)(Hydrido)Iridium Complex and Its Reaction with Arenes and Alkanes. Sequential Intermolecular C-H Oxidative Addition and Hydride-to-Alkene Migratory Insertion Reactions," submitted to J. Am. Chem. Soc.; LBL-24231.
7. P.O. Stoutland (Ph.D. Thesis), "Reactive Intermediates in Organometallic Chemistry," LBL-24359.
8. W.D. McGhee (Ph.D. Thesis), "The Synthesis and Chemistry of Organoiridium Allyl and Oxo Complexes," LBL-24230.

Invited Talks

9. R.G. Bergman, "Alkane C-H Activation Using Organotransition Complexes," Department of Chemistry, California State University, Hayward, CA, Jan. 14, 1987.
10. R.G. Bergman, "Organic Transformations Mediated by Organotransition Metal Complexes," Herbert C. Brown Lectures in Organic Chemistry, Department of Chemistry, Purdue University, West Lafayette, IN, Apr. 4, 1987.
11. R.G. Bergman, "Reactions of Transition Metal Enolates," Department of Chemistry, University of Pennsylvania, Philadelphia, Mar. 31, 1987.
12. R.G. Bergman, "Carbon-Carbon Bond Forming Reactions Using Organotransition Metal Enolates," Department of Chemistry, Indiana University, Bloomington, Apr. 1, 1987.
13. R.B. Bergman, "Synthesis and Chemistry of Metal Alkoxide Complexes," Department of Chemistry, Indiana University, Bloomington, Apr. 2, 1987.
14. R.G. Bergman, 1987 Frontiers in Chemistry Lecture, Department of Chemistry, University of Toledo, OH: "Values in Science," May 20, 1987; "Activation of Carbon-Hydrogen Bonds in Organic Molecules Using Organotransition Metal Complexes," May 21, 1987; "Synthesis of Electron-Rich Metal Alkoxide Complexes and their Reactions with Organic Compounds," May 22, 1987.
15. R.G. Bergman, "Transformations of Organic Compounds Mediated by Organotransition Metal Complexes," Department of Chemistry, Harvard University, Cambridge, MA, July 10, 1987.
16. R.G. Bergman, "Perspectives In the Selective Activation of C-H and C-C Bonds in Saturated Hydrocarbons," Nato Workshop, Bonas, Gers, France, July 3, 1987.
17. R.G. Bergman, "Reactions of Metal Alkoxides with Organic Compounds," Laboratoire de Chemie Organique et Organometallique, University of Bordeaux I, France, June 25, 1987.
18. R.G. Bergman, "Carbon-Carbon Bond-Forming Reactions of Organotransition Metal Enolate Complexes," Fourth IUPAC Symposium on Organometallic Chemistry Directed Toward Organic Synthesis, Vancouver, BC, July 27, 1987.
19. R.G. Bergman, "Reactions of Late-Transition Metal Complexes With Metal-Oxygen Bonds," Gordon Conference on Organometallic Chemistry, Salve Regina College, Newport, RI, July 24, 1987.
20. R.G. Bergman, "Summary of Activation of Alkanes in Homogenous Solution Using Organotransition Metals," Symposium on Molecular Phenomena at Electrode Surfaces, Division of Colloid and Surface Chemistry, New Orleans, LA, Sept. 2, 1987.
21. R.G. Bergman, "Reactions of Organic Compounds Mediated by Organotransition Metal Complexes," ACS Arthur Cope Scholar Award Address, New Orleans, LA, Sept. 1, 1987.
22. R.G. Bergman, "Reactions of Metal Oxo and Alkoxide Complexes With Organic Compounds," Department of Chemistry, University of Miami, Coral Gables, FL, Nov. 13, 1987; Department of Chemistry, University of Puerto Rico, Rio Piedras, Puerto Rico, Nov. 16, 1987.
23. R.G. Bergman, 1987 Lemieux Lectures, Department of Chemistry, University of Ottawa, Ontario: "Activation of Carbon-Hydrogen Bonds Using Organotransition Metal Enolates," Dec. 7, 1987; "Carbon-Carbon Bond-Forming Reactions of Organotransition Metal Enolates," Dec. 8, 1987; "Synthesis of Metal Alkoxides and their Reactions with Organic Compounds," Dec. 9, 1987.
24. R.G. Bergman, "Synthesis of Metal Alkoxides and their Reactions with Organic Compounds," Department of Chemistry, University of Virginia, Charlottesville, VA, Dec. 11, 1987.

CHEMICAL ENGINEERING SCIENCES

High-Pressure Phase Equilibria in Hydrocarbon-Water (Brine) Systems*

John M. Prausnitz, Investigator

INTRODUCTION

Phase equilibria are required for efficient design of large-scale separation processes (e.g., distillation and extraction) in the chemical and related industries. In this context, "efficient" refers to optimum use of raw materials and to conservation of energy.

Since the variety of technologically important fluid mixtures is extremely large, it is not possible to obtain all desired equilibria from experiment. Therefore, the objective of this research is the development of molecular thermodynamics for the interpretation and correlation of selected phase-equilibrium data toward reliable prediction of phase equilibria for computer-aided engineering design. The correlations are expressed through semitheoretical physicochemical models. In this research, particular attention is given to those systems that are of primary interest in energy-related industries, especially those concerned with fossil fuels, aqueous mixtures containing electrolytes, fossil-fuel/water mixtures, agricultural products, and mixtures encountered in biotechnology.

Development of molecular thermodynamics calls for a combination of theoretical, computational, and experimental work. Further, it demands simultaneous awareness first, of progress in molecular science and second, of realistic requirements for engineering design.

*This work was supported by the Director, Office of Energy Research, Office of Basic Energy Sciences, Chemical Sciences Division of the U.S. Department of Energy under Contract No. DE-AC03-76SF00098.

1. Molecular Thermodynamics of Aqueous Solutions Containing Electrolytes and Nonelectrolytes (Publication 18)

R.K. Kruppa,† A.H. Harvey, and J.M. Prausnitz

To measure phase-equilibrium data in mixtures containing electrolytes and nonelectrolytes, an experimental apparatus has been designed and constructed. The composition of both phases is analyzed from small samples. A circulation system mixes the components to ensure equilibrium. The equipment can withstand conditions of 250°C and 140 MPa. Experimental safety is a key element of the design. It can be used for systems containing combustible gases; the first application is to measure the solubility of CH_4 in NaCl solutions at high pressures.

Phase equilibria are predicted from a new equation of state applicable to high pressures and all practical fluid densities. The Helmholtz energy of a mixture of electrolytes and nonelectrolytes is calculated from molecular theory. Pure-component and binary parameters are used to adjust the equation of state to experimental data. The model predicts the solubility of CO_2 in pure water at pressures to 100 MPa with a maximum deviation of less than 0.3 mole%. When applied to ternary mixtures containing electrolytes, the salting-out effect is represented correctly even at high pressures.

†Present address: Lehrstuhl B für Thermodynamik, Technische Universität München, 8000 Munich, Federal Republic of Germany.

2. Extraction of Fatty-Acid Methyl Esters with Supercritical Carbon Dioxide (Publication 17)

A.H. Wu, A. Stammer,† and J.M. Prausnitz

A flow apparatus was constructed to measure vapor-phase compositions of systems containing fatty-acid methyl esters as solute and supercritical carbon dioxide as solvent at 65 to 200 bar. The equilibrium cell consists of a packed bed of liquid

(or solid) solute coated on an inert solid support that is commonly used in gas-chromatographic columns.

Experimental measurements were obtained for five binary systems containing methyl myristate, methyl stearate, methyl oleate, methyl linoleate, or methyl laurate. Each system was measured at 40 and 60°C and at a pressure below the critical pressure of the mixture. In addition, a ternary system containing carbon dioxide, methyl oleate, and methyl linoleate was measured at 60°C and 107 bar.

The measured solubility data were correlated using an equation of state that has a perturbation term of the van der Waals form and a reference system proposed by Boublik and Mansoori. A quadratic mixing rule with one binary parameter is suitable for these mixtures.

---

†Present address: Institut für Thermische Verfahrenstechnik, Universität Karlsruhe, 7500 Karlsruhe, Federal Republic of Germany.

3. A Cubic Equation of State for High-Pressure Phase Equilibria of Mixtures Containing Polymers and Volatile Fluids (Publication 22)

T. Sako,† A.H. Wu, and J.M. Prausnitz

Generalized van der Waals theory is used to obtain a three-parameter cubic equation of state that is applicable to fluids containing small or large molecules, including polymers. Upon extension to mixtures, the equation of state is used to calculate high-pressure phase equilibria for the ethylene-polyethylene system. The relatively simple equation may be useful for engineering-design calculations for fluid mixtures containing polymers.

---

†Present address: National Chemical Laboratory for Industry, Yatabe, Ibaraki 305, Japan.

4. Liquid-Liquid Equilibria for Water-Toluene-Phenol Mixtures at 150 and 200°C (Publication 20)

H.H. Hooper, S. Michel, and J.M. Prausnitz

Mutual solubilities at the three-phase equilibrium pressure have been measured for ternary aqueous mixtures containing toluene and phenol. The equilibrium compositions of both liquid phases, and the three-phase equilibrium pressures are reported in the temperature range 150–200°C.

5. Molecular Thermodynamics of Partially Ordered Fluids: Phase Behavior of Microemulsions (Publication 21)

Y. Hu† and J.M. Prausnitz

Mixtures of water, oil, and surfactant often form microemulsions where tiny drops of oil (or water) are dispersed in a matrix of water (or oil). A microemulsion is a partially ordered fluid where the surfactant molecules exist in an oriented layer at the boundary between the continuous phase and the discontinuous phase. This work proposes a molecular-thermodynamic model that is useful for calculating a variety of phase diagrams observed in microemulsion-forming systems.

The model is based on a revised form of Widom's abstract representation of a microemulsion; that representation provides a procedure for calculating essential contributions to the configurational entropy. In Widom's representation, all molecules are difunctional dumbbells such that all the hydrophilic ends are situated together in some lattice sites and all the lipophilic ends are situated together in other sites. A form of Guggenheim's quasichemical theory is used to evaluate the combinatorial contributions that correspond to Widom's picture. Chemical association of surfactant molecules and physical interactions are also taken into account. Minimization of the Gibbs energy yields a distribution function for representing micelle sizes.

Calculated ternary phase diagrams are in good agreement with experimental results. Different types of diagrams can be obtained upon changing physically significant model parameters. A study of how these parameters affect phase behavior provides insight on microemulsion stability.

---

†Present address: East China Institute of Technology, Shanghai, People's Republic of China.

6. Thermodynamics of Liquid-Liquid Equilibria Including the Critical Region: Binary and Ternary Mixtures (Publication 19)

J.J. de Pablo and J.M. Prausnitz

To obtain good representation in the critical region, a semitheoretical correction is added to a conventional expression (e.g., van Laar or NRTL) for the excess Gibbs energy of a binary or ternary system. This correction is an exponential function

of a carefully defined distance from the critical point; it is appreciable in the critical region but not elsewhere. In the exponential argument, two parameters are determined from theoretical scaling laws. While the coordinates of the critical point must be known (or estimated), no phase-equilibrium data in the critical region are required to determine parameters. The semiclassical method presented here provides an excellent continuous approximation for phase equilibria close to and remote from critical conditions. Further, the method allows simultaneous representation of vapor-liquid equilibria and liquid-liquid equilibria including the critical region.

7. Thermodynamic Properties of Polar Fluids from a Perturbed-Dipolar-Hard-Sphere Equation of State (Publication 10)

P.F. Bryan[†] and J.M. Prausnitz

Based on theoretical results for a system of hard spheres with dipoles, a new equation of state is applied to the correlation of thermodynamic properties for four fluids: argon, ammonia, water, and acetonitrile. The reference system has the same dependence on density as that given by the Carnahan-Starling equation, but the coefficients are now functions of temperature through the reduced dipole moment. These coefficients are chosen to match the Padé approximant developed by Rushbrooke, Stell, and Høye for the Helmholtz energy of dipolar hard spheres. The reference system proposed here shows a phase transition for reduced dipole moments greater than 1.9. A simple empirical perturbation term is added to the reference system to account for induction and dispersion forces. For polar fluids, the equation gives results significantly better than those obtained from conventional cubic equations of state, when using the same limited experimental data for determining equation-of-state parameters.

[†]Present address: Chemical Engineering and Petroleum Refining Department, Colorado School of Mines, Golden, CO.

8. A Correlation for Thermodynamic Properties of Heavy Fossil-Fuel Fractions (Publication 16)

B.J. Schwarz and J.M. Prausnitz

A correlation is developed for calculation of thermodynamic properties of heavy fossil fuels, based on a recent version of the perturbed-hard-chain equation of state. Since the correlation does not require experimental vapor pressures or densities as input data, it is useful for heavy fossil fuels where vapor pressures and densities are difficult or impossible to measure. For fossil-fuel fractions, equation-of-state parameters are found from approximate molecular-structure (characterization) data coupled with a calibration based on pure-component (model compound) data. Interaction parameters are given for mixtures of fossil fuels with methane, ethane, carbon dioxide, hydrogen, and hydrogen sulfide. While the correlation presented here is useful for calculating vapor-liquid equilibria, it is not intended for conventional fossil fuels, where other correlations are satisfactory. Instead, it is intended for heavy fossil fuels, where conventional correlations are often not reliable and where the usual input data are often unavailable.

9. Work in Progress

Efforts are directed at experimental and molecular-thermodynamic studies of (a) high-pressure vapor-liquid equilibria in multicomponent aqueous systems containing salts and common gases; (b) liquid-liquid equilibria for ternary mixtures of water, thiophene, and pyridine; (c) high-pressure liquid-liquid equilibria in aqueous systems containing polymers, salts, and carbon dioxide; (d) solubilities of agricultural products in compressed carbon dioxide; (e) phase equilibria in aqueous mixtures containing water-soluble polymers and biomolecules; (f) enzyme-catalyzed transesterification in compressed carbon dioxide; (g) phase equilibria in the critical region of binary and ternary mixtures; and (h) enzyme-catalyzed production of high-value chemicals using a reversed-micelle reactor.

1987 PUBLICATIONS AND REPORTS

Refereed Journals

1. F.E. Anderson and J.M. Prausnitz, "Mutual Solubilities and Vapor Pressures for Binary and Ternary Aqueous Systems Containing Benzene, Toluene, m-Xylene, Thiophene, and Pyridine in the Region 100–200°C," Fluid Phase Equilib. **32**, 63 (1986); LBL-20851.
2. M. Radosz, R.L. Cotterman, and J.M. Prausnitz, "Phase Equilibria in Supercritical Propane Systems for Separation of Continuous Oil Mixtures," Ind. Eng. Chem. Res. **26**, 731 (1987); LBL-20868.
3. P.A. Rodgers, A.L. Creagh, M.M. Prange, and J.M. Prausnitz, "Molecular-Weight Distributions for Heavy Fossil Fuels from Gel-Permeation Chromatography and Characterization Data," Ind. Eng. Chem. Res. **26**, 2312 (1987); LBL-22000.
4. B.J. Schwarz, J.A. Wilhelm, and J.M. Prausnitz, "Vapor Pressures and Saturated-Liquid Densities of Heavy Fossil-Fuel Fractions," Ind. Eng. Chem. Res. **26**, 2353 (1987); LBL-22250.
5. B.J. Schwarz and J.M. Prausnitz, "Solubilities of Methane, Ethane and Carbon Dioxide in Heavy Fossil-Fuel Fractions," Ind. Eng. Chem. Res. **26**, 2360 (1987); LBL-22383.
6. K. Kawazuishi and J.M. Prausnitz, "Correlation of Vapor-Liquid Equilibria for the System Ammonia–Carbon Dioxide–Water," Ind. Eng. Chem. Res. **26**, 1482 (1987); LBL-22402.
7. A.H. Harvey and J.M. Prausnitz, "Dielectric Constants of Fluid Mixtures over a Wide Range of Temperature and Density," J. Soln. Chem. **16**, 857 (1987); LBL-22520.
8. S.F. Sciamanna and J.M. Prausnitz, "Thermodynamics of Highly Dilute Solutions and the Quest for Ultrapurity," AIChE J. **33**, 1315 (1987); LBL-22521.
9. W. Raatschen, A.H. Harvey, and J.M. Prausnitz, "Equation of State for Solutions of Electrolytes in Mixed Solvents," Fluid Phase Equilib. **38**, 19 (1987); LBL-22646.
10. P.F. Bryan and J.M. Prausnitz, "Thermodynamic Properties of Polar Fluids from a Perturbed-Dipolar-Hard-Sphere Equation of State," Fluid Phase Equilib. **38**, 201 (1987); LBL-22693.
11. M. Zou and J.M. Prausnitz, "Vapor-Liquid and Liquid-Liquid Equilibria in Binary Aqueous Systems," J. Chem. Eng. Data **32**, 34 (1987).
12. M.M. Abbott and J.M. Prausnitz, "Generalized van der Waals Theory: A Classical Perspective," Fluid Phase Equilib. **37**, 29 (1987).

Other Publications

13. R.C. Reid, J.M. Prausnitz, and B.E. Poling, *The Properties of Gases and Liquids*, 4th Edition, McGraw-Hill, New York, 1987.
14. M.M. Abbott and J.M. Prausnitz, "Phase Equilibria," in *Handbook of Separation Process Technology*, R.W. Rousseau, Ed., Wiley-Interscience, New York, 1987, p. 3.

LBL Reports

15. Y. Liu and J.M. Prausnitz, "Thermodynamics of Concentrated Electrolyte Solutions," LBL-22763.
16. B.J. Schwarz and J.M. Prausnitz, "A Correlation for Thermodynamic Properties of Heavy Fossil-Fuel Fractions," accepted by Ind. Eng. Chem. Res.; LBL-23918.
17. A.H. Wu, A. Stammer, and J.M. Prausnitz, "Extraction of Fatty-Acid Methyl Esters with Supercritical Carbon Dioxide," LBL-24201.
18. R.K. Kruppa, A.H. Harvey, and J.M. Prausnitz, "Molecular Thermodynamics of Aqueous Solutions Containing Electrolytes and Nonelectrolytes," LBL-24206.
19. J.J. de Pablo and J.M. Prausnitz, "Thermodynamics of Liquid-Liquid Equilibria Including the Critical Region: Binary and Ternary Mixtures," accepted by AIChE J.; LBL-24207.
20. H.H. Hooper, S. Michel, and J.M. Prausnitz, "Liquid-Liquid Equilibria for Water-Toluene-Phenol Mixtures at 150 and 200°C," LBL-24245.
21. Y. Hu and J.M. Prausnitz, "Molecular Thermodynamics of Partially-Ordered Fluids: Phase Behavior of Microemulsions," submitted to AIChE J.; LBL-24266.
22. T. Sako, A.H. Wu, and J.M. Prausnitz, "A Cubic Equation of State for High-Pressure Phase Equilibria of Mixtures Containing Polymers and Volatile Fluids," LBL-24276.

Invited Talks

23. J.M. Prausnitz, "Molecular Thermodynamics for Chemical Process Design," University of Wisconsin, Madison, Apr. 1987, University of Missouri, Rolla, Oct. 1987.
24. J.M. Prausnitz, "Phase Equilibria in Aqueous Polymer Systems," European Society for Chemical Engineering Thermodynamics, Solstrand, Norway, June 1987.
25. J.M. Prausnitz, "Thermodynamic Properties of Polar Fluids from a Dipole-Hard-Sphere Equation of State," Technical University of Berlin, Federal Republic of Germany, June 1987.
26. J.M. Prausnitz, "The Legacy of Carl von Linde," Deutscher Kältetechnischer Verein, Cologne, Federal Republic of Germany, Nov. 1987.
27. A.H. Harvey (speaker) and J.M. Prausnitz, "Vapor-Liquid Equilibria for Systems Containing Electrolytes and Nonelectrolytes from a Single Equation of State," 8th International Symposium on Solute-Solute-Solvent Interactions, Regensburg, Federal Republic of Germany, Aug. 1987.
28. J.J. de Pablo (speaker) and J.M. Prausnitz, "Thermodynamics of Liquid-Liquid Equilibria Including the Critical Region: Binary and Ternary Systems," American Institute of Chemical Engineers Annual Meeting, New York, Nov. 1987.

Nuclear Sciences

LOW-ENERGY NUCLEAR SCIENCES

HEAVY-ELEMENT CHEMISTRY

Actinide Chemistry*

Norman M. Edelstein, Richard A. Andersen, Kenneth N. Raymond, Glenn T. Seaborg, Andrew Streitwieser, Jr., David H. Templeton, and Alan Zalkin, Investigators

INTRODUCTION

The purpose of this project is to study actinide materials in order to provide the basic knowledge necessary for their safe and economic utilization in present and future technology. The program includes the preparation of new gaseous, liquid, and solid phases and studies of their physical and chemical properties. Techniques for characterization include x-ray diffraction, optical and vibrational spectroscopy, magnetic resonance, and magnetic susceptibility. Equilibrium and kinetic data for complex formation are measured. From these complementary studies, new insights into the structural and chemical principles of actinide compounds are obtained with which to design new synthetic schemes to produce new materials.

A major aspect of the program is the design and synthesis of sequestering agents for actinide ions. These compounds are intended for use in the treatment of actinide poisoning and for possible application in the treatment of spent reactor fuels. Preparative, structural, and physical studies of new types of organoactinide, related organolanthanide, and new actinide inorganic complexes are continuing. Studies on optical spectra of free ions and actinide ions in crystals are being pursued in order to understand their electronic structure.

ACTINIDE-SPECIFIC SEQUESTERING AGENTS

The purpose of this work is the preparation and characterization of a series of encapsulated, kinetically inert lanthanide amine complexes. Such complexes are of interest in nuclear medicine (diagnosis and radiation therapy) and can serve as models for the synthesis of sequestering agents for the actinides. A novel template approach is used for the encapsulation of the lanthanide ion. The resulting complexes are characterized by spectroscopic methods, including single-crystal x-ray diffraction, and by electrochemical techniques.

1. Kinetically Inert Lanthanide Amine Complexes (Publication 43)

P.H. Smith† and K.N. Raymond

The purpose of this work is to answer three basic questions: (1) Is it possible to encapsulate a lanthanide ion in a ligand cage, thereby rendering it kinetically inert to ligand exchange? (2) If so, what are the properties of such materials? (3) Using amine ligation, what can be learned about the lanthanide amine coordination chemistry?

To answer these questions, complexes of La, Ce, Pr, Eu, and Yb with 1,9-bis(2-aminoethyl)-1,4,6,9,12,14-hexaazacyclohexadecane (L) (Figure 1-1) have been prepared, using a previously described template approach, involving the reaction of the metal trifluoromethanesulfonate (trif) salt as the template source with two equivalents of the tetradentate amine 2, 2′, 2″-tris(2-aminoethyl)amine (tren) and an excess of the formaldehyde derivative bis(dimethylamino)methane. An analogous lanthanum triflate complex, $[La(L')](trif)_3$ [L′ = N,N′-bis(tris-2-aminoethylamino)methane], has been prepared and structurally characterized (see Figure 1-2). The structure is similar to the previously described dibridged complex $[LaL](trif)_3 \cdot CH_3CN$, and a comparison of these structures suggests possible explanations for the difficulties in obtaining the fully encapsulated lanthanide complex.

The preparation and structure of the first example of a mixed ligand lanthanide amine complex, $[Pr(tren)(trien)](trif)_3$ [trien = triethylenetetramine] (Figure 1-3), was investigated in an attempt to characterize the preferred geometry and appropriate bridging units for interconnecting the amine groups.

*This work was supported by the Director, Office of Energy Research, Office of Basic Energy Sciences, Chemical Sciences Division of the U.S. Department of Energy under Contract No. DE-AC03-76SF00098.

†Present address: Los Alamos National Laboratory, Los Alamos, NM.

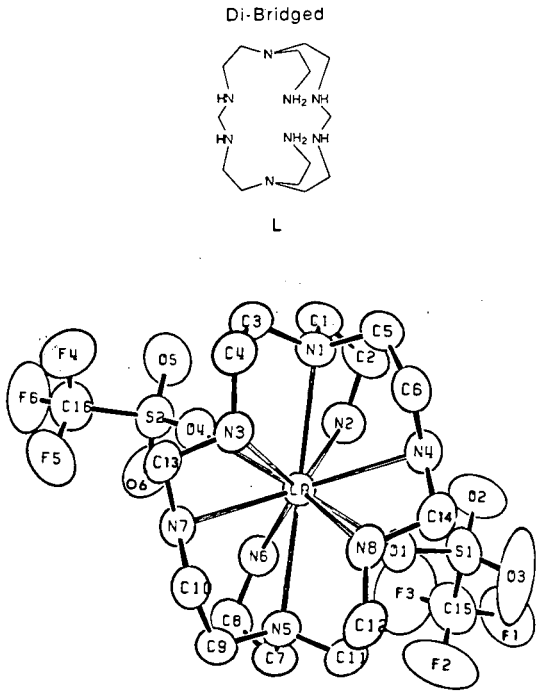

Figure 1-1. ORTEP drawing of the dibridged cation $[La(L)(trif)]^{2+}$, along with a schematic drawing of the dibridged ligand. (XBL 8712-5355)

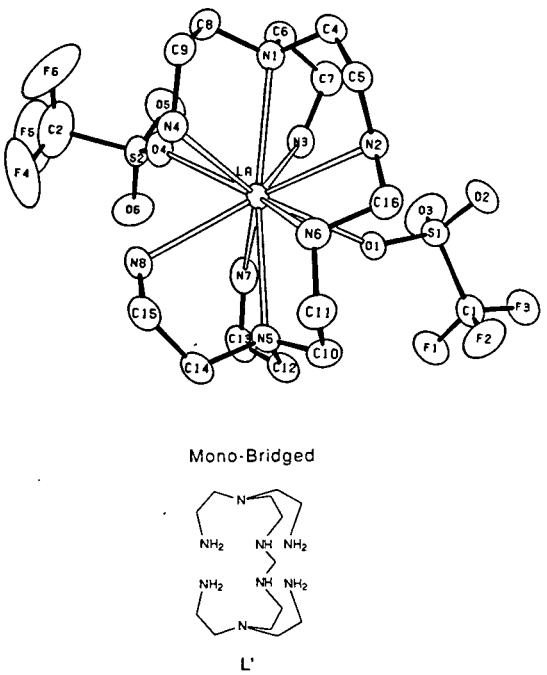

Figure 1-2. ORTEP drawing of the monobridged cation $[La(L')(trif)_2]^+$, along with a schematic drawing of the monobridged ligand. (XBL 8712-5356)

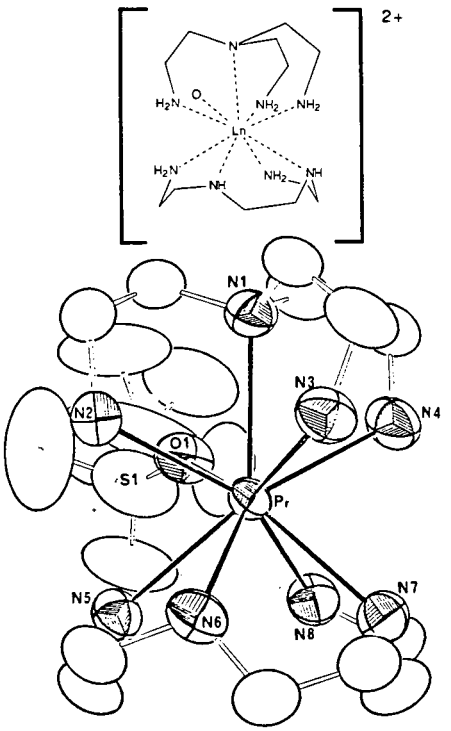

Figure 1-3. ORTEP drawing of the cation $[Pr(tren)(trien)(trif)]^{2+}$, along with a schematic drawing of the complex. (XBL 8712-5357)

SYNTHETIC AND STRUCTURAL STUDIES OF ACTINIDES AND OTHER COMPOUNDS

2. Electron-Transfer Reactions of Divalent Ytterbium Metallocenes; Synthesis of the Series $[(Me_5C_5)_2Yb]_2$ [μ-E], where E is O, S, Se, or Te, and Crystal Structure of $[(Me_5C_5)_2Yb]_2$ [μ-Se] (Publication 34)

D.J. Berg, C.J. Burns, R.A. Andersen, and A. Zalkin

The preparation of the divalent, base-free compounds $(Me_5C_5)_2M$, where M = Eu or Sm, from their respective diethyl ether complexes is described. Reaction of $(Me_5C_5)_2M$, where M = Yb or Sm, with N_2O gives $[(Me_5C_5)_2M]_2$ [μ-O] in high yield. Additionally, $(Me_5C_5)_2Yb$ reacts with Ph_3PS or As_2S_3 or COS, Ph_3PSe or elemental Se, n-Bu_3PTe or elemental Te, to give the bridging chalcogenides $[(Me_5C_5)_2Yb]_2$ [μ-E], where E is S, Se, or Te, respectively. Magnetic susceptibility studies show that there is no magnetic exchange between the paramagnetic f-metals across the bridging group-16 dianions. The variable-temperature magnetic studies also show

LOW-ENERGY NUCLEAR SCIENCES

HEAVY-ELEMENT CHEMISTRY

Actinide Chemistry*

Norman M. Edelstein, Richard A. Andersen, Kenneth N. Raymond, Glenn T. Seaborg, Andrew Streitwieser, Jr., David H. Templeton, and Alan Zalkin, Investigators

INTRODUCTION

The purpose of this project is to study actinide materials in order to provide the basic knowledge necessary for their safe and economic utilization in present and future technology. The program includes the preparation of new gaseous, liquid, and solid phases and studies of their physical and chemical properties. Techniques for characterization include x-ray diffraction, optical and vibrational spectroscopy, magnetic resonance, and magnetic susceptibility. Equilibrium and kinetic data for complex formation are measured. From these complementary studies, new insights into the structural and chemical principles of actinide compounds are obtained with which to design new synthetic schemes to produce new materials.

A major aspect of the program is the design and synthesis of sequestering agents for actinide ions. These compounds are intended for use in the treatment of actinide poisoning and for possible application in the treatment of spent reactor fuels. Preparative, structural, and physical studies of new types of organoactinide, related organolanthanide, and new actinide inorganic complexes are continuing. Studies on optical spectra of free ions and actinide ions in crystals are being pursued in order to understand their electronic structure.

ACTINIDE-SPECIFIC SEQUESTERING AGENTS

The purpose of this work is the preparation and characterization of a series of encapsulated, kinetically inert lanthanide amine complexes. Such complexes are of interest in nuclear medicine (diagnosis and radiation therapy) and can serve as models for the synthesis of sequestering agents for the actinides. A novel template approach is used for the encapsulation of the lanthanide ion. The resulting complexes are characterized by spectroscopic methods, including single-crystal x-ray diffraction, and by electrochemical techniques.

1. Kinetically Inert Lanthanide Amine Complexes (Publication 43)

P.H. Smith† and K.N. Raymond

The purpose of this work is to answer three basic questions: (1) Is it possible to encapsulate a lanthanide ion in a ligand cage, thereby rendering it kinetically inert to ligand exchange? (2) If so, what are the properties of such materials? (3) Using amine ligation, what can be learned about the lanthanide amine coordination chemistry?

To answer these questions, complexes of La, Ce, Pr, Eu, and Yb with 1,9-bis(2-aminoethyl)-1,4,6,9,12,14-hexaazacyclohexadecane (L) (Figure 1-1) have been prepared, using a previously described template approach, involving the reaction of the metal trifluoromethanesulfonate (trif) salt as the template source with two equivalents of the tetradentate amine 2, 2′, 2″-tris(2-aminoethyl)amine (tren) and an excess of the formaldehyde derivative bis(dimethylamino)methane. An analogous lanthanum triflate complex, $[La(L')](trif)_3$ [L′ = N,N′-bis(tris-2-aminoethylamino)methane], has been prepared and structurally characterized (see Figure 1-2). The structure is similar to the previously described dibridged complex $[LaL](trif)_3 \cdot CH_3CN$, and a comparison of these structures suggests possible explanations for the difficulties in obtaining the fully encapsulated lanthanide complex.

The preparation and structure of the first example of a mixed ligand lanthanide amine complex, $[Pr(tren)(trien)](trif)_3$ [trien = triethylenetetramine] (Figure 1-3), was investigated in an attempt to characterize the preferred geometry and appropriate bridging units for interconnecting the amine groups.

*This work was supported by the Director, Office of Energy Research, Office of Basic Energy Sciences, Chemical Sciences Division of the U.S. Department of Energy under Contract No. DE-AC03-76SF00098.

†Present address: Los Alamos National Laboratory, Los Alamos, NM.

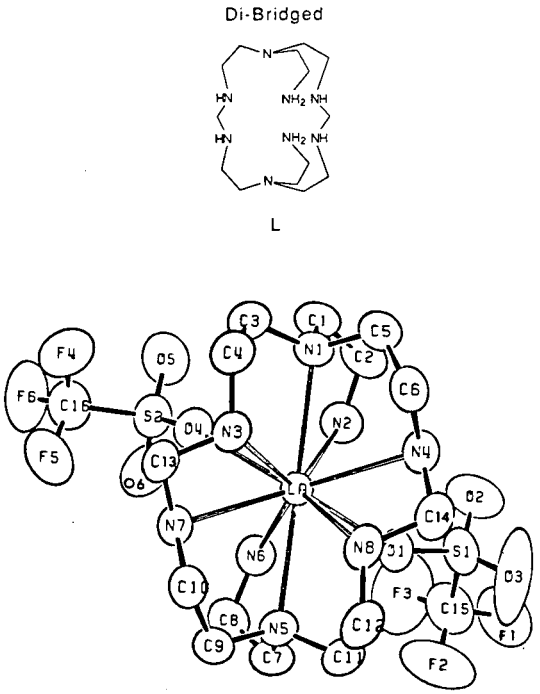

Figure 1-1. ORTEP drawing of the dibridged cation $[La(L)(trif)]^{2+}$, along with a schematic drawing of the dibridged ligand. (XBL 8712-5355)

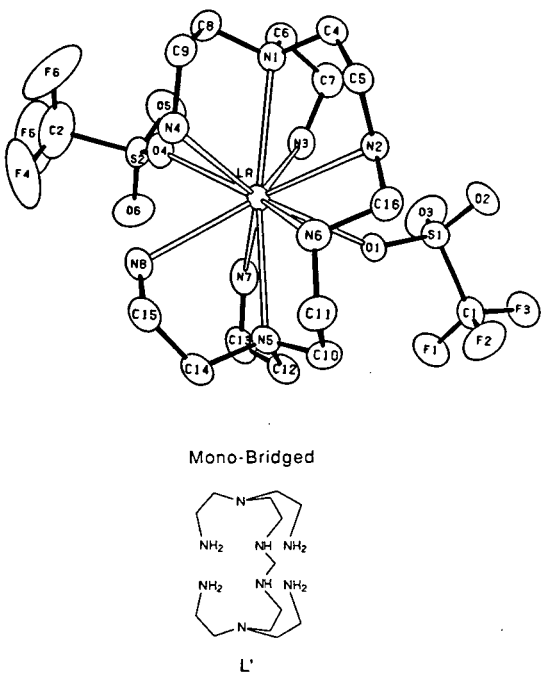

Figure 1-2. ORTEP drawing of the monobridged cation $[La(L')(trif)_2]^+$, along with a schematic drawing of the monobridged ligand. (XBL 8712-5356)

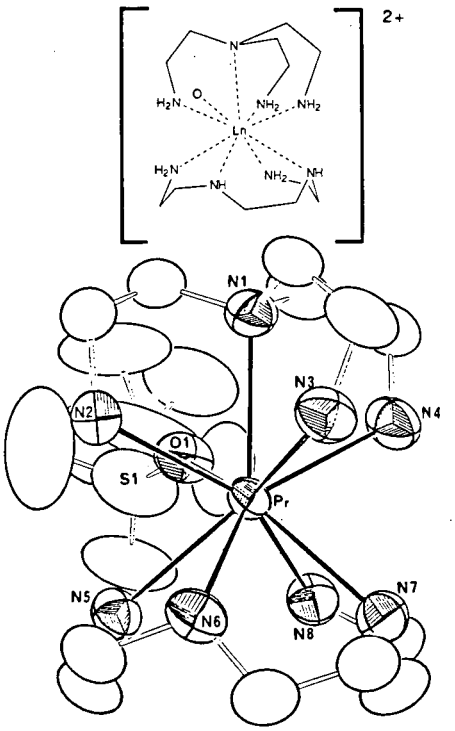

Figure 1-3. ORTEP drawing of the cation $[Pr(tren)(trien)(trif)]^{2+}$, along with a schematic drawing of the complex. (XBL 8712-5357)

SYNTHETIC AND STRUCTURAL STUDIES OF ACTINIDES AND OTHER COMPOUNDS

2. Electron-Transfer Reactions of Divalent Ytterbium Metallocenes; Synthesis of the Series $[(Me_5C_5)_2Yb]_2$ [μ-E], where E is O, S, Se, or Te, and Crystal Structure of $[(Me_5C_5)_2Yb]_2$ [μ-Se] (Publication 34)

D.J. Berg, C.J. Burns, R.A. Andersen, and A. Zalkin

The preparation of the divalent, base-free compounds $(Me_5C_5)_2M$, where M = Eu or Sm, from their respective diethyl ether complexes is described. Reaction of $(Me_5C_5)_2M$, where M = Yb or Sm, with N_2O gives $[(Me_5C_5)_2M]_2$ [μ-O] in high yield. Additionally, $(Me_5C_5)_2Yb$ reacts with Ph_3PS or As_2S_3 or COS, Ph_3PSe or elemental Se, n-Bu_3PTe or elemental Te, to give the bridging chalcogenides $[(Me_5C_5)_2Yb]_2$ [μ-E], where E is S, Se, or Te, respectively. Magnetic susceptibility studies show that there is no magnetic exchange between the paramagnetic f-metals across the bridging group-16 dianions. The variable-temperature magnetic studies also show

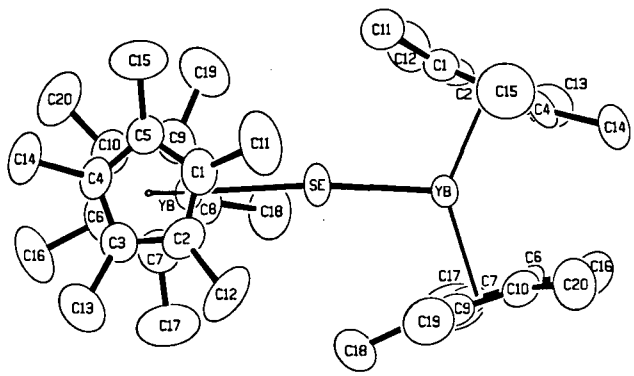

Figure 2-1. $[(Me_5C_5)_2Yb]_2[\mu\text{-Se}]$ viewed down a line connecting the centroids of the Cp rings; 50% probability ellipsoids. (XBL 8711-4920)

that $(Me_5C_5)_2Sm$ and $[(Me_5C_5)_2Sm]_2$ $[\mu\text{-O}]$ display temperature-independent paramagnetism, as predicted by Van Vleck.[1] The crystal structure of $[(Me_5C_5)_2Yb]_2$ $[\mu\text{-Se}]$ is tetragonal, $P\bar{4}2_1c$, with a = 14.984(5) Å and c = 19.165(9) Å. For Z = 4 the calculated density is 1.491 g/cm^3. The structure was refined by full-matrix least squares to a conventional R factor of 0.031 [3797 data, $F^2 > 2\sigma(f^2)$] (see Figure 2-1). The selenium atom is on a twofold axis and bonds to two Yb atoms in a nearly linear structure [Yb-Se-Yb angle: 171.09(6)°]. The Yb atom is η^5-bonded to two cyclopentadienyl rings and is on a plane defined by the centers of the two rings and the selenium atom. Distances are Yb-Se: 2.621(1) Å; Yb-C (avg): 2.609(7) Å; Yb-Cp (ring centroid): 2.319(2) Å.

1. J.H. Van Vleck, *The Theory of Electron and Magnetic Susceptibilities*, Clarendon Press, Oxford, 1932.

3. Preparation and Crystal Structure of Addition Compound MeLi·U[OCH(CMe$_3$)$_2$]$_4$, a Compound with a Uranium-to-Carbon Sigma Bond (Publication 35)

J.L. Stewart and R.A. Andersen

Reaction of MeLi and U[OCH(CMe$_3$)$_2$]$_4$ gives the addition compound LiU(Me)[OCH(CMe$_3$)$_2$]$_4$, which in the solid state has a geometry based on square pyramidal uranium with the apical site occupied by a methyl group and the four basal sites occupied by

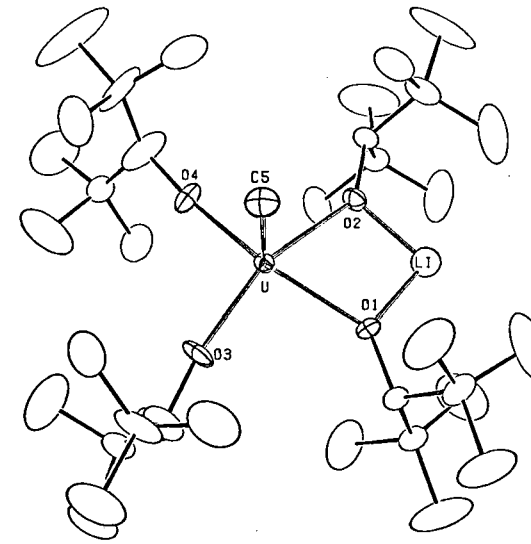

Figure 3-1. ORTEP drawing of LiU(Me)[(OCH)(CMe$_3$)$_2$]$_4$. (XBL 874-1668)

oxygen atoms of the alkoxide ligand, two of which form bridges to the lithium atom. An ORTEP drawing of the compound is shown in Figure 3-1.

4. Crystal Structures of $(MeC_5H_4)_4U_2(\mu\text{-NR})_2$. Unsymmetrical Bridging, R = Ph, and Symmetrical Bridging, R = SiMe$_3$, Organoimide Ligands in Organoactinide Compounds (Publication 36)

J.G. Brennan, R.A. Andersen, and A. Zalkin

The tetravalent uranium complexes with bridging organoimide ligands, $(MeC_5H_4)_2U$ $(\mu\text{-NR})_2$, have been prepared by the valence conproportionation reaction of $(MeC_5H_4)_3U\cdot thf$ and $(MeC_5H_4)_3UNR$. X-ray crystallographic study of R = Ph and SiMe$_3$ shows that the NPh group asymmetrically bridges the two uranium fragments, whereas the NSiMe$_3$ group symmetrically bridges the two uranium fragments. Crystals of $(MeC_5H_4)_4U_2(NPh)_2$ are monoclinic, $P2_1/n$, with a = 14.738(3) Å, b = 9.933(2) Å, c = 10.612(2) Å, and β = 102.11(2)° at 23°C. For Z = 2 (dimers), the calculated density is 2.13 g/cm^3. The structure was refined by full-matrix least squares to a conventional R factor of 0.029 [1600 data, $F^2 > 2\sigma(F^2)$] (see Figure 4-1). Crystals of $(MeC_5H_4)_4U_2(NSiMe_3)_2$ also are monoclinic, $P2_1/n$,

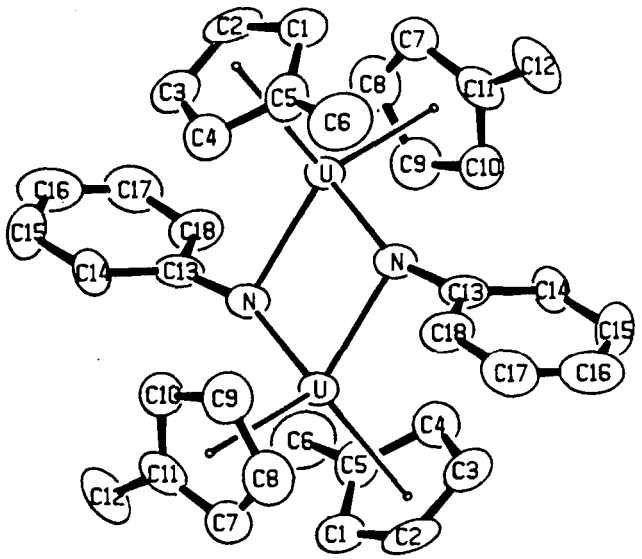

Figure 4-1. ORTEP drawing of $(MeC_5H_4)_4U_2(NPh)_2$; thermal ellipsoids at 50% probability level. (XBL 8711-4922)

with a = 15.761(6) Å, b = 9.389(4) Å, c = 11.052(4) Å, and β = 101.36(3)° at 23°C. For Z = 2 (dimers), the calculated density is 2.00 g/cm^3 (see Figure 4-2). The structure was refined by full-matrix least squares to a conventional R factor of 0.023 [2544 data, $F^2 > 2\sigma(F^2)$]. Both complexes are dimers in which the two $(MeC_5H_4)_2U$ fragments are bridged by the organoimide group so that an inversion center is located in the center of the U_2N_2 ring. The bridging U-N distances are 2.156(8) Å and 2.315(8) Å in the NPh complex and 2.217(4) Å and 2.230(4) Å in the $NSiMe_3$ complex.

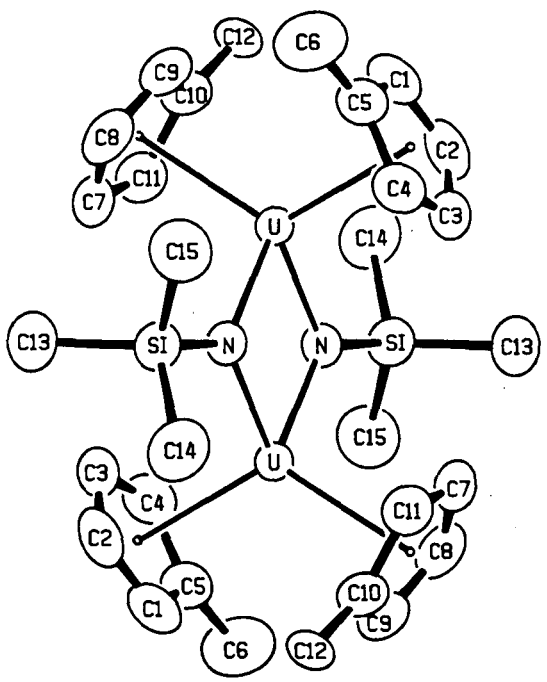

Figure 4-2. ORTEP drawing of $(MeC_5H_4)_4U_2(NSiMe_3)_2$; thermal ellipsoids at 50% probability level. (XBL 8711-4923)

5. Crystal Structures of $(MeC_5H_4)_3M(L)$, where M is Uranium or Cerium and L is Quinuclidine or $P(OCH_2)_3CEt$; Evidence for Uranium to Phosphorus π-Backbonding (Publication 37)

J.G. Brennan, S.D. Stults, R.A. Andersen, and A. Zalkin

The synthesis and x-ray crystal structure of $(MeC_5H_4)_3M(L)$, where M is Ce or U and L is $N(CH_2CH_2)_3CH$ or $P(OCH_2)_3CEt$, is described. Crystals of $(MeC_5H_4)_3UN(CH_2CH_2)_3CH$ are triclinic, $P\bar{1}$, with a = 10.604(4) Å, b = 13.552(6) Å, c = 8.333(4) Å, α = 100.20(4)°, β = 74.78(4)°, and γ = 104.13(4)° at 23°C. For Z = 2, the calculated density is 1.751 g/cm^3. The structure was refined by full-matrix least squares to a conventional R factor of 0.022 [4209 data, $F^2 > 2\sigma(F^2)$]. Crystals of $(MeC_5H_4)_3CeN(CH_2CH_2)_3CH$ are triclinic, $P\bar{1}$, with a = 10.609(4) Å, b = 13.586(5) Å, c = 8.348(5) Å, α = 100.15(4)°, β = 74.75(4)° and γ = 104.01(3)° at 23°C. For Z = 2 the calculated density is 1.451 g/cm^3. The structure was refined by full-matrix least squares to a conventional R factor of 0.024 [4516 data, $F^2 > 2\sigma(F^2)$] (see Figure 5-1). The uranium(III) and cerium(III) atoms are each bonded to three cyclopentadienyl rings; the average U-C and Ce-C distances are 2.82 ± 0.03 Å and 2.85 ± 0.03 Å, respectively. The U-N and Ce-N distances are 2.764(4) Å and 2.789(3) Å, respectively. Crystals of $(MeC_5H_4)_3UP(OCH_2)_3CEt$ (see Figure 5-2) and

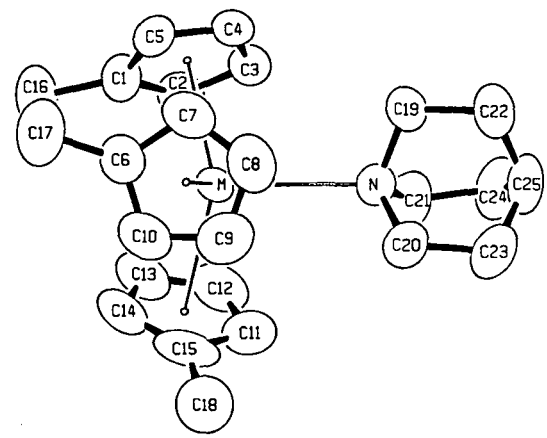

Figure 5-1. ORTEP drawing of $(CH_3C_5H_4)_3U{\cdot}N(CH_2CH_2)_3CH$. (XBL 8711-4918)

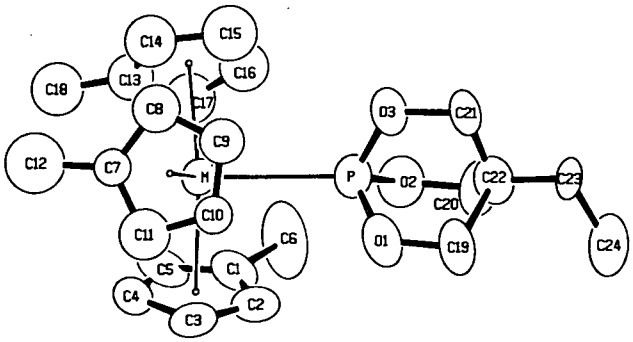

Figure 5-2. ORTEP drawing of $(CH_3C_5H_4)_3U{\cdot}P(OCH_2)_3CC_2H_5$, M = U. Only one conformation of the disordered ring C(7)–C(11) is shown. (XBL 8711-4919)

$(MeC_5H_4)_3CeP(OCH_2)_3CEt$ are orthorhombic, $P2_12_12_1$, Z = 4. The structures of the two isomorphous complexes were determined by single-crystal x-ray diffraction methods and refined by full-matrix least squares. For the uranium complex, a = 13.122(5) Å, b = 16.363(5) Å, and c = 10.922(4) Å at 23°C; the calculated density is 1.806 g/cm^3; the final R factor is 0.044 [2292 data, $F^2 > 3\sigma(F^2)$]. For the cerium complex, a = 13.163(7) Å, b = 16.443(7) Å, and c = 10.976(4) Å at 23°C; the calculated density is 1.509 g/cm^3; the final R factor is 0.046 [3195 data, $F^2 > 3\sigma(F^2)$]. The metal atom is tetrahedrally bound to the three cyclopentadienyl rings and a phosphorus atom. The U-P and Ce-P distances are 2.988(6) Å and 3.086(3) Å, respectively; the average U-C and Ce-C distances are 2.80 ± 0.05 Å and 2.82 ± 0.03 Å, respectively. The metal-to-Lewis-base bond lengths are rationalized in terms of U-P π-backbonding and the lack of π-backbonding in both of the amine complexes and in the cerium phosphite complex.

6. $(Me_5C_5)_2Yb(\mu\text{-}Me)Be(C_5Me_5)$: A Model for Methane Coordination? (Publication 7)

C.J. Burns and R.A. Andersen

The concept of NH_3 or CH_3^- acting as a Lewis base by donating a pair of electrons in a σ-symmetry orbital to a vacant σ-symmetry orbital on a metal fragment is a fundamental principle of inorganic coordination and organometallic chemistry. The frontier orbitals of the Lewis base are of σ-symmetry, and therefore they are called σ-donors. In principle, the methyl group in a compound such as CH_3X could act as a σ-donor towards a Lewis acid provided that X is more electropositive than the methyl group, such as in the molecule $MeBe(C_5Me_5)$, in which the dipole moment is in the direction of the σ-methyl group. Such a complex, $(Me_5C_5)_2Yb(\mu\text{-}Me)Be(C_5Me_5)$, may be prepared from $(Me_5C_5)_2Yb$ and $MeBe(C_5Me_5)$. A single-crystal x-ray diffraction study at −80°C (see Figure 6-1) shows that the Yb-C(Me)-Be angle is 177.2(3)°; the averaged Yb-C-H, Be-C-H, and H-C-H angles are 69.6 ± 5.7°, 110.6 ± 4.7°, and 108.3 ± 8.2°, respectively; and the Yb-C(Me) distance is 2.766(4) Å.

7. Tris(methylcyclopentadienyl)uranium(III) (p-Dimethylaminopyridine) (Publication 13)

A. Zalkin and J.G. Brennan

The complex $(C_5H_4Me)_3U{\cdot}(p\text{-}Me_2NC_5H_4N)$ was synthesized. The crystals are triclinic, P1, with a = 15.541(6) Å, b = 17.155(7) Å, c = 10.303(4) Å, α = 106.83(4)°, β = 106.52(4)°, and γ = 67.04(4)° at 23°C (see Figure 7-1). For Z = 4, D_x = 1.671 g/cm^3. The structure was refined by full-matrix least squares to an R factor of 0.033. Two independent but chemically similar molecules are found in the unit cell. The U(III) is at the center of a distorted tetrahedron consisting of the pyridine N atom and the centroids of the three cyclopentadienyl rings. Distances are: U-N, 2.662(13) Å and 2.627(12) Å; average U-C(ring): 2.82(4) Å; average U-Cp: 2.56(2) Å.

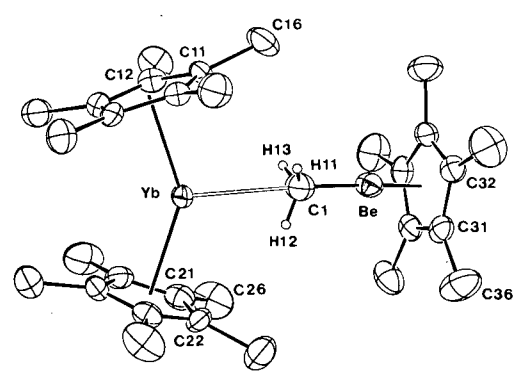

Yb - C1	2.766(4) Å	Yb - C1 - Be	177.2(3)°
Be - C1	1.705(6) Å		
Yb··· H11	2.54(4) Å	Be - C1 - H11	115.2(2.4)°
H12	2.51(5) Å	H12	113.0(3.1)°
H13	2.71(6) Å	H13	103.5(5.0)°

Figure 6-1. ORTEP drawing of $(Me_5C_5)_2Yb(\mu\text{-}Me)Be(C_5Me_5)$. (XBL 874-1666)

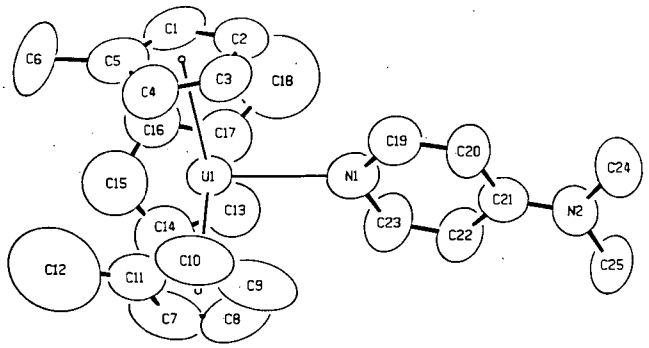

Figure 7-1. ORTEP drawing of $(MeC_5H_4)_3U{\cdot}(NC_5H_4NMe_2)$; 50% probability ellipsoids. (XBL 8711-4921)

8. Preparation and Crystal Structures of Tetrakis(methyltrihydroborato)uranium(IV) Bis(tetrahydrofuranate) and Tetrakis(methyltrihydroborato)uranium(IV) Tetrahydrothiophenate (Publication 22)

R. Shinomoto, A. Zalkin, and N.M. Edelstein

The U(IV) complexes $U(B_3H_3)_4{\cdot}2OC_4H_8$ (I) and $[(BH_3CH_3)_4U{\cdot}SC_4H_8]_2$ (II) were synthesized and their structures determined. Crystals of (I) are orthorhombic, Aba2, with a = 12.911(3) Å, b = 16.072(4) Å, and c = 10.116(4) Å at 23°C (see Figure 8-1); for Z = 2 the calculated density is 1.574 g/cm^3. Crystals of (II) are monoclinic, $P2_1/c$, with a =12.054(2) Å, b = 16.372(3) Å, c = 18.545(3) Å, and β = 108.82(2)° at 23°C (see Figure 8-2); for Z = 4 the calculated density is 1.694 g/cm^3. The structures were refined by full-matrix least squares to a conventional R factor of 0.028 (I) and 0.038 (II). The tetrahydrofuran

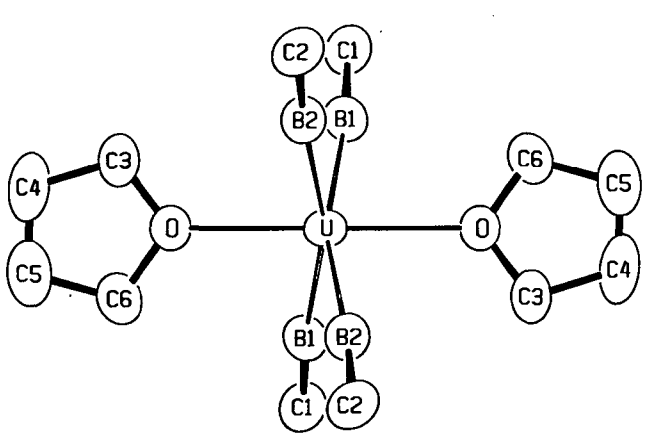

Figure 8-1. ORTEP drawing of $U(BH_3CH_3)_4{\cdot}2(OC_4H_8)$; 50% probability ellipsoids. (XBL 8410-4299)

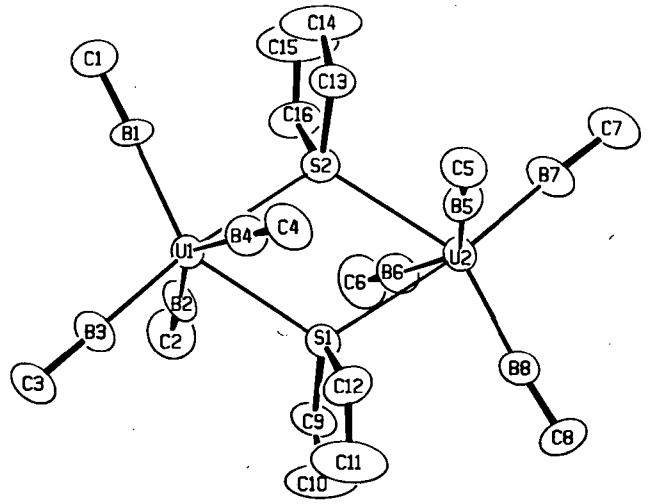

Figure 8-2. ORTEP drawing of $[U(BH_3CH_3)_4{\cdot}SC_4H_8]_2$; 50% probability ellipsoids. (XBL 8410-4301)

complex is monomolecular, with the uranium atom on a twofold axis and coordinated to four methyltrihydroborato and two tetrahydrofuran ligands; the U-B distances are 2.55(2) Å and 2.58(2) Å, and the U-O distance is 2.485(6) Å. The tetrahydrothiophene complex is a dimer in which two sulfur atoms bridge the uranium atoms of two tetra(methyltrihydroborato)uranium(IV) molecules; the U-B distances range from 2.468(2) to 2.591(2) Å, and the U-S distances are 3.120(4) and 3.239(5) Å; the S-S and U-U distances in the bridge are 3.477(5) and 5.374(1) Å, respectively.

9. Preparation of Some Lewis Base Adducts of Tris(methyltrihydroborato)Ho and Yb and Crystal Structures of Tris(methyltrihydroborato)ytterbium(III) Etherate and Tris(methyltrihydroborato)holmium(III)bis(pyridine) (Publication 23)

R. Shinomoto, A. Zalkin, and N.M. Edelstein

The complexes $M(B_3H_3)_3{\cdot}O(C_2H_5)_2$ (M = Lu, Yb, or Ho), $M(B_3H_3)_3{\cdot}OC_4H_8$ (M = Lu, Yb, or Ho), $M(B_3H_3)_3{\cdot}2OC_4H_8$ (M = Lu or Yb), and $Ho(BH_3CH_3)_3{\cdot}2C_6H_5N$ were prepared and characterized. Crystals of $(CH_3BH_3)_3Yb(III){\cdot}O(C_2H_5)$ are monoclinic, $P2_1/n$, with a = 10.745(4) Å, b = 15.647(4) Å, c = 9.215(3) Å, and β = 90.78(2)° at 23°C (see Figure 9-1); for Z = 4 the calculated density is 1.431 g/cm^3. Crystals of

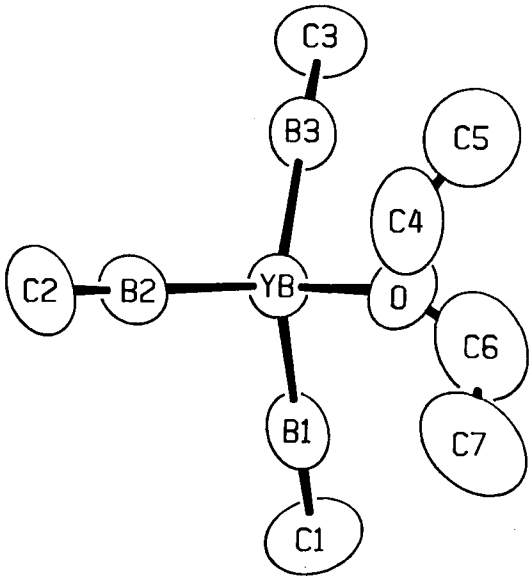

Figure 9-1. ORTEP drawing of $(CH_3BH_3)_3Yb{\cdot}OEt_2$; 50% probability ellipsoids. (XBL 8410-4298)

$(CH_3BH_3)_3Ho(III){\cdot}2(C_5NH_5)$ are triclinic, $P\bar{1}$, with a = 9.370(4) Å, b = 12.155(2) Å, c = 8.840(2) Å, α = 80.47(2)°, β = 107.41(2)°, and γ = 95.15(2)° at 23°C (see Figure 9-2); for Z = 2 the calculated density is 1.324 g/cm^3. The structures were refined by full-matrix least squares to conventional R factors of 0.040 and 0.023, respectively. The ytterbium complex is monomeric with the ytterbium atom tetrahedrally coordinated to three boron atoms and an ethyl oxygen atom; the Yb-B distances are 2.40(2) Å, 2.41(2) Å, and 2.43(2) Å, and the Yb-O distance is 2.23(1) Å. The holmium complex is a monomer with the holmium atom at the center of a trigonal bipyramid that has three boron atoms on the equator and two nitrogen atoms at the apices; the Ho-B distances are 2.483(6) Å, 2.495(6) Å, and 2.520(5) Å, and the Ho-N distances are 2.535(4) Å and 2.555(4) Å.

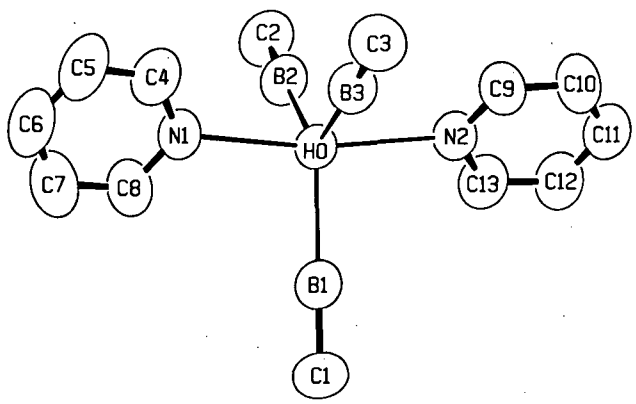

Figure 9-2. ORTEP drawing of $(CH_3BH_3)_3{\cdot}2(NC_5H_5)$; 50% probability ellipsoids. (XBL 8410-4300)

10. Preparation and Crystal Structures of Complexes of $U(BH_3CH_3)_4$ with 1,2-Dimethoxyethane, N,N,N′,N′-Tetramethylethylenediamine, and 1,2-Bis(methylthio)ethane (Publication 21)

R. Shinomoto, A. Zalkin, N.M. Edelstein, and D. Zhang

Complexes of $U(BH_3CH_3)_4$ with $MeOCH_2CH_2OMe$ (I), $Me_2NCH_2CH_2NMe_2$ (II), and $MeSCH_2CH_2SMe$ (III) were synthesized and their molecular structures determined. Complex (I) is tetragonal, P4/n, with a = 21.822(8) Å, c = 7.681(5) Å, Z = 8, d_x = 1.61 g/cm^3, and R = 0.028 (see Figure 10-1). Complex (II) is monoclinic, $P2_1/n$, with a = 10.206(4) Å, b = 15.436(6) Å, c = 12.880(5) Å, β = 92.25(3)°, d_x = 1.54 g/cm^3, and R = 0.029 (see Figure 10-2). Complex (III) is triclinic, $P\bar{1}$, with a = 8.937(4) Å, b = 13.692(4) Å, c = 8.186(3) Å, α = 96.46(4)°, β = 97.64(4)°, γ = 74.07(4)°, d_x = 1.66 g/cm^3, and R = 0.023 (see Figure 10-3). With one exception, all BH_3CH_3 groups are coordinated to the uranium atoms by tridentate hydrogen bridges with a U-B bond distance of 2.55(2) Å. For (II), one B atom is coordinated to the uranium atom through a bindentate hydrogen bridge with a U-B distance of

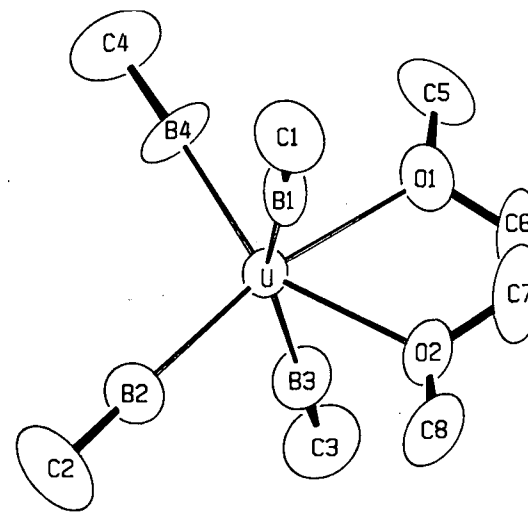

Figure 10-1. ORTEP drawing of $U(BH_3CH_3)_4{\cdot}MeOCH_2CH_2OMe$; 50% probability ellipsoids. (XBL 843-1027)

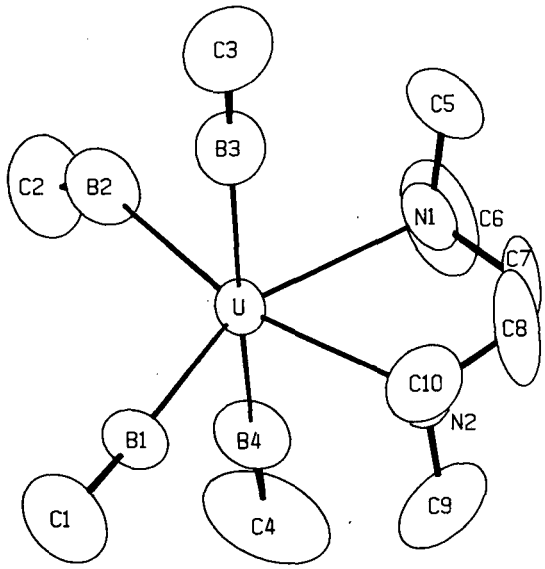

Figure 10-2. ORTEP drawing of $U(BH_3CH_3)_4 \cdot Me_2NCH_2CH_2NMe_2$; 50% probability ellipsoids. (XBL 843-1028)

2.72(2) Å and a U-B-C angle of 142(2)°. Uranium is coordinated to the O, N, or S atoms with average distances of 2.58, 2.73, and 3.07 Å, respectively.

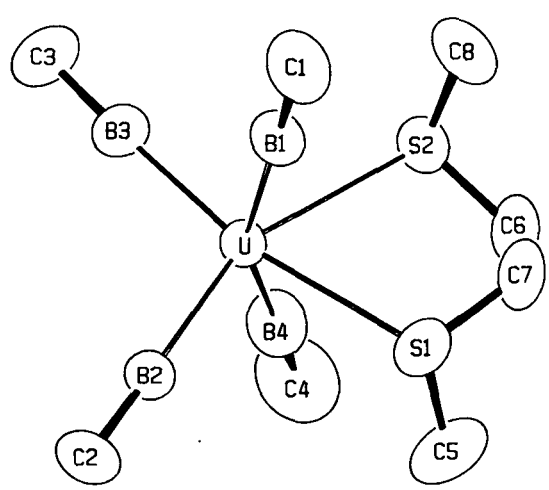

Figure 10-3. ORTEP drawing of $U(BH_3CH_3)_4 \cdot MeSCH_2CH_2SMe$; 50% probability ellipsoids. (XBL 843-1026)

11. Synthesis of Bis(η-1,3,5-tri-t-butylbenzene) Sandwich Complexes of Yttrium(0) and Gadolinium(0); the X-Ray Crystal Structure of the First Authentic Lanthanide(0) Complex, $[Gd(\eta\text{-}^tBu_3C_6H_3)_2]$ (Publication 12)

J.G. Brennan, F.G.N. Cloke, A.A. Sameh, and A. Zalkin

The vapors of yttrium and gadolinium react with 1,3,5-tri-t-butylbenzene to produce the metal(0) complexes $[M(\eta\text{-}^tBu_3C_6H_3)_2]$, where M = Y or Gd. The x-ray crystal structure of the gadolinium complex shows the molecule to possess a parallel-ring sandwich structure (see Figure 11-1). The crystals of $Gd[(t\text{-}C_4H_9)_3C_3]_2$ are triclinic, $P\bar{1}$, with a = 10.387 Å, b = 10.579 Å, c = 9.847 Å, α = 72.45(5)°, β = 61.78(4)°, and γ = 66.14(4)°; for Z = 1, d_x = 1.250 g/cm^3. The structure was refined by full-matrix least squares to an R factor of 0.033. The Gd atom is on the center of symmetry and is sandwiched by two cyclopentadienyl rings at a distance of 2.219 Å; the Gd-C range is 2.59–2.66 Å.

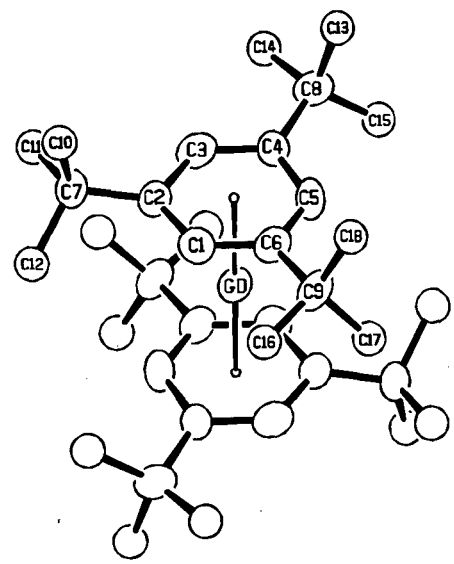

Figure 11-1. ORTEP drawing of $[^tBu_3C_6H_3)]_2Gd$; 50% probability ellipsoids. (XBL 8711-4925)

12. Phases in the System XeF_2/XeF_5AsF_6 and Structural and Vibrational Evidence for the Ionization Pathway: $XeF_2 \rightarrow XeF^+ + F^-$ (Publication 26)

B. Zemva, A. Jesih, D.H. Templeton, A. Zalkin, A.K. Cheetham, and N. Bartlett

A fusion-temperature versus composition curve has been obtained for the system XeF_2/XeF_5AsF_6 (see Figure 12-1). The fusion-temperature/composition curve indicates compound formation at XeF_2-to-SeF_5AsF_6 ratios of 1:2 at 89.5°C, 2:1 at 59.5°C, and 3:1 at 74.0°C. Other simple-integer ratios are also suggested: 1:1 at 56.5°C and 3:2 at 56.0°C. The crystal structures of $XeF_2 \cdot 2(XeF_5AsF_6)$ (I), $XeF_2 \cdot XeF_5AsF_6$ (II), and $2XeF_2 \cdot XeF_5AsF_6$ (III) were determined. All three crystallize in the monoclinic system. The XeF_2 molecule in all three compounds is linear, with Xe-F bond distances in the 1.97–2.06 Å range. In (I) the XeF species are coordinated via their F ligands to two XeF_5^+ ions that are bridge-bonded to two AsF_6^- ions to form a three-dimensional polymer (see Figure 12-2). In (II) the structural unit is the formula unit, and these units are not interconnected; the XeF_2 and the AsF_6^- each are coordinated via a fluorine bridge bond to the XeF_5^+ (see Figure 12-3). In (III) the formula unit is again a structural unit, and these units are not interconnected (see Figure 12-4). The three bridged flourine bonds to the XeF_5^+ come from each of the XeF_2 molecules and from the AsF_6^- ion. In all cases the Xe-F distance in XeF_2 is foreshortened by about 0.05 Å when it is not involved in a bridge bond. Differences in the coordination number of the XeF_5^+ cation in these complexes account for the polymeric or nonpolymeric nature of the complexes. Such differences are determined by the extent of ionization of the XeF_2 species. The observed, essentially linear distortions of XeF_2 are interpreted as points on the ionization pathway $XeF_2 \rightarrow XeF^+ + F^-$. From the force constants and associated interatomic distances, the isolated XeF^+ ion is predicted to have a bond length of ~1.92 Å and a force constant of ≤ 4.48 mdyne/Å.

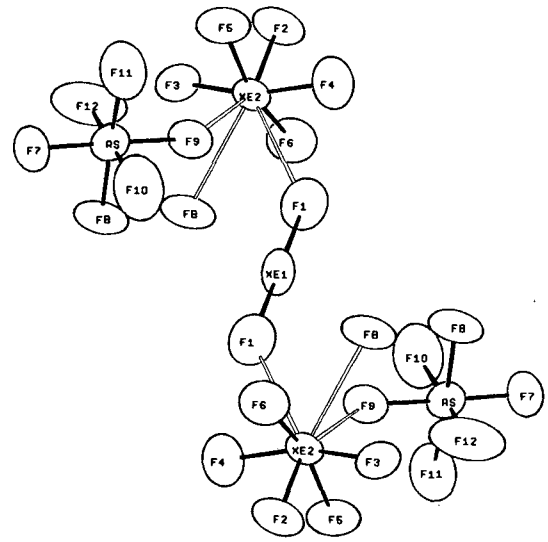

Figure 12-2. ORTEP drawing of $XeF_2 \cdot 2(XeF_5^+ \; AsF_6^-)$; 50% probability ellipsoids. (XBL 792-8266)

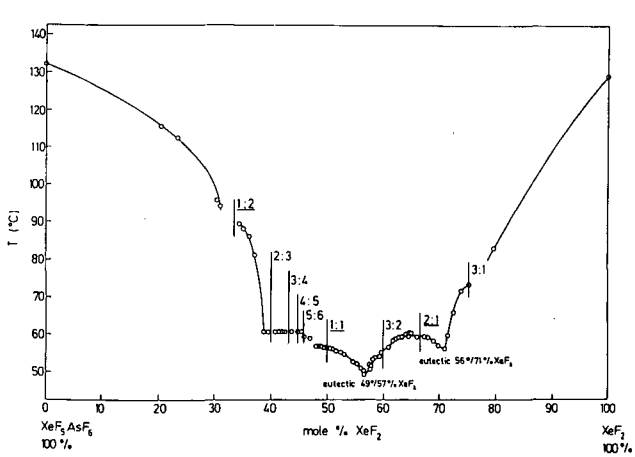

Figure 12-1. Fusion-temperature composition curve for XeF_2/XeF_5AsF_6. (XBL 8711-4924)

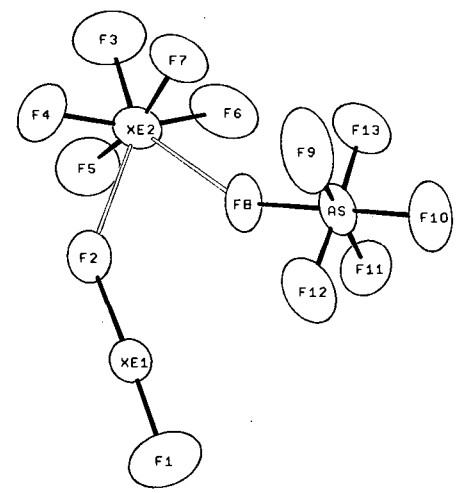

Figure 12-3. ORTEP drawing of $XeF_2 \cdot (XeF_5^+ \; AsF_6^-)$; 50% probability ellipsoids. (XBL 792-8267)

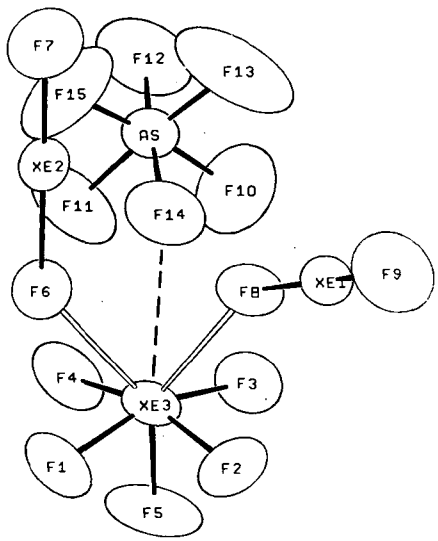

Figure 12-4. ORTEP drawing of $2XeF_2 \cdot (XeF_5^+ \ AsF_6^-)$; 50% probability ellipsoids. (XBL 793-8719)

PHYSICAL AND SPECTROSCOPIC PROPERTIES

13. $\{Th(III)[\eta^5\text{-}C_5H_3(SiMe_3)_2]_3\}$, an Actinide Compound With a $6d^1$ Ground State (Publication 42)

W.K. Kot, G.V. Shalimoff, N.M. Edelstein, M.A. Edelman,† and M.F. Lappert†

The free ion of trivalent thorium [Th(III)] has a $5f^1$ ground configuration whose center of gravity is 9897 cm^{-1} below the center of gravity of the excited $6d^1$ configuration. The $7s^1$ level is at 23,120 cm^{-1}, while the $7p_{1/2,3/2}$ levels are found at energies greater than 60,000 cm^{-1} above the ground state. Although the free-ion spectrum of the isoelectronic ion Pa(IV) is not known, the difference between the centers of gravity of the ground $5f^1$ configuration and the excited $6d^1$ configuration for this ion is estimated to be ~50,000 cm^{-1} from the interpolation of the known free-ion data for the isoelectronic series Ra(I), Ac(II), Th(III), and U(V). Optical spectra of $Pa(IV)/ThBr_4$ and $PaCl_6^{2-}$ showed that the lowest $5f^1 \rightarrow 6d^1$ crystal-field transition appeared at ~20,000 cm^{-1}. Assuming that the total crystal-field splitting for the $6d^1$ orbitals for $PaCl_6^{2-}$ is ~20,000 cm^{-1}, we estimate the splitting between the centers of gravity of the $5f^1$ and $6d^1$ configuration for $PaCl_6^{2-}$ to be ~25,000 cm^{-1}. Thus in this compound, the Pa(IV) $5f^1 \rightarrow 6d^1$ (centers of gravity) splitting is lowered by 25,000 cm^{-1} from the free ion to the crystal. These arguments suggest that for Th(III) in a crystal field, the ground state could arise from the $6d^1$ configuration.

The Th(III) compound $ThCp''_3$ [$Cp'' = \eta^5\text{-}C_5H_3(SiMe_2)_3\text{-}1,3$] has recently been synthesized and structurally characterized. Electron paramagnetic resonance (EPR) spectra of powdered samples and of solutions in dry, degassed methylcyclohexane were obtained at 10–300 K. The spectra obtained could be fit with the parameters of the spin-Hamiltonian

$$\mathscr{H} = g_{||}\beta H_z S_z + g_{\perp}\beta(H_x S_x + H_y S_y) \ .$$

Representative values of the g-tensor components at various temperatures are given in Table 13-1.

An analysis of these g-tensor data is only consistent with a $6d^1$ ground state for this Th(III) compound.

†Permanent address: School of Chemistry and Molecular Sciences, University of Sussex, Brighton BN1 9QJ, United Kingdom.

Table 13-1
Spin Hamiltonian parameters for $Th[\eta^5\text{-}C_5H_3(SiMe_3)_2]_3$ as a function of temperature.

	g	$g_{\perp}$	$g_{Avg.}$	Temp.(K)
Methylcyclohexane solution	—	—	1.910 ± 0.001	300
Methylcyclohexane solution	1.9725 ± 0.001	1.879 ± 0.001	1.910[a]	10–110
Powdered solid	1.972 ± 0.001	1.878 ± 0.001	1.909[a]	10–300

a. Calculated from $1/3(g + 2g_{\perp})$.

14. Optical and EPR Investigations of Np^{4+} in Single Crystals of $ZrSiO_4$ (Publication 40)

I. Poirot, W. Kot, G. Shalimoff, N. Edelstein, M.M. Abraham,† C.B. Finch,† and L.A. Boatner†

Polarized optical spectroscopy has been used to investigate the electronic structure of tetravalent neptunium incorporated as a dilute impurity in single crystals of the tetragonal host $ZrSiO_4$. Thirty-one levels were assigned from 30 intense polarized optical transitions and used to obtain a fit to a parametric Hamiltonian to within an rms deviation of 34 cm^{-1}. Thirteen other levels with comparable intensities and good polarization characteristics were observed. Inclusion of these levels using the parameters from the 31-level fit, however, resulted in an increase of the rms deviation to approximately 100 cm^{-1}. EPR spectra of the ground crystal-field state were obtained at 4.2 K. The spin-Hamiltonian parameters, $|g_{\parallel}| = 0.8 \pm 0.6$, $|g_{\perp}| = 2.59 \pm 0.02$, are in reasonable agreement with the values calculated from the wave functions obtained from the optical data analysis.

†Permanent address: Solid State Division, Oak Ridge National Laboratory, Oak Ridge, TN 37831.

15. EPR and Optical-Absorption Studies of Cm^{3+} in YPO_4 and $LuPO_4$ Single Crystals (Publication 17)

M.M. Abraham,† L.A. Boatner,† C.B. Finch,† W.K. Kot, J.G. Conway, G.V. Shalimoff, and N.M. Edelstein

$^{244}Cm^{3+}$ has been incorporated as a dilute impurity in single crystals of the tetragonal-symmetry lanthanide orthophosphate hosts $LuPO_4$ and YPO_4. EPR spectroscopic observations were made of all of the excited doublets in the ground $^8S_{7/2}$ multiplet of Cm^{3+} in both host crystals. Excited-state resonances were observed at both 77 and 4.2 K by use of X-band frequencies. The observed axial g values were used to compute the admixed wave functions for all four doublet levels in the ground manifold of Cm^{3+} and to calculate the g value expected for the lowest-lying doublet that could not be observed by EPR spectroscopy. Optical-absorption and Zeeman-effect investigations were carried out for Cm^{3+} in YPO_4, and a ground-state g value was obtained for the lowest-lying doublet in the ground-state manifold. The value was in excellent agreement with the value predicted by use of EPR results for the three excited-doublet levels. The Mohr-circle construction was used to obtain additional information regarding the nature of the crystal-field interaction for Cm^{3+} in the two crystal systems. In particular, the tetragonal crystal-field interaction was found to be stronger in the YPO_4 host than in $LuPO_4$. Additionally, the crystal-field-induced admixtures were found to be smaller at 77 K than at 4.2 K for both hosts, and the signs of the Steven's parameters were determined to be positive for b_4^0 and negative for b_2^0.

†Permanent address: Solid State Division, Oak Ridge National Laboratory, Oak Ridge, TN 37831.

16. Reduced Biuranocenylene — a Mixed-Valence Organoactinide Compound? (Publication 15)

D. Eisenberg and A. Streitwieser, Jr.

Bis(bicyclooctatetraenyl)diuranium, biuranocenylene (see Figure 16-1), was partially reduced with potassium in THF-d_8. The ^1H nuclear magnetic resonance (NMR) spectrum of the resulting mixture indicates that the remaining biuranocenylene undergoes fast electron exchange on the ^1H NMR time scale with its reduction product. Complete reduction results in a product that appears to be the mixed-valence (III-IV) biuranocenylene whose NMR spectrum of seven different peaks indicates that it has equivalent cyclooctatetraene rings on the NMR time scale. If the structure was that of the U(III)-U(IV) compound with rapid intramolecular electron transfer on the NMR time scale, the visible spectrum would be expected to be a superposition of that of a uranocene with the uranocene reduction product; the latter is a featureless spectrum with a long tail. The visible spectrum of biuranocenylene is that of a typical uranocene; on reduction the characteristic uranocene cascade of peaks diminishes and finally disappears, and the tail into the visible increases, indicat-

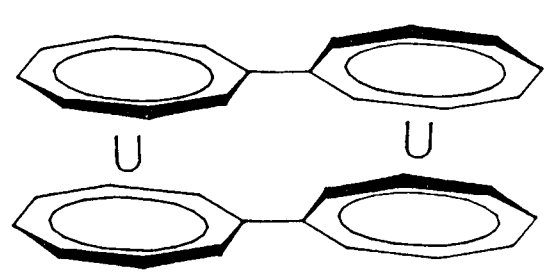

Figure 16-1. Biuranocenylene. (XBL 8712-5354)

ing that the mixed-valence compound is not valence localized on the visible time scale. That is, the reduction product has electronically equivalent uraniums in which the five 5f electrons are delocalized such that each uranium has an intermediate oxidation state of 3 1/2.

17. The Structures and Energies of Main Group Metal Formyl Complexes. The Mechanism of the Reaction of LiH with CO. An *Ab Initio* Study (Publication 29)

E. Kaufmann,† P. Schleyer, S. Gronert, A. Streitwieser, Jr., and M. Halpern

Direct insertions of carbon monoxide are now common in early transition metal and actinide compounds; for example, Marks[1] has demonstrated rapid reversible addition of CO to alkoxybis(pentamethylcyclopentadienyl)thorium hydrides to generate formyl-thorium complexes. Spectrometric data, such as the low C=O frequencies of about 1477 cm^{-1}, imply $[\eta]^2$ coordination of the formyl ligand to the metal, and such $[\eta]^2$ coordination has been used commonly in reaction mechanisms of such reactions. Thus, the nature of the bonding in such structures is of interest; in particular, since bonding to actinides frequently tends to be highly ionic, the important question is whether such $[\eta]^2$ coordination can result from purely ionic interactions or whether novel types of covalent interactions are required. Theoretical calculation of actinide compounds is still generally a formidable problem, but this question could be addressed by *ab initio* calculations of suitable lighter elements.

In collaboration with the research group of Professor Paul Schleyer of the University of Erlangen-Nurnberg, formyl complexes, MCHO, of first- and second-row metals and metal hydrides were investigated by *ab initio* calculations (MP2/6-31+G*//6-31G* and lower levels). Both $[\eta]^2$ (i.e., bridged structures) and $[\eta]^1$ coordination of the metals were found, but the former are favored for electropositive metals. Electron-density analysis shows that the formyl-metal bonding in such compounds is predominantly ionic. Figure 17-1 shows a projected electron density map of formyllithium with the 3-21G* basis set. The minimum contour levels are used to demark the boundaries between atoms and are shown as dotted lines in the figure. The numbers indicate the integrated electron populations for each fragment and give a lithium charge of +0.88.

Comparable structures are given for all of the $[\eta]^2$-coordinated compounds with long C-O bond lengths of 1.24–1.25 Å and small O-C-M bond angles

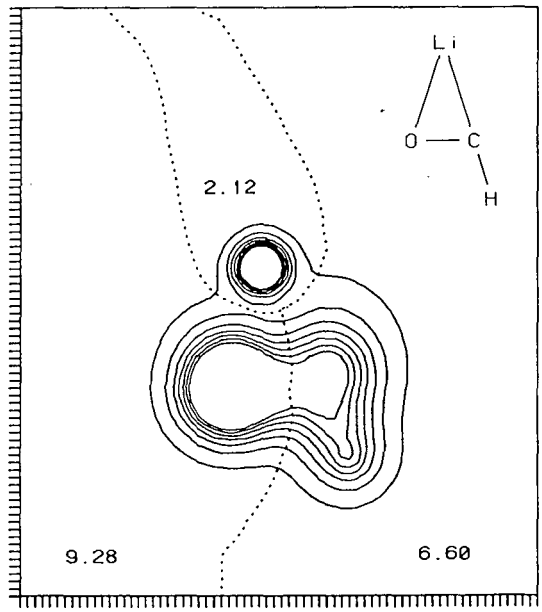

Figure 17-1. Projected electron-density map of formyllithium at 3-21G*, showing demarkation into atomic-like regions and integrated electron populations. (XBL 8712-5353)

of about 65°. Optimization of HCOLi with correlation correction at the MP2/6-31G* level had minor effects on the structure; the largest effect was a lengthening of the C-O bond length from 1.243 to 1.277 Å and the O-Li bond from 1.782 to 1.835 Å. Natural populations also gave metal populations of about +0.85. Finally, if the interaction between the lithium cation and the formyl anion were completely ionic, then the 2s and 2p shell on lithium would be empty. By limiting the lithium to a basis set that contains only a 1s shell, the lithium can be forced to interact completely ionically. This drastic change in basis sets results in only small changes in geometry.

These results demonstrate that the $[\eta]^2$ coordination observed for acyl derivatives of actinides is a normal consequence of ionic bonding and does not necessarily represent unusual bonding modes. Of course, this does not mean that covalent effects are necessarily negligible; for example, semiempirical extended Hückel theory results show that orbital overlap effects can explain significant stereochemical aspects of CO insertion into Th-H bonds.[2]

---

†Permanent address: Institute of Organic Chemistry, University of Erlangen-Nurnberg, Federal Republic of Germany.

1. P.J. Fagan, K.G. Moloy, and T.J. Marks, J. Am. Chem. Soc. **103**, 6959 (1981); K.G. Moloy and T.J. Marks, J. Am. Chem. Soc. **106**, 7051 (1984).

2. K. Tatsumi, A. Nakamura, P. Hofmann, P. Stauffert, and R. Hoffmann, J. Am. Chem. Soc. **107**, 4440 (1985); P. Hofmann, M. Frede, P. Stauffert, W. Lasser, and U. Thewalt, Angew. Chem. **97**, 693 (1985); K. Tatsumi, A. Nakamura, P. Hofmann, R. Hoffmann, K.G. Moloy, and T.J. Marks, J. Am. Chem. Soc. **108**, 4467 (1986).

1987 PUBLICATIONS AND REPORTS

Refereed Journals

1. S.F. Haddad and K.N. Raymond, "The Structure and Properties of Tetrakis(tironate)cerate(IV), $Na_{12}[Ce(C_6H_2O_2\ (SO_3)_2)_4]\cdot 9H_2O\cdot 6C_3H_7NO$," Inorg. Chim. Acta **122**, 111 (1986).
2. K.N. Raymond, M.E. Cass, and S.L. Evans, "Metal Sequestering Agents in Bioinorganic Chemistry: Enterobactin Mediated Iron Transport in E. Coli and Biomimetic Applications," Pure & Appl. Chem. **59**, 771 (1987).
3. C.J. Burns and R.A. Andersen, "Preparation of the First Molecular η^2-Acetylene Complex of a 4f-Transition Metal, $(Me_5C_5)_2Yb(\eta^2\text{-}MeC{\equiv}CMe)$," J. Am. Chem. Soc. **109**, 941 (1987); LBL-22127.
4. C.J. Burns and R.A. Andersen, "Preparation of the First η^2-Olefin Complex of a 4f-Transition Metal, $(Me_5C_5)_2Yb(\mu\text{-}C_2H_4)Pt(PPh_3)_2$," J. Am. Chem. Soc. **109**, 917 (1987); LBL-22245.
5. C.J. Burns, D.J. Berg, and R.A. Andersen, "Preparation and Crystal Structure of the Mixed-Valence [Yb(III,II)] Tetranuclear Complex, $(Me_5C_5)_6Yb_4(\mu\text{-}F)_4$," J. Chem. Soc. Chem. Comm., 272 (1987); LBL-22007.
6. R.A. Andersen, R. Blom, J.M. Boncella, C.J. Burns, and H.V. Volden, "The Thermal Average Molecular Structures of Bis(pentamethylcyclopentadienyl)-Magnesium(II), -Calcium(II), and -Ytterbium(II) in the Gas Phase," Acta Chem. Scand. A **41**, 24 (1987); LBL-22585.
7. C.J. Burns and R.A. Andersen, "$(Me_5C_5)_2Yb(\mu\text{-}Me)Be(C_5Me_5)$: A Model for Methane Coordination?" J. Am. Chem. Soc. **109**, 5853 (1987); LBL-23392.
8. A. Zalkin, T.J. Henly, and R.A. Andersen, "Amminebis (pentamethylcyclopentadienyl)(thiophenolato)ytterbium(III)," Acta Crystallogr. C **43**, 233 (1987); LBL-21445.
9. A. Zalkin, J.G. Brennan, and R.A. Andersen, "Dibenzyl[1,2-bis-(dimethylphosphino)ethane]bis(cyclopentadienyl)thorium(IV)," Acta Crystallogr. C **43**, 421 (1987); LBL-22312.
10. A. Zalkin, J. G. Brennan, and R.A. Andersen, "[1,2-Bis(dimethylphosphino)ethane]bis(cyclopentadienyl)-dimethylthorium(IV) and [1,2-Bis(dimethylphosphino)ethane]dichlorobis(cyclopentadienyl)thorium-(IV)," Acta Crystallogr. C **43**, 418 (1987); LBL-22313.
11. S. Stults and A. Zalkin, "Structure of Tris(η-methylcyclopentadienyl)(trimethylphosphine)cerium-(III)," Acta Crystallogr. C **43**, 430 (1987); LBL-21333.
12. J.G. Brennan, F.G.N. Cloke, A.A. Sameh, and A. Zalkin, "Synthesis of Bis(η-1,3,5-tri-t-butylbenzene) Sandwich Complexes of Yttrium(0) and Gadolinium(0); the X-Ray Crystal Structure of the First Authentic Lanthanide(0) Complex, $[Gd(\eta\text{-}^tBu_3C_6H_3)_2]$" J. Chem. Soc. Chem. Commun., 1668 (1987).
13. A. Zalkin and J.G. Brennan, "(4-Dimethylaminopyridine)tris(η-methylcyclopentadienyl)uranium(III)," Acta Crystallogr. C **43**, 1919 (1987); LBL-22955.
14. L. Gong, A. Streitwieser, Jr., and A. Zalkin, "Structure of $([\eta]^5\text{-}C_5Me_5)_2LuCl(C_4H_8O)$ and Exchange of Coordinated Solvent," J. Chem. Soc. Chem. Comm., 460 (1987).
15. D. Eisenberg and A. Streitwieser, Jr., "Reduced Biuranocenylene — A Mixed Valence Organoactinide Compound?" Inorg. Chim. Acta **139**, 193 (1987).
16. L.R. Morss, J. Fuger, J. Goffart, N. Edelstein, and G.V. Shalimoff, "Enthalpy of Formation and Magnetic Susceptibility of Californium Sesquioxide, Cf_2O_3," J. Less-Common Metals **127**, 251 (1987); LBL-22710.
17. M.M. Abraham, L.A. Boatner, C.B. Finch, W.K. Kot, J.G. Conway, G.V. Shalimoff, and N.M. Edelstein, "EPR and Optical-Absorption Studies of Cm^{3+} in YPO_4 and $LuPO_4$ Single Crystals," Phys. Rev. B **35**, 3057 (1987); LBL-23490.
18. W.K. Kot, N.M. Edelstein, and A. Zalkin, "Structure and Characterization of $(C_5H_5)_2Zr(H)BH_3CH_3$," Inorg. Chem. **26**, 1339 (1987); LBL-22223.
19. N.M. Edelstein, "Optical and Magnetic Properties of Tetravalent Actinide Ions and Compounds," J. Less-Common Metals **133**, 39 (1987); LBL-22319.
20. E. Gamp, R. Shinomoto, N. Edelstein, and B.R. McGarvey, "Multinuclear NMR Spectroscopy of the Tetrahedral Uranium(IV) Complex $U(BH_3CH_3)_4$," Inorg. Chem. **26**, 2177 (1987); LBL-22310.
21. R. Shinomoto, A. Zalkin, N.M. Edelstein, and D. Zhang, "Preparation and Crystal Structures of Complexes of $U(BH_3CH_3)_4$ with 1,2-Dimethoxyethane, N,N,N′,N′-Tetramethylethylenediamine, and 1,2-Bis(methylthio)ethane," Inorg. Chem. **26**, 2868 (1987); LBL-22925.
22. R. Shinomoto, A. Zalkin, and N.M. Edelstein, "Preparation and Crystal Structures of Tetrakis-(methyltrihydroborato)uranium(IV)bis(tetrahydrofuranate) and Tetrakis(methylhydroborato)uranium (IV)tetrahydrothiophenate," Inorg. Chim. Acta **139**, 91 (1987); LBL-23297.
23. R. Shinomoto, A. Zalkin, and N. Edelstein, "Preparation of Some Lewis Base Adducts of Tris(methyltrihydroborato)Ho and Yb and Crystal Structures of Tris(methyltrihydroborato)ytterbium(III)-(Etherate and Tris(methyltrihydroborato) holmium(III)bis(pyridine)," Inorg. Chim. Acta **139**, 97 (1987); LBL-23296.
24. H.-D. Amberger, H. Reddmann, G. Shalimoff, and N.M. Edelstein, "The Electronic Structure of Organometallic Complexes of the f Elements–XIX. Parameterization of the Crystal Field Splitting Patterns of Quasi Trigonal Bi-pyramidal Anionic Complexes Involving the Tris(η^5-cyclopentadienyl)-uranium(IV) Moiety," Inorg. Chim. Acta **139**, 335 (1987); LBL-22073.
25. A. Zalkin, D.H. Templeton, D. Eimerl, and S.P. Velsko, "Trithallium(I) Phosphate, an Optical Second-

Harmonic Generator," Acta Crystallogr. C **42**, 1687 (1986); LBL-21314.

26. B. Zemva, A. Jesih, D.H. Templeton, A. Zalkin, A.K. Cheetham, and N. Bartlett, "Phases in the System XeF_2/XeF_5AsF_6 and Structural and Vibrational Evidence for the Ionization Pathway: $XeF_2 \rightarrow XeF^+ + F^-$," J. Am. Chem. Soc. **109**, 7420 (1987).
27. D.H. Templeton and L.K. Templeton, "X-ray Birefringence, Forbidden Reflections, and Direct Observation of Structure-Factor Phases," Acta Crystallogr. A **43**, 573 (1987).†
28. D. Eimerl, L. Davis, S. Velsko, E.K. Graham, and A. Zalkin, "Optical, Mechanical, and Thermal Properties of Barium Borate," J. Appl. Phys. **62**, 1968 (1987).
29. E. Kaufmann, P. Schleyer, S. Gronert, A. Streitwieser, Jr., and M. Halpern, "The Structures and Energies of Main Group Metal Formyl Complexes. The Mechanism of the Reaction of LiH with CO. An *Ab Initio* Study," J. Am. Chem. Soc. **109**, 2553 (1987).

Other Publications

30. D.L. White, P.W. Durbin, N. Jeung, and K.N. Raymond, "Specific Sequestering Agents for the Actinides. 16. Initial Biological Testing of Synthesis and Polydentate Hydroxypyridonate Ligands," J. Med. Chem. (in press).
31. P.H. Smith and K.N. Raymond, "Biomimetic Ligands: Metal Ion Specificity and Encapsulation," XXVth ICCC, Nanjing, People's Republic of China, July 26–31, 1987; IUPAC J. (in press).
32. D. Zhu, M.J. Kappel, and K.N. Raymond, "Coordination Chemistry of Lanthanide Catechcolates," submitted to Inorg. Chim. Acta.
33. G. S. Smith, Q.C. Johnson, D.E. Cox, R.L. Snyder, D.K. Smith, and A. Zalkin, "Synchotron Radiation Applied to Computer Indexing," in *Advances in X-Ray Analysis*, Vol. 30, Lawrence Livermore National Laboratory; UCRL-94599.

LBL Reports

34. D.J. Berg, C.J. Burns, R.A. Andersen, and A. Zalkin, "Electron-Transfer Reactions of Divalent Ytterbium Metallocenes: Synthesis of the Series $[(Me_5C_5)_2Yb]_2[\mu\text{-}E]$ Where E is O, S, Se, or Te and the Crystal Structure of $[(Me_5C_5)_2Yb]_2[\mu\text{-}Se]$," LBL-22934.
35. J.L. Stewart and R.A. Andersen, "Preparation and Crystal Structure of Addition Compound $MeLi{\cdot}U[OCH(CMe_3)_2]_4$, a Compound with a Uranium to Carbon Sigma Bond," LBL-23513.
36. J.G. Brennan, R.A. Andersen, and A. Zalkin, "Crystal Structures of $(MeC_5H_4)_4U_2(\mu\text{-}NR)_2$. Unsymmetrical Bridging, R=Ph, and Symmetrical Bridging, R=$SiMe_3$, Organoimide Ligands in Organoactinide Compounds," LBL-24055.
37. J.G. Brennan, S.D. Stults, R.A. Andersen, and A. Zalkin, "Crystal Structures of $(MeC_5H_4)_3M(L)$ Where M is Uranium or Cerium and L is Quinuclidine or $P(OCH_2)_3CEt$; Evidence for Uranium to Phosphorus π-Backbonding," LBL-22025.
38. C.J. Burns (Ph.D. Thesis), "The Coordination Chemistry of Divalent Bis(Pentamethylcyclopentadienyl)Lanthanide Complexes with Non-Classical Ligands," LBL-24110.
39. D.J. Berg (Ph.D. Thesis), "Bis(Pentacyclopentadienyl)Ytterbium: Reactions with Organic Compounds and Related Molecules," LBL-24153.
40. I. Poirot, W. Kot, G. Shalimoff, N. Edelstein, M.M. Abraham, C.B. Finch, and L.A. Boatner, "Optical and EPR Investigations of Np^{4+} in Single Crystals of $ZrSiO_4$," Phys. Rev. B (in press); LBL-23518.
41. N.M. Edelstein, "Optical Properties of Tetravalent Uranium in the Solid State," in *Proc. 2nd Int. Conf. Basic and Applied Chem. of f-Transition (Lanthanide and Actinide) and Related Elements*, Lisbon, Portugal, April 6–10, 1987; submitted to Inorg. Chim. Acta; LBL-24003.
42. W. Kot, G.V. Shalimoff, N. Edelstein, M.A. Edelman, and M.F. Lappert, "$[Th(III)\{\eta^5\text{-}C_5H_3(SiMe_3)_2\}_3]$, An Actinide Compound With a $6d^1$ Ground State," J. Am. Chem. Soc. (in press); LBL-24136.
43. P.H. Smith, Z.E. Reyes, C.-W. Lee, and K.N. Raymond, "Characterization of a Series of Lanthanide Amine Cage Complexes," submitted to Inorg. Chem.; LBL-24530.

Invited Talks

44. K.N. Raymond, "Specific Sequestering Agents for Iron and Actinides," Department of Chemistry, Iowa State University of Science and Technology, Ames, Mar. 19–20, 1987.
45. K.N. Raymond, "Metal Sequestering Agents in Bioinorganic Chemistry," Leiden, The Netherlands, July 6–10, 1987.
46. K.N. Raymond, "Biomimetic Ligands: Metal Ion Specificity and Encapsulation," XXV International Conference on Coordination Chemistry, Nanjing, People's Republic of China, July 26–31, 1987.
47. K.N. Raymond, "Actinide Specific Sequestering Agents," Institute of Atomic Energy, Beijing, People's Republic of China, Aug. 4, 1987.
48. R.A. Andersen, "Bis(pentamethylcyclopentadienyl)-Ytterbium Chemistry," University of Texas, Austin, June 30, 1987; Stanford University, Stanford, CA, Nov. 3, 1987.
49. N. Edelstein, "Optical Properties of Tetravalent Uranium in the Solid State," presented at "Trends on Fundamental Research on Uranium as a Nonnuclear Element," 2nd International Conference on Lanthanides and Actinides (ICLA), Lisbon, Portugal, Apr. 6–10, 1987.
50. N. Edelstein, "Electronic Structure and Optical Spectroscopy of Lanthanide and Actinide Ions," Montana State University, Bozeman, May 15, 1987.
51. L.K. Templeton and D.H. Templeton, "Anomalous Scattering of Synchrotron Radiation" and "X-ray

Birefringence, Forbidden Reflections, and Direct Observation of Diffraction Phases," Patterson Award Lectures, American Crystallographic Association Meeting, Austin, TX, Mar. 16, 1987.

52. D.H. Templeton, "Service Crystallography — A Critical View," American Crystallographic Association Meeting, Austin, Texas, Mar. 18, 1987.
53. D.H. Templeton and L.K. Templeton, "X-ray Birefringence, Anomalous Scattering, and the Phase Problem," XIVth International Union of Crystallographers Congress, Perth, Australia, Aug. 14, 1987.
54. D.H. Templeton, "Lattice Sums and the Madelung Constant; Ewald in America," XIVth International Union of Crystallographers Congress, Perth, Australia, Aug. 15, 1987.
55. D.H. Templeton and L.K. Templeton, "Anomalous Scattering Factors," Symposium on Accuracy in Structure Factor Measurements, Warburton, Australia, Aug. 26, 1987.
56. D.H. Templeton and L.K. Templeton, "X-Ray Birefringence and Anomalous Scattering," Stanford Synchrotron Radiation Laboratory Users' Conference, Stanford, CA, Oct. 22, 1987.

†Supported by NSF Grant No. CHE-821-7443.

Fossil
Energy

Studies of Materials Erosion in Coal Conversion and Utilization Systems*

Alan V. Levy, Investigator

INTRODUCTION

The erosion and erosion-corrosion of materials were investigated at test conditions that related to the operating conditions in fluidized bed combustors, coal gasifiers, and steam turbines. Alternate, chromium containing steels were tested with both round and angular shaped particles to determine the effects of the morphology of the scales that formed on them and the resulting metal wastage rates. The erosivity of various size bed material particles from an atmospheric fluidized bed was determined at elevated temperatures. The effect of solid solution strengthening of iron and copper base alloys on their erosion rates was investigated. Erosion protection coatings were studied over a range of test variables. The erosion-corrosion rates and mechanisms of tubing steels tested in a laboratory nozzle tester were compared to the metal wastage that occurred on in-bed tubes in an atmospheric fluidized bed combustor. A first attempt was made to identify a possible tradeoff between test variables to achieve an erosion severity parameter that would be common to both laboratory and in-service test exposures.

1. Erosion-Corrosion of Scales on Alternate Steel Tubing Alloys (Publication 16)

W. Bu-Qian

The metal wastage mechanisms of commercial, chromium containing alloy steels were used as the basis for selecting and testing alternate compositions with lower chromium contents. Alloys containing small amounts of added silicon were tested and their metal loss rates were compared to similar compositions that contained normal amounts of silicon. The oxide scales that formed on the alternate alloys during erosion-corrosion tests at 650°C and 850°C were determined to retain the segmented scale morphology that was demonstrated in earlier work to result in low metal wastage rates. Standard silicon content chromium alloy steels formed consolidated scales at the same test conditions that were removed by a faster, metal wastage mechanism. The differences in metal wastage rates were significant with the higher silicon content, 2–5% chromium alloys performing better than standard steels containing up to 20% chromium. The amount of difference in metal wastage between the higher silicon and standard silicon content alloys decreased as the angularity of the erodent particles increased. The potential for the lower cost, alternate alloys to reduce metal wastage rates in erosion-corrosion environments is promising.

2. The Erosivity of Fluidized Bed Combustor Bed Material (Publication 17)

S. Zheng-Rong

The bed material in fluidized bed combustors (FBCs) contains hard particles such as SiO_2 and Al_2O_3, as well as CaO and $CaSO_4$ that cause metal wastage of in-bed heat exchanger tubes. An investigation was carried out using a laboratory nozzle tester to determine the effect of the particles on the nature of the surface degradation. Bed material from the Canadian CANMET Pt. Tupper atmospheric FBC was obtained for testing and used as erodent with three particle sizes: 600, 250, and 130 μm in dia. Three alloys were tested: 9Cr1Mo steel and 304 and 310 stainless steels. It was determined that the largest size particles used were generally more erosive than smaller particles. The angular shaped bed material was more erosive than angular Al_2O_3 and SiC erodent particles used at the same elevated temperature erosion-corrosion test conditions in a laboratory nozzle tester. The 130 and 250 μm size particles formed a deposit on the surface of the test specimens at lower particle velocities that protected the surface somewhat, as occurs on in-bed tubes of FBCs. All metal loss was the result of erosion of oxide scale and its continual replacement by the oxidation of the base metal.

3. Erosion of Solid Solution Strengthened Alloys (Publication 18)

S. Zheng-Rong and W. Bu-Qian

The hardening of many iron, nickel, and cobalt base structural alloys by various mechanical or ther-

*This work was supported by the U.S. Department of Energy under DOE/FE AA 15 10 10 0, Advanced Research and Technical Development, Fossil Energy Materials Program, Work Breakdown Structure Element LBL-3, and under Contract No. DE-AC03-76SF00098.

mal processes to improve their erosion resistance has been investigated and has been found to not increase their erosion resistance. In order to determine whether the last possible general strengthening mechanism for structural alloys that could be tried—solid solution strengthening—improved erosion resistance, both iron and copper base alloys were melted and room temperature erosion tested in the as-cast and rolled forms. It was determined that solid solution strengthening of eight different alloys did not improve their erosion resistance and, to some degree, had a small negative effect on their performance. There was relatively little difference in their erosion rates over a wide range of hardness. There was also essentially no difference in the erosion rates of as-cast and rolled versions of the same alloys. It appears that the solid particle erosion wear mechanism in ductile structural alloys transcends the strengthening mechanisms that generally increase the degradation resistance of alloys subjected to other types of forces.

4. The Effects of Test Variables on the Erosion of Protective Coatings (Publication 19)

W. Bu-Qian

The use of coating systems to protect structural metal surfaces from elevated temperature small, solid particle erosion and erosion-corrosion can extend component life and permit operation in more severe environments. The room and elevated temperature erosion behavior of several hard material coating systems—i.e., carbides, borides, and nitrides—was determined over a range of test conditions. Particle velocities from 70 to 150 m/sec and test temperatures from 25°C to 540°C were used. Mechanisms of erosion were established and related to erosion rates in a manner that defined the requirements of composition, morphology, and defect levels of coating systems for long term service. It was determined that small grain size, low porosity, and the absence of cracks were microstructural features that enhanced erosion resistance. Hardness levels and the composition and distribution of second phase, hard particles had less effect on coating performance. Angular silicon carbide particles were considerably more erosive than either alumina or mixed oxide, round shaped particles; and the ranking of the coatings' performances were different for each erodent and set of test conditions.

5. The Relationships Between Laboratory and In-Service Erosion-Corrosion Tests (Publication 20)

M. Yong-Fa and N. Jee

The comparative erosion-corrosion behavior of steels that are used in coal burning energy generation equipment as determined in both laboratory nozzle tester and FBC in-service exposures at elevated temperatures was analyzed. It was determined that the steels tested in both environments had the same types of metal wastage mechanisms and, generally, similar metal wastage rates. At shallow impingement angles and low particle velocities, scales formed on the steel surfaces that were segmented and were removed by a slow cracking and chipping mechanism. At steeper impingement angles and higher particle velocities, consolidated scales occurred that were removed by a higher rate, spalling mechanism. As the chromium content of the steels was increased, the scales became thinner but were still removed by the same mechanisms. At lower particle velocities, protective erodent buildups occurred on the surface of alloys in both the laboratory and in-service tests.

6. Work in Progress

Determination of Erosion-Corrosion Test Variable Tradeoffs (G. Gangquang)

The possible development of an "erosion severity" parameter based on tradeoffs between primary test conditions such as particle shape and velocity and test temperature is being investigated. Earlier work has indicated that combinations of various levels of test variables such as more rounded particles in combination with a higher test temperature could result in the same metal wastage rates as a more angular particle at a lower test temperature. The objective of the study will be to determine test variable tradeoff combinations that will make it possible to equate erosion severity in laboratory tests to in-service exposures without having to closely simulate the total in-service environment.

Development of Low Velocity Erosion Tester (S. MacAdam)

An erosion tester is being developed that can test specimens at particle velocities from <1 to 10

m/sec. The tester is designed to rotate flat surface specimens in a fluidized bed of erodent particles at elevated temperatures in a neutral or reactive gas atmosphere.

Behavior of Alternate Alloy Steels at Low Elevated Temperatures (G. Gangquang)

The very promising results obtained using alternate, low chromium content steels in erosion-corrosion tests at higher elevated temperatures to 850°C will be pursued at lower test temperatures down to 300°C to determine if the low metal wastage rates happen at temperatures that occur in fluidized bed combustors.

Erosion and Erosion-Corrosion of Materials (A.V. Levy)

The knowledge of the erosion and erosion-corrosion of materials in gas and liquid, solid particle flows gained over the last decade of experimental work at LBL is being consolidated into a book.

1987 PUBLICATIONS AND REPORTS

Refereed Journals

1. A.V. Levy, N. Jee, and P. Yau, "Erosion of Steels in Coal-Solvent Slurries," Wear **117**, 115 (1987); LBL-17238.
2. A.V. Levy and G. Hickey, "Liquid-Solid Particle Slurry Erosion of Steels," Wear **117**, 129 (1987); LBL-17239.

Other Publications

3. A.V. Levy and N. Jee, "The Erosion-Corrosion of Scales on Heat Exchanger Alloys," in *NACE Corrosion 87*, San Francisco, CA, Mar. 1987, Paper No. 475.
4. A.V. Levy and M. Yong-Fa, "Effect of Test Variables on the Erosion-Corrosion of Chromium Steel," in *NACE Corrosion 87*, San Francisco, CA, Mar. 1987, Paper No. 17.
5. A.V. Levy and W. Bu-Qian, "Erosion-Corrosion of Protective Scales on Alloy Steels," in *Proc. Int. Conf. Metallurgical Coatings*, San Diego, CA, Mar. 1987.
6. A. Ninham and A.V. Levy, "The Erosion of Carbide-Metal Composites," in *Proc. ASME Conf. Wear of Materials 1987*, Houston, TX, Apr. 1987, p. 825.
7. A. Ninham, "The Effect of Mechanical Properties on Erosion," in *Proc. ASME Conf. Wear of Materials 1987*, Houston TX, Apr. 1987, p. 813.
8. A.V. Levy and W. Bu-Qian, "Erosion of Hard Materials Coating Systems," in *Proc. ASME Conf. Wear of Materials 1987*, Houston, TX, Apr. 1987, p. 477.
9. A.V. Levy, M. Yong-Fa, and N. Jee, "The Erosion-Corrosion of Heat Exchanger Tubes in Fluidized Bed Combustors," in *Proc. ASME 1987 Int. Conf. Fluidized Bed Combustion*, Boston, MA, May 1987, p. 637.
10. A.V. Levy, "Studies of Materials Erosion in Coal Conversion and Utilizations Systems," in *Proc. DOE-ORNL Fossil Energy Materials Program Conf.*, Oak Ridge, TN, May 1987, p. 467.
11. A.V. Levy, S. Zheng-Rong, and W. Bu-Qian, "Erosion of Solid Solution Strengthened Alloys," in *Proc. Seventh Int. Conf. Erosion by Liquid and Solid Impact*, Cambridge, England, Sept. 1987, Paper No. 51.
12. A.V. Levy, W. Bu-Qian, M. Yong-Fa, and N. Jee, "Erosion-Corrosion of Steels in Simulated and Actual Fluidized Bed Combustor Environments," in *Proc. Seventh Int. Conf. Erosion by Liquid and Solid Impact*, Cambridge, England, Sept. 1987, Paper No. 72.
13. A.V. Levy and W. Bu-Qian, "Erosion-Corrosion of Scales on Low Alloy Steels," in *Proc. ASM Symp. Tribological Mechanisms and Wear Problems in Materials*, Cincinnati, OH, Oct. 1987.
14. A.V. Levy, S. Zheng-Rong, and W. Bu-Qian, "Erosivity of Fluidized Bed Combustor Bed Material," in *Proc. ASM Symp. Materials Performance in Fluidized Bed Combustion Environments*, Cincinnati, OH, Oct. 1987.
15. A.V. Levy, "The Erosion-Corrosion of FBC, In-Bed Tubing Alloys," in *Proc. ANL-EPRI Workshop on Wastage of In-Bed Surfaces in Fluidized Bed Combustors*, Argonne, IL, Nov. 1987.

LBL Reports

16. A.V. Levy and W. Bu-Qian, "Erosion-Corrosion of Alternate Low Alloy Steel Tubing Alloys," LBL-24608.
17. A.V. Levy, S. Zheng-Rong, and W. Bu-Qian, "The Erosivity of FBC Bed Material," LBL-24609.
18. A.V. Levy, S. Zheng-Rong, and W. Bu-Qian, "Erosion of Solid Solution Strengthened Alloys," LBL-24610.
19. A.V. Levy and W. Bu-Qian, "Erosion of Hard Material Coating Systems," LBL-24611.
20. A.V. Levy, N. Jee, L. Sun, and S. Zheng-Rong, "Analysis of Scales Formed on AFBC In-Bed Tubes," LBL-24612.

Invited Talks

21. A.V. Levy, "Erosion and Erosion-Corrosion Rates and Mechanisms of Metals and Coatings," Combustion Engineering Co., Chattanooga, TN, June 1987.

22. A.V. Levy, "Erosion Behavior of Metals and Ceramics," Vanderbilt University, Nashville, TN, May 1987.

23. A.V. Levy, "Mechanisms of Material Removal in Erosion and Erosion-Corrosion," Kentucky Energy Cabinet Laboratory, Lexington, KY, May 1987.

24. A.V. Levy, "Erosion-Corrosion of Alternate, Chromium Alloy Steels," Oak Ridge National Laboratory, Oak Ridge, TN, Oct. 1987.

25. A.V. Levy, "Metal Wastage Mechanisms in Fluidized Bed Combustor, In-Bed Heat Exchanger Tubes," National Research Council of Canada, Montreal, Quebec, Oct. 1987.

26. A.V. Levy, "Erosion of Protective Coatings," Brown Boveri Co., Baden, Switzerland, Sept. 1987.

Fundamental Studies of Catalytic Gasification*

Heinz Heinemann, Investigator, with G.A. Somorjai, Investigator, and J. Carrazza

INTRODUCTION

This program studies the basic chemistry of the reaction of carbonaceous materials with water in the presence of catalysts to produce hydrogen and/or synthesis gas. In the past this program has investigated the role of catalysts in the relatively low-temperature steam gasification of graphite and of chars. New mechanisms have been demonstrated, and it has been shown that combinations of alkali hydroxide with transition metal oxides form compounds that act as the true catalyst to produce mostly hydrogen and carbon dioxide. This has been further confirmed by surface science studies and by transmission electron microscopy. At the lower temperatures used (~800 K), hydrogen and CO_2 are the predominant products formed from graphite, but the effect of temperature and of the exact composition of the NiO/KOH catalyst that has been studied in the greatest detail on the CO_2/CO ratio remains to be defined. Similarly, a clear definition of the advantages of different alkali–transition metal oxide compositions is required. It appears possible that with the right catalyst and conditions, either syngas or $H_2 + CO_2$ can be produced.

1. Kinetics of the Steam Gasification of Chars (Publications 4 and 5)

H. Heinemann

Activation energies for K/Ni catalyzed steam gasification of graphite and of chars are identical, indicating that the same mechanism prevails though rates are much higher for chars. This result permits extrapolation of findings in high-vacuum equipment from graphite to chars.

The kinetic properties of a catalyst derived from a mixture of KOH and $Ni(NO_3)_2$ for steam gasification of three chars have been determined. H_2, CO_2, smaller amounts of CO, and negligible amounts of CH_4 are the reaction products. The product distribution is controlled by the activation energies for formation of the gases. The activation energies for H_2 and CO_2 formation are 29 and 36 Kcal/mol, respectively. The catalyst derived from the $KOH/Ni(NO_3)_2$ mixture has better catalytic properties, due to a cooperative effect between nickel and potassium, than the catalyst derived by loading the components alone. The mixture has a higher activity and lower activation energies for H_2 and CO_2 production than does KOH alone, and it has a higher resistance to deactivation than does $Ni(NO_3)_2$ alone.

The CO/CO_2 ratio of gases produced in the presence of a K/Ni catalyst along with hydrogen varies with different chars. The ratio is 0.8 for Illinois #6 char and 0.08 for North Dakota char. Methane production is several orders of magnitude smaller and ceases after about 2 hours. North Dakota char, which has the highest ash content of all chars tested, showed higher gasification rates than the other chars tested and exhibited some activity even in the absence of an added K/Ni catalyst. However, this innate activity died within a few hours. North Dakota char was treated with steam until it was inactive, and then a K/Ni catalyst was added. Gasification now occurred at a higher rate than the initial one with the untreated char, and deactivation was extremely slow. About 40% of the char was gasified in 2 hours. A totally demineralized char (by treatment with HF/HCl) had no activity. Ni on this char had only slight activity, but Ni/K allowed 100% char consumption in 2 hours (see Figure 1-1).

Deactivation of Ni/K containing char does not appear to be a function of reduced porosity or surface of the char during gasification, but of catalyst poisoning by ash components that can be deactivated by steaming. Potassium appears to interact with calcium in the ash, giving a eutecticum that wets the carbon and acts as a gasification catalyst, which is superior to either potassium or calcium alone in the absence of ash. Alkali earth–alkali mixtures must therefore be investigated as potential catalysts. Nickel alone is very sensitive to the ash content of the char, apparently due to the interaction between nickel and either calcium or sulfur. It has almost no activity for gasifying the North Dakota char, in contrast to a short-lived high-level activity in the gasification of graphite and of low-ash chars.

*This work was supported by the Assistant Secretary of Fossil Energy, Office of Management, Planning, and Technical Coordination, Technical Coordination Division of the U.S. Department of Energy under Contract No. DE-AC03-76SF00098, through Morgantown Energy Technology Center, Morgantown, WV 26505.

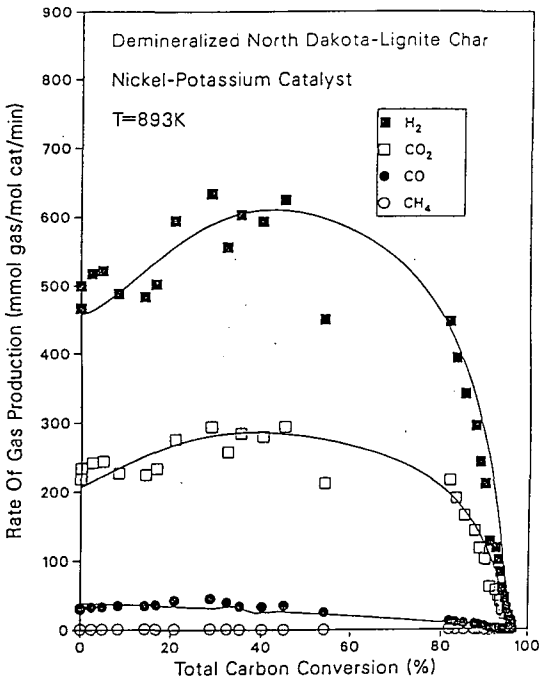

Figure 1-1. Rate of gas production as a function of carbon conversion, for all the gases formed from the steam gasification of demineralized char at 893 K, catalyzed by the nickel-potassium mixture. The molar ratio of nickel to potassium was equal to 0.9, and the catalyst loading was equal to 2.0 mmol cat/g char. The initial weight of char was 0.5 g. (XBL 884-1330)

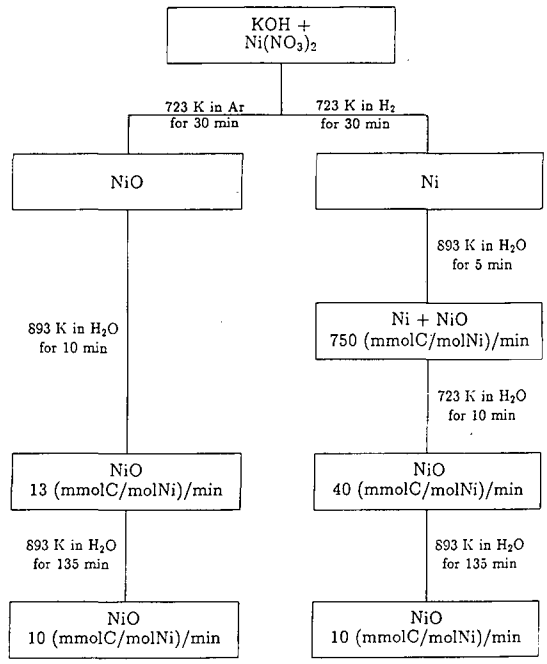

Figure 2-1. Summary of the results obtained with the catalyst derived from a mixture of KOH and $Ni(NO_3)_2$. (XBL 884-1337)

2. Surface Science Studies of Catalyst Components (Publications 4 and 5)

H. Heinemann

An x-ray photoelectron spectroscopy (XPS) study of surface species on graphite after impregnation with KOH and/or $NiNO_3$ before and after gasification confirmed the chemical interaction of potassium and nickel compounds. The following results were found: (a) Nickel stabilizes potassium on the surface and prevents its vaporization at reaction temperature. (b) Nickel alone, a brief-lived very active catalyst, becomes deactivated because it cannot wet the carbon surface. In the presence of potassium, wetting takes place. (c) Most of the nickel in the K/Ni catalyst is present in the Ni(+2) form, which is not reduced by carbon or hydrogen. It is possible that there is a very small amount (>2%) of metallic nickel present in the NiO. It is also possible that under the influence of KOH or NiO(OH) a Ni(+3) is formed, which may dissociate water (see Figure 2-1).

3. Reaction of Graphite with Various Gases (Publications 2 and 3)

B. Marchon, G.A. Somorjai, and H. Heinemann

Prior to an attempt to determine the surface species on carbonaceous materials formed by reaction with either CO, CO_2, O_2, or H_2O, experiments on adsorption and temperature-programmed desorption (TPD) were carried out with graphite. CO, CO_2, O_2, and H_2O chemisorption yield the same CO desorption precursor on three different sites, decomposing at 700, 820, and 980°C. This species has been tentatively assigned to a semi-quinone functional group. As byproducts of the CO precursor, CO_2 adsorption gives gaseous CO, and H_2O adsorption gives hydrogen atoms that either recombine to form H_2 or form carbon-hydrogen bonds of two types, aromatic-like and aliphatic-like. The first type decomposes around 1000°C to produce H_2, and the second produces hydrocarbons below 500°C.

A small fraction of the CO precursors reacts with the adsorbing gas to produce the CO_2 precursor, which then decomposes thermally between 200 and 600°C. A lactone species has been proposed as the CO_2 surface precursor.

CO adsorbed at room temperature leads to the formation of a weakly bound species, assigned to a carbonyl group, and desorbs at 200°C as CO. Physical wetting by water also leads to a weakly bound species, suggested to be a hydrate, and desorbs at 350°C as H_2O.

4. Work in Progress

Work for the immediate future involves essentially two tasks: (1) A set of seven chars and their analyses have been received from Illinois Institute of Gas Technology. These chars vary in derivation, and in ash and sulfur content. The interaction of mineral matter and catalysts will be further studied with these samples. (2) Mixtures of earth alkali and alkali salts will be studied as potential gasification catalysts.

1987 PUBLICATIONS AND REPORTS

Refereed Journals

1. J. Carrazza, J.J. Chludinsky, Jr., H. Heinemann, G.A. Somorjai, and R.T.K. Baker, "Controlled Atmosphere Electron Microscopy Study of the Gasification of Graphite by Water, Hydrogen and Oxygen Catalyzed by a Nickel/Potassium Mixture," J. Catal. **110**, 1 (1988); LBL-23337.

LBL Reports

2. B. Marchon, W.T. Tysoe, J. Carrazza, H. Heinemann, and G.A. Somorjai, "The Reactive and Kinetic Properties of Carbon Monoxide and Carbon Dioxide on Graphite Surface," submitted to J. Phys. Chem.; LBL-24184.
3. B. Marchon, J. Carrazza, H. Heinemann, and G.A. Somorjai, "TPD and XPS Studies of O_2, CO_2 and H_2O Adsorption on Clean Polycrystalline Graphite," Carbon (in press); LBL-24185.
4. H. Heinemann, "Fundamental Studies of Catalytic Gasification: Quarterly Report, April 1, 1987–June 30, 1987," LBL-23649.
5. H. Heinemann, "Fundamental Studies of Catalytic Gasification: Annual Report, October 1, 1986–September 30, 1987," LBL-23930.

Invited Talks

6. H. Heinemann, "Catalytic Gasification Fundamentals," Morgantown Energy Technology Center, Morgantown, WV, June 1987.
7. H. Heinemann, "Gasification Mechanisms," Mobil Research and Development Corp., Princeton, NJ, Apr. 1987.
8. H. Heinemann, "Steam Gasification of Carbonaceous Solids Catalyzed by a Mixture of Potassium and Nickel Oxides below 1000 K," American Chemical Society, Anaheim, CA, Apr. 1987.

Energy Storage Systems

ELECTROCHEMICAL ENERGY STORAGE

Lutgard C. DeJonghe, James W. Evans, Rolf H. Muller, John Newman, Philip N. Ross, Jr., and Charles W. Tobias, Investigators

Surface Morphology of Metals in Electrodeposition*

Charles W. Tobias, Investigator

INTRODUCTION

The objective of this project is to gain understanding of the partial processes and their interactions involved in the deposition and dissolution of metals by electrolysis. Of particular interest is the influence of hydrodynamic flow on electrocrystallization, and the distribution of charge-transfer rates on advancing and receding metal profiles, as determined by the electric and concentration fields in the solution, and by the kinetics of the charge-transfer reaction. Control of the morphology of metallic deposits has been traditionally effected by addition agents that interfere with the crystallization process. In energy-storage applications, however, other means may have to be employed for the control of morphology.

- Rotating-disk electrodes and planar electrodes in channel-type electrolyzers are used for the preparation of metal deposits, over large ranges of solution properties and hydrodynamic conditions, with potentiostatic or galvanostatic control. The genesis of surface textures is studied, using *in situ* motion-picture microphotography, videorecording, and *post mortem* examination by electron microscopy.
- Developing surface contours are simulated by solving the Laplace equation, using either the finite-difference, finite-element, or boundary-element method.

*This work was supported by the Assistant Secretary of Conservation and Renewable Energy, Office of Energy Storage and Distribution of the U.S. Department of Energy under Contract No. DE-AC03-76SF00098.

1. Mechanism of Leveling in Electrodeposition (Publication 10)

J.O. Dukovic, K.G. Jordan, and C.W. Tobias

According to the adsorption theory of leveling and brightening, the lower rate of diffusion of inhibitors into recesses, relative to transport to the more accessible areas on the surface, results in accelerated smoothing and evening of the electrodeposits. Simulation of advancing profiles based on the simultaneous solution of the Laplace equation for the electric fields, however, predicts a more rapid leveling action than is generally found by measuring actual deposit profile thicknesses. In our view this discrepancy is caused by a neglect of microscopic flows into recesses (notches, V-grooves) in computer-implemented simulations.

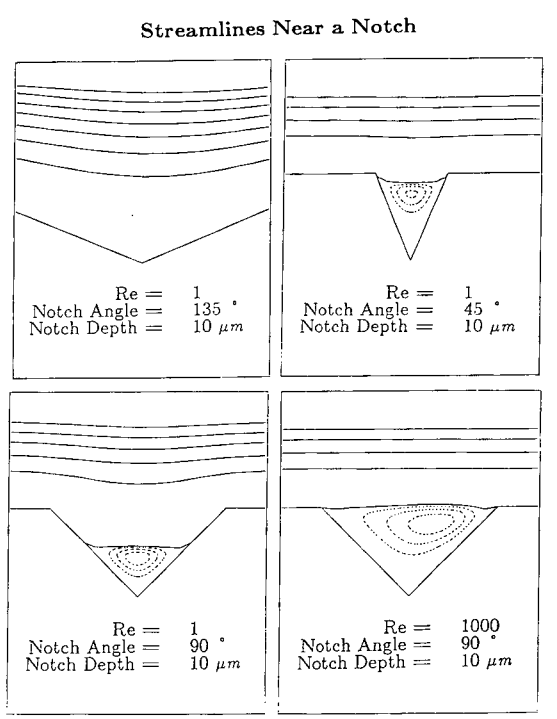

Figure 1-1. Streamlines in a notch resulting from Couette flow. Fluid motion originates from solid plane moving parallel to electrode at a distance of ten times the notch depth. Movement of electrolyte improves transport of inhibitor, thereby reducing leveling action. (XBL 884-1323)

Enhanced transport of inhibitors into recesses would tend to decrease the leveling action by interference with the deposition process in the more remote areas. As a first approach to the elucidation of this problem, we have solved the flow field in Couette and Poiseuille flows past angular notches over a range of Reynolds numbers and notch angles. The Polyflow program was used for the finite-element routine. Results indicate that there is a recirculation pattern in notches below a critical angle. As the Reynolds number is increased, the recirculation region grows in strength and eventually becomes asymmetrical (see Figure 1-1). The solution of the convective diffusion equation based on the results of the hydrodynamic analysis indicates that these recirculation flows can indeed explain the decrease in leveling action when compared to a condition of stagnant electrolyte. Thus, while effective convective transport is essential for the transport of the reacting metal ion, the same condition has an adverse effect on leveling.

Engineering Analysis of Electrolytic Gas Evolution

Charles W. Tobias, Investigator

INTRODUCTION

Electrolytic gas evolution is among the most common reaction types in electrolysis and in advanced rechargeable batteries. Modern applications in energy storage and transmission (e.g., hydrogen) require much higher energy efficiency and lower capital cost than achieved in gas-generating processes in the past. This project is directed toward the quantitative description of partial processes and their interactions involved in the nucleation, coalescence, and detachment of gas bubbles. Of special interest are the effects of moving individual bubbles and of gas-electrolyte emulsions on ohmic-cell resistance and on mass transport of charged and uncharged species to and from electrode surfaces. A thorough understanding of the physical processes involved in the liberation and movement of gases at electrodes and in the electrolyte should lead to improved energy efficiency and lower capital costs in process and device technology.

1. Experimental Observations of Free-Convection Mass Transfer to a Horizontal Surface with a Micromosaic Electrode (Publication 1)

D.W. Dees and C.W. Tobias

The classical limiting-current method was employed in performing mass-transfer experiments on a 1-mm square micromosaic electrode facing upward in a horizontal position. The reduction of ferric to ferrous ions ($Fe^{3+} + e = Fe^{2+}$) in the presence of 1.0M H_2SO_4 served as the indicator reaction. All 100 segments were polarized cathodically in the mass-transfer limiting region, but only to potentials less negative than necessary for the reduction of hydrogen ions. The current to each segment was measured, providing a direct quantitative measure of the mass-transfer rate of all individual segments.

To monitor the current to each segment required computer data acquisition and control. A 128-channel multiplexer connected to a current follower and a potentiostat were used for this purpose. Data sample rates range from 1.0 to 10 kHz. The change in limiting current to a segment after a potential step follows the Cottrell behavior (diffusion from a semi-infinite column), but after about 20 seconds the Raleigh stability criterion is reached; the density gradient next to the electrode becomes large enough for free convection to commence. The current to each segment demonstrates regular periodic variation, with a period of 29 ± 1 sec. While the period of fluctuations remains constant, those of neighboring segments are not in phase with each other. An almost linear lag between distance and phase lag has been observed. In Figure 1-1 lines of constant phase lag are plotted every two seconds; the arrow points in the direction of increasing phase lag. This illustrates the nature of the flow across the surface. From the distance between lines, a phase lag velocity of 40 μm/sec was determined.

The periodicity indicates a repetitive fluid-flow pattern next to the electrode. The size of this pattern can be estimated from the period of fluctuations and the velocity with which it travels across. This velocity multiplied by the period yields 1.1 mm for the characteristic length. The picture emerging from this analysis of the microhydrodynamic events at a horizontal electrode facing upward confirms the existence of Bernard-type cellular flows, a very effective mechanism of fluid motion that enhances mass transfer to the surface in an otherwise stagnant pool of electrolyte.

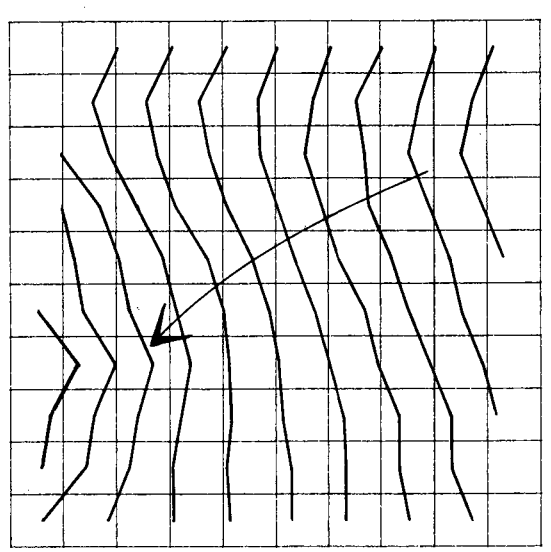

Figure 1-1. Lines of constant phase lag of fluctuations in the free convection limiting current to hundred matrix segments, covering a 1 × 1 mm area. Lines are plotted every two seconds; the arrow indicates increasing phase lag. Electrode reaction: $Fe^{3+} + e = Fe^{2+}$. (XBL 838-6114)

2. The Shape and Stability of Axisymmetric Gas Bubbles Attached to a Curved Surface (Publications 8 and 11)

G.M. Whitney and C.W. Tobias

The equation of Bashforth and Adams has been used to calculate the configurations of axisymmetric bubbles formed on a curved surface, such as on a hemispherical solid. The volume of the largest stable equilibrium bubbles that can adhere to a flat horizontal surface is a function of the characteristic length of the system,

$$L_c \equiv \left[\frac{\gamma}{\rho g}\right]^{1/2} ,$$

and the equilibrium contact angle θ and is given by

$$\frac{V_{max,\,flat}}{\pi L_c^3} = 0.285\,\theta^{2.96} \quad (\theta \text{ in radians}) \quad ,$$

where γ is surface tension, ρ is density, and g is acceleration of gravity.

The bubble configurations of maximum volume for contact angles greater than 60° have re-entrant contact angles. A stability analysis that accounts for axisymmetric disturbances in bubble shape extending over the entire surface of the bubble shows that, although re-entrant contact angles usually indicate instability, the profiles with re-entrant contact angles at the point of maximum volume are stable.

The determination of maximum bubble volume has been extended to account for the destabilizing effect of the solid support curving away from the bubble. The situation described applies exactly to a bubble growing on a hemispherical protrusion on the surface, and by extension, to a bubble growing on a wire or screen. The reduction in the maximum stable bubble volume (V_{max}, r_w) for such a case can be described by the simple function

$$\frac{V_{max,\,r_w}}{V_{max,flat}} = \left[\frac{r_w}{r_w + L_c}\right]^{0.95\,\theta} \quad (\theta \text{ in radians}) \quad ;$$

where r_w is the radius of the protrusion (see Figure 2-1).

This result is the first step in accounting for the role of the morphology of the substrate on bubble size, which profoundly affects the dynamics of gas evolution on electrode surfaces. In practice, gas is often evolved on more complex electrode geometries and on orientations other than horizontal, and further extensions of the classical theory to describe these cases will prove valuable to understanding the factors affecting electrolytic gas evolution, and also nucleate boiling and mineral flotation.

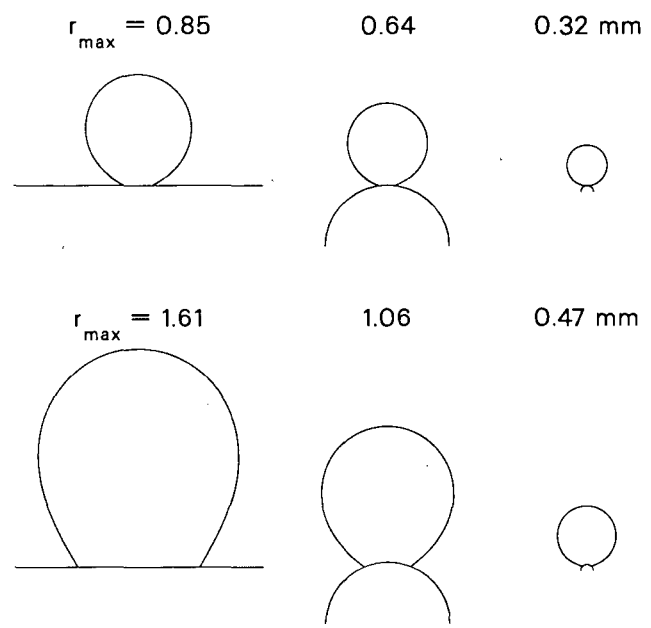

Figure 2-1. Largest stable equilibrium bubble configurations with a contact angle of 30° (top row) and 60° (bottom row) on a flat horizontal surface facing upward; surface curvature r_w = 1.0 mm (middle) and r_w = 0.1 mm (right). (XBL 876-2824)

1987 PUBLICATIONS AND REPORTS

Refereed Journals

1. D.W. Dees and C.W. Tobias, "Experimental Observations of Free Convection Mass Transfer to a Horizontal Surface with a Micromosaic Electrode," J. Electrochem. Soc. **134**, 369 (1987); LBL-21229.
2. J.O. Dukovic and C.W. Tobias, "The Influence of Attached Bubbles on Potential Drop and Current Distribution at Gas Evolving Electrodes," J. Electrochem. Soc. **134**, 331 (1987); LBL-18818.
3. D.W. Dees and C.W. Tobias, "Mass Transfer at Gas Evolving Surfaces," J. Electrochem. Soc. **134**, 1702 (1987); LBL-22311.
4. R.T. Atanasoski, H.H. Law, R.C. McIntosh, and C.W. Tobias, "Electrochemical Analysis of Trace Amounts of Water in Propylene Carbonate Electrolytes," Electrochim. Acta **32**, 887 (1987); LBL-22467.
5. K.J. Hanson and C.W. Tobias, "Electrochemistry of Iodide in Propylene Carbonate I. Cyclic Voltammetry Monitored by Optical Spectroscopy," J. Electrochem. Soc. **134**, 2204 (1987); LBL-22088.

6. K.J. Hanson, M.J. Matlosz, J. Newman, and C.W. Tobias, "Electrochemistry of Iodide in Propylene Carbonate. Part II—Theoretical Model," J. Electrochem. Soc. **134**, 2210 (1987); LBL-22009.
7. G.M. Whitney and C.W. Tobias, "The Onset of Buoyancy-Induced Convection at a Micro-Mosaic Electrode," J. Electroanal. Chem. **229**, 429 (1986); "The Limiting Current Technique at a Sectioned Electrode for the Study of Buoyancy-Induced Convection," ASME, HTD, Vol. 60, p. 105; LBL-22036.

Other Publications

8. G.M. Whitney and C.W. Tobias, "The Shape and Stability of Electrolytic Gas Bubbles Formed on Axisymmetric Surfaces," in *Extended Abstracts of the Electrochemical Society*, Vol. 87–1, No. 358, May 1987.
9. G.M. Whitney and C.W. Tobias, "Mass Transfer Effects of Bubble Streams Rising Past Vertical Electrodes," in *Extended Abstracts of the Electrochemical Society*, Vol. 87–1, No. 363, May 1987.
10. J.O. Dukovic and C.W. Tobias, "Simulation of Leveling in Electrodeposition," in *Extended Abstracts of the Electrochemical Society*, Vol. 87–2, Oct. 1987.

LBL Reports

11. G.M. Whitney (Ph.D. Thesis), with C.W. Tobias, "Microscale Resolution of Interfacial Mass-transfer Rates in Electrode Processes," LBL-23596.
12. G.M. Whitney and C.W. Tobias, "Mass Transfer Effects of Bubble Streams Rising Near Vertical Electrodes," accepted by AIChE J.; LBL-24618.

Invited Talks

13. G.M. Whitney and C.W. Tobias, "The Shape and Stability of Electrolytic Gas Bubbles Formed on Axisymmetric Curved Surfaces," The Electrochemical Society 171st National Meeting, Philadelphia, PA, May 10–15, 1987.
14. G.M. Whitney and C.W. Tobias, "Mass Transfer Effects of Bubble Streams Rising Past Vertical Electrodes," The Electrochemical Society 171st National Meeting, Philadelphia, PA, May 10–15, 1987.
15. J.O. Dukovic and C.W. Tobias, "The Electrochemical Society 172nd National Meeting, Honolulu, HI, Oct. 15–18, 1987.
16. C.W. Tobias, "Propagation of Surface Roughness," opening address, Round Table Discussion on Electrodeposition in Electronics, Nuova Samim Research Center, Venice, Italy, Oct. 2, 1987.
17. C.W. Tobias, "On the Leveling Phenomena in Electrolytic Metal Deposition," University of Ferrara, Italy, Oct. 2, 1987.
18. C.W. Tobias, "In Pursuit of Electrolytic Gas Evolution," McCabe Lecture, North Carolina State University, Raleigh, Nov. 9, 1987.

Surface Layers on Battery Materials*

Rolf H. Muller, Investigator

INTRODUCTION

Direct experimental information is obtained on the formation of surface layers on battery-electrode materials to determine factors responsible for enhanced cell performance. Present studies concern the formation of anodic oxides. A more broadly based program, conducted in part in collaboration with C.W. Tobias, is reported under "Electrochemical Phase Boundaries" and "Electrochemical Processes."

1. Nucleation of Silver Oxide (Publication 3)

S.T. Mayer and R.H. Muller

A new mechanism for the anodic formation of silver oxide on silver has been derived from spectroscopic ellipsometer measurements. The mechanism involves the rapid formation of an oxide monolayer followed by the slower growth of a thin primary layer and simultaneous film dissolution; the latter process accounts for most of the oxidized material generated at low potentials. At sufficiently high potentials, the primary layer reaches a critical thickness (100–200 Å) at which secondary crystals are nucleated. These crystals initially grow by the transfer of oxide materials from the primary layer, resulting in a sharp decrease in its thickness (see Figure 1-1). After the crystals have grown to a point where their solubility no longer depends on size, the thickness of the primary layer before nucleation is re-established.

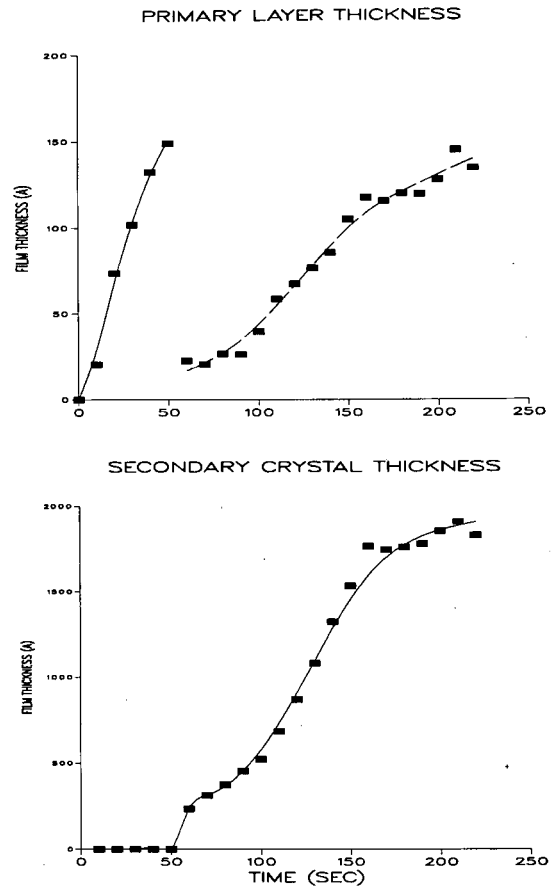

Figure 1-1. Thickness of primary or underlayer (A) and secondary or crystal layer (B) of silver oxide on silver derived from ellipsometer measurements for a film formed by a potential step at time zero to 200 mV versus Ag/AgI, 4M KCl. Note decrease of primary layer thickness at onset of secondary layer growth. (XBL 876-3024)

2. Work in Progress

A study of the anodic oxidation of copper in alkaline media by spectroscopic ellipsometry and scanning electron microscopy has been found to result in the initial growth of a compact Cu_2O layer, followed, at higher potential, by the formation of a highly porous $Cu(OH)_2$ layer. The compositions of these films have been identified by the use of newly developed Raman spectroscopy equipment for *in situ* measurements and by *ex situ* x-ray diffraction. Predictions of optical models agree well with measurements (see Figure 2-1). Angularly resolved elastic light scattering is also being developed to investigate the nucleation of anodic oxides.

Ellipsometer measurements of anodic oxides with a 20-μm probe beam have revealed local variations of film thickness and composition on a scale much smaller than the grain size (see Figure 2-2). For the further investigation of spatially varying surface layers, an analysis of different principles for the operation of an imaging ellipsometer with high spatial resolution has resulted in a preferred design that employs an array detector for photometric measurement.

*This work was supported by the Assistant Secretary of Conservation and Renewable Energy, Office of Energy Storage and Distribution of the U.S. Department of Energy under Contract No. DE-AC03-76SF00098.

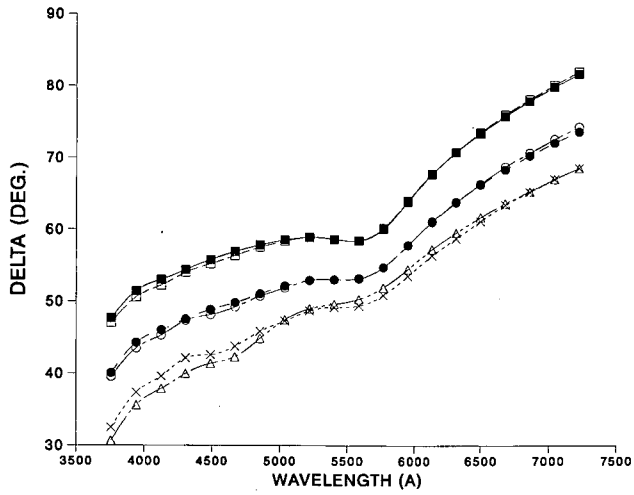

Figure 2-1. Spectroscopic ellipsometer measurements (Δ, ●, ■) and corresponding model predictions (×, ○ , □) for the anodic oxidation of copper in 1M KOH at 22 $\mu A/cm^2$ for 150 sec (■, □), 320 sec (●, ○), and 493 sec (Δ, ×). (XBL 884-1339)

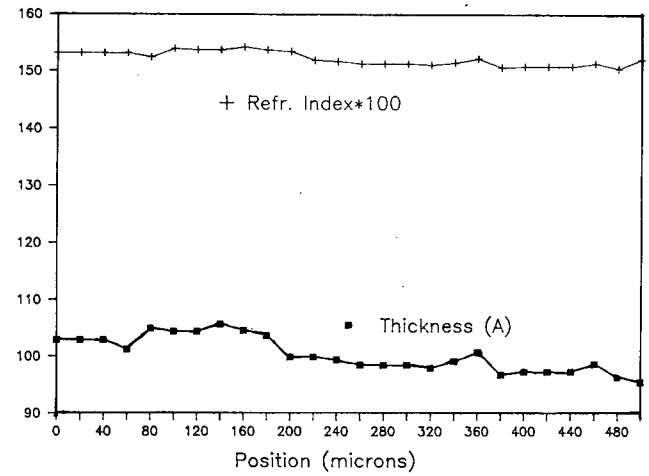

Figure 2-2. Ellipsometric profilometry of $Ni(OH)_2$ with a 20-μm probe beam. Locally varying refractive index and thickness on polycrystalline nickel of 200–300 μm grain size. Reduced form of 102 Å film after 5 potential cycles between −0.2 and +0.4 V vs Hg/HgO in 1M KOH at 50mV/sec. (XBL 884-1340)

1987 PUBLICATIONS AND REPORTS

Refereed Journals

1. J.G. Thevenin and R.H. Muller, "Impedance of Lithium Electrodes in a Propylene Carbonate Electrolyte," J. Electrochem. Soc. **134**, 273 (1987); LBL-21192.
2. J.G. Thevinin and R.H. Muller, "Study of the Li/Li_3N Electrode in an Organic Electrolyte," J. Electrochem. Soc. **134**, 2650 (1987); LBL-21191.

LBL Reports

3. S.T. Mayer and R.H. Muller, "Nucleation of Silver (1) Oxide Investigated by Spectroscopic Ellipsometry," submitted to J. Electrochem. Soc.; LBL-23844.

Electrode Kinetics and Electrocatalysis*

P.N. Ross, Investigator

INTRODUCTION

Complex electrochemical reactions in which chemical bonds are broken and/or formed are invariably catalytic, with electrode kinetics varying by many orders of magnitude for different electrode materials. The structural conformation of the electrode material can also have a pronounced effect on electrode kinetics. The structural effects complicate the optimization of catalytic materials for technological applications, and they are not effects that are well understood. The study of structure-related effects in electrocatalysis is a central theme in our research.

Metal/metal-ion (Me/Me^{Z+}) couples form the largest class of negative-electrode types for batteries. The kinetics of Me/Me^{Z+} couples used in batteries are relatively rapid, but they are not usually controlled by only a charge-transfer step. These reactions are often quasi-reversible, in the sense that they proceed at high rate and small overpotential, but they do not follow "ideal" charge-transfer rate expressions. Phenomena frequently cited as contributing to the "nonideal" behavior of Me/Me^{Z+} systems are critical nucleation, intermediate or precursor formation, and impurity adsorption. The structural transformations to the metallic surface as a result of cyclic Me^{Z+} formation are not well known, particularly at the atomic scales of structure. Yet these structural transformations may control critical phenomena in Me/Me^{Z+} cyclability.

Bifunctional air electrodes, which both consume and evolve oxygen, are especially attractive positive electrodes that can be coupled with Zn negative electrodes to form high-energy-density (150–200 Wh/kg) ambient-temperature batteries. Bifunctional air electrodes require the development of catalytic materials that are both active and corrosion-resistant over a demanding range of electrode potentials. Electrode structures based on catalyzed carbon black appear attractive on the basis of cost. The corrosion resistance of carbons is under investigation.

*This work was supported by the Assistant Secretary of Conservation and Renewable Energy, Office of Energy Storage and Distribution of the U.S. Department of Energy under Contract No. DE-AC03-76SF00098.

1. Structure-Property Relations for Surface Processes at the Metal/Solution Interface (Publication 1)

P.N. Ross

The recent development of a special apparatus coupling electroanalytical cells directly to ultrahigh-vacuum (UHV) surface analytical chambers has made possible definitive determination of structure-property relations for processes at metal-electrode surfaces. Low-energy electron diffraction (LEED) analyses of emersed platinum electrodes have provided direct evidence for place-exchange processes accompanying anodic oxidation, and combined with recent x-ray photoelectron spectroscopy and thermal desorption spectroscopy results, these studies have refined our understanding of aqueous oxidation phenomena. The use of UHV annealed well-ordered single-crystal surfaces has produced some surprising results. The process of submonolayer metal-ion deposition (so-called underpotential deposition) exhibits unexpected sensitivity to long-range order in the substrate, indicating that lateral bonding forces are of the same magnitude as the perpendicular bonding force. On a well-ordered Pt(111) surface, unexpected new surface processes have been observed that are unique to this surface, i.e., that are not seen on either (100) or (110) surfaces, nor on polycrystalline surfaces. It appears that the new processes are associated with atomically flat regions of the (111) surface with a critical region size that is quite large, at least 2 nm. It is suggested that cooperative interactions in the double layer form a critical ensemble that reacts to form the new surface species. However, much further study utilizing *in situ* spectroscopy will be required to understand this new surface process in Pt(111).

2. Long-Range Structural Effects in the Anomalous Voltammetry on Ultrahigh-Vacuum-Prepared Pt(111) (Publication 4)

F.T. Wagner† and P.N. Ross, Jr.

The cyclic voltammetry of Pt(111) in three different structural states (well-ordered, restructured by electrochemical redox cycling, and restructured by Ar^+ sputtering) was studied in aqueous acidic and basic electrolytes using a UHV–electrochemical transfer system. The well-ordered surface gave dis-

tinctive voltammograms characterized by reduced pseudocapacity in the "normal" hydrogen adsorption potential region, anomalous features in the potential range normally ascribed to double-layer charging, and a sharp peak [around 1080 mV reversible hydrogen electrode (RHE) in HF] shown by Auger electron spectroscopy to correspond to oxidation of the surface. The anomalous features were identical to those first reported by Clavilier using flame-annealed (111) surfaces transferred through the air while hot. Cycling the well-annealed (111) surface to potentials above the sharp oxidation peak removed the anomalous voltammetric features. LEED showed that such cycling introduced randomly spaced monatomic steps to the surface. Similarly restructured surfaces were produced in UHV by Ar^+ sputtering, and the voltammogram of these surfaces reproduced the voltammograms of annealed surfaces electrochemically restructured by extensive cycling. This agreement clearly demonstrates that the mechanism whereby electrochemical cycling drastically altered the voltammogram of Pt(111) is a disruption of the long-range (>5 atomic spacings) order of the surface, rather than a simple irreversible oxidation of adventitious impurities. The anomalous features were observed on well-ordered Pt(111) electrode surfaces in a variety of electrolytes over a wide range of pH (0–11), but the potentials at which the features appear and the detailed shapes of the features changed considerably. Based on the pH and anion-concentration dependencies, we conclude that the anomalous features in sulfate and chloride acid solutions are associated with the process of specific adsorption of these anions. We present a rationalization of the extreme structure sensitivity of the specific adsorption process based on the relative strengths of interactions between water, sulfate (chloride) ions, and Pt atoms in various states of coordination in the surface. The identity of the species and processes involved in the anomalous features in perchlorate, fluoride, bicarbonate, and hydroxide electrolytes remains uncertain.

†Present address: General Motors Research Laboratory, Warren, MI 48090.

3. The Corrosion of Carbon Black Anodes in Alkaline Electrolyte: III. The Effect of Graphitization on the Corrosion Resistance of Furnace Blacks (Publication 5)

P.N. Ross and M. Sattler

A selection of furnace black carbons of varying surface area and industry type were heat-treated in purified helium at 2700°C and the corrosion resistance measured under conditions of oxygen evolution in 30% KOH at 55°C. The extent of graphitization was determined qualitatively by x-ray diffraction and by transmission electron microscopy (TEM). Separate linear correlations of the corrosion rate per unit mass with the Brunauer-Emmett-Teller (BET) surface area were observed for furnace blacks and for graphitized furnace blacks, with the rate for the graphitized blacks being a factor of ~2.5 lower on a unit area basis. The correlations had a relatively high standard deviation, however, indicating that the BET area was probably not the only physical property affecting the corrosion rate. TEM analysis of the carbons after extended corrosion indicated a strong preferential attack of the ungraphitized regions, i.e., much greater selectivity that the factor of 2.5 indicated by the BET correlation (see Figure 3-1). A unifying correlation was observed for both the furnace blacks and their graphitized forms using the corrosion rate per unit mass and the iodine adsorption number. It was concluded that there are specific sites on the carbon surface (titrated by iodide) that serve as the initiators for dissolution of carbon atoms from the bulk of the material. One particular type of furnace black, SRF (N774), appears to be an especially good precursor for forming a highly graphitized and very corrosion-resistant carbon black.

4. Work in Progress

New work is being started on catalysts for the direct oxidation of methanol in fuel cells. These studies will use modern surface-analytical methods coupled with electrochemical methods to determine the

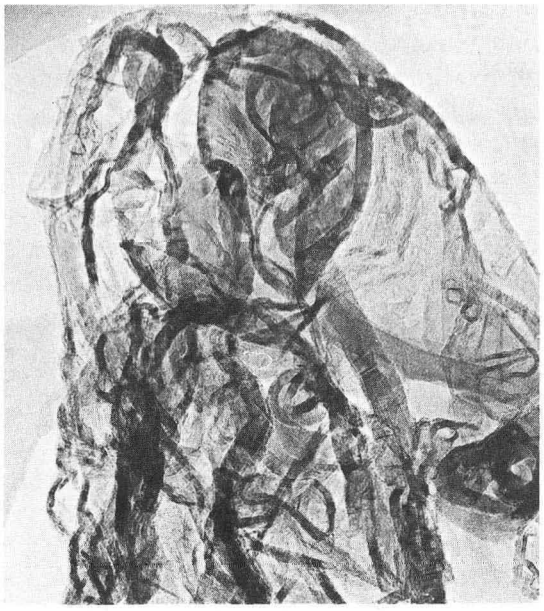

Figure 3-1. Transmission electron micrograph of acetylene black showing preferential dissolution of amorphous (nongraphitic) microstructure during oxygen evolution in KOH electrolyte at 55°C. (XBB 874-3153A)

surface composition dependence of the catalytic activity for selected platinum alloys. Two of the most promising catalysts for methanol oxidation are Pt-Sn and Pt-Ru, but the surface composition of these alloys in electrolyte is not known, nor is there a consistent theory about why these alloys are more active than platinum alone. In addition, we are studying the effect of the electrolyte on methanol-oxidation kinetics, as there are new fluorosulfonic acid electrolytes available that have very different properties from the inorganic (e.g., sulfuric) acids used previously.

1987 PUBLICATIONS AND REPORTS

Refereed Journals

1. P.N. Ross, "Structure-Property Relations for Surface Processes at the Metal/Solution Interface," J. Vac. Sci. Technol. **A5**, 948 (1987); LBL-22105.
2. A. D'Agostino and P.N. Ross, "LEED/Electrochemical Analysis of Gold Single Crystals: Stability of the UHV Prepared Surfaces of Au(111) and Au(100) in Aqueous Electrolyte," Surf. Sci. **185**, 88 (1987); LBL-21792.

Other Publications

3. W. Cieslak, A. Brown, V. Dantam, B. Lichter, W. Baden, S. Pensabone, and P. Ross, "Corrosion in Batteries and Fuel Cell Power Sources," in *The New Metals Handbook, Vol. 13: Corrosion*, ASM International, Metals Park, OH, 1987, p. 1317; LBL-22489.

LBL Reports

4. F.T. Wagner and P.N. Ross, "Long-Range Structural Effects in the Anomalous Voltammetry on Ultra-High Vacuum Prepared Pt(111)," J. Electroanal. Chem. (in press); LBL-22488.
5. P.N. Ross and M. Sattler, "The Corrosion of Carbon Black Anodes in Alkaline Electrolyte: III. The Effect of Graphitization on the Corrosion Resistance of Furnace Blacks," J. Electrochem. Soc. (in press); LBL-24232.

Electrical and Electrochemical Behavior of Particulate Electrodes*

James W. Evans, Investigator

INTRODUCTION

This work is concerned with the use of particulate electrodes (especially zinc) in the storage of electrical energy. One of the major difficulties encountered in the use of monolithic (e.g., slablike) zinc electrodes in batteries is the change in the morphology of the electrode as the battery is cycled. For example, there is a tendency for zinc to form nodular or dendritic growths; this growth can have an impact on battery performance by forming shorts or by penetrating cell diaphragms. These problems might be overcome by use of a particulate electrode where the zinc is present either as particles or as a thick coating on a particle substrate; the morphology and mechanical integrity of the particle is then of less concern.

Possible particulate electrodes are slurry electrodes (where the particles move into and out of the cell in suspension in the electrolyte), fluidized-bed electrodes, and moving-bed electrodes. The last two are under investigation at LBL, and investigations of the fundamental electrical and electrochemical behavior of fluidized-bed electrodes have been completed (see publications 1–3, 6, and 7). The present focus of investigation is the moving-bed electrode, which appears most suitable for use in discharging (electrodissolution) of zinc particles. Moving beds have low requirements for electrolyte pumping. Of major interest is the performance of a cell discharging a zinc moving-bed electrode against an air cathode.

1. Particulate Electrodes (Publications 1–3, 6, and 7)

J.W. Evans, H. Choi,[†] T. Huh,[‡] and V. Jiricny[§]

A bed of zinc or zinc-coated particles can be electrochemically discharged against an air electrode, varieties of which are commercially available, driving current through an external circuit. One type of particulate electrode that appears suitable for this kind of cell is a moving-bed electrode. LBL investigations have shown that a moving bed of zinc particles has little resistance (minimizing parasitic voltage drops across the electrode itself), and (superficial) current densities of several hundred mA/cm^2 can be maintained at these electrodes. The objective of research in 1987 has been the development and improvement of a laboratory cell with a moving-bed zinc electrode and a commercial air cathode. Figure 1-1 shows the best performance to date for the cell discharged at two different currents (2.5 A, corresponding to a superficial current density of 100 mA/cm^2, and 5 A). The horizontal line at 1.7 V and the vertical line at 35 Ah indicate the theoretically expected performance. The area of this rectangle is therefore the expected energy of the cell, and the areas under the two curves form a ratio to this area that is the energy efficiency on discharge. These energy efficiencies require improvement, which is possible with modification of the cell design. For example, the better result of Figure 1-1 is an improvement on the 31% discharge efficiency achieved in earlier cells.

[†]Present address: McGill University, Montreal, Quebec.

[‡]Present address: Pusan National University, Pusan, Republic of Korea.

[§]Present address: Institute of Chemical Process Fundamentals, Prague, Czechoslovakia.

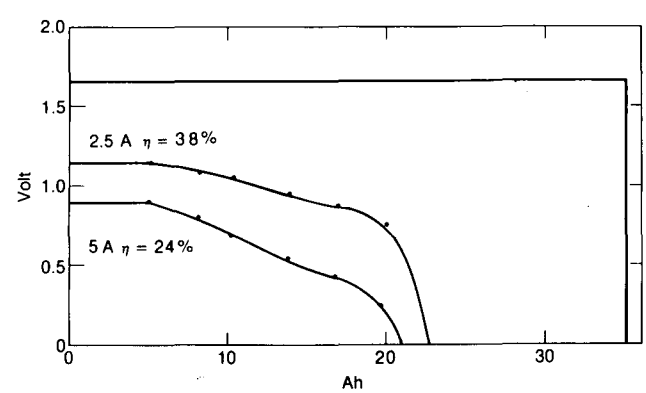

Figure 1-1. Results of constant current discharge experiments for a cell with a moving-bed zinc anode and a commercially available air cathode. (XBL 878-3618)

*This work was supported by the Assistant Secretary of Conservation and Renewable Energy, Office of Energy Storage and Distribution of the U.S. Department of Energy under Contract No. DE-AC03-76SF00098.

2. Other Electrochemical Investigations (Publications 4, 5, and 8)

J.W. Evans and D.D. Macdonald[†]

A theoretical investigation of the response of an electrode to a nonideal step change in potential has been completed in collaboration with Dr. D.D. Macdonald of SRI International. Stepping the potential (using a potentiostat) and observing the current transient is a widely used technique for studying the kinetics of electrochemical reactions or diffusion of electroactive species to (or from) the electrode. Real potentiostats are incapable of a true step changes; instead they typically "overshoot" the final potential, and this overshoot is then followed by decaying oscillations leading to the final value. The investigation showed that these departures from an ideal step change can result in spurious currents that are comparable with those due to the step change itself.

Publication 8 is a reinterpretation of computed results published in 1984 by Alkire, Reiser, and Sani.[1] Those investigators used finite-element techniques to calculate the concentration field and mass fluxes from small cavities such as those encountered in electrochemical processing of electronic circuits or in pitting corrosion. The reinterpretation of Publication 8 makes the results more accessible by employing fluid mechanics to show that dimensionless groups used by Alkire and coworkers can be recast in terms of bulk parameters (such as the velocity outside a turbulent boundary layer). It was also shown how the results can be applied to electrodeposition (as well as to the electrodissolution treated by Alkire and coworkers).

[†]Present address: SRI International, Menlo Park, CA.

1. R.C. Alkire, D.B. Reiser, and R.L. Sani, J. Electrochem. Soc. **131**, 2795 (1984).

3. Work in Progress

The further improvement of cells for discharge of zinc particles is in progress, as is the study of zinc electrodeposition from various alkaline electrolytes onto a fluidized cathode.

1987 PUBLICATIONS AND REPORTS

Refereed Journals

1. V. Jiricny, H. Choi, and J.W. Evans, "Zinc Electrodeposit Morphology Under Conditions of Fluctuating Current Density," J. Appl. Electrochem. **17**, 91 (1987); LBL-21986.
2. T. Huh and J.W. Evans, "Electrical and Electrochemical Behavior of Fluidized Bed Electrodes, I. Potential Transients and Time-Averaged Values," J. Electrochem. Soc. **134**, 308 (1987); LBL-20840.
3. T. Huh and J.W. Evans, "Electrical and Electrochemical Behavior of Fluidized Bed Electrodes, II. Effective Bed Resistivities," J. Electrochem. Soc. **134**, 317 (1987); LBL-20841.
4. J.W. Evans and D.D. Macdonald, "Transient Response Under Nonideal Potential Control, I. Reversible Charge Transfer Reaction," J. Electrochem. Soc. **134**, 2234 (1987); LBL-24460.
5. J.W. Evans and D.D. Macdonald, "Transient Response Under Nonideal Potential Control, II. Irreversible Charge Transfer Reaction," J. Electrochem. Soc. **134**, 2238 (1987); LBL-24461.

Other Publications

6. J.W. Evans, "Fluidized Bed Electrodes," in *Proc. Symp. Electrochemistry and Solid State Science Education at the Graduate and Undergraduate Level*, W.H. Smyrl and F. McLarnon, Eds., The Electrochemical Society, Pennington, NJ, 1987, p. 241.
7. J.W. Evans, "Particulate Zinc Electrodes," in *Proc. 9th Battery and Electrochem. Contractors Conf.*, Washington, DC, Nov. 1987.

LBL Reports

8. J.W. Evans, "Effect of Fluid Flow on Mass Transport Within Small Cavities — A Reinterpretation of the Results of Alkire and Coworkers," LBL-24500.

Invited Talks

9. J.W. Evans and V. Jiricny, "Fluidized Bed Electrodes," 9th International Congress of Chemical Engineering, Chemical Equipment Design and Automation, CHISA '87, Prague, Czechoslovakia, Aug. 30–Sept. 4, 1987.
10. J.W. Evans, "Mathematical Modeling: Expectations Failures and Successes," keynote address, The Metallurgical Society Fall Extractive Meeting, Palm Springs, CA, Nov. 29–Dec. 20, 1987.

Electrochemical Properties of Solid Electrolytes*

Lutgard C. De Jonghe, Investigator

INTRODUCTION

The development of high-temperature battery systems such as the Na/Na_2S_x and Li/FeS_2 cells has progressed to a point where batteries demonstrating high specific power as well as long cycle life are possible. Still, issues of cost and safety have prompted other researchers to investigate alternative systems operating at more moderate temperatures. The recent introduction of sodium/organosulfur batteries, resulting from work in this laboratory, has generated research on a wide variety of novel high-energy-density cells operating between ambient and intermediate temperatures (25 to 150°C). At present the majority of advanced and conventional batteries are derived exclusively from inorganic electrochemical couples: Pb/PbO_2, Zn/MnO_2, Li/Ti_2, Na/S, etc. The organosulfur electrodes present a departure from this tradition in that they are based on the general redox reaction for organic disulfides,

$$RSSR + 2\,e^- \rightleftarrows 2\,RS^- \quad ,$$

where R is an organic moiety such as CH_3, C_6H_5, $CH_3OCH_2CH_2$, etc. The thio/disulfide redox reaction is an important biochemical reaction, and the organic disulfides are well known for their industrial applications. Among the advantages of such a generic redox couple for energy storage is the ability to control the physical, chemical, and electrochemical properties of organosulfur species by appropriate choice of the organic moiety. Many organic disulfides are available commercially, and although they share some chemical and electrochemical similarities due to the disulfide linkage, their physical properties are as different as the organic moieties attached to the sulfur-sulfur bond.

1. A Novel Class of Organosulfur Electrodes for Energy Storage (Publication 6)

S.J. Visco, C.C. Mailhe, L.C. De Jonghe, and M.B. Armand

Sodium/organosulfur (Na/RSSR) batteries are tested in cells having epoxy and elastomeric O-ring seals, allowing access to the positive organodisulfide electrode (RSSR) compartment for injection of solvents or other additives, and/or allowing the positive electrode to be renewed when desired. Na/beta″-alumina/RSSR cells (see Table 1-1) are cycled galvanostatically under computer control, with continuous monitoring of internal cell resistance, open circuit voltage, cell temperature, and positive electrode pressure as a function of current density and state of charge. One of the earliest cells tested was the sodium/tetraethylthiuram disulfide (Na/TETD) battery. Na/TETD cells have been assembled with maximum practical energy densities of over

Table 1-1
Theoretical energy densities of sodium/organosulfur cells.

Organosulfur compound	Equivalent weight (equiv/mol)	Melting point (°C)	Theoretical energy density (Whr/Kg)
$(C_2H_5NCSS)_2$	148	74	360
CH_3SSCH_3	47	−85	770
$(CH_3OCH_2CH_2S)_2$	91	<25	490
$(HOCH_2CH_2S)_2$	77	25	560
$-(SCH_2CH_2OCH_2CH_2S)-_n$	68	?	590
$C_6H_5SSC_6H_5$	109	58	406
$F-C_6H_4SSC_6H_4-F$	127	<25	430

*This work was supported the Assistant Secretary of Conservation and Renewable Energy, Office of Energy Storage and Distribution of the U.S. Department of Energy under Contract No. DE-AC03-76SF00098.

110 Whr/Kg at zero current drain. At 130°C, Na/TETD batteries are cycled between 10 and 90% of available capacity at power densities of 6 W/Kg at an overall energy efficiency of 75% and a realized energy density of 80 Whr/Kg. Carefully assembled cells are capable of delivering peak current densities of 100 to 150 mA/cm^2 for one minute or more, corresponding to peak power densities of 40 to 60 W/Kg (see Figure 1-1). Unfortunately, the TETD electrode is unable to sustain these peak rates of discharge for an appreciable fraction of available capacity. This is most likely due to slow mass transport in the positive electrode melt, as confirmed by viscosity measurements. Viscosity of the positive electrode can be substantially lowered by the addition of a low-viscosity solvent or by the use of a lower-viscosity organosulfur compound (see Table 1-1), resulting in higher cycling rates.

2. Ionic Conductivity of Organosulfur Melts for Advanced Storage Electrodes (Publication 7)

S.J. Visco and L.C. De Jonghe

The attainable energy efficiency and power density of a secondary battery is directly related to polarization losses in the cell under load. One of the contributing factors to polarization of an organosulfur electrode is the rate of ionic transport in the melt. Among the sodium/beta″-alumina/organosulfur (Na/RSSR) batteries under investigation in this laboratory is the Na/TETD cell, in which the product of cell discharge is the thiolate salt, sodium diethyldithiocarbamate (NaDEDC). Accordingly, the ionic conductivity of NaDEDC and related electrolytes in molten TETD has been studied as a function of composition and temperature. The ionic conductivity of the TETD electrode increases by 3 orders of magnitude in going from the neat melt to about 10% discharge composition of a Na/TETD battery. The equivalent conductivity of the NaDEDC/TETD melts implies significant ion pairing and formation of triplet ions, which is expected for electrolytes dissolved in solvents of low dielectric constant (see Figure 2-1). The dielectric constant for TETD was estimated from the conductivity data to be approximately 12. The low values of equivalent conductivity in TETD are also explained by the high measured values of viscosity leading to low ion mobilities. As a solvent, TETD appears to be very effective at dissolving salts having the dithiocarbamate anion, but ineffective at dissolving other strong electrolytes. The addition of species — tetracyanoethylene and tetracyanoquinodimethane —known to form charge-transfer complexes with disulfides, strongly increased the conductivity of the melts, but the nature of that increase requires further study.

3. A Novel Class of Positive Electrodes for Rechargeable Batteries (Publication 8)

C.C. Mailhe

The organosulfur electrodes are derived from a large class of organic disulfides, including the thiuram disulfides, aliphatic disulfides, aromatic disulfides, polymeric disulfides, etc. Although some of

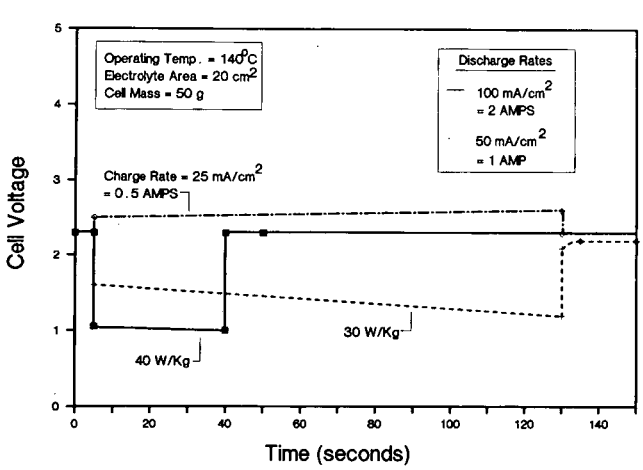

Figure 1-1. Transient power capabilities of the Na/beta″-alumina/TETD battery. Negative electrode is liquid sodium metal. Positive electrode is graphite felt impregnated with pure molten TETD. (XBL 876-2508)

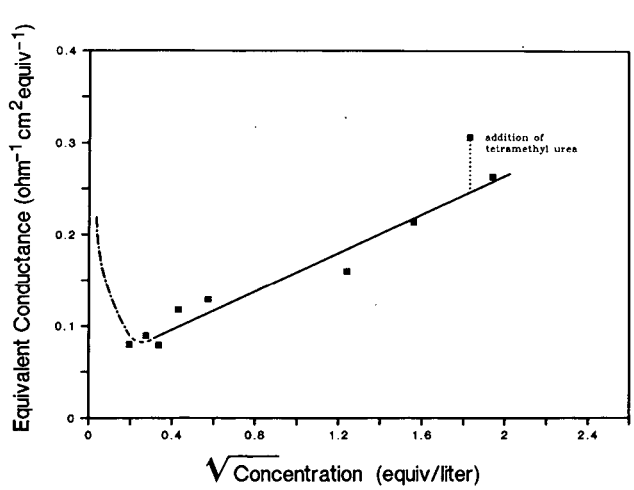

Figure 2-1. Equivalent conductivity of NaDEDC in TETD as a function of (concentration)$^{1/2}$ at 130°C; —·—·—: expected behavior at dilute concentrations; ·····: effect on equivalent conductance by the addition of the solvent tetramethylurea. (XBL 8712-5258)

the organosulfur electrodes such as the thiuram disulfides or hydroxyalkyl disulfides are capable of dissolving the thiolate salts generated on cell discharge, others, such as the alkyl or aryl disulfides, cannot. In this case it is necessary to choose an appropriate solvent to facilitate cell discharge. In fact, the thiuram disulfide electrodes also benefit from the incorporation of solvents, as this is a way of increasing the dielectric constant and/or reducing the viscosity of the melt, thus increasing the rates of mass transport in the electrode. The effects of various solvents on the performance of Na/RSSR cells are determined for a variety of organosulfur electrodes, by the response of the Na/RSSR cells to galvanostatic cycling. The best results for cycling of the Na/TETD battery are obtained with the addition of 10 to 20 wt% dimethyl sulfoxide or sulfolane to the positive electrode, allowing charge/discharge cycling at 5 mA/cm^2 at an operating temperature of 120°C. Simple aliphatic disulfides were also tested in Na/RSSR cells. Na/CH_3SSCH_3 cells with DMSO solvent in the positive electrode are capable of very high rates, up to 50 mA/cm^2 for half of available capacity (see Figure 3-1). Hydroxyethyl disulfide (HEDS) demonstrates high sodium-ion solubilities and high Na/HEDS discharge rates. Laboratory Na/HEDS cells have been assembled with maximum practical energy densities of 200 Whr/Kg, of which half can be discharged at a current density of 10 mA/cm^2 at 120°C. The most promising electrodes may be the alkoxyalkyl disulfides, RORSSROR. These electrodes have been cycled at 10 to 15 mA/cm^2 at 120°C, using DMSO as solvent, and appear to be very thermally and electrochemically stable.

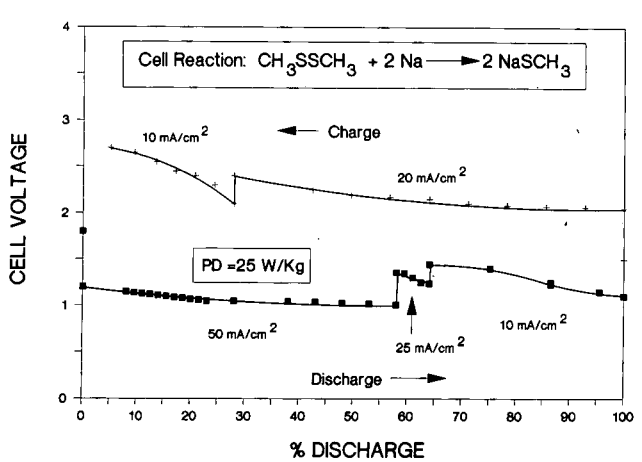

Figure 3-1. High-rate Na/CH_3SSCH_3 cell operating at 110°C. Positive electrode is composed of graphite felt immersed in 25 wt% CH_3SSCH_3/74 wt% DMSO with 1 wt% cobalt phthalocyanine as an electrocatalyst. (XBL 885-1874)

4. Work in Progress

Synthesis of fluorinated and/or perfluorinated organic disulfides is currently under way. High Na/RSSR cell voltages attainable with fluorinated electrodes should boost the power density of the cell. In addition, the use of electrocatalysts to minimize charge-transfer polarization in organosulfur electrodes is being pursued in more detail. The use of highly oxidizing low-viscosity organosulfur electrodes in combination with electrocatalysts should lead to cells of both high specific energy and power. Other organosulfur electrodes such as the alkoxyalkyl disulfides, which should have high sodium ion solubilities as well as low viscosities and reasonable oxidizing power, are also currently being studied. The majority of the organosulfur electrodes being investigated for intermediate-temperature cells are also being tested in lithium room-temperature cells, particularly those disulfides that are liquid at room temperature, allowing the assembly of very high specific energy cells. A key issue for all organosulfur cells at this time is to demonstrate long cycle life at reasonable power densities, with high demonstrated peak power densities. For the lithium batteries, studies are also under way to determine the reversibility of the lithium electrode in Li/RSSR cells.

1987 PUBLICATIONS AND REPORTS

Refereed Journals

1. C.C. Mailhe, S. Visco, and L.C. De Jonghe, "Oxygen Activity and Asymmetric Polarization at the Sodium/Beta″-Alumina Interface," J. Electrochem. Soc. **134**, 1121 (1987); LBL-19359.

Other Publications

2. S.J. Visco, C.C. Mailhe, L.C. De Jonghe, and M.B. Armand, "A New Class of High Energy Density, Intermediate Temperature, Batteries," in *Proc. 171st Meeting of The Electrochemical Society*, Philadelphia, PA, May 10–15, 1987.
3. C.C. Mailhe, S.J. Visco, and L.C. De Jonghe, "Performance Characteristics of Novel, High Energy Density, Intermediate Temperature Batteries," in *Proc. 171st Meeting of The Electrochemical Society*, Philadelphia, PA, May 10–15, 1987.
4. S.J. Visco, C.C. Mailhe, and L.C. De Jonghe, "Extension of the Novel Class of Positive Electrodes to Systems Having Theoretical Energy Densities Between 500 and 800 Whrs/Kg," in *Proc. 171st Meeting of The Electrochemical Society*, Philadelphia, PA, May 10–15, 1987.

5. S.J. Visco, C.C. Mailhe, and L.C. De Jonghe, "Electrochemical Studies of Novel Positive Electrode Compounds," in *Proc. 171st Meeting of The Electrochemical Society*, Philadelphia, PA, May 10–15, 1987.

LBL Reports

6. S.J. Visco, C.C. Mailhe, L.C. De Jonghe, and M.B. Armand, "A Novel Class of Organosulfur Electrodes for Energy Storage," submitted to J. Electrochem. Soc.; LBL-23598.
7. S.J. Visco and L.C. De Jonghe, "Ionic Conductivity of Organosulfur Melts for Advanced Storage Electrodes," submitted to J. Electrochem. Soc.; LBL-24462.
8. C.C. Mailhe (Ph.D. Thesis), "A Novel Class of Positive Electrodes for Rechargeable Batteries," LBL-24244.

Invited Talks

9. S.J. Visco, C.C. Mailhe, M. Liu, M.B. Armand, and L.C. De Jonghe, "A Novel Class of Organosulfur Electrodes for Energy Storage," American Chemical Society, Pacific Conference on Chemistry and Spectroscopy, Irvine, CA, Oct. 28–30, 1987.
10. C.C. Mailhe, S.J. Visco, and L.C. De Jonghe, "Organosulfur Cell Performance," American Chemical Society, Pacific Conference on Chemistry and Spectroscopy, Irvine, CA, Oct. 28–30, 1987.
11. M. Liu, S.J. Visco, and L.C. De Jonghe, "Charge Transfer Kinetics of a Group of Organosulfur Electrode Materials," American Chemical Society, Pacific Conference on Chemistry and Spectroscopy, Irvine, CA, Oct. 28–30, 1987.

Analysis and Simulation of Electrochemical Systems*

John Newman, Investigator

INTRODUCTION

This program involves fundamental investigations of the transport and interfacial phenomena important in electrochemical systems. Results of this work are used to analyze experimental data, to identify important system parameters, and to aid in the design and scale-up of electrochemical systems. Specific projects include analysis of the thin-gap flow cell for electrochemical synthesis and energy storage, mathematical modeling of the Li–Al/FeS battery and the Li–Si/FeS_2 battery, an investigation of porous electrodes with applications to molten-salt systems, and an ac impedance analysis of both zinc and iron corrosion.

1. Design of Thin-Gap Channel Flow Cells (Publication 3)

V. Edwards and J. Newman

A model for predicting the current, concentration, and potential distributions in a thin-gap channel flow cell is presented. The model does not invoke the thin-diffusion-layer assumption or the assumption of straight current lines, and it allows for multiple reactions. The model, however, does not include the effect of migration; thus, it is only valid for systems with excess supporting electrolyte. This model can be used for the design and scale-up of channel-flow electrochemical reactors. Results are presented for a single reaction to show the effects of interacting diffusion boundary layers and of the axial component of current.

2. Anodic Dissolution of Iron in Acidic Sulfate Solutions. II. Mathematical Model of Current Oscillations Observed under Potentiostatic Conditions (Publication 2)

P. Russell and J. Newman

A mathematical model describing sustained current oscillations observed in the iron–sulfuric acid system, under potentiostatic conditions, is presented. This model assumes that the sustained oscillations are due to a continuous cycling of a portion of the electrode between the active and the passive states. The electrode surface is covered by a porous ferrous sulfate film. Transient changes in the potential and concentration profiles in the pores of the salt film and in the diffusion layer are responsible for the continuous cycling. A one-dimensional model that describes these processes is presented. Results from this model are compared to the experimental current-time curves. The calculated current-time curve shows oscillatory behavior. The characteristics of the calculated current-time curve differ from experimental results. The calculated ferrous sulfate film thickness is substantially thinner than expected from a steady-state analysis and from the previously reported work of others.

Due to lack of quantitative agreement between experimental and calculated results, two modifications to the present model are proposed in a qualitative manner. These modifications suggest that one may wish to (i) remove the requirement of passivation and assume that the current oscillations are caused by continuous cycling in the fraction of the electrode surface area that is covered by ferrous sulfate, or (ii) assume that the current oscillations are caused by continuous cycling in the porosity of the salt film in combination with changes in the amount of active area. Both proposed modifications would include kinetics of salt-film precipitation and dissolution. It is anticipated that finite precipitation and dissolution kinetics will increase the calculated salt-

*This work was supported by the Assistant Secretary of Conservation and Renewable Energy, Office of Energy Systems Research, Energy Storage Division of The U.S. Department of Energy under Contract No. DE-AC03-76SF00098.

film thickness. Further work would be required to incorporate either modification into the model in a quantitative way.

3. Mathematical Modeling of LiAl/LiCl, KCl/FeS Cells (Publication 9)

D. Bernardi, E.M. Pawlikowski, and J. Newman

The behavior of the thermodynamic, open-circuit potential of the LiAl/LiCl,KCl/FeS cell is investigated, and nonequilibrium results obtained from a computer model of the cell are presented. The nonequilibrium computer model predicts the cell voltage, temperature, and heat-generation rate during cell operation. Position-dependent behavior such as reaction rates and concentrations within the cell are also calculated. The effects of state of discharge, electrolyte composition, porosity, KCl precipitation, and temperature on cell behavior are investigated. Factors that can limit a cell during operation are identified, and the influence of changes in design parameters on cell performance is discussed. The results of the model compare favorably with available experimental data.

4. Differential Diffusion Coefficients of Sodium Polysulfide Melts (Publication 11)

S.D. Thompson and J. Newman

The method of restricted diffusion has been applied to sodium polysulfide melts in order to determine differential diffusion coefficients spanning the composition range of the single-phase liquid region (Na_2S_3 to Na_2S_5), at temperatures between 300 and 350°C. Molybdenum electrodes at the ends of the cell gave open-circuit potentials in response to the transient concentration difference. The shape of the potential-*versus*-time plots showed the expected dependence on the initial concentration profile.

The following expression summarizes the experimental data:

$$D = 0.0153 \exp(-5890/T) \exp(5.30x_e) \text{ cm}^2/\text{sec}.$$

The diffusion coefficients showed a temperature dependence in harmony with viscosity data, but not in harmony with conductivity data.

5. Current Distributions at Electrode Edges at High Current Densities (Publication 12)

W.H. Smyrl and J. Newman

At current densities large in magnitude and also large compared to the exchange-current density, a conducting disk in an insulating plane has a very nonuniform current distribution across the surface. The current distribution near the center is governed predominantly by ohmic effects, but near the edge, electrode kinetics become important. This paper describes the treatment of the current and potential distributions on the electrode, especially near the edge of the electrode where the nonuniformity is most extreme. The electrode kinetics are taken to be in the Tafel region. The results are valid for any and all large values of current density and provide a definitive description of the way in which the current and potential distributions approach the purely ohmically controlled (primary) distributions as the current is increased. The current density at the edge of the disk is found to increase with the square of the average current density.

These results for the edge region of a disk at high currents and those of an earlier paper for high exchange currents can be applied to electrodes of more general geometry.

6. Work in Progress

Past work in the optimization of the Li(alloy)/FeS battery is being extended to the Li(alloy)/FeS_2 system. In addition to the investigation of stacks of rectangular cells, cylindrical cells with multiple positive electrodes are being considered. Work will be continued with new experimental data obtained from Argonne National Laboratory.

A model that uses Duhamel's theorem to simulate cyclic voltammetry experiments at stationary and rotating-disk electrodes is being improved. The model can account for mass-transfer effects, Faradaic reactions, and adsorption phenomena, which will permit the quantitative interpretation of data. In particular, it is being used to study linear sweep voltammograms of the reduction of nitrate in acidic nickel solutions.

A mathematical model of the electrode/electrolyte interface is being developed to calculate the frequency response of a rotating disk. The working algorithm accounts for the effect of surface coverage owing to specific adsorption and

charge-transfer reactions. Double-layer theory is used to calculate the potentials at the interfacial planes and the surface excesses of all the electroactive species present in the solution. Presently, the microscopic model of the interface qualitatively predicts the measured complex impedance for the zinc chloride system. This mechanistic approach allows the proposed reaction process to be changed to account for the experimental observations. Finally, the generalized model can be used to identify system limitations and to guide further experimental research. This microscopic model of the interface will be coupled with the previously developed macroscopic model accounting for convection, migration, and multicomponent diffusion in concentrated solutions, in addition to homogeneous and heterogeneous reactions.

An experimental investigation of porous ferrous sulfate films is under way. Specifically, the reaction kinetics of film dissolution and precipitation and estimates of the film thickness are being investigated.

Double-layer adsorption is an important phenomenon in heavy-metal ion removal from waste streams and in discharge transients in high-pulse-power battery systems. An experimental investigation of double-layer adsorption of zinc ions on high-surface-area porous carbon and on planar carbon electrodes is being completed.

The solution of Laplace's equation is important to many modeling efforts. Its solution is often expensive and difficult to obtain accurately. The feasibility of a boundary-integral technique for use in current-distribution problems is being investigated. Preliminary observations appear promising. This technique is being applied to primary and secondary current distributions and can be used for more general problems involving Laplace's equation.

Additional work includes an experimental and theoretical ac impedance study of transport phenomena through membranes and an investigation of the effects of induced magnetic fields on battery performance during high rates of discharge.

1987 PUBLICATIONS AND REPORTS

Refereed Journals

1. M. Matlosz and J. Newman, "Solving 1-D Boundary-Value Problems with Bandaid: A Functional Programming Style and a Complementary Software Tool," Comput. Chem. Eng. **11**, 45 (1987); LBL-21589.
2. P. Russell and J. Newman, "Anodic Dissolution of Iron in Acidic Sulfate Electrolytes. II. Mathematical Model of Current Oscillations Observed under Potentiostatic Conditions," J. Electrochem. Soc. **134**, 1051 (1987); LBL-19773.
3. V. Edwards and J. Newman, "Design of Thin-Gap Channel Flow Cells," J. Electrochem. Soc. **134**, 1181 (1987); LBL-19959.
4. D. Bernardi and J. Newman, "Mathematical Modeling of Lithium (alloy), Iron Disulfide Cells," J. Electrochem. Soc. **134**, 1309 (1987); LBL-21764.
5. K.J. Hanson, M.J. Matlosz, J. Newman, and C.W. Tobias, "Electrochemistry of Iodide in Propylene Carbonate. II. Theoretical Model," J. Electrochem. Soc. **134**, 2210 (1987); LBL-22009.
6. J.L. Bomben, J. Newman, and C.J. King, "Growth of Radially Symmetric Ice in a Supercooled Sucrose Solution," Ind. Eng. Chem. Res. **26**, 23 (1987).
7. P.S. Fedkiw and J. Newman, "Friction Factors for Creeping Flow in Sinusoidal Periodically Constricted Tubes," Chem. Engr. Sci. **42**, 2962 (1987).

Other Publications

8. M.E. Orazem and J. Newman, "Photoelectrochemical Devices for Solar Energy Conversion," in *Modern Aspects of Electrochemistry*, No. 18, R.E. White, J.O'M. Bockris, and B.E. Conway, Eds., Plenum Press, New York, 1986, p. 61; LBL-18766.

LBL Reports

9. D. Bernardi, E.M. Pawlikowski, and J. Newman, "Mathematical Modeling of LiAl/LiCl,KCl/FeS Cells," submitted to J. Electrochem. Soc.; LBL-22265.
10. J. Newman, "Mass Transport and Potential Distribution in the Geometries of Localized Corrosion," submitted to *Proc. Int. Conf. on Localized Corrosion*, June, 1987, H.S. Isaacs, Ed.; LBL-23474.
11. S.D. Thompson and J. Newman, "Differential Diffusion Coefficients of Sodium Polysulfide Melts," submitted to J. Electrochem. Soc.; LBL-23820.
12. W.H. Smyrl and J. Newman, "Current Distribution at Electrode Edges at High Current Densities," submitted to J. Electrochem. Soc.; LBL-23905.
13. C.C. Haili (M.S. Thesis), "The Corrosion of Iron Rotating Hemispheres in 1 M Sulfuic Acid: An Electrochemical Impedance Study," LBL-23776.
14. G. Sisler (M.S. Thesis), "Adsorption of Dilute-Aqueous Zinc Ions in the Electrical Double Layer of a Porous-Carbon Electrode," LBL-24406.
15. A.C. West and J. Newman, "Corrections to Kinetic Measurements Taken on a Disk Electrode," submitted to J. Electrochem. Soc.; LBL-24416.

Invited Talks

16. J. Newman, "Theory of Battery Design and Optimization," Second Annual Battery Conference on Applications and Advances, Long Beach, CA, Jan. 13, 1987.

17. J. Newman, "Mass Transport and Current Distribution in the Geometries of Localized Corrosion," International Conference on Localized Corrosion, National Association of Corrosion Engineers, Orlando, FL, June 3, 1987.
18. A.K. Hauser and J. Newman, "A Microscopic Impedance Model of the Electrode/Electrolyte Interface—Adsorption Mechanism for Zinc Dissolution in Chloride Solutions," Honolulu meeting of The Electrochemical Society, Oct. 22, 1987.
19. V. Edwards and J. Newman, "Modeling Thin-Gap Channel Flow Cells," New York meeting of the American Institute of Chemical Engineers, Nov. 19, 1987.

Health and Environmental Sciences

Semiconductor Materials and Devices*

Eugene E. Haller, Investigator

INTRODUCTION

The recently achieved ultrahigh purity and crystalline perfection of large germanium single crystals and, to a lesser degree, silicon single crystals have led to the discovery of a large number of novel impurity and defect complexes that exhibit energy levels in the band gap of these semiconductors. Understanding the composition and electronic structure of these novel acceptors and donors through the use of sensitive far-infrared spectroscopy techniques and novel radioactive tracer schemes represents one component of this research effort. Another closely coupled component focuses on the formation of these centers during crystal growth.

Two factors have helped greatly in identifying the composition of these novel acceptors and donors: (1) correlations between concentration and electronic-structure effects of a given center, and (2) control of the materials involved in the crystal growth and purification, such as the crucible material (typically synthetic silica or graphite) and the ambient (typically H_2, N_2, or vacuum). One of the major findings is that atomic hydrogen plays an important role in the formation and composition of many of the new impurity complexes. The information gained through this research is of immediate use to LBL's semiconductor radiation-detector program, which originated this research.

The use of ultrapure crystals as starting material for specially doped crystals is studied in connection with the development of sensitive far-infrared photoconductors for low-photon-flux applications in outer space and neutron-transmutation-doped germanium bolometers. The high ratio of intentional-dopant concentrations and residual-impurity concentrations has led to photoconductors with very high responsivity working at close to the photon noise limits.

The close coupling between crystal synthesis and analysis has enabled us to effectively study and use these extremely pure and structurally perfect materials.

*This work was supported by the Director, Office of Energy Research, Office of Health and Environmental Research, U.S. Department of Energy under Contract No. DE-AC03-76SF00098; and in part by NASA Contract No. W-14,606 under Interagency Agreement with the U.S. Department of Energy.

1. Trigonal Hydrogen-Related Acceptor Complexes in Germanium (Publication 16)

J.M. Kahn,† R.E. McMurray, Jr., E.E. Haller, and L.M. Falicov

In germanium, an interstitial hydrogen atom may bind at a substitutional atom of carbon, silicon, beryllium, or zinc to form a shallow, monovalent acceptor complex. Photothermal ionization spectroscopy under uniaxial stress reveals that the complexes A(H,C), A(H,Si), A(Be,H), and A(Zn,H) have trigonal (C_{3v}) symmetry. Each has two (1s)-like acceptor levels that shift, but do not split, under stress. In the fourfold basis for an $\Gamma_8(T_d)$ level, simultaneous diagonalization of the perturbations of applied stress, and of a trigonal lowering of symmetry, yields theoretical piezospectroscopic behavior in quantitative agreement with all available experimental data. This procedure has been extended to predict the stress-induced shifts of (1s)-like shallow acceptor levels associated with tetragonal (D_{2d}) and rhombic I (C_{2v}) complexes in germanium, should these ever be observed experimentally. The four trigonal complexes in germanium are to be contrasted with A(Be,H) in silicon, in which the rapid tunneling of hydrogen leads to recovery of tetrahedral symmetry and a much more complicated energy-level structure. Figure 1-1 shows the photothermal ionization spectra of the D transitions of the acceptors $A(H,Si)_1$, $A(H,Si)_2$, and aluminum under [111] uniaxial compression. The numbers 1 and 2 in square brackets refer to $A(H,Si)_1$ and $A(H,Si)_2$, respectively. Note the difference between the highly symmetric splitting of the D lines of aluminum and boron and the assymetric splitting of the lines associated with A(H,Si).

†Present address: AT&T Bell Laboratories, Crawford Hill Laboratory, Holmdel, NJ 07733.

2. Diamond-Like Antireflective Coatings for Far-Infrared Photoconductors (Publication 27)

J.W. Beeman, A.R. Nyaiesh,† E.E. Haller, W.L. Hansen and E.L. Garwin†

Diamond-like films have been used as antireflective coatings on far-infrared semiconductor photoconductors. An average increase in the detector responsivity of 28% was realized for optimally coated gallium-doped germanium photoconductors compared to uncoated devices. The photoconductors

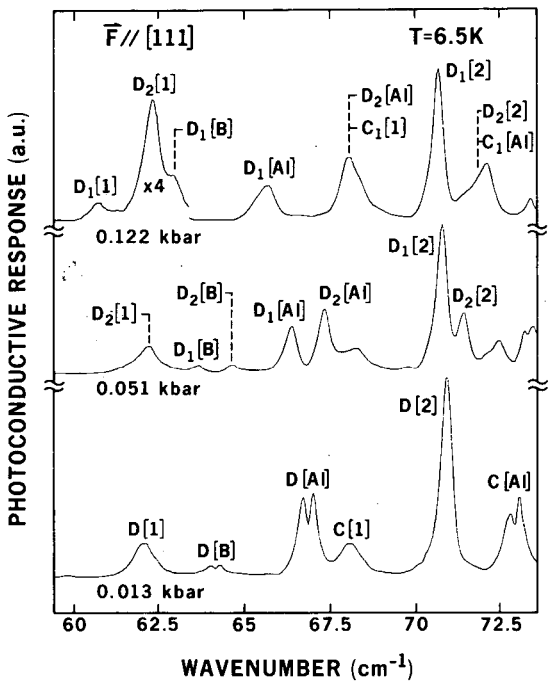

Figure 1-1. PTI spectra of the D transitions of $A(H,Si)_1$, $A(H,Si)_2$, and aluminum, under [111] uniaxial compression. The numbers "1" and "2" in square brackets refer to $A(H,Si)_1$ and $A(H,Si)_2$, respectively. (XBL 874-1719)

were operated at 3 K without cavity in a narrow wavelength range from 98.45 to 99.35 mm. The films survived repeated thermal cycling between room temperature and 2.5 K. Any increase in dark current caused by the coating is $\leq 10^{-14}$ A, a value given by instrumentation. The protective qualities of the film are explored. The potential applications of diamond-like coated photoconductors in large, unstressed and stressed arrays that will be used in future, satellite-born astrophysics missions will be discussed.

---

†Permanent address: Stanford Linear Accelerator Center, Stanford University, Stanford, CA 94305.

3. Ion Implantation of Boron in Germanium (Publication 9)

K.S. Jones† and E.E. Haller

The activation of boron implanted at room temperature into germanium has been studied. In sharp contrast to all other group III elements, boron forms a *p*-type layer before any postimplant annealing steps. Variable-temperature Hall-effect measurements and deep-level transient-spectroscopy experiments indicate that all of the boron ions are electrically active as shallow acceptor centers over the entire dose range ($5 \times 10^{11}/cm^2$ to $1 \times 10^{14}/cm^2$) and energy range (25–100 keV) investigated, without any postimplant annealing. The concentration of damage-related acceptor centers is only 10% of the boron-related, shallow acceptor center concentration for low-energy implants (25 keV), but becomes dominant at high energies (100 keV) and low doses ($<1 \times 10^{12}/cm^2$). Three damage-related hole traps are produced by ion implantation of $^{11}B^+$. Two of these hole traps have also been observed in g-irradiated Ge, and three traps anneal out at low temperatures (<300°C). Room-temperature implantation of BF_{2+} into Ge does not lead to substitutionally active boron without annealing. A thermal cycle of 350°C for 30 min activates 100% of the boron. Figure 3-1 shows the Hall-effect sample geometry used for our experiments. In order to isolate the *p*-type implanted layer from the substrate, the latter was chosen to be lightly n-type. Figure 3-2 shows the log of the hole concentration as a function of the inverse absolute temperature. The slope at low temperature corresponds to one half of the boron acceptor binding energy, as expected for low-compensation *p*-type material. The thermal annealing only affects the higher-temperature range, in which deep-level holes are thermally activated. The shallow-level concentrations before and after annealing are identical,

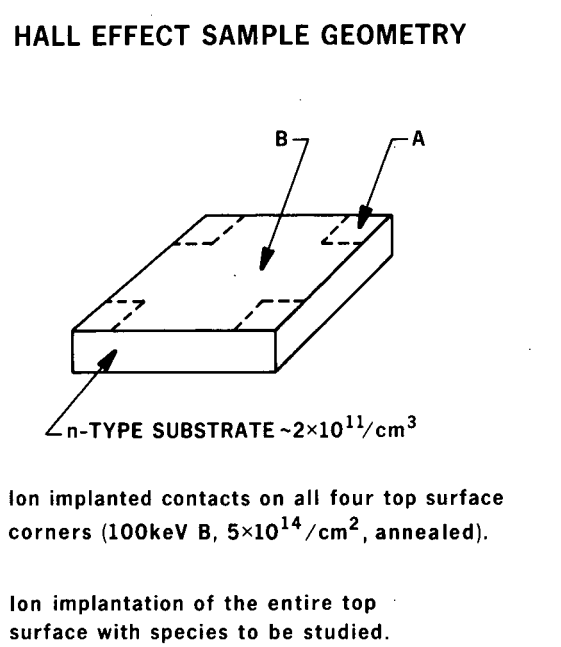

Figure 3-1. Van der Pauw Hall effect sample geometry for studying implanted layers. (XBL 8410-4377)

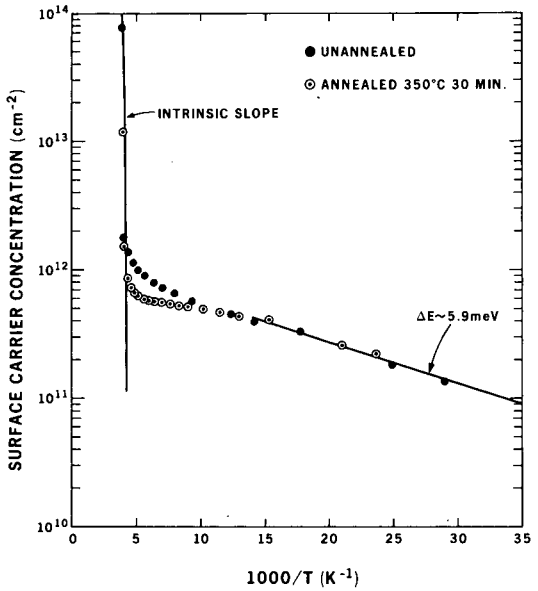

Figure 3-2. Carrier freezeout as a function of inverse absolute temperature for a 100-keV boron implant into Ge at a dose of $5 \times 10^{11}/cm^2$. (XBL 853-1612)

which means that boron is electrically active in Ge "as-implanted."

---

†Permanent address: Department of Materials Science, University of Florida, Gainesville, FL.

1987 PUBLICATIONS AND REPORTS

Refereed Journals

1. R.E. McMurray, Jr., N.M. Haegel, J.M. Kahn, and E.E. Haller, "Beryllium-Hydrogen and Zinc-Hydrogen Shallow Acceptors Complexes in Germanium," Solid State Commun. **61**, 27 (1987); LBL-20881.
2. D.D. Nolte, E.E. Haller, and P. Omling, "Uniaxial Stress DLTS Measurements on Iron Acceptor Pairs in Silicon," in *Proc. 14th ICDS*, H.J. Von Bardeleben, Ed., Mat. Sci. Forum **10-12**, 457 (1987); LBL-21988.
3. J.C. Culbertson, R.M. Westervelt, and E.E. Haller, "Free Exciton Diffusion and Decay in Zero Stress Ge," Phys. Rev. B **34**, 6980 (1986).
4. E.E. Haller, "Infrared Spectroscopy of Impurity Complexes in Germanium," in *Proc. 2nd Int. Conf. Shallow Impurity Centers*, Physica **146 B**, 201 (1987); LBL-21955.
5. K.-M. Yu, S.K. Cheung, T. Sands, J.M. Jaklevic, and E.E. Haller, "Correlation Between Solid State Reaction and Electrical Properties of the Rh/GaAs Schottky Contact," J. Appl. Phys. **61**, 1099 (1987); LBL-21889.
6. M.L.W. Thewalt, D. Labrie, I.J. Booth, B.P. Clayman, E.C. Lightowlers, and E.E. Haller, "Photoluminescence and Infrared Absorption Studies of Double Acceptors in Germanium," in *Proc. 2nd Int. Conf. Shallow Impurity Centers*, Physica **146 B**, 47 (1987).
7. K.-M. Yu, T. Sands, J.M. Jaklevic, and E.E. Haller, "Interfacial Interactions of Evaporated Iridium Thin Films with (100) GaAs," J. Appl. Phys. **62**, 1815 (1987); LBL-22376.
8. M.L.W. Thewalt, D. Labrie, E.C. Lightowlers, and E.E. Haller, "Effects of <001> Uniaxial Stress on the Photoluminescence Spectrum of Ge Doped with Zn," Solid State Commun. **60**, 327 (1986).
9. K.S. Jones and E.E. Haller, "Ion Implantation of Boron in Germanium," J. Appl. Phys. **61**, 2469 (1987).
10. E.D. Bourret, J.B. Guitron, and E.E. Haller, "Evaluation of the Mellen 'EDG' Furnace for Growth of Large Diameter GaAs Single Crystals in a Horizontal Configuration," J. Cryst. Growth **85**, 124 (1987).
11. E.D. Bourret, J.B. Guitron, and E.E. Haller, "Imaging and Analysis of Carbon Distribution in GaAs Using Radioactive Tracer ^{14}C," J. Cryst. Growth **85**, 290 (1987).
12. K.-M. Yu, W. Walukiewicz, J.M. Jaklevic, and E.E. Haller, "Effects of Interface Reactions on Electrical Characteristics of Metal-GaAs Contacts," Appl Phys. Lett. **51**, 189 (1987); LBL-23067.
13. D.D. Nolte and E.E. Haller, "The Optimization of Energy Resolution of Deep Level Transient Spectroscopy," J. Appl. Phys. **62**, 900 (1987); LBL-22206.
14. K.-M. Yu, J.M. Jaklevic, and E.E. Haller, "Solid Phase Reactions Between (100) GaAs and Thin Film Refractory Metals (Ti, Zr, V, Nb, Cr, Mo and W)," J. Appl. Phys. **A44**, 177 (1987); LBL-23282.
15. D.D. Nolte, W. Walukiewicz, and E.E. Haller, "Band-Edge Hydrostatic Deformation Potentials in III-V Semiconductors," Phys. Rev. Lett. **59**, 501 (1987); LBL-23238.
16. J.M. Kahn, R.E. McMurray, Jr., E.E. Haller, and L.M. Falicov, "Trigonal Hydrogen-Related Acceptor Complexes in Germanium," Phys. Rev. B **36**, 8001 (1987); LBL-23305.
17. D.D. Nolte, W. Walukiewicz, and E.E. Haller, "Critical Criterion for Axial Models of Defects in as-Grown n-GaAs," Phys. Rev. B **36**, 9374 (1987); LBL-23857.
18. D.D. Nolte, W. Walukiewicz, and E.E. Haller, "Deep Level Defects in Silicon and the Band-Edge Hydrostatic Deformation Potentials," Phys. Rev. B **36**, 9392 (1987); LBL-23963.

Other Publications

19. N.M. Haegel and E.E. Haller, "Extrinsic Germanium Photoconductor Material: Crystal Growth and Characterization," presented at Materials Technologies for IR Detectors Session of the Third Int. Symp. on Optical and Optoelectronic Appl. Sci. and Engr.,

Innsbruck, Austria, April 14–24, 1986; APIE Proc. **659**, 188 (1986); LBL-20515.

20. J.M. Kahn, E.E. Haller, and L.M. Falicov, "Copper-Dihydrogen Acceptors in High-Purity Germanium," in *Proc. 18th Int. Conf. Physics of Semiconductors*, O. Engstroem, Ed., World Scientific Publ. Co., Singapore, 1987, p. 1003; LBL-21183.
21. E.E. Haller, H. Navarro, and F. Keilmann, "Intrinsic Linewidths of 1s-np Donor Transitions in Ultra-Pure Germanium," in *Proc. 18th Int. Conf. Physics of Semiconductors*, O. Engstroem, Ed., World Scientific Pub. Co., Singapore, 1987, p. 837; LBL-22120.
22. H. Navarro, J. Griffin, and E.E. Haller, "The Zeeman Spectra of Phosphorus and the D(H,O) Donor Complex in Ultrapure Germanium," in *Proc. 2nd Int. Conf. Shallow Impurity Centers*, Trieste, Italy, 1986.
23. E.E. Haller and L.M. Falicov, "Hydrogen-Related Impurity Complexes in Germanium and Silicon," in *Proc. 3rd Brazilian School of Semiconductor Physics*, C.E.T. Goncalves da Silva, L.E. Oliveira, and J.R. Leite, Eds., World Scientific Publ. Co., Singapore, 1987, p. 132; LBL-22976.
24. E.E. Haller, "Up-Close: Max-Planck-Institute for Solid State Research in Stuttgart," MRS Bulletin **12**, 34 (1987).
25. E. Kreysa, G. Haslam, and E.E. Haller, "A ^{3}He-Cooled Bolometer Array for the IRAM 30 m Telescope," in *Proc. Int. Conf. Array Detectors for Ground-Based Infrared Astronomy*, Univ. of Hawaii, C.G. Wynn-Williams and E.E. Becklin, Eds., 1987, p. 263.
26. D. Labrie, I.J. Booth, M.L.W. Thewalt, and E.E. Haller, "Piezospectroscopy of the Ground and Excited States of Zinc Double Acceptors in Germanium," accepted by Phys. Rev. B.
27. J.W. Beeman, A.R. Nyaiesh, E.E. Haller, W.L. Hansen, and E.L. Garwin, "Diamond-Like Antireflective Coatings for Far Infrared Photoconductors," Proc. E., Mat. Res. Soc. (in press); SLAC-PUB-4309.
28. M. Helm, K. Unterrainer, E. Gornik, and E.E. Haller, "New Results on Stimulated Emission From p-Germanium in Crossed Fields," to appear in *Proc. Fifth Int. Conf. Hot Carriers in Semiconductors*, Boston, MA, July 20–24, 1987.

LBL Reports

29. W. Walukiewicz, E. Bourret, W.F. Yau, R.E. McMurray, Jr., E.E. Haller, and D. Bliss, "Spatial Distribution of Carbon and Native Defects in Large-Diameter Bulk-Grown GaAs," submitted to DRIP II, Monterey, CA, Apr. 27–29, 1987; LBL-22751.
30. E.D. Bourret, J.B. Guitron, and E.E. Haller, "A New Approach to Vertical Seeded Growth of Large-Diameter GaAs Crystals," submitted to ACCG-7/II-VI-87 Conf., Amer. Assoc. for Crystal Growth, Monterey, CA, July 12–17,1987; LBL-22902.
31. D.D. Nolte, W. Walukiewicz, and E.E. Haller, "Absolute Pressure Derivatives of Deep Level Defects in III-V Semiconductors," submitted to 1987 Fall Meeting of Mat. Res. Soc., Boston, MA, Nov. 30–Dec. 4, 1987; LBL-23599.
32. E.E. Haller, "Far Infrared Fourier Transform Spectroscopy of Semiconductors," presented at the 6th FTS Conference 1987, Vienna, Austria, Aug. 24–28, 1987, accepted by Microchim. Acta; LBL-23244.
33. K.-M. Yu, J.M. Jaklevic, and E.E. Haller, "Investigations of Thin Films on GaAs Using the Proton Resonant Scattering Technique," submitted to Nucl. Instrum. Meth. B; LBL-24023.

Invited Talks

34. E.E. Haller, "Hydrogen Related Impurity Complexes in Germanium and Silicon," 3rd Brazilian School on Semiconductor Physics, Campinas, Brazil, Feb. 17, 1987.
35. E.E. Haller, "Dynamic Impurities in Ultra-Pure Germanium," H.C. Oersted Institute, Physics Dept., University of Kopenhagen, Denmark, Aug. 19, 1987.
36. E.E. Haller, "Far Infrared Fourier Transform Spectroscopy in Semiconductors," 6th International Conference on FTIR, Vienna, Austria, Aug. 27, 1987.
37. E.E. Haller, "Spectroscopy of Hydrogen Related Complexes in Semiconductors," XEROX Palo Alto Research Center, Oct. 9, 1987.
38. E.E. Haller, "Semiconductor Materials for Radiation Detection," IEEE Nuclear Science Symposium Short Course, San Francisco, CA, Oct. 20, 1987.
39. E.E. Haller, "Hydrogen in Semiconductors," Department of Materials Science and Mineral Engineering, University of California, Berkeley, Nov. 5, 1987.
40. J.M. Kahn, "H-Related Complexes in Si and Ge: Static or Dynamic Defects?" Gordon Research Conference on Point Defects, Line Defects and Interfaces in Semiconductors, Plymouth State College, Plymouth, NH, July 24,1987.
41. J.M. Kahn, "Hydrogen Related Impurity Complexes in Semiconductors," Boeing Corporation, Seattle, WA, Feb. 13, 1987; AT&T Bell Laboratories, Murray Hill, NJ, Feb. 16, 1987; AT&T Bell Laboratories, Holmdel, NJ, Feb. 17, 1987; Sandia National Laboratory, Albuquerque, NM, Mar. 4, 1987.

Program Development Funds

Raman Studies of Surface Processes*

Gerd M. Rosenblatt, Investigator

INTRODUCTION

This project is designed to utilize and develop new instrumentation for the study of surfaces using unenhanced surface Raman spectroscopy (SRS). The project's goals are to use SRS to study surface composition; to provide new information concerning rotational and vibrational energy levels, dynamics, and reactivity of molecules adsorbed on a variety of surfaces; to study fundamental processes under ultrahigh-vacuum (UHV) conditions; and to extend the technique to a range of chemically important pressures, temperatures, and interfaces. An apparatus has been completed that uses an imaging photomultiplier tube (PMT) to obtain Raman spectra that have unprecedented sensitivity and that yield a one-dimensional Raman image of sample composition along a few millimeters of an illuminating, focused laser beam. The Raman system is coupled to an UHV chamber that enables Raman spectra to be obtained from solid samples and films at temperatures between 15 K and 800 K. The UHV chamber has low-energy electron diffraction (LEED) and Auger surface analysis capabilities. This project provides a dramatic new analytical capability that compliments and contributes to other LBL surface science projects.

1. Raman Spectroscopy Applications of an Imaging Photomultiplier Tube (Publication 1)

D.K. Veirs, V.K.F. Chia, and G.M. Rosenblatt

A Raman spectroscopy system having an unprecedented combination of high sensitivity and low noise has been built incorporating an imaging (2D) photomultiplier tube. The number of photons detected for a vibrational band approaches the theoretical limit set by the Raman cross section and experimental configuration. A detector dark count of 10^{-4} counts/sec/pixel is the major electronic source of noise. The spectrum of air reveals low-concentration gas components, specifically $^{16}O^{18}O$ and CO_2. Vibrational Raman spectra are obtained from solid samples as thin as 20 nm with low laser powers, e.g., 6.5 mW. The imaging photomultiplier yields 1D (along the focused laser beam) Raman images of interfaces (see Figure 1-1) or concentration gradients.

2. Ultrahigh-Vacuum Apparatus for Unenhanced Raman Spectroscopy at Cryogenic Temperatures (Publication 3)

V.K.F. Chia, D.K. Veirs, and G.M. Rosenblatt

An UHV apparatus for studying submonolayer molecular coverages on well-defined single crystals by means of unenhanced SRS is described. Surface studies at controlled temperatures from 13 K to 900 K are possible. Sample cooling is achieved with a flexible thermal braid and closed-cycle helium refrigerator. Sample manipulation includes translation in the XYZ directions, tilt, and two degrees of rotation. This wide range of sample movement allows SRS, LEED, and Auger spectroscopy to be carried out while maintaining a controlled temperature. Optical ports, at two incident angles, permit the study of a variety of substrates with differing optical properties. Unenhanced Raman spectra of nitrogen physisorbed on silver are presented in Figure 2-1.

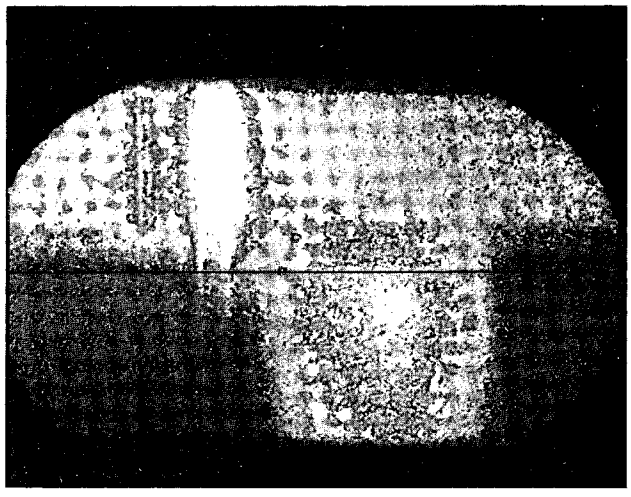

Figure 1-1. Gray-scale image of the data array from a water-cyclohexane mixture. The gray scale represents the number of counts in a pixel. The x axis is wavelength dispersion, and the y axis is along the laser beam waist. (CBB 875-3689)

*This work was supported by the Director's Program Development Funds of Lawrence Berkeley Laboratory under Contract No. DE-AC03-76SF00098

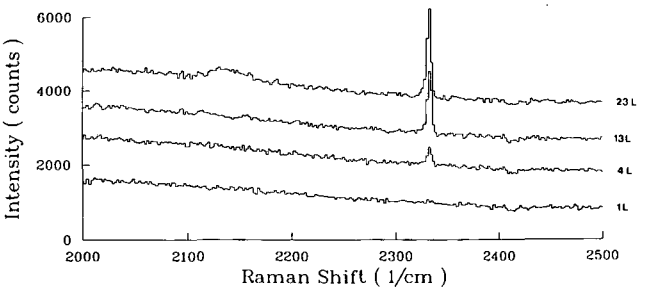

Figure 2-1. Raman spectra of physisorbed N_2 on the (111) face of clean, single-crystal Ag at 15 K with increasing exposure: (a) 1 Langmuir, (b) 4 Langmuirs, (c) 13 Langmuirs, and (d) 23 Langmuirs. The data for b, c, and d have an increasing offset for clarity. The observed frequency, 2329 cm^{-1}, is shifted from the liquid N_2 frequency (2326.5 cm^{-1})[1] and coincides with the frequency of the α-phase of solid N_2 (2329 cm^{-1}).[2] (XBL 881-301)

1. S.A. Akhmanor, F.N. Gadzhiev, N.I. Koroteev, R. Yu. Orlov, and I.L. Shvmai, JETP Lett. **27**, 243 (1978).
2. A. Anderson, T.S. Sun, and M.C.A. Donkersloot, Can. J. Phys. **48**, 2265 (1971).

3. Application of Spatially Resolved Raman Spectroscopy in the Study of Transformed Zones in Partially Stabilized Zirconia (Publication 5)

D.K. Veirs, R.O. Ritchie, and R.H. Dauskardt

Raman vibrational spectroscopy provides an effective phase-characterization technique in materials systems containing particle dispersions of the three polymorphs of ZrO_2, each of which yields a unique Raman spectrum. An investigation is reported to assess the capabilities of a novel, spatially resolved Raman spectroscopy system in the study of phase-transformation zones around crack tips in partially stabilized ZrO_2 (PSZ). The experimental arrangement makes use of an imaging (2D) photomultiplier tube that produces a 1D map of chemical composition along a laser beam without translating either the sample or the laser beam and without scanning the spectrometer. Results from phase-characterization studies of size, frontal morphology, extent of transformation, and degree of reversibility of the transformation zone surrounding cracks produced under monotonic and cyclic loading conditions are presented.

4. Work in Progress

Forces between physisorbed molecules and surfaces are being examined using Raman spectroscopy of N_2 and H_2 physisorbed on clean, well-characterized single-crystal silver surfaces. Preliminary investigations indicate that N_2 forms an ordered structure on Ag much like the low-temperature α-phase of solid N_2 (see Figure 2-1). Further studies are under way to determine the low coverage limit of unenhanced SRS of this system. Other collaborative projects that are being actively investigated with this apparatus include: (1) Raman studies of hard carbon films and of "diamond-like" films; (2) Raman studies of 90 K transition temperature superconductors as a function of temperature, oxygen isotope, and sample-preparation conditions; and (3) use of spatially resolved Raman spectroscopy to ascertain the extent of the phase-transformation zone in PSZ caused by crack propagation and subsequent relaxation.

1987 PUBLICATIONS AND REPORTS

Refereed Journals

1. D.K. Veirs, V.K.F. Chia, and G.M. Rosenblatt, "Raman Spectroscopy Applications of an Imaging Photomultiplier Tube," Appl. Opt. **26**, 3530 (1987); LBL-22853.

LBL Reports

2. H.-c. Tsai, D.B. Bogy, M.K. Kundmann, D.K. Veirs, M.R. Hilton, and S.T. Mayer, "Structure and Properties of Sputtered Carbon Overcoats on Rigid Magnetic Media Disks," J. Vac. Sci. Technol. A. (in press); LBL-22762.
3. V.K.F. Chia, D.K. Veirs, and G.M. Rosenblatt, "Ultrahigh Vacuum Apparatus for Unenhanced Raman Spectroscopy at Cryogenic Temperatures," LBL-24567.
4. D.K. Veirs, V.K.F. Chia, and G.M. Rosenblatt, "Unenhanced Surface Raman Spectroscopy of Adsorbed Films," abstract submitted to 62nd Colloid and Surface Science Symposium; LBL-24566abs.
5. D.K. Veirs, R.O. Ritchie, and R.H. Dauskardt, "Application of Spatially Resolved Raman Spectroscopy in the Study of Transformed Zones in PSZ," abstract submitted to March 1988 meeting, American Physical Society; LBL-24565abs.

Invited Talks

6. D.K. Veirs, V.K.F. Chia, and G.M. Rosenblatt, "Applications of Position-Sensitive, Photon-Counting Detectors in Raman Spectroscopy," topical meeting, Optical Society of America, Incline Village, NV, Jan. 1987.

7. G.M. Rosenblatt, "Recent Developments in Optical Methods for the Study of Adsorbed Species," Third Annual Meeting on Chemical Analysis, Brussels, Belgium, May, 1987, and Physics Colloquium, University of California, Riverside, Nov. 1987.

Structure Determination at the Metal/Solution Interface*

P.N. Ross, Investigator†

INTRODUCTION

Within the last decade, a number of research groups have developed a new type of apparatus uniting ultrahigh-vacuum (UHV) surface analytical techniques with electroanalytical cells. An apparatus of this type permits UHV surface preparation and characterization with maintenance of the UHV structure up to the moment of contact of the surface to the liquid phase. Structural transformations to the surface as a result of the liquid/solid interaction can be determined *ex situ* by removing the bulk liquid from the surface and analyzing the solid surface in vacuum with low-energy electron diffraction (LEED) or reflected high-energy electron diffraction (RHEED). Such experiments have the intrinsic limitation that they can never reveal the structure of the interface, nor even the structure of the solid surface in contact with liquid, i.e. the *in situ* structure. Recognizing these limitations, many of these same groups are pursuing the development of methods for determining the structure of the solid surface *in situ*. Among the methods being developed at LBL are scanning tunneling microscopy (STM) and grazing incidence x-ray scattering (GIXS). The latter method encompasses a number of techniques, including surface diffraction (grazing-incidence diffraction, or GID), in-plane wide-angle scattering (WAXS), and surface extended x-ray absorption fine structure (SEXAFS).

*This work was supported by the Director's Program Development Funds of the Lawrence Berkeley Laboratory under Contract No. DE-AC03-76SF00098.

†Work performed in collaboration with M. Van Hove (MCSD), J. Kortright (Accelerator and Fusion Research Division), and O. Melroy of IBM Almaden Research Center, San Jose, CA.

1. An *In Situ* Grazing Incidence X-Ray Scattering Study of the Initial Stages of Electrochemical Growth of Lead on Silver (111) (Publication 1)

O.R. Melroy,† *M.F. Toney,*† *G.L. Borges,*† *M.G. Samant,*† *J.B. Kortright, P.N. Ross, and L. Blum*‡

The potential-dependent structure of underpotentially deposited lead on silver (111) and the initial stages of bulk lead deposition on the ad-layer have been studied using GIXS. Measurements were made *in situ* and under potential control. The closed-packed hexagonal lattice formed by the underpotential deposition of lead (at full monolayer coverage) is compressed 1.4% relative to bulk lead. This strain increases linearly with applied potential until the onset of bulk deposition, where the ad-layer is compressed 2.8%. Bulk lead is not deposited epitaxially on this template because of the large strain. Instead, it grows as islands with (111) texture that are randomly oriented in the plane of the substrate. After the deposition of approximately five equivalent monolayers of bulk lead, the initial ad-layer reconstructs, apparently becoming disordered in the plane of the silver substrate.

†Permanent address: IBM Almaden Research Center, San Jose, CA 95120.

‡Permanent address: Physics Department, College of Natural Sciences, Rio Piedras, Puerto Rico 00931.

2. Work in Progress

Ex situ LEED analyses of emersed (removed from electrolyte under potentiostatic control) single-crystal electrodes have provided direct observations of place-exchange during the anodic oxidation of both Pt and Au surfaces. These recent surface-structure determinations have confirmed, and refined, our understanding of anodic oxidation and place-exchange developed previously from purely electrochemical methods. The use of *ex situ* LEED to observe more subtle changes in surface structure has, however, proven to be problematic. In particular, the stability of the UHV reconstructed surfaces of Au in electrolyte cannot be established in a definitive way by use of LEED due to changes in surface excess charge (the effective potential of the electrode in vacuum) during emersion and evacuation. These changes are described more fully in Publication 3. GID, which we used successfully to determine the *in situ* structure of a Pd monolayer on silver (111) (Publications 1 and 2), is capable of providing the

in situ structure determination essential for determining the stability of the UHV-reconstructed surfaces in electrolyte. These studies are in progress using the synchrotron from beamline VI at the Stanford Synchrotron Research Laboratory.

1987 PUBLICATIONS AND REPORTS

LBL Reports

1. O. Melroy, M. Toney, G. Borges, M. Samant, J. Kortright, P. Ross, and L. Blum, "An *In Situ* Grazing Incidence X-Ray Scattering Study of the Initial Stages of Electrochemical Growth of Lead on Silver (111)," submitted to Surf. Sci.; LBL-24455.
2. O. Melroy, M. Toney, G. Borges, M. Samant, J. Kortright, P. Ross, and L. Blum, "The Two-Dimensional Compressibility of Electrochemically Adsorbed Lead on Silver (111)," submitted to Phys. Rev. Lett.; LBL-24454.
3. P. Ross, "Potential Induced Structural Transformations of the Au(100) and (111) Surfaces," LBL-24442.

Novel Properties of Matter at Megabars of Pressure*

Marvin L. Cohen, Raymond Jeanloz, and Peter Y. Yu, Investigators

INTRODUCTION

The purpose of this research project is to investigate the properties of matter at megabars of pressure both experimentally and theoretically. The objective is to combine the expertise of experimentalists and theorists in the area of high-pressure technology, materials characterization techniques, inorganic synthesis, and theoretical computation of properties of matter to synthesize and investigate new materials with unusual properties or with potential applications to energy technology. Examples of these new materials are ultrahard solids with strength comparable to or exceeding that of diamond, and solids with unusual electrical, superconducting, optical, and magnetic properties.

1. Synthesis of New Alloys of C-B-N with Diamond Structure (Publications 3, 6, and 7)

R.M. Wentzcovitch, M.L. Cohen, P.K. Lam, K.J. Chang, and G. Martinez

A new model in which the bulk moduli of solids with diamond and zinc-blende structure scale with only the nearest-neighbor bond length has been proposed. Results obtained from this empirical approach were found to compare favorably with values calculated by a full *ab initio* pseudopotential method. Based on this method, it was predicted that a compound with the formula of BCN and the structure of diamond will be more densely packed and therefore harder than diamond. A new material with the composition $C_x(BN)_{1-x}$ has been synthesized under pressures of 10 to 30 GPa and temperatures of between 1000–2000 K inside a laser-heated diamond anvil cell using graphite and boron nitride as the starting materials. X-ray diffraction has shown that these new alloys have the diamond structure. The lattice parameters and bulk moduli of these alloys have been measured as a function of x. Contrary to Vegard's law, the lattice parameter for values of x between 0 and 1 was found to be larger than the value obtained by a linear interpolation between the end-point values. This was contrary to expectations based on theoretical calculations of Cohen. These calculations have suggested a normal behavior according to Vegard's law, where the lattice parameters should be smaller than a linear interpolation. The bulk moduli also varied nonlinearly with x, suggesting that the alloys have bulk moduli lower than that of diamond. Although these binary alloys probably will not be harder than diamond, they may still have important applications in electronics and machine tool manufacturing.

2. Pressure Dependence of the New High-T_c Superconductors (Publications 1, 2, and 8)

D. Erskine, P.Y. Yu, G. Martinez, E. Hess, A.M. Stacy, A. Zettl, and M.L. Cohen

Using diamond anvil cells, we have studied the pressure dependence of both the room temperature resistance and T_c in LaBaCuO, LaSrCuO, and YBaCuO compounds up to 20 GPa. Typically we found that the room-temperature resistance of these ceramic superconductors decreased by several orders of magnitude at pressures ranging from 8 GPa in LaSrCuO to 5 GPa in YBaCuO. The transition temperature in the LaBaCuO and LaSrCuO compounds showed strongly nonlinear pressure dependence. At pressures below 3–5 GPa, T_c increased rapidly with pressure. At pressures of above 5 GPa, T_c tended to saturate and then decrease with pressure. In YBaCuO, T_c was almost independent of pressure and then decreased with pressure. In both YBaCuO and LaSrCuO, above a well-defined pressure the sample became a better metal at room temperature but also lost its superconducting properties. These results suggest that the high superconducting temperatures in these materials are very sensitive to bond lengths. There is an optimal bond length for the highest superconducting temperature. In YBaCuO this optimal bond length is achieved at atmospheric pressure. When the materials are compressed beyond this optimal bond length, superconductivity is quickly destroyed, while the sample also becomes a better normal metal.

3. Work in Progress

For the first time a theoretical study of the bulk modulus of solids based on first-principles calcula-

*This work was supported by the Director's Program Development Funds of the Lawrence Berkeley Laboratory under Contract No. DE-AC03-76SF00098.

tion has been performed and used to guide experimental work in the search for new materials with unusual mechanical properties. Based on a systematic investigation of the electronic structure, bulk moduli, lattice constants, and lattice vibrational spectra of hard materials, such as diamond, BN, SiC, and BP, the theoretical group of Marvin Cohen has concluded that materials synthesized from carbon and BN under high temperature and pressure can have a bulk modulus higher than or comparable to diamond. The resulting experimental investigation carried out by the group of Raymond Jeanloz has shown that alloys of the composition $C_x(BN)_{1-x}$ can be formed with new interesting properties. The mechanical properties and lattice constant of these new alloys are still being investigated.

1987 PUBLICATIONS AND REPORTS

Refereed Journals

1. D. Erskine, P.Y. Yu, and G. Martinez, "A New Technique for High-Pressure Electrical Conductivity Measurements in Diamond Anvil Cell at Cryogenic Temperatures," Rev. Sci. Instrum. **58**, 406 (1987); LBL-22485.
2. D. Erskine, E. Hess, P.Y. Yu, and A.M. Stacy, "Pressure Dependence of the Superconducting Transition Temperature in $La_{1.85}Sr_{0.15}CuO_4$ to 8 GPa," J. Mater. Res. **2**, 783 (1987); LBL-23808.
3. R.M. Wentzcovitch, K.J. Chang, and M.L. Cohen, "Electronic and Structural Properties of BN and BP," Phys. Rev. B **34**, 1071 (1986).
4. R.M. Wentzcovitch and M.L. Cohen, "Theory of Structural and Electronic Properties of BAs," J. Phys. C **34**, 6791 (1986).
5. S. Fahy, K.J. Chang, S.G. Louie, and M.L. Cohen, "Pressure Coefficients of Band Gaps of Diamond," Phys. Rev. B **35**, 8196 (1987).
6. P.K. Lam, M.L. Cohen, and G. Martinez, "Analytic Relation Between Bulk Moduli and Lattice Constants," Phys. Rev. B **35**, 9190 (1987).
7. R.M. Wentzcovitch, M.L. Cohen, and P.K. Lam, "Theoretical Study of BN, BP, and BAs at High Pressures," Phys. Rev. B **36**, 6058 (1987).

LBL Reports

8. D. Erskine, E. Hess, P.Y. Yu, A.M. Stacy, A. Zettl, and M.L. Cohen, "Electrical Properties of High T_c Superconductors under High Pressures," LBL-23692.
9. D. Erskine, P.Y. Yu, and S.C. Freilich, "High Pressure Visible Spectroscopy of Polyimide Film," LBL-24553.

Electron Electric Dipole Moment*

Eugene Commins and Harvey Gould, Investigators

INTRODUCTION

This project is an experiment to search for an electric dipole moment (EDM) of the electron. An electron EDM can exist only if the product of charge conjugation (C) and parity (P) are not conserved. CP nonconservation has been observed in neutral K decay and in no other system: it is not explained by the conventional models and is one of the most important unsolved problems in physics.

A large number of models based on new physics predict an electron EDM at values up to about 10^{-25} cm $\times$ e. Among these are calculations based on left-right-symmetric models, lepton family mixing, supersymmetry, and superstring-inspired models. Our experiment is designed to ultimately be sensitive to an electron EDM of 10^{-28} cm $\times$ e, a factor of 10,000 below the current upper limit.

1. Work in Progress

We have completed extensive calculations of systematic effects and of noise sources at the most sensitive level of the experiment. We have considered vXE/c effects from electric and magnetic field misalignments in three directions; misalignments and vXE/c effects due to gravitational deflection, misalignments of the laser, the atomic beam, and the rf fields; electric and magnetic field inhomogeneity effects; electric field switching effects; effects caused by possible inclusions of magnetic material; and other effects. Our most important finding is that gravitational deflection of a horizontal beam, especially in the presence of electric or magnetic field inhomogeneities, would lead to incomplete cancellation of vXE/C effects. To eliminate problems caused by gravitational deflection, we have built a vertical apparatus.

We have completed a design for the entire apparatus. The vacuum system, consisting of five chambers spanning 10 feet from floor to ceiling, has been completed, installed, and pumped down to a pressure of a few microtorr. The laser optical pumping system has been set up and has achieved the design power in single mode of 378 nm. The fluorescence detectors were constructed and installed. A thallium beam has been produced and fluorescence radiation detected. Simple laser spectroscopy was performed on the thallium atoms.

1987 PUBLICATIONS AND REPORTS

Invited Talks

1. E. Commins, "Experiments on P and T Nonconservation at Berkeley," Soviet Academy of Science, All Union Conference on Laser Spectroscopy, Novosibirsk, USSR, June 16, 1987.
2. E. Commins, "P and T Nonconservation Experiments at Berkeley," 8th International Conference on Laser Spectroscopy, Åre, Sweden, June 27, 1987.

*This work was supported by the Director's Program Development Funds of the Lawrence Berkeley Laboratory under Contract No. DE-AC03-76SF00098.

Work for Others

UNITED STATES OFFICE OF NAVAL RESEARCH

Quantum Monte Carlo for Molecular Studies*

William A. Lester, Jr., Investigator

INTRODUCTION

We are pursuing the use of the quantum Monte Carlo (QMC) method for the computation of molecular properties. This approach, borrowed from statistical mechanics, allows one to calculate essentially exact quantum-mechanical expectation values. Thus, it provides an alternative to traditional *ab initio* quantum chemical approaches. The method takes advantages of the formal similarity of the Schrödinger equation in imaginary time to a diffusion equation.

1. Auxiliary Walks for Atomic and Molecular Properties (Publication 1)

R.N. Barnett,† P.J. Reynolds, and W.A. Lester, Jr.†

Monte Carlo methods have been used previously in computing accurate energies for small atomic and molecular systems. However, it is also of interest to compute additional properties, such as electric dipole and quadrupole moments. In this work two methods for computing moments using QMC are studied. Each approach involves determining the asymptotic population of points sampled in a QMC "walk." Using one of these methods, the dipole moment of LiH and the quadrupole moment of H_2 and LiH are obtained. The other method in certain cases provides a more efficient estimator for the dipole moment. The resulting dipole moment for LiH is 2.315 ± 0.008 a.u., to be compared with the exact value (experiment minus vibrational effects) of 2.293 a.u. The quadrupole moment for H_2 agrees with the exact Born-Oppenheimer value of Kolos and Wolniewicz while that of LiH, with respect to the center of mass, is −3.004 ± 0.037 a.u., as compared to recent complete active space self-consistent field and coupled-cluster results of −3.070 and −3.192 a.u., respectively.

*This work was supported by the Office of Naval Research through an agreement with the U.S. Department of Energy under Contract No. DE-AC03-76SF00098.

†Also at the Department of Chemistry, University of California, Berkeley, CA 94720.

2. Transition Dipole Moments: Quantum Monte Carlo Methods and Results (Publication 2)

R.N. Barnett,† P.J. Reynolds, and W.A. Lester, Jr.†

Three Monte Carlo methods for computing transition dipole moments are studied. To evaluate the quality of each method, the transition dipole moment between the 1s and the $2p_x$ states of the hydrogen atom is calculated. It is found that one of the methods, the use of a variational walk with fixed-node side walks, yields an accurate transition dipole moment most efficiently. This method is used to compute the transition dipole moment between the lowest-energy S and P states of the lithium atom. The total energies of each state are also obtained from QMC calculations. These energies, −7.47809 ± 0.00024 hartrees for the ground state and −7.41031 ± 0.00022 hartrees for the excited state, are in excellent agreement with the nonrelativistic limit energies of −7.47807 and −7.41016 hartrees, respectively. The QMC transition dipole moment is 2.349 ± 0.012 a.u. This value, together with the QMC energies above, are used to obtain 0.7480 ± 0.0084 for the oscillator strength and 27.17 ± 0.40 ns for the mean lifetime of the P state. The QMC results are in excellent agreement with the experimental values of the oscillator strength, 0.7416 ± 0.0012, and the mean lifetime of the P state, 27.29 ± 0.04 ns.

†Also at the Department of Chemistry, University of California, Berkeley, CA 94720.

3. Bounded Vibrational Energies by Quantum Monte Carlo (Publication 3)

B. Bernu,[†] *D.M. Ceperley,*[‡] *and W.A. Lester, Jr.*[§]

QMC is an attractive alternative to the conventional variational and perturbation-theoretic techniques used in physics and chemistry. With it one can obtain excited states using a trial function Ψ_T that is orthogonal to the exact lowest-energy state. Convergence (in the QMC sense) is then to the next-lowest energy. However, when studying states of the same symmetry, it is generally not possible to find a trial wave function exactly orthogonal to all the lower-energy states of that symmetry. Thus one is not guaranteed an upper bound to the energy.

An alternative approach is developed that allows a significant number of excited states, typically 10–15, to be found in a single calculation. At the present time, in order to avoid problems with Fermi statistics, vibrational and rotational states have been studied through the use of potential energy surfaces. This restriction can be lifted, and excited electronic states will be explored shortly. The method involves the calculation of two matrices of correlation functions. The eigenvalues obtained from the ratio of the two matrices provide bounded energy estimates for all the eigenstates represented in the matrices. With this method the molecules H_2O, SO_2, and H_2CO have been studied with the use of good-quality potential surfaces from the literature. Results are compared with other theoretical and experimental results on vibrational excited states. Good agreement with these results has been obtained.

[†]Permanent address: Laboratoire de Physique, Theorique des Liquides, Université Pierre et Marie Curie, 75230 Paris Cedex 05, France.

[‡]Present address: Department of Physics, University of Illinois, Urbana.

[§]Also at the Department of Chemistry, University of California, Berkeley, CA 94720.

1987 PUBLICATIONS AND REPORTS

LBL Reports

1. R.N. Barnett, P.J. Reynolds, and W.A. Lester, Jr., "Auxilliary Walks for Atomic and Molecular Properties," submitted to J. Chem. Phys.; LBL-24848.
2. R.N. Barnett, P.J. Reynolds, and W.A. Lester, Jr., "Transition Dipole Moments: Quantum Monte Carlo Methods and Results," submitted to J. Chem. Phys.; LBL-24849.
3. B. Bernu, D.M. Ceperley, and W.A. Lester, Jr., "Bounded Vibrational Energies by Quantum Monte Carlo," submitted to J. Chem. Phys.; LBL-24850.

Invited Talk

4. P.J. Reynolds, "How to Calculate Molecular Properties with Random Numbers," Physical Chemistry Seminar, San Francisco State University, San Francisco, CA, Dec. 16, 1987.

Properties of Superconducting Thin Films; Electron-Phonon and Non-Phonon Coupling*

Vladimir Z. Kresin, Investigator

INTRODUCTION

The main goal of this research is to develop the theory of high-T_c superconductivity. The research is carried out in two directions: (1) analysis of normal and superconducting properties that do not depend on the precise mechanisms of high-T_c superconductivity (evaluation of the main parameters of the new high-T_c oxides, fermiology, multigap structure, proximity effect, etc.); and (2) origin of high T_c.

1. Parameters and Exotic Properties of High-T_c Superconductors (Publication 5)

V.Z. Kresin

A method of determining the values of main parameters, such as effective mass, Fermi energy, and coherence length, for the new high-T_c superconductors is developed. The method is based on specific-heat data. The new high-T_c materials are highly anisotropic systems, and this feature plays a crucial role in the analysis. Particularly interesting is the small values of the Fermi energy E_F. The results of the analysis show that we are dealing with unusual systems. The energy gap appears to be comparable with E_F, and the coherence length is small. Contrary to the usual case, a large fraction of carriers is paired.

2. Strong Electron-Phonon Coupling. Multigap Structure (Publications 3 and 4)

V.Z. Kresin and S.A. Wolf

It is shown that the ratio $\beta = \epsilon/T_c$ (where ϵ is the energy gap at $T = 0$ K) saturates with increasing strength of the electron-phonon interaction: the value β_{max} is calculated. The special case of a multigap superconductor is discussed. New high-T_c superconductors present a unique opportunity to observe a multigap structure.

A simple analytical expression describing T_c for any strength of electron-phonon coupling is derived directly from the Eliashberg equation.

3. Coexistence of Phonon and Nonphonon Mechanisms of Superconductivity. Concept of Coexistence and High T_c (Publications 6 and 9)

V.Z. Kresin

A quantitative test is presented that allows one to separate phononic from nonphononic contributions to the superconductivity in Nb_3Ge. This test is based on analysis of heat capacity and tunneling $\alpha^2F(\omega)$ data and neutron scattering data. Evidence was obtained that the superconductivity in Nb_3Ge is caused in part by a substantial nonphononic mechanism. In contrast, our results suggest that the superconducting state in Pb and V_3Si is due to phonons.

The analysis of recent experimental data shows that high T_c is due to the coexistence of phonon and nonphonon mechanisms.

4. Plasmons and Phonons in New High-T_c Materials (Publication 2)

V.Z. Kresin

High-T_c superconductivity is caused by the coexistence of two mechanisms: (1) strong electron-phonon coupling and (2) plasmon mechanisms. Anisotropy, the presence of layer and chain structures, leads to an appearance of low-lying plasmon branches. One can distinguish two physically distinct branches. An additional increase in T_c is due to the hybridization of plasmons with optical phonon modes.

5. Proximity Effect (Publications 10 and 12)

V.Z. Kresin

A proximity system containing a high-T_c superconductor can be used in order to strengthen the field effect. The use of the proximity contact S_h-Nb in the Josephson junction S_h-Nb-InAs-Nb-S_h (S_h is a

*This work was supported by the U.S. Office of Naval Research under Contract No. N00014-86-F0015 through an agreement with the U.S. Department of Energy under Contract No. DE-AC03-76SF00098.

high-T_c film) is promising from the point of view of making a three-terminal device.

The proximity effect can also be used in order to increase the values of the parameters of a conventional superconductor, such as T_c, critical field, and critical current.

1987 PUBLICATIONS AND REPORTS

Refereed Journals

1. V.Z. Kresin, "Critical Temperatures of Superconductors with Low Dimensionality," Phys. Rev. B **35**, 8716 (1987); LBL-22737.
2. V.Z. Kresin, "On the Critical Temperature for Any Strength of the Electron-Phonon Coupling," Phys. Lett. **122**, 434 (1987); LBL-23063.
3. V.Z. Kresin, "On the Relation between the Energy Gap and the Critical Temperature," Solid State Comm. **63**, 725 (1987); LBL-23416.
4. V.Z. Kresin and S.A. Wolf, "Effect of Low Dimensionality on the Parameters of High T_c Superconductors," Solid State Comm. **63**, 1141 (1987); LBL-23336.
5. V.Z. Kresin, "On the Coexistence of Phonon and Non-Phonon (Plasmon) Mechanisms in New High T_c Superconductors," Int. J. Modern Phys. B **1**; 945 (1987); LBL-24094.
6. V.Z. Kresin, "Mechanisms of High T_c Superconductivity in Low-Dimensional Materials," J. Mater. Res. **2**, 793 (1987); LBL-23417.

Other Publications

7. V.Z. Kresin, "Mechanisms of High T_c Superconductivity in Low Dimensional Materials," in *Proc. Meeting Mater. Res. Soc.*, Anaheim, CA, April 1987, p. 19; LBL-23602.
8. V.Z. Kresin, "Non-Phonon Mechanisms of Superconductivity in High T_c Superconducting Oxides and Other Materials and Their Manifestation," in *Novel Superconductivity*, S. Wolf and V.Z. Kresin, Eds., Plenum, New York, 1987, p. 309; LBL-24073.
9. V.Z. Kresin, "Tunneling Junction and the Field Effect," in *Proc. 1987 Int. Superconductivity Electronics Conf.*, Tokyo, August 1987, p. 365; LBL-25443.
10. V.Z. Kresin, "Field Effect and Josephson Junction," IEEE Trans. Magn. **MAG-23**, 707 (1987); LBL-22185.
11. S. Wolf and V.Z. Kresin, Eds., *Novel Superconductivity*, Plenum Press, NY, 1987.

Invited Talks

12. V.Z. Kresin, "Mechanisms of High T_c," Special Session, APS, New York, NY, Mar. 1987.
13. V.Z. Kresin, "High T_c in Low Dimensional Materials," Materials Research Society Meeting, Anaheim, CA, Apr. 1987.
14. V.Z. Kresin, "Non-Phonon Mechanisms of Superconductivity in High T_c Oxides and Other Materials and Their Manifestations," International Workshop on Novel Mechanisms of Superconductivity, Berkeley, CA, June 1987.
15. V.Z. Kresin, "Coexistence of Phonon and Non-Phonon Mechanisms," International Conference on High T_c Superconductivity, Trieste, Italy, July 1987.
16. V.Z. Kresin, "New Superconducting Materials," International Conference on RF Superconductivity, Argonne, IL, Sept. 1987.
17. V.Z. Kresin, "Mechanisms of High T_c," Naval Research Laboratory, Washington, DC, Feb. 1987.
18. V.Z. Kresin, "New Superconductors," Jet Propulsion Laboratory and California Institute of Technology, Pasadena, CA, May 1987.
19. V.Z. Kresin, "Theory of High T_c," Frascati Laboratory, Frascati, Italy, July 1987.
20. V.Z. Kresin, "Exotic Properties of New High T_c Materials," IBM Research Laboratory, Yorktown Heights, NY, Sept. 1987.
21. V.Z. Kresin, "High T_c and the Multigap Structure," University of Wisconsin, Milwaukee, Sept. 1987.

UNITED STATES AIR FORCE

Quantum Monte Carlo Study of Tetrahydrogen*

William A. Lester, Jr., Investigator

INTRODUCTION

The purpose of this project is to investigate properties of tetrahydrogen (H_4) using the fixed-node quantum Monte Carlo (FNQMC) method. Properties of interest include formation mechanisms, potential-energy surfaces, lifetimes, and decay channels. At long range, the H_4 species of interest correlates with $H_2(^1\Sigma_2^+) + H_2(B\,^1\Sigma_u^+)$ at one asymptote and $H + H_3$ at the other asymptote. Efforts are directed at confirming the existence and stability of the maximum-ionicity excited state (MIES) using multireference configuration-interaction wave functions.[1] The FNQMC approach will be used to determine decomposition pathways and, in particular, classical barriers to formation of the MIES and other excited forms. Hartree-Fock, multiconfiguration Hartree-Fock, and configuration-interaction wave functions will be used, where appropriate, as importance functions in FNQMC study.

1. C. A. Nicolaides, G. Theodorakopoulos, and I. D. Petsalakis, J. Chem. Phys. **80**, 1705 (1984).

*This work was supported by the U.S. Air Force Rocket Propulsion Laboratory under Contract No. F04611-85-X-0068, through an agreement with the U.S. Department of Energy under Contract No. DE-AC03-76SF00098.

1987 PUBLICATIONS AND REPORTS

Invited Talk

1. W.A. Lester, Jr., "Quantum Monte Carlo Study of the MIES Associated with $H_2(X\,^1\Sigma_g^+)$ and $H_2(B\,^1\Sigma_u^+)$," University of Dayton-sponsored Cooling Condensation and Storage of Hydrogen Cluster Ions Workshop, SRI International, Menlo Park, CA, Jan. 8–9, 1987.

UNITED STATES DEPARTMENT OF TRANSPORTATION

Materials for Enhanced Heavy Fuel Capability Marine Diesels—Part 1*

Alan V. Levy Investigator

1. The Durability of Thermal Barrier Coatings in Diesel Engines (Publication 3)

A.V. Levy and S. MacAdam

A representative selection of diesel engine combustion zone components coated with plasma sprayed zirconia thermal barrier systems was analyzed after 14,000 hours of practical engine service. The coating systems under investigation included a flame stabilized and a pre-alloyed 8% Y_2O_3-ZrO_2 coating and a flame stabilized 22% MgO-ZrO_2 coating. All three of these systems applied to piston crowns survived engine service with no noticeable deterioration of any kind. Coating performance on valve faces was mixed. The 22% MgO-ZrO_2 valve coating consistently spalled at or near the interface, with the expansion associated with the observed phase transformation of the zirconia to the monoclinic structure. The flame stabilized 8% Y_2O_3-ZrO_2 coating on the valves consistently failed over large regions while a pre-alloyed coating of the same composition survived with only minimal loss. This strongly suggests that the successful coating system–engine component combinations indicated have the durability to reliably serve through the overhaul lifetime in this type of service (18,000 to 22,000 hours).

1987 PUBLICATIONS AND REPORTS

Refereed Journals

1. A.V. Levy and S. MacAdam, "The Behavior of Ceramic Thermal Barrier Coatings on Diesel Engine Combustion Zone Components," Surface and Coatings Technology **30**, 51 (1987).

Other Publications

2. A.V. Levy and S. MacAdam, "Performance Analysis of Ceramic Thermal Barrier Coatings After 9000 Hours Service in a Marine Diesel Engine," ASME Paper No. 87-ICE-14.
3. A.V. Levy and S. MacAdam, "Durability of Ceramic Coatings in 14,000 Hours Service in a Marine Diesel Engine," ASME Paper No.88-ICE-19.

*This work was supported by the U.S. Department of Transportation, Maritime Administration, P.O. No. 400-49002, through an agreement with the U.S. Department of Energy under Contract No. DE-AC03-76SF00098.

Materials for Enhanced Heavy Fuel Capability Marine Diesels—Part 2*

Alan V. Levy, Investigator

1. The Performance of Thin Y_2O_3-ZrO_2 Coatings in the DDA 149 Engine (Publication 1)

A.V. Levy

Combustion zone components and exhaust manifolds of a DDA 149 diesel engine were coated and tested on an engine test stand for 150 hours to determine engine performance characteristics and gain some indication of coating durability. A pre-alloyed 8%Y_2O_3-ZrO_2 coating was plasma sprayed on the test parts. The coating performed well on the piston domes and exhaust manifold components. There was a small amount of spallation of the coatings inward from the edges of some of the exhaust valve faces due to thermal-mechanical stresses that developed at the abrupt termination of the the coating. Feathering of coating near the valve face edge would eliminate the type of minor coating loss that occurred. This is the first test segment in this project whose objective is to determine the performance of thin ceramic thermal barrier coatings in a variety of service applications.

1987 PUBLICATIONS AND REPORTS

Other Publications

1. A.V. Levy, "Behavior of Y_2O_3-ZrO_2 Plasma Sprayed Coatings on Combustion Zone Components of a DDA 149 Engine," report to Detroit Diesel Allison Corp., Apr. 1987.

*This work was supported by the U.S. Department of Transportation, Maritime Administration, P.O. No. 400-49002, through an agreement with the U.S. Department of Energy under Contract No. DE-AC03-76SF00098.

U.S.-SPAIN JOINT COMMITTEE FOR SCIENTIFIC AND TECHNOLOGICAL COOPERATION

Improved Emission Control Catalysts*

Heinz Heinemann, Investigator, with J. Odriozola and J. Marti

INTRODUCTION

This program aims to investigate the catalytic removal of NO_x from power plant stack gases by reaction with ammonia in the presence of vanadia-titania catalysts. It seeks to determine a reaction mechanism and means to improve catalyst performance. It is a joint program with the Catalysis Institute of the Consejo Superior d'Investigaciones Scientificas in Madrid, Spain. Dr. Juan Garcia de la Banda is the Spanish principal investigator. Work is performed both in Madrid and at LBL according to an agreed upon work plan. Only the work at LBL is reported here.

1. Work in Progress

Surface Science Studies of V_2O_5/TiO_2 Catalysts

XPS, Auger, and TPS studies of pure vanadium pentoxide have shown that ammonia reduces V(V) to V(IV) while being oxidized to N_2O. V_2O_5 does not sorb NO, but V(IV) can be oxidized to V(V) by NO, which in turn is reduced to N_2. N_2O can react with surface vacancies to decompose to nitrogen. Oxygen is needed in the feed gas stream, and the overall reaction is

$$4NO + 4NH_3 + O_2 \rightarrow 4N_2 + 6H_2O.$$

Titania in the anatase form sorbs NO readily, though there are differences in the amount of adsorption for different titania preparations. It appears that NO adsorbed on titania spills over to V_2O_5 that has been reduced by NH_3 to V(IV).

Dispersion of V_2O_5 on titania is another important factor for catalytic activity. Catalyst improvements can probably be made by choosing a well-dispersed V_2O_5 on a highly NO-adsorbing titania.

Some commercial catalysts are prepared by using phosphoric acid as a binder during extrusion. This work has shown that, in the presence of phosphorus compounds, the vanadia surface is greatly reduced. Extrusion with organic binders that can be burned out appears to be preferable.

*This work is supported by the U.S.-Spain Joint Committee for Scientific and Technological Cooperation through Register Number CCA-8411-018.

ELECTRIC POWER RESEARCH INSTITUTE

Erosion-Corrosion of Materials in Coal-Water Slurries*

Alan V. Levy, Investigator

1. Erosion-Corrosion of Materials in Coal-Water Slurries (Publication 2)

A.V. Levy and S. MacAdam

Pulverized coal can be carried into coal gasifiers in a water slurry. The carbon steel pipes used to contain the slurry are subjected to erosion-corrosion. The potential use of erosion resistant liner materials to prevent an unacceptable metal loss rate of the carbon steel was investigated by determining the room and elevated temperature erosion rates of mild steel and a number of protective layer materials. The tests were carried out in a slurry pot tester using neutral and acidic waters for test durations that caused steady state material loss rates to occur. It was determined that the materials' behaviors were in three performance levels. The corrosion resistance of materials, even in neutral slurries, was the primary factor in establishing their metal wastage rates. Hard, basically nonmetallic materials such as alumina and fused basalt had very low loss rates in the range 3–7 mils/yr. Iron-based materials with a high chromium content that formed carbides had low loss rates of 15 to 20 mils/yr. The third level of materials tested was basically lower chromium content, thermally hardened steel surfaces that eroded at high rates of 200–250 mils/yr, the same as the mild steel piping material used as a comparative standard. The mechanisms of material loss were determined for each material and correlated well with the three different material loss rate regimes.

1987 PUBLICATIONS AND REPORTS

Other Publications

1. S. MacAdam and A.V. Levy, "Erosion of Materials by Coal-Water Slurries," in *Proc. ASM Symp. on Materials for Coal Gasification*, Cincinnati, OH, Oct. 1987.

LBL Reports

2. A.V Levy and S. MacAdam, "Erosion-Corrosion of Materials in Coal-Water Slurries," EPRI Report; LBL-24613.

*This work was supported by the Electric Power Research Institute.

A Cold Model Study of Wear on Fluidized Bed Combustor Tubes*

Alan V. Levy, Investigator

1. Work in Progress

Energy production from the fluidized bed combustion of coal has many advantages over conventional coal burning methods. A large reduction in emissions of pollutants believed to cause acid rain, as well as a greater operating efficiency and wider fuel tolerance, make fluidized bed combustion an attractive technology. A major problem encountered in the combustion of coal by this process has been the material wastage of heat exchanger tubes immersed in the burning fluidized bed. This wastage is the result of a combination of material wear, due to particle/tube interactions, and corrosion, resulting from a favorable thermal and chemical environment. Erosion/corrosion of in-bed tubes has resulted in unacceptable wastage rates often as high as 1 mm/1000 hours.

Wear in fluidized beds can result from many causes. It is believed that a major contribution to wear arises from the impact of blocks of essentially unfluidized particles on the tubes as a result of either bubble passage or a cooperative bed particle motion. Optical experiments have shown such particle blocks impacting tube bottoms and sliding across their surfaces. In an effort to investigate this process, isolated from other effects and in a controlled environment, a cold fluidized bed unit has been designed and built with the unique feature of a specimen tube that can be quickly actuated a short distance vertically within a minimally fluidized bed. The downward specimen motion is of similar frequency and velocity to that of the impacting particle blocks in an operating fluidized bed. Because the bed is minimally fluidized during testing, all other contributions to wear are essentially eliminated.

Results of the cold model study have thus far strongly supported the particle block impact theory. Material wastage rates agree very well with the results of other cold bed tests carried out under typical fluidizing conditions. Furthermore, the wastage pattern around the exposed tubes duplicates that which has often been found in practice. The mechanism of material removal was found to be one of a combination of ploughing and micro-machining due to the dragging of partially constrained particles across the tube surface. Study of tube wear behavior in a cold bed environment will continue so that the effects of material properties and particle loading conditions on wastage rates and distribution can be determined. The testing unit will then be modified to operate at a temperature under which the combined effects of corrosion and wear can be investigated.

*This work was supported by Electric Power Research Institute through Agreement No. RP8000-6.

Appendices

APPENDIX A

DIVISION PERSONNEL

1987 Scientific Staff

Investigators	Postdoctoral and Other Scientists	Graduate Students		Participating Guests
Neil Bartlett	R. Hagiwara	K. Kourtakis M. Lerner	S. Mayorga B. Shen	T. Richardson T. Sasaki
Alexis Bell	M. Sattler	J. Brown D. Jordan K. Krishna	S. Lombardo G. Went G. Yokomizo	R. June R. Rosin
Robert Bergman		K. Bharucha E. Burkhardt J. Chang T. Foo D. Glueck K. Goldberg J. Hartwig D. Johnson	D. Klein W. McGhee R. Simpson P. Stoutland M. Trost P. Walsh E. Wasserman	
Robert Bragg	Y. Kaburagi A. Lachter	M. Tidjani		J. Aladekomo
Leo Brewer	C. Meyer	J. Bularzik B. Ebbinghaus J. Kouvetakis	K. Krushwitz S. Leonard	
John Clarke		A. Cleland N. Fan M. Ferrari M. Heaney	J. Pelz J. Schmidt F. Wellstood	R. Dalven
Marvin Cohen	K. Chang	S. Zhang		
Eugene Commins		K. Abdullah		
Robert Connick	R. Adamic			
Didier de Fontaine	J. Kulik L. Wille	A. Berera J. Hoyt	P. Huang	C. Burmester B. Davis M. Kraitchman M. Wiedenmeier
Lutgard De Jonghe	M. Armand A. Garg M. Rahaman S. Varanasi S. Visco	Y. Boiteux T. Buchanan M. Chu D. Kapolnek T. Kueper M. Lin	M. Liu C. Mailhe E. Reiner C. Sheu M. Weiser	S. Shinde

Investigators	Postdoctoral and Other Scientists	Graduate Students		Participating Guests
Norman Edelstein	B. Attenberg	T. Boussie	J. Rigsbee	T. Allyn
	S. Beshouri	D. Eisenberg	R. Rosen	A. Bulls
Richard Andersen	J. Brennan	M. Fabiano	P. Smith	C. Burns
Kenneth Raymond	J. Bucher	T. Franczyk	J. Stewart	S. Evans
Andrew Streitwieser, Jr.	J. Chambron	L. Gong	S. Stults	M. Ganz
David Templeton	G. Feige	W. Kot	B. Tansy	S. Gokcen
Allan Zalkin	I. Poirot	W. Mallet	L. Uhlir	E. Hahn
	G. Shalimoff	P. Matsunaga	G. Williams	J. Koningstein
		D. Piehler		S. Kretchmar
				J. Krupa
				M. Silva
				L. Templeton
				D. White
				S. Xia
James Evans		L. Feng	O. Rego-Monterio	H. Lee
		B. Li	G. Savaskan	E. Luh
				S. Siv
				H. Tsai
Leo Falicov		D. Chrzan	A. Reich	
Andreas Glaeser		W. Carter	J. Roedel	
		L. Edelson	M. Shalz	
Harvey Gould	C. Bengtsson	C. Munger		
	J. Schweppe			
Ronald Gronsky				J. Camberos
				M. Fendorf
				M. Kundmann
				S. Packer
				J. Punglia
				C. Shim
				W. Soffa
				L. Yamamoto
Eugene Haller*				
Charles Harris		M. Arndt		E. Haas
		J. Brown		R. Hoff
		R. Jordan		W. Merry
		E. Peterson		M. Paige
				D. Pennington
				M. Prisant
				D. Russell
				B. Schwartz
				D. Smith
Heinz Heinemann	J. Odriozola			J. Munoz
Carson Jeffries		P. Bryant	Q. Lam	
		Y. Kim		
Harold Johnston	A. Young	J. Burley	C. Miller	
		P. Hunter	B. Oh	
		B. Kim	K. Patten	
		D. Kinnison	W. Sisk	
William Jolly				

*Also affiliated with the Engineering Division

Investigators	Postdoctoral and Other Scientists	Graduate Students		Participating Guests
Yuan Lee	G. Nathanson Q. Zhu	J. Allman B. Balko R. Brudzynski P. Chu R. Continetti M. Covinsky E. Cromwell H. Davis M. Helfand	E. Hintsa J. Meyers J. Price G. Robinson A. Schmoltner A. Suits M. Vrakking L. Yeh X. Zhao	R. Ferrieri J. Mestdagh W. Miller D. Neumark T. Trickl A. Yokoyama
William Lester, Jr.	V. Kresin P. Reynolds	R. Barnett C. Dateo B. Hammond	S. Huang R. Owen	B. Bernu J. Dixon K. Pape P. Pernot M. Srinavasan C. Young
Alan Levy	S. MacAdam			Z. Shui B. Wang
Steven Louie	J. Northrup	S. Fahy		H. Lin
William Miller	J. Chang	Y. Chang T. Gray J. Tromp	A. Makri B. Ruf	B. Jansen J. Zhang
C. Bradley Moore		T. Butenhoff I. Chen Y. Choi D. Darwin M. Foltz	J. Frisoli W. Green Y. Guo V. Venturo	M. Chuang A. Kung M. Ochsner
Rolf Muller	H. Gerischer	M. Armstrong D. Barkey R. Crocker	J. Gyory S. Mayer	G. Burgess
John Newman		V. Battaglia T. Fuller C. Haili A. Hauser	A. Mason P. Shain G. Sisler A. West	
Donald Olander	M. Derzon F. Tehranian	J. Abrefah K. Kim M. Moalem	A. Motta K. Park D. Sherman	M. Ballooch H. Harrell T. Wonnell S. Yagnik
Norman Phillips	C. Marcenant	S. Kim S. Lacy	J. Olsen	R. Fisher J. Gordon
Alexander Pines	J. Anandan G. Chingas D. Suter K. Takegoshi T. Terao	D. Caplan J. Chang C. Connor M. Gochin T. Jarvie C. Lee K. Mueller	J. Pearson M. Raferty S. Rucker D. Shykind A. Thayer M. Trecoske	H. Cho L. DeMenorval H. Huber S. Liu M. Luzar S. Matsui K. Neidig A. Shaka C. Schmidt A. Somoson U. Werner
Kenneth Pitzer	D. Schreiber R. Singh J. Tanger			J. Yang
John Prausnitz		R. Cotterman A. Harvey	A. Wu	

Investigators	Postdoctoral and Other Scientists	Graduate Students		Participating Guests
Michael Prior				H. Berg J. Pederson H. Schmidt-Bocking H. Shugart
Paul Richards		G. Bernstein M. Fischer A. Lange	D. Miller R. Phelps S. Verghese	P. Timbie
Robert Ritchie		R. Dauskardt J. Mason	T. Oh J. Shang	J. Cullinan G. Doi F. Haubensak H. Hayashigatani J. Miwa P. Spencer W. Yu
Gerd Rosenblatt	K. Viers	V. Chia		
Philip Ross	K. Gaugler A. Haner C. Pender H. Saffarian			L. Johnson
Richard Saykally		K. Busarow R. Cohen D. Gwo D. Hovde	K. Laughlin R. Robinson D. Steyert	
Alan Searcy	P. Hou D. Meschi	J. Bierach R. Cinque		
Y. Ron Shen		W. Chen M. Feller A. Karn	C. Mullin X. Xiao X. Zhu	P. Guyot-Sionnest M. Haner L. Martinez-Miranda R. Pan T. Stehlin J. Tapie
David Shirley	S. Kim	P. Heimann Z. Huang L. Huckabee E. Hudson L. Medhurst B. Niu	A. Schach von Wittenau L. Terminello R. Vanzee L. Wang J. Zhang	P. Gresser K. Leung S. Liu Z. Yang X. Zhang
Gabor Somorjai	M. Van Hove M. Xu	G. Blackman M. Bussell J. Carrazza S. Fu D. Godbey C. Kao	D. Kelly C. Knight K. Lewis P. McAnally T. Rucker G. Vurens	J. Adams P. Bernhardt F. Garin I. Harrison J. Houlihan M. Khader R. Nix J. Novskov H. Ohtani R. Pande E. Sowa D. Sullivan P. Xu
Angelica Stacy		J. Badding M. Dixon M. Geselbracht W. Ham R. Hoskins	S. Keller P. Vernody J. Womack H. zur Loye	G. Holland

Investigators	Postdoctoral and Other Scientists	Graduate Students		Participating Guests
Gareth Thomas	H. Zandbergen	L. Chan M. Chandramouli J. Chen M. Dass	H. Ho T. Huynh S. Miyasato R. Ramesh	T. Bielicki D. Bradley D. Callahan K. Gupte J. Kim J. Kim C. Koestler V. Radmilovic L. Sidjanin K. Srikrishna
Charles Tobias		P. Andersen S. Hessami K. Jordan L. McVay	D. Sutija G. Whitney B. Wines	R. Anderson
K. Peter Vollhardt		M. Huffman P. McGovern R. Myrabo	D. Newman W. Tolman M. West	
Jack Washburn	Z. Liliental J. Mazur N. Newman	L. Allen R. Caron J. Ding	C. Jou J. Lou D. Olson	D. Ah Tye W. Swider
Kenneth Westmacott	U. Dahmen C. Hetherington R. Kilaas K. Krishnan M. O'Keefe			J. Dobson P McDougall J. Penisson J. Posthill M. Whitcomb
Peter Yu	D. Erskine	H. Goldstein E. Hess Y. Haung	D. Kim Q. Williams	M. Li G. Martinez W. Shan
Alex Zettl		S. Hoen		W. Creager

Support Staff

Division Administrative Staff

M. Alper — Associate Division Head
Division Administrators: L. Maio, M. Montgomery

Administration

L. English
J. Leonard
R. Rodriguez

Personnel/Financial

C. Coolahan
R. Hunt
P. Paladini
G. Solomon
S. Waters

Purchasing

S. Stewart
J. Leonard

Technical Editor

R. Albert

Travel

S. Quarello

Administrative/Secretarial Staff

T. Allyn
R. Arcol
M. Atkinson
C. Becker
H. Benson
M. Bishop
M. Borgrink
G. Brazil
D. Carmichael
H. Conti
N. Corwin
J. Denney
L. Dory
E. Edelson
S. Ewing
S. Gangwer
C. Gliebe
L. Gloria
R. Jones
B. Kuchinsky
E. Lemos
M. Momii
M. Moore
L. Mori
B. Moriguchi
T. Narasimhan
M. Noyd
G. Osterloh
M. Penton
P. Ray
R. Rodriguez
B. Tung
A. Weightman
A. Wingfield
K. Wong
S. Yamagishi
C. Yoder
B. Zambrano
J. Zissler

Technical Staff

Technical Coordinator: M. Moebus/J. Holthuis

D. Ackland
H. Ackler
D. Ah Tye
H. Brendel
R. Cardenas
N. Claytor
D. Colomb
K. Desai
C. Echer
C. Flor
G. Gager
L. Gill
A. Gronsky
J. Holthuis
J. Jacobsen
D. Jurica
E. Mah
J. Miles
E. Nelson
M. Ng
T. Prussin
R. Ruegg
L. Rumaner
J. Severns
W. Smith
H. Sokol
B. Sun
L. Sun
G. Tabler
J. Turner
J. Wu

APPENDIX B

DIVISION COMMITTEES

DIVISIONAL COUNCIL

A. Bell
L. De Jonghe
H. Johnston
S. Louie
K. Raymond
R. Ritchie
P. Ross
G. Thomas
K. Westmacott

DIVISIONAL RESEARCH STAFF COMMITTEE

N. Edelstein
L. Falicov
R. Muller*
K. Westmacott

ELECTRON MICROSCOPE USERS COMMITTEE

R. Gronsky
P. Ross*
K. Westmacott

EQUIPMENT REVIEW COMMITTEE

J. Clarke
H. Johnston
R. Muller*
R. Ritchie
P. Yu

TECHNICAL STAFF AND SHARED FACILITIES COMMITTEE

L. De Jonghe*
R. Gronsky
P. Ross
G. Somorjai

ADMINISTRATIVE STAFF COMMITTEE

C. Peterson*
M. Van Hove
P. Yu

MCSD SAFETY COORDINATOR

D. Meschi/R. Ellis

SAFETY AND LABORATORY STANDARDS COMMITTEE

Buildings 62, 66, and 72

D. Ackland
H. Brendel
D. Colomb
R. Ellis*
L. English
K. Gaugler
J. Haley
J. Holthuis
J. Jacobsen
L. Johnson
D. Jurica
D. Krieger
J. Leonard
E. (Fong) Mah
D. Meschi
M. Moebus
B. Muhammad
R. Muller
E. Perez
C. Peterson
P. Ruegg
M. Salmeron
J. Severns
G. Shalimoff
S. Stewart
W. Wong
J. Wu

Building 70A

D. Lindle
T. Minton
G. Shalimoff*
A. Weightman

CERAMICS PROGRAM ADVISORY COMMITTEE

R. Gronsky
R. Ritchie
A. Searcy

BUILDING AND SPACE COMMITTEE

R. Gronsky
D. Meschi
R. Muller*
A. Zalkin

Buildings 62 and 66 Building Manager:
D. Meschi/R. Ellis
(Alternate: C. Peterson)

Building 72 Building Manager:
K. Westmacott
(Alternate: D. Ackland)

---

*Chairman

APPENDIX C

LIST OF DIVISIONAL SEMINARS

Surface Science and Catalysis Seminars

Date	Speaker and Affiliation	Seminar Title
1-8-87	V. Akhmedov, Azerbaidjan State University, Baku, USSR	Catalytic Oligomerization of Dienes and Olefins with Catalysts Derived Directly from Metal Atoms
1-15-87	T.L. Einstein, University of Maryland	Phase Transitions of Chemisorbed Atoms: What Can Be Learned About and From 2-D Critical Properties
1-22-87	T. Gentle, Dow, Midland, MI	Recent Developments in Silicon Surface Chemistry
1-27-87	S.C. Fain, University of Washington, Seattle	Incommensurate Hydrogen Molecular Layers on Graphite
1-29-87	E. Sutcliffe, IBM, Yorktown Heights, NY	Controlled Modification and Etching of Organic Polymer Films by Pulsed UV Laser Radiation
2-5-87	D. Auerbach, IBM Almaden Research Center, San Jose, CA	Molecular Beam Studies of Dissociative Chemisorption
2-12-87	R. Bastasz, Sandia National Laboratory, Livermore, CA	Hydrogen at Palladium Interfaces Studied with Semiconductor Devices
2-19-87	B.E. Koel, University of Colorado, Boulder	Chemistry of Nitrogen Dioxide on Metal Surfaces
2-26-87	J. Whitten, SUNY, Stony Brook, NY	Chemisorption on Metals: CH Fragments
3-9-87	F. Hansen, University of Utah	Syngas Conversion to Olefins over Raney Fe-Mn Catalysts: A Process Variable Study
3-12-87	J.W. Larsen, Lehigh University, Bethlehem, PA	The Macromolecular Structure of Coals
3-19-87	T. Oyama, Catalytica Associates	Structure Sensitivity of Propylene Oxidation on Oriented MoO_3 Crystallites
3-20-87	A. Inspektor, Nuclear Research Center, Negev, Israel	Plasma-Assisted Chemical Vapor Deposition of Hard Wear-Resistant Coatings
4-2-87	J.R. Anderson, CSIRO, Australia	Hydrogenolysis Reactions: New Light; Old Problems
4-8-87	J. McLaren, Imperial College, London	Catalytic Implications of Surface Electronic Structure and Perturbations Induced by Coadsorbates
4-9-87	H. Ibach, KFA Jülich, Federal Republic of Germany	Surface Phonons, Surface Stress, and Surface Reconstruction

Date	Speaker and Affiliation	Seminar Title
4-23-87	D. Smith, IBM, Yorktown Heights, NY	The Effect of Mismatch on the Epitaxy of Metal Films
4-30-87	A. Ignatiev, Space Vacuum Epitaxy Center, University of Houston	Epitaxial Crystal Growth in Outer Space
5-7-87	R. Prins, Technical University, Eindhoven, The Netherlands	EXAFS Study of the Metal Particle Size and Metal-Support Interface of Rh, Pt, and Ir on Al_2O_3, SiO_2, and TiO_2 Catalysts
5-13-87	B.J. Kip, Eindhoven University, The Netherlands	Selective Formation of Oxy-Products in Synthesis Gas Reactions over Rh/SiO_2 Promoted by V_2O_3, MoO, and ThO_2
5-14-87	J. Oudar, Université Pierre et Marie Curie, Paris	Butadiene Hydrogenation on Platinum Single Crystals
5-21-87	F. Parmigiani, CISE Research Center, Milan, Italy	Electronic Structure of Small Metal Clusters and Their Interaction With a Substrate
6-4-87	M. Geusic, Battelle Pacific Northwest Laboratories, Richland, WA	Cluster Studies Within a Supersonic Molecular Beam
6-11-87	F. Garin, Laboratoire de Catalyse et Chemie des Surfaces, Strasbourg, France	A Study of Reforming Reactions on Supported Metallic Platinum and Single Crystal Catalysts by the Use of Labelled Hydrocarbons
7-9-87	J. Norskov, Nordita, Copenhagen	Adsorbate-Induced Reconstructions of fcc(110) Metal Surfaces
7-14-87	G. Maire, CNRS, Strasbourg, France	Catalytic Properties of Small Particles and Surface Crystals of Platinum—Extension to Alloys
7-16-87	A.A. Lucas, Namur, Belgium, and IBM Almaden, San Jose, CA	Theory of Tunneling Through Localized Barriers: Application to Scanning Tunneling Microscopy
7-30-87	Prof. D. Olivier, Université Pierre et Marie Curie, Paris	Dimerization of Olefins by Tailor-Made Supported Nickel Complexes. Selectivity Control by Electronic and Steric Ligand Effect
8-13-87	C.M. Mate, IBM Almaden Research Center, San Jose, CA	The Atomic-Force Microscope
8-20-87	H.P. Boehm, Institute of Inorganic Chemistry, University of Munich	Metal on Titania Catalysts, Photochemical Preparation and Observations of Their Catalytic Behavior
8-25-87	C. Minot, University of Paris, Orsay, France	Benzene and Toluene Adsorption on Hexagonally Packed Ru(0001), Rh(111), Pd(111), and Pt(111)
8-27-87	M. Asscher, Hebrew University, Jerusalem, Israel	Structure-Sensitive Gas-Surface Interactions
9-3-87	S. Chiang, IBM Almaden Research Center, San Jose, CA	Scanning Tunneling Microscopy of Metals on Semiconductors
9-10-87	J.G. Tobin, University of Wisconsin, Madison	Photoemission and Inverse Photoemission of Metal Overlayers Systems

Date	Speaker and Affiliation	Seminar Title
9-17-87	C.R. Henry, University of Marseilles, France	Adsorption Kinetics on Stepped Surfaces by Molecular Beam Techniques
9-24-87	P. Pfeifer, University of Missouri, Columbia	Critical Phenomena on Fractal Surfaces
10-1-87	P. Williams, National Tritium Labeling Facility, LBL	Tritium Labeling and Tritium NMR
10-8-87	J.P. Cowin, University of California, Santa Barbara	Photodynamics of Molecules on a Metal Surface
10-15-87	S. Kaiser, Union Carbide, Charleston, SC	Methanol Conversion to C_2-C_4 Olefins Over Aluminophosphate Molecular Sieves
10-22-87	A.T. Hubbard, University of Cincinnati	Electrochemistry of Well-Defined Surfaces
10-23-87	G. Comsa, Jülich, Federal Republic of Germany	Hydrogen Does Not Dissociate on Pt(111)-Terraces
10-29-87	D. Gruen, Argonne National Laboratory	Depth of Origin of Sputtered Atoms
11-5-87	N. Spencer, W.R. Grace & Co., Maryland	Partial Oxidation of Methane
11-6-87	H.P. Bonzel, Jülich, Federal Republic of Germany	Surface Energy Anisotropy and Surface Reconstruction
11-12-87	K.M. Ho, Iowa State University, Ames	Theory of the Missing Row Reconstruction on Transition Metals
11-19-87	G. Kubiak, Sandia National Laboratory, Livermore, CA	Characterization of Normally Unoccupied Bands on Cu(111) and C(111) (2×1) (diamond) Via Two-Photon Photoemission
12-3-87	L.L. Kesmodel, University of Indiana, Bloomington	High-Resolution EELS Studies of CO and Hydrocarbon Adsorption on Supported Platinum Particles
12-10-87	H.C. Siegmann, ETH-Zürich and IBM Almaden	Magnetism in Epitaxial Films
12-17-87	G.B. Fisher, General Motors Research Laboratory, Warren, MI	CO Oxidation and NO Reduction Over Rhodium Catalysts. High-Pressure Rates Explained Using UHV Surface Science

Chemical Dynamics Seminars

1-28-87	D.J. Kouri, Dept. of Chemistry, University of Houston	Amplitude Density Approach to Reactive Scattering
1-30-87	R. Gordon, Dept. of Chemistry, Harvard University	Chemical Vapor Deposition
2-12-87	G.S. Ezra, Dept. of Chemistry, Cornell University, Ithaca, NY	Resonances, Antiresonances, and Bottlenecks: A Phase Space View of Vibrational Relaxation
3-30-87	J.J. Murrell, University of Sussex, England	Non-Adiabatic Transitions for Polyatomic Molecules

Date	Speaker and Affiliation	Seminar Title
4-20-87	S.L. Anderson, Dept. of Chemistry, State University of NY, Stony Brook	Physical and Chemical Properties of Aluminum Cluster Ions
4-22-87	S. Nordholm, School of Chemistry, University of Sydney, Australia	An Explanation of Covalet Bonding Using Nonergodic Thomas-Fermi Theory
4-29-87	E. Pollak, Israel	
7-10-87	L. Holmlid, Dept. of Physical Chemistry, University of Goteborg, Sweden	
7-16-87	R. McGreevy, Clarendon Laboratory, Oxford, England	Structure and Dynamics of Molten Salts: Experiments and Computer Simulations

Electron Microscopy Seminars

1-15-87	R. Geiss, IBM, San Jose	Transmission Electron Microscopy of Thin Magnetic Media
1-29-87	D. Attwood, LBL	Coherent Radiation at X-ray Wavelengths: Optics and Applications
2-12-87	F. Ponce, Xerox Palo Alto Research Center	Application of HREM to the Study of Semiconductors
2-13-87	S. Das, Allied Signal, NJ	Microstructure and Properties of RSP Light Alloys
2-19-87	M. Ruhle, UC Santa Barbara	Structure and Chemistry of Metal-Ceramic Interfaces
3-3-87	D. Ayrault, École des Mines, Paris	Laser Shock Loading Effects in Nickel-Base Superalloys
3-12-87	B. Stacy, Philips/Signetics	Microstructural Studies of Silicon Integrated Circuits
3-26-87	J. Bastacky, LBL	HVEM and AEM of the Lung
4-2-87	J. Clarke, LBL	The Scanning Tunnelling Microscope Looks at the Graphite Surface
4-16-87	H.R. Wenk, UC Berkeley	Microstructures in Minerals and their Geological Interpretations
5-1-87	G. Van Tendeloo, University of Antwerp, Belgium	HREM of Different Sublattices in Complex Materials
5-7-87	R. Sinclair, Stanford	Interpretation of Semiconductor Interface Reactions using Ternary Phase Diagrams
5-14-87	W.A. Soffa, University of Pittsburgh	The Relationship Between Microstructure and Mechanisms of Magnetic Reversal in Hard Magnetic Materials

Date	Speaker and Affiliation	Seminar Title
6-22-87	R. Egerton, SUNY, Stony Brook, NY	Recent Developments in Electron Energy-Loss Spectroscopy
10-12-87	K.H. Downing, LBL	TEM Studies of Organic Materials—Reducing the Effects of Radiation Damage
10-19-87	I. McFadyen, IBM, San Jose	Characterization of Magnetic Materials Using Electron Microscopy
10-26-87	J.B. Kortright, LBL	Grazing Incidence X-ray Scattering Studies of GaAs on Si and Other Systems
10-28-87	A. Loiseau, ONERA, Paris	High Resolution Studies of Al-Cu-Li-Mg Quasicrystals
11-2-87	H. Zandbergen, University of Leiden, The Netherlands	HREM Studies of High T_c Superconductors, Structure-Property Relationships
11-9-87	D.F. Blake, NASA Ames Research Laboratories, Mountain View, CA	Analytical Microscopy of the Nature and the Origin of Interstellar Diamond
11-17-87	J.M. Gibson, ATT Bell Laboratories	*In situ* Studies of Molecular Beam Epitaxy by TEM
11-23-87	O. Krivanek, Gatan	Parallel Detection EELS
12-7-87	D. Howitt, UC Davis	Electron Beam Damage in Electron Microscopy
12-14-87	C.W.T. Bulle-Lieuwma, Philips Research, Eindhoven, The Netherlands	Nucleation and Growth of $CoSi_2$ on (100) and (111)Si

Other Seminars Hosted

3-9-87	A.L. Johnson, National Bureau of Standards, Gaithersburg, MD	Recent Work on the Chemisorption of First Row Protic Hydrides on Si(100) Using ESDIAD
3-10-87	D.W. Lindle, National Bureau of Standards, Gaithersburg, MD	Fluorescence Spectroscopy
4-10-87	B. Zemva	New Synthetic Routes to Fluorometallates
8-26-87	O. Glemser	Studies about Positive Electrodes for the Alkaline Accumulator Together with Some Aspects of Electrotraction

APPENDIX D

INDEX OF INVESTIGATORS*

Andersen, Richard A. **203**

Bartlett, Neil **192**, **203**
Bell, Alexis T. **185**
Bergman, Robert G. **195**
Bragg, Robert H. **66**
Brewer, Leo **111**

Carrazza, J. **223**
Clarke, John **86**, 134
Cohen, Marvin L. 86, **94**, 99, 102, 103, 138, **256**
Commins, Eugene **258**
Connick, Robert E. **184**
Conway, John G. **203**

de Fontaine, Didier 27, 32, **39**, **41**
De Jonghe, Lutgard C. 30, **62**, **227**, **239**

Edelstein, Norman M. **203**
Evans, James W. **37**, **227**, **237**

Falicov, Leo M. **41**, **91**, 247

Glaeser, Andreas M. **68**
Gould, Harvey **179**, **258**
Gronsky, Ronald **1**, 12, **19**, 56, 58

Haller, Eugene E. 72, **247**
Harris, Charles B. **145**
Heinemann, Heinz **223**, **266**

Jeanloz, Raymond 146, **256**
Jeffries, Carson D. **81**
Johnston, Harold S. **143**
Jolly, William L. **191**

Kresin, Vladimir Z. **261**

Lee, Yuan T. 76, 78, 161, 169, **173**
Lester, William A., Jr. **155**, **259**, **263**
Levy, Alan V. **219**, **264**, **265**, **267**, **268**
Louie, Steven G. 94, 95, **98**, 138

Marti, J. **266**
Miller, William H. **162**
Moore, C. Bradley **148**
Muller, Rolf H. 107, **117**, **227**, **232**

Newman, John **227**, **243**

Odriozola, J. **266**
Olander, Donald R. **114**

Phillips, Norman E. **105**
Pines, Alexander **131**
Pitzer, Kenneth S. **151**
Prausnitz, John M. **199**
Prior, Michael H. **181**

Raymond, Kenneth N. **203**
Richards, Paul L. **71**, 102
Ritchie, Robert O. **45**, 252
Rosenblatt, Gerd M. **251**
Ross, Philip N., Jr. **227**, **234**, **254**

Saykally, Richard J. **160**
Seaborg, Glenn T. **203**
Searcy, Alan W. 26, **52**
Shen, Yuen-Ron **76**, 123, 173, 174, 175
Shirley, David A. **165**, 175
Somorjai, Gabor A. **121**, **141**, 186, **223**
Stacy, Angelica M. . 71, 84, 86, 99, 102, 103, 105, **138**, 256
Streitwieser, Andrew, Jr. **203**

Templeton, David H. **203**
Thomas, Gareth **5**, **19**
Tobias, Charles W. **107**, 118, **227**, **229**

Vollhardt, K. Peter C. **188**

Washburn, Jack **56**
Westmacott, Kenneth H. **16**, **19**

Yu, Peter Y. **84**, **256**

Zalkin, Allan **203**
Zettl, Alex 71, 84, 86, 99, **102**, 138, 256

*Boldface numbers indicate investigators' main programs.

LAWRENCE BERKELEY LABORATORY
TECHNICAL INFORMATION DEPARTMENT
UNIVERSITY OF CALIFORNIA
BERKELEY, CALIFORNIA 94720